



<https://theses.gla.ac.uk/>

Theses Digitisation:

<https://www.gla.ac.uk/myglasgow/research/enlighten/theses/digitisation/>

This is a digitised version of the original print thesis.

Copyright and moral rights for this work are retained by the author

A copy can be downloaded for personal non-commercial research or study,
without prior permission or charge

This work cannot be reproduced or quoted extensively from without first
obtaining permission in writing from the author

The content must not be changed in any way or sold commercially in any
format or medium without the formal permission of the author

When referring to this work, full bibliographic details including the author,
title, awarding institution and date of the thesis must be given

Enlighten: Theses

<https://theses.gla.ac.uk/>
research-enlighten@glasgow.ac.uk

**PHYSIOLOGICAL STUDIES ON MICRO-ALGAE
CULTURED IN A MULTI-PASS FLAT PLATE
AIR LIFT PHOTOBIOREACTOR**

By

IAIN A J RATCHFORD MSc

A thesis submitted for the degree of
Doctor of Philosophy
in the University of Glasgow.

Department of Biochemical Sciences
Scottish Agricultural College
Auchincruive, Ayr, KA6 5HW

February 1994.

ProQuest Number: 10647137

All rights reserved

INFORMATION TO ALL USERS

The quality of this reproduction is dependent upon the quality of the copy submitted.

In the unlikely event that the author did not send a complete manuscript and there are missing pages, these will be noted. Also, if material had to be removed, a note will indicate the deletion.



ProQuest 10647137

Published by ProQuest LLC (2017). Copyright of the Dissertation is held by the Author.

All rights reserved.

This work is protected against unauthorized copying under Title 17, United States Code
Microform Edition © ProQuest LLC.

ProQuest LLC.
789 East Eisenhower Parkway
P.O. Box 1346
Ann Arbor, MI 48106 – 1346

Thesis
9905
Cp 2

GLASGOW
UNIVERSITY
LIBRARY

ACKNOWLEDGEMENTS

Firstly I must thank Howard (stick it in the onion bag) Fallowfield for devising and supervising the entire research project after surprisingly having it accepted by the Ministry of Agriculture Fisheries and Food. His firm belief that Tranmere Rovers will one day be at the top the Premier Division shows what a sense of humour he really has. Equal thanks go to Nancy JUDITH, (Whalette on the starboard bow, starboard bow, starboard bow) Cromar for her proof reading ability of my references.

Secondly I must thank Jim Clark for without his help in the construction of the photobioreactor and other aspects of engineering and electronics, the research could have not been carried out.

Thirdly I must thank the Ministry of Agriculture Fisheries and Food for the financial support and in particular the extra 1 year support given after accepting my appeal. I must not forget to thank all the staff at the Biochemical Sciences Department and in particular Archie Gillespie and Philip Simpson for their help ordering items and in finding items which Susan had hidden away in far off places.

Finally I am grateful Nick Martin, Bootser cat, Emma cat and Olly cat for helping to ensure that my lift went and still does go up to the top floor. The help of Huey, Duey and Luey along with Mary Mungo and Midge is also appreciated.

Abstract

A flat plate air lift photobioreactor (FPALR) has been designed, constructed and patented which facilitates the growth and photosynthetic studies of micro-algae and cyanobacteria in a very accurately defined light field of known photon flux density and spectral radiant flux. Whilst being culture in the photobioreactor biomass concentrations of micro-algae were 2-5 times higher than those obtained using chemostats. Concentrations of between 6 and 8% carbon dioxide v/v were found to be toxic to cells of *Chlorella vulgaris* 211/11c and *Scenedesmus sp.* when cultured in the CSTR compared to the FPALR.

The FPALR was found to significantly affect the cellular dynamics of *Chlorella vulgaris* 211/11c when cultured at different Reynolds numbers. At a Reynolds number of 6000 cells of *Chlorella vulgaris* 211/11c had approximately half the volume size of similar cells grown at a Reynolds number of 2500.

The photosynthetic kinetics of unicellular green micro-algae were generally unaffected by the presence of HCO_3^- , however, *Synechococcus* 1479/5 was found to have a higher light saturated rate of photosynthesis in the presence of HCO_3^- . Species of micro-algae and cyanobacteria were found to exhibit different photosynthetic kinetics when incubated in the presence of phosphate buffer compared to ASM. The presence of nitrate in the incubating medium of irradiated cells of both micro-algae and cyanobacteria was found to have a significant affect on preventing the onset of photoinhibition.

Centrifugation prior to P/I measurement was found to increase the respiration rates of all micro-algae and cyanobacteria, the levels of which, however, were species dependent. Increases in photon flux density were found to increase the respiration rates of both micro-algae and cyanobacteria during photosynthesis / irradiance response measurements.

Increases in P/I incubation temperature on cells of micro-algae and cyanobacteria cultured at low growth temperatures of 15°C and 23°C was found to increase the light saturated rates of photosynthesis. The relationship between the natural log of the rate of photosynthesis measured at a PFD of $100\mu\text{mol s}^{-1} \text{m}^{-2}$ and temperature was found to be linear for *Chlorella vulgaris* 211/11c, *Nannochloris atomus*, *Scenedesmus sp.*, *Ankistrodesmus antarcticus*, *Synechococcus sp.* and *Synechococcus* 1479/5. Each of the aforementioned organisms had a higher Q_{10} at a temperature between 20°C and 25°C when grown at a PFD of $100\mu\text{mol s}^{-1} \text{m}^{-2}$ compared to 30°C and 35°C. Cells of *Chlorella vulgaris* 211/11c, *Scenedesmus sp.* and

Synechococcus 1479/5, however, showed a decreasing rate of Q_{10} with increasing temperature when grown at a PFD of $200\mu\text{mol s}^{-1} \text{m}^{-2}$.

Cells of *Chlorella vulgaris* 211/11c and *Synechococcus* 1479/5 were shown to require an increasingly longer period of time in the dark with increasing exposure time and intensity to light at photoinhibitive intensities.

Cells of *Chlorella vulgaris* 211/11c and *Synechococcus* 1479/5 increased their dry matter content and decreased their chlorophyll a content when exposed to increases in PFD. The chlorophyll a content of both *Chlorella vulgaris* 211/11c was found to generally decrease with increasing PFD whilst the maximum rate of photosynthesis was found to increase. Dark respiration and light enhanced dark respiration rates were found to increase sharply when the cells of *Chlorella vulgaris* 211/11c were irradiated at increasing PFD from 100 to $750\mu\text{mol s}^{-1} \text{m}^{-2}$.

Light / dark cycles of medium frequency (seconds to minutes) were found to affect the overall cell productivity of both *Chlorella vulgaris* 211/11c and *Synechococcus* 1479/5. Maintaining the light duration fraction and decreasing the dark duration fraction time whilst increasing the overall frequency of the total light / dark cycle duration was found to decrease cellular productivity.

Light of red wavelengths (600-800nm) were found to significantly increase the LEDR rates of *Chlorella vulgaris* 211/11c, *Scenedesmus sp.* and *Synechococcus* 1479/5 compared to either blue (375-550) or white (300-800nm) light. The incubation of *Chlorella vulgaris* 211/11c and *Scenedesmus sp.* in the presence of $50\mu\text{mol}$ 3(3,4-Dichloro-phenyl)-1,1-Dimethylurea was found to inhibit photosynthesis. Incubations of between 10 and $100\mu\text{mol}$ potassium cyanide (KCN) were found to significantly reduce the LEDR rate of *Chlorella vulgaris* 211/11c, however, some resistance to the CN^- was clearly evident. The LEDR rate of *Scenedesmus sp.* was completely inhibited in the presence of $10\mu\text{mol}$ KCN. Both the LEDR rates of *Chlorella vulgaris* 211/11c and *Scenedesmus sp.* were unaffected by the addition of salicylic hydroxamic acid (SHAM).

Table of Contents.

Acknowledgements		I
Abstract		II
1.0	Introduction	1
2.0	Methods and Materials	23
2.1	Flat Plate Air Lift Reactor (FPALR)	23
2.1.1	Construction	23
2.1.2	Hydraulic characteristics	25
2.1.3	Changing the light / dark cycle	26
2.2	Growth of Micro-algae and Cyanobacterial Cultures	26
2.2.1	Culture media	26
2.2.2	Axenic cultures	27
2.2.3	Effect of spectral radiant flux	27
2.3	The Measurement of Photon Flux Density (PFD)	28
2.4	Biochemical Analysis	28
2.4.1	Optical density determination	28
2.4.2	Dry weight measurement	28
2.4.3	Chlorophyll analysis	28
2.4.4	Protein determination	28
2.4.5	Carbohydrate determination	29
2.4.6	Nitrate analysis	29
2.4.7	Phosphate analysis	29
2.5	Growth of Micro-algae and Cyanobacteria in the FPALR and CSTR.	29
2.5.1	Growth rate calculation	29
2.5.2	Determination of dilution rates	30
2.5.3	Growth of micro-algae and cyanobacteria under Batch Kinetics	31
2.5.4	Growth of micro-algae and cyanobacteria in the FPALR under different light sources	31

2.5.5	Growth of micro-algae and cyanobacteria in the FPALR under different light intensities	32
2.5.6	Growth of micro-algae and cyanobacteria in the FPALR and CSTR under different concentrations of carbon dioxide	32
2.5.7	Growth of micro-algae and cyanobacteria in the FPALR and CSTR under different temperatures	32
2.6	Micro-algae and Cyanobacteria grown in the FPALR under continuous kinetics	33
2.6.1	Light / Dark Cycling	33
2.7.	Growth of micro-algae and cyanobacteria in the FPALR in gradients of light	33
2.7.1	Light gradients	33
2.8	Oxygen Electrode Analysis	34
2.8.1	Measurement of Photosynthesis / irradiance response curves	34
2.8.2	Interpretation of photosynthesis / irradiance data	36
2.8.3	Nutrients / buffers	36
2.8.4	Centrifugation	36
2.8.5	Light / dark cycling	36
2.8.6	Temperature	37
2.8.7	Spectral radiant flux	38
2.9	Light Enhanced Dark Respiration (LEDR)	39
2.9.1	Inhibitors of photosynthetic and respiration	39
2.10	Microscopic Examination	40
2.10.1	Image analysis	40
3.0	Results and Discussions	41
3.1	Design and construction of a Flat Plate Air Lift Reactor	41
3.2	Growth of Micro-algae and Cyanobacteria operating under Batch Kinetics	41
3.2.1	The effect of Quartz-Halogen Lamps / High Pressure Sodium Lights on micro-algae and cyanobacterial growth in the FPALR.	42

3.2.2	The effect of Photon Flux Density on micro-algal and cyanobacterial growth kinetics in the FPALR	45
3.2.3	The effect of Carbon Dioxide Concentration on micro-algal / cyanobacterial growth kinetics in the FPALR and CSTR	48
3.2.4	The effect of Temperature on micro-algal / cyanobacterial growth kinetics in the FPALR and CSTR	53
3.2.5	Nutrient uptake and cellular physiology of <i>Chlorella vulgaris</i> 211/11c and <i>Scenedesmus sp.</i> cultured in FPALR	59
3.2.6	The effect of Reynolds number on the cell dynamics of <i>Chlorella vulgaris</i> 211/11c	64
3.2.6.1	Macro programming for the cellular analysis of <i>Chlorella vulgaris</i> 21/11c	65
3.3	Measurement of Photosynthesis / irradiance curves	69
3.3.1	Comparison of photosynthesis / irradiance response curves measured in the presence and absence of bicarbonate	69
3.3.2	Comparison of photosynthesis / irradiance response curves measured in phosphate buffer or ASM	73
3.3.3	The effect of the presence and absence of nitrate on the measurement of photosynthesis / irradiance curves	77
3.3.4	The effect of trace elements on the measurement of photosynthesis / irradiance response curves	81
3.3.5	The effect of centrifugation on the measurement of photosynthesis / irradiance response curves	81
3.3.6	The effect of LEDR on the measurement of photosynthesis irradiance response curves	87
3.4	The effect of culture temperature and P/I incubation temperature on the photosynthetic kinetics of micro algae and cyanobacteria	92
3.4.1	The effect of culture temperature and P/I incubation temperature on cells of micro-algae and cyanobacteria grown at a PFD of $100\mu\text{mol s}^{-1} \text{m}^{-2}$.	92
3.4.2	The effect of culture temperature and P/I incubation temperature on cells of micro-algae and cyanobacteria grown at a PFD of $200\mu\text{mol s}^{-1} \text{m}^{-2}$.	139
3.5	Light / dark cycling	162
3.5.1	The effect of light / dark cycles of medium frequency on the photosynthesis of <i>Chlorella vulgaris</i> 211/11c	162
3.6	The growth of Micro-algae and Cyanobacteria in light / dark cycles of medium frequency in the FPALR under continuous kinetics	173
3.6.1	The effect of light / dark cycles of medium frequency on the	

	growth of cells of <i>Chlorella vulgaris</i> 211/11c	173
3.6.2	The effect of light / dark cycles of medium frequency on the growth of cells of <i>Synechococcus</i> 1479/5	180
3.7	The effect of Light / Dark cycling on the photosynthetic parameters, respiration and light enhanced dark respiration of cells of micro-algae cultured in the FPALR under continuous kinetics	185
3.7.1	The effect of light / dark cycles of medium frequency on the photosynthetic kinetics of <i>Chlorella vulgaris</i> 211/11c	186
3.8	The effect of light gradients on the growth kinetics of micro-algae and cyanobacteria	197
3.8.1	The effect of light gradients on the growth kinetics and productivity of <i>Chlorella vulgaris</i> 211/11c and <i>Synechococcus</i> 1479/5	197
3.9	The effect of spectral radiant flux on the growth and photosynthesis of micro-algae and cyanobacteria	208
3.9.1	The effect of spectral radiant flux on the growth kinetics of micro-algae and cyanobacteria	208
3.9.2	The effect of spectral radiant flux on the photosynthesis / irradiance curves of micro-algae and cyanobacteria	214
3.10	Effect of spectral radiant flux on the light enhanced dark respiration of micro-algae and cyanobacteria	226
3.10.1	The effect of spectral radiant flux on the light enhanced dark respiration of <i>Chlorella vulgaris</i> 211/11c, <i>Scenedesmus sp.</i> , and <i>Synechococcus</i> 1479/5	226
3.10.2	The effect of inhibitors on the light enhanced dark respiration rate of <i>Chlorella vulgaris</i> 211/11c and <i>Scenedesmus sp.</i>	234
3.11	Overall Discussion	244
	References	258

LIST OF FIGURES

	Preceding Page
Figure 1. A typical continuously stirred tank reactor for the growth of micro-organisms.	1
Figure 2. A helical photostage airlift photobioreactor.	1
Figure 3. A 450 litre peristaltic pump driven tubular biocoil.	4
Figure 4. A novel photobioreactor feeding light into the heart of a micro-algal culture.	4
Figure 5. A novel multi-pass flat plate air lift photobioreactor.	5
Figure 6. The biochemical processes occurring during the treatment of wastes by micro-algal culture in a high rate algal pond.	5
Figure 7. Changes in photosynthesis throughout the depth of a high rate algal pond.	5
Figure 8. A novel oxygen electrode system.	9
Figure 9. Photograph of novel oxygen electrode system including probe port and incubation chambers	9
Figure 10. A schematic representation of a typical P/I curve and the parameters that can be measured from it.	10
Figure 11a. A schematic diagram of a P/I curve where $\text{Beta} > 0$.	12
Figure 11b. A schematic diagram of a P/I curve where $\text{Beta} = 0$.	12
Figure 12. The reactions associated with the dark pathways of micro-algae.	18
Figure 13. The construction of the curved internally partitioned channels of the flat plate air lift photobioreactor.	23
Figure 14. A light gradient calculated for $200\mu\text{mol s}^{-1} \text{m}^{-2}$.	34
Figure 15a. A light gradient calculated for $400\mu\text{mol s}^{-1} \text{m}^{-2}$.	34
Figure 15b. A light gradient calculated for $800\mu\text{mol s}^{-1} \text{m}^{-2}$.	34
Figure 16. A solenoid relay switch for light / dark simulation.	35
Figure 17. Spectral characteristics of the green filter.	38
Figure 18. Spectral characteristics of the blue filter.	38
Figure 19. Spectral characteristics of the red filter.	38
Figure 20. Spectral characteristics of the chrome orange filter.	38
Figure 21. Spectral characteristics of the orange filter.	38
Figure 22. Spectral characteristics of the yellow filter.	38
Figure 23. Change in optical density (560nm) of <i>C. vulgaris</i> 211/11c irradiated with quartz-halogen lights and high pressure sodium lamps	42
Figure 24. Change in dry weight of <i>C. vulgaris</i> 211/11c irradiated with quartz-halogen lights and high pressure sodium lamps	42
Figure 25. Change in chlorophyll a content of <i>C. vulgaris</i> 211/11c irradiated with quartz-halogen lights and high pressure sodium lamps.	42

Figure 26. Change in chlorophyll b content of <i>C. vulgaris</i> 211/11c irradiated with quartz-halogen lights and high pressure sodium lamps.	42
Figure 27. Change in dry weight of <i>Scenedesmus sp.</i> irradiated with quartz-halogen lights and high pressure sodium lamps.	42
Figure 28. Change in chlorophyll a content of <i>Scenedesmus sp.</i> irradiated with quartz-halogen lights and high pressure sodium lamps.	42
Figure 29. Change in chlorophyll b content of <i>Scenedesmus sp.</i> irradiated with quartz-halogen lights and high pressure sodium lamps.	43
Figure 30. Change in dry weight of <i>Synechococcus</i> 1479/5 irradiated with quartz-halogen lights and high pressure sodium lamps.	43
Figure 31. Change in chlorophyll a content of <i>Synechococcus</i> 1479/5 irradiated with quartz-halogen lights and high pressure sodium lamps.	43
Figure 33. The change in spectral energy with wavelength of a high pressure sodium lamp.	43
Figure 34. Change in dry weight of <i>C. vulgaris</i> 211/11c irradiated at a PFD of $200\mu\text{mol s}^{-1} \text{m}^{-2}$.	45
Figure 35. Change in dry weight of <i>Scenedesmus sp.</i> irradiated at a PFD of $200\mu\text{mol s}^{-1} \text{m}^{-2}$.	45
Figure 36. Change in dry weight of <i>Synechococcus</i> 1479/5 irradiated at a PFD of $200\mu\text{mol s}^{-1} \text{m}^{-2}$.	45
Figure 37. The effect of carbon dioxide concentration on the dry weight of <i>Chlorella vulgaris</i> 211/11c (air-4%) cultured in the FPALR.	48
Figure 38. The effect of carbon dioxide concentration on the dry weight of <i>Chlorella vulgaris</i> 211/11c (6-10%) cultured in the FPALR.	48
Figure 39. The effect of carbon dioxide concentration on the dry weight of <i>Chlorella vulgaris</i> 211/11c (air-4%) cultured in the CSTR.	48
Figure 40. The effect of carbon dioxide concentration on the dry weight of <i>Chlorella vulgaris</i> 211/11c (6-10%) cultured in the CSTR.	48
Figure 41. The effect of carbon dioxide concentration on the dry weight of <i>Scenedesmus sp.</i> (air-4%) cultured in the FPALR.	51
Figure 42. The effect of carbon dioxide concentration on the dry weight of <i>Scenedesmus sp.</i> (6-10%) cultured in the FPALR.	51
Figure 43. The effect of carbon dioxide concentration on the dry weight of <i>Scenedesmus sp.</i> (air-4%) cultured in the CSTR.	51
Figure 44. The effect of carbon dioxide concentration on the dry weight of <i>Scenedesmus sp.</i> (6-10%) cultured in the CSTR.	51
Figure 45. The effect of carbon dioxide concentration on the dry weight of <i>Synechococcus</i> 1479/5 (air-4%) cultured in the FPALR.	51

Figure 46. The effect of carbon dioxide concentration on the dry weight of <i>Synechococcus</i> 1479/5 (6-10%) cultured in the FPALR.	51
Figure 47. The effect of carbon dioxide concentration on the dry weight of <i>Synechococcus</i> 1479/5 (air-4%) cultured in the CSTR	51
Figure 48. The effect of carbon dioxide concentration on the dry weight of <i>Synechococcus</i> 1479/5 (6-10%) cultured in the CSTR	51
Figure 49. The effect of temperature on the dry weight of <i>C. vulgaris</i> 211/11c cultured in the FPALR.	53
Figure 50. The effect of temperature on the dry weight of <i>C. vulgaris</i> 211/11c cultured in the CSTR.	53
Figure 51. The effect of temperature on the dry weight of <i>Scenedesmus</i> sp. cultured in the FPALR.	54
Figure 52. The effect of temperature on the dry weight of <i>Scenedesmus</i> sp. cultured in the CSTR.	54
Figure 53. The effect of temperature on the dry weight of <i>Synechococcus</i> 1479/5 cultured in the FPALR.	56
Figure 54. The effect of temperature on the dry weight of <i>Synechococcus</i> 1479/5 cultured in the CSTR.	56
Figure 55. The percentage change in nitrate and phosphate content of ASM whilst culturing <i>C. vulgaris</i> 211/11c in the FPALR at a concentration of 2% v/v at a PFD of $100\mu\text{mol s}^{-1} \text{m}^{-2}$.	59
Figure 56. The variation in protein and carbohydrate content of <i>C. vulgaris</i> 211/11c cultured in the FPALR at a CO_2 of 2% v/v at a PFD of $100\mu\text{mol s}^{-1} \text{m}^{-2}$.	59
Figure 57. The percentage change in nitrate and phosphate content of ASM whilst culturing <i>C. vulgaris</i> 211/11c in the FPALR at a CO_2 concentration of 2% v/v at a PFD of $200\mu\text{mol s}^{-1} \text{m}^{-2}$.	60
Figure 58. The variation in protein and carbohydrate content of <i>C. vulgaris</i> 211/11c in the FPALR at a CO_2 concentration of 2% v/v at a PFD of $200\mu\text{mol s}^{-1} \text{m}^{-2}$.	60
Figure 59. The percentage change in nitrate and phosphate content of ASM whilst culturing <i>Scenedesmus</i> sp. in the FPALR at a CO_2 concentration of 2% v/v at a PFD of $100\mu\text{mol s}^{-1} \text{m}^{-2}$.	60
Figure 60. The variation in protein and carbohydrate content of <i>Scenedesmus</i> sp. cultured in the FPALR at a CO_2 concentration of 2% v/v at a PFD of $100\mu\text{mol s}^{-1} \text{m}^{-2}$.	60
Figure 61. The percentage change in nitrate and phosphate content of ASM whilst culturing <i>Scenedesmus</i> sp. in the FPALR at a CO_2 concentration of 2% v/v at a PFD of $200\mu\text{mol s}^{-1} \text{m}^{-2}$.	61
Figure 62. The variation in protein and carbohydrate content of <i>Scenedesmus</i> sp. cultured in the FPALR at a CO_2 concentration of 2% v/v at a PFD of $200\mu\text{mol s}^{-1} \text{m}^{-2}$.	61

Figure 63. The variation in protein and carbohydrate content of <i>C. vulgaris</i> 211/11c cultured in the FPALR at a PFD of $100\mu\text{mol s}^{-1} \text{m}^{-2}$ with air.	61
Figure 64. The variation in protein and carbohydrate content of <i>C. vulgaris</i> 211/11c cultured in the FPALR at a PFD of $100\mu\text{mol s}^{-1} \text{m}^{-2}$ with 4% v/v CO_2 .	61
Figure 65. The variation in protein and carbohydrate content of <i>Scenedesmus sp.</i> cultured in the FPALR at a PFD of $100\mu\text{mol s}^{-1} \text{m}^{-2}$ with air.	61
Figure 66. The variation in protein and carbohydrate content of <i>Scenedesmus sp.</i> cultured in the FPALR at a CO_2 concentration of 4% v/v at a PFD of $100\mu\text{mol s}^{-1} \text{m}^{-2}$.	61
Figure 67. The variation in protein and carbohydrate content of <i>C. vulgaris</i> 211/11c cultured in the FPALR at a PFD of $100\mu\text{mol s}^{-1} \text{m}^{-2}$ with 10% v/v CO_2 .	62
Figure 68. The variation in protein and carbohydrate content of <i>Scenedesmus sp.</i> cultured in the FPALR at a PFD of $100\mu\text{mol s}^{-1} \text{m}^{-2}$ with 10% v/v CO_2 .	62
Figure 69. The effect of Reynolds number on the cell dynamics of <i>C. vulgaris</i> 211/11c.	64
Figure 70. The effect of Reynolds number on the cell volume of <i>C. vulgaris</i> 211/11c.	64
Figure 71. The effect of bicarbonate on the P/I curves of <i>C. vulgaris</i> 211/11c.	69
Figure 72. The effect of bicarbonate on the P/I curves of <i>Scenedesmus sp.</i>	69
Figure 73. The effect of bicarbonate on the P/I curves of <i>Synechococcus</i> 1479/5.	71
Figure 74. The effect of measuring P/I curves of <i>Chlorella vulgaris</i> 211/11c incubated in phosphate buffer and ASM.	71
Figure 75. The effect of measuring P/I curves of <i>Scenedesmus sp.</i> incubated in phosphate buffer and ASM.	73
Figure 76. The effect of measuring P/I curves of <i>Synechococcus</i> 1479/5 incubated in phosphate buffer and ASM.	73
Figure 77. The effect of measuring P/I curves of <i>Ankistrodesmus antarcticus</i> incubated in phosphate buffer and ASM.	76
Figure 78. The effect of nitrate absence and presence on the P/I curves of <i>Scenedesmus sp.</i>	76
Figure 79. The effect of nitrate absence and presence on the P/I curves of <i>Ankistrodesmus antarcticus</i> .	77
Figure 80. The effect of nitrate absence and presence on the P/I curves of <i>Synechococcus sp.</i>	77
Figure 81. The effect of nitrate absence and presence on the P/I curves of <i>Synechococcus</i> 1479/5.	79

Figure 82. The effect of trace elements on the P/I curves of <i>C. vulgaris</i> 211/11c.	79
Figure 83. The effect of trace elements on the P/I curves of <i>Scenedesmus</i> sp.	81
Figure 84. The effect of centrifugation on the P/I curves of <i>C. vulgaris</i> 211/11c.	81
Figure 85. The effect of centrifugation on the P/I curves of <i>Synechococcus</i> 1479/5.	83
Figure 86. The effect of centrifugation on the P/I curves of <i>Scenedesmus</i> sp.	83
Figure 87. The effect of irradiance on the light enhanced dark respiration of <i>Chlorella vulgaris</i> 211/11c and the subsequent effect on a P/I curve.	87
Figure 88. The effect of irradiance on the light enhanced dark respiration of <i>Scenedesmus</i> sp. and the subsequent effect on a P/I curve	89
Figure 89. The effect of irradiance on the light enhanced dark respiration of <i>Synechococcus</i> 1479/5 and the subsequent effect on a P/I curve	89
Figure 90. The effect of P/I incubation temperature on the P/I response curves of <i>C. vulgaris</i> 211/11c cultured at 15°C.	92
Figure 91. The effect of P/I incubation temperature on the P/I response curves of <i>C. vulgaris</i> 211/11c cultured at 23°C.	92
Figure 92. The effect of P/I incubation temperature on the P/I response curves of <i>C. vulgaris</i> 211/11c cultured at 30°C.	92
Figure 93. The effect of P/I incubation temperature on the P/I response curves of <i>C. vulgaris</i> 211/11c cultured at 35°C.	92
Figure 94. The effect of P/I incubation temperature on the respiration rates of <i>C. vulgaris</i> 211/11c cultured at 15°C.	96
Figure 95. The effect of P/I incubation temperature on the respiration rates of <i>C. vulgaris</i> 211/11c cultured at 23°C.	96
Figure 96. The effect of P/I incubation temperature on the respiration rates of <i>C. vulgaris</i> 211/11c cultured at 30°C.	96
Figure 97. The effect of P/I incubation temperature on the respiration rates of <i>C. vulgaris</i> 211/11c cultured at 35°C.	96
Figure 98. Ahrenius plot of photosynthesis measured at a PFD of 100 $\mu\text{mol s}^{-1} \text{m}^{-2}$ against increasing P/I incubation temperature of <i>C. vulgaris</i> 211/11c cultured at 15°C.	98
Figure 99. Ahrenius plot of photosynthesis measured at a PFD of 100 $\mu\text{mol s}^{-1} \text{m}^{-2}$ against increasing P/I incubation temperature of <i>C. vulgaris</i> 211/11c cultured at 23°C.	98
Figure 100. Ahrenius plot of photosynthesis measured at a PFD of 100 $\mu\text{mol s}^{-1} \text{m}^{-2}$ against increasing P/I incubation temperature of <i>C. vulgaris</i> 211/11c cultured at 30°C.	98

Figure 101. Ahrenius plot of photosynthesis measured at a PFD of 100 $\mu\text{mol s}^{-1} \text{m}^{-2}$ against increasing P/I incubation temperature of <i>C. vulgaris</i> 211/11c cultured at 35°C.	98
Figure 102. The effect of P/I incubation temperature on the P/I response curves of <i>Nannochloris atomus</i> cultured at 15°C.	98
Figure 103. The effect of P/I incubation temperature on the P/I response curves of <i>Nannochloris atomus</i> cultured at 23°C.	98
Figure 104. The effect of P/I incubation temperature on the P/I response curves of <i>Nannochloris atomus</i> cultured at 30°C.	98
Figure 105. The effect of P/I incubation temperature on the P/I response curves of <i>Nannochloris atomus</i> cultured at 35°C.	98
Figure 106. The effect of P/I incubation temperature on the respiration rates of <i>Nannochloris atomus</i> cultured at 15°C.	101
Figure 107. The effect of P/I incubation temperature on the respiration rates of <i>Nannochloris atomus</i> cultured at 23°C.	101
Figure 108. The effect of P/I incubation temperature on the respiration rates of <i>Nannochloris atomus</i> cultured at 30°C.	101
Figure 109. The effect of P/I incubation temperature on the respiration rates of <i>Nannochloris atomus</i> cultured at 35°C.	101
Figure 110. Ahrenius plot of photosynthesis measured at a PFD of 100 $\mu\text{mol s}^{-1} \text{m}^{-2}$ against increasing P/I incubation temperature of <i>Nannochloris atomus</i> cultured at 15°C.	104
Figure 111. Ahrenius plot of photosynthesis measured at a PFD of 100 $\mu\text{mol s}^{-1} \text{m}^{-2}$ against increasing P/I incubation temperature of <i>Nannochloris atomus</i> cultured at 23°C.	104
Figure 112. Ahrenius plot of photosynthesis measured at a PFD of 100 $\mu\text{mol s}^{-1} \text{m}^{-2}$ against increasing P/I incubation temperature of <i>Nannochloris atomus</i> cultured at 30°C.	104
Figure 113. Ahrenius plot of photosynthesis measured at a PFD of 100 $\mu\text{mol s}^{-1} \text{m}^{-2}$ against increasing P/I incubation temperature of <i>Nannochloris atomus</i> cultured at 35°C.	104
Figure 114. The effect of P/I incubation temperature on the P/I response curves of <i>Scenedesmus sp.</i> cultured at 15°C.	104
Figure 115. The effect of P/I incubation temperature on the P/I response curves of <i>Scenedesmus sp.</i> cultured at 23°C.	104
Figure 116. The effect of P/I incubation temperature on the P/I response curves of <i>Scenedesmus sp.</i> cultured at 30°C.	104
Figure 117. The effect of P/I incubation temperature on the P/I response curves of <i>Scenedesmus sp.</i> cultured at 35°C.	104
Figure 118. The effect of P/I incubation temperature on the respiration rates of <i>Scenedesmus sp.</i> cultured at 15°C.	107

Figure 119. The effect of P/I incubation temperature on the respiration rates of <i>Scenedesmus sp.</i> cultured at 23°C.	107
Figure 120. The effect of P/I incubation temperature on the respiration rates of <i>Scenedesmus sp.</i> cultured at 30°C.	107
Figure 121. The effect of P/I incubation temperature on the respiration rates of <i>Scenedesmus sp.</i> cultured at 35°C.	107
Figure 122. Ahrenius plot of photosynthesis measured at a PFD of 100 $\mu\text{mol s}^{-1} \text{m}^{-2}$ against increasing P/I incubation temperature of <i>Scenedesmus sp.</i> cultured at 15°C.	109
Figure 123. Ahrenius plot of photosynthesis measured at a PFD of 100 $\mu\text{mol s}^{-1} \text{m}^{-2}$ against increasing P/I incubation temperature of <i>Scenedesmus sp.</i> cultured at 23°C.	109
Figure 124. Ahrenius plot of photosynthesis measured at a PFD of 100 $\mu\text{mol s}^{-1} \text{m}^{-2}$ against increasing P/I incubation temperature of <i>Scenedesmus sp.</i> cultured at 30°C.	109
Figure 125. Ahrenius plot of photosynthesis measured at a PFD of 100 $\mu\text{mol s}^{-1} \text{m}^{-2}$ against increasing P/I incubation temperature of <i>Scenedesmus sp.</i> cultured at 35°C.	109
Figure 126. The effect of P/I incubation temperature on the photosynthesis / irradiance response curves of <i>Ankistrodesmus antarcticus</i> cultured at 15°C.	109
Figure 127. The effect of P/I incubation temperature on the photosynthesis / irradiance response curves of <i>Ankistrodesmus antarcticus</i> cultured at 23°C.	109
Figure 128. The effect of P/I incubation temperature on the photosynthesis / irradiance response curves of <i>Ankistrodesmus antarcticus</i> cultured at 30°C.	109
Figure 129. The effect of P/I incubation temperature on the photosynthesis / irradiance response curves of <i>Ankistrodesmus antarcticus</i> cultured at 35°C.	109
Figure 130. The effect of P/I incubation temperature on the respiration rates of <i>Ankistrodesmus antarcticus</i> cultured at 15°C.	113
Figure 131. The effect of P/I incubation temperature on the respiration rates of <i>Ankistrodesmus antarcticus</i> cultured at 23°C.	113
Figure 132. The effect of P/I incubation temperature on the respiration rates of <i>Ankistrodesmus antarcticus</i> cultured at 30°C.	113
Figure 133. The effect of P/I incubation temperature on the respiration rates of <i>Ankistrodesmus antarcticus</i> cultured at 35°C.	113
Figure 134. Ahrenius plot of photosynthesis measured at a PFD of 100 $\mu\text{mol s}^{-1} \text{m}^{-2}$ against increasing P/I incubation temperature of <i>Ankistrodesmus antarcticus</i> cultured at 15°C.	115
Figure 135. Ahrenius plot of photosynthesis measured at a PFD of 100	

$\mu\text{mol s}^{-1} \text{m}^{-2}$ against increasing P/I incubation temperature of <i>Ankistrodesmus antarcticus</i> cultured at 23°C.	115
Figure 136. Ahrenius plot of photosynthesis measured at a PFD of 100 $\mu\text{mol s}^{-1} \text{m}^{-2}$ against increasing P/I incubation temperature of <i>Ankistrodesmus antarcticus</i> cultured at 30°C.	115
Figure 137. Ahrenius plot of photosynthesis measured at a PFD of 100 $\mu\text{mol s}^{-1} \text{m}^{-2}$ against increasing P/I incubation temperature of <i>Ankistrodesmus antarcticus</i> cultured at 35°C.	115
Figure 138. The effect of P/I incubation temperature on the photosynthesis / irradiance response curves of <i>Synechococcus</i> 1479/5 cultured at 15°C.	115
Figure 139. The effect of P/I incubation temperature on the photosynthesis / irradiance response curves of <i>Synechococcus</i> 1479/5 cultured at 23°C.	115
Figure 140. The effect of P/I incubation temperature on the photosynthesis / irradiance response curves of <i>Synechococcus</i> 1479/5 cultured at 30°C.	115
Figure 141. The effect of P/I incubation temperature on the photosynthesis / irradiance response curves of <i>Synechococcus</i> 1479/5 cultured at 35°C.	115
Figure 142. The effect of P/I incubation temperature on the respiration rates of <i>Synechococcus</i> 1479/5 cultured at 15°C.	118
Figure 143. The effect of P/I incubation temperature on the respiration rates of <i>Synechococcus</i> 1479/5 cultured at 23°C.	118
Figure 144. The effect of P/I incubation temperature on the respiration rates of <i>Synechococcus</i> 1479/5 cultured at 30°C.	118
Figure 145. The effect of P/I incubation temperature on the respiration rates of <i>Synechococcus</i> 1479/5 cultured at 35°C.	118
Figure 146. Ahrenius plot of photosynthesis measured at a PFD of 100 $\mu\text{mol s}^{-1} \text{m}^{-2}$ against increasing P/I incubation temperature of <i>Synechococcus</i> 1479/5 cultured at 15°C.	120
Figure 147. Ahrenius plot of photosynthesis measured at a PFD of 100 $\mu\text{mol s}^{-1} \text{m}^{-2}$ against increasing P/I incubation temperature of <i>Synechococcus</i> 1479/5 cultured at 23°C.	120
Figure 148. Ahrenius plot of photosynthesis measured at a PFD of 100 $\mu\text{mol s}^{-1} \text{m}^{-2}$ against increasing P/I incubation temperature of <i>Synechococcus</i> 1479/5 cultured at 30°C.	120
Figure 149. Ahrenius plot of photosynthesis measured at a PFD of 100 $\mu\text{mol s}^{-1} \text{m}^{-2}$ against increasing P/I incubation temperature of <i>Synechococcus</i> 1479/5 cultured at 35°C.	120

Figure 150. The effect of P/I incubation temperature on the photosynthesis / irradiance response curves of <i>Synechococcus sp.</i> cultured at 15°C.	121
Figure 151. The effect of P/I incubation temperature on the photosynthesis / irradiance response curves of <i>Synechococcus sp.</i> cultured at 23°C.	121
Figure 152. The effect of P/I incubation temperature on the photosynthesis / irradiance response curves of <i>Synechococcus sp.</i> cultured at 30°C.	121
Figure 153. The effect of P/I incubation temperature on the photosynthesis / irradiance response curves of <i>Synechococcus sp.</i> cultured at 35°C.	121
Figure 154. The effect of P/I incubation temperature on the respiration rates of <i>Synechococcus sp.</i> cultured at 15°C.	124
Figure 155. The effect of P/I incubation temperature on the respiration rates of <i>Synechococcus sp.</i> cultured at 23°C.	124
Figure 156. The effect of P/I incubation temperature on the respiration rates of <i>Synechococcus sp.</i> cultured at 30°C.	124
Figure 157. The effect of P/I incubation temperature on the respiration rates of <i>Synechococcus sp.</i> cultured at 35°C.	124
Figure 158. Ahrenius plot of photosynthesis measured at a PFD of 100 $\mu\text{mol s}^{-1} \text{m}^{-2}$ against increasing P/I incubation temperature of <i>Synechococcus sp.</i> cultured at 15°C.	126
Figure 159. Ahrenius plot of photosynthesis measured at a PFD of 100 $\mu\text{mol s}^{-1} \text{m}^{-2}$ against increasing P/I incubation temperature of <i>Synechococcus sp.</i> cultured at 23°C.	126
Figure 160. Ahrenius plot of photosynthesis measured at a PFD of 100 $\mu\text{mol s}^{-1} \text{m}^{-2}$ against increasing P/I incubation temperature of <i>Synechococcus sp.</i> cultured at 30°C.	126
Figure 161. Ahrenius plot of photosynthesis measured at a PFD of 100 $\mu\text{mol s}^{-1} \text{m}^{-2}$ against increasing P/I incubation temperature of <i>Synechococcus sp.</i> cultured at 35°C.	126
Figure 162. Variation in Q_{10} of <i>C. vulgaris</i> 211/11c.	137
Figure 163. Variation in Q_{10} of <i>Nannochloris atomus</i> .	137
Figure 164. Variation in Q_{10} of <i>Scenedesmus sp.</i>	137
Figure 165. Variation in Q_{10} of <i>Ankistrodesmus antarcticus</i> .	137
Figure 166. Variation in Q_{10} of <i>Synechococcus</i> 1479/5.	138
Figure 167. Variation in Q_{10} of <i>Synechococcus sp.</i>	138
Figure 168. The effect of P/I incubation temperature on the photosynthesis / irradiance response curves of <i>C. vulgaris</i> 211/11c cultured at 15°C.	140

Figure 169. The effect of P/I incubation temperature on the photosynthesis / irradiance response curves of <i>C. vulgaris</i> 211/11c cultured at 23°C.	140
Figure 170. The effect of P/I incubation temperature on the photosynthesis / irradiance response curves of <i>C. vulgaris</i> 211/11c cultured at 30°C.	142
Figure 171. The effect of P/I incubation temperature on the photosynthesis / irradiance response curves of <i>C. vulgaris</i> 211/11c cultured at 35°C.	142
Figure 172. The effect of P/I incubation temperature on the photosynthesis / irradiance response curves of <i>Scenedesmus sp.</i> cultured at 15°C.	143
Figure 173. The effect of P/I incubation temperature on the photosynthesis / irradiance response curves of <i>Scenedesmus sp.</i> cultured at 23°C.	143
Figure 174. The effect of P/I incubation temperature on the photosynthesis / irradiance response curves of <i>Scenedesmus sp.</i> cultured at 30°C.	144
Figure 175. The effect of P/I incubation temperature on the photosynthesis / irradiance response curves of <i>Scenedesmus sp.</i> cultured at 35°C.	144
Figure 176. The effect of P/I incubation temperature on the photosynthesis / irradiance response curves of <i>Synechococcus</i> 1479/5 cultured at 15°C.	147
Figure 177. The effect of P/I incubation temperature on the photosynthesis / irradiance response curves of <i>Synechococcus</i> 1479/5 cultured at 23°C.	147
Figure 178. The effect of P/I incubation temperature on the photosynthesis / irradiance response curves of <i>Synechococcus</i> 1479/5 cultured at 30°C.	149
Figure 179. The effect of P/I incubation temperature on the photosynthesis / irradiance response curves of <i>Synechococcus</i> 1479/5 cultured at 35°C.	149
Figure 180. Ahrenius plot of ln photosynthetic rate vs. P/I incubation temperature for <i>C. vulgaris</i> 211/11c cultured at 15°C.	156
Figure 181. Ahrenius plot of ln photosynthetic rate vs. P/I incubation temperature for <i>C. vulgaris</i> 211/11c cultured at 23°C.	156
Figure 182. Ahrenius plot of ln photosynthetic rate vs. P/I incubation temperature for <i>C. vulgaris</i> 211/11c cultured at 30°C.	156
Figure 183. Ahrenius plot of ln photosynthetic rate vs. P/I incubation temperature for <i>C. vulgaris</i> 211/11c cultured at 35°C.	156
Figure 184. Ahrenius plot of ln photosynthetic rate vs. P/I incubation temperature for <i>Scenedesmus sp.</i> cultured at 15°C.	156

Figure 185. Ahrenius plot of ln photosynthetic rate vs. P/I incubation temperature for <i>Scenedesmus sp.</i> cultured at 23°C.	156
Figure 186. Ahrenius plot of ln photosynthetic rate vs. P/I incubation temperature for <i>Scenedesmus sp.</i> cultured at 30°C.	156
Figure 187. Ahrenius plot of ln photosynthetic rate vs. P/I incubation temperature for <i>Scenedesmus sp.</i> cultured at 35°C.	156
Figure 188. Ahrenius plot of ln photosynthetic rate vs. P/I incubation temperature for <i>Synechococcus</i> 1479/5 cultured at 15°C.	156
Figure 189. Ahrenius plot of ln photosynthetic rate vs. P/I incubation temperature for <i>Synechococcus</i> 1479/5 cultured at 23°C.	156
Figure 190. Ahrenius plot of ln photosynthetic rate vs. P/I incubation temperature for <i>Synechococcus</i> 1479/5 cultured at 30°C.	156
Figure 191. Ahrenius plot of ln photosynthetic rate vs. P/I incubation temperature for <i>Synechococcus</i> 1479/5 cultured at 35°C.	156
Figure 192. Variation in Q ₁₀ values with temperature for <i>C. vulgaris</i> 211/11c.	156
Figure 193. Variation in Q ₁₀ values with temperature for <i>Scenedesmus sp.</i>	156
Figure 194. Variation in Q ₁₀ values with temperature for <i>Synechococcus</i> 1479/5.	156
Figure 195. Light / dark cycles at a PFD of 300µmol s ⁻¹ m ⁻² on photosynthesis of <i>C. vulgaris</i> 211/11c.	162
Figure 195a. Light / dark cycles at a PFD of 300µmol s ⁻¹ m ⁻² on photosynthesis of <i>C. vulgaris</i> 211/11c.	163
Figure 196. Light / dark cycles at a PFD of 300µmol s ⁻¹ m ⁻² on photosynthesis and respiration of <i>C. vulgaris</i> 211/11c.	163
Figure 197. Light / dark cycles at a PFD of 300µmol s ⁻¹ m ⁻² on photosynthesis of <i>C. vulgaris</i> 211/11c.	163
Figure 198. Light / dark cycles at a PFD of 300µmol s ⁻¹ m ⁻² on photosynthesis of <i>C. vulgaris</i> 211/11c.	163
Figure 199. Light / dark cycles at a PFD of 300µmol s ⁻¹ m ⁻² on photosynthesis of <i>C. vulgaris</i> 211/11c.	164
Figure 200. Light / dark cycles at a PFD of 500µmol s ⁻¹ m ⁻² on photosynthesis of <i>C. vulgaris</i> 211/11c.	164
Figure 201. Light / dark cycles at a PFD of 500µmol s ⁻¹ m ⁻² on photosynthesis of <i>C. vulgaris</i> 211/11c.	164
Figure 202. Light / dark cycles at a PFD of 500µmol s ⁻¹ m ⁻² on photosynthesis of <i>C. vulgaris</i> 211/11c.	165
Figure 203. Light / dark cycles at a PFD of 500µmol s ⁻¹ m ⁻² on photosynthesis of <i>C. vulgaris</i> 211/11c.	165
Figure 204. Light / dark cycles at a PFD of 750µmol s ⁻¹ m ⁻² on photosynthesis of <i>C. vulgaris</i> 211/11c.	165
Figure 205. Light / dark cycles at a PFD of 750µmol s ⁻¹ m ⁻² on photosynthesis of <i>C. vulgaris</i> 211/11c.	165

Figure 206. Light / dark cycles at a PFD of $200\mu\text{mol s}^{-1} \text{m}^{-2}$ on photosynthesis of <i>Synechococcus</i> 1479/5.	166
Figure 207. Light / dark cycles at a PFD of $300\mu\text{mol s}^{-1} \text{m}^{-2}$ on photosynthesis of <i>Synechococcus</i> 1479/5.	166
Figure 208. Light / dark cycles at a PFD of $300\mu\text{mol s}^{-1} \text{m}^{-2}$ on photosynthesis of <i>Synechococcus</i> 1479/5.	166
Figure 209. Light / dark cycles at a PFD of $300\mu\text{mol s}^{-1} \text{m}^{-2}$ on photosynthesis of <i>Synechococcus</i> 1479/5.	167
Figure 210. Light / dark cycles at a PFD of $500\mu\text{mol s}^{-1} \text{m}^{-2}$ on photosynthesis of <i>Synechococcus</i> 1479/5.	167
Figure 211. Light / dark cycles at a PFD of $500\mu\text{mol s}^{-1} \text{m}^{-2}$ on photosynthesis of <i>Synechococcus</i> 1479/5.	167
Figure 212. Light / dark cycles at a PFD of $500\mu\text{mol s}^{-1} \text{m}^{-2}$ on photosynthesis of <i>Synechococcus</i> 1479/5.	167
Figure 213. Light / dark cycles at a PFD of $750\mu\text{mol s}^{-1} \text{m}^{-2}$ on photosynthesis of <i>Synechococcus</i> 1479/5.	167
Figure 214. Light / dark cycles at a PFD of $750\mu\text{mol s}^{-1} \text{m}^{-2}$ on photosynthesis of <i>Synechococcus</i> 1479/5.	168
Figure 215. Light / dark cycles at different PFDs on the photosynthesis of <i>Synechococcus</i> 1479/5.	168
Figure 216. The effect of light / dark cycles and dosage on the photosynthesis of <i>Synechococcus</i> 1479/5.	168
Figure 217. The effect of light / dark cycles and dosage on the photosynthesis of <i>Synechococcus</i> 1479/5.	168
Figure 218. A plot of recovery ratio vs. PFD for <i>C. vulgaris</i> 211/11c and <i>Synechococcus</i> 1479/5.	168
Figure 219. The variation in optical density of <i>C. vulgaris</i> 211/11c cultured in the FPALR operating under continuous kinetics.	175
Figure 220. The change in chlorophyll a of <i>C. vulgaris</i> 211/11c cultured in the FPALR operating under continuous kinetics.	175
Figure 221. The variation in protein concentration of <i>C. vulgaris</i> 211/11c cultured in the FPALR operating under continuous kinetics.	178
Figure 222. The variation in protein to chlorophyll a ratio of <i>C. vulgaris</i> 211/11c cultured in the FPALR operating under continuous kinetics.	179
Figure 223. The variation in carbohydrate content of <i>C. vulgaris</i> 211/11c cultured in the FPALR operating under continuous kinetics.	180
Figure 224. The variation in optical density of <i>Synechococcus</i> 1479/5 cultured in the FPALR operating under continuous kinetics.	180
Figure 225. The variation in chlorophyll a content of <i>Synechococcus</i> 1479/5 cultured in the FPALR operating under continuous kinetics.	183
Figure 226. The variation in protein content of <i>Synechococcus</i> 1479/5 cultured in the FPALR operating under continuous kinetics.	183
Figure 227. The variation in carbohydrate content of <i>Synechococcus</i> 1479/5 cultured in the FPALR operating under continuous kinetics.	183

Figure 228. The effect of light / dark cycles on P_{\max} of <i>C. vulgaris</i> 211/11c.	186
Figure 229. The effect of light / dark cycles on I_k of <i>C. vulgaris</i> 211/11c.	189
Figure 230. The effect of light / dark cycles on alpha of <i>C. vulgaris</i> 211/11c.	190
Figure 231. The effect of light / dark cycles on respiration of <i>C. vulgaris</i> 211/11c.	190
Figure 232. The effect of light / dark cycles on nutrient uptake of <i>C. vulgaris</i> 211/11c	192
Figure 233. Change in light attenuation with increasing depth.	197
Figure 234. The effect of light / dark cycles of medium frequency on the growth kinetics of <i>C. vulgaris</i> 211/11c.	198
Figure 235. The effect of light / dark cycles of medium frequency on the growth kinetics of <i>Synechococcus</i> 1479/5.	198
Figure 236. The effect of light / dark cycles of medium frequency on the growth kinetics of <i>C. vulgaris</i> 211/11c.	201
Figure 237. The effect of light / dark cycles of medium frequency on the growth kinetics of <i>C. vulgaris</i> 211/11c.	201
Figure 238. The effect of spectral radiant flux on the growth of <i>C. vulgaris</i> 211/11c.	209
Figure 239. The effect of spectral radiant flux on the growth of <i>C. vulgaris</i> 211/11c.	209
Figure 240. The effect of spectral radiant flux on the growth of <i>Scenedesmus</i> sp.	211
Figure 241. The effect of spectral radiant flux on the growth of <i>Scenedesmus</i> sp.	211
Figure 242. The effect of spectral radiant flux on the growth of <i>Synechococcus</i> 1479/5	212
Figure 243. The effect of spectral radiant flux on the growth of <i>Synechococcus</i> 1479/5	212
Figure 244. The effect of white light (control) on the growth of <i>C. vulgaris</i> 211/11c, <i>Scenedesmus</i> sp. and <i>Synechococcus</i> 1479/5.	213
Figure 245. The effect of spectral radiant flux on the photosynthesis of <i>Chlorella vulgaris</i> 211/11c cultured in red light.	216
Figure 246. The effect of spectral radiant flux on the photosynthesis of <i>Chlorella vulgaris</i> 211/11c cultured in red light.	216
Figure 247. The effect of spectral radiant flux on the photosynthesis of <i>Chlorella vulgaris</i> 211/11c cultured in blue light.	216
Figure 248. The effect of spectral radiant flux on the photosynthesis of <i>Chlorella vulgaris</i> 211/11c cultured in blue light.	216
Figure 249. The effect of spectral radiant flux on the photosynthesis of <i>Scenedesmus</i> sp. cultured in red light.	216

Figure 250. The effect of spectral radiant flux on the photosynthesis of <i>Scenedesmus</i> sp. cultured in red light.	216
Figure 251. The effect of spectral radiant flux on the photosynthesis of <i>Scenedesmus</i> sp. cultured in blue light.	217
Figure 252. The effect of spectral radiant flux on the photosynthesis of <i>Scenedesmus</i> sp. cultured in blue light.	217
Figure 253. The effect of spectral radiant flux on the photosynthesis of <i>Synechococcus</i> sp. cultured in red light.	219
Figure 254. The effect of spectral radiant flux on the photosynthesis of <i>Synechococcus</i> sp. cultured in red light.	219
Figure 255. The effect of spectral radiant flux on the photosynthesis of <i>Synechococcus</i> sp. cultured in blue light	219
Figure 256. The effect of spectral radiant flux on the photosynthesis of <i>Synechococcus</i> sp. cultured in blue light	219
Figure 257. The effect of spectral radiant flux on the photosynthesis of <i>Synechococcus</i> 1479/5 cultured in red light	221
Figure 258. The effect of spectral radiant flux on the photosynthesis of <i>Synechococcus</i> 1479/5 cultured in blue light	221
Figure 259. The variation in spectral composition with depth in Lake Constance.	221
Figure 260. The effect of spectral radiant flux on the photosynthesis of <i>Chlorella vulgaris</i> 211/11c cultured in white light.	223
Figure 261. The effect of spectral radiant flux on the photosynthesis of <i>Chlorella vulgaris</i> 211/11c cultured in white light.	223
Figure 262. The effect of spectral radiant flux on the photosynthesis of <i>Scenedesmus</i> sp. cultured in white light.	223
Figure 263. The effect of spectral radiant flux on the photosynthesis of <i>Scenedesmus</i> sp. cultured in white light.	223
Figure 264. The effect of spectral radiant flux on the photosynthesis of <i>Synechococcus</i> sp. cultured in white light.	223
Figure 265. The effect of spectral radiant flux on the photosynthesis of <i>Synechococcus</i> sp. cultured in white light.	223
Figure 266. The effect of spectral radiant flux on the photosynthesis of <i>Synechococcus</i> 1479/5 cultured in white light.	223
Figure 267. The effect of DCMU on the photosynthesis of <i>Scenedesmus</i> sp.	234
Figure 268. The effect of CN ⁻ on the photosynthesis of <i>Scenedesmus</i> sp.	236
Figure 269. The effect of SHAM on the photosynthesis of <i>Scenedesmus</i> sp.	236
Figure 270. The effect of DCMU on the photosynthesis of <i>C. vulgaris</i> 211/11c	236
Figure 271. The effect of CN ⁻ on the photosynthesis of <i>C. vulgaris</i> 211/11c	237
Figure 272. The effect of SHAM on the photosynthesis of <i>C. vulgaris</i> 211/11c	237

LIST OF TABLES

	Page
Table 1.0. Mathematical equations developed to describe photosynthesis irradiance curves	13
Table 1. The effect of photon flux density on the growth kinetics of <i>Chlorella vulgaris</i> 211/11c, <i>Scenedesmus sp.</i> and <i>Synechococcus</i> 1479/5	46
Table 2. The effect of carbon dioxide on the growth kinetics of <i>Chlorella vulgaris</i> 211/11c cultured in the FPALR compared to the CSTR	46
Table 3. The effect of carbon dioxide on the growth kinetics of <i>Scenedesmus sp.</i> cultured in the FPALR compared to the CSTR	49
Table 4. The effect of carbon dioxide on the growth kinetics of <i>Synechococcus</i> 1479/5 cultured in the FPALR compared to the CSTR	49
Table 5. The cellular doubling times of <i>Chlorella vulgaris</i> 211/11c cultured at different carbon dioxide concentrations in the FPALR and CSTR	51
Table 6. The cellular doubling times of <i>Scenedesmus sp.</i> cultured at different carbon dioxide concentrations in the FPALR and CSTR	51
Table 7. The cellular doubling times of <i>Synechococcus</i> 1479/5 cultured at different carbon dioxide concentrations in the FPALR and CSTR	51
Table 8. The effect of temperature on the growth kinetics of <i>Chlorella vulgaris</i> 211/11c cultured in the FPALR and CSTR	54
Table 9. The effect of temperature on the growth kinetics of <i>Scenedesmus sp.</i> cultured in the FPALR and CSTR	54
Table 10. The effect of temperature on the growth kinetics of <i>Synechococcus</i> 1479/5 cultured in the FPALR and CSTR	54
Table 11. The cellular doubling times of <i>Chlorella vulgaris</i> 211/11c cultured at different temperatures in the FPALR and CSTR	56
Table 12. The cellular doubling times of <i>Scenedesmus sp.</i> cultured at different temperatures in the FPALR and CSTR	56
Table 13. The cellular doubling times of <i>Synechococcus</i> 1479/5 cultured at different temperatures in the FPALR and CSTR	56
Table 14. The effect of bicarbonate on the photosynthesis / irradiance response curves of <i>Chlorella vulgaris</i> 211/11c	70

Table 15. The effect of bicarbonate on the photosynthesis / irradiance response curves of <i>Scenedesmus sp.</i>	70
Table 16. The effect of bicarbonate on the photosynthesis / irradiance response curves of <i>Synechococcus</i> 1479/5	70
Table 17. The effect of phosphate buffer on the photosynthetic parameters of <i>Chlorella vulgaris</i> 211/11c	72
Table 18. The effect of phosphate buffer on the photosynthetic parameters of <i>Scenedesmus sp.</i>	74
Table 19. The effect of phosphate buffer on the photosynthetic parameters of <i>Synechococcus</i> 1479/5	74
Table 20. The effect of phosphate buffer on the photosynthetic parameters of <i>Ankistrodesmus antarcticus</i>	76
Table 21. The effect of nitrate on the photosynthesis / irradiance curves of <i>Scenedesmus sp.</i>	76
Table 22. The effect of nitrate on the photosynthesis / irradiance curves of <i>Ankistrodesmus antarcticus</i>	78
Table 23. The effect of nitrate on the photosynthesis / irradiance curves of <i>Synechococcus</i> 1479/5	78
Table 24. The effect of nitrate on the photosynthesis / irradiance curves of <i>Synechococcus sp.</i>	80
Table 25. The effect of trace elements on the photosynthesis / irradiance curves of <i>Chlorella vulgaris</i> 211/11c	80
Table 26. The effect of trace elements on the photosynthesis / irradiance curves of <i>Scenedesmus sp.</i>	82
Table 27. The effect of centrifugation on the photosynthesis / irradiance curves of <i>Chlorella vulgaris</i> 211/11c	82
Table 28. The effect of centrifugation on the photosynthesis / irradiance curves of <i>Scenedesmus sp.</i>	84
Table 29. The effect of centrifugation on the photosynthesis / irradiance curves of <i>Synechococcus</i> 1479/5	84
Table 30. The effect of increasing dark respiration on the photosynthetic parameters of <i>Chlorella vulgaris</i> 211/11c	88
Table 31. The effect of increasing dark respiration on the photosynthetic parameters of <i>Scenedesmus sp.</i>	88
Table 32. The effect of increasing dark respiration on the photosynthetic parameters of <i>Synechococcus</i> 1479/5	91
Table 33. The effect of temperature on the photosynthetic parameters of <i>Chlorella vulgaris</i> 211/11c cultured at 15°C	94
Table 34. The effect of temperature on the photosynthetic parameters of <i>Chlorella vulgaris</i> 211/11c cultured at 23°C	94
Table 35. The effect of temperature on the photosynthetic parameters of <i>Chlorella vulgaris</i> 211/11c cultured at 30°C	95
Table 36. The effect of temperature on the photosynthetic parameters of <i>Chlorella vulgaris</i> 211/11c cultured at 35°C	95

Table 37. The effect of temperature on the photosynthetic parameters of <i>Nannochloris atomus</i> cultured at 15°C	100
Table 38. The effect of temperature on the photosynthetic parameters of <i>Nannochloris atomus</i> cultured at 23°C	100
Table 39. The effect of temperature on the photosynthetic parameters of <i>Nannochloris atomus</i> cultured at 30°C	101
Table 40. The effect of temperature on the photosynthetic parameters of <i>Nannochloris atomus</i> cultured at 35°C	101
Table 41. The effect of temperature on the photosynthetic parameters of <i>Scenedesmus sp.</i> cultured at 15°C	106
Table 42. The effect of temperature on the photosynthetic parameters of <i>Scenedesmus sp.</i> cultured at 23°C	106
Table 43. The effect of temperature on the photosynthetic parameters of <i>Scenedesmus sp.</i> cultured at 30°C	107
Table 44. The effect of temperature on the photosynthetic parameters of <i>Scenedesmus sp.</i> cultured at 35°C	107
Table 45. The effect of temperature on the photosynthetic parameters of <i>Ankistrodesmus antarcticus</i> cultured at 15°C	111
Table 46. The effect of temperature on the photosynthetic parameters of <i>Ankistrodesmus antarcticus</i> cultured at 23°C	111
Table 47. The effect of temperature on the photosynthetic parameters of <i>Ankistrodesmus antarcticus</i> cultured at 30°C	112
Table 48. The effect of temperature on the photosynthetic parameters of <i>Ankistrodesmus antarcticus</i> cultured at 35°C	112
Table 49. The effect of temperature on the photosynthetic parameters of <i>Synechococcus</i> 1479/5 cultured at 15°C	117
Table 50. The effect of temperature on the photosynthetic parameters of <i>Synechococcus</i> 1479/5 cultured at 23°C	117
Table 51. The effect of temperature on the photosynthetic parameters of <i>Synechococcus</i> 1479/5 cultured at 30°C	118
Table 52. The effect of temperature on the photosynthetic parameters of <i>Synechococcus</i> 1479/5 cultured at 35°C	118
Table 53. The effect of temperature on the photosynthetic parameters of <i>Synechococcus sp.</i> cultured at 15°C	123
Table 54. The effect of temperature on the photosynthetic parameters of <i>Synechococcus sp.</i> cultured at 23°C	123
Table 55. The effect of temperature on the photosynthetic parameters of <i>Synechococcus sp.</i> cultured at 30°C	124
Table 56. The effect of temperature on the photosynthetic parameters of <i>Synechococcus sp.</i> cultured at 35°C	124
Table 57. Maximum rate of photosynthesis / dark respiration ratio of <i>Chlorella vulgaris</i> 211/11c	128

Table 58. Maximum rate of photosynthesis / dark respiration ratio of <i>Nannochloris atomus</i>	128
Table 59. Maximum rate of photosynthesis / dark respiration ratio of <i>Scenedesmus sp.</i>	128
Table 60. Maximum rate of photosynthesis / dark respiration ratio of <i>Ankistrodesmus antarcticus</i>	129
Table 61. Maximum rate of photosynthesis / dark respiration ratio of <i>Synechococcus</i> 1479/5	129
Table 62. Maximum rate of photosynthesis / dark respiration ratio of <i>Synechococcus sp.</i>	129
Table 63. The effect of temperature on the LEDR / DR ratio of <i>Chlorella vulgaris</i> 211/11c	132
Table 64. The effect of temperature on the LEDR / DR ratio of <i>Nannochloris atomus</i>	133
Table 65. The effect of temperature on the LEDR / DR ratio of <i>Scenedesmus sp.</i>	134
Table 66. The effect of temperature on the LEDR / DR ratio of <i>Ankistrodesmus antarcticus</i>	135
Table 67. The effect of temperature on the LEDR / DR ratio of <i>Synechococcus</i> 1479/5	136
Table 68. The effect of temperature on the LEDR / DR ratio of <i>Synechococcus sp.</i>	137
Table 69. The effect of temperature on the photosynthetic parameters of <i>Chlorella vulgaris</i> 211/11c cultured at 15°C	140
Table 70. The effect of temperature on the photosynthetic parameters of <i>Chlorella vulgaris</i> 211/11c cultured at 23°C	140
Table 71. The effect of temperature on the photosynthetic parameters of <i>Chlorella vulgaris</i> 211/11c cultured at 30°C	141
Table 72. The effect of temperature on the photosynthetic parameters of <i>Chlorella vulgaris</i> 211/11c cultured at 35°C	141
Table 73. The effect of temperature on the photosynthetic parameters of <i>Scenedesmus sp.</i> cultured at 15°C	145
Table 74. The effect of temperature on the photosynthetic parameters of <i>Scenedesmus sp.</i> cultured at 23°C	145
Table 75. The effect of temperature on the photosynthetic parameters of <i>Scenedesmus sp.</i> cultured at 30°C	146
Table 76. The effect of temperature on the photosynthetic parameters of <i>Scenedesmus sp.</i> cultured at 35°C	146
Table 77. The effect of temperature on the photosynthetic parameters of <i>Synechococcus</i> 1479/5 cultured at 15°C	149
Table 78. The effect of temperature on the photosynthetic parameters of <i>Synechococcus</i> 1479/5 cultured at 23°C	149

Table 79. The effect of temperature on the photosynthetic parameters of <i>Synechococcus</i> 1479/5 cultured at 30°C	150
Table 80. The effect of temperature on the photosynthetic parameters of <i>Synechococcus</i> 1479/5 cultured at 35°C	150
Table 81. Maximum rate of photosynthesis / dark respiration ratio of <i>Chlorella vulgaris</i> 211/11c	152
Table 82. Maximum rate of photosynthesis / dark respiration ratio of <i>Scenedesmus sp.</i>	152
Table 83. Maximum rate of photosynthesis / dark respiration ratio of <i>Synechococcus</i> 1479/5	152
Table 84. The effect of temperature on the LEDR / DR ratio of <i>Chlorella vulgaris</i> 211/11c	155
Table 85. The effect of temperature on the LEDR / DR ratio of <i>Scenedesmus sp.</i>	155
Table 86. The effect of temperature on the LEDR / DR ratio of <i>Synechococcus</i> 1479/5	156
Table 87. The effect of changing PFD on the chlorophyll a content of <i>Chlorella vulgaris</i> 211/11c cultured in the FPALR	175
Table 88. The effect of changing PFD on the chlorophyll a content of <i>Synechococcus</i> 1479/5 cultured in the FPALR	175
Table 89. The effect of increasing PFD on the P_{\max}^{PFD} of <i>Chlorella vulgaris</i> 211/11c cultured in the FPALR	187
Table 90. The effect of light gradients on the growth kinetics of <i>Chlorella vulgaris</i> 211/11c cultured in the FPALR	199
Table 91. The effect of light gradients on the growth kinetics of <i>Synechococcus</i> 1479/5 cultured in the FPALR	199
Table 92. The effect of light gradients (light / dark cycle 58:18 seconds) on the growth kinetics of <i>Chlorella vulgaris</i> 211/11c cultured in the FPALR	202
Table 93. The effect of light gradients (light / dark cycle 70:18 seconds) on the growth kinetics of <i>Chlorella vulgaris</i> 211/11c cultured in the FPALR	202
Table 94. The effect of wavelength on the growth kinetics of <i>Chlorella vulgaris</i> 211/11c	210
Table 95. The effect of wavelength on the growth kinetics of <i>Scenedesmus sp.</i>	210
Table 96. The effect of wavelength on the growth kinetics of <i>Synechococcus</i> 1479/5	213
Table 97. The effect of wavelength on the photosynthesis of <i>Chlorella vulgaris</i> 211/11c cultured in red light	216
Table 98. The effect of wavelength on the photosynthesis of <i>Chlorella vulgaris</i> 211/11c cultured in blue light	216
Table 99. The effect of wavelength on the photosynthesis of <i>Scenedesmus sp.</i> cultured in red light	218

Table 100. The effect of wavelength on the photosynthesis of <i>Scenedesmus sp.</i> cultured in blue light	218
Table 101. The effect of wavelength on the photosynthesis of <i>Synechococcus sp.</i> cultured in red light	219
Table 102. The effect of wavelength on the photosynthesis of <i>Synechococcus sp.</i> cultured in blue light	219
Table 103. The effect of wavelength on the photosynthesis of <i>Synechococcus</i> 1479/5 cultured in red light	221
Table 104. The effect of wavelength on the photosynthesis of <i>Synechococcus</i> 1479/5 cultured in blue light	221
Table 105. The effect of spectral radiant flux on the light enhanced dark respiration of <i>Chlorella vulgaris</i> 211/11c cultured in blue light	227
Table 106. The effect of spectral radiant flux on the light enhanced dark respiration of <i>Chlorella vulgaris</i> 211/11c cultured in red light	227
Table 107. The effect of spectral radiant flux on the light enhanced dark respiration of <i>Scenedesmus sp.</i> cultured in blue light	229
Table 108. The effect of spectral radiant flux on the light enhanced dark respiration of <i>Scenedesmus sp.</i> cultured in red light	229
Table 109. The effect of spectral radiant flux on the light enhanced dark respiration of <i>Synechococcus</i> 1479/5 cultured in blue light	231
Table 110. The effect of spectral radiant flux on the light enhanced dark respiration of <i>Synechococcus</i> 1479/5 cultured in red light	231
Table 111. The effect of DCMU concentration on the respiration of <i>Scenedesmus sp.</i>	235
Table 112. The effect of KCN concentration on the respiration of <i>Scenedesmus sp.</i>	235
Table 113. The effect of SHAM concentration on the respiration of <i>Scenedesmus sp.</i>	237
Table 114. The effect of DCMU concentration on the respiration of <i>Chlorella vulgaris</i> 211/11c	237
Table 115. The effect of KCN concentration on the respiration of <i>Chlorella vulgaris</i> 211/11c	239
Table 116. The effect of SHAM concentration on the respiration of <i>Chlorella vulgaris</i> 211/11c	239
Table 117. Reversibility of cyanide oxidase enzyme complex in <i>Scenedesmus sp.</i> and <i>Chlorella vulgaris</i> 211/11c	240

INTRODUCTION

For centuries man has used micro-organisms as a source of food (Stanbury and Whitaker, 1984). The most common use was for the fermentation of wine and other spirits using crude culturing vessels and non aseptic techniques (Corran, 1975). The cultivation of the microbe, however, has now reached high levels of sophistication. Pure, pyrogen free products derived from the microbe has demanded technology to develop artificial environments in which parameters such as pH, temperature, nutrients, dissolved gasses, redox etc. can be controlled externally and maintained aseptically (Figure 1). These artificial environments or bioreactors are common throughout the world of industry and research and used for the cultivation and production of micro-organisms. Bacteria, yeast and fungi have been used to produce fine intracellular / extracellular chemicals and pharmaceutical products as well as to manipulate biochemical conversions (Boing, 1982). Both free and immobilised cell / enzyme systems have been used in attempts to obtain alternate and more efficient methods for optimising production rates and purity of the final product. For most processes the simple chemostat is able to satisfy these criteria and so is still used throughout the biotechnology industry.

Biotechnological exploitation of micro-algae and cyanobacteria.

Large scale industrial systems utilising mixing vessels up to 150,000 litres are quite common place, however, there are larger vessels e.g. ICI, who operate a continuous 3000,000 litre pressure cycle fermenter (Smith, 1981). These industrial scale bioreactors and indeed pilot scale systems, however, do not use photosynthetic organisms. There are currently only a handful of bioreactors designed and constructed specifically for the production of fine chemicals by micro-algae or cyanobacteria. Compared to bacteria and yeast, micro-algae present several problems, including long cell doubling times (typically >24 hours), lower active biomass concentration (typical micro-algal biomass concentrations of the order 1-5 g l^{-1} (Ratchford and Fallowfield, 1991), compared to yeast which can readily achieve >80 g l^{-1} (Pyle verbal communication 1989), less well known and understood physiology and finally a

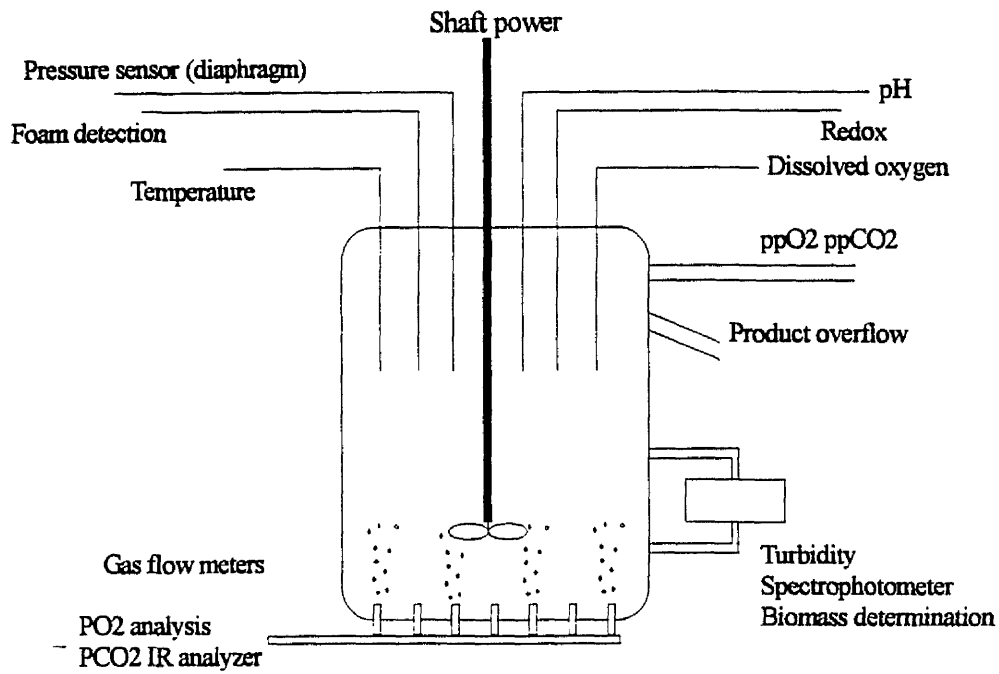


Figure 1. A typical continuously stirred tank reactor for the growth of micro-organisms.

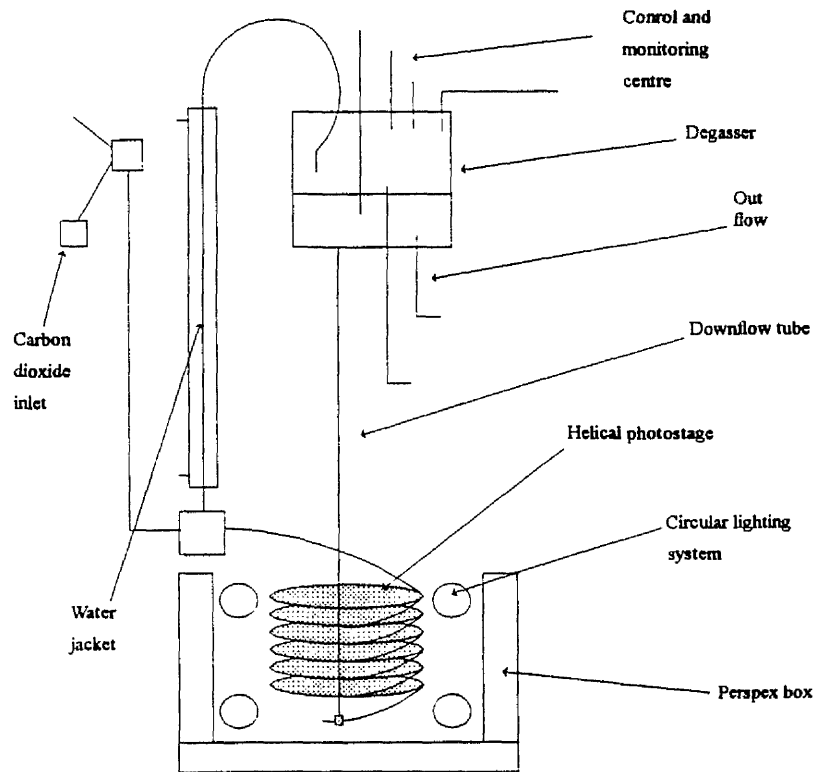


Figure 2. A helical tubular photostage airlift photobioreactor.

requirement of light. Unlike bacteria and fungi whose growth rate and metabolism is governed by the presence of nutrients and a suitable temperature, micro-algae and cyanobacteria require an added input of light. The main objective of all types of photobioreactor is to maximise algal growth rates under conditions of nutrient sufficiency and light limitation.

Scaling up a chemostat from laboratory to pilot scale is accompanied with a decrease in biomass output caused by light limited growth (Watts-Pirt and Pirt, 1977). To overcome this problem it is possible to increase the light incident on the reactor surface in order for it to penetrate further into the vessel. If the photon flux density (PFD) is increased to a level beyond that required for the maximum rate of photosynthesis problems of photoinhibition can also lead to a decline in biomass production, cellular photodamage and photooxidation (Sironval and Kandler, 1958; Jensen and Knutsen, 1993). Cellular photodamage has also been attributed as the reason why cells of *Chlorella vulgaris* 211/11c adhere to the surface of bioreactor vessels which further reduces the penetration of the light (Ratchford and Fallowfield unpublished data). Increasing the surface light incident on the bioreactor vessel requires an increase in the energy costs to irradiate the vessel which ultimately leads to an increase in the reactor cooling requirements. Changes in the internal energy of a photobioreactor must be maintained efficiently if cellular maintenance energies are to be kept at a minimum.

Attempts to overcome the problem of light limitation have resulted in several innovative concepts of design and construction. Pirt *et al.*, (1983) designed a 52 meter glass tubing photobioreactor with a 1 cm bore giving the system a very high surface area to volume ratio of 200m^{-1} . The culture was circulated by either a mechanically driven pump (centrifugal and peristaltic) or by an air lift mechanism. Biomass concentrations of up to 20g l^{-1} were claimed to be readily obtainable from a *Chlorella* type organism (CCAP MA003) when grown using this system.

Lee and Bazin (1990) designed and constructed a 0.315 litre helical photobioreactor driven an airlift mechanism (Figure 2). The helical photostage was designed so that the area to volume ratio of 127m^{-1} was relatively high compared to the ordinary chemostat (a typical 1 litre continually stirred tank reactor (CSTR) has surface area to volume ratio of $20\text{-}40\text{m}^{-1}$). The photobioreactor achieved a biomass output of 4.6g l^{-1} .

l compared to 1.7 g l^{-1} using a conventional stirred tank. Other researchers have developed similar tubular systems, all of which attempted to increase the light availability and increase biomass production e.g. Davis *et al.*, (1953); Panikov and Lee (1979); Pirt *et al.*, (1983).

Attempts to reduce the shearing rates of mechanical pumps lead to the construction of a glass centrifugal pump by Kruger and Eloff (1981). The complete photobioreactor and pump system was made entirely out of glass. A further advantage of such a system was that the photobioreactor and all its components could be steam sterilised in an autoclave. Tubular photobioreactors constructed out of P.V.C (Lee and Bazin, 1990), silicone rubber (Pirt *et al.*, 1983), polycarbonate (Fallowfield *et al.*, 1990) and acrylic (Ratchford and Fallowfield, 1992a) depend on using chemical agents to clean the systems which does not completely sterilise the vessel. Due to the high shear forces created when using conventional centrifugal pumps and the high costs and maintenance requirements of similar pumps (gear, lobe, centrifugal and peristaltic), the use of mechanical systems to drive cell cultures in bioreactor vessels has been all but abandoned. Most photobioreactors can be driven by an air lift mechanism which has several advantages compared to reactors driven by mechanical devices. Firstly cells cultured in air lift driven reactors based on tubular design can be circulated through the system without the requirement for any mechanical moving parts. This reduces energy and maintenance costs but more importantly removes an obstacle to the flow which increases the head and pressure losses due to friction. Minimising head and pressure losses is necessary for the efficient flow of a fluid within a system at high Reynolds numbers corresponding to full turbulent flow. Secondly, in order to avoid a problem of carbon limitation of photosynthetic organisms, carbon dioxide can be introduced into the air lift stream at the desired concentration in gas risers similar to those of Pirt *et al.*, (1983); Lee and Bazin (1990) and Ratchford and Fallowfield (1992a).

Most of the laboratory scale photobioreactors have been designed to have very large surface area to volume ratios. This has been primarily achieved by having a small culture volume of 1 to 3.5 litres (Pirt *et al.*, 1983; Lee and Bazin, 1990). In order to achieve high concentrations of biomass, photobioreactors have been scaled from 10 to 450 litres in capacity. In systems of this kind the effect of light limited growth becomes a major problem. The biomass concentration of 20 g l^{-1} obtained with the

bioreactor of Pirt *et al.*, (1983) is not possible in large volume systems of 450 litres (Ratchford and Fallowfield unpublished data). Kruger and Eloff, (1981) reported that biomass concentrations of 1.02 g l^{-1} were obtainable when growing *Microcystis* in 15-60 litre volumes in the glass photobioreactor. Ratchford and Fallowfield (1991), obtained 2.75 g l^{-1} of *Scenedesmus sp.* cells when culturing the organism in an 11 litre flat plate air lift reactor (FPALR). Biomass concentrations of 0.8 g l^{-1} of *Chlorella vulgaris* 211/11c have been obtained from a 450 litre biocoil photobioreactor (Figure 3; Ratchford and Fallowfield unpublished data). The explanation for such reduced biomass production in large volume vessels is due to light being a growth limiting factor. As scale up of a photobioreactor is carried out the surface area to volume ratio decreases and there is an overall reduction in the incident light energy per unit volume (Lee and Bazin, 1990).

Photobioreactors based on circular geometry present a major problem in determining the accurate measurement of PFD of light that is being intercepted by micro-algal and cyanobacteria. In tubular reactors, it is not unusual to find the maximum illuminated surface area of the culture determined by half the circumference at the inner diameter of the tubing multiplied by the length of the tubing (Pirt *et al.*, 1983). The radius of the tube is used since only half the tube is irradiated by light from one side. This calculation, however, does not take into account the light absorption by the tubing and the internal (glass) and external reflection of light at the surface. This uncertainty in quantifying the accurate measurement of the PFD actually incident on reactor surface displays that systems based on circular geometry are inefficient for the growth and study of high biomass production from photosynthetic organisms. Attempts to overcome the problem of accurately measuring and defining the light field combined with reducing the level of self shading and light limited growth has lead to the design of novel photobioreactors which are not based on the typical circular geometry of tubular systems and CSTRs.

The culture vessel constructed by Mori *et al.*, (1989) concentrated on the reduction of light limited growth and self shading by micro-algal cells. The photobioreactor (Figure 4), although irradiated by a conventional lighting placed outside the vessel, housed a secondary unit in which a Hesner lens system was used to concentrate light and feed it down optical fibres to acrylic radiator rods placed within the algal culture. By feeding light into the central core of the photobioreactor the system went some way to

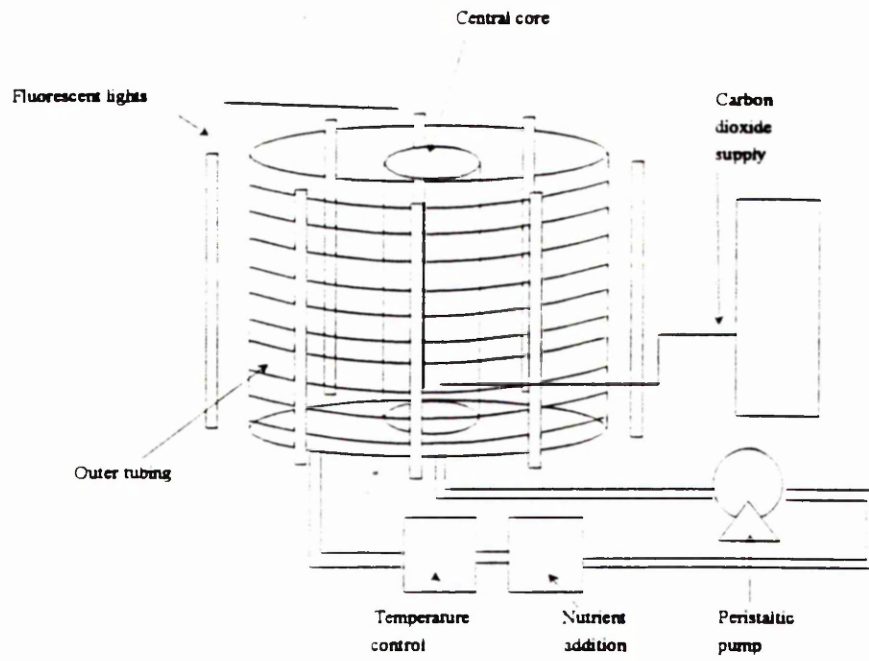


Figure 3. A 450 litre peristaltic pump driven tubular biocoil

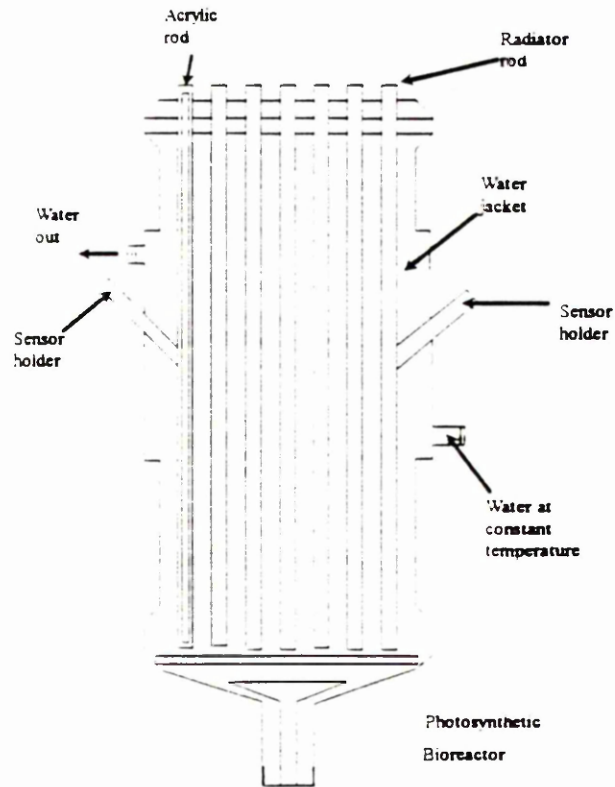


Figure 4. A novel photobioreactor feeding light into the heart of a micro-algal culture.

drastically reducing the level of self shading and light limited growth. This design was developed primarily for use in space as a life support system. The oxygen produced by the photosynthetic cells was used by an aerobic life form which in turn provided the micro-algae / cyanobacteria with carbon dioxide.

Ratchford and Fallowfield, (1992a) designed a photobioreactor based on a flat plate (Figure 5) of acrylic which was internally partitioned to give a continuous path length in which the culture of micro- algae or cyanobacteria could be circulated through an accurately defined light field of known PFD and spectral radiant flux. The system was driven using air injection into a gas riser column allowing very high Reynolds numbers to be obtained within the channels. This high degree of turbulence ensured that self shading by cells of micro-algae and cyanobacteria was minimised.

Vessels have been designed to simulate the light / dark cycles of medium frequency often found in lakes and reservoirs. These vessels include an algal cyclostat with a computer controlled light regime designed and constructed by Kroon *et al.*, (1992a). This photobioreactor used venetian blinds whose blades could be angled independently in order to obtain the required PFD. As the system was computer controlled the system could be run automatically and was extremely flexible since neutral density filters were not required. One major drawback to the culture vessel was the poor mixing ability of the air driven rectangular tank. Being 30mm thick the culture growing in the vessel may have suffered from some degree of self shading which may help explain why the biomass concentration decreased.

The development of photobioreactors and advanced reactor technology for mass algal culture has facilitated research on micro-algal photosynthesis, biochemistry and cellular interaction.

Vertical Attenuation and Light / Dark Cycling

Cells of micro-algae and cyanobacteria play an important role in the production of oxygen in high rate algal pond (HRAP) waste water treatment systems (Oswald, 1976; Fallowfield and Martin 1988). Figure 6 summarises the biochemical exchanges

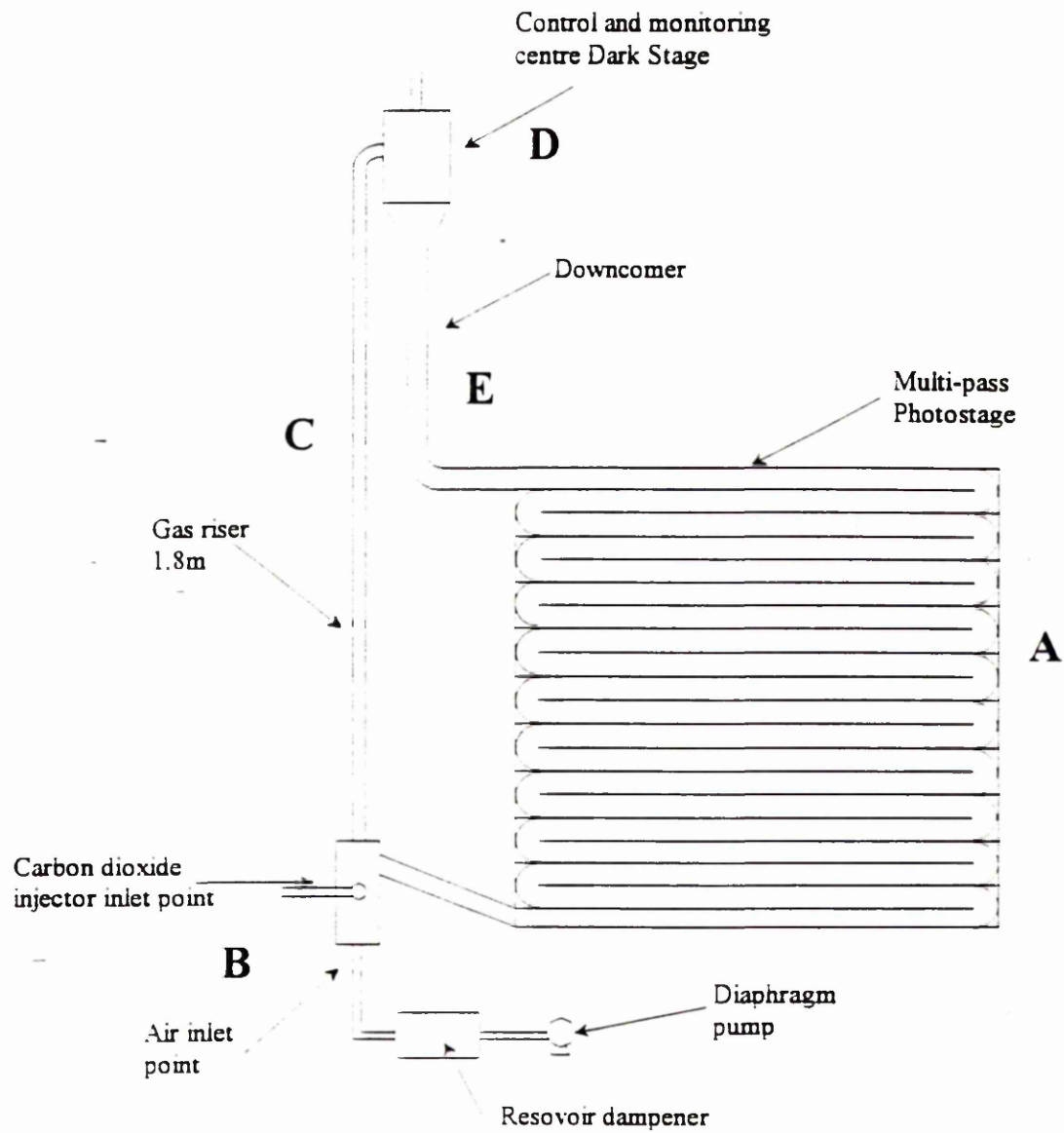


Figure 5. A novel multi-pass flat plate airlift photobioreactor

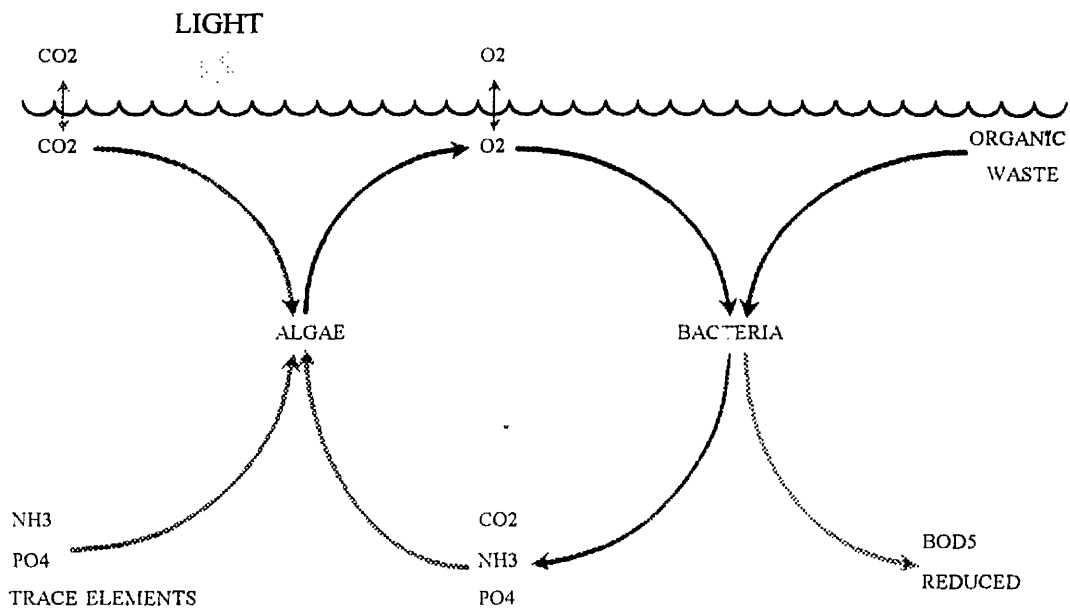


Figure 6. The biochemical processes occurring during the treatment of wastes by micro-algal culture in a high rate algal pond.

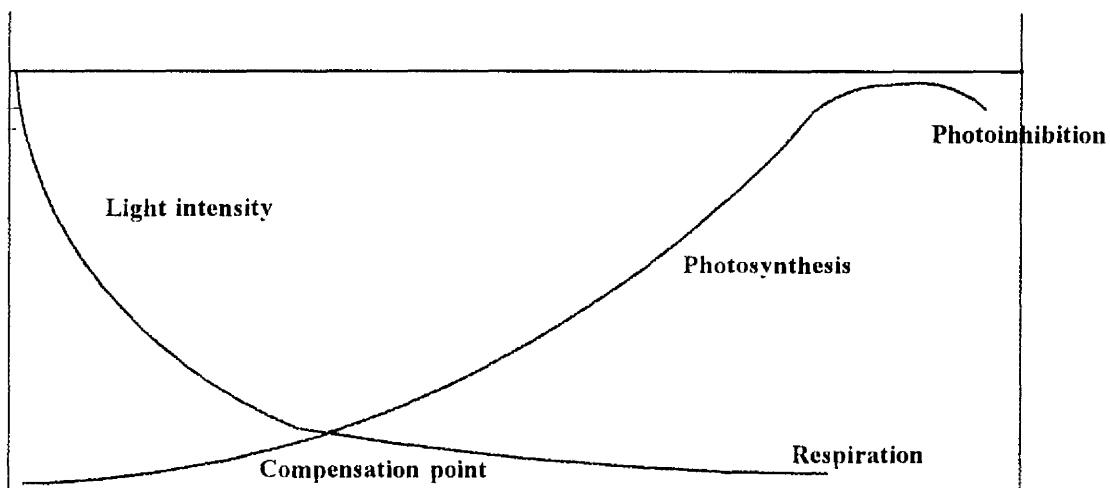


Figure 7. Schematic changes in photosynthesis throughout the depth of a high rate algal pond.

between photosynthetic cells and bacteria that co-exist together in these treatment systems. The photosynthetic organisms use light to split water and evolve molecular oxygen which is used by bacteria to degrade organic matter. In return the bacteria evolve carbon dioxide which is absorbed by the micro-algal / cyanobacteria cells during photosynthesis. For the efficient treatment of waste water, the system design must ensure that it can, under conditions of time and temperature, support the growth of cells of micro-algae at a sufficient level to release enough oxygen to meet the biological oxygen demand B.O.D. (Oswald, 1988).

HRAPs have been used for several years to remove the BOD from the waste water of both animals and humans (Oswald, 1976; Fallowfield and Martin, 1988). Research into the optimum design and operation of these ponds has led to a greater understanding of the complex relationship that exists between the photosynthetic cells and the microbial cells that dwell in such systems.

Cells of micro-algae and cyanobacteria are mixed within a HRAP by means of a single or several large paddle wheels (Soeder, *et al.*, 1970; Stengal, 1970; Oswald, 1976; Fallowfield and Martin 1988). This maintains a well mixed environment throughout the pond depth. The cell motion brought about by the paddle wheel is considered to be circular but does not provide enough oxygen to satisfy the BOD loading (Fallowfield verbal communication). The cell is believed to move throughout the entire depth of the pond from the surface to the very bottom of the HRAP (Fallowfield and Martin, 1988). Both the movement pattern of the cell and the speed of the circulation throughout the depth play an important role in the both the photosynthesis and productivity of cells of micro-algae and cyanobacteria.

In order to understand and predict the mechanisms governing productivity, it is necessary to determine the separate forms of water motion and relate them to the external driving force (Hutter *et al.*, 1991). Little information has been published concerning the effect of light / dark cycles of medium frequency whilst in a vertical attenuation gradient on the growth and photosynthesis of photosynthetic cells. The time scale of the movement and the depth to which the movement occurs ultimately affect a cell's photosynthetic status. In the upper surface of the water column, phytoplankton thrive where sunlight acts as an energy source for photosynthesis (Prezelin *et al.*, 1991). Gibson, (1984) reported that the level of accumulated

carbohydrate increased with increasing light intensity when cell samples obtained from Lough Neagh were incubated in an artificial light gradient. Sunlight, however, may be at a PFD photoinhibitory to cells (Figure 7 after Fallowfield and Martin, 1988). Light at high PFD can be photodamaging to a cell but the degree of photoinhibition with PFD varies between species. *Chlorella vulgaris* 211/11c has been found to have a maximum rate of photosynthesis at a PFD of 200-300 $\mu\text{mol s}^{-1} \text{m}^{-2}$ (23°C, 100mM HCO_3^-) (Ratchford and Fallowfield 1992a). Irradiances above this PFD are photoinhibitory to the cells and result in a decrease in the photosynthetic rate. The onset of photoinhibition, however, has been shown to be prevented by placing the cells in a dark phase in which the photosynthetic apparatus is allowed to recover (Samuelsson *et al.*, 1985; Ratchford and Fallowfield unpublished). The effect of light / dark cycles whilst irradiated at photoinhibitive light intensities, however, is less well understood and published. Light / dark cycles created by the movement of a cell through the light gradient associated with the depth of a water body such as a HRAP, play a crucial role in the cellular productivity of a photosynthetic organism and research is required to establish whether cycling is critical to HRAP performance. These unstable environments can restrict phytoplankton growth and even threaten a cell's survival. Although the PFD of the light gradient (Figure 7) changes as the cell moves through the depth of the HRAP, the available photosynthetically active radiation (PAR), temperature profile and the availability of inorganic nutrients also changes (Prezelin *et al.*, 1991). In lake systems the degree of PAR becomes increasingly important with the level of dead particulate matter. Dead particulate matter is known to strongly absorb light of wavelengths associated with the blue and ultraviolet regions of the spectrum (Kirk, 1983) but has low absorption with the red regions of the spectrum. The main absorption peaks of the chlorophyll a and chlorophyll b pigments associated with the Chlorophyceae and Cyanophyceae are mainly in both the blue and red regions of the spectrum (Kirk, 1983). As the PFD of light decreases with increasing depth the degree to which the wavelengths of light are absorbed is more important than the PFD of the light itself since light of high PFD is of little use to the eukaryotic green micro- algae and cyanobacteria if the wavelength of that light is at 500nm. Jones and Kok, (1966) examined the effect of photoinhibition on oceanic phytoplankton and found that the 50% of the photoinhibition measured at the surface of the water body was attributed to light of wavelengths below 390nm.

The duration of cycle times in which cells of phytoplankton move through water

bodies, can be split into three discreet different time scale. At the upper end of the cycle time of the order days to years, are those created by storms and seasonal changes in very large water bodies (Ferris and Christian, 1991). Determining the productivity of large bodies of phytoplankton over such a time scale is extremely difficult as these cycle times generally affect the phytoplankton community as a whole. At the lower end of the cycle time (seconds) are the conditions created by surface waves (Walsh and Legendre, 1983). Wind blowing across the surface of a water body can induce a circulation movement associated with the water surface. These circulation's occur as unit cells termed Langmuir cells after Irving Langmuir who first studied them. Typical Langmuir cells can have surface speeds of 1.5cm s^{-1} and diameters ranging from centimetres to meters (Kirk, 1983). Photosynthetic cells trapped in the movement of a Langmuir cell would not reside at the surface of a body of water for very long. The time of duration being mainly dependent on the wind speed. Harris and Piccinin, (1977) observed that in the Great Lakes of North America, the average monthly wind speed was great enough to generate Langmuir cells of sufficient size and movement to ensure photosynthetic cells were not subject to irradiance from high light intensities long enough for photoinhibition to occur.

Research examining the flashing effect has been shown to increase the light utilisation of phytoplankton (Laws *et al.*, 1983). The cycle times used have been as low as micro-seconds (Clendenning and Ehrmantraut, 1950) to milli-seconds (Marra, 1978; Terry, 1986). The flashing affect has also been used to quantify the photosynthetic unit of cells of *Chlorella pyrenoidosa* (Myers and Graham, 1971). The effect of medium scale cycle time (seconds to minutes) however, is the least understood and has caused much controversy. Gibson, (1984) examined the effect of circulating phytoplankton through a water column, on cellular carbohydrate content. The results showed no increase in carbon fixation in cells that were circulated through a light gradient. Other researchers, however, have reported increases in cellular productivity when incubating cells in light gradients of medium light / dark cycles. Mann *et al.*, (1972) recorded a 30% increase in overall cellular productivity when incubation bottles were rotated through a light gradient. Marra, (1978) also observed an increase in cellular productivity when using bottles cycled through a vertical gradient. Grobbelaar, (1989), however found no conclusive evidence for increases in productivity when comparing static incubations and mixed systems.

Photosynthesis / irradiance measurements

Photosynthesis is usually determined by the measurement of carbon fixed or oxygen gas released from micro-algal or cyanobacteria cells (Osborne and Geider, 1992). The accurate and ease of use of the oxygen electrode has made it a useful and popular tool for photosynthetic measurements. Figure 8 shows the basic apparatus used for the determination of oxygen consumption and evolution from cells of micro-algae and cyanobacteria. The oxygen electrode has been used to examine the effects of light, (Herbert, 1990); carbon dioxide, (Sukenik *et al.*, 1990); nutrients (Aparicio and Quiñones, 1991); chemical inhibitors (Wang *et al.*, 1992), temperature (Lin and Markhart, 1990) and light / dark cycles (Ratchford and Fallowfield unpublished data) on the photosynthesis and respiration of a given organism. Figure 8 shows the light source used to irradiate cells and is usually a standard slide projector with a quartz-iodide source. Figure 9 shows the electrode chamber in more detail as a flat plate cylindrical vessel in which the cells are suspended with a high speed magnetic stirrer. The oxygen electrode is inserted at right angles to the chamber which is maintained at constant temperature using water circulated from a water bath. The photosynthesis response curve obtained from such gaseous exchange measurements plays the central role in measuring, modelling and predicting the photosynthesis and productivity of a micro-algae or cyanobacterium. Ultimately the measurement of photosynthesis / irradiance response curves displays an indication of the physiology and biochemistry status of the cell.

A schematic plot of a typical photosynthesis / irradiance curve showing the various photosynthetic parameters that can be determined from the curve is shown in Figure 10. The relationship between oxygen evolution and irradiance of Figure 10 is split into 3 very distinct regions. Section (A) shows that the cells are light limited and the rate of photosynthesis increases with increasing PFD. The light limited slope of the photosynthesis / irradiance curve (α) gives an indication of the cells photosynthetic index. As the PFD is increased there comes a point at which the photosynthetic oxygen evolution equals that consumed by respiration. The point I_c is referred to as the light compensation point. Typically the I_c for cells of micro-algae and cyanobacteria lies between 4 and $20 \mu\text{mol s}^{-1} \text{m}^{-2}$ Falkowski and Owens, (1980). In the marine diatom *Skeletonema costatum*, however, the value of I_c has been measured at $0.2 \mu\text{mol s}^{-1} \text{m}^{-2}$ irrespective of the PFD the organism was cultured with (Falkowski and Owens, 1980).

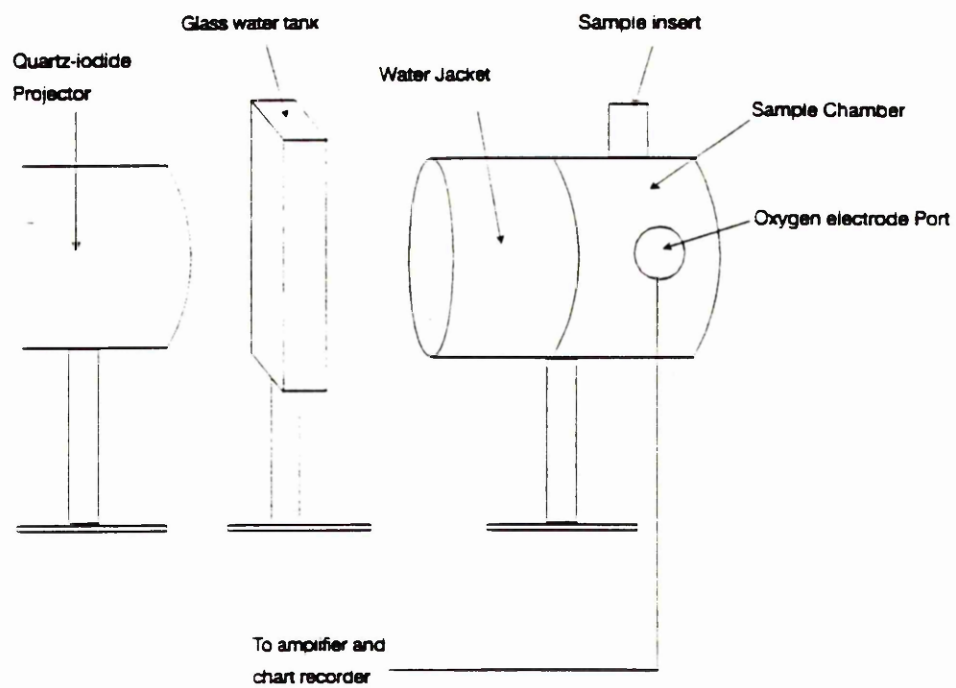


Figure 8. A novel oxygen electrode system.

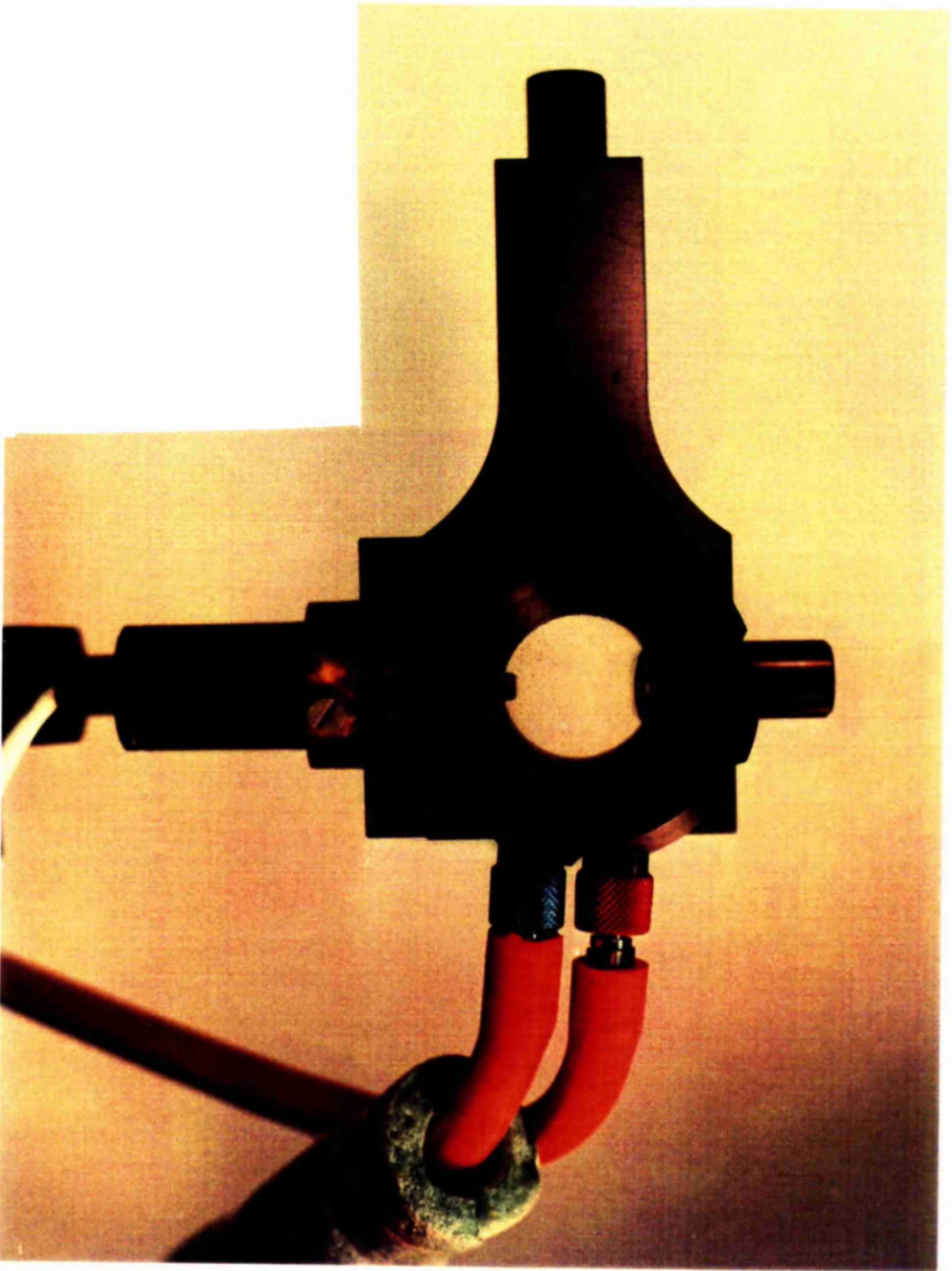


Figure 9. Novel oxygen electrode chamber including probe port and incubation chambers

It has been reported that an intermediate region exists between light limited and light saturated photosynthesis (Sharkey, 1989). Very little information has, however, been reported on this transition state. It has been observed, however, that an abrupt transition occurs between the light limited and light saturated region of the photosynthesis / irradiance curve. Although it is still unclear it is thought to be due to changes in reaction centre light absorption and energy transfer during photosynthesis at low light levels. Sharkey, (1989) considers most abrupt transitions in photosynthesis / irradiance curves to be directly due to very efficient enzyme regulation especially that of Rubisco which can constitute 20-30% of total cell nitrogen (Falkowski *et al.*, 1989). A second region of interest on photosynthesis / irradiance response curves is known to occur near the light compensation point. It has been reported that the slope of the curve close to I_c often increases sharply at low irradiances. The change in the gradient of the curve is referred to as the Kok effect (Kok, 1948). The intersection of the gradient (light limited slope) with the maximum rate of photosynthesis or P_{max} / α (Figure 10) provides us with the value I_k interpolated from the X-axis. Often referred to as the Talling constant, I_k is a measure of the PFD prior to the onset of light saturation. It can be used to show the maximum PFD at which the photosynthetic capacity of cells can be maintained indefinitely if there are no other limiting factors. I_k is also indicative of the photoadaptive state of a phytoplankton community (Prezelin *et al.*, 1991).

The curve reaches a peak plateau (section (B) Figure 10) at which point it is referred to as the maximum rate of photosynthesis P_{max} . The plateau can either immediately fall off or be maintained with increasing PFD up to point at which it begins to decline. Since the value of P_{max} occurs over a range of PFDs and is maintained with increasing PFD, it is often difficult to determine the exact irradiance at which light saturated photosynthesis begins. A term rarely used in photosynthesis / irradiance description is P_{max}^{PFD} i.e. the PFD at which the maximum rate of photosynthesis occurs. This gives an indication of the degree of photoadaptation of the culture irradiance compared to the previous light history.

Beta is used to define the negative slope of the photoinhibition (section (B) Figure 10). The term I_b is a measure of the PFD necessary to bring about the onset of photoinhibition and is calculated by P_{max} / β . The degree to which photoinhibition occurs has also been linked to the rate of degradation and subsequent repair of the photo reaction centre. Photosystem II as opposed to photosystem I, of micro-algae and cyanobacteria has long been associated with susceptibility to damage by light

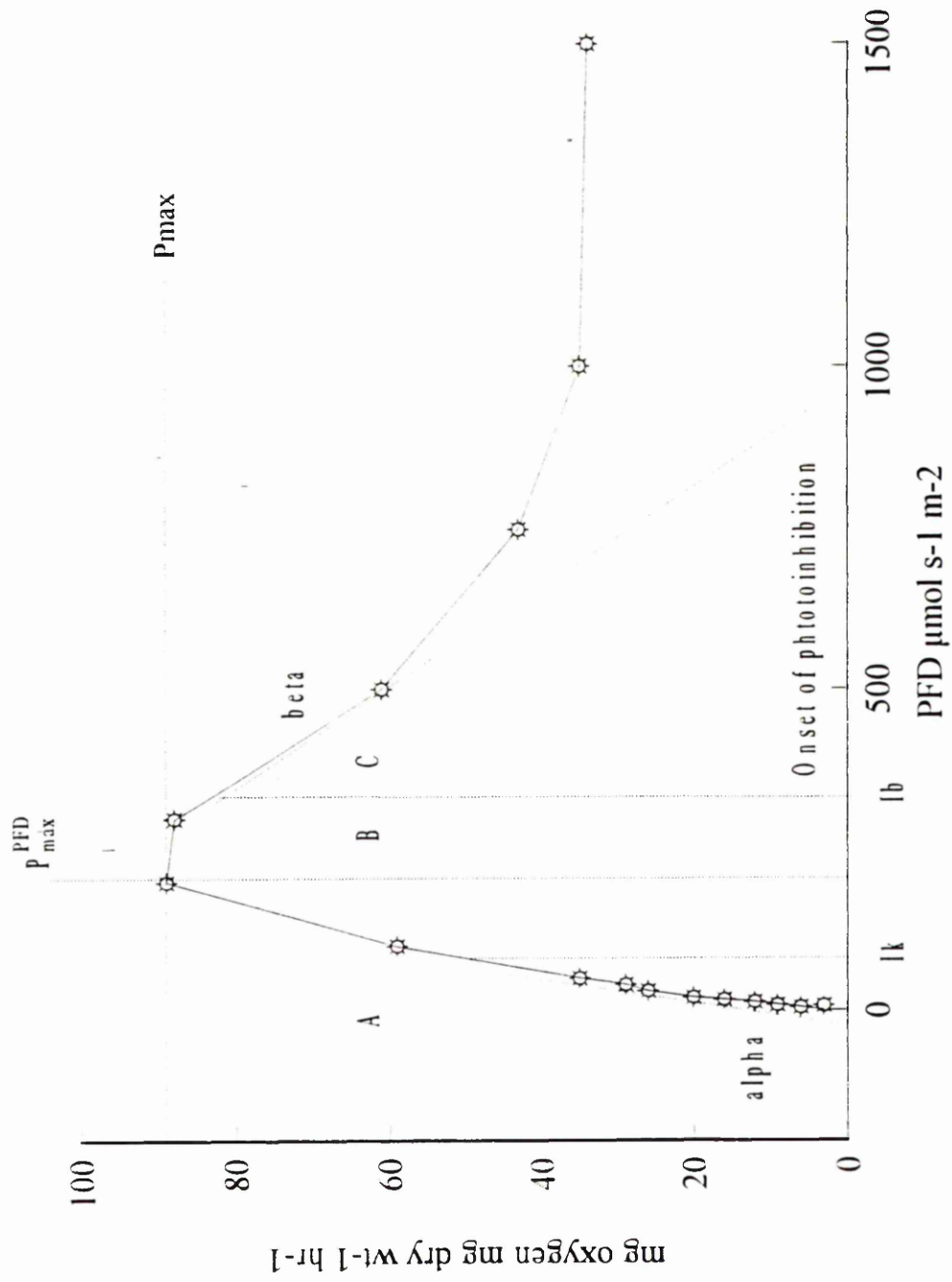


Figure 10. A schematic representation of a typical photosynthesis / irradiance curve and the parameters that can be measured from it.

(Wang *et al.*, 1992). The decrease in photosynthetic oxygen evolution (section (C) Figure 10) at high irradiance PFDs is indicative of photoinhibition. The occurrence and influence of photoinhibition is dependent on several factors including temperature. It has been demonstrated that *Asterionella* cells, (precultured at a temperature of 18°C and 200 $\mu\text{mol s}^{-1} \text{m}^{-2}$), when exposed to light at a PFD of 2000 $\mu\text{mol s}^{-1} \text{m}^{-2}$ for 1 hour at 18 and 23°C had decreased photosynthetic rates of 10 and 50% respectively (Kirk, 1983). Both previous light history and the exposure time is also known to play a crucial role in determining the onset, duration and recovery from photoinhibition. Takahashi *et al.*, (1971) found that photoinhibition in cells of *Phaeodactylum tricornerutum* was far more marked in cells grown in low light compared to cells cultured in high light. The degree of photoinhibition was greater in cells exposed for a time length of 3 hours compared to shorter time periods. Although the mechanism of photoinhibition is known to occur in most cells of micro-algae and cyanobacteria, there are reports of an absence of photoinhibition at PFDs above 2000 $\mu\text{mol s}^{-1} \text{m}^{-2}$. Coudret and Jupin, (1985) reported the absence of photosynthetic inhibition at PFDs above 2000 $\mu\text{mol s}^{-1} \text{m}^{-2}$ whilst working on fixed and surface forms of the diatom *Cystoseira elegans*. The different types of photosynthesis / irradiance response curves that can be obtained vary between photosynthetic organisms. Figure 11a and 11b show two of the classic curves obtained from micro-algae and cyanobacteria. The lack of photoinhibition shown in Figure 10 results in the photosynthesis / irradiance curve obtained in Figure 11b. Although Figure 11b follows a similar trend as Figure 10, section (C) differs markedly. Although cells of micro-algae and cyanobacteria usually display some elements of photoinhibition, the effects of high light intensity have been shown to be fully reversible. Samuelsson *et al.*, (1985) reported that there were two stages of photoinhibition associated with the cyanobacterium *Anacystis nidulans*. Initially exposure of the cells to light of 1000 $\mu\text{mol s}^{-1} \text{m}^{-2}$ resulted in a rapid decrease in oxygen evolution, but this was soon followed by a quasi steady state reduction. This quasi steady state was reached within 30 minutes of the photoinhibitory treatment. A reduction in oxygen evolution at photoinhibitive light intensities has been attributed to the processes of photoinhibition of PSII and photorespiration (Wang *et al.*, 1992). The mechanism of photorespiration, however, can be ruled out in most photosynthesis / irradiance response measurements provided the cells of micro-algae and cyanobacteria are saturated with carbon in the form of carbon dioxide or HCO_3^- (the carbon concentrating mechanism associated with the suppression of photorespiration is discussed below). No data has been produced to determine the effect of high light intensities on cell respiration and its overall effect on photosynthesis and productivity.

Dark respiration (DR) is measured to be oxygen consumption rate. This has been considered to be a constant throughout the measurement of a photosynthesis / irradiance curve (Fallowfield and Martin, 1988; Grobbelaar, 1989; Kroon *et al.*, 1992). Measurement of oxygen evolution involves the gradient changes in mV output from an oxygen electrode. As photosynthesis occurs, respiration is also carried out, hence the actual photosynthetic oxygen evolution is the sum of the oxygen production measured by the electrode plus that which is lost due to dark respiration. There are no reports of the effect of changing respiration on subsequent photosynthesis / irradiance response curve determinations. Light enhanced dark respiration (LEDR) is the term which has been applied to changes in dark respiration after cells of micro-algae or cyanobacteria have been irradiated with light (Falkowski, *et al.*, 1985; Reddy, *et al.*, 1991; Ratchford and Fallowfield, 1992b) and is measured after a photosynthesis / irradiance response curve has been determined.

Simple mathematical models have been developed to describe photosynthetic response curves. However each of these models is simplified in its empirical formulation of not being able to describe all of the external factors that can alter its shape. The early mathematical equations were determined using plants (Blackman, 1905). Table 1 displays the various equations that have been developed and modified since Blackman, (modified from Geider and Osborne, 1992) With the exception of equation 9, all of the remaining equations are satisfactory in determining P_{max} , α and I_k for values of I such that $I < I_b$ i.e. for photosynthetic rates below those associated with photoinhibition. Equation 9, however, can be used to obtain photoinhibition parameters of β and I_b where $I > I_b$. In equation 8 of Platt *et al.*, (1980) P_{max} does not necessarily equal P_s . As β approaches zero the plot of P vs. I becomes that of Figure 11b and hence P_{max} becomes constant over a range of increasing irradiances. Equation 8 has since been modified to account for photoinhibition (Equation 11)

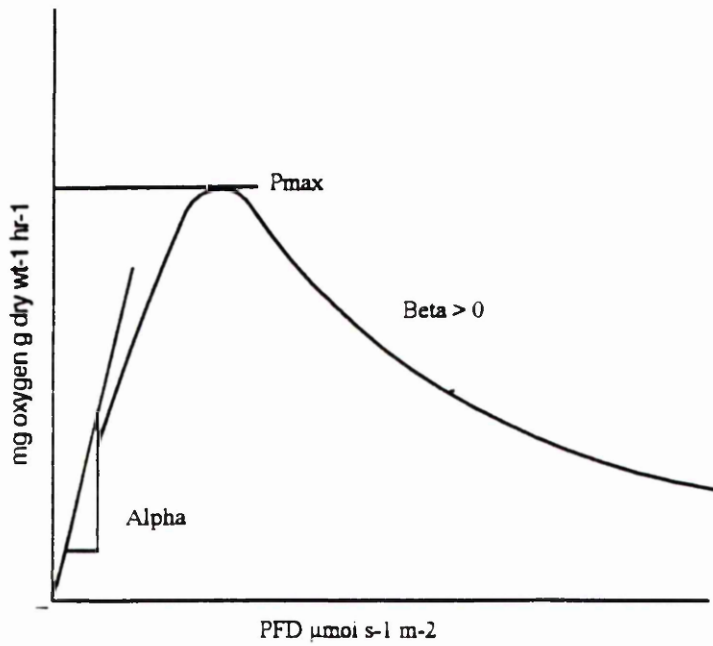


Figure 11a. A schematic diagram of a photosynthesis / irradiance curve when $\text{Beta} > 0$.

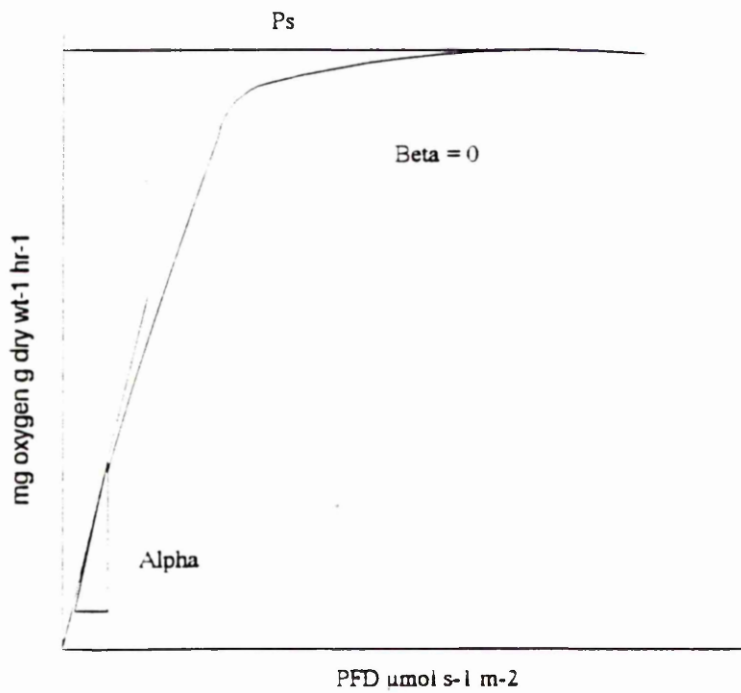


Figure 11b. A schematic diagram of a photosynthesis / irradiance curve $\text{Beta} = 0$.

Table 1.0. Mathematical equations developed to describe the photosynthesis / irradiance response curve (modified from Geider and Osborne, 1992).

$P = \alpha I$	$I < \frac{P_{\max}}{\alpha}$	Blackman, (1905)	(0)
$P = P_{\max}$	$I > \frac{P_{\max}}{\alpha}$	Blackman, (1905)	(1)
$P = \frac{P_{\max} \alpha I}{(P_{\max} + \alpha I)}$		Baly, (1935)	(2)
$P = P_m \left(\frac{\alpha I}{\sqrt{P_m^2 + (\alpha I)^2}} \right) + R$		Smith, (1936) and Talling, (1957)	(2a)
$P = \alpha I e^{\left(\frac{-\alpha I}{P_{\max} e}\right)}$		Steele, (1962)	(3)
$P = P_{\max} \left[1 - e^{\left(\frac{-\alpha I}{P_{\max}}\right)} \right]$		Webb <i>et al.</i> , (1974)	(4)
$P = \alpha I - \frac{(\alpha I)^2}{4P_{\max}}$	$I < \frac{2P_{\max}}{\alpha}$	Platt <i>et al.</i> , (1975)	(5)
$P = P_{\max}$	$I > \frac{2P_{\max}}{\alpha}$	Platt <i>et al.</i> , (1975)	(6)
$P = P_{\max} \tanh\left(\frac{\alpha I}{P_{\max}}\right)$		Jassby and Platt, (1976)	(7)
$P = P_s [1 - e^{-a}] e^{-b}$		(Platt <i>et al.</i> , 1980)	(8)
$P = P_{\max} \tanh\left(\frac{I}{I_k}\right) + rb$		Gallegos and Platt, (1981)	(9)
$P_{\text{net}} = \tanh\left(\frac{\alpha I}{P_{\max}}\right) - R$		Kroon <i>et al.</i> , (1992a)	(10)
$P = P_s [1 - e^{(-aE)}] e^{(-bE)}$		Platt <i>et al.</i> , (1981)	(11)

$$a = \frac{\alpha}{P_s} \quad \text{and} \quad b = \frac{\beta}{P_s}$$

where

P = the photosynthetic rate at a given irradiance

I = irradiance

P_{\max} = maximum rate of photosynthesis

\tanh = hyperbolic function

α = light limited slope

If photoinhibition is not observed and P_s equals P_{\max} , then:

$$a = \frac{1}{I_k} \quad \text{since} \quad I_k = \frac{P_{\max}}{\alpha}$$

$$b = \frac{1}{I_b} \quad \text{since} \quad I_b = \frac{P_{\max}}{\beta}$$

One of the most recent attempts to describe the photosynthetic curve including elements of photoinhibition was that of Megard *et al.*, (1984).

$$P = \frac{P_s}{(K_1 + E + E^2 / K^2)} \quad (\text{Megard } et al., (1984) \quad (12)$$

P = photosynthetic rate at given irradiance (mg oxygen g dry wt⁻¹ hr⁻¹)

P_{\max} = maximum rate of photosynthesis (mg oxygen g dry wt⁻¹ hr⁻¹)

I = irradiance photon flux density (mol s⁻¹ m⁻²)

I_k = photon flux density prior to onset of light saturation (μmol s⁻¹ m⁻²)

α = light limited slope (mg oxygen g dry wt⁻¹ hr⁻¹/μmol s⁻¹ m⁻²)

b = relative baseline (y intercept)

K = constant

It has been observed that the value of α for both chlorophyll a and dry matter specific photosynthesis / irradiance curves of cells of *Chlorella* cultures does not change with the PFD at which the cells were grown at (Myers, 1970). The maximum rate of

photosynthesis, however, was found to increase with increase growth irradiance. The differences in photosynthetic parameters obtained from cells of micro-algae and cyanobacteria cultured at different light intensities has been an area of close examination. The response of micro-algae and cyanobacteria to increasing light intensity is usually accompanied by a reduction in photosynthetic pigment content (Geider, 1987). The results reported by Beardall and Morris, (1976), however, showed decreasing chlorophyll a specific light saturated photosynthetic rates in micro-algae cultured at low PFDs.

Most photosynthesis response curves are expressed as the photosynthetic oxygen evolution (net) per unit dry weight (Arnold and Murray, 1980; Baghdadli *et al.*, 1990; Ratchford and Fallowfield, 1992a); oxygen evolution per cell, (Falkowski and Owens, 1978; Marra, 1978;) or oxygen evolution per unit chlorophyll (Sueltemeyer *et al.*, 1986; Glidewell and Raven, 1975; Peltier and Thibault, 1985; Reddy *et al.*, 1991). The conditions under which the measurement of photosynthesis response curve occurs differ widely. The more common method being to incubate the cell sample in a buffer of known pH and temperature. Temperature, pH and a great number of external factors can affect both the measurement and interpretation of a photosynthesis / irradiance curve. The external factors usually have an influence on different components of the photosynthetic apparatus (Geider and Osborne, 1992). The rate of photosynthesis by a micro-algal or cyanobacteria cell depends on the interception of quanta from the light source from which the intensity and spectral radiant flux has a major contribution.

Although light can be considered to be a major limiting factor for primary productivity, carbon and other nutrients can be limiting the photosynthetic rates. The light reactions of photosynthesis include the production of ATP and NADPH₂. These products are required for the carbon fixation mechanisms that occur in the dark. At very high light intensities the formation of ATP and NADPH₂ can be at its maximum for the given conditions, however, the utilisation of these two products may be limited in the reactions associated with the dark stages of photosynthesis, namely carbon limitation. The affinity for carbon has been demonstrated to be linked to the previous conditions under which the cell was cultured. Badger and Andrews, (1982) found that air grown cells of a *Synechococcus sp.* had a much higher affinity for bicarbonate than similar cells grown at 5% carbon dioxide. The data, however, also showed that carbon dioxide grown cells achieved higher rates of photosynthetic oxygen evolution in the higher inorganic carbon incubation experiments than air grown cells. Equation 13

shows the different forms that carbon can exist when present in water.



The form that carbon takes is directly affected by the pH of the surrounding medium. As the pH increases then the equilibrium moves to the right of equation 11 and carbon readily takes the form of carbonate. Lloyd *et al.*, (1977) observed that the photosynthetic rates of *Chlorella pyrenoidosa* measured at a constant $270\mu\text{mol s}^{-1}\text{m}^{-2}$ were increased 2 fold by the presence of $200\mu\text{l l}^{-1}$ carbon in the form of carbon dioxide. The uptake form of carbon by cells of micro-algae and cyanobacteria has been the centre of great interest (Miller and Colman, 1980; Kaplan, 1981; Badger and Andrews, 1982; Badger *et al.*, 1985; Sueltemeyer *et al.*, 1986; Palmqvist *et al.*, 1990; Thielmann *et al.*, 1990; Espie *et al.*, 1991; Espie and Kandasamy, 1992). It is known that carbon utilised by the ribulose diphosphate carboxylase enzyme is in the form of carbon dioxide but the entry of carbon, into the cell, however, has been demonstrated to be in the form of HCO_3^- ; *Coccochloris peniocystis*, (Miller and Colman, 1980; *Chlamydomonas renhardtii*, Palmqvist *et al.*, 1990; *Synechococcus sp.*, Espie and Kandasamy, 1992). Further evidence for the active transport of the HCO_3^- ion across the cell membrane comes from the measurements of inorganic carbon present within the cell and comparisons made with the amount of carbon that could exist in the cell if the movement of carbon dioxide was by means of a passive carbon dioxide equilibration across the plasmalemma (Kaplan *et al.*, 1980; Coleman and Colman, 1981; Badger and Andrews, 1982). Espie and Kandasamy, (1992), reported that the accumulation and transport of carbon was also affected by the presence of Na^+ ions.

Working with the cyanobacterium *Synechococcus* UTEX 625, it was observed that the active transport and accumulation of intracellular carbon in air grown cells (air bubbled through culture 70ml min^{-1}) was promoted by the presence of 25mM Na^+ . This transport and accumulation resulted in an increase in photosynthetic oxygen evolution rates and carbon fixation. However it was also found that the active transport and accumulation of carbon in free standing cells (cultured on orbital shakers with no air addition) was reduced in the presence of 25mM Na^+ . This requirement for the presence of Na^+ for air grown cells displays that the metal ion plays an acute role the uptake and concentrating of dissolved inorganic carbon in the transport system of cyanobacteria.

The observations of Espie and Kandasamy, (1992), however, suggest that some cyanobacteria possess a Na^+ independent uptake mechanism. It has also been recorded that the cyanobacterium *Synechococcus* UTEX 625 cellular carbon dioxide transporting system, is inhibited by the presence of carbonyl sulphide (Espie *et al.*, 1991). The presence of carbonyl sulphide, however, was not found to significantly affect the Na^+ dependent transport process. They proposed that two different paths existed for the entry of dissolved inorganic carbon into the cyanobacterium, the first of which was a constitutive and functioned around the carbon dioxide molecule whereas the second was inducible and concentrated on the HCO_3^- molecule.

Inorganic nutrients have been shown to affect the rates of photosynthesis as it has been reported that reduced levels of nitrate have been associated with decreases in the chlorophyll content of *Chlorella* (Kirk, 1983). Chlorophyll a specific maximum rates of photosynthesis decrease rapidly with decreasing nitrate and phosphate (Herzig and Falkowski, 1989). Changes in photosynthesis with respect to varying nitrogen levels can be mainly attributed to the functions of the enzyme Rubisco and the repair / maintenance enzymes of the cell. At photoinhibitive irradiances, the cell requirement for nitrogen increases, paralleled with an increase in the oxygen consumption. Falkowski *et al.*, (1989) calculated that between 20 and 30% of the total cell nitrogen was in the form of the enzyme Rubisco. The presence of various types and concentrations of nutrients has not been examined on photosynthesis / irradiance curve parameters.

Respiration Pathways in Micro-algal Cells

Primary productivity is the light dependent assimilation of carbon and inorganic nutrients processed by the thylakoid in the chloroplast (Beardall and Raven, 1990). The light energy intercepted and absorbed by the chlorophyll pigments is used to generate adenosine triphosphate (ATP) and nicotinamide adenine di-nucleotide hydrogen phosphate (NADPH). For the fixation of carbon to occur, carbon has to be processed via 3 major pathways leading to the oxidation of organic substrates (Beardall and Raven, 1990).

Eukaryotic green micro-algae carry out the oxidation of carbon via the processes of glycolysis (carried out in the cytosol), oxidative pentose phosphate pathway (carried out in the inner mitochondrial membrane and thylakoids) and the tricarboxylic acid pathway (carried out in the mitochondria) combined with oxidative phosphorylation (Figure 12). The mechanisms of respiration in micro-algae and cyanobacteria has been extensively reviewed by Gibbs, (1962); Danforth, (1967); Lloyd, (1974); Raven, (1984); Beardall, (1989) and Beardall and Raven, (1990). Briefly, the process of glycolysis breaks down glucose to form pyruvic acid and acetyl -CoA. The biproducts of the pathway include carbon dioxide, ATP and NADH. The acetyl-CoA produced at the end of glycolysis is then used to provide the carbon skeletons necessary to drive the TCA cycle (Figure 12). The TCA cycle produces useful intermediary carbon structures and biproducts including carbon dioxide, ATP, and NADH. Raven, (1972a) showed that although the pentose phosphate pathway produced carbon dioxide and NADPH₂, it had no obligatory role in the process of carbon synthesis. Early work carried out by Mangat *et al.*, (1974) indicated that the substrates of light and dark respiration were different in the higher plants. This difference in the respiratory processes that occur in the light and dark has been confirmed by Buchanan, (1980). It was found that two of the key enzymes of the glycolytic pathway (phospho-fructokinase) and the pentose phosphate pathway (glucose 6 phosphate dehydrogenase) were inhibited by light. This suggested that the carbon assimilation and movement through the upper region of glycolysis and the oxidative pentose phosphate pathway was not possible. Kanazawa *et al.*, (1972) and Raven, (1972), however, reported that the carbon flux for the TCA cycle was the same in the light as it was in the dark. It was therefore suggested that carbon in the form of triose could enter the TCA cycle from the Calvin cycle recycle. As Beardall and Raven, (1990) pointed out, cells of micro-algae grow continuously in the light and so must have a fully functioning TCA cycle in order to meet the necessary biosynthetic need of the cell.

Cells of micro-algae have the ability to consume oxygen via several pathways. These include the Mehler reaction, thylakoid electron transport and the recently understood mechanism of 'chlororespiration' where oxygen acts as a terminal electron acceptor (Beardall and Raven, 1990). The Mehler reaction involves the use of oxygen which acts as terminal electron acceptor to combine 2 protons and an oxygen molecule to form hydrogen peroxide which is then detoxified by catalase, ascorbate peroxidase or

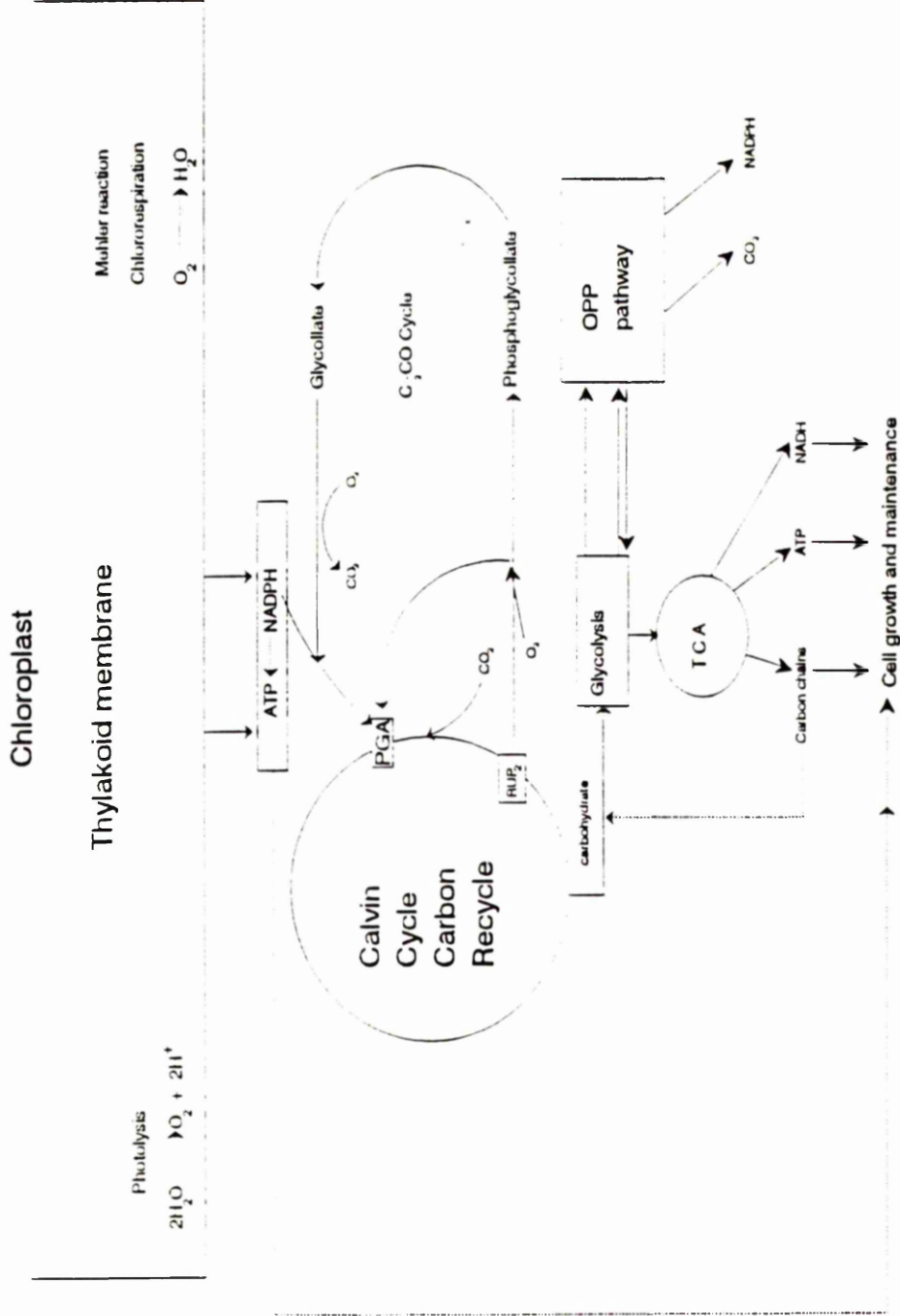
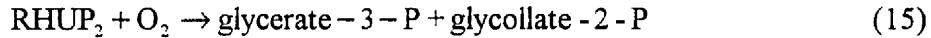
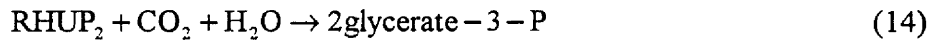


Figure 12. The biochemical reactions associated with the dark pathways of micro-algae.

Ribulose 1-5 diphosphate carboxylase / oxygenase has two functions, one of which is the combining of carbon dioxide and water (Equation 14) and the other is the reaction with oxygen (Equation 1.15; Beardall and Raven, 1990).



Although the mechanism of photorespiration is known to occur in higher plants, very little is known about whether or not the process occurs in cells of micro-algae and cyanobacteria. Photorespiration has been defined as the oxygen sensitive loss of carbon dioxide during photosynthesis (Brendan *et al.*, 1982). Attempts to detect and measure the process of photorespiration have lead to a great deal of controversy about the demonstration of carbon dioxide evolution from cells incubated in the light. Brendan *et al.*, (1982), however, showed that an oxygen sensitive carbon dioxide release in the light did exist in cells of the unicellular micro-algae of *Chlorella vulgaris*, *Chlamydomonas reinhardtii* and *Navicula pelliculosa* as well as in the cyanobacteria *Anabaena flos aquae* and *Anacystis nidulans*. It should be noted, however, that photorespiration was only recorded under conditions of very low dissolved inorganic carbon. The level dissolved inorganic carbon is now believed to hold the key to determining whether or not the process of photorespiration occurs in cells of micro-algae and cyanobacteria. Badger *et al.*, (1980) first demonstrated that a carbon concentrating mechanism was present in cell in the form of active transport of HCO_3^- ions. Evidence for this process arose from the observations that the $K_{1/2}$ for carbon dioxide in *Chlamydomonas reinhardtii* decreased with increasing pH which as shown in Equation 13, forces carbon to exist as HCO_3^- ions. Raven, (1970) and Birmingham and Colman, (1979) all reported that micro-algal cells were capable of directly uptaking dissolved inorganic carbon in the form of HCO_3^- . Other researchers had recorded different levels of the enzyme carbonic anhydrase in cells that were particularly prone to exhibiting photorespiration (Hogetsu and Miyachi, 1979a; Pronina *et al.*, 1981). Spalding *et al.*, (1983a) used a mutant of *Chlamydomonas reinhardtii* which required high levels of carbon dioxide (>5% for photoautotrophic growth). The organism had a defective gene which reduced the level of inorganic

carbon accumulation and transport (gene *pmp-1-16-5K*). It was reported that the mutant cells had higher levels of carbonic anhydrase than the wild type cells and exhibited photorespiration. This suggested that the mechanism of photorespiration was associated with the presence of an inorganic carbon transporting mechanism. It is now generally thought that an active transport mechanism exists (Beardall, 1989; Beardall and Raven, 1990), for the movement of dissolved inorganic carbon into the cells which when concentrated on the other side of the plasmalemma create high carbon dioxide to oxygen ratios which in turn decrease the oxygenase activity of the Rubisco enzyme which suppresses the process of photorespiration.

The consumption of oxygen in the dark by cells of micro-algae and cyanobacteria has long been considered to be equal to that consumed in the light. Brown, (1953) used $^{18}\text{O}_2$ to examine the consumption of oxygen by *Chlorella pyrenoidosa* in the light and dark. No difference was measured between the rates of oxygen consumption in either the light or the dark. Similar observations have been recorded by other researchers including Peltier and Thibault, (1985). Heichel, 1972; Glidewell and Raven, 1975); Falkowski *et al.*, (1985); Reddy *et al.*, (1991), however, have all reported enhanced rates of respiration in cells of micro-algae and cyanobacteria whilst irradiated with light. Using specific respiration inhibitors, it has been shown that the increase in oxygen uptake in the light can be attributed to the Mehler reaction when the cells are incubated under high carbon dioxide concentrations and attributed to the Mehler reaction plus photorespiration when present in low carbon dioxide concentrations. The ratio of light to dark respiration has been recorded to vary with species. Grande *et al.*, (1989) reported that the respiration measured during the dark was greater than that measured in the light. The problem with long term ^{14}C incubations is the excretion and re-assimilation of the labelled carbon having already passed through the cell and it is difficult to measure respiration in these experiments. Brown and Tregunna, (1966), showed that cells of *Chlorella pyrenoidosa*, *Chlamydomonas reinhardtii* and *Anabaena flos aquae* lacked conventional photorespiration, however they reported that the organisms may continue to carry out normal dark type respiration in the light but that the rate was equal or below the original dark respiration, suggesting that there was an inhibition of dark type respiration in the presence of light. Oxygen consumption in the light has been recorded to be 0.75 to 10 times the rate of dark respiration (taken from Geider and Osborne, 1992). It has been reported that the wavelength of light which cells are irradiated with and the wavelength of light which the cells are cultured under also has an influence on the rate of LEDR (Ratchford and Fallowfield, 1992b). Cells of

Chlorella vulgaris 211/11c, *Scenedesmus sp.* and *Synechococcus* 1479/5 cultured in blue (350-550nm), red (600-800nm) and full spectrum light (300-800nm), all showed increases in LEDR rates when subsequently irradiated with blue (350-550nm) light. Stone and Ganf, (1981) examined the effect of light exposure on two green micro-algae and two cyanobacteria. After 10 minutes of exposure to a PFD of $550\mu\text{mol s}^{-1} \text{m}^{-2}$, the cells showed increases of 65 to 275% in the enhanced dark respiration rate compared to the initial dark respiration rate. Increasing the exposure time to this high PFD to 4 to 8 hours resulted in enhanced post illumination respiration rates of 400 to 600% that of the initial dark respiration rate. It was also recorded that the time taken for the LEDR rate to return to the original dark respiration rate following an exposure of $550\mu\text{mol s}^{-1} \text{m}^{-2}$ for 10 minutes required 40 minutes. The process of LEDR, however, is not confined to cells of micro-algae and cyanobacteria. The process of LEDR has been observed to occur in mesophyl protoplasts from leaves of *Pisum sativum* L. cv Arkel more commonly known as Pea (Reddy *et al.*, 1991). It was found that respiratory oxygen uptake was increased 3 fold after cells were irradiated with light of PFD $1250\text{mol s}^{-1} \text{m}^{-2}$. It was also found that in a similar pattern to cells of micro-algae and cyanobacteria the rate of LEDR and duration was determined by the exposure irradiance and duration.

Research Objectives

- (1). To design, construct and optimise a multi-pass flat plate air lift reactor for the growth of micro-algae and cyanobacteria.
- (2). To investigate the effect of light source, irradiance, carbon dioxide concentration, temperature and gradients of light on the growth kinetics and physiology of micro-algae and cyanobacteria grown with batch kinetics in the flat plate air lift reactor and a continually stirred tank reactor.
- (3). Examine the effect of irradiance and light / dark cycles on the growth, physiology and photosynthetic kinetics of micro-algal and cyanobacterial cultured in the flat plate air lift reactor.
- (4). Investigate the effects of photoinhibitory irradiances and light / dark cycles of medium frequency on the photosynthesis, respiration and recovery times of micro-algal and cyanobacterial cells with the aid of an oxygen electrode system.
- (5). Investigate the effect of temperature, nutrients, centrifugation, spectral radiant flux and culture irradiance on the photosynthesis / irradiance curves of micro-algae and cyanobacteria.
- (6). Determine the effect of spectral radiant flux on the growth kinetics and photosynthesis / irradiance response curves of micro-algae and cyanobacteria.
- (7). Examine the effect of spectral radiant flux on the light enhanced dark respiration of cells of microalgae and cyanobacteria.

2.0 METHODS AND MATERIALS

2.1 Flat Plate Air Lift Reactor

To facilitate closer examination of micro-algal cellular responses to light, wavelength, temperature and nutrient availability, a flat plate air lift reactor (FPALR) was constructed. The general design of the FPALR is shown in Figure 5. The micro-algal culture was circulated through the channels of the photostage (A), into the gas injection facility (B), up through the gas riser column (C), into the dark stage (D), down through the downcomer tube (E) and finally returned to the photostage (A) to repeat the cycle. The culture was circulated solely by an air lift mechanism.

2.1.1 Construction

A Flat Plate Air Lift Reactor (FPALR), was constructed out of acrylic and poly vinyl chloride (P.V.C.). The photostage (A of Figure 5) had dimensions of 760mm x 700mm x 15mm and was constructed out of a twin walled, internally partitioned acrylic sheet. The surface area of the photostage was 0.5 m² and housed 23 channels of dimensions 32mm x 16mm. As the flat plate had endings at right angles to the channels (1 of Figure 13) it was necessary to reduce energy losses from within the circulating fluid and to minimise shearing stresses on the micro-algal cells. This was achieved by making curved endings (180° U turn) and fitting them to each horizontal channel (3 of Figure 13), from which 2.5 cm of acrylic (2 of Figure 13) had been removed using a flat soldering iron. The sides of each channel were protected from the heat of the soldering iron using small metal inserts. The curved strip inserts were made from acrylic and had dimensions of 100mm x 13mm x 2.5mm. Each strip was examined for signs of stress or the presence of internal / external fractures prior to use. The curved strips were placed into the partitioned channels at a distance Hd from the centre (4 of Figure 13). This process was repeated in alternate channels down both sides of the photostage. On completion the photostage had a continuous path length of 14.5 meters.

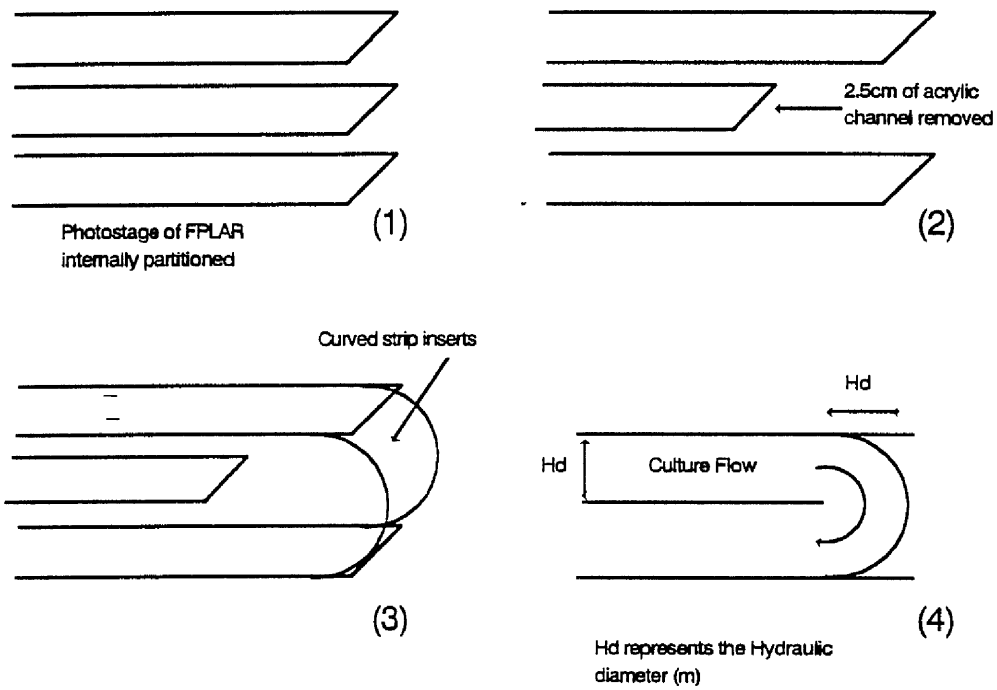


Figure 13. The construction of the curved internally partitioned channels of the flat plate air lift photobioreactor.

When all the subsequent parts were in position, an Acrifix agent was applied and the system made water tight. The FPALR was left for 3 days to allow the Acrifix agent time to seal completely. After 3 days the flat plate was filled with cold water and checked for leakage from within the channels. Upon completion the flat plate was placed under an ultra-violet lamp for 24 hours to cure the system to remove stress points.

A cylindrical cross section 162mm in diameter was milled out of PVC which housed the reactor controls and monitoring centre (D of Figure 5). A cone shaped PVC downcomer was used to facilitate the smooth passage of the recycled culture back into the photostage. The control and monitoring centre acted as a dark stage for the photobioreactor. The top of the dark stage was covered with a P.V.C. circular lid which was removable allowing access to the system if it became necessary. Holes were drilled into the cover to allow probe inserts which could then be sealed to maintain aseptic conditions within the system. The top section housed both the monitoring and control of pH, temperature, anti-foaming, pressure relief valve, feed inlet and outlet. Culture temperature was maintained at $23 \pm 0.5^\circ\text{C}$ using an electrically thermostatic cartridge heater and a refrigerated circulating Churchill chiller unit. Water was circulated through a large glass tank placed in front of the photostage to further facilitate the removal of heat. The pH of the culture was continuously monitored and controlled by the automatic addition of either 1 M NaOH or 1 M HCl via an automatic pH controller (Kent Industrial Instruments; EIL9142). All cultures of micro-algae and cyanobacteria were monitored every 24 hours for the presence of foam. Foam accumulation was controlled by the manual addition of polypropylene glycol (MW 400; $400 \mu\text{l l}^{-1}$) when necessary.

The down comer was attached to the photostage via 1.75 inch diameter reinforced nylon tubing 0.712m in length. Special inserts made out of PVC were constructed to connect the downcomer tubing to the top channel of the photostage. These inserts were designed to reduce fluid energy losses and cell shearing.

All cells cultured in the FPALR were circulated by an air lift mechanism (B of Figure 5) placed at the end of the photostage. The hydraulic diameter of the cross section of each channel of the photostage was approximately 15 mm. To keep pressure and head losses

due to friction to a minimum, a gas riser of the same diameter was incorporated into the design. Calculations based on bubble gravity theory suggested that the maximum height for this column should be approximately 2.0 meters (Joshi and Sharma, 1979). This allowed the input of high gas flow rates into the column without resulting in bubble collapse. The gas riser (1.82 m x 0.013 m) was made from acrylic (C of Figure 5). The gas riser entered the dark stage via a curved right angle.

The gas input was located at the base of the column (B of Figure 5). The forces controlling the movement of fluid throughout the reactor were greatly influenced at this point. Fluid from the photostage was introduced into the gas riser system at an angle of 30°. This facilitated the smooth movement of the culture into the column under highly turbulent conditions. For reasons of optimum mixing, the air and carbon dioxide gases entered the reactor at this stage since there is a higher degree of turbulence within the column than in any other part of the reactor. Air was delivered from a diaphragm pump via a 4 litre reservoir to dampen the air pulsation caused by the pump. A pressure relief valve was fitted to the reservoir to prevent any form of compression occurring within the reservoir. A glass sparger was situated below the main path of fluid to enhance the air lift effect. Carbon dioxide was delivered through a threaded insert situated halfway up the air input stage and at right angles to the flow. To reduce the problem of back pressures carbon dioxide was introduced into the column via a small hypodermic needle placed through a small rubber bung.

The reactor was cleaned by circulating a solution of 2% w/v of sodium hypochlorite within the FPALR. This solution was then discarded and residual chlorine was neutralised by circulating sodium thiosulphate. The FPALR was then rinsed 3 times with sterile distilled water.

2.1.2 Hydraulic Characteristics.

The FPALR was hydraulically characterised (Ratchford and Fallowfield, 1992a). A copy of the paper is presented at the back of the thesis.

2.1.3 Changing the Light / Dark Cycle

The light / dark cycle was normally set and maintained at 58:26 seconds with a Reynolds number of 5800 unless otherwise stated.

The light / dark cycle in the FPALR was changed according to three methods. Firstly, the volume of media in the FPALR was decreased from 10 litres to 8.9 litres to change the length of time spent in the dark stage of the reactor from 26 seconds to 1 second (based on operating the FPALR at a Reynolds number of 5800). Secondly the light / dark cycle in the FPALR was manipulated by varying the gas flow rate into the gas riser and so varying the Reynolds number. The variation in Reynolds number with gas flow rate can be found in Ratchford and Fallowfield, (1992a). The third method to change the light / dark cycles was to shield specific channels in the FPALR from the incident light using thick white card.

2.2 Growth of Micro-algal / Cyanobacteria Cultures

The organisms used throughout the research were *Chlorella vulgaris* 211/11c, *Pseudochlorella*, *Nannochloris atomus*, *Scenedesmus sp.*, *Ankistrodesmus antarcticus*, *Synechococcus* 1479/5 and *Synechococcus sp.*

2.2.1 Culture Media

All cultures of micro-algae and cyanobacteria were grown in modified, sterile (121°C for 15 min) ASM medium containing the following ingredients (mg per litre distilled water) K₂HPO₄, 7.4 mg; FeCl₃, 3.2 mg; Na₂EDTA, 7.4 mg; MgCl₂, 19.0 mg; MgSO₄·7H₂O, 49.0 mg; CaCl₂·2H₂O, 85.0 mg; NaNO₃, 303.5 mg; NaMoO₄·2H₂O, 0.504 mg; CoCl₂·6H₂O, 0.08 mg; ZnSO₄·10H₂O, 0.088 mg; MnCl₂·4H₂O, 0.72 mg. The pH of the resulting solution was adjusted to 8.0 with sodium hydroxide (1M). All algae were

cultured in 250 cm⁻³ Erlenmeyer flasks, on an orbital shaker (100 r.p.m.), at a constant PFD (40 Watt cool white fluorescent tubes) 70 $\mu\text{mol s}^{-1} \text{m}^{-2}$ at 23°C.

Stock cultures of algae were maintained on slopes of ASM solidified with 2% w/v Agar No2.

2.2.2 Axenic Cultures

To obtain axenic cultures of *Chlorella vulgaris* 211/11c, *Scenedesmus sp.* and *Synechococcus* 1479/5, it was necessary to remove heterotrophic contaminating bacteria every few months from stock cultures. This was carried out by adding Penicillin G (1000 units ml⁻¹) and Streptomycin Sulphate (1mg ml⁻¹) to sterile ASM under aseptic conditions. Growth kinetics, photosynthesis response curves and cell physiology were examined against control flasks with no antibiotic additions.

2.2.3 Effect of Spectral Radiant Flux

The effects of spectral quality on the growth and photosynthesis of *Chlorella vulgaris* 211/11c, *Scenedesmus sp.* and *Synechococcus* 1479/5 were examined using small Erlenmeyer flasks (250 ml). Flasks of ASM were wrapped with a single layer of filter of known spectral quality (Blacklite, Edinburgh). The flasks were then inoculated with 1ml of cells previously cultured under 50 $\mu\text{mol s}^{-1} \text{m}^{-2}$ full spectrum light on an orbital shaker at 100 r.p.m. The maximum PFD received by the cells was 50 $\mu\text{mol s}^{-1} \text{m}^{-2}$. Flasks wrapped with blue filters required an extra fluorescent tube in order to obtain a PFD of 50 $\mu\text{mol s}^{-1} \text{m}^{-2}$. Cells were cultured for 10 days at 23°C. Growth was monitored via dry matter content every 24 hours. Upon reaching late exponential phase of growth 1ml of culture was removed and used to inoculate an identical flask covered with the same wavelength filter and incubated as above. This process was repeated 3 times in order to obtain cells that had photoadapted themselves to the particular wavelength, in which the culture had been grown. Samples were removed after 7 days exponential growth for analysis in an oxygen electrode system. All experiments were carried out in duplicate.

2.3 The Measurement of Photon Flux Density (PFD)

The PFD of all light was determined using a Skye Instruments (Llandrindod Wells, Wales) SKP215 PAR (400-700nm), cosine corrected, quantum sensor

2.4 Biochemical Analysis

2.4.1 Optical Density Determination

Optical densities were measured at 560nm on a Unicam SP1800 UV Spectrophotometer against a distilled water blank using 1 cm path length glass cuvettes.

2.4.2 Dry Weight Measurement

The dry weight content was determined in triplicate by filtering 10 ml of algal sample through predried, pre weighed Whatman GF/C (2.5 cm) filter pads. The filters were dried over night at 105°C and the dry matter content calculated by the difference.

2.4.3 Chlorophyll Analysis

Chlorophyll content was extracted at 5°C in the dark using a dimethyl sulphoxide / 90% acetone extraction (3:1 v/v). Chlorophyll content was determined spectrophotometrically using a Philips Pye Unicam SP8-500 UV/VIS Spectrophotometer and determined via the trichromatic equation of Jeffrey and Humphrey (1975).

2.4.4 Protein Determination

Protein was determined using the Coomassie Blue dye binding protein method of (Bradford, 1976). Bovine serum albumin (BSA) was used as the standard.

2.4.5 Carbohydrate Determination

Carbohydrates were determined using the anthrone reagent method of Herbert, (1971). Calibration curves were determined using glucose as the standard.

2.4.6 Nitrate Analysis

Nitrates were determined as nitrites following the reduction with spongy cadmium (APHA, 1985). Nitrate / nitrite test strips (BDH) were used to determine the necessary dilution series required for the measurement. Potassium nitrate was used as the standard.

2.4.7 Phosphorus Analysis

Total phosphorus was determined using the "stannous chloride / molybdate" (APHA, 1985). Samples were digested with sulphuric acid (2.5M), ammonium persulphate solution at 121°C, 15 p.s.i. for 60 minutes). The standard line was produced using potassium dihydrogen phosphate (ANALAR).

2.5 **Growth of Micro-Algae and Cyanobacteria in the Flat plate air lift reactor (FPALR) and Continually stirred tank reactor (CSTR).**

2.5.1 Growth rate calculation.

The cellular growth rates of the micro-algae and cyanobacteria were determined by plotting the natural log of the biomass against time (Eq 17). A least square regression was then performed on the straight line section of the plot (Pirt, 1975).

$$dx = \mu x . dt \quad (16)$$

$$\ln x = \ln x_0 + \mu t \quad (17)$$

Cellular doubling times were determined from equations 18 and 19 respectively

$$x = x_0 e^{\mu t} \quad (18)$$

$$t_d = \frac{\ln 2}{\mu} \quad (19)$$

dx = increase in biomass

dt = time interval

μ = growth rate

t_d = doubling time

2.5.2 Determination of Dilution rates.

The dilution rate (D) for cells cultured in the FPALR operating under continuous kinetics was determined from the growth rates of *Chlorella vulgaris* 211/11c and *Synechococcus* 1479/5 measured during experiments operating the FPALR under batch kinetics.

By setting the dilution rate below the growth rate, the problem of cell wash out was removed. The growth rate was determined to be that measured at a PFD of $100 \mu\text{mol s}^{-1} \text{m}^{-2}$, at a carbon dioxide concentration of 4% and at a temperature of 23°C . The dilution rate was then calculated from equation 20

$$D = \frac{F}{V} \quad (20)$$

D = Dilution rate equal to growth rate (day^{-1})

F = Flow rate (litres day^{-1})

V = Reactor volume (litres)

2.5.3 Growth of micro-algae and cyanobacteria under Batch kinetics

Micro-algae and cyanobacteria were cultured in the FPALR under a very accurately defined light field of known PFD and spectral quality (Ratchford and Fallowfield, 1992a). Using neutral density filters, accurate light fields were obtained across the flat plate for PFDs 100, 200 and 400 $\mu\text{mol s}^{-1} \text{m}^{-2}$ respectively. In each experiment the operating volume of the FPALR was 10 litres (unless otherwise stated), inoculated with 200 cm^{-3} of a 7 day old exponential growth phase starter culture. Carbon was supplied via a carbon dioxide cylinder run at 5 p.s.i. and mixed with 2000 cm^{-3} of air at 2% v/v CO_2 . The pH was controlled automatically and set to pH 6.9-7.2.

The CSTR experiments were carried out in a glass cylindrical chemostat with an operating volume of 20 litres. The light fields of 100 and 200 $\mu\text{mol s}^{-1} \text{m}^{-2}$ were obtained using neutral density filters. The CSTR was mixed by a large multi-blade paddle system. Mixing was further aided with the introduction of 4000 $\text{cm}^3 \text{min}^{-1}$ of air with 2% v/v CO_2 through a glass sparger placed at the base of the vessel. The pH was controlled automatically and set to pH 6.9-7.2. All experiments were monitored until late stationary phase was achieved. All experiments (unless otherwise stated) were carried out in duplicate.

2.5.4 Growth of micro-algae and cyanobacteria in the FPALR under different light sources.

The effects of two different light sources, Quartz Halogen lamps and High pressure sodium lights (QHL and HPSL) were used to determine the effect on the growth curves of *Chlorella vulgaris* 211/11c. The FPALR was operated at a Reynolds number of 5800, with 2% v/v carbon dioxide (2000 $\text{cm}^3 \text{min}^{-1}$ air), at a temperature of 23°C and a PFD of 100 $\mu\text{mol s}^{-1} \text{m}^{-2}$ provided by either a single 400W HPSL or 4 quartz-halogen lights.

2.5.5 Growth of micro-algae and cyanobacteria in the FPALR under different light intensities.

Experiments were conducted to examine the effect of light intensity on the batch kinetics of micro-algal and cyanobacterial cells. *Chlorella vulgaris* 211/11c, *Scenedesmus sp.* and *Synechococcus* 1479/5 were irradiated at 100 and 200 $\mu\text{mol s}^{-1} \text{m}^{-2}$ in the FPALR. Each experiment was operated at 23°C, Reynolds number 5800 (determined according to the method of Ratchford and Fallowfield, 1992a), 2000 $\text{cm}^3 \text{min}^{-1}$ air with 2% carbon dioxide v/v. Each experiment was carried out in duplicate unless otherwise stated.

2.5.6 Growth of micro-algae and cyanobacteria in the FPALR and CSTR under different concentrations of carbon dioxide .

The effects of carbon dioxide on the growth curves of *Chlorella vulgaris* 211/11c, *Scenedesmus sp.* and *Synechococcus* 1479/5 was investigated to determine the optimum CO_2 concentration for each organism. Carbon dioxide concentrations of 2-10% v/v (2000 $\text{cm}^3 \text{min}^{-1}$ air) were used accordingly. The FPALR was operated under batch kinetics at a temperature of 23°C, with a Reynolds number of 5800, at a PFD of 200 $\mu\text{mol s}^{-1} \text{m}^{-2}$. Light was provided by a single 400W HPSL. Unless otherwise stated all experiments were carried out in duplicate. For comparison purposes a CSTR was operated under the same conditions as the FPALR.

2.5.7 Growth of micro-algae and cyanobacteria in the FPALR and CSTR under different temperatures.

The optimum growth temperatures of *Chlorella vulgaris* 211/11c, *Scenedesmus sp.* and *Synechococcus* 1479/5 were examined in both the FPALR and CSTR. The temperature examined were 23, 30 and 35°C. The FPALR was operated at a Reynolds number of 5800, PFD 200 $\mu\text{mol s}^{-1} \text{m}^{-2}$ and 4% carbon dioxide v/v (air input 2000 $\text{cm}^3 \text{min}^{-1}$). A single 400W HPSL was used to provide light. The CSTR was operated under the same conditions as the FPALR for comparison purposes.

2.6 Micro-algae and Cyanobacteria grown in the FPALR under continuous kinetics.

The effects of stepped increase in PFD was examined on the growth kinetics of *Chlorella vulgaris* 211/11c and *Synechococcus* 1479/5. Experiments were performed at a Reynolds number of 5800, with 4% carbon dioxide v/v (air 2000cm³ min⁻¹) at a temperature of 23 °C. A single 600W HPSL was used to irradiate the FPALR at the desired PFD. Prior to inoculation all continuous feed tubes were sterilised via autoclaving at 121°C, 15 p.s.i. for 15 minutes. The photobioreactor was chemically cleaned as previously described.

2.6.1 Light / Dark Cycling.

Accurate light fields of known PFD were constructed at 100, 200, 400 and 800µmol s⁻¹ m⁻² respectively. After inoculation each organism was allowed to grow under batch kinetics for 5 days prior to switching to continuous culture. Dilution rates were determined from the results of the batch kinetics experiments. These were set below the growth rate required to prevent wash out. The FPALR was fed with 100% ASM from two feed tanks (20 and 8 litres respectively). To prevent the growth of algae within the delivery and removal tubes, all tubes were wrapped in aluminium foil. Samples were removed aseptically every 24 hours from the continuous output line.

2.7 Growth of micro-algae and cyanobacteria in the FPALR in gradients of light.

2.7.1 Light Gradients

In order to simulate the effect of light attenuation found in natural lake and high rate algal pond systems, a series of experiments were carried out in the FPALR using gradients of light constructed out of neutral density filters. By varying the thickness of the filter, the

gradients shown in Figures 14, 15a and 15b were produced. The PFDs at the relative depths were calculated using equation (21 pers. comm Martin).

$$S_{id} = S_i \times 0.79 \times e^{\frac{(-d \times (0.63 \times O.D_{560} + 0.0301))}{2.303}} \quad (21)$$

S_{id}	Irradiance PFD ($\mu\text{mol s}^{-1} \text{m}^{-2}$) at depth (d)
S_i	Surface irradiance PFD ($\mu\text{mol s}^{-1} \text{m}^{-2}$)
d	Depth of water system (cm)
OD	Optical density (560nm) of operating system (1.0 for this study)

The top channel of the photostage of the FPALR was irradiated at or below the set PFD of the 200 (Figure 14), 400 (Figure 15a) and $800 \mu\text{mol s}^{-1} \text{m}^{-2}$ (Figure 15b) gradient. The gas riser column of the FPALR was covered with aluminium foil. To simulate the effects of attenuation found in natural lake and ponds systems, cells of *Chlorella vulgaris* 211/11c and *Synechococcus* 1479/5 were cultured in the FPALR through a light gradient. Based an optical density of 1.0 PFDs were calculated with increasing depth and neutral density filters were used to produce this gradient. The FPALR was operated at a Reynolds number of 5800, with a temperature of 23°C and a 4% v/v carbon dioxide (air $2000 \text{cm}^3 \text{min}^{-1}$). A single 600W HPSL was used to irradiate the photostage. The effects of these conditions on algal cell physiology and productivity was monitored. Samples were also examined to determine physical parameters of main object cell length, breadth, perimeter and area. These were measured from cells chosen at random using a macro program written with the Bioscan Optimas software.

2.8 Oxygen Electrode Analysis

2.8.1 Measurement of Photosynthesis / irradiance response curves.

Using the method of Ratchford and Fallowfield (1992a), similar to that of Dubinsky *et al* (1987) photosynthesis response curves were determined for *Chlorella vulgaris* 211/11c,

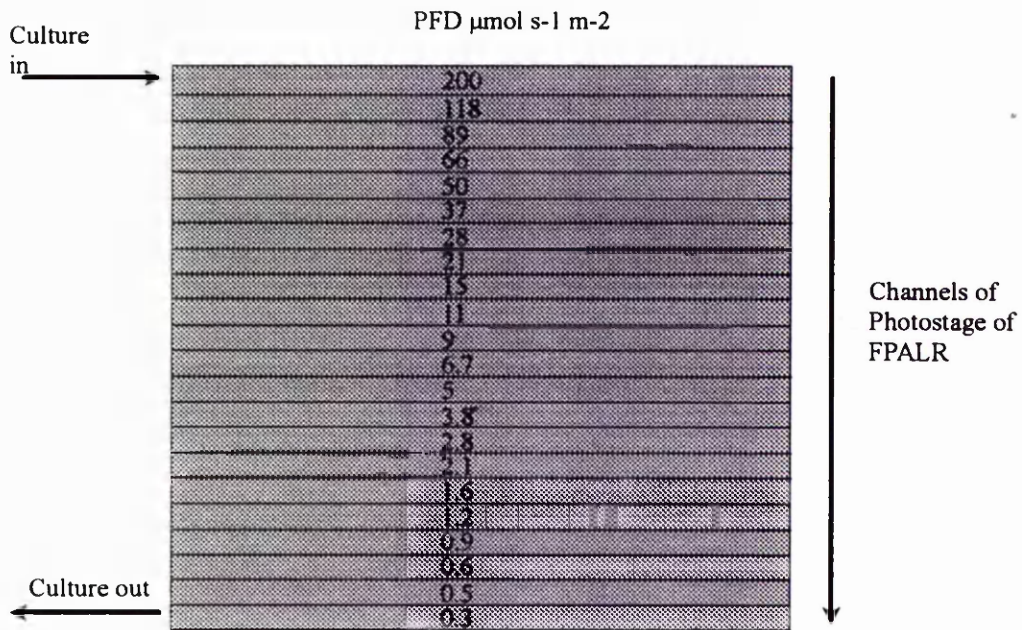


Figure 14. A light gradient calculated for $200\mu\text{mol s}^{-1}\text{m}^{-2}$.

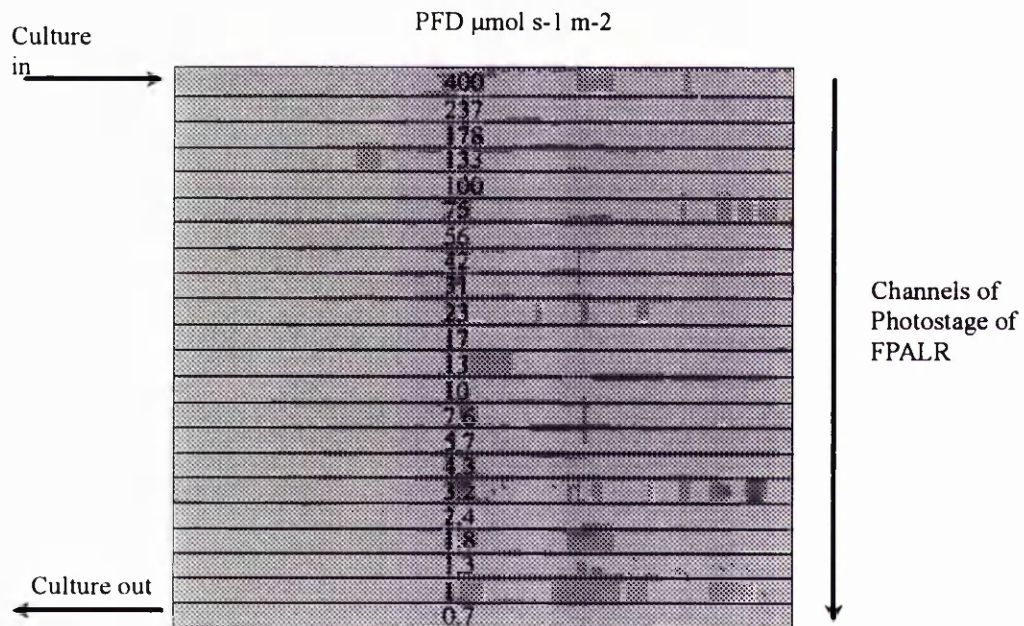


Figure 15a. A light gradient calculated for $400\mu\text{mol s}^{-1}\text{m}^{-2}$

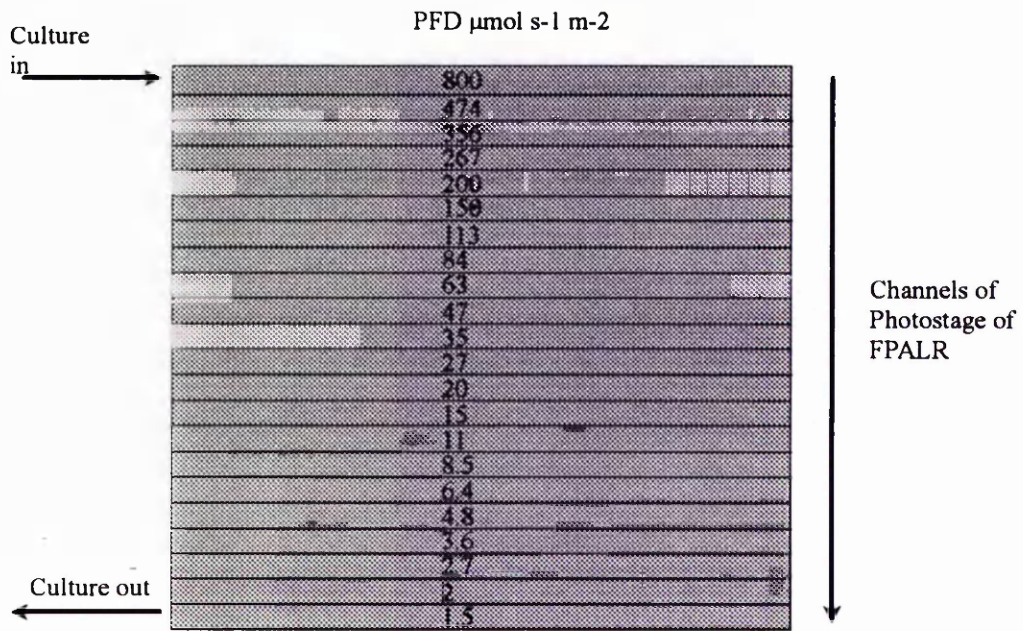


Figure 15b. A light gradient calculated for $800\mu\text{mol s}^{-1}\text{m}^{-2}$.

Nannochloris atomus, *Ankistrodesmus antarcticus*, *Scenedesmus sp.*, *Synechococcus* 1479/5 and *Synechococcus sp.*

Figure 16 displays the oxygen electrode chamber used for the measurement of photosynthetic / irradiance response curves.

An oxygen electrode chamber was constructed out of P.V.C. to form a small cylindrical cross section. This chamber was internally partitioned via a glass disc on one side creating a second chamber in which circulating water was pumped through from a water bath. Temperature was maintained at a constant $\pm 0.1^{\circ}\text{C}$ within the sample chamber. A small hole at right angles to the sample chamber allowed the insertion of an oxygen electrode (Clark polarographic, YSI Instrumentation, Yellow Springs Ohio). A small magnetic flea was used within the chamber to ensure the system was mixed. The electrode was calibrated at 0% using a solution of sodium sulphite (cobalt chloride catalysed) and at 100% using a saturated solution of distilled water. The electrode was zeroed at several gain settings increasing in amplification (gain 5-8). The electrode was only used when all the rates obtained at different gain settings were identical.

Samples of micro-algae and cyanobacteria were diluted with the appropriate medium to an optical density (560nm) of approximately 0.15. The diluted sample was then placed in the chamber. Prior to the measurement of all photosynthesis / response curves each sample was placed in the dark to obtain a steady dark respiration rate and to allow the culture to temperature equilibrate. After a constant respiration rate was obtained the sample was exposed to a light source at a PFD of $4\mu\text{mol s}^{-1} \text{m}^{-2}$ (quartz-iodide projector 150W) for 6 minutes. The rates of photosynthesis were then measured for 6 minutes at the following PFDs; 8, 12, 16, 20, 30, 50, 100, 200, 300, 500, 750, 1000, 1500, 2000 $\mu\text{mol s}^{-1} \text{m}^{-2}$. Unless otherwise stated all photosynthesis / irradiance response curves were determined at 23 C.

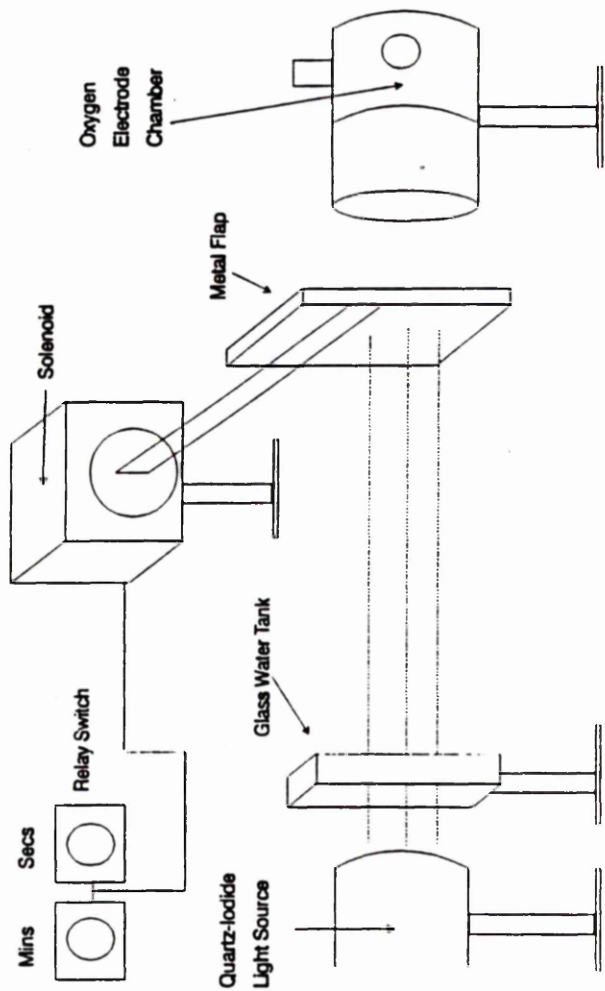


Figure 16. A solenoid relay switch connected to a timer mechanism allowing the simulation of light / dark cycles (seconds to minutes).

2.8.2 Interpretation of photosynthesis / irradiance data.

Photosynthetic parameters of P_{\max} , I_k , α , β and I_B were measured and calculated directly from the raw analogue data. This procedure was used throughout to ensure no biased interpretations resulted from the photosynthesis / irradiance curves analysis.

2.8.3 Nutrients / Buffers

The following micro-algae and cyanobacteria were used to study the effects of nutrients and buffers on photosynthesis response curves; *Chlorella vulgaris* 211/11c, *Nannochloris atomus*, *Scenedesmus sp.*, *Ankistrodesmus antarcticus*, *Synechococcus sp.* and *Synechococcus* 1479/5. Seven day old samples were taken during exponential growth and were centrifuged down at 2500g before being re suspended in the test media. The following treatments were used in the experiments; ASM including trace elements, ASM - trace elements, Phosphate buffer (pH 7.0), ASM including nitrate, ASM - Nitrate and ASM + Na HCO₃ (200mM).

2.8.4 Centrifugation

Prior to photosynthesis / irradiance response curve measurement, samples of micro-algae and cyanobacteria were centrifuged in a Sorvall RT6000 Refrigerated Centrifuge, Du Pont, Stevenage, at 2500g for 15 minutes at a temperature of 23°C. The cells were then resuspended in ASM medium and diluted with ASM to an optical density (560nm) of 0.15 prior to oxygen exchange measurements.

2.8.5 Light / Dark Cycling

A novel solenoid connected to a relay timer was constructed to form controllable switch. This device was used in front of the projector to interrupt the light beam and place an oxygen electrode culture sample immediately in the dark (Figure 16). The metal flap on Figure 16 acted as a shutter mechanism and was controlled by the timer which allowed

the controlled exposure of cells to light / dark cycles at light of known photoinhibitive PFD.

The effects of light / dark cycling on oxygen evolution / consumption and LEDR of *Chlorella vulgaris* 211/11c and *Synechococcus* 1479/5 was examined. By varying the times from seconds to minutes it was possible to examine the effects of long term light / dark cycles of medium frequency.

To ensure carbon limitation did not occur in the oxygen chamber a fine hypodermic needle placed through a small hole in the sample chamber and fresh sterile ASM was injected every 8 hours containing 1mM to 50mM sodium bicarbonate to ensure nutrient limitation did not occur over the length of the study (2-24 hours).

2.8.6 Temperature

In order to determine the optimum growth temperature for cells of micro-algae and cyanobacteria in the FPALR and CSTR and to determine the effects of temperature variation on photosynthesis and respiration rates, experiments were conducted in which cells of micro-algae and cyanobacteria were cultured at 4 different temperatures through a 10 day growth cycle. A 30 litre water filled incubator was used to create a constant temperature environment, maintained at $\pm 0.5^{\circ}\text{C}$ using a small Nova Solid State Electronic Thermostat (non submersible) regulator which was run against a Churchill chiller unit.

Chlorella vulgaris 211/11c, *Synechococcus* 1479/5, *Scenedesmus sp.*, *Ankistrodesmus antarcticus*, *Synechococcus sp.* and *Nannochloris atomus* were used in the study.

The growth temperatures of the organisms were 15, 23, 30 and 40°C . In the first set of experiments illumination was provided by 4 cool 40W fluorescent tubes at a PFD of $80 \text{ mol s}^{-1} \text{ m}^{-2}$ at the flask surface. Growth was monitored by optical density (560nm). When the cells were in their 7th day of growth, samples were removed for photosynthesis / irradiance measurement at each of the 4 temperatures. All measurements were performed within 24 hours to ensure the cells were in an exponential phase of growth and

at similar physiological state during the growth cycle. Temperature incubations and oxygen electrode experiments were carried out in duplicate.

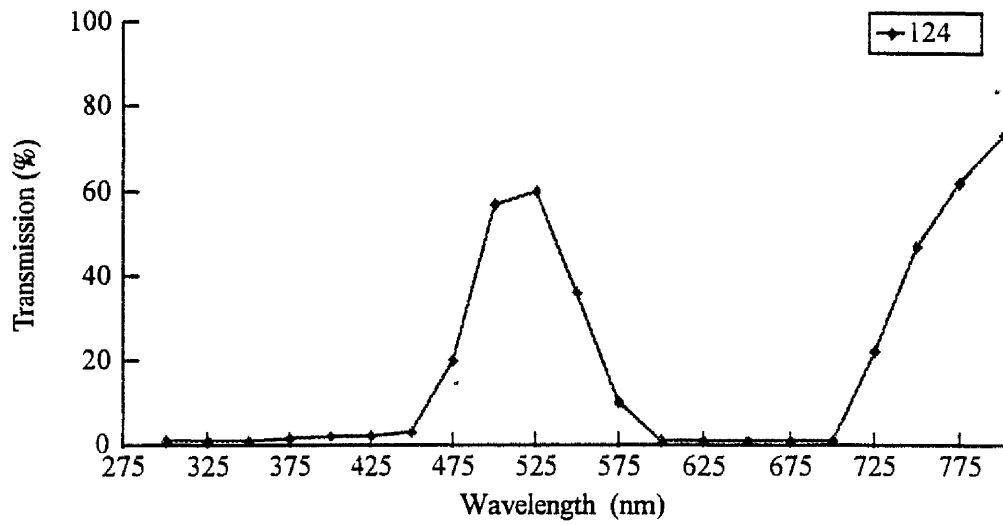
In the second set of temperature studies, the method used was identical to the above except that the flasks were illuminated by 2, 500W quartz halogen lights at the same PFD of $80 \text{ mol s}^{-1} \text{ m}^{-2}$.

In the final set of temperature experiments, flasks containing *Chlorella vulgaris* 211/11c and *Synechococcus* 1479/5 were cultured under the same conditions as the experiment described above except that the PFD was increased to $200 \text{ mol s}^{-1} \text{ m}^{-2}$. Due to problems of overheating the experiments involving 15°C culturing were not performed since the refrigeration unit was unable to lower the culture temperature down to this value.

2.8.7 Spectral Radiant Flux

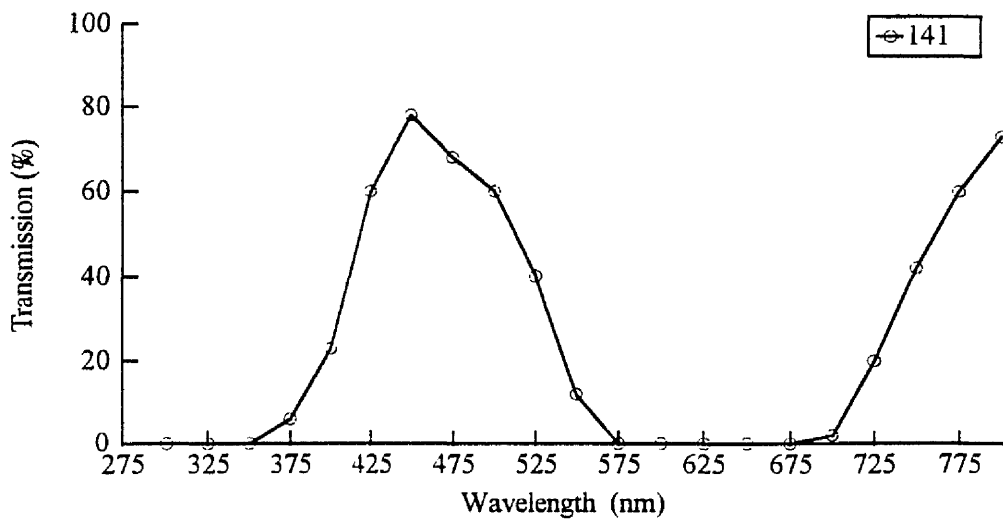
Chlorella vulgaris 211/11c, *Synechococcus* 1479/5, and *Scenedesmus sp.* were used to examine the effect of spectral radiant flux on photosynthesis / irradiance curves of photoadapted cultures. Using cells of *Chlorella vulgaris* 211/11c, *Synechococcus* 1479/5 and *Scenedesmus sp.* grown in red (Figure 19), photosynthesis / irradiance response curves were measured using blue (Figure 18), red (Figure 19), and full spectrum light (300-800nm).

Photosynthesis / irradiance curves were also determined using the following micro-algae and cyanobacteria cultured for 7 days under full spectrum light; *Chlorella vulgaris* 211/11c, *Synechococcus* 1479/5, *Scenedesmus sp.*, *Synechococcus sp.*, *Ankistrodesmus antarcticus* and *Pseudochlorella*. The wavelengths employed included the following green (Figure 17), blue (Figure 18), red (Figure 19), orange (Figure 20), chrome orange (Figure 21) and yellow (Figure 22). Respiration rates and light enhanced dark respiration (LEDR) values were also determined for *Chlorella vulgaris* 211/11c, *Synechococcus* 1479/5, *Scenedesmus sp.* The respiration rate of cells was determined to be the oxygen consumption of cells incubated in the dark prior to photosynthesis / irradiance measurement. The LEDR rate was the increased oxygen consumption determined after a photosynthesis / irradiance curve had been measured.



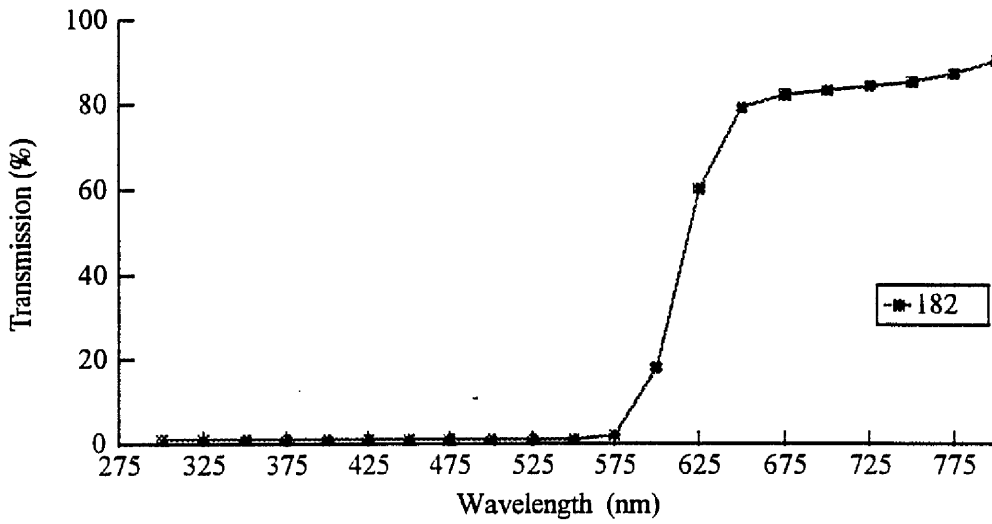
Y=31.01%

Figure 17. Spectral characteristics of the green filter.



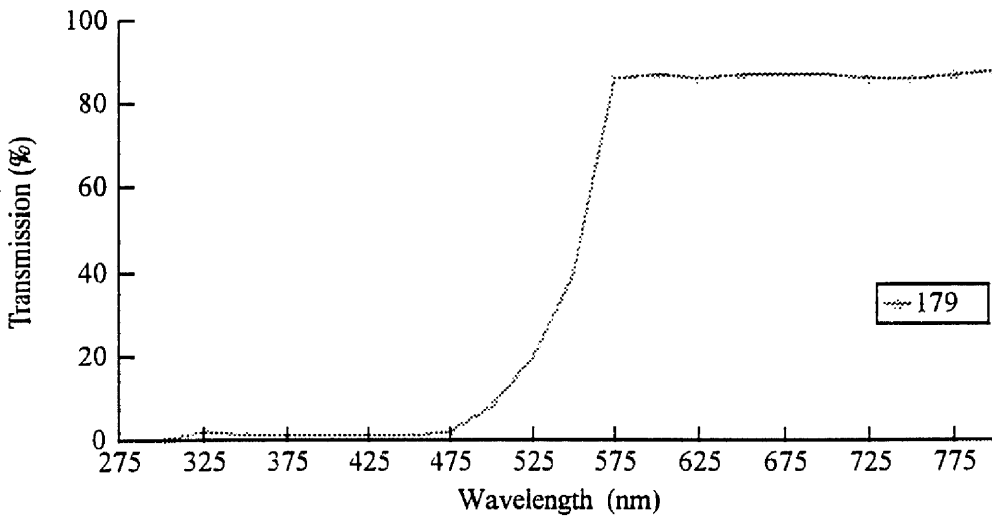
Y=17.88%

Figure 18. Spectral characteristics of the blue filter



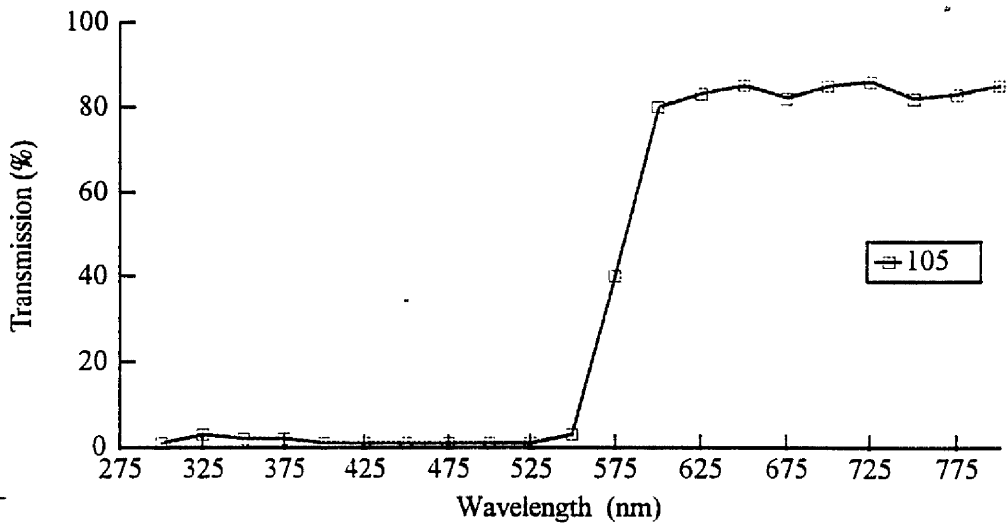
Y=11.04%

Figure 19. Spectral characteristics of the red filter.



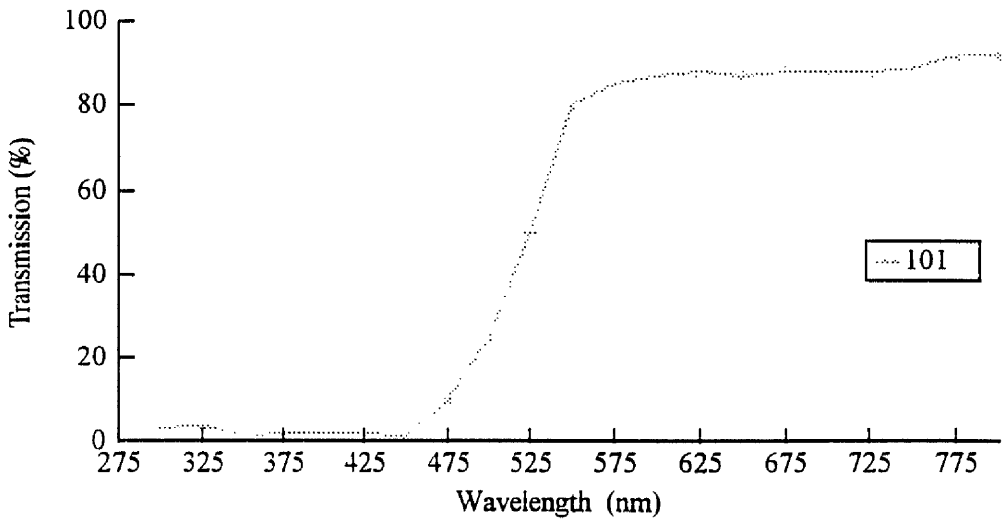
Y=53.97%

Figure 20. Spectral characteristics of the chrome orange filter.



Y=41.28%

Figure 21. Spectral characteristics of the orange filter.



Y=80.00%

Figure 22. Spectral characteristics of the yellow filter.

2.9 Light Enhanced Dark Respiration (LEDR)

Using samples of *Chlorella vulgaris* 211/11c and *Scenedesmus sp.*, the effects of light on dark respiration was investigated using the oxygen electrode system.

Cells having undergone a full photosynthesis / irradiance response curve measurement were placed in the dark immediately after the final 6 minute illumination at $2000 \text{ mol s}^{-1} \text{ m}^{-2}$. Dark respiration was measured until the rate of oxygen consumption returned to the original respiration rate measured at the start of the experiment. Cells of *Chlorella vulgaris* 211/11c, *Scenedesmus sp.* and *Synechococcus* 1479/5, were used in a second set of experiments in which a sample was placed in the oxygen electrode chamber and its dark respiration rate measured. The sample was then irradiated with light at $4 \mu\text{mol s}^{-1} \text{ m}^{-2}$ for 6 minutes before having its dark respiration re-measured. That sample was then replaced by a fresh sample and the dark respiration rate was measured. This time the sample was irradiated at 4 and then $8 \mu\text{mol s}^{-1} \text{ m}^{-2}$ before having its dark respiration rate measured. After having been irradiated for 6 minutes to a PFD of $8 \mu\text{mol s}^{-1} \text{ m}^{-2}$ the LEDR was again measured. This process was repeated to until a full photosynthesis / irradiance response curve had been determine.

2.9.1 Inhibitors of Photosynthesis and Respiration

Salicylhydroxamic acid (SHAM) (1-100 μmol), 3-(3,4-DichloroPhenyl)-1,1- Dimethylurea (DCMU) (5-100 μmol) and Potassium cyanide (KCN) (1-100 μmol), were used to examine the effect of their addition on the respiration and LEDR of *Chlorella vulgaris* 211/11c and *Synechococcus* 1479/5. Cells were incubated with the test compound using two methods. Firstly, the cells were incubated in the presence of the test substance for 30 mins prior to photosynthesis response measurement. Secondly, the cells were placed in the oxygen electrode chamber and the test substance was injected into the chamber via a hypodermic needle at the same concentration as the incubation experiment.

2.10 Microscopic examination.

2.10.1 Image Analysis.

Experimental samples of *Chlorella vulgaris* 211/11c were examined using an Olympus Vanox Microscope with Nomarsky optics to determine the cells physical characteristics. Cell main objective length, breadth, perimeter and area were measured using an image analysis system. Using a Panasonic wvCL700 colour video camera, a microscopic image of the cells was captured via a frame grabbing processor board (Imaging Technology Incorporated, MA, USA). The frame grabbing board was controlled via image analysis software obtained from Bioscan Optimas v3.01 (Bioscan Inc. Edmonds, Washington, USA). The captured image was then sent to a Barco monitor (Barco Video and Communications Kortrijk, Belgium). The entire system was controlled from an Elonex 386DX, 25MHz, 4Mb RAM computer using Microsoft Disk Operating System v5 and Microsoft Windows v3.1. Macro-programs to repeat user actions were written accordingly.

3.0 RESULTS AND DISCUSSIONS

3.1 Design and construction of a flat plate air lift photobioreactor.

The flat plate air lift reactor was hydraulically characterised and its performance discussed against that of a conventional chemostat in the paper of Ratchford and Fallowfield (1992a). A copy of this paper is attached at the back of this thesis.

3.2 Growth of Micro-algae and Cyanobacteria in a FPALR operating under batch kinetics.

The FPALR had been designed and constructed to facilitate the study of growing photosynthetic cells in an accurately defined light field of known photon flux density and spectral quality. In an attempt to examine the growth kinetics of micro-algae and cyanobacteria, cells were cultured in the FPALR operating under batch kinetics. As cellular photosynthesis and productivity are governed primarily by light, cells were cultured in 2 different field of known PFD. Neutral density filters were employed to ensure an even distribution of photosynthetically active radiation across the surface of the flat plate.

The FPALR design housed a gas injector system constructed to provide efficient mixing of carbon dioxide. To determine both the optimum concentration for growth and the possible toxic concentration of carbon dioxide, cells of micro-algae and cyanobacteria were culture in the FPALR operating under batch kinetics.

Temperature is known to play an active role in the photosynthesis of both micro-algae and cyanobacteria. The combined effect of temperature and the high shear forces that were known to exist in the FPALR, required examination.

Although the constant cylindrical cross sectional area to volume ratio makes the CSTR available for comparison with the FPALR, the batch processing of the FPALR was slightly different to the CSTR since it operated with a light / dark cycle. The experiments examining the effect of photon flux density, carbon dioxide concentration

and temperature on the growth kinetics of cells of *Chlorella vulgaris* 211/11c, *Scenedesmus sp.* and *Synechococcus* 1479/5 in the FPALR, contained a light / dark cycle of 58:23 seconds respectively.

3.2.1 The effect of Quartz-Halogen Lamps / High Pressure Sodium Lights on micro-algal and cyanobacterial growth in the FPALR.

In an attempt to determine the optimum light source for growing micro-algae and cyanobacterial cells in the FPALR, two different kinds of light source were investigated. Figure 23 shows the results of culturing cells of *Chlorella vulgaris* in the FPALR irradiated by 4 x 500W Quartz-Halogen lights (QHL) or 1 x 400W High Pressure Sodium Lamp (HPSL). From Figure 23 it can be seen that cells grew slightly better when irradiated with light from the HPSL. Cells of *Chlorella vulgaris* 211/11c, irradiated with HPSL achieved a higher growth rate of 1.17 day^{-1} compared to 1.06 day^{-1} with cells irradiated with QHL (Figure 24). At these respective growth rates the cells had mean doubling times of 1.19 days and 1.14 days. Cultured cells irradiated with the HPSL were also found to reach a higher stationary phase biomass level of 1.71 g l^{-1} compared to 1.62 g l^{-1} for cells irradiated with QHL.

Figure 25 shows the variation in chlorophyll a and b content of *Chlorella vulgaris* 211/11c cells when cultured in the FPALR, irradiated by QHL and HPSL. It can be seen that the maximum chlorophyll a content of $24.55 \mu\text{g ml}^{-1}$ was achieved at late stationary phase of 240 hours when the cells were irradiated by QHL compared to $16.78 \mu\text{g ml}^{-1}$ when irradiated by HPSL. The cells irradiated by QHL also had a higher chlorophyll b content when irradiated with QHL compared to HPSL (Figure 26).

Figure 27 shows the increase in dry weight with increasing time for cells of *Scenedesmus sp.* when cultured in the FPALR using QHL and HPSL respectively. Unlike the observations made with *Chlorella vulgaris* 211/11c, *Scenedesmus sp.* cells did not show any difference in stationary phase biomass levels when irradiated with QHL or HPSL. Both the growth rates and the stationary phase biomass levels were similar regardless of the light source. Chlorophyll a and b levels (Figures 28 and 29), however, did show significant differences in cells cultured with QHL and HPSL. In

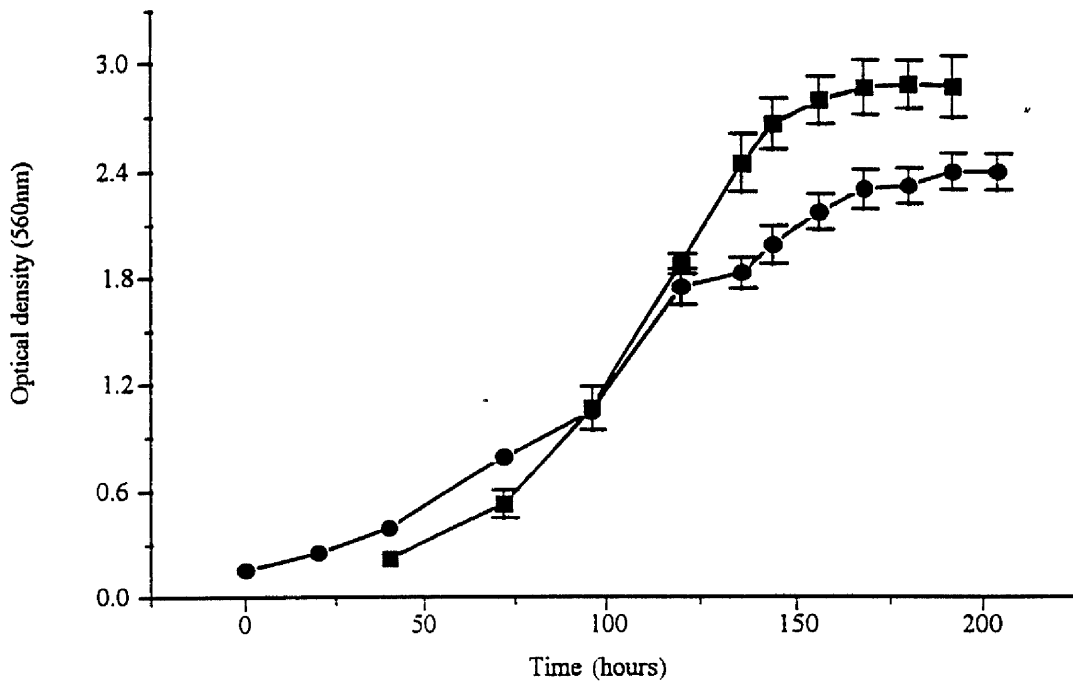


Figure 23. Change in optical density (560nm) of *Chlorella vulgaris* 211/11c, ■—■ irradiated with Quartz-halogen lights, ●—● irradiated with a High pressure sodium lamp.

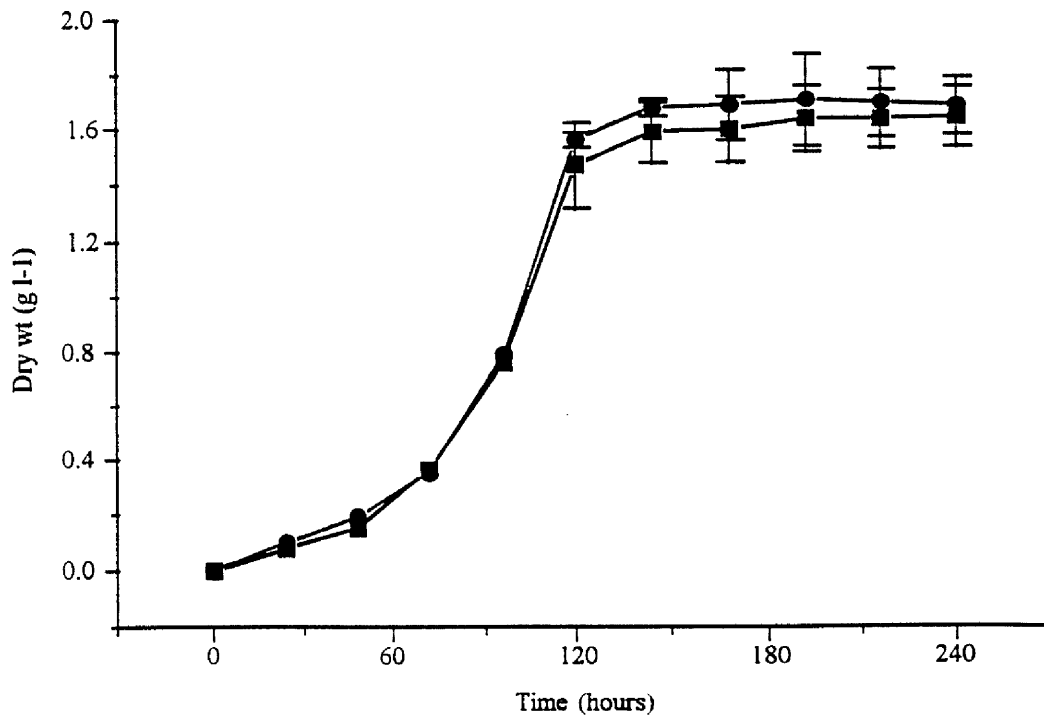


Figure 24. Change in dry weight (g l^{-1}) of *Chlorella vulgaris* 211/11c, ■—■ irradiated with Quartz-halogen lights, ●—● irradiated with a High pressure sodium lamp.

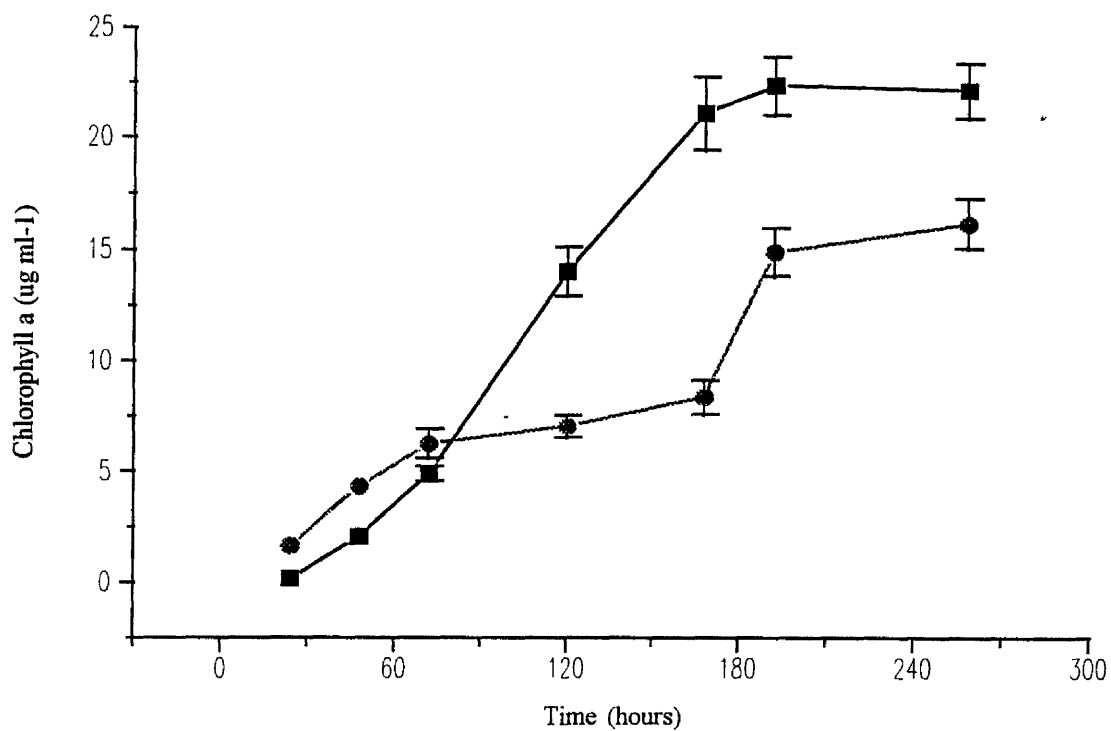


Figure 25. Change in chlorophyll a content of *Chlorella vulgaris* 211/11c, ■—■ irradiated with Quartz-halogen light, ●—● irradiated with a High pressure sodium lamp.

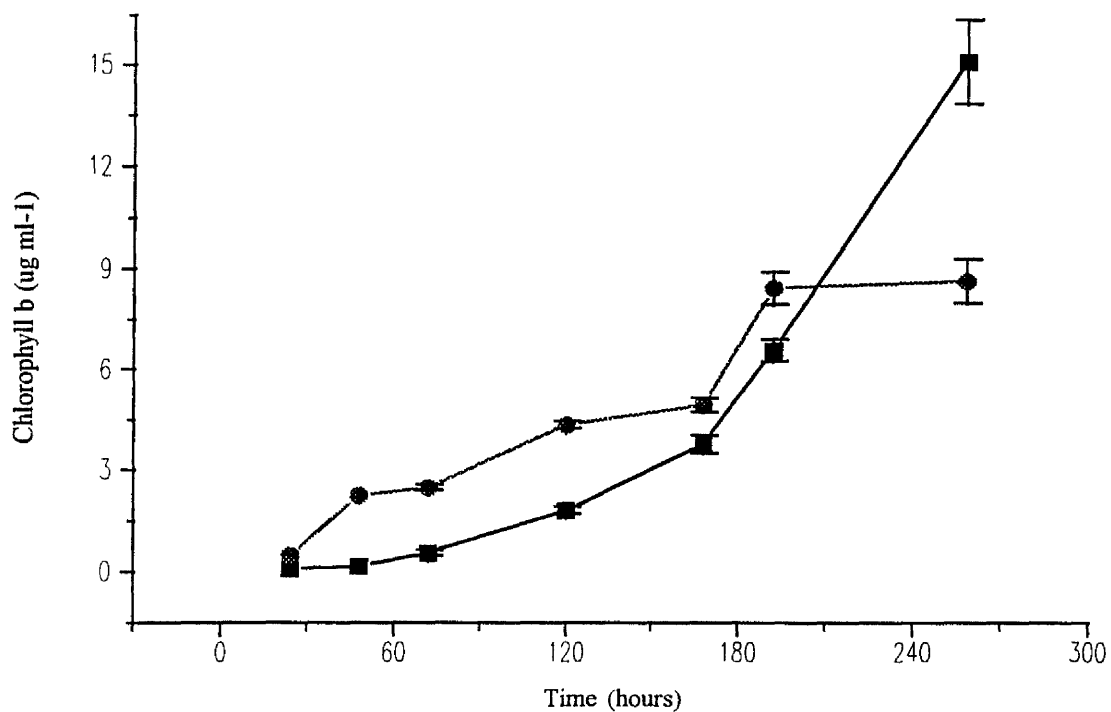


Figure 26. Change in chlorophyll b content of *Chlorella vulgaris* 211/11c, ■—■ irradiated with Quartz-halogen lights, ●—● irradiated with a High pressure sodium lamp.

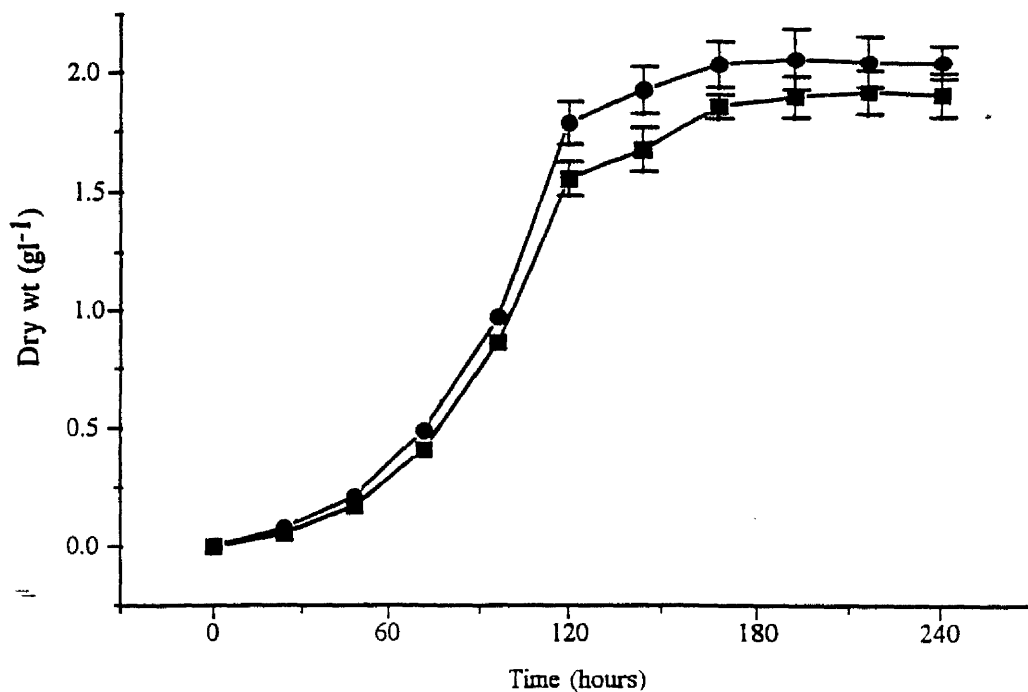


Figure 27. Change in dry weight (gl⁻¹) of *Scenedesmus sp.* 211/11c, ■—■ irradiated with Quartz-halogen lights, ●—● irradiated with a High pressure sodium lamp.

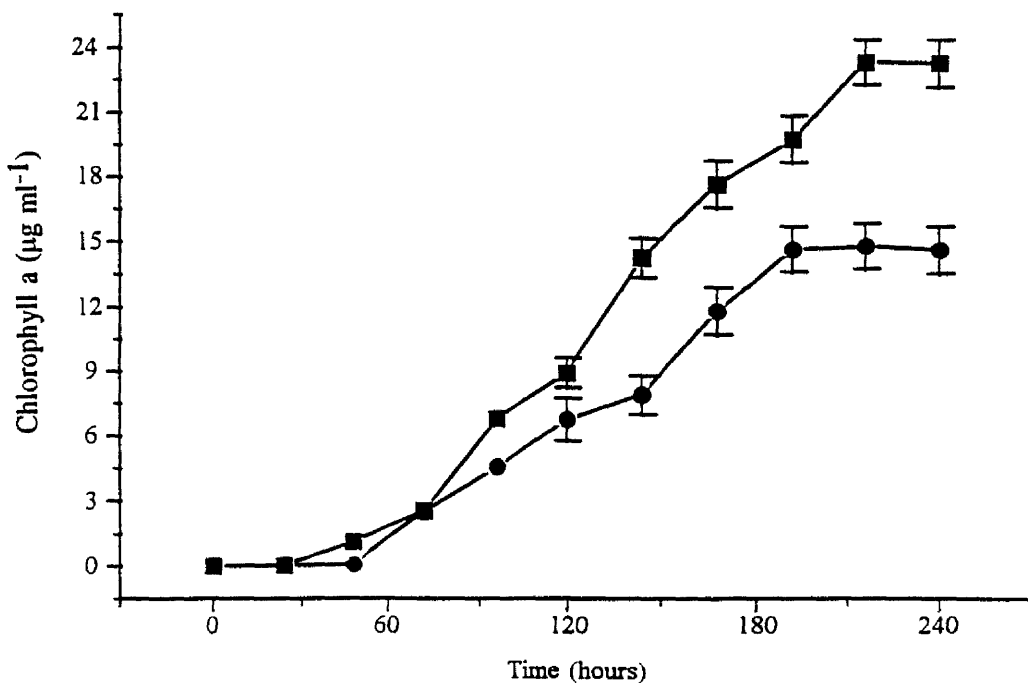


Figure 28. Change in chlorophyll a content of *Scenedesmus sp.* 211/11c, ■—■ irradiated with Quartz-halogen light, ●—● irradiated with a High pressure sodium lamp.

each case cells irradiated with QHL had a higher chlorophyll content than similar cells irradiated with HPSL.

Synechococcus 1479/5 did not show a similar pattern to that of either *Chlorella vulgaris* 211/11c or *Scenedesmus* sp. The growth of cells of *Synechococcus* 1479/5 (Figure 30) was higher when irradiated with QHL as opposed to cells irradiated with HPSL. Figure 31 and 32 show the changes in the chlorophyll a and b content of *Synechococcus* 1479/5 respectively. It was observed that the chlorophyll a and b content of cells irradiated with HPSL was higher in the early to mid exponential phase of growth compared to cells irradiated with QHL. In each case, however, towards the late exponential growth phase the chlorophyll a and b content of *Synechococcus* 1479/5 increased in cells irradiated with QHL compared to cells irradiated with HPSL.

Cells cultured in the FPALR irradiated by QHL produced a lower stationary phase biomass level than similar cells irradiated by HPSL. However cells irradiated with QHL were found to produce twice as much chlorophyll a and 3 times as much chlorophyll b as the cells irradiated with HPSL. Although the growth of cells irradiated with HPSL has reached stationary phase after 160 hours, cells irradiated with QHL were found to continue to approximately 200-240 hours. Figure 33 shows the relative spectral energy of HPSL of respective wavelength. It can be seen that HPSLs have strong energy emissions in the 400-450nm, 525nm and 600nm wavelength bands (Geider and Osborne, 1992). The maximum absorption peaks of chlorophyll a and b are known to lie in the 400-475nm and 625-675nm regions (Kirk, 1983). It is known that QHLs suffer from a major drawback in their respective energy distribution output. This is caused by a low output in the blue region of the spectrum (375-500nm) (Geider and Osborne 1992). Since 2 of the 4 major absorption peaks of chlorophyll a and b lie in the blue region of the spectrum, it is suggested that this was the underlying reason behind the slightly lower growth rates, reduced maximum stationary phase biomass levels and the low cell doubling times obtained when cells of *Chlorella vulgaris* 211/11c were irradiated in the FPALR using QHL compared to HPSL. It is unclear why the chlorophyll a and b content of *Chlorella vulgaris* 211/11c and *Scenedesmus* sp. were higher when irradiated with QHL compared to HPSL. It may be that since the blue wavelengths of light (350-500nm) emitted by the QHL were very low or absent, the cells responded by increasing the chlorophyll content of a and b in order to compensate by intercepting more light in the red end of the

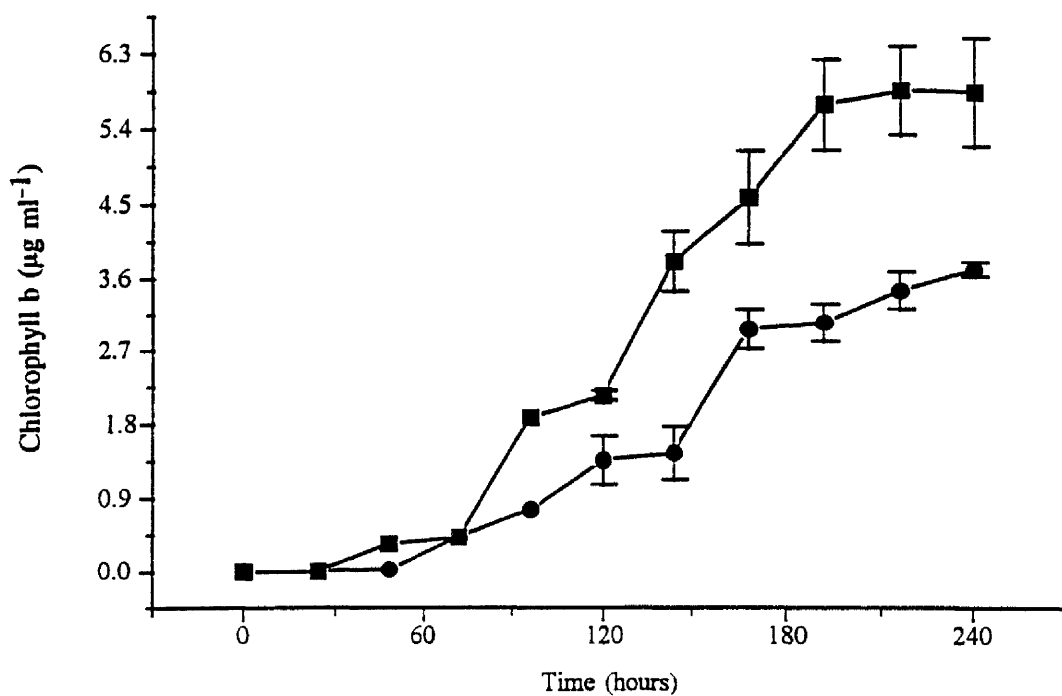


Figure 29. Change in chlorophyll b content of *Scenedesmus sp.* 211/11c, ■—■ irradiated with Quartz-halogen lights, ●—● irradiated with a High pressure sodium lamp.

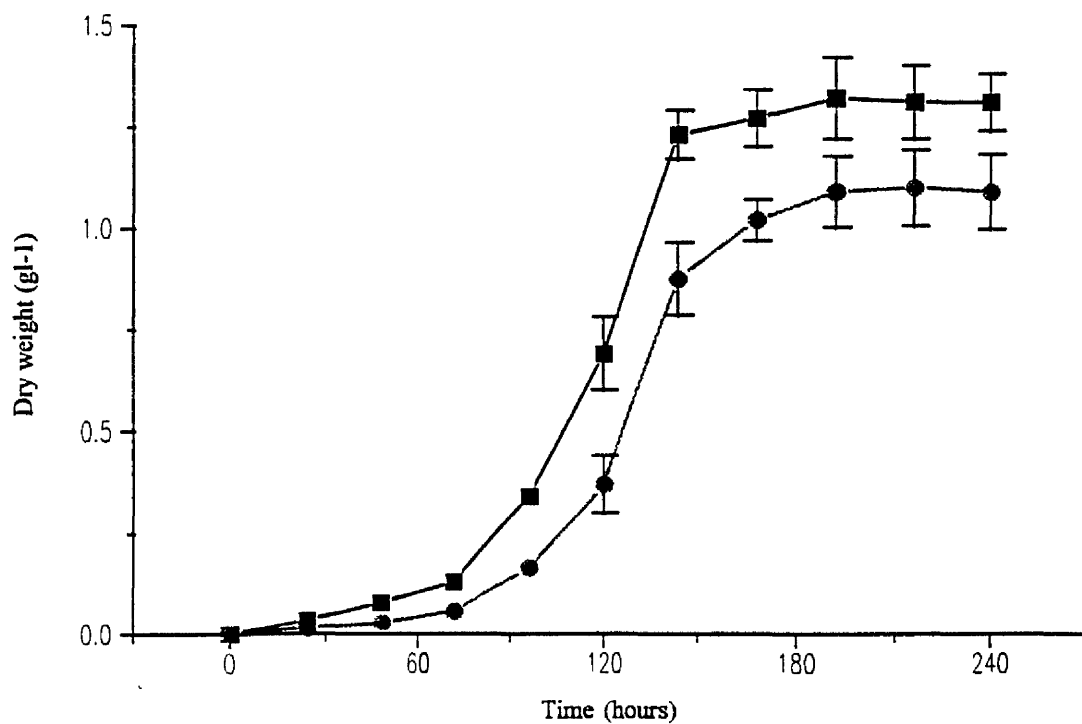


Figure 30. Change in dry weight (g l⁻¹) of *Synechococcus* 1479/5, ■—■ irradiated with Quartz-halogen lights, ●—● irradiated with a High pressure sodium lamp.

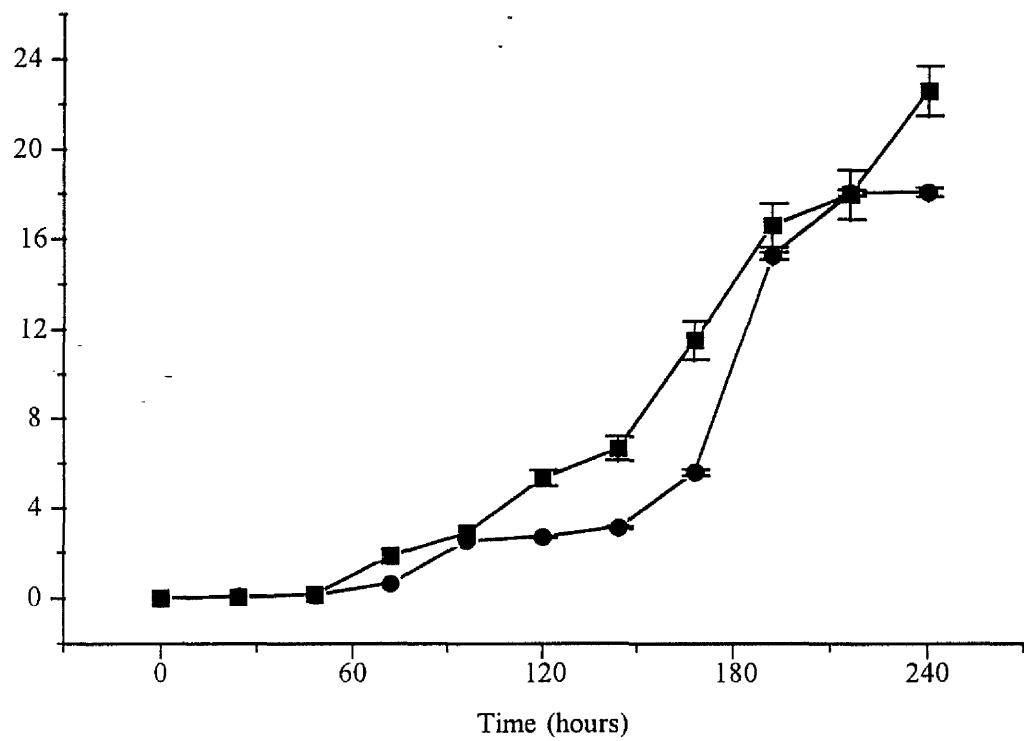


Figure 31. Change in chlorophyll a content of *Synechococcus* 1479/5, ■—■ irradiated with Quartz-halogen light, ●—● irradiated with a High pressure sodium lamp.

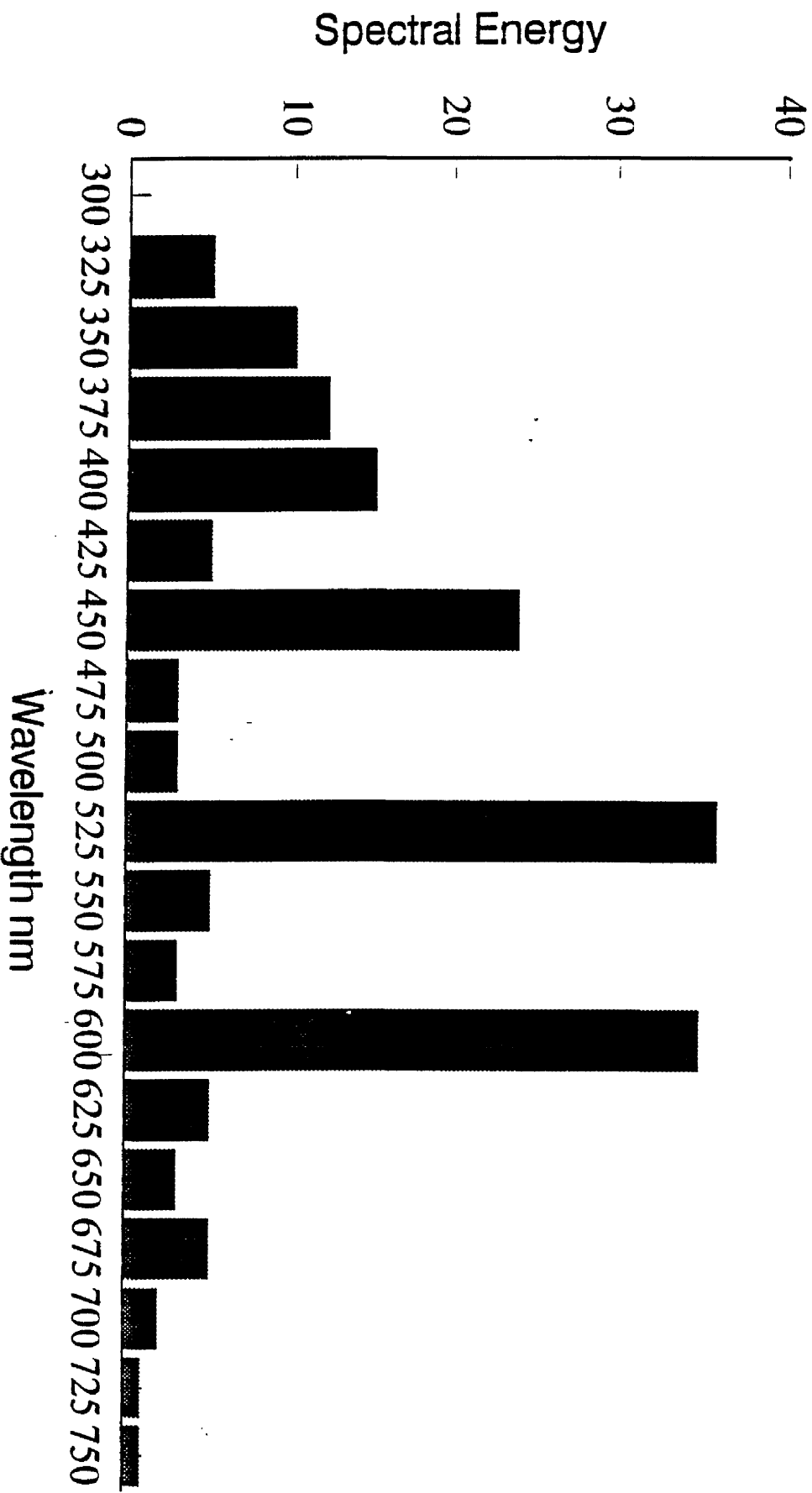


Figure 33. The output spectral energy of a High Pressure Sodium Lamp

spectrum. *Synechococcus* 1479/5, however, does not contain light intercepting pigments at the blue end of the spectrum apart from chlorophyll a. It does, however, contain other minor absorbing pigments as well as chlorophyll a in the red region and far red region of the spectrum which may be the reason why the cells grew better when irradiated with QHL compared to HPSL. A discussion on the effect of spectral radiant flux on the changes in metabolite production and cellular physiology of microalgae and cyanobacteria is presented in Section 3.9.

In conclusion cells of *Chlorella vulgaris* 211/11c, *Scenedesmus sp.* and *Synechococcus* 1479/5 all displayed different growth rates and stationary phase biomass levels when cultured in the FPALR irradiated with HPSLs compared to QHLs. *Chlorella vulgaris* 211/11c grew slightly better (not significant) when irradiated with a HPSL compared to the QHL whereas, *Synechococcus* 1479/5 preferred the QHLs. *Scenedesmus sp.* showed no significant difference in growth rates for either light source.

Chlorophyll a and b contents, however, were higher for each organism when irradiated by the QHL compared to the HPSL. This suggested that growth and photosynthesis were possibly uncoupled since the higher maximum rates of photosynthesis would be expected from those cells with a higher pigment content assuming that the efficiency of the light harvesting reaction centres and utilisation are similar (see Section 3.4.1 and 3.4.2). Although the light sources were measured to be at identical PFDs, the cells of *Chlorella vulgaris* 211/11c and *Scenedesmus sp.* increased their chlorophyll a and b content when irradiated by the QHL suggesting that they were at a lower PFD, a process normally observed when cells irradiated at a high PFD are placed in a light regime at a lower PFD. This will be discussed further in Section 3.6.

Since the differences obtained in the growth rates of the organisms when irradiated by the two different light sources was marginal at best, the FPALR was irradiated with a single 600W HPSL for all further experiments since it provided a more uniform light field.

Experiments were performed to assess the design of the photostage of the FPALR at minimising the degree of cellular self shading and to assess the effect of increased PFD on the growth kinetics and cell physiology of micro-algae and cyanobacteria.

3.2.2 The effect of photon flux density on Micro-algal / cyanobacterial growth kinetics in the FPALR.

To assess the effect of increases photon flux density on the growth kinetics of micro-algae and cyanobacteria, cells of *Chlorella vulgaris* 211/11c, *Scenedesmus sp.* and *Synechococcus* 1479/5 were cultured in the FPALR under two light regimes of PFD 100 and 200 $\mu\text{mol s}^{-1} \text{m}^{-2}$. The light in each case was provided by a 600W HPSL. The FPALR was operated under conditions of 23°C, at a Reynolds number of 5800 and 2% carbon dioxide v/v (2000 $\text{cm}^3 \text{min}^{-1}$ air)

It was found that *Chlorella vulgaris* 211/11c, *Scenedesmus sp.* and *Synechococcus* 1479/5 had higher growth rates and maximum stationary phase biomass levels when cultured in the FPALR at a PFD of 200 $\mu\text{mol s}^{-1} \text{m}^{-2}$ compared to a PFD of 100 $\mu\text{mol s}^{-1} \text{m}^{-2}$ (Table 1). The variation in the biomass produced by cells of *Chlorella vulgaris* 211/11c cultured in the FPALR is shown in Figure 34. *Chlorella vulgaris* 211/11c was found to have a mean growth rate of 0.46 day^{-1} measured at mid exponential growth phase at a PFD of 100 $\mu\text{mol s}^{-1} \text{m}^{-2}$. This growth rate was observed to increase to 0.782 day^{-1} when the PFD was increased to 200 $\mu\text{mol s}^{-1} \text{m}^{-2}$. Increasing the PFD from 100-200 $\mu\text{mol s}^{-1} \text{m}^{-2}$ was also found to increase the maximum stationary phase biomass from 1.53 to 1.77 gl^{-1} measured at 175 hours. The maximum cell doubling time of 21.26 hours was measured when the cells were irradiated at a PFD of 100 $\mu\text{mol s}^{-1} \text{m}^{-2}$.

Figure 35 shows the increase in cellular biomass of cells of *Scenedesmus sp.* cultured in the FPALR. *Scenedesmus sp.* had a growth rate of 0.72 day^{-1} when cultured in the FPALR at a PFD of 100 $\mu\text{mol s}^{-1} \text{m}^{-2}$. This growth rate subsequently increased to 0.95 day^{-1} when the PFD was increased to 200 $\mu\text{mol s}^{-1} \text{m}^{-2}$. The maximum stationary phase biomass level measured after 190 hours increased from 2.29 gl^{-1} to 2.59 gl^{-1} when the PFD was increased from 100 to 200 $\mu\text{mol s}^{-1} \text{m}^{-2}$. It was found that *Scenedesmus sp.* had a cell doubling time of 17.5 hours (Table 1).

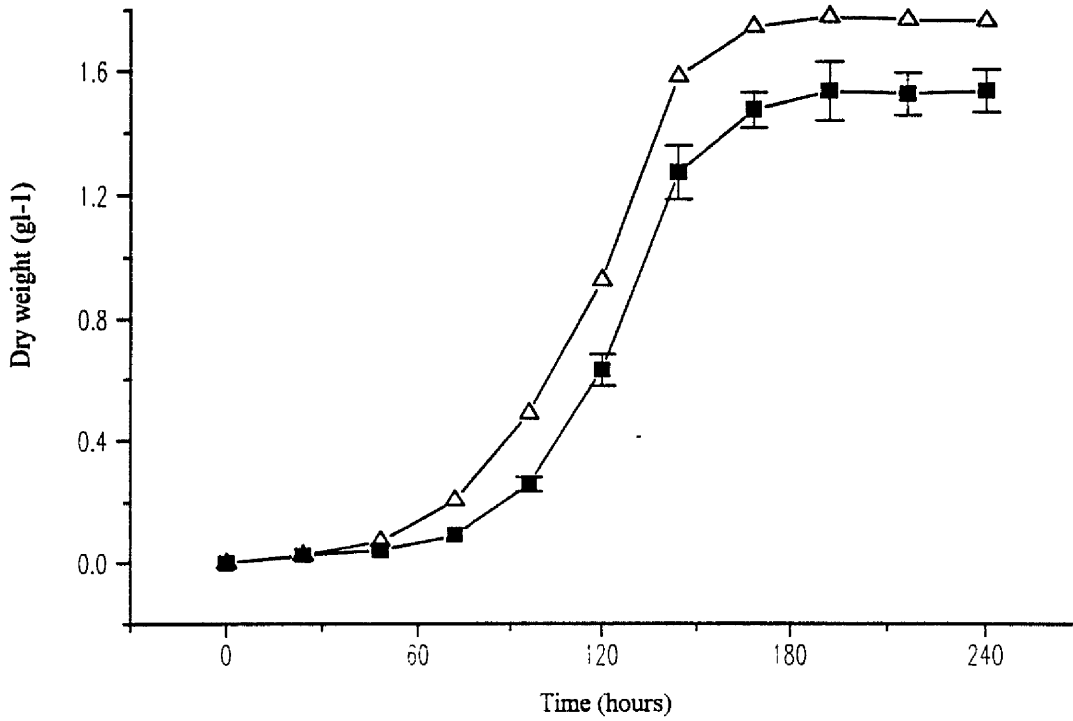


Figure 34. Change in dry weight (g l^{-1}) of *Chlorella vulgaris* 211/11c, Δ — Δ irradiated at a PFD of $200\mu\text{mol s}^{-1} \text{m}^{-2}$ using a high pressure sodium lamp, \blacksquare — \blacksquare irradiated at a PFD of $100\mu\text{mol s}^{-1} \text{m}^{-2}$ using a high pressure sodium lamp.

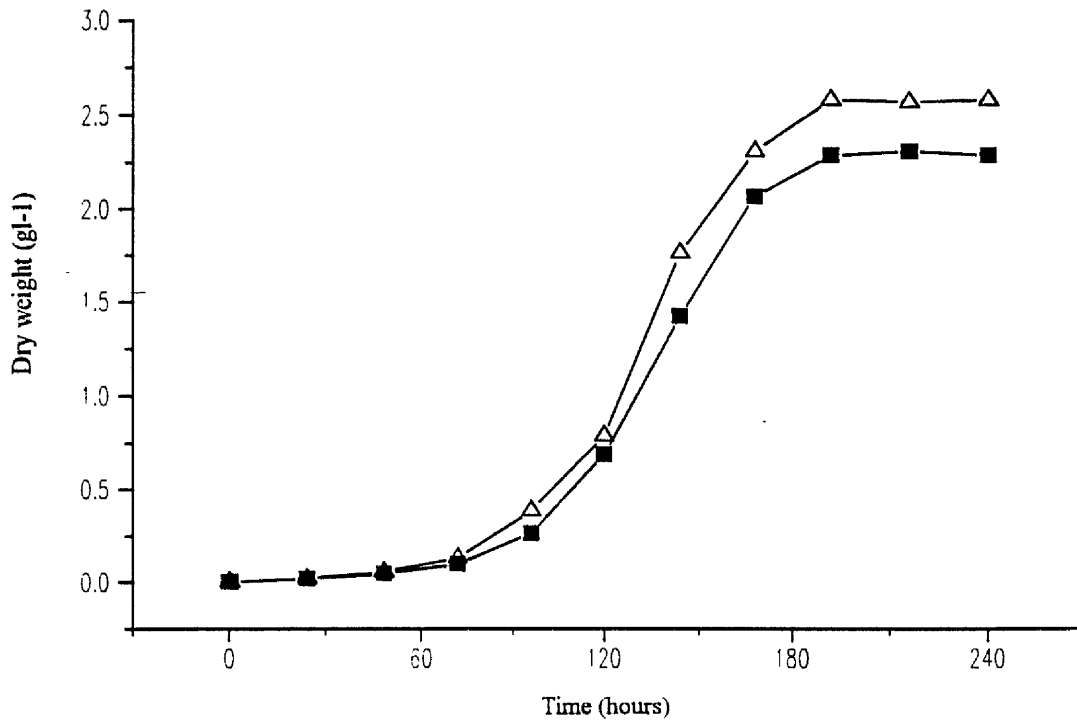


Figure 35. Change in dry weight (g l^{-1}) of *Scenedesmus* sp., Δ — Δ irradiated at a PFD of $200\mu\text{mol s}^{-1} \text{m}^{-2}$ using a high pressure sodium lamp, \blacksquare — \blacksquare irradiated at a PFD of $100\mu\text{mol s}^{-1} \text{m}^{-2}$ using a high pressure sodium lamp.

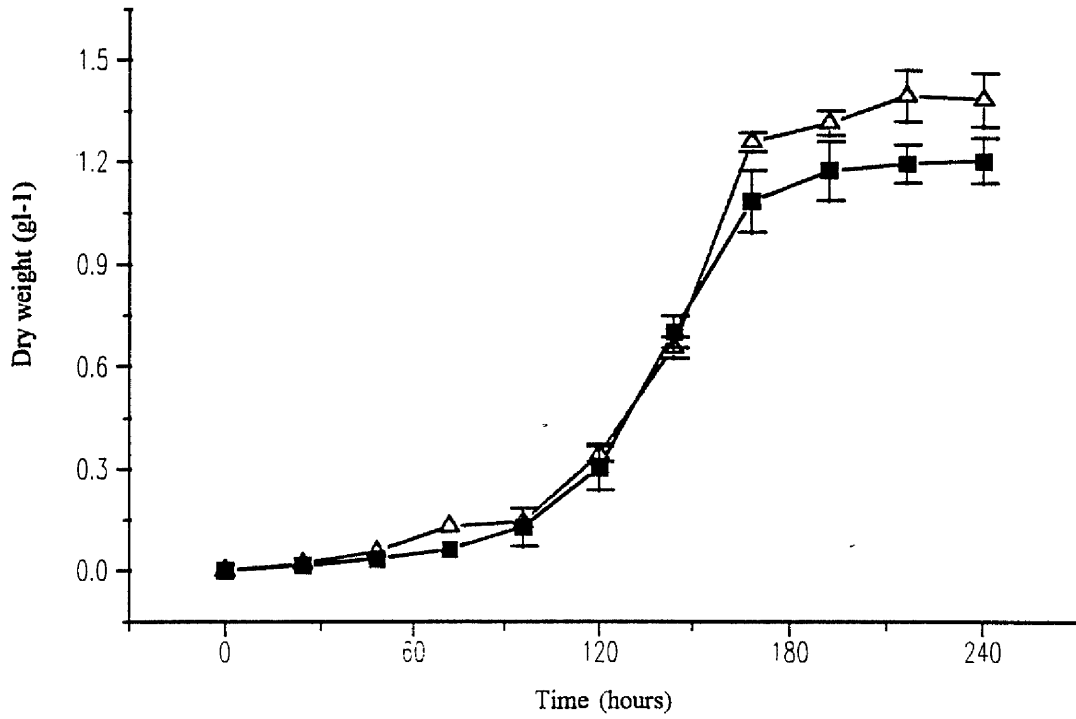


Figure 36. Change in dry weight (g l^{-1}) of *Synechococcus* 1479/5, Δ — Δ irradiated at a PFD of $200\mu\text{mol s}^{-1} \text{m}^{-2}$ using a high pressure sodium lamp, \blacksquare — \blacksquare irradiated at a PFD of $100\mu\text{mol s}^{-1} \text{m}^{-2}$ using a high pressure sodium lamp.

Table 1. The effect of photon flux density on the growth rates, stationary phase biomass and cell doubling times of *Chlorella vulgaris* 211/11c, *Scenedesmus sp.* and *Synechococcus* 1479/5.

	FPALR PFD100 Growth rate day ⁻¹	FPALR PFD100 Maximum Stationary Phase Biomass g l ⁻¹	Doubling Time (hours)	FPALR PFD200 Growth rate day ⁻¹	FPALR PFD200 Maximum Stationary Phase Biomass g l ⁻¹	Doubling Time (hours)
<i>C. vulgaris</i> 211/11c	0.46	1.53	35.9	0.78	1.77	21.26
<i>Scenedes</i> <i>mus sp.</i>	0.72	2.29	23.16	0.95	2.59	17.5
<i>Synechoc</i> <i>occus</i> 1479/5	0.59	1.21	28.33	0.978	1.58	17.06

Table 2. The effect of carbon dioxide concentration on the growth kinetics of *C. vulgaris* 211/11c cultured in the FPALR compared to the CSTR.

Carbon dioxide % air v/v.	FPALR Growth rate day ⁻¹	Maximum Stationary Phase Biomass g l ⁻¹	CSTR Growth rate day ⁻¹	Maximum Stationary Phase Biomass g l ⁻¹
Air Grown	0.379	0.88	0.24	0.67
2%	0.48	1.47	0.36	1.21
4%	1.05	1.59	0.78	1.42
6%	1.04	1.62	0.79	1.46
8%	0.59	0.91	0.46	1.34
10%	0.42	0.67	0.28	0.39

The increase in biomass of *Synechococcus* 1479/5 with time, in the FPALR is shown in Figure 36. *Synechococcus* 1479/5 had a growth rate of 0.59 day^{-1} when irradiated at a PFD of $100 \mu\text{mol s}^{-1} \text{ m}^{-2}$. The growth rate, however, increased to 0.978 day^{-1} when the PFD was increased to $200 \mu\text{mol s}^{-1} \text{ m}^{-2}$. The maximum stationary phase biomass level measured after 180 hours increased from 1.21 g l^{-1} to 1.58 g l^{-1} after the PFD was increased from 100 to $200 \mu\text{mol s}^{-1} \text{ m}^{-2}$. The mean cell doubling time of cells cultured in the FPALR at a PFD of $200 \mu\text{mol s}^{-1} \text{ m}^{-2}$ was measured to be 17.06 hours.

Subsequent chemical analysis of the spent culture medium used to grow cells of *Chlorella vulgaris* 211/11c in the FPALR at a PFD of $100 \mu\text{mol s}^{-1} \text{ m}^{-2}$, sampled during the stationary phases of growth revealed that the phosphate had been depleted from the medium. This suggested that the cells cultured in the FPALR at a PFD of $100 \mu\text{mol s}^{-1} \text{ m}^{-2}$ were possibly substrate limited. However, continuous sequential additions of phosphate (0.15 g l^{-1}), nitrate (0.5 g l^{-1}) and trace elements (ASM components) and increasing the carbon dioxide concentration to 4%v/v in the FPALR whilst cells were in the exponential and stationary phases of growth was not found to increase biomass levels whilst operating at a PFD of $100 \mu\text{mol s}^{-1} \text{ m}^{-2}$. It was only when cells were cultured in the FPALR at an increased PFD of $200 \mu\text{mol s}^{-1} \text{ m}^{-2}$ that an increase in growth rate was observed indicating that the cells were light limited at a PFD of $100 \mu\text{mol s}^{-1} \text{ m}^{-2}$.

In conclusion cells of *Chlorella vulgaris* 211/11c, *Scenedesmus sp.* and *Synechococcus* 1479/5 exhibited higher growth rates and stationary phase biomass levels when cultured in the FPALR at a PFD of $200 \mu\text{mol s}^{-1} \text{ m}^{-2}$ compared to a PFD of $100 \mu\text{mol s}^{-1} \text{ m}^{-2}$. Although the cells of *Synechococcus* 1479/5 were found to have the highest growth rates of 0.72 and 0.978 day^{-1} and cell doubling times of 23.16 and 17.06 hours (cultured at a PFDs of 100 and $200 \mu\text{mol s}^{-1} \text{ m}^{-2}$ respectively), it attained the lowest maximum stationary phase biomass levels of 1.21 and 1.58 g l^{-1} at both irradiances. *Scenedesmus sp.* reached the highest maximum stationary phase biomass of 2.29 g l^{-1} and 2.59 g l^{-1} at a PFD of 100 and $200 \mu\text{mol s}^{-1} \text{ m}^{-2}$ respectively (Figure 35).

3.2.3. The effect of Carbon dioxide Concentration on Micro-algal / Cyanobacterial growth kinetics in the FPALR and CSTR.

Chlorella vulgaris 211/11c, *Scenedesmus sp.* and *Synechococcus* 1479/5 were cultured in the FPALR and CSTR to examine the effects of different concentrations of carbon dioxide on growth kinetics. The FPALR was operated under conditions of 23°C, at a Reynolds number 5800 and irradiated at a PFD of $100\mu\text{mol s}^{-1} \text{m}^{-2}$. The CSTR was operated under conditions of 23°C and at a PFD $100\mu\text{mol s}^{-1} \text{m}^{-2}$. The results of the experiments are presented in Tables 2, 3 and 4 for *Chlorella vulgaris* 211/11c, *Scenedesmus sp.* and *Synechococcus* 1479/5 respectively.

It was found that cells of *Chlorella vulgaris* 211/11c showed much higher growth rates in the FPALR compared to the CSTR when cultured under the same conditions of carbon dioxide concentration apart from cells cultured in air (Table 2). In the air grown cultures it was found that the growth rates in the FPALR and CSTR were 0.379 and 0.24 day^{-1} respectively. It should be noted, however, that when the FPALR was operating at 0% v/v carbon dioxide the air stream was $2000\text{cm}^3 \text{ min}^{-1}$ compared to the CSTR which had an operating air input of $4000\text{cm}^3 \text{ min}^{-1}$ to aid mixing. Thus the CSTR had twice as much atmospheric carbon dioxide entering the vessel compared to the FPALR. Nevertheless it was found that cells grown in the FPALR reached early exponential growth phase and maximum stationary growth phase 2-3 days ahead of cells cultured in the CSTR under similar conditions (Figures 37 and 39). *Chlorella vulgaris* 211/11c/ achieved a maximum growth rate of 1.005 day^{-1} in the FPALR at a carbon dioxide concentration of 4-6% (Table 2, Figures 37 and 38) displaying a cell mean doubling time of approximately 15.84 hours (Table 5). The highest maximum stationary biomass of 1.62 gl^{-1} , however, was observed at 6% carbon dioxide in the FPALR suggesting that the optimum CO_2 concentration was about 5% for this organism. The optimum carbon dioxide concentration in the CSTR was also observed at 4-6% where cells had a maximum growth rate of approximately 0.785 day^{-1} and mean doubling time of 21.05 hours (Table 5). In air grown cultures cells cultured in both the FPALR and CSTR displayed severe carbon limited growth (Figure 37 and 39). Cells cultured in both the FPALR and CSTR at 10% carbon dioxide (Figures 38 and 40) displayed decreased growth rates (0.42 and 0.28 day^{-1} respectively) and maximum stationary phase biomass (0.67 and 0.39 gl^{-1}

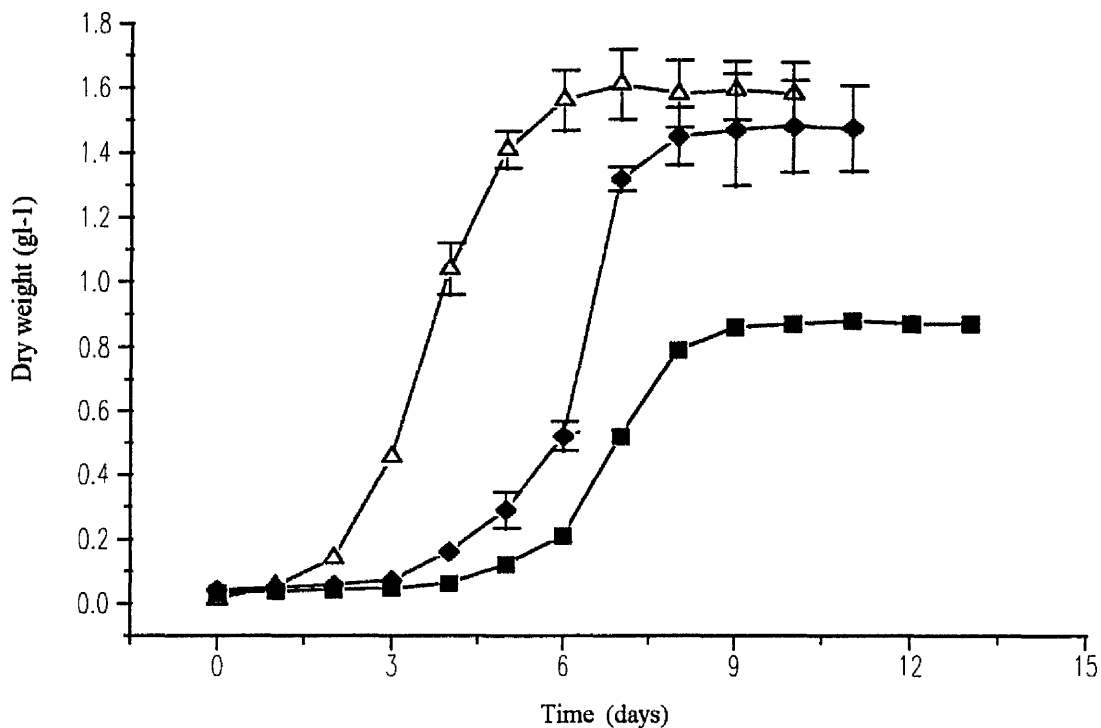


Figure 37. The effect of carbon dioxide concentration on the dry weight (g l^{-1}) of *Chlorella vulgaris* 211/11c cultured in the FPALR, Δ — Δ 4%v/v CO_2 , \blacklozenge — \blacklozenge 2%v/v CO_2 , \blacksquare — \blacksquare air grown.

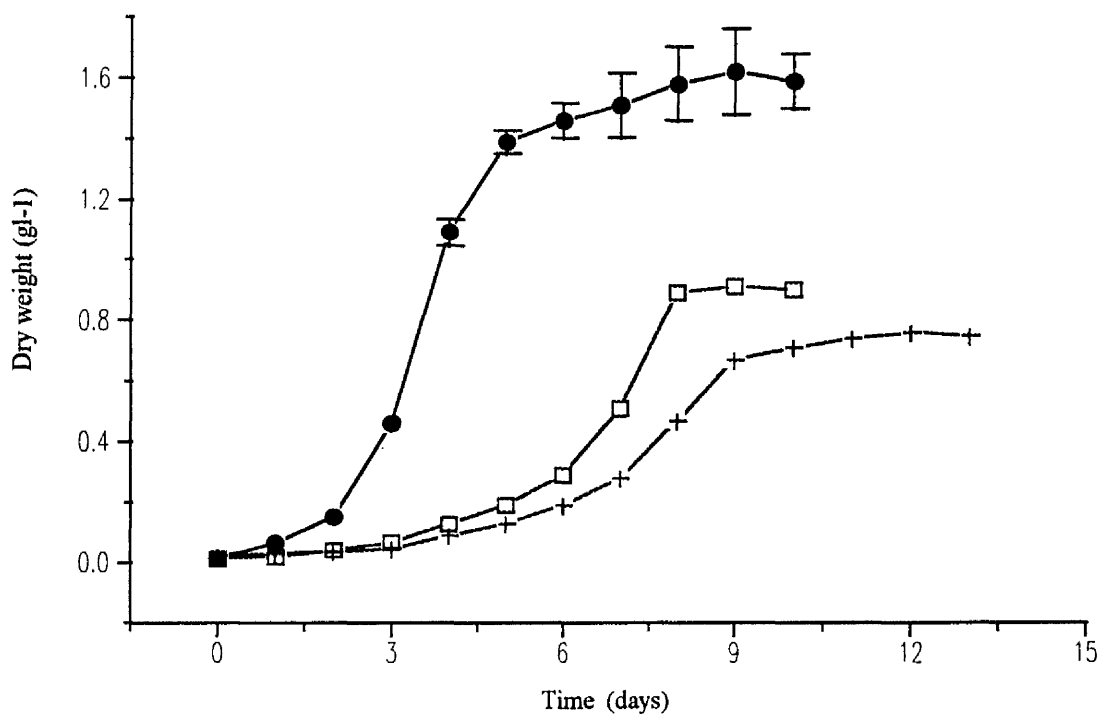


Figure 38. The effect of carbon dioxide concentration on the dry weight (g l^{-1}) of *Chlorella vulgaris* 211/11c cultured in the FPALR, \bullet — \bullet 6%v/v CO_2 , \square — \square 8%v/v CO_2 , $+$ — $+$ 10%v/v CO_2 .

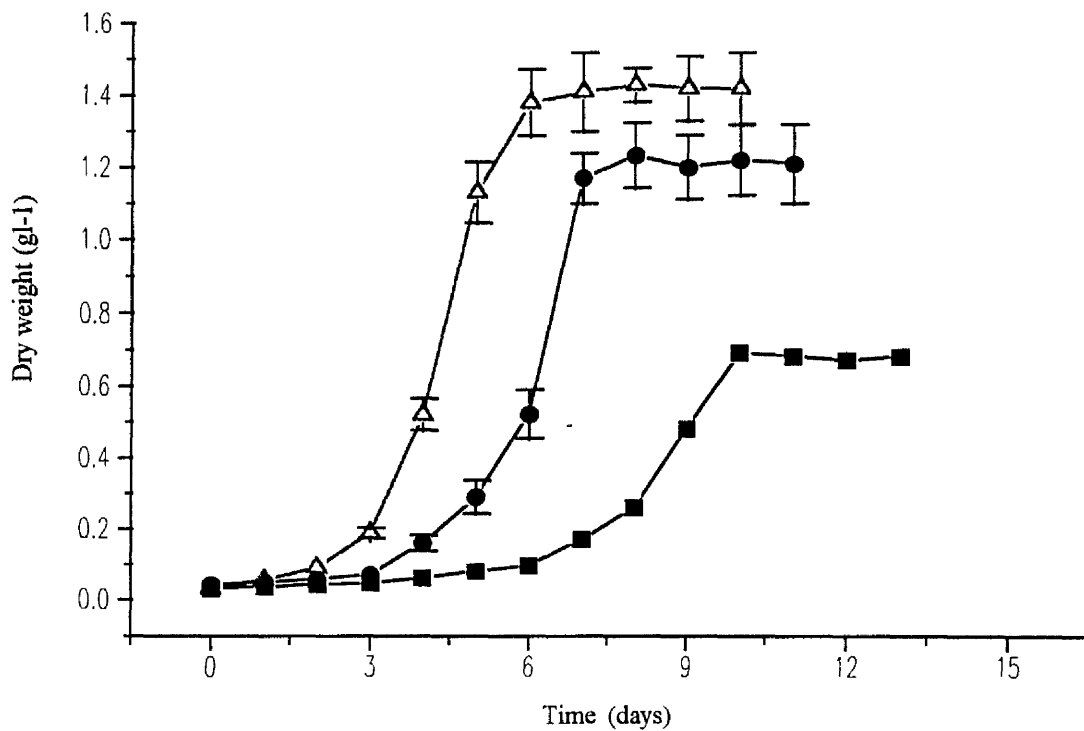


Figure 39. The effect of carbon dioxide concentration on the dry weight (g l⁻¹) of *Chlorella vulgaris* 211/11c cultured in the CSTR, Δ — Δ 4%v/v CO₂, \bullet — \bullet 2%v/v CO₂, \blacksquare — \blacksquare air grown.

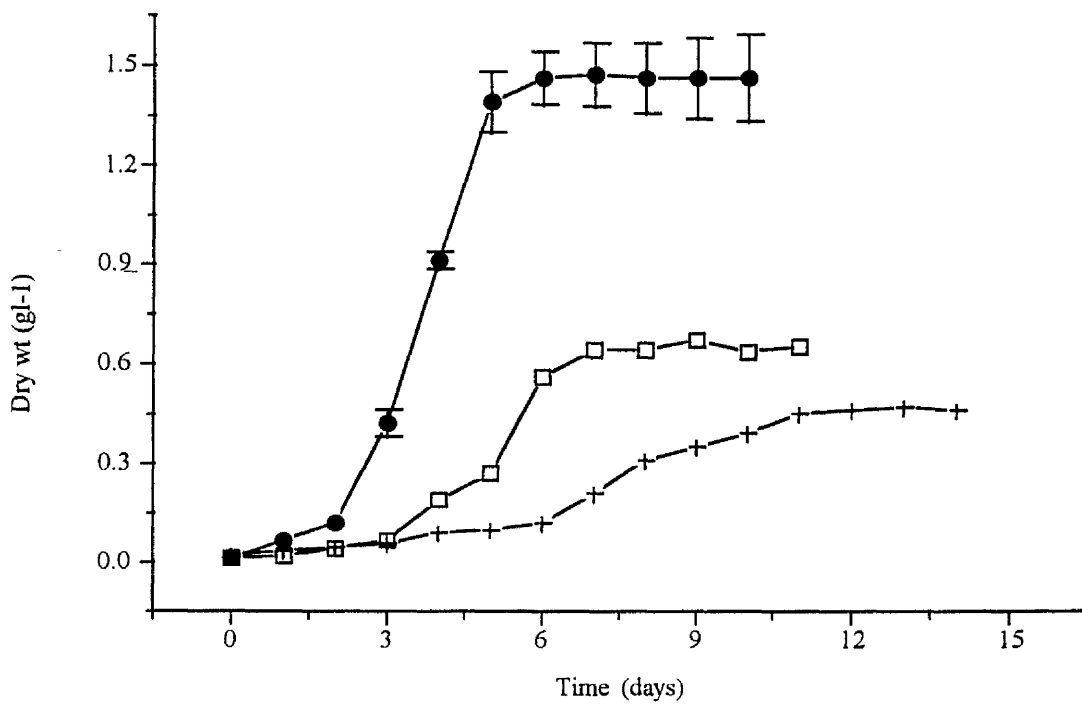


Figure 40. The effect of carbon dioxide concentration on the dry weight (g l⁻¹) of *Chlorella vulgaris* 211/11c cultured in the CSTR, \bullet — \bullet 6%v/v CO₂, \square — \square 8%v/v CO₂, +—+ 10%v/v CO₂.

Table 3. The effect of carbon dioxide concentration on the growth kinetics of *Scenedesmus sp.* cultured in the FPALR compared to the CSTR.

Carbon dioxide % air v/v.	FPALR Growth rate day ⁻¹	Maximum Stationary Phase Biomass g l ⁻¹	CSTR Growth rate day ⁻¹	Maximum Stationary Phase Biomass g l ⁻¹
Air Grown	0.46	1.26	0.27	0.79
2%	0.72	1.31	0.56	1.21
4%	1.34	1.63	0.86	1.46
6%	1.41	1.89	0.93	1.57
8%	0.89	1.69	0.51	0.9
10%	0.42	1.13	0.3	0.67

Table 4. The effect of carbon dioxide concentration on the growth kinetics of *Synechococcus 1479/5* cultured in the FPALR compared to the CSTR.

Carbon dioxide % air v/v.	FPALR Growth rate day ⁻¹	Maximum Stationary Phase Biomass g l ⁻¹	CSTR Growth rate day ⁻¹	Maximum Stationary Phase Biomass g l ⁻¹
Air Grown	0.41	1.1	0.33	0.79
2%	0.62	1.43	0.51	0.96
4%	0.89	1.67	0.77	1.27
6%	1.03	1.82	0.89	1.62
8%	1.01	1.74	0.72	1.21
10%	0.48	0.45	0.32	0.33

respectively), suggesting that the carbon dioxide concentration was possibly at toxic levels to the cells.

Scenedesmus sp. showed a similar pattern to that observed with *Chlorella vulgaris* 211/11c. The optimum carbon dioxide concentration was approximately 6% in the FPALR and CSTR (Table 3). At a carbon dioxide concentration of 6% cells cultured in the FPALR and CSTR had very high growth rates of 1.41 and 0.93 day⁻¹ respectively. The average cell doubling time at these high growth rates were measured to be 11.79 in the FPALR and 17.88 hours in the CSTR (Table 6). As was found with cells of *Chlorella vulgaris* 211/11c, *Scenedesmus sp.* showed a decrease in both growth rates and stationary phase biomass in both the FPALR and CSTR at the higher carbon dioxide concentration of 10%, (Figure 42, 44 and Table 3). At a concentration of 10% carbon dioxide cells of *Scenedesmus sp.* had very low growth rates of 0.42 and 0.3 day⁻¹ in the FPALR and CSTR respectively. At this high carbon dioxide concentration of 10% the average cell doubling times were 39.6 and 55 hours respectively (Table 6).

Figures 45, 46 and 47, 48 show the growth curves of *Synechococcus* 1479/5 cultured in the FPALR and CSTR respectively at various concentrations of carbon dioxide. Cells of *Synechococcus* 1479/5 were found to grow to very high biomass levels in the FPALR at all carbon dioxide concentrations with the exception of 10% (Table 4). The cells displayed the highest growth rate of 1.03 day⁻¹ in the FPALR and 0.89 day⁻¹ in the CSTR under conditions of 6% carbon dioxide. The average cell doubling time in the FPALR during which the highest growth rate was measured, was 16.14 hours (Table 7). The cells were found to have an optimum carbon dioxide requirement of 6%, based on the measured growth rates in the FPALR (Figure 46). A sharp reduction in both growth rate and stationary phase biomass levels were recorded in the FPALR and CSTR at the 10% carbon dioxide concentration (Figures 46 and 48).

It was found that the effect of high concentrations of carbon dioxide on growth and stationary phase biomass levels was strictly species dependent. The growth rates and stationary phase biomass levels of *Chlorella vulgaris* 211/11c, *Scenedesmus sp.* and *Synechococcus* 1479/5 measured in the FPALR were higher than those found in the CSTR. To a large degree this difference may be attributed to a superior light environment created by its design and turbulence that existed in the FPALR. However

Table 5. The cellular doubling times of *Chlorella vulgaris* 211/11c cultured at different Carbon dioxide concentrations in the FPALR and CSTR.

Carbon Dioxide %v/v Air	Mean Cell Doubling Time (Hours) FPALR	Mean Cell Doubling Time (Hours) CSTR
Air Grown	43.8	69.3
2%	34.65	46.2
4%	15.84	21.32
6%	15.99	21.05
8%	28.18	36.15
10%	39.6	59.4

Table 6. The cellular doubling times of *Scenedesmus sp.* cultured at different Carbon dioxide concentrations in the FPALR and CSTR.

Carbon Dioxide %v/v Air	Mean Cell Doubling Time (Hours) FPALR	Mean Cell Doubling Time (Hours) CSTR
Air Grown	36.15	61.6
2%	23.1	29.7
4%	12.4	19.33
6%	11.79	17.88
8%	18.68	32.6
10%	39.6	55.44

Table 7. The cellular doubling times of *Synechococcus* 1479/5 cultured at different Carbon dioxide concentrations in the FPALR and CSTR.

Carbon Dioxide %v/v Air	Mean Cell Doubling Time (Hours) FPALR	Mean Cell Doubling Time (Hours) CSTR
Air Grown	40.5	50.4
2%	26.8	32.6
4%	18.68	21.6
6%	16.14	18.68
8%	16.46	23.1
10%	34.6	51.97

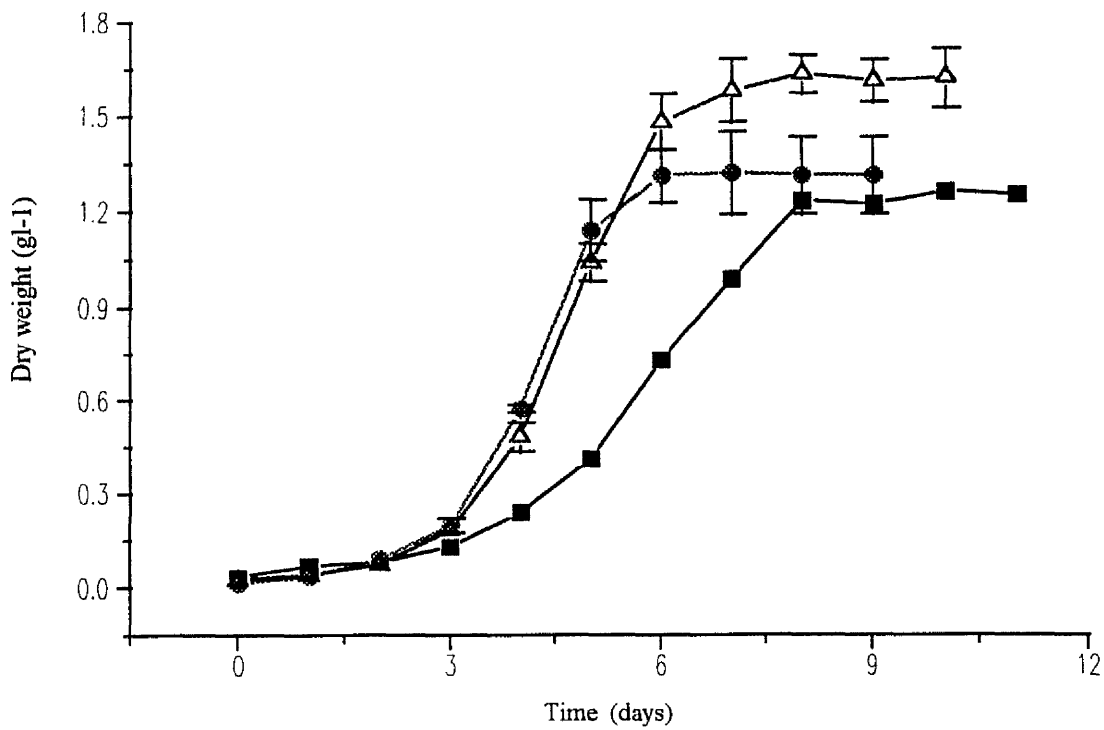


Figure 41. The effect of carbon dioxide concentration on the dry weight (g l^{-1}) of *Scenedesmus* sp. cultured in the FPALR. Δ — Δ 4%v/v CO_2 , \bullet — \bullet 2%v/v CO_2 , \blacksquare — \blacksquare air grown.

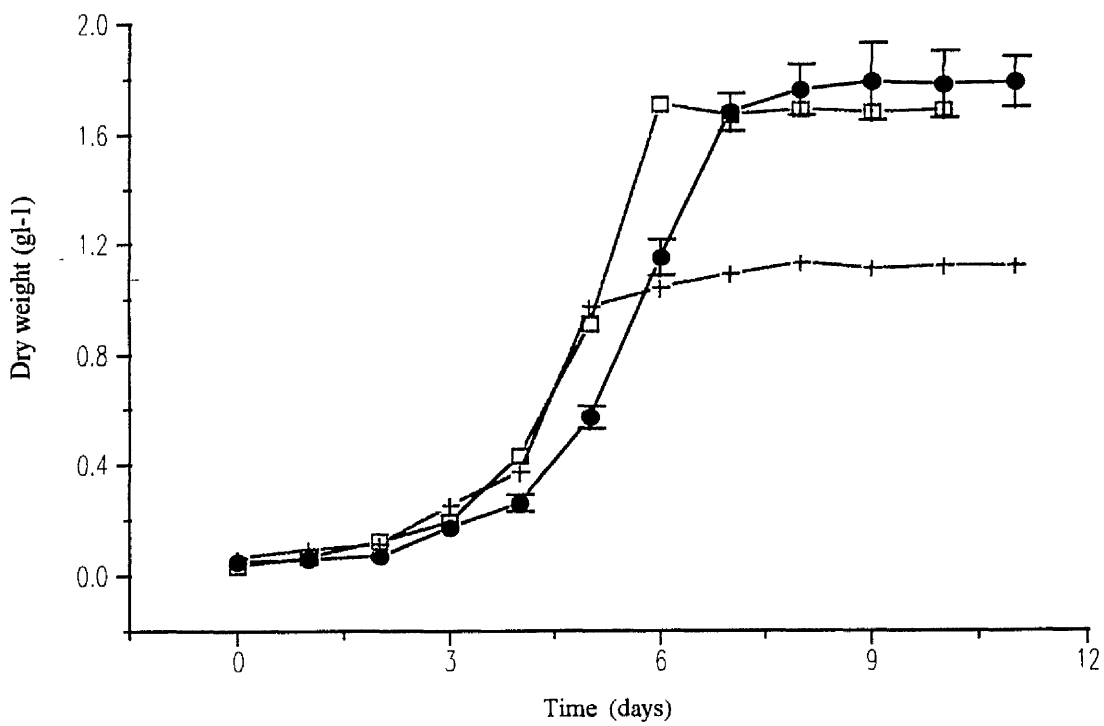


Figure 42. The effect of carbon dioxide concentration on the dry weight (g l^{-1}) of *Scenedesmus* sp. cultured in the FPALR. \bullet — \bullet 6%v/v CO_2 , \square — \square 8%v/v CO_2 , $+$ — $+$ 10%v/v CO_2 .

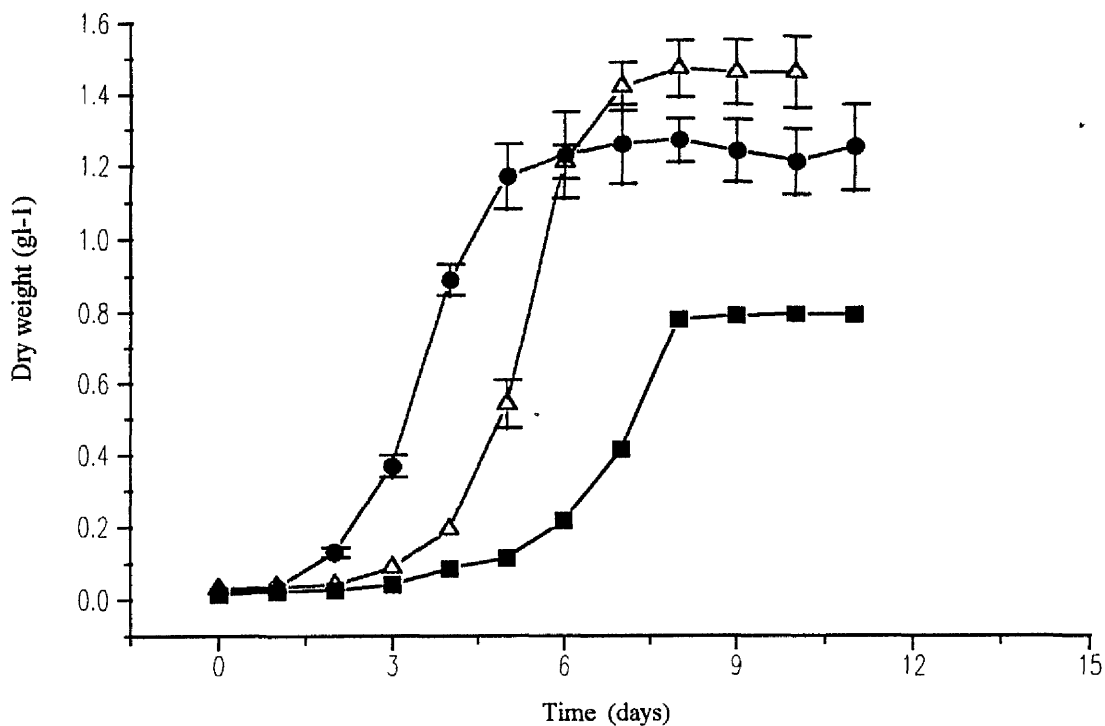


Figure 43. The effect of carbon dioxide concentration on the dry weight (g l^{-1}) of *Scenedesmus* sp. cultured in the CSTR. Δ — Δ 4%v/v CO_2 , \bullet — \bullet 2%v/v CO_2 , \blacksquare — \blacksquare air grown.

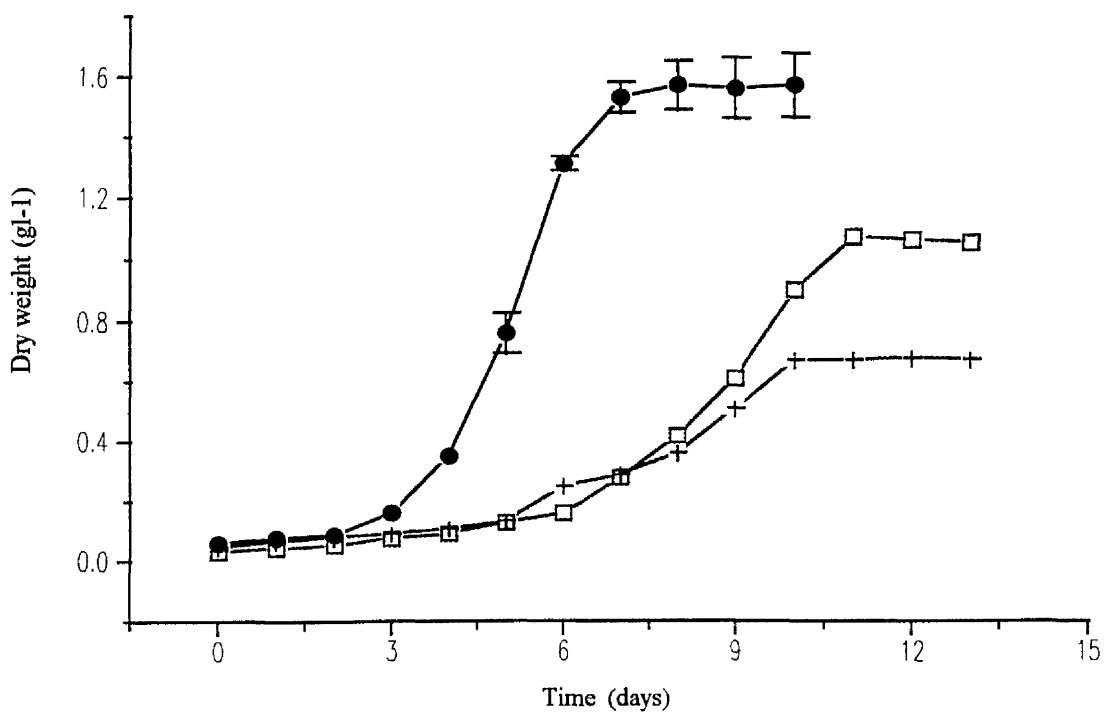


Figure 44. The effect of carbon dioxide concentration on the dry weight (g l^{-1}) of *Scenedesmus* sp. cultured in the CSTR. \bullet — \bullet 6%v/v CO_2 , \square — \square 8%v/v CO_2 , +—+ 10%v/v CO_2 .

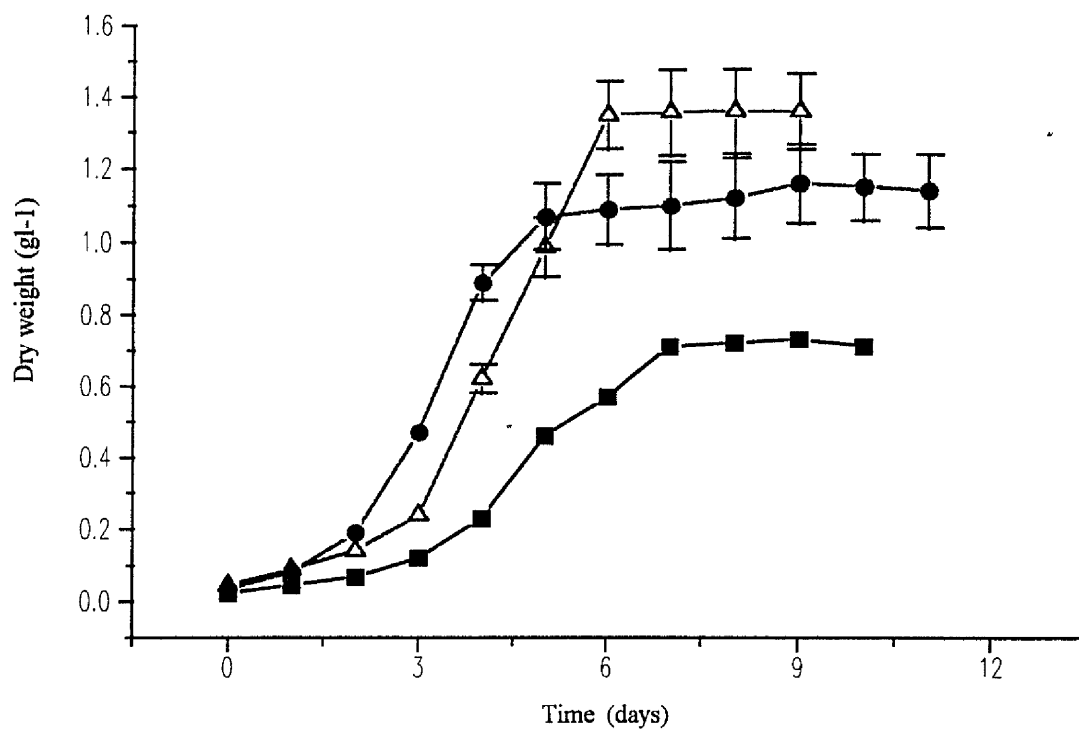


Figure 45. The effect of carbon dioxide concentration on the dry weight (g l^{-1}) of *Synechococcus* 1479/5 cultured in the FPALR, Δ — Δ 4%v/v CO_2 , \bullet — \bullet 2%v/v CO_2 , \blacksquare — \blacksquare air grown.

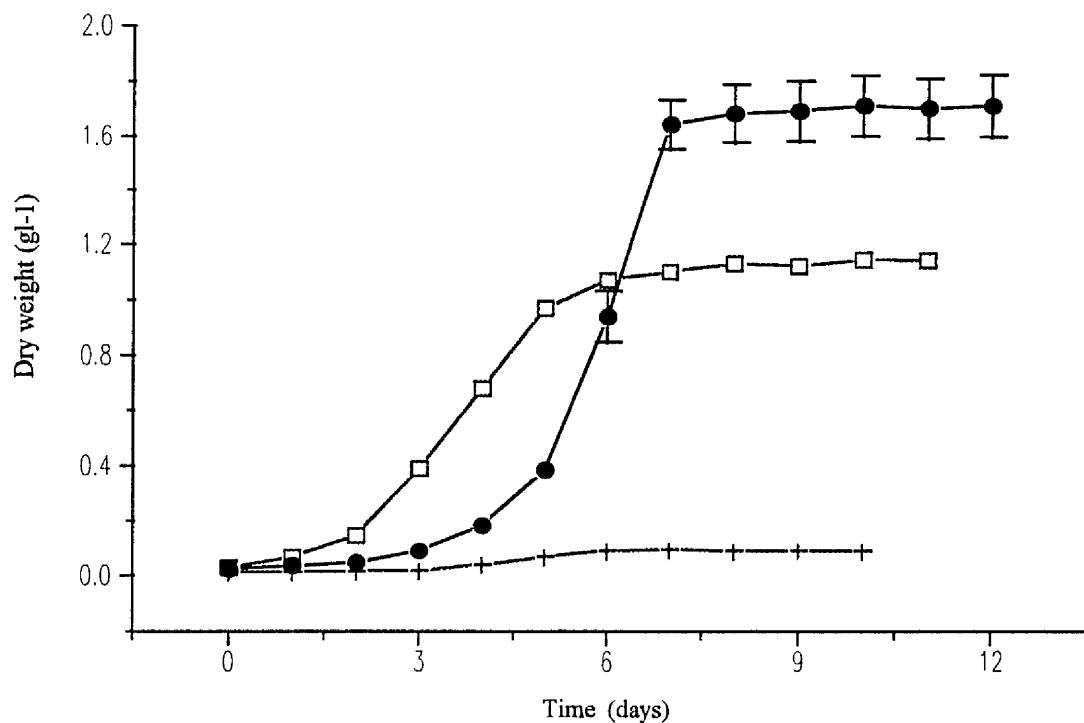


Figure 46. The effect of carbon dioxide concentration on the dry weight (g l^{-1}) of *Synechococcus* 1479/5 cultured in the FPALR, \bullet — \bullet 6%v/v CO_2 , \square — \square 8%v/v CO_2 , $+$ — $+$ 10%v/v CO_2 .

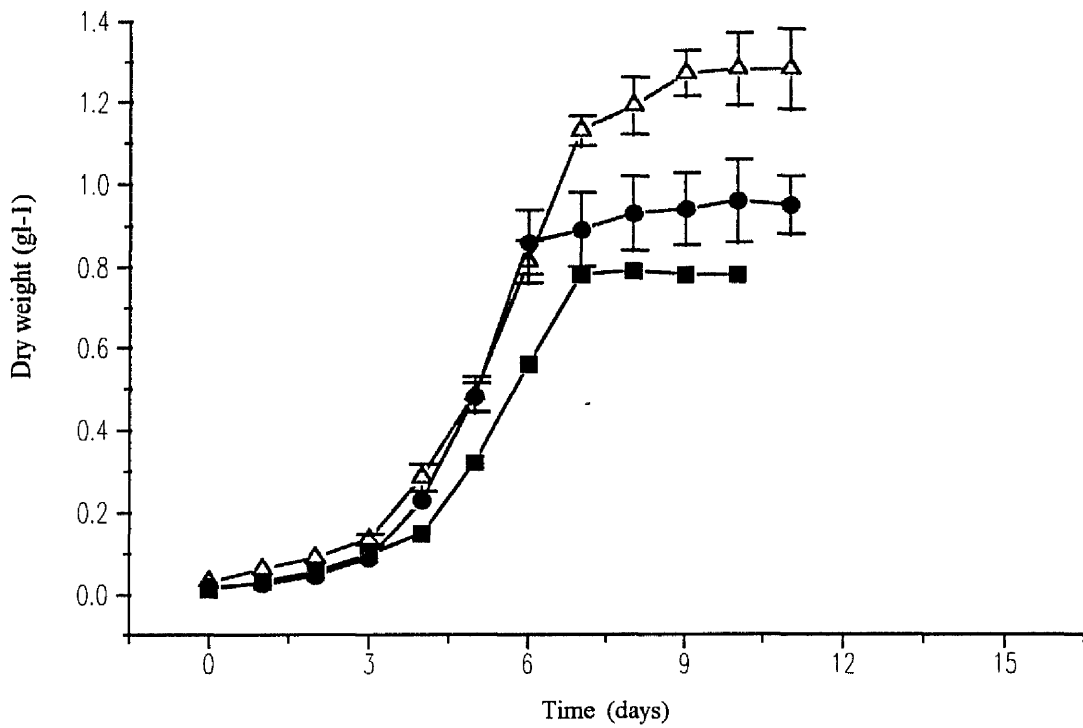


Figure 47. The effect of carbon dioxide concentration on the dry weight (g l^{-1}) of *Synechococcus* 1479/5 cultured in the CSTR, Δ — Δ 4%v/v CO_2 , \bullet — \bullet 2%v/v CO_2 , \blacksquare — \blacksquare air grown.

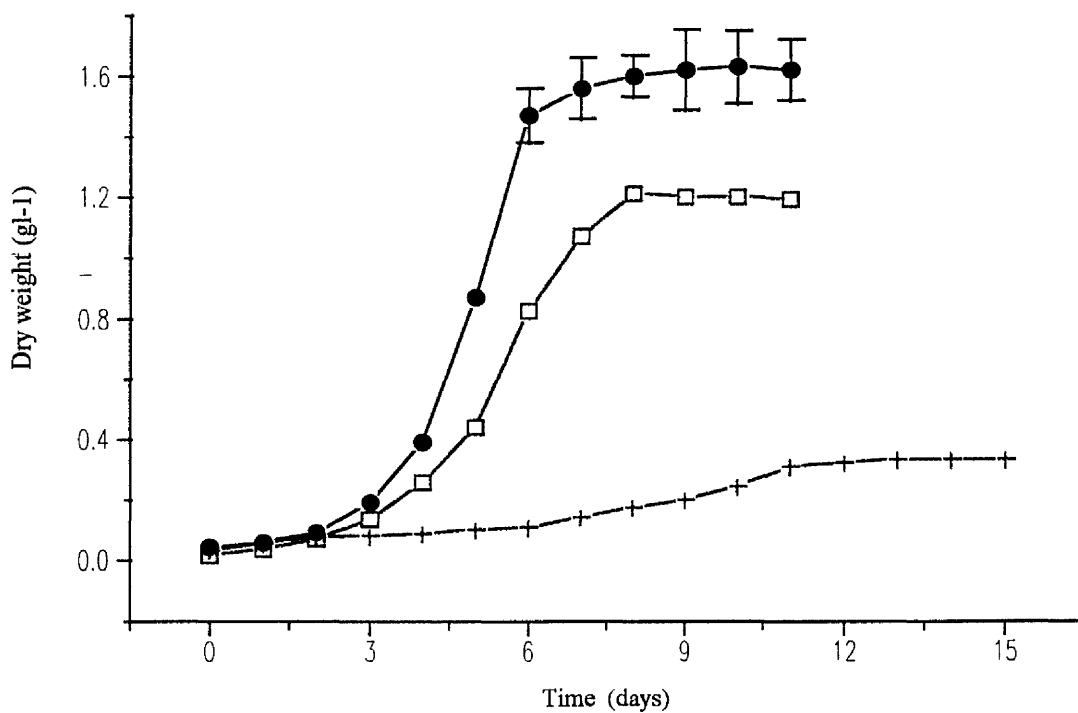


Figure 48. The effect of carbon dioxide concentration on the dry weight (g l^{-1}) of *Synechococcus* 1479/5 cultured in the CSTR, \bullet — \bullet 6%v/v CO_2 , \square — \square 8%v/v CO_2 , $+$ — $+$ 10%v/v CO_2 .

the superior gas handling and mixing facilities of the FPALR compared to the CSTR may have played a minor but crucial role. This was particularly noticeable at the high carbon dioxide concentration experiments (8-10% v/v). In the FPALR and CSTR (Figures 46 and 48), cells of *Synechococcus* 1479/5 had very high growth rates of 1.01 day^{-1} in the FPALR compared to 0.72 day^{-1} in the CSTR under similar conditions of 8% v/v carbon dioxide. This difference in growth rates of cells of *Synechococcus* 1479/5 in the FPALR and CSTR may be explained by the differences in fluid / gas mixing between the systems and the lesser degree of self shading that existed in the FPALR. The FPALR gas injector system produced very small diameter bubbles at high pressure with a greater mass transfer coefficient (kl_a) at the gas liquid interface. This meant that the movement of gas molecules was down a pressure gradient of the carbon dioxide containing bubble until it reached the interfacial membrane before crossing over to the liquid side. The coefficient kl_a is much larger at this point and so resulted in a greater mass transfer in the FPALR compared to the CSTR. The concentration gradient from the interfacial membrane controls the overall mechanism (Botton *et al.*, 1980). When delivering carbon dioxide to micro-algae or cyanobacteria there can be up to eight different resistance's to the movement of the gas molecules (Moo-Young and Blanch, 1981) These are summarised below:

1. in a gas film inside the bubble
2. at the gas-liquid interface
3. in the liquid film at the gas-liquid interface
4. in the bulk fluid
5. in the liquid film surrounding the cell
6. at the cell liquid
- 7. the internal cell resistance
8. the resistance at the site of biochemical reaction

However only the first 4 of the above are directly dependent on a systems design and construction. The CSTR was designed to mix cultures (mainly bacteria and yeast), using stirring paddles rotating above a glass sparger. The glass sparger allowed air to be pumped through creating large bubbles ranging from several mm to a few cm in diameter. This method of gas supply and mixing may have exposed the cultured cells to high levels of carbon dioxide by direct contact, causing a reduction in both growth rates and stationary phase biomass levels. However the FPALR uses a 1.8 metre

acrylic column in which to mix the gases at high pressure and turbulence. The bubble formation at the gas injector point was found have diameters of 1 mm or less. These very small diameter bubbles moving at high velocity resulted in very high magnitudes of $k_L a$. The result of which increased the overall mass transfer of carbon dioxide across the liquid phase from the gas phase and then to the cell.

The FPALR operated at a Reynolds number of 5800 which meant that the system was fully turbulent. Coupled to the flat plate design of the photostage and high degree of turbulence that existed in the channels, the degree of self shading was minimal. The light field determined for the CSTR only existed at the surface of the vessel. As the optical density of the culture increased the degree of self shading increased. It is suggested that cells in the CSTR may have been light limited even during the exponential phase of growth.

3.2.4 The effect of Temperature on Micro-algal / Cyanobacterial growth kinetics in the FPALR and the CSTR.

The effect of temperature on the growth kinetics of cells of *Chlorella vulgaris* 211/11c, *Scenedesmus sp.* and *Synechococcus* 1479/5 was examined in the FPALR and CSTR. The conditions of operation in the FPALR were 2% v/v carbon dioxide (2000cm³ min⁻¹ air) and a PFD of 100µmol s⁻¹ m⁻². The CSTR was operated with 2% carbon dioxide v/v (4000cm³ min⁻¹ air) at a PFD 100µmol s⁻¹ m⁻².

Figures 49 and 50 show the increase in the biomass of *Chlorella vulgaris* 211/11c cultured in the FPALR and CSTR respectively. *Chlorella vulgaris* 211/11c had higher growth rates and stationary phase biomass levels in the FPALR (Table 8) when cultured at 35°C (0.87 day⁻¹ and 2.32 gl⁻¹) compared cells cultured in the CSTR at the same temperature (0.612 day⁻¹ and 1.75 gl⁻¹). The shortest cell doubling time was found to be 19.8 hours in the FPALR at a temperature of 35°C compared to 27.18 hours in the CSTR at the same temperature (Table 11).

Scenedesmus sp. was found to have an optimum growth temperature of 35°C in the FPALR and the CSTR (Table 9). Figures 51 and 52 show that *Scenedesmus sp.* attained higher stationary phase biomass levels of 2.6 and 1.65 gl⁻¹ in both the

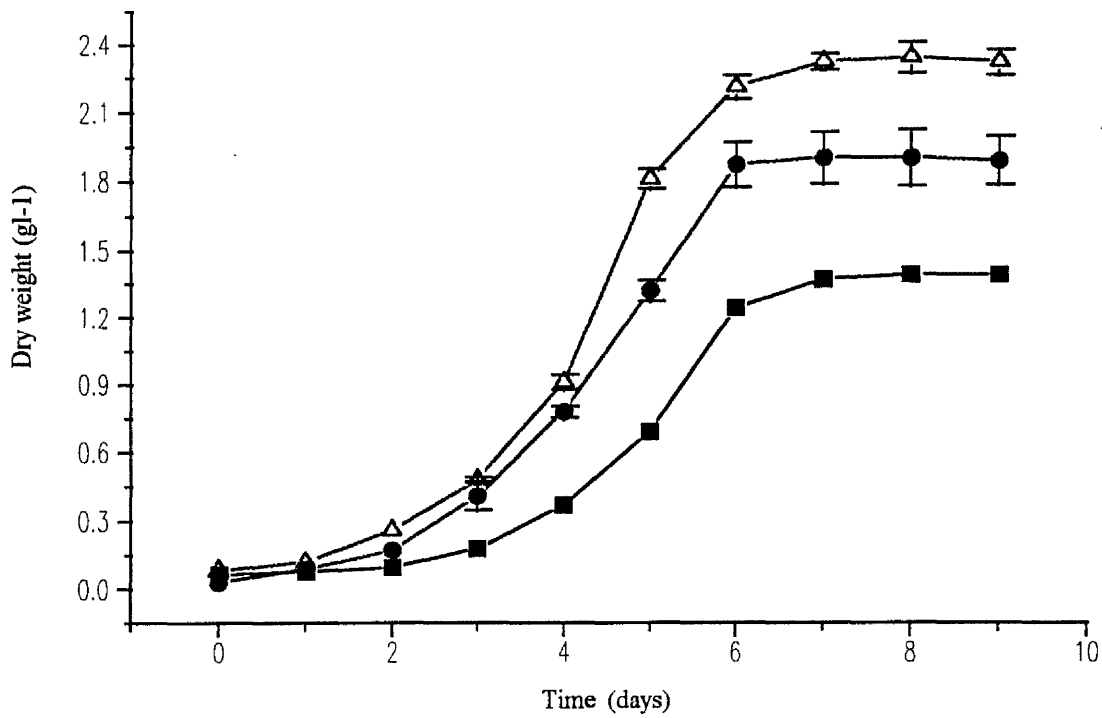


Figure 49. The effect of temperature on the dry weight (g l^{-1}) of *Chlorella vulgaris* 211/11c cultured in the FPALR. Δ — Δ 35°C, \bullet — \bullet 30°C, \blacksquare — \blacksquare 23°C.

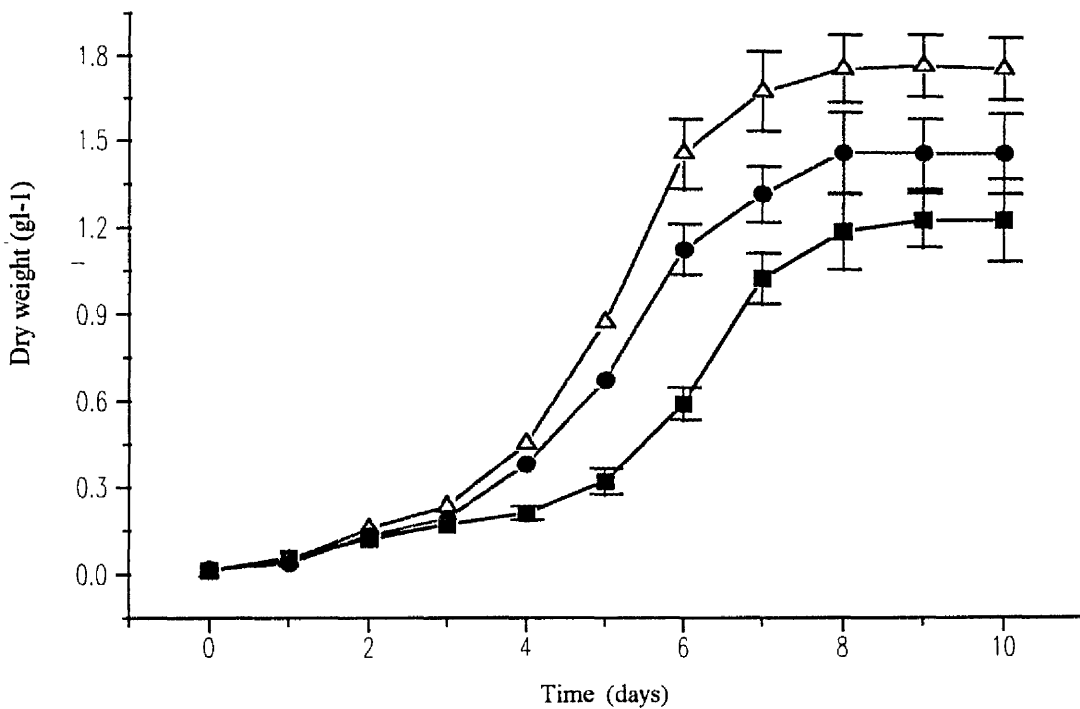


Figure 50. The effect of temperature on the dry weight (g l^{-1}) of *Chlorella vulgaris* 211/11c cultured in the CSTR. Δ — Δ 35°C, \bullet — \bullet 30°C, \blacksquare — \blacksquare 23°C.

Table 8. The effect of temperature on the growth kinetics of *Chlorella vulgaris* 211/11c cultured in the FPALR and CSTR.

	FPALR Growth rate day ⁻¹	Maximum Stationary Phase Biomass g l ⁻¹	CSTR Growth rate day ⁻¹	Maximum Stationary Phase Biomass g l ⁻¹
23	0.45	1.39	0.41	1.2
30	0.682	1.89	0.55	1.45
35	0.87	2.32	0.612	1.75

Table 9. The effect of temperature on the growth kinetics of *Scenedesmus sp.* 211/11c cultured in the FPALR and CSTR.

	FPALR Growth rate day ⁻¹	Maximum Stationary Phase Biomass g l ⁻¹	CSTR Growth rate day ⁻¹	Maximum Stationary Phase Biomass g l ⁻¹
23	0.69	1.38	0.54	1.23
30	0.892	1.85	0.69	1.51
35	1.12	2.6	0.712	1.65

Table 10. The effect of temperature on the growth kinetics of *Synechococcus* 1479/5 211/11c cultured in the FPALR and CSTR.

	FPALR Growth rate day ⁻¹	Maximum Stationary Phase Biomass g l ⁻¹	CSTR Growth rate day ⁻¹	Maximum Stationary Phase Biomass g l ⁻¹
23	0.61	1.46	0.52	0.88
30	0.78	1.86	0.64	1.27
35	0.858	2.15	0.71	1.57

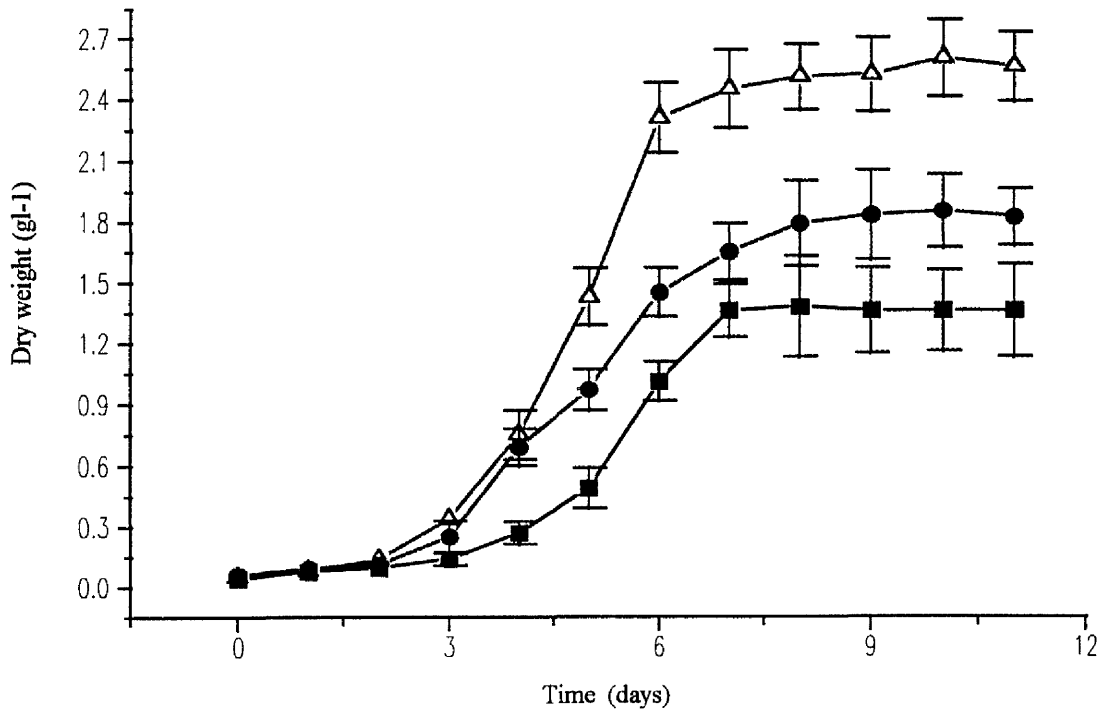


Figure 51. The effect of temperature on the dry weight (g l^{-1}) of *Scenedesmus sp.* cultured in the FPALR, Δ — Δ 35°C, \bullet — \bullet 30°C, \blacksquare — \blacksquare 23°C.

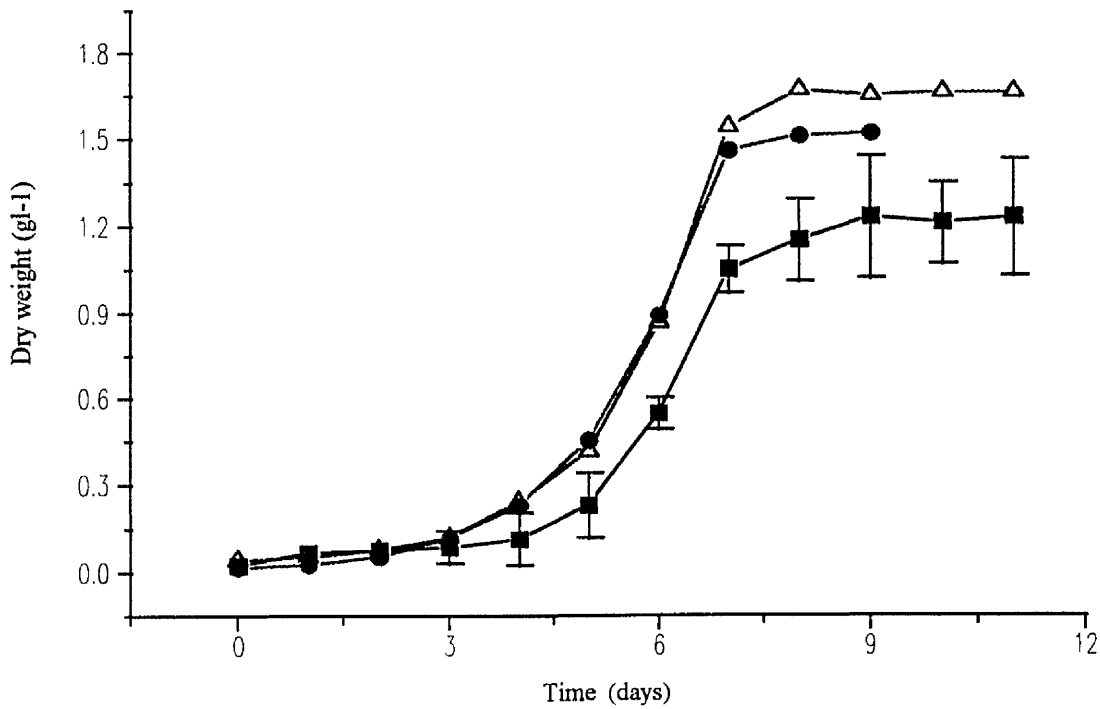


Figure 52. The effect of temperature on the dry weight (g l^{-1}) of *Scenedesmus sp.* cultured in the CSTR, Δ — Δ 35°C, \bullet — \bullet 30°C, \blacksquare — \blacksquare 23°C.

FPALR and CSTR at the higher temperature of 35°C. The maximum stationary phase biomass of 1.38 gl^{-1} measured from cells cultured in the FPALR at 23°C doubled to 2.6 gl^{-1} when cells were cultured in the same vessel at an increased temperature of 35°C (Table 9). *Scenedesmus sp.* cells were found to have an average cell doubling time of 14.85 and 23.36 hours when cultured in the FPALR and CSTR (Table 12).

Cells of *Synechococcus* 1479/5 were found to have an optimum growth temperature of 35°C in both the FPALR and CSTR. At this temperature the recorded growth rates of 0.858 and 0.71 day^{-1} (Table 10) were measured giving rise to cell doubling times of 19.38 and 23.4 hours (Table 13) in the FPALR and CSTR respectively. The maximum stationary phase biomass levels were found to be higher in both the FPALR and CSTR at a temperature of 35°C (Figures 53 and 54). It was found that culturing the cells in the CSTR at 35°C resulted in a 5-6 day lag phase prior to the onset of early exponential phase. No lag phase was evident in the FPALR at the same temperature. The stationary phase biomass produced at a temperature of 23°C in the CSTR was almost half that produced at 35°C.

From the results of Sections 3.2.1 to 3.2.4 it can be concluded that cells of *Chlorella vulgaris* 211/11c, *Scenedesmus sp.* and *Synechococcus* 1479/5 grew with higher growth rates and produced higher stationary phase biomass levels when cultured in both the FPALR and CSTR at a PFD of 200 $\mu\text{mol s}^{-1} \text{m}^{-2}$ compared to a PFD of 100 $\mu\text{mol m}^{-2} \text{s}^{-1}$. The optimum requirement for carbon dioxide of cells of *Chlorella vulgaris* 211/11c was found to be 4-6% in both the FPALR and CSTR. The optimum carbon dioxide requirement for *Scenedesmus sp.* however, was found to be 6% in both the FPALR and CSTR. *Synechococcus* 1479/5 was found to have an optimum requirement of carbon dioxide of between 6 and 8% in the FPALR compared to 6% in the CSTR. All three photosynthetic organisms were found to have higher growth rates in the FPALR and CSTR at a temperature of 35°C.

Cells of micro-algae and cyanobacteria cultured in the FPALR were found to have significantly higher growth rates, stationary phase biomass levels and doubling times throughout all of the experiments examining PFD, carbon dioxide concentration and temperature, compared to cells cultured in the CSTR under similar conditions. Increases in biomass without a necessary increase in growth rate has been observed in

Table 11. The cellular doubling times of *Chlorella vulgaris* 211/11c cultured at different temperatures in the FPALR and CSTR.

Temperature °C	Mean Cell Doubling Time (Hours) FPALR	Mean Cell Doubling Time (Hours) CSTR
23	36.96	40.57
30	24.39	30.24
35	19.8	27.18

Table 12. The cellular doubling times of *Scenedesmus* sp. cultured at different temperatures in the FPALR and CSTR.

Temperature °C	Mean Cell Doubling Time (Hours) FPALR	Mean Cell Doubling Time (Hours) CSTR
23	24.1	30.1
30	18.64	24.1
35	14.85	23.36

Table 13. The cellular doubling times of *Synechococcus* 1479/5 cultured at different temperatures in the FPALR and CSTR.

Temperature °C	Mean Cell Doubling Time (Hours) FPALR	Mean Cell Doubling Time (Hours) CSTR
23	27.37	31.99
30	21.32	25.99
35	19.38	23.4

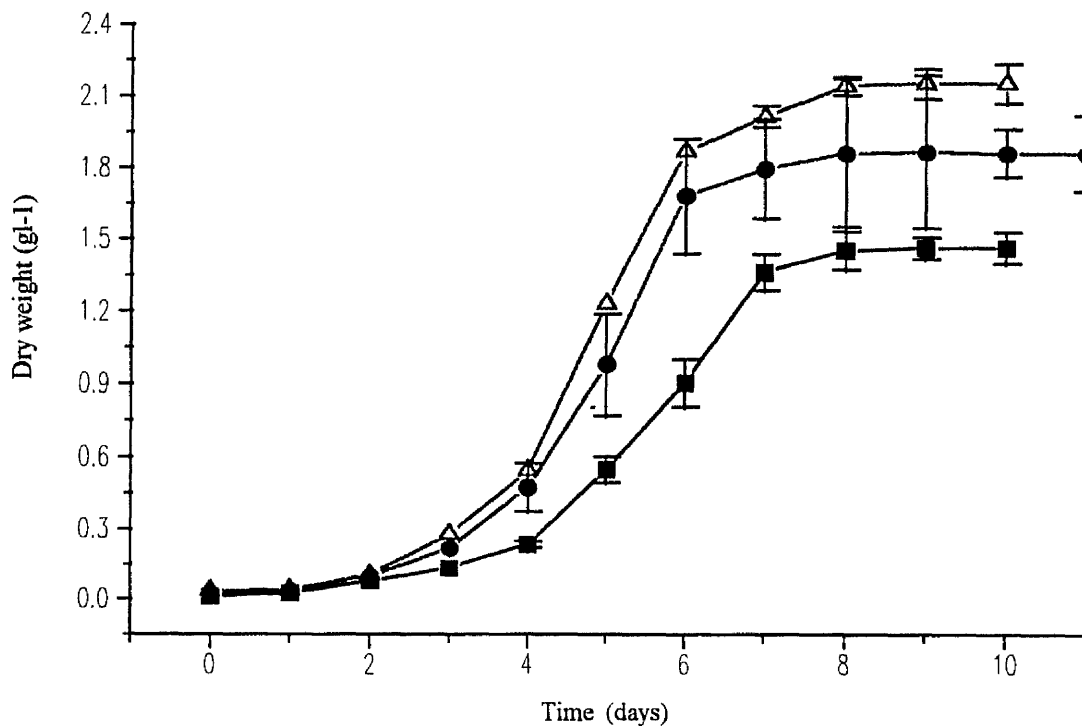


Figure 53. The effect of temperature on the dry weight (g l^{-1}) of *Synechococcus* 1479/5 cultured in the FPALR, Δ — Δ 35°C, \bullet — \bullet 30°C, \blacksquare — \blacksquare 23°C.

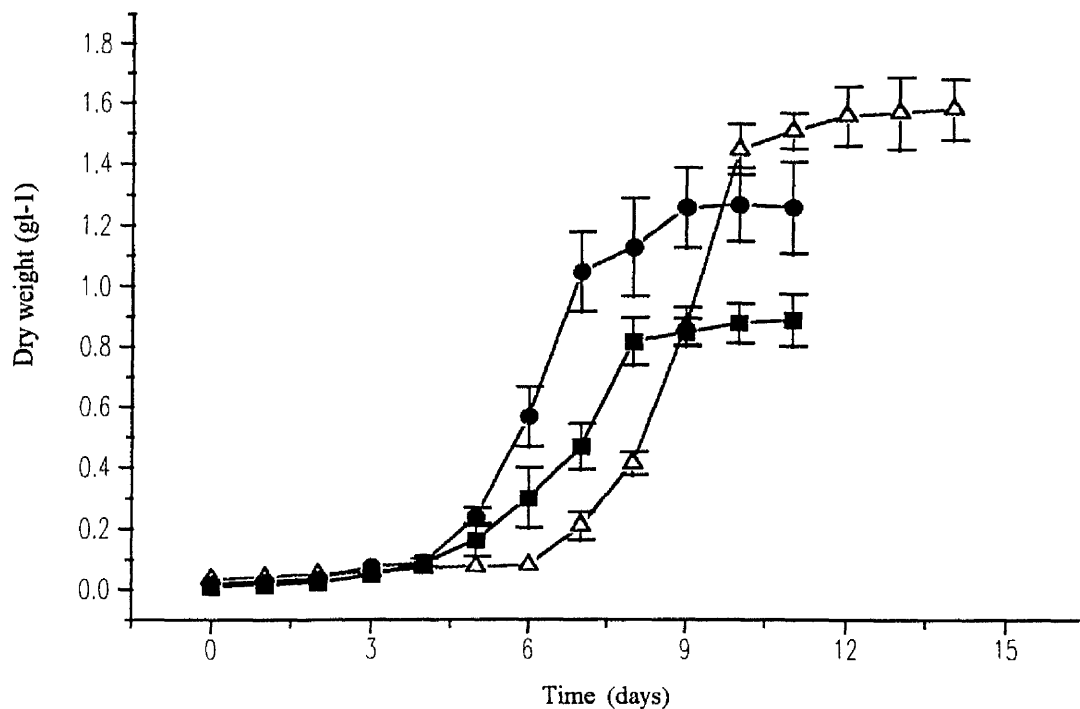


Figure 54. The effect of temperature on the dry weight (g l^{-1}) of *Synechococcus* 1479/5 cultured in the CSTR, Δ — Δ 35°C, \bullet — \bullet 30°C, \blacksquare — \blacksquare 23°C.

Chlamydomonas reinhardtii (Coleman and Colman, 1980). It was found that increasing the temperature from 15 to 35°C resulted in an increased affinity for carbon dioxide. This increase in temperature changed the K_m CO₂ from 0.55µM at 15°C to 1.10µM at 35°C. It was found that the K_m CO₂ was sensitive to changes in oxygen and that it remained unchanged with increasing temperature if kept at low oxygen saturations.

It was observed that as the temperature of the culture was increased in the FPALR to the optimum values for each organism, there was a marked development in the formation of gas bubbles within the reactor channels. These gas bubbles presented a problem since they restricted the flow of the culture and so aided the adhering of cells to the surface walls of the plate. It was possible to remove the gas by stopping the flow for a few minutes to allow the movement of the bubbles to the dark stage degasser. This was performed at least once during each FPALR temperature experimental run. Increased input of the polyethylene glycol to quell the foaming had no effect. The production of increased foam with increased temperature in the CSTR was observed but manual addition of anti-foaming agent reduced this significantly.

Although the formation and persistence of gas bubbles in the channels of the FPALR, primarily restricted the turbulent flow of the culture, high oxygen saturation has been shown to inhibit cellular photosynthesis (Zelitch, 1971; Laing *et al.*, 1974; Radmer and Kok, 1976; Ku and Edwards, 1977; Shelp and Canvin, 1980; Richmond *et al.*, 1992). The use of air-lift mechanisms designed to circulate cultures of microbial cells has a relatively unknown advantage in that the introduction of air into gas rise columns helps disrupt oxygen super saturated fluid prior to the processing via the degasser (Richmond *et al.*, 1992).

Although the mechanism of oxygen inhibition of photosynthesis remains unclear, it has been suggested that the process involves the enzyme ribulose di-phosphate carboxylase-oxygenase (Ku and Edwards, 1977). Evidence for the proposed mechanism is derived from the observation that photosynthesis is more sensitive to oxygen concentration at increased temperatures. It is thought that the enzyme ribulose di-phosphate carboxylase-oxygenase, has different activation energies for each of the oxygenase and carboxylase activities. Badger and Andrews, (1974), observed that the activation energy of the oxygenase component was significantly higher than the

carboxylase part. Hence the explanation of why the oxygenase reaction is considerably affected by a change in temperature. However this observation of the different activation energies of the enzyme ribulose di-phosphate carboxylase-oxygenase, has not been found in other cells (Laing *et al.*, 1974). Although a large amount of research has been geared towards plant cells, similar observations of oxygen inhibition of photosynthesis has been found in micro-algae. Shelp and Canvin, (1980) examined the role of oxygen saturation on the photosynthesis of *Chlorella pyrenoidosa*. They determined that oxygen did not affect the cellular rates of photosynthesis until saturation levels of 50% were achieved. No change in the rates of photosynthesis were recorded when the oxygen saturation level of 21% was subsequently decreased to 2%. When the oxygen saturation level was increased to 50%, the rate of photosynthesis of cells of *Chlorella pyrenoidosa* displayed a 12% inhibition. Increasing the oxygen concentration to 100% saturation reduced the photosynthetic rate by 24%. Although the cellular V_{max} was reduced, no detected change in the K_m (CO_2) was measured. The effect of oxygen on photosynthesis was not affected by the presence or absence of either carbon dioxide or bicarbonate ions.

The competition between the oxygenase and carboxylase components of ribulose di-phosphate carboxylase-oxygenase has been thought to be the main contributor to oxygen inhibition in C_3 plants (Cholet and Ogren, 1975). However with cells of micro-algae, the oxygenase activity of the enzyme has been shown to be suppressed in the presence of carbon concentrating mechanisms, (Beardall and Raven, 1990). This suppression completely disables the mechanism of photorespiration. Photorespiration is the light dependant increase in the rate of carbon -dioxide production that is usually associated with the production of glycolate. It is usually extremely difficult to measure in the light since the carbon dioxide consumed in the pentose phosphate pathway is far greater than the production via glycolate. Photorespiration has been reported to continue for several minutes after the cells have been placed in the dark (Decker, 1955). It has been demonstrated that the mechanism of photorespiration can be prevented by having cells saturated with internal carbon (Beardall, 1989). This concentrating mechanism was first thought to occur via a "biochemical carbon dioxide pump" in which auxiliary carboxylation of phosphoenolpyruvate occurs (Edwards and Walker, 1983). However no evidence exists for this mechanism to occur in micro-algae and it is now thought that there is an active transport of in-organic carbon into

the cell which is then stored and concentrated, thus suppressing the action of the oxygenase activity of Rubisco.

Culturing cells of micro-algae and cyanobacteria in the FPALR operating under batch kinetics was necessary in order to determine the cellular growth rates of *Chlorella vulgaris* 211/11c and *Synechococcus* 1479/5. The generated data was used to determine the maximum dilution rates that the cells could withstand prior to wash out from within the system. The effect of light, carbon dioxide concentration and culture temperature was only examined on the growth kinetics of the micro-algae and cyanobacteria. Further analysis was required to examine the effects of these parameters on the nutrient uptake and cellular physiology.

3.2.5 Nutrient uptake and cellular physiology of *Chlorella vulgaris* 211/11c and *Scenedesmus sp.* cultured in the FPALR.

Cells of *Chlorella vulgaris* 211/11c and *Scenedesmus sp.* were cultured in the FPALR to examine the effect of photon flux density and carbon dioxide concentration on the uptake rates of phosphate and nitrate and in particular the protein and carbohydrate content. The micro-algal culture media ASM, contained 7.4 mg l^{-1} phosphate (as K_2HPO_4) and 303.5 mg l^{-1} nitrate (as NaNO_3).

Figure 55 shows the increase in the dry matter content of *Chlorella vulgaris* 211/11c grown in the FPALR at a PFD of $100 \mu\text{mol s}^{-1} \text{ m}^{-2}$ with a carbon dioxide concentration of 2%, at a temperature of 23°C and a Reynolds number of 5800. The changes in the phosphate and nitrate content of ASM are also shown in Figure 55. The maximum removal rates of both phosphate and nitrate occurred when the cells were in the exponential growth phase (100-150 hours after inoculation). During this growth phase the phosphate and nitrate content of ASM decreased from 6.29 and 273.15 mg l^{-1} to 0.74 and 224.59 mg l^{-1} respectively. It was also found that removal of phosphate continued whilst cells were in the early and late stationary phases of growth (200-250 hours) whilst the removal of nitrate during this growth phase stopped. The minimum levels of phosphate and nitrate measured in the FPALR after cells of *Chlorella vulgaris* 211/11c had been cultured for 240 hours were found to be 0.07 and 200 mg l^{-1} respectively.

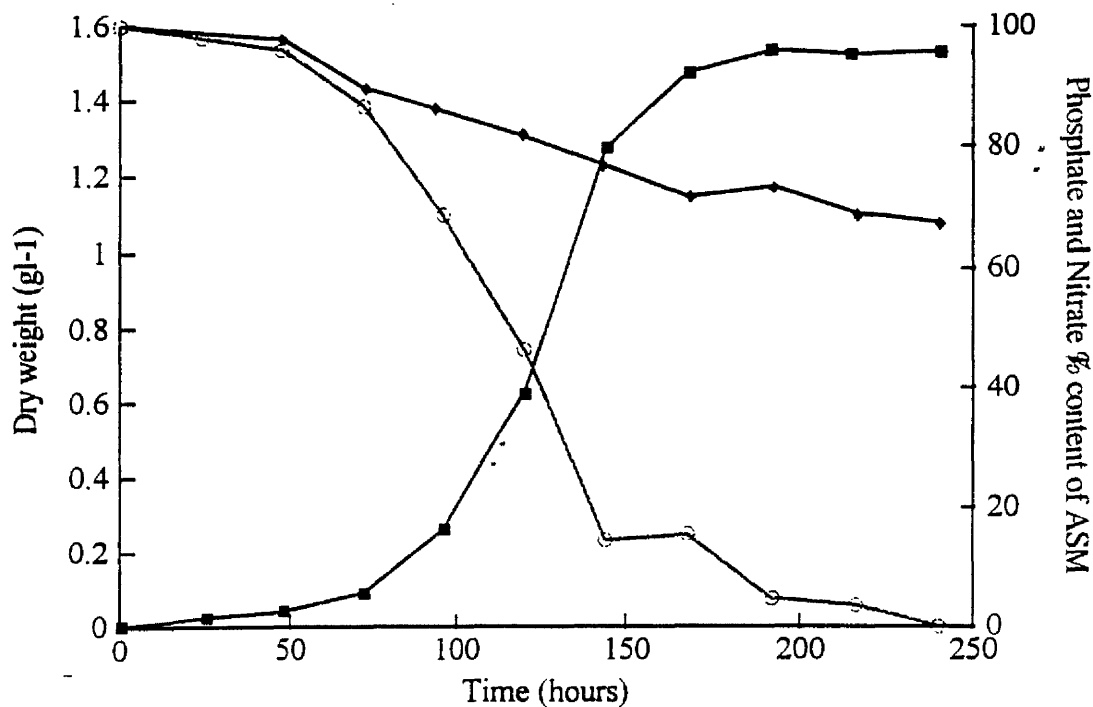


Figure 55. The percentage change in the nitrate and phosphate content of ASM whilst culturing *Chlorella vulgaris* 211/11c in the FPALR at a PFD of $100\mu\text{mol s}^{-1} \text{m}^{-2}$ at a carbon dioxide concentration of 2% v/v. ■—■ increase in dry matter, ◆—◆ change in nitrate, O—O change in phosphate.

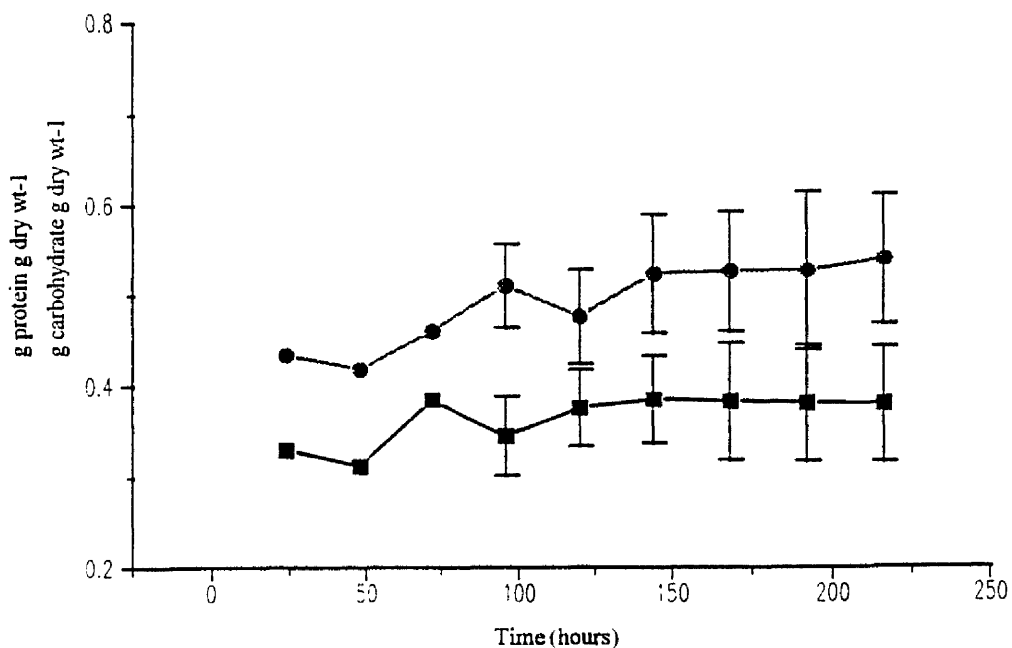


Figure 56. The variation in the carbohydrate and protein content of *Chlorella vulgaris* 211/11c cells cultured in the FPALR at a PFD of $100\mu\text{mol s}^{-1} \text{m}^{-2}$ at a carbon dioxide concentration of 2% v/v. ●—● change in carbohydrate, ■—■ change in protein.

Figure 56 shows the changes in the protein and carbohydrate content of cells of *Chlorella vulgaris* 211/11c when cultured in the FPALR in the conditions described for Figure 55. The carbohydrate content increased from 0.43 to 0.5 g carbohydrate per gram dry weight during a period of 8 days, whereas, the protein showed a small increase from 0.3 to 0.35 g protein per gram dry weight.

Figure 57 shows the change in the phosphate and nitrate content of ASM whilst cells of *Chlorella vulgaris* 211/11c were cultured in the FPALR with a PFD of $200\mu\text{mol s}^{-1}\text{ m}^{-2}$ in a carbon dioxide concentration of 2% v/v, in a Reynolds number of 5800 and a temperature of 23°C. As was observed in Figure 55, the phosphate and nitrate content of the ASM fell rapidly during the exponential growth phase (50-135 hours). This rate of removal, however, was higher as the phosphate content of the ASM was measured to be 0.148mg l^{-1} after 150 hours compared to 1.184mg l^{-1} for the culture irradiated at a PFD of $100\mu\text{mol s}^{-1}\text{ m}^{-2}$. The nitrate content of the ASM was also found to have decreased from 273.15 to 182.1 mg l^{-1} during the exponential growth phase.

Figure 58 shows the changes in the protein and carbohydrate content of cells cultured under the same conditions as described for Figure 57. After a time period of 150 hours when the cells were approaching late exponential growth phase, the carbohydrate content of the cells was $0.48\text{ g g dry wt}^{-1}$. The protein content of the cells increased from 0.32 to $0.46\text{ g g dry wt}^{-1}$ from 24 to 175 hours. During the stationary phase (175-225 hours) the protein level decreased to $0.42\text{ g g dry wt}^{-1}$.

The changes in phosphate and nitrate content of ASM in the presence of *Scenedesmus sp.* cultured in the FPALR under conditions PFD $100\mu\text{mol s}^{-1}\text{ m}^{-2}$ with a carbon dioxide concentration of 2% v/v at a temperature of 23°C with a Reynolds number of 5800 (Figure 59). Whereas with *Chlorella vulgaris* 211/11c, the phosphate content of the ASM was exhausted after 200-225 hours, *Scenedesmus sp.* had reduced the level of phosphate to approximately zero after 170 hours. The nitrate level in the ASM decreased to a minimum of 182.1 mg l^{-1} after 240 hours.

The changes in *Scenedesmus sp.* cellular protein and carbohydrate are shown in Figure 60. It can be seen that the protein levels showed a steady increase from 0.42 g g dry

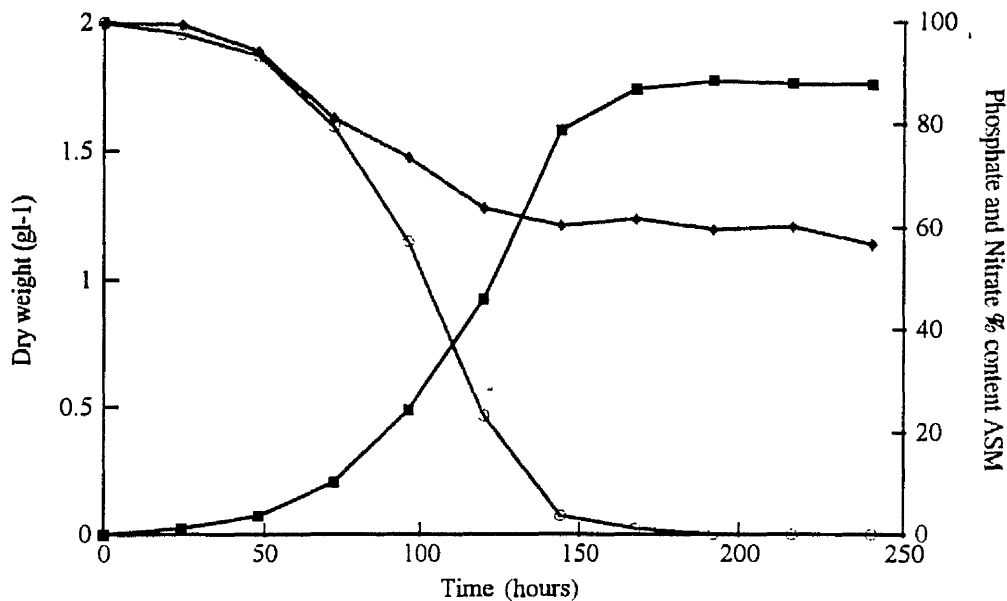


Figure 57. The percentage change in the nitrate and phosphate content of ASM whilst culturing *Chlorella vulgaris* 211/11c in the FPALR at a PFD of $200\mu\text{mol s}^{-1} \text{m}^{-2}$ at a carbon dioxide concentration of 2% v/v. ○—○ change in phosphate content, ◆—◆ change in nitrate content, ■—■ change in dry matter.

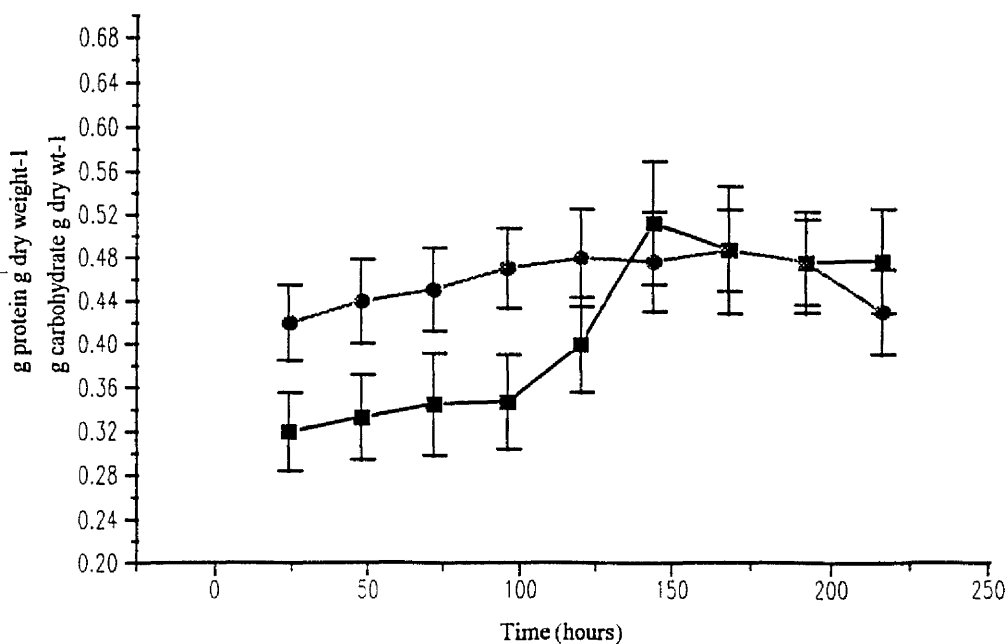


Figure 58. The variation in the carbohydrate and protein content of *Chlorella vulgaris* 211/11c cells cultured in the FPALR at a PFD of $200\mu\text{mol s}^{-1} \text{m}^{-2}$ at a carbon dioxide concentration of 2% v/v. ●—● change in carbohydrate, ■—■ change in protein.

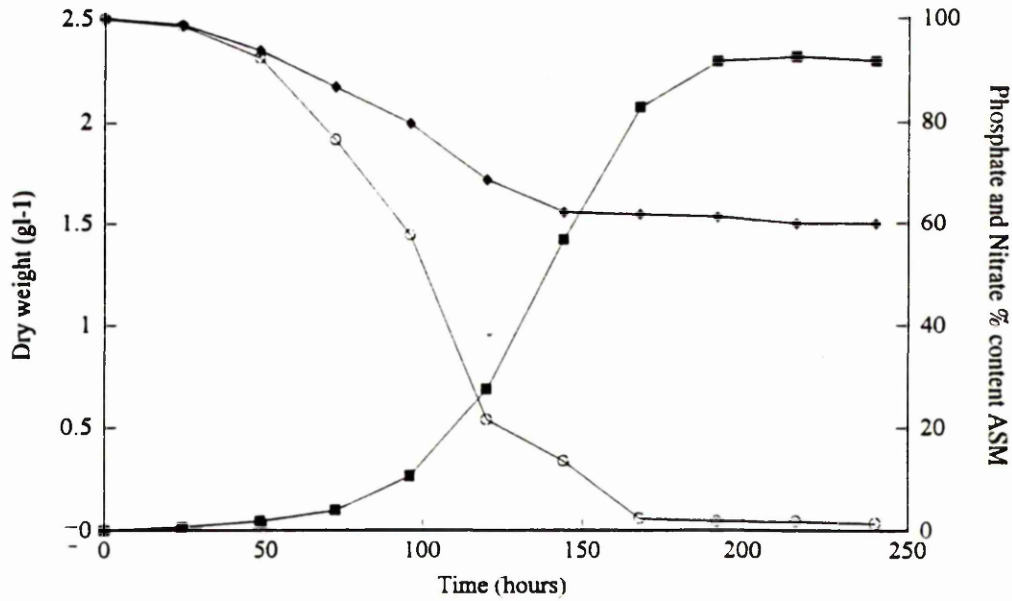


Figure 59. The percentage change in the nitrate and phosphate content of ASM whilst culturing *Scenedesmus sp.* in the FPALR at a PFD of $100\mu\text{mol s}^{-1} \text{m}^{-2}$ at a carbon dioxide concentration of 2% v/v. ○—○ change in phosphate content, ◆—◆ change in nitrate content, ■—■ change in dry matter.

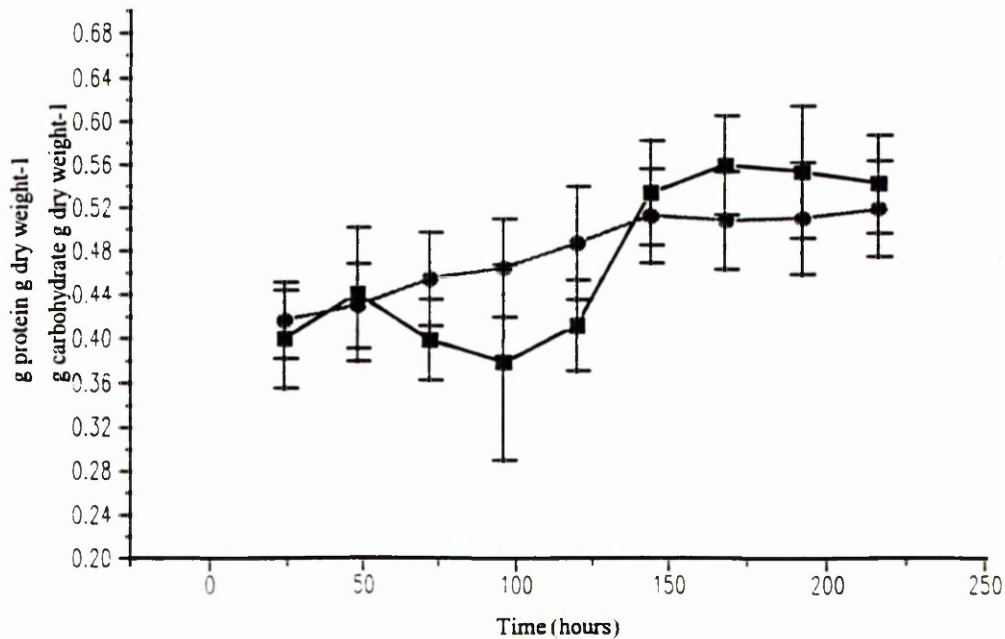


Figure 60. The variation in the carbohydrate and protein content of *Scenedesmus sp.* cells cultured in the FPALR at a PFD of $100\mu\text{mol s}^{-1} \text{m}^{-2}$ at a carbon dioxide concentration of 2% v/v. ●—● change in carbohydrate, ■—■ change in protein.

wt⁻¹ at 24 hours to 0.51 g g dry wt⁻¹ after 225 hours. The carbohydrate content, however, only showed a clear increase when the cells were in late exponential phase of growth, during which the carbohydrate increased from 0.37 g g dry wt⁻¹ at 100 hours to 0.54 g g dry wt⁻¹ after 175 hours.

Figure 61 shows the changes in phosphate and nitrate content of ASM during the culturing of *Scenedesmus sp.* At the elevated PFD of 200 μmol s⁻¹ m⁻², the phosphate content of ASM was completely removed after 175-200 hours. The phosphate uptake rate was no different from that measured from similar cells cultured at a reduced PFD of 100 μmol s⁻¹ m⁻². The nitrate uptake, however was greater from the culture irradiated at the higher PFD of 200 μmol s⁻¹ m⁻² compared to 100 μmol s⁻¹ m⁻² (Figure 59). The late stationary phase nitrate content of ASM was 157.8 mg l⁻¹. The changes in protein and carbohydrate from cells irradiated at 200 μmol s⁻¹ m⁻² are shown in Figure 62. The carbohydrate content was consistently higher than the protein content over the entire growth phase. Both carbohydrate and protein content increased with increasing time.

Figure 63 and 64 show the changes in the protein and carbohydrate content of cells of *Chlorella vulgaris* 211/11c cultured at a PFD of 100 μmol s⁻¹ m⁻², at Reynolds number of 5800 and a temperature of 23°C; the carbon dioxide concentrations were 0% (air grown) and 4% respectively. The carbohydrate content of air grown cells (Figure 63) was higher than that of cells cultured in a carbon dioxide concentration of 4% v/v (Figure 64). The maximum carbohydrate content was 0.47 g g dry wt⁻¹ during the mid exponential growth phase. As the culture approached stationary phase, this content decreased to 0.42 g g dry wt⁻¹, whereas, the protein content increased 0.33 g g dry wt⁻¹. Cells cultured in the same conditions but at 4% v/v carbon dioxide showed a different response (Figure 64). Carbohydrate content was significantly higher than the protein content. The maximum carbohydrate content was measure to be 0.48 g g dry wt⁻¹ during stationary phase of growth, whereas, the maximum protein content of 0.33 g g dry wt⁻¹ was measured during the mid exponential growth phase.

Figures 65 and 66 show the effect of air and air plus 4% carbon dioxide on the carbohydrate and protein content of *Scenedesmus sp.* grown under identical conditions as *Chlorella vulgaris* 211/11c. The air grown culture (Figure 65) had a

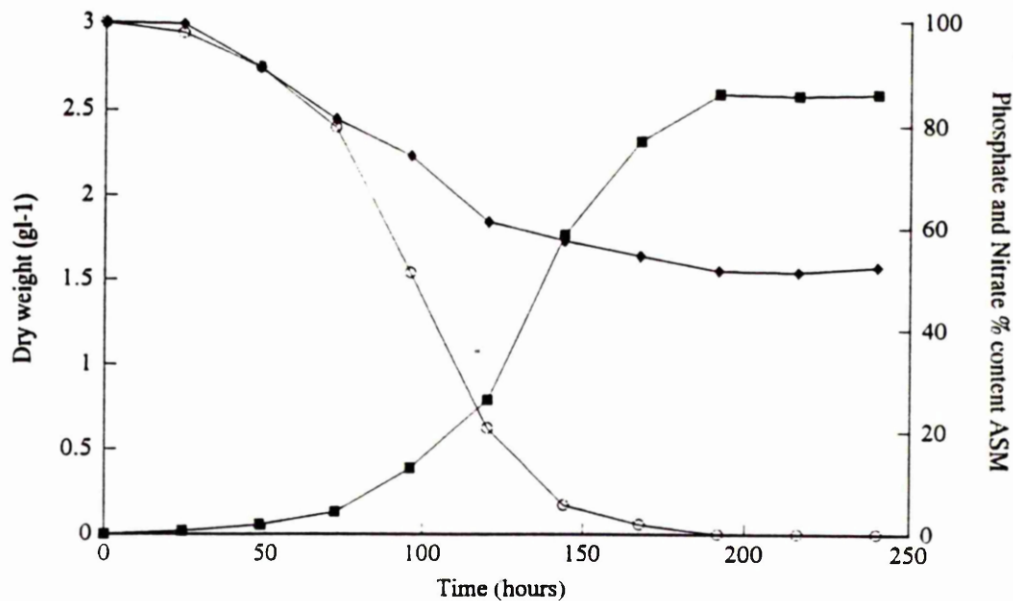


Figure 61. The percentage change in the nitrate and phosphate content of ASM whilst culturing *Scenedesmus sp.* in the FPALR at a PFD of $200\mu\text{mol s}^{-1} \text{m}^{-2}$ at a carbon dioxide concentration of 2% v/v. $\circ-\circ$ change in phosphate content, $\blacklozenge-\blacklozenge$ change in nitrate content, $\blacksquare-\blacksquare$ change in dry matter.

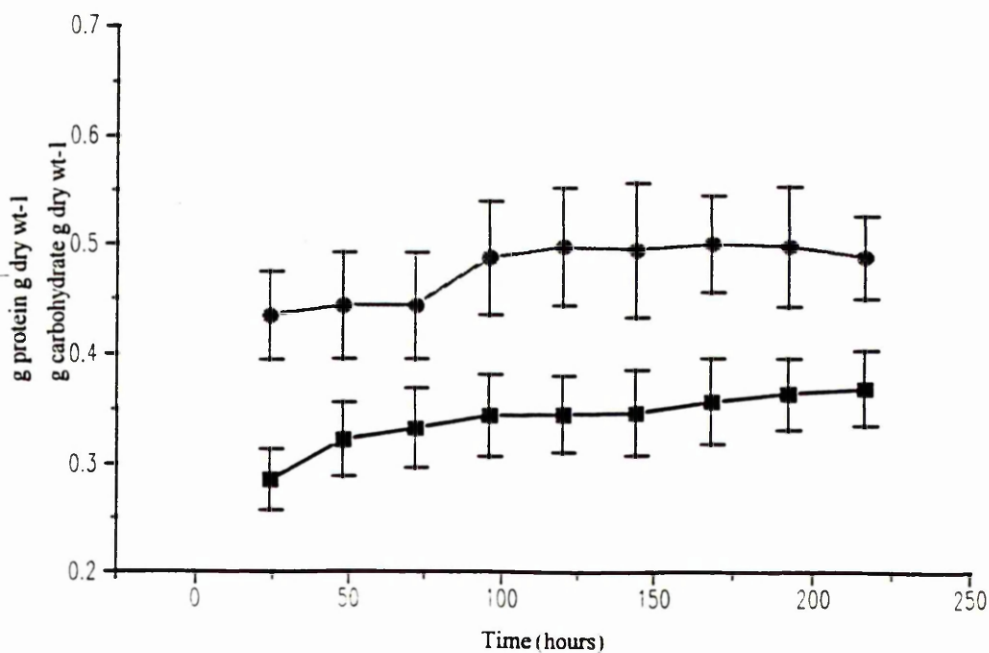


Figure 62. The variation in the carbohydrate and protein content of *Scenedesmus sp.* cells cultured in the FPALR at a PFD of $200\mu\text{mol s}^{-1} \text{m}^{-2}$ at a carbon dioxide concentration of 2% v/v. $\bullet-\bullet$ change in carbohydrate, $\blacksquare-\blacksquare$ change in protein.

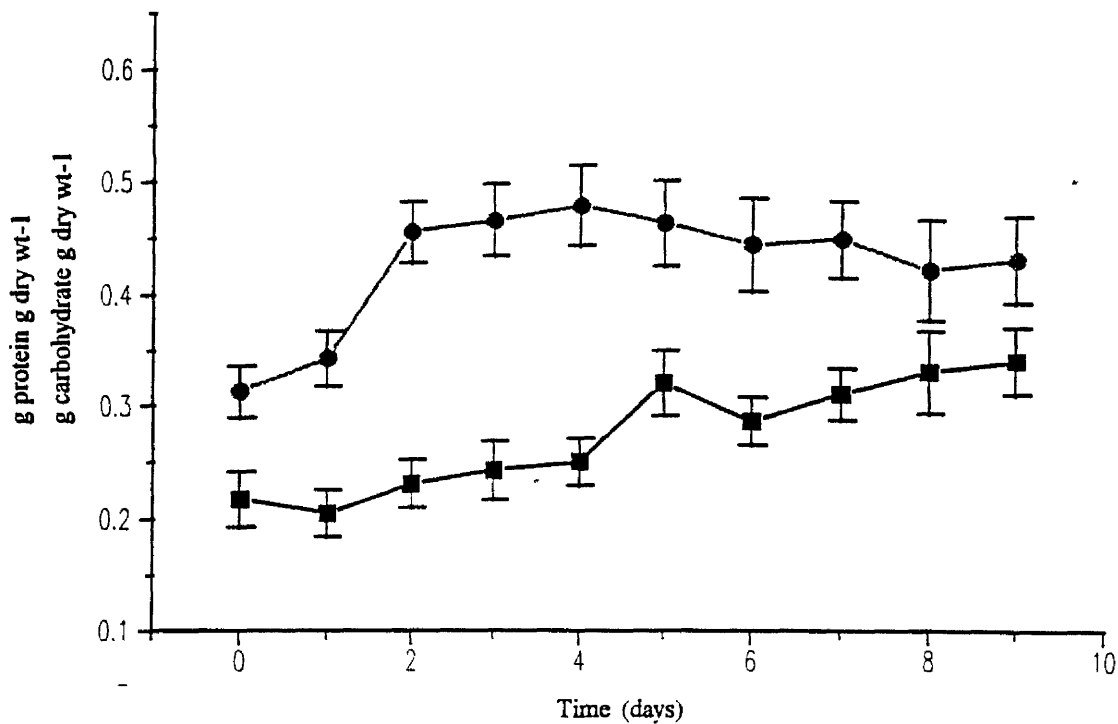


Figure 63. The variation in the carbohydrate and protein content of *Chlorella vulgaris* 211/11c cultured in the FPALR at a PFD of $100\mu\text{mol s}^{-1} \text{m}^{-2}$ with air. ●—● change in carbohydrate, ■—■ change in protein

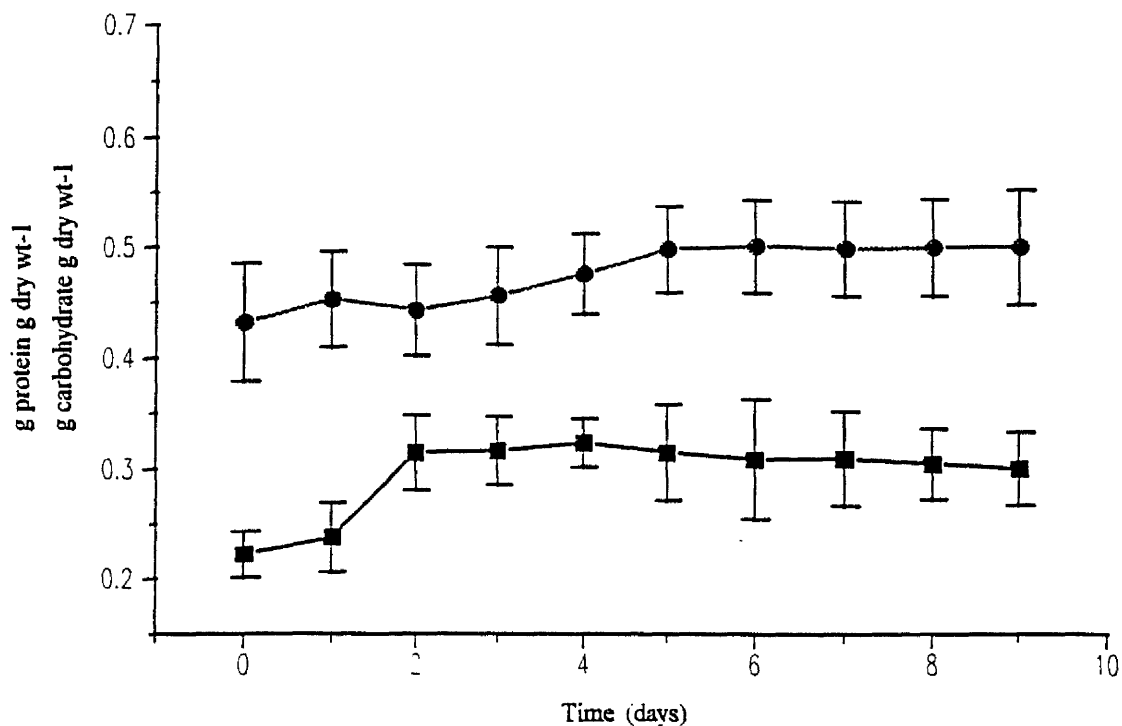


Figure 64. The variation in the carbohydrate and protein content of *Chlorella vulgaris* 211/11c cells cultured in the FPALR at a PFD of $200\mu\text{mol s}^{-1} \text{m}^{-2}$ at a carbon dioxide concentration of 4% v/v. ●—● change in carbohydrate, ■—■ change in protein.

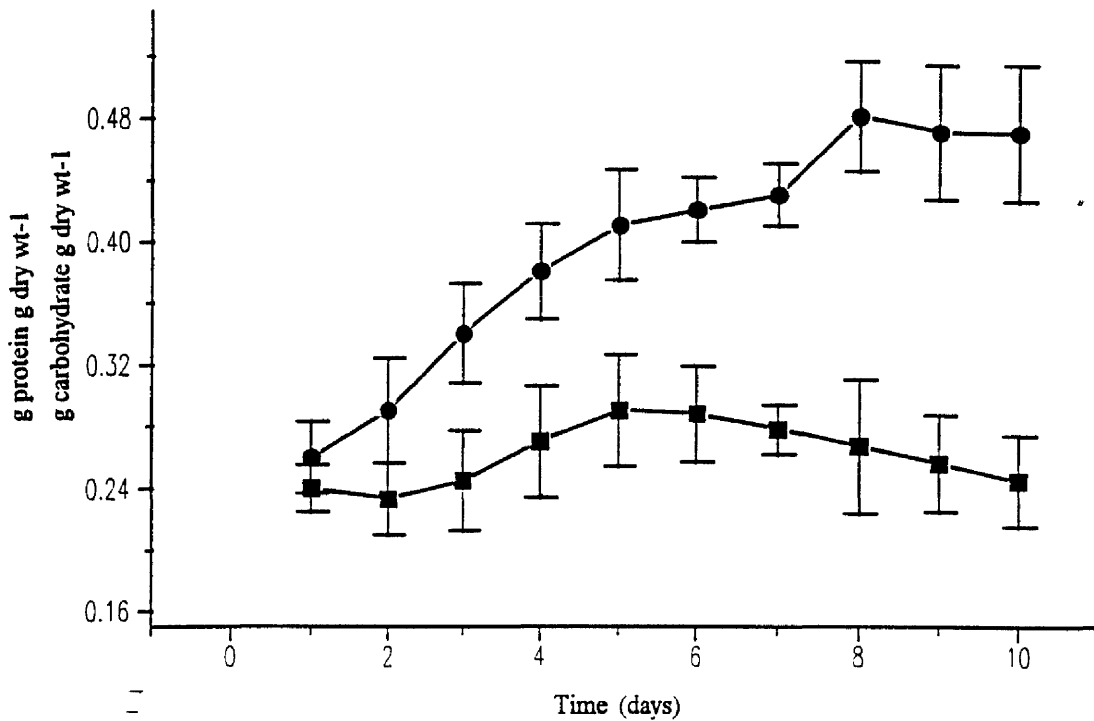


Figure 65. The variation in the carbohydrate and protein content of *Scenedesmus sp.* cultured in the FPALR at a PFD of $100\mu\text{mol s}^{-1} \text{m}^{-2}$ with air. ●—● change in carbohydrate, ■—■ change in protein

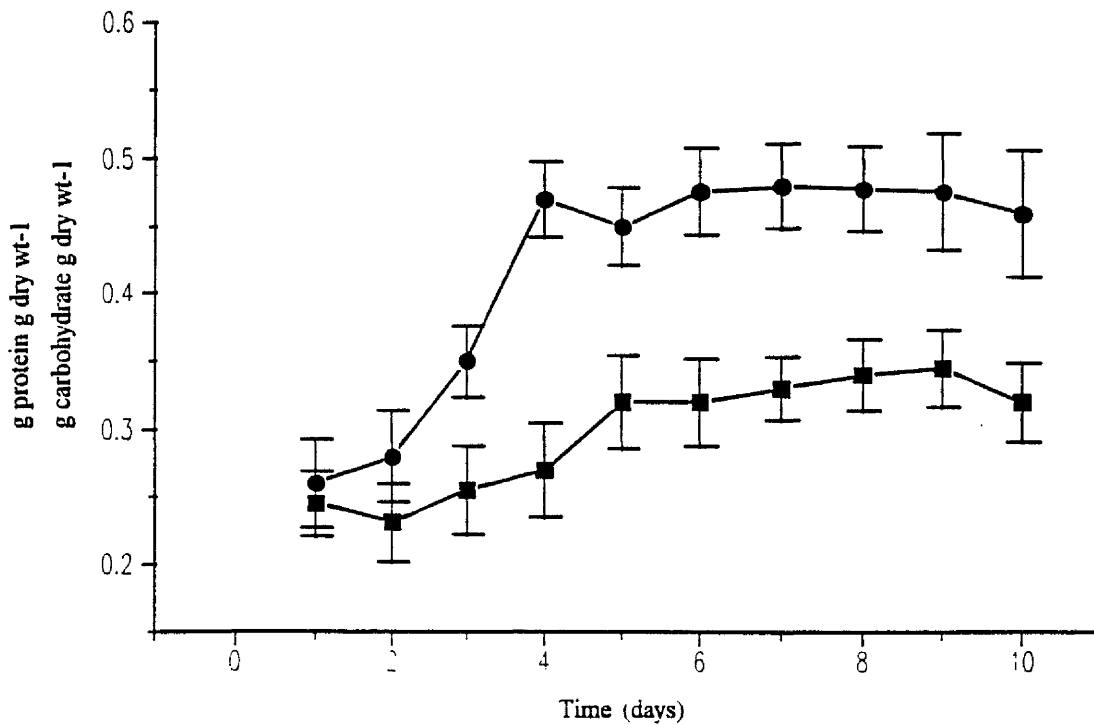


Figure 66. The variation in the carbohydrate and protein content of *Scenedesmus sp.* cells cultured in the FPALR at a PFD of $100\mu\text{mol s}^{-1} \text{m}^{-2}$ at a carbon dioxide concentration of 4% v/v. ●—● change in carbohydrate, ■—■ change in protein.

much higher carbohydrate content compared to protein. During the growth cycle, carbohydrate increased from 0.26 to 0.48 g g dry wt⁻¹ (day 1 to day 8). The maximum carbohydrate content was 0.48 g g dry wt⁻¹ measured at day 8, after which the carbohydrate content decreased to 0.46 g g dry wt⁻¹ during the stationary growth phase. The protein content increased steadily from 0.24 to a maximum of 0.28 g g dry wt⁻¹ (day 1 to day 5) at the mid exponential phase of growth. As the cells approached stationary growth phase the protein content decreased to 0.25 g g dry wt⁻¹.

Figures 67 and 68 show the variations in protein and carbohydrate content of *Chlorella vulgaris* 211/11c and *Scenedesmus sp.* respectively cultured in the presence of 10% v/v carbon dioxide. The protein content of *Chlorella vulgaris* 211/11c (Figure 67) increased from 0.2 g g dry wt⁻¹ measured at day 1 to 0.47 g g dry wt⁻¹ measured during the late stationary growth phase (day 10), whereas carbohydrate remained steady from day 1 to day 8 at a level of 0.41 g g dry wt⁻¹ before decreasing after day 8 to 0.35 g g dry wt⁻¹. *Scenedesmus sp.* (Figure 68), however, showed a different response to being grown in the presence of 10% v/v carbon dioxide. The carbohydrate content of the cells showed a small increase from 0.34 g g dry wt⁻¹ at day 1 to 0.44 g g dry wt⁻¹ at day 10. The protein content also showed a small increase over the entire growth stage, increasing from 0.17 g g dry wt⁻¹ at day 1 to 0.22 g g dry wt⁻¹ at day 10.

It was generally found that cells of *Chlorella vulgaris* 211/11c and *Scenedesmus sp.* showed an increase in carbohydrate content towards the stationary growth phase (Figures 56, 60, 63, 64, 65,66 and 68). When the cells of *Chlorella vulgaris* 211/11c were cultured in the presence of 10% v/v carbon dioxide (Figure 67) there was a marked change in the cellular contents compared to that of *Scenedesmus sp.* (Figure 68). In *Chlorella vulgaris* 211/11c, the protein content surpassed the carbohydrate content towards the stationary growth phase where as previously noted, an increase in carbohydrate was more common. This may reflect that the carbon dioxide concentration was at toxic levels to the cells indicated by low growth rates (Figure 38). *Scenedesmus sp.*, however, showed no toxic response to a carbon dioxide concentration of 10%. The protein content of the cells was clearly much lower than the carbohydrate content.

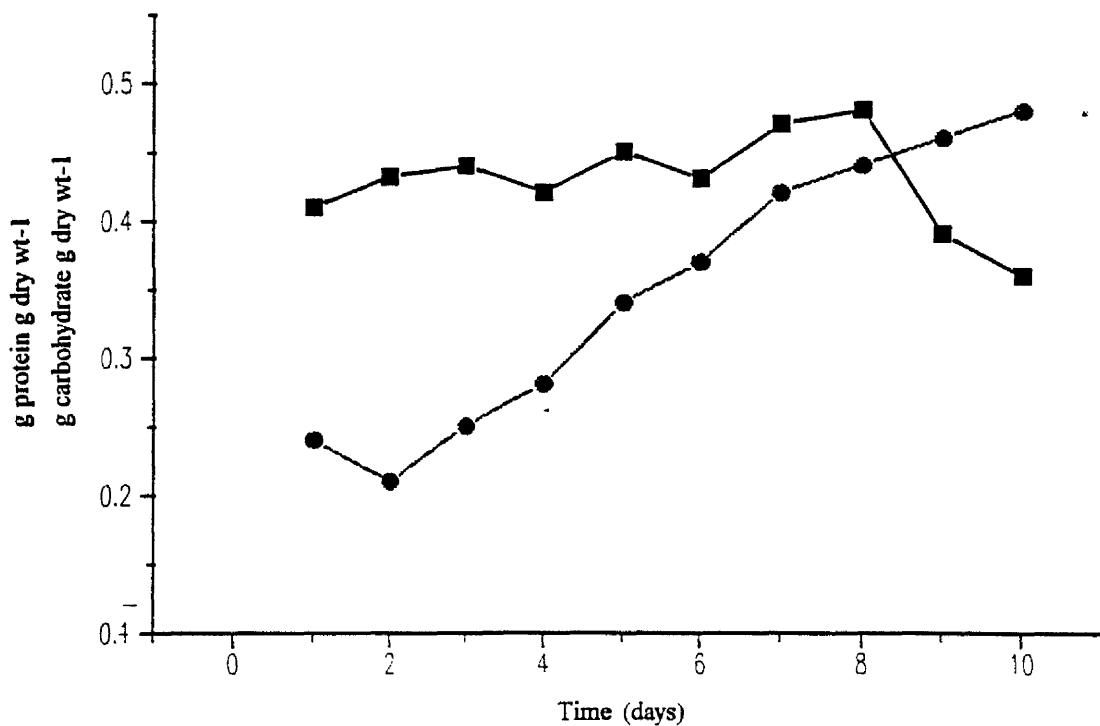


Figure 67. The variation in the carbohydrate and protein content of *Chlorella vulgaris* 211/11c cultured in the FPALR at a PFD of $100\mu\text{mol s}^{-1} \text{m}^{-2}$ with 10% v/v carbon dioxide. ●—● change in carbohydrate, ■—■ change in protein

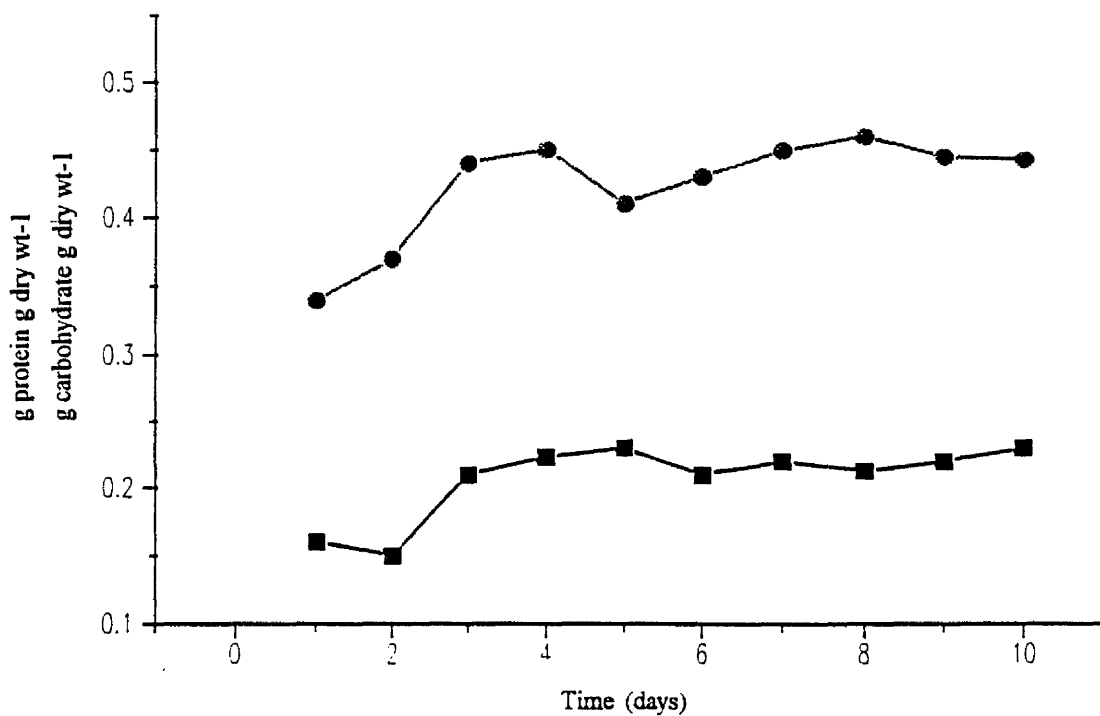


Figure 68. The variation in the carbohydrate and protein content of *Scenedesmus sp.* cells cultured in the FPALR at a PFD of $100\mu\text{mol s}^{-1} \text{m}^{-2}$ at a carbon dioxide concentration of 10% v/v. ●—● change in carbohydrate, ■—■ change in protein.

Nutrient availability and uptake has a major affect on both the productivity of the organism but also on its internal physiology. Behrens *et al.*, (1989), reported that cells of *Chlorella vulgaris* 211/11c which became nitrogen limited channelled carbon into carbohydrate storage and were found to contain 55% starch, whereas cells cultured under nitrogen rich conditions contained 20% starch. The research also found that the formation of starch was affected by the pH of the system and that the optimum starch production was at pH 7.5 to 8.0 although the optimum growth rates were measured at pH 7.0. The findings of the experiments carried out in this Section (3.2.5) support the work of Behrens *et al.*, (1989) which showed that between 30% and 50% of the cells of *Chlorella vulgaris* 211/11c, *Scenedesmus sp.* and *Synechococcus* 1479/5 was in the form of carbohydrate. It was also shown that the protein content in the cells of *Chlorella vulgaris* 211/11c could contain protein levels as high as 40% protein when nitrogen was in plentiful supply compared to 19% protein of biomass when the cells were nitrogen limited. Nitrate was chosen as the sole source of nitrogen since Borowitzka and Borowitzka, (1988b) reported that under conditions of acidification by carbon dioxide input, the ammonium (NH_4^+ ion) was capable of causing cell death because of the rapid acidification of the medium resulting in ammonium uptake and metabolism. The above observations (Figures 55 and 57) support the findings of Kanda *et al.*, (1989) and Vincent, (1992), who reported that nitrate uptake increased with increasing light intensity. Nutrients have also been shown to affect the periodicity of some photosynthetic organisms. Putt and Prezelin, (1988) found that the photosynthetic periodicity of *Thalassiosira weissflogii* was not evident when placed in fluctuating light intensity. Changing nutrients and in particular the addition of nitrogen in the form of ammonium, however, was found to dramatically produce changes in the maximum rate of photosynthesis.

Cellular storage of protein and carbohydrate is greatly affected by the external conditions in which the cells are cultured. Warr *et al* (1985) determined that the storage process of cells of the cyanobacteria *Synechocystis* PCC 6714 was dependent on the salinity and temperature; low salinity and high temperatures resulted in carbohydrate being stored as sucrose. Philippis *et al.*, (1993), reported that the protein and carbohydrate storage ability of *Cyanothece sp.* was affected greatly by the presence of particular elements. In the absence of magnesium, potassium and calcium ions the synthesis of proteins and carbohydrates was close to 50% lower compared to cells culture in the presence of these ions. Although the FPALR was run under batch

kinetics in which phosphate ions were reduced to approximately zero, the addition of further phosphate was not found to affect the growth of micro-algae or cyanobacteria. This suggested that the cells were taking up phosphate merely for storage and possible future division.

3.2.6 The effect of Reynolds number on the cell dynamics of *Chlorella vulgaris* 211/11c.

The FPALR was primarily designed for the study of micro-algal / cyanobacterial photosynthesis and physiology. However due to the complexity of the system's design in optimising the light environment and gas mixing capability, the response of the photosynthetic cells to the high shear forces that exist in the FPALR required examination. An image analysis system was used to examine cells of *Chlorella vulgaris* 211/11c cultured in the FPALR at different Reynolds numbers to determine the effects of high turbulence on cellular dynamics. Image analysis and other forms of direct measurement e.g. flow cytometry are being increasingly used as a method of rapid counting and size analysis of cells and particles (Balfort *et al.*, 1992).

Figure 69 shows the effects of increasing Reynolds number on the cellular dynamics (breadth, area and main objective length) of cells of *Chlorella vulgaris* 211/11c. Figure 70 displays the effect of Reynolds number on the overall cellular volume. It was found that increasing the Reynolds number from 2500 to 3500 resulted in an increase in cell breadth, length and area. However area, breadth and main objective cell length were observed to decrease as the Reynolds number increased above 3500.

It is suggested that the peak cells size at a Reynolds number of 3500 indicated that this was the optimum flow rate for cells of *Chlorella vulgaris* 211/11c. The difference between cellular dynamics measured at a Reynolds number of 3500 and 6200 were statistically significant at $P=0.001$ level ($n=6$).

Running the FPALR at very high Reynolds numbers was considered to be essential since it was necessary to ensure that cells in the system were fully mixed and in turbulent conditions in which the degree of self shading was at a minimum. This was

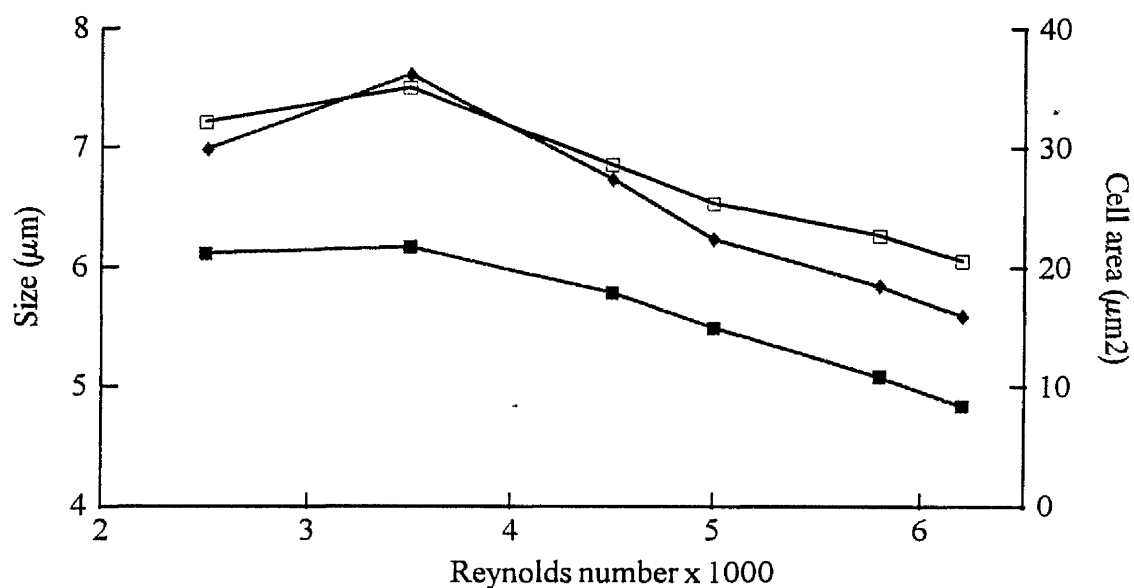
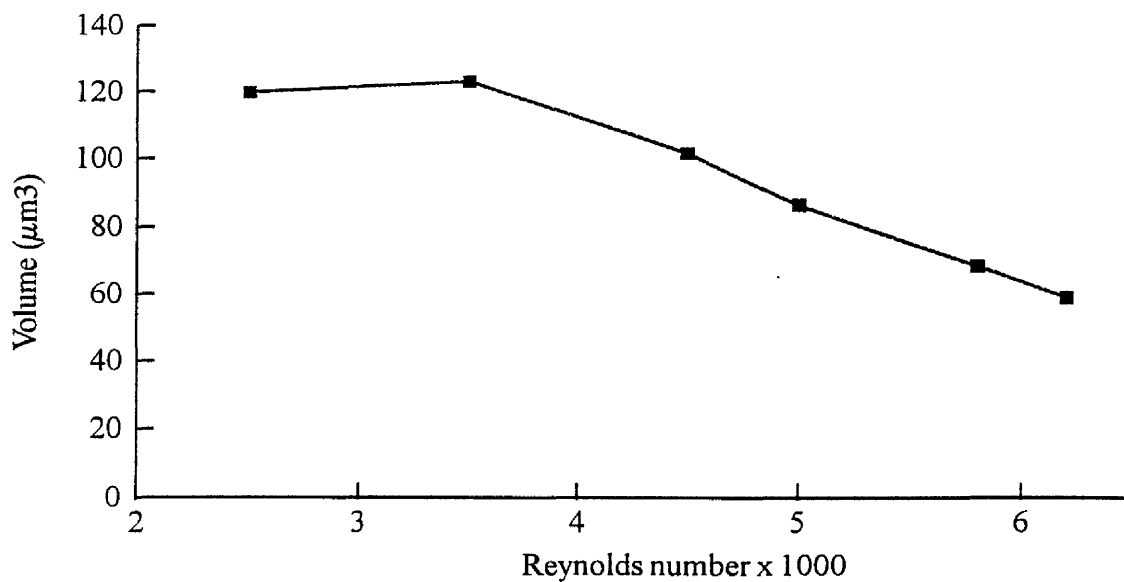


Figure 69. The effect of Reynolds number on the cell dynamics of *Chlorella vulgaris* 211/11c cultured in the FPALR. ◆—◆ cell main objective length (µm), ■—■ cell breadth (µm), (□—□) cell area (µm²).



4% CO₂ 23°C PFD 200µmol s⁻¹ m⁻²

Figure 70. The effect of Reynolds number on the cell volume (µm³) of *Chlorella vulgaris* 211/11c cultured in the FPALR.

important since increasing external factors such as temperature, light etc. may have given incorrect interpretations on the metabolic status of the micro-algal cells. The effect of photon flux density ($\mu\text{mol s}^{-1} \text{m}^{-2}$) and carbon dioxide concentration were not found to significantly affect cellular dynamics (data not shown). It is suggested that the changes in cell size created by changes in Reynolds number were entirely due to the physical forces that were active on the cells in FPALR. At very high Reynolds numbers cells were significantly smaller since in this flow regime the impact energy of the cell on the sides of the FPALR and the fluid on the cell was higher. It is unclear as to whether the cells responded by creating a smaller tighter more robust structure. Further analysis of cell stress levels is required.

3.2.6.1 Macro programming for the cellular analysis of *Chlorella vulgaris* 211/11c.

The following macro program was written for the frame capture, stop motion, filter, automatic extract / export and subsequent cellular measurement of *Chlorella vulgaris* 211/11c cells taken from the FPALR. The program contains two key routines: Firstly KEY.MAC contains all the routines for opening configuration files, activating the calibration file and setting the threshold limits. This routine also handles the exportation of data into the appropriate file format. Secondly ROI.MAC is the program that generates the random fields and determines the screen width and the pan / scrolling that is required.

KEY.MAC

```
if (Prompt("Ready to initialise standard settings"));
    OpenConfiguration ("C:/OPTIMAS/TAI1.CFG");

    if (prompt("The current calibration is" : ActiveCalibration : " \n Do you want
to change it?" ) )

        Calibrate ();
        while (IsWindow("Calibration"));

    if (prompt("Now ready to check threshold"));
```

```

MySetVal= Threshold ();
    Show (MySetVal);

    if (Prompt("Remember that this will create a new datafile"));
    RunMacro ("C:/mac/format.mac");
DataFile ("C:/OPTIMAS/NEW.OPS");
    if (prompt("The following MACRO will acquire a new
image"));
beep (40,6);

if (prompt("Remember, this program will export data and acquire new fields until you
press any key"));
    beep (40,9);
    BOOLEAN bAcquireForever = TRUE;
RunMacro ( "c:/mac/roi.mac");
SetExport (NULL, 0, FALSE);

    SetExport (NULL, 1, FALSE);
        SetExport (, 0, TRUE);
            SetExport (, 1, TRUE);

SetExport (ArArea, 1, TRUE);
    SetExport (ArBreadth, 1, TRUE);
        SetExport (ArMajorAxisLength, 1, TRUE);
            SetExport (ArPerimeter, 1, TRUE);

AutoClassify = TRUE;

{
    Local INTEGER count = 0;
        Local REAL myroi[,] = ROI;
            PositionWindow ("Macro - KEY.MAC", 100, 139, 401,
201);

                if (!IsWindow ("ArPoints"))
                    viewbox (ArPoints);

```

```

if (!IsWindow ("MyROI"))
    viewbox (myroi);
    PositionWindow ("myroi", -5, 58, 401, 201);
if (!IsWindow ("Count"))
    viewbox (count);
    PositionWindow ("count", 223, 262, 401, 201);
if (!IsWindow ("ArArea"))
    viewbox (ArArea);
    PositionWindow ("ArArea",200, 200);
    PositionWindow ("data", 517, 118, 98, 118);
if(prompt ("Okay to place viewboxes. Use mouse to click on okay as Return will be
a keypress and will terminate the MACRO");

    keyhit ();
    while (Keyhit() == 0)
        beep ((Integer) RAND () % 68);
        filters (StopMotion );
        if (bAcquireForever)
            Acquire();
Filters(StopMotion );
count += 1;
myroi = RandRoi ();
myroipix = ConvertCalibToPixels (myroi);
scroll (myroipix[1] - 80);
pan (myroipix[0]);
CreateArea (, -1, TRUE);
}

delete (bAcquireForever);
}
ROI.MAC
/*
RANDROI.MAC

```

Entry Points:

```
    RandROI ();
*/

define RandROI ()
{
    LOCAL REAL FullScreenDimensions[2];
    LOCAL REAL NewROI[4];

    FullScreenDimensions =
        (ROIFullScreen[2] - ROIFullScreen[0]) :
        (ROIFullScreen[3] - ROIFullScreen[1]);

    NewROI = FullScreenDimensions * (REAL) rand (2) / 32000
        + ROIFullScreen [0 : 1];
    NewROI := FullScreenDimensions * (REAL) rand(2) / 32000
        + ROIFullScreen [0 : 1];
    SelectROI (NewROI);
    return (NewROI);
}
DeleteProtect( RandROI );

while (TRUE) {
    RandROI ();
}
```

The macro program runs independently of the user but a single key stroke will stop the running in order to obtain a new field. The macro FORMAT.MAC determines which values are to be exported and the format. FORMAT also sets up the initial data link up enabling data transfer between the datafile and the export configuration. The macro routine was found to be invaluable for the automatic measurement and export of data to ASCII code.

3.3 The measurement of Photosynthesis / irradiance curves.

The photosynthesis response curve, whether it is photosynthesis / irradiance (P/ I), photosynthesis / carbon dioxide, photosynthesis / pigment or photosynthesis / temperature has been used throughout research experiments to describe / determine a cell's response and metabolic status to various set conditions. The methodology used for measuring photosynthesis / response curves and more importantly the interpretation of the generated data has been an area of great interest. There are still no commonly agreed protocols for measuring photosynthesis response curves. Factors such as temperature, suspending medium, initial oxygen saturation, nutrient availability (carbon, nitrate, phosphate and trace elements), pH, light source (spectral quality), time of exposure to irradiance, time interval between irradiance steps, optical density of culture in analysis chamber, culture growth stage, sample preparation and previous light history all affect the nature of the photosynthesis response curve.

3.3.1 Comparison of photosynthesis / irradiance response curves measured in the presence and absence of Bicarbonate.

Photosynthesis / irradiance curves were normally determined for micro-algae and cyanobacteria in ASM medium in the oxygen electrode chamber. Preliminary investigations were undertaken to investigate the effect of various nutrients upon the photosynthesis / irradiance response curve.

Cells of *Chlorella vulgaris* 211/11c, *Scenedesmus sp.* and *Synechococcus* 1479/5 were used to examine the affect of bicarbonate on their respective photosynthesis / irradiance curves. All photosynthesis response curves were measured in triplicate from duplicate micro-algal / cyanobacterial cultures.

Figure 71 shows the photosynthesis / irradiance curves of cells of *Chlorella vulgaris* 211/11c measured in the presence and absence of 2mM NaHCO₃, photosynthetic parameters are presented in Table 14. It can be seen (Figure 71) that the addition of

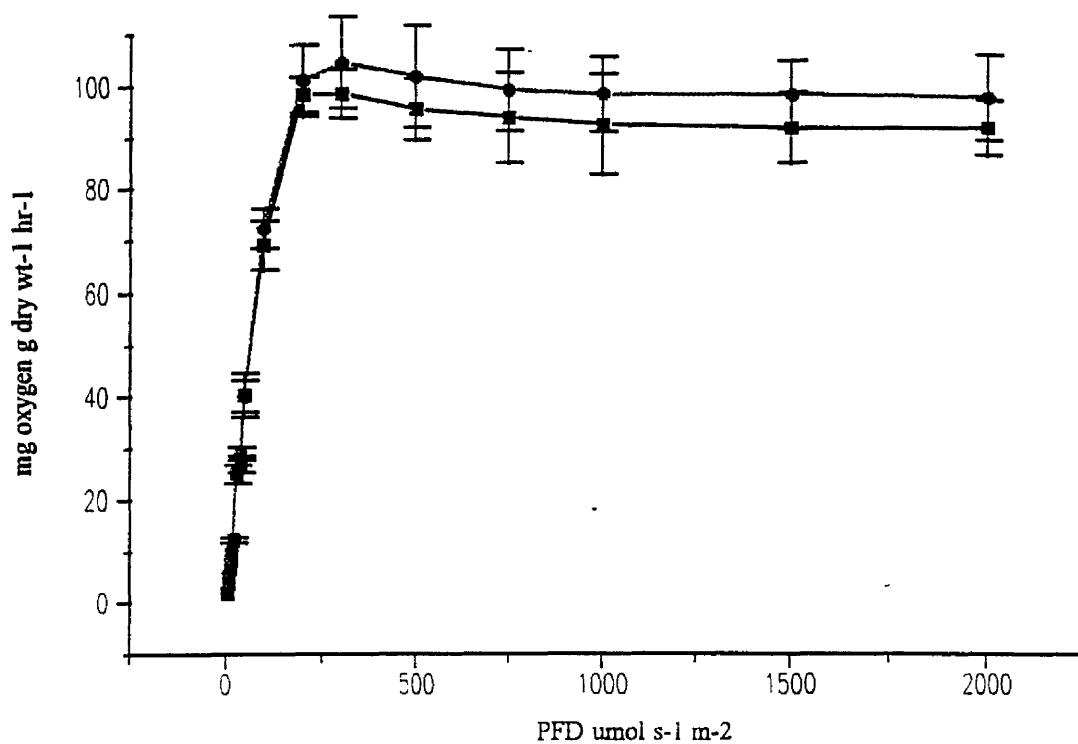


Figure 71. The effect of bicarbonate addition on the photosynthesis / irradiance response curves of *Chlorella vulgaris* 211/11c, ●—● ASM and 2mM HCO₃⁻, ■—■ ASM.

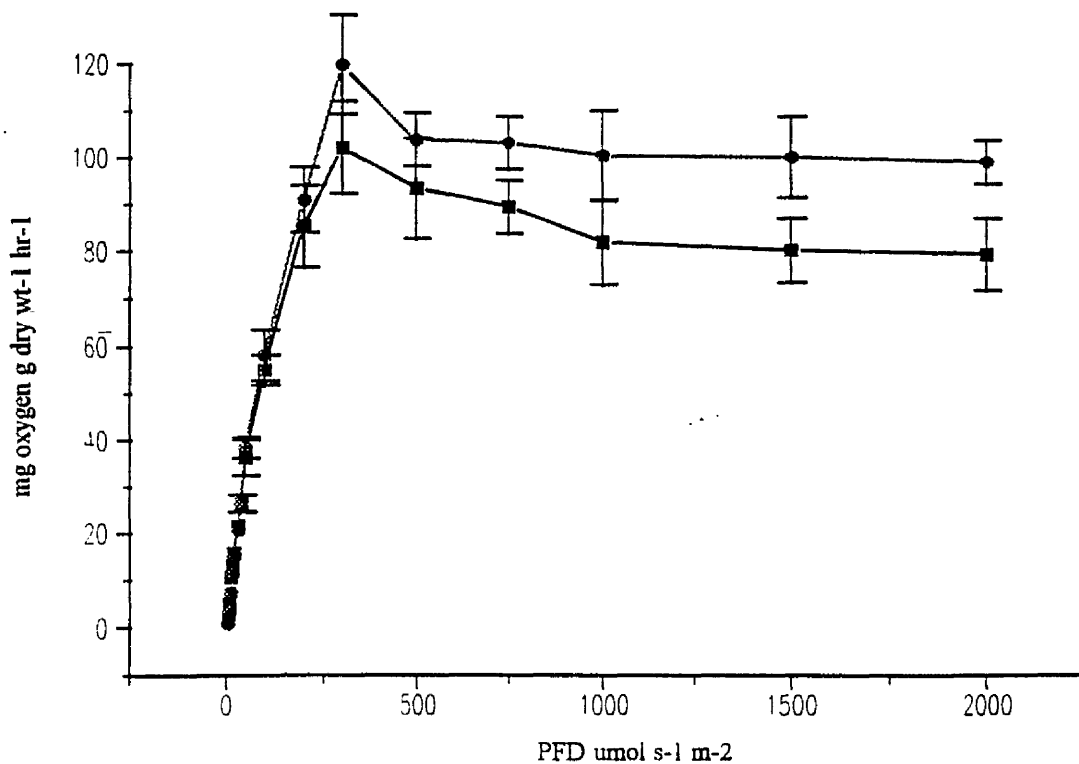


Figure 72. The effect of bicarbonate addition on the photosynthesis / irradiance response curves of *Scenedesmus* sp., ●—● ASM and 2mM HCO₃⁻, ■—■ ASM.

Table 14. The effect of bicarbonate on the photosynthesis / irradiance curve measurements of cells of *Chlorella vulgaris* 211/11c.

P / I parameter	ASM	ASM + 2mM Bicarbonate
α (mg oxygen g dry wt ⁻¹ hr ⁻¹ / $\mu\text{mol s}^{-1} \text{m}^{-2}$)	0.554	0.615
P_{max} (mg oxygen g dry wt ⁻¹ hr ⁻¹)	98.45	104.45
I_k ($\mu\text{mol s}^{-1} \text{m}^{-2}$)	177.7	169.8
$P_{\text{max}}^{\text{PPFD}}$ ($\mu\text{mol s}^{-1} \text{m}^{-2}$)	300	300
Initial dark respiration (mg oxygen g dry wt ⁻¹ hr ⁻¹)	19.072 ± 2.35	20.48 ± 3.2
LEDR (mg oxygen g dry wt ⁻¹ hr ⁻¹)	59.425 ± 3.67	60.75 ± 4.2

Table 15. The effect of the presence and absence of 2mM NaHCO₃ on the photosynthetic parameters of cells of *Scenedesmus* sp.

P / I parameter	ASM	ASM + 2mM Bicarbonate
α (mg oxygen g dry wt ⁻¹ hr ⁻¹ / $\mu\text{mol s}^{-1} \text{m}^{-2}$)	0.9677	0.8814
P_{max} (mg oxygen g dry wt ⁻¹ hr ⁻¹)	102.07	119.06
I_k ($\mu\text{mol s}^{-1} \text{m}^{-2}$)	105.47	135.08
$P_{\text{max}}^{\text{PPFD}}$ ($\mu\text{mol s}^{-1} \text{m}^{-2}$)	300	300
Initial dark respiration (mg oxygen g dry wt ⁻¹ hr ⁻¹)	14.65 ± 1.23	14.58 ± 1.98
LEDR (mg oxygen g dry wt ⁻¹ hr ⁻¹)	66.75 ± 2.44	78.39 ± 4.6

2mM NaHCO₃ had only a very slight effect on the photosynthesis / irradiance curves of *Chlorella vulgaris* 211/11c. The presence of NaHCO₃ resulted in an increase in the light limited slope (α) from 0.554 to 0.615 $\mu\text{mol s}^{-1} \text{m}^{-2}$. The values of P_{max}, initial dark respiration and light enhanced dark respiration rates were not affected by NaHCO₃ (Table 14).

The photosynthesis / irradiance curves of cells of *Scenedesmus sp.* measured in the presence and absence of 2mM NaHCO₃ are shown in Figure 72.

The photosynthetic parameters determined from the photosynthesis / irradiance curves are presented in Table 15. From Figure 72 it can be seen that the presence of NaHCO₃ increased the photosynthetic rates of this organism. The value of α decreased from 0.9677 to 0.8814 mg oxygen g dry wt⁻¹ hr⁻¹ / $\mu\text{mol s}^{-1} \text{m}^{-2}$ in the presence of 100mM NaHCO₃. The maximum rate of photosynthesis P_{max} increased from 102.07 to 119.06 $\mu\text{mol s}^{-1} \text{m}^{-2}$ in the presence of 2mM NaHCO₃. The value of I_k increase as a direct result of the changes in alpha and P_{max}. The presence of 100mM NaHCO₃ had no effect on the initial dark respiration rate measured to be approximately 14 mg oxygen g dry wt⁻¹ hr⁻¹. The LEDR rate, however, increased from 66.75 to 78.39 mg oxygen g dry wt⁻¹ hr⁻¹.

Figure 73 shows the effect of the presence and the absence of 2mM NaHCO₃ on the photosynthesis / irradiance curves of *Synechococcus* 1479/5. The photosynthetic parameters determined from Figure 73 are presented in Table 16. In contrast to Figures 71 and 56 cells of *Synechococcus* 1479/5 responded to the presence 2mM NaHCO₃, and increased their photosynthetic rates.

Unlike cells of *Scenedesmus sp.* it can be seen from Table 16 that the value of α almost doubled from 0.492 to 0.909 mg oxygen g dry wt⁻¹ hr⁻¹ / $\mu\text{mol s}^{-1} \text{m}^{-2}$, as a consequence of incubating cells in the presence of 2mM NaHCO₃. The maximum rate of photosynthesis (P_{max}) was found to have increased from 89.55 to 105.4 mg oxygen g dry wt⁻¹ hr⁻¹. As a result of the changes in α and P_{max}, I_k was found to decrease from 182.62 to 115.95 $\mu\text{mol s}^{-1} \text{m}^{-2}$.

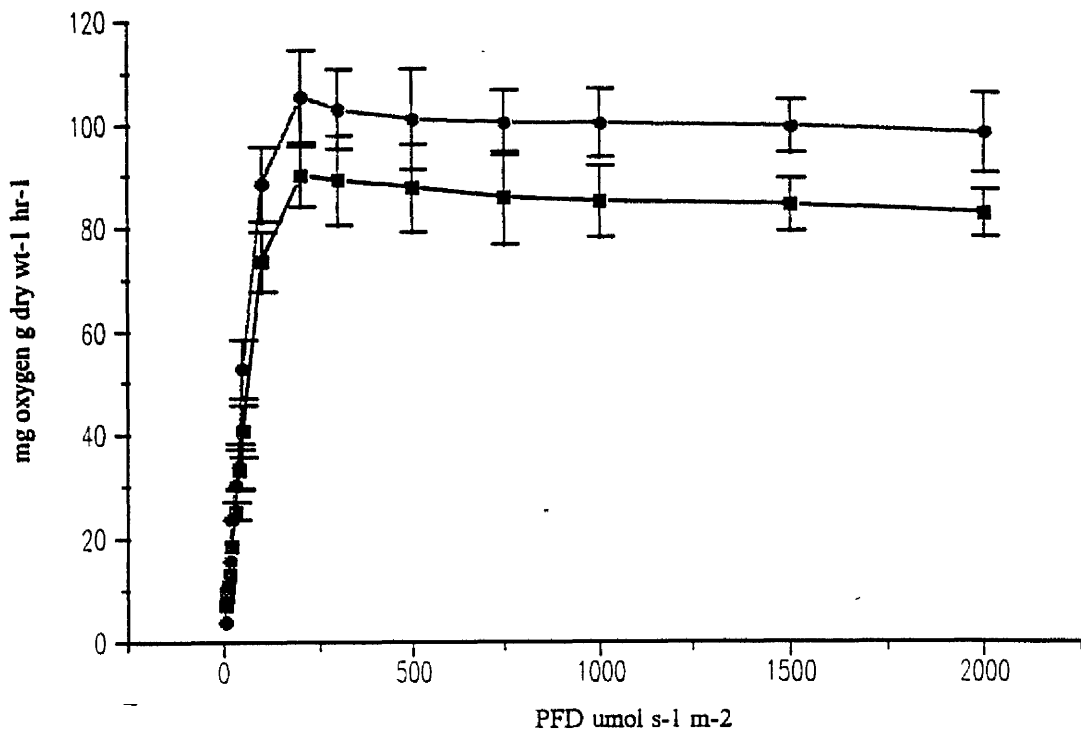


Figure 73. The effect of bicarbonate addition on the photosynthesis / irradiance response curves of *Synechococcus* 1479/5, ●—● ASM and 2mM HCO₃⁻, ■—■ ASM.

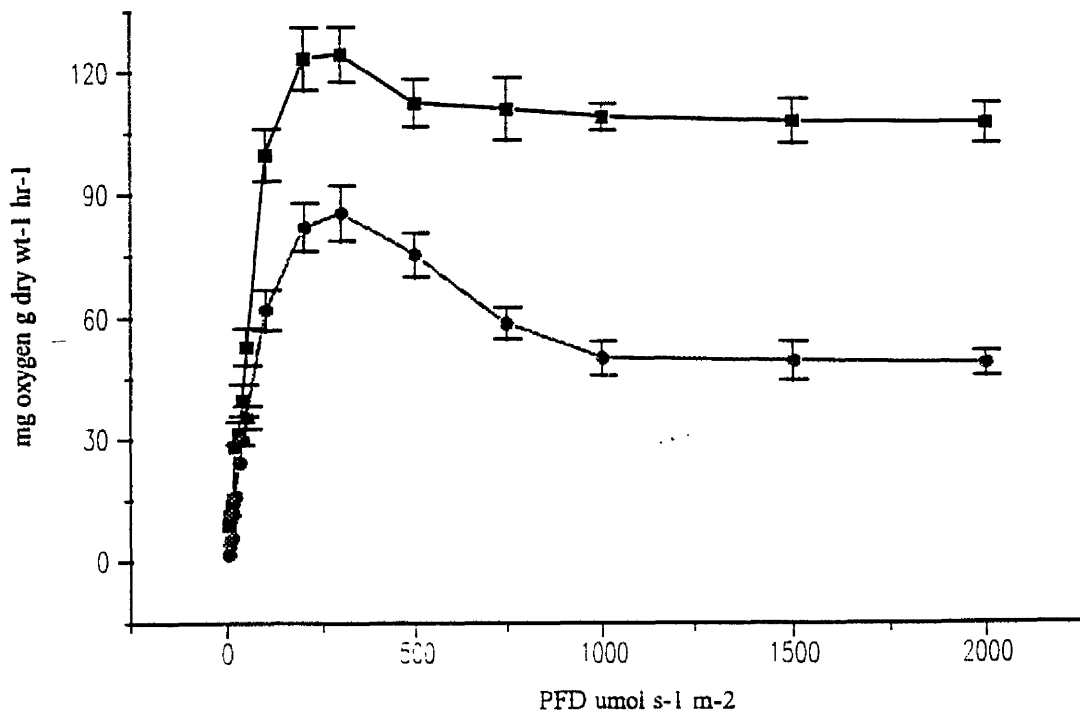


Figure 74. The effect of measuring photosynthesis / irradiance response curves from cells of *Chlorella vulgaris* 211/11c incubated in phosphate buffer (pH 7.0) against ASM (pH 7.0), ●—● phosphate buffer, ■—■ ASM.

Table 16. The effect of the presence and absence of 2mM NaHCO₃ on the photosynthetic parameters of cells of *Synechococcus* 1479/5.

P / I parameter	ASM	ASM + 2mM Bicarbonate
α (mg oxygen g dry wt ⁻¹ hr ⁻¹ / $\mu\text{mol s}^{-1} \text{m}^{-2}$)	0.492	0.909
P_{max} (mg oxygen g dry wt ⁻¹ hr ⁻¹)	89.85	105.4
I_{k} ($\mu\text{mol s}^{-1} \text{m}^{-2}$)	182.62	115.95
$P_{\text{max}}^{\text{PPFD}}$ ($\mu\text{mol s}^{-1} \text{m}^{-2}$)	200	200
Initial dark respiration (mg oxygen g dry wt ⁻¹ hr ⁻¹)	24.02 ± 2.23	26.56 ± 1.94
LEDR (mg oxygen g dry wt ⁻¹ hr ⁻¹)	62.46 ± 7.5	65.31 ± 3.78

Table 17. The effect of phosphate buffer on the photosynthetic parameters of *Chlorella vulgaris* 211/11c.

P / I parameter	ASM (pH 7.0)	Phosphate buffer (pH 7.0)
α (mg oxygen g dry wt ⁻¹ hr ⁻¹ / $\mu\text{mol s}^{-1} \text{m}^{-2}$)	0.552	0.773
P_{max} (mg oxygen g dry wt ⁻¹ hr ⁻¹)	124.39	85.31
I_{k} ($\mu\text{mol s}^{-1} \text{m}^{-2}$)	225.34	110.36
$P_{\text{max}}^{\text{PPFD}}$ ($\mu\text{mol s}^{-1} \text{m}^{-2}$)	300	300
β (mg oxygen g dry wt ⁻¹ hr ⁻¹ / $\mu\text{mol s}^{-1} \text{m}^{-2}$)	no data	-0.059
I_{β} ($\mu\text{mol s}^{-1} \text{m}^{-2}$)	no data	1445.9
Initial dark respiration (mg oxygen g dry wt ⁻¹ hr ⁻¹)	29.82 ± 3.43	24.26 ± 3.2
LEDR (mg oxygen g dry wt ⁻¹ hr ⁻¹)	81.25 ± 5.4	71.88 ± 4.2

3.3.2 Comparison of photosynthesis / irradiance response curves measured in Phosphate Buffer or ASM.

Cells of micro-algae and cyanobacteria are normally resuspended in an incubating buffered medium prior to placement in an oxygen electrode chamber for photosynthesis / irradiance measurements (Miller and Colman, 1980; Shelp and Canvin, 1985; Hettler *et al.*, 1991; Espie and Kandasamy, 1992; Pollio *et al.*, 1993). The following section shows the results of incubating cells of *Chlorella vulgaris* 211/11c, *Scenedesmus sp.*, *Synechococcus* 1479/5 and *Ankistrodesmus antarcticus* in phosphate buffer (pH 7.0) and 100% ASM (pH 7.0) during photosynthesis / irradiance measurement.

The photosynthesis / irradiance curves of *Chlorella vulgaris* 211/11c determined in phosphate buffer and ASM medium are given in Figure 74. It can be seen that the photosynthetic rates at all photon flux densities were lower when the cells were incubated in phosphate buffer. The photosynthetic parameters determined from Figure 74 are presented in Table 17. The value of α increased from 0.552 mg oxygen g dry wt⁻¹ hr⁻¹ in ASM medium to 0.773 mg oxygen g dry wt⁻¹ hr⁻¹ in the presence of phosphate buffer, however, the most obvious effect of phosphate buffer on photosynthesis was on the maximum rate of photosynthesis. In ASM the cells had a measured P_{\max} of 124.9 mg oxygen g dry wt⁻¹ hr⁻¹ whereas cells in phosphate buffer showed a sharp decrease in P_{\max} to 85.31 mg oxygen g dry wt⁻¹ hr⁻¹. Phosphate buffer was not found to have any significant affect on cellular respiration or light enhanced dark respiration. Figure 74 also shows that cells incubated in phosphate buffer had a measurable value for β and I_{β} since they showed indications of photoinhibition. The PFD at which P_{\max} was measured (P_{\max}^{PFD}) was found to be the same for cells incubated in ASM and phosphate buffer.

Figure 75 shows the photosynthesis / irradiance curves of cells of *Scenedesmus sp.* measured in phosphate buffer (pH 7.0) and ASM (pH 7.0). Similar to the results obtained for *Chlorella vulgaris* 211/11c, the photosynthetic rates of *Scenedesmus sp.* cells measured in ASM were considerably higher than those from cells measured in phosphate buffer. The photosynthetic parameters determined from Figure 75 are presented in Table 18. Unlike *Chlorella vulgaris* 211/11c, the value of α decreased (1.004-0.6233 mg oxygen g dry wt⁻¹ hr⁻¹ / $\mu\text{mol s}^{-1} \text{m}^{-2}$) when *Scenedesmus sp.* was

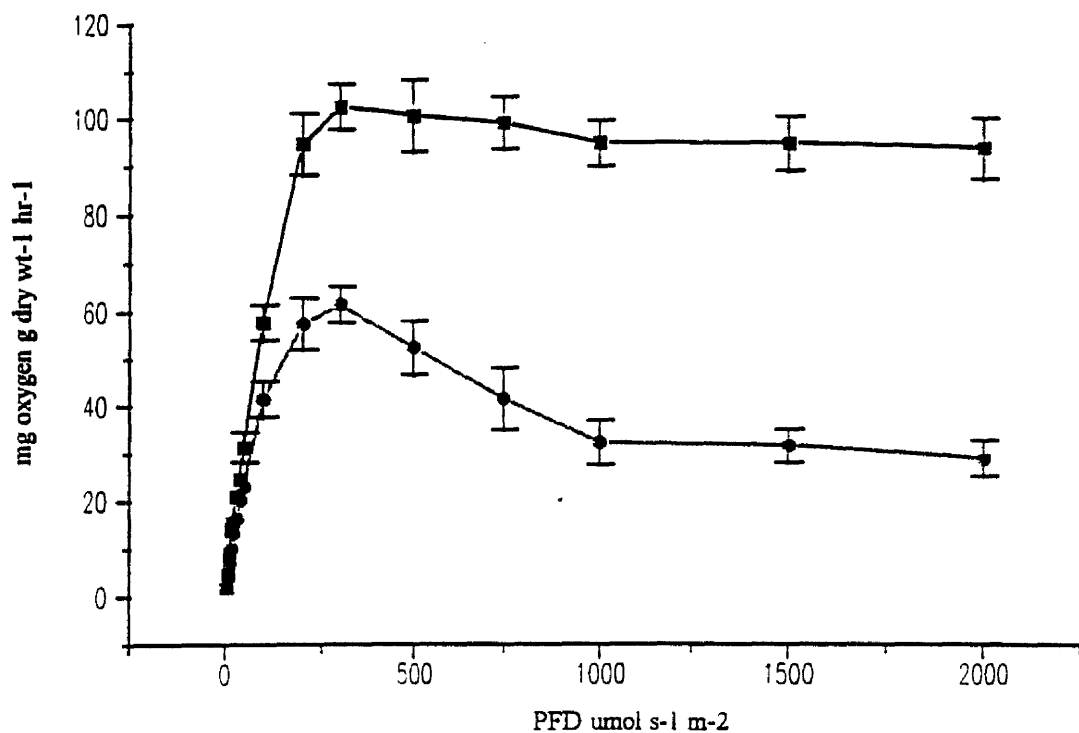


Figure 75. The effect of measuring photosynthesis / irradiance response curves from cells of *Scenedesmus sp.* incubated in phosphate buffer (pH 7.0) against ASM (pH 7.0), ●—● phosphate buffer, ■—■ ASM.

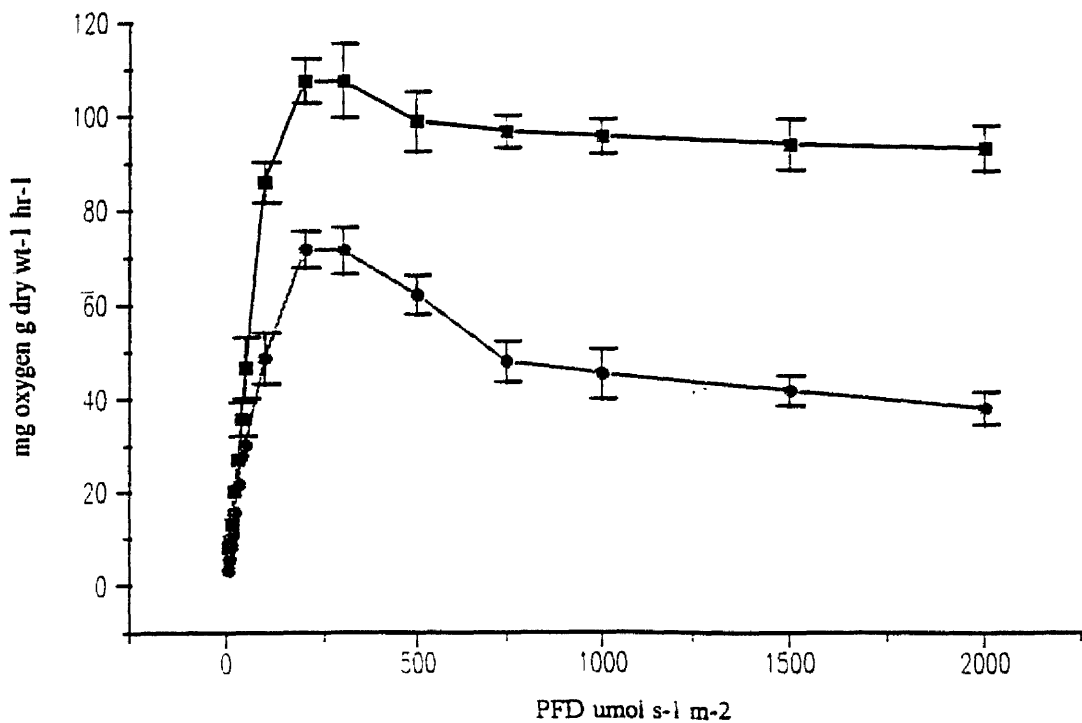


Figure 76. The effect of measuring photosynthesis / irradiance response curves from cells of *Synechococcus 1479/5* incubated in phosphate buffer (pH 7.0) against ASM (pH 7.0), ●—● phosphate buffer, ■—■ ASM.

Table 18. The effect of phosphate buffer on the photosynthetic parameters of cells of *Scenedesmus sp.*

P / I parameter	ASM (pH 7.0)	Phosphate buffer (pH 7.0)
α (mg oxygen g dry wt ⁻¹ hr ⁻¹ / $\mu\text{mol s}^{-1} \text{m}^{-2}$)	1.04	0.62
P_{max} (mg oxygen g dry wt ⁻¹ hr ⁻¹)	102.47	61.29
I_k ($\mu\text{mol s}^{-1} \text{m}^{-2}$)	102.06	98.33
β (mg oxygen g dry wt ⁻¹ hr ⁻¹ / $\mu\text{mol s}^{-1} \text{m}^{-2}$)	no data	-0.044
I_β ($\mu\text{mol s}^{-1} \text{m}^{-2}$)	no data	1392.9
$P_{\text{max}}^{\text{PFD}}$ ($\mu\text{mol s}^{-1} \text{m}^{-2}$)	300	300
Initial dark respiration (mg oxygen g dry wt ⁻¹ hr ⁻¹)	15.41 ± 1.67	14.59 ± 3.7
LEDR (mg oxygen g dry wt ⁻¹ hr ⁻¹)	68.35 ± 3.5	61.04 ± 5.3

Table 19. The effect of phosphate buffer on the photosynthetic parameters of cells *Synechococcus 1479/5.*

P / I parameter	ASM (pH 7.0)	Phosphate buffer (pH 7.0)
α (mg oxygen g dry wt ⁻¹ hr ⁻¹ / $\mu\text{mol s}^{-1} \text{m}^{-2}$)	0.453	0.615
P_{max} (mg oxygen g dry wt ⁻¹ hr ⁻¹)	107.5	71.64
I_k ($\mu\text{mol s}^{-1} \text{m}^{-2}$)	237.3	116.48
β (mg oxygen g dry wt ⁻¹ hr ⁻¹ / $\mu\text{mol s}^{-1} \text{m}^{-2}$)	no data	-0.0526
I_β ($\mu\text{mol s}^{-1} \text{m}^{-2}$)	no data	1361.9
$P_{\text{max}}^{\text{PFD}}$ ($\mu\text{mol s}^{-1} \text{m}^{-2}$)	300	200
Initial dark respiration (mg oxygen g dry wt ⁻¹ hr ⁻¹)	26.85 ± 3.1	22.66 ± 2.7
LEDR (mg oxygen g dry wt ⁻¹ hr ⁻¹)	75.59 ± 6.4	66.33 ± 4.8

suspended in phosphate buffer. The measured value of P_{\max} was found to be nearly 2 fold higher in ASM (102.47 mg oxygen g dry wt⁻¹ hr⁻¹) than in phosphate buffer (61.29 mg oxygen g dry wt⁻¹ hr⁻¹). The values of I_k and P_{\max}^{PFD} were the same for cells suspended in ASM and phosphate buffer. Phosphate buffer was not found to significantly influence the respiration or LEDR rates. However similar to the results obtained with cells of *Chlorella vulgaris* 211/11c, *Scenedesmus sp.* cells showed typical indicators of photoinhibition at high irradiances when incubated in phosphate buffer. The value of β was -0.044 mg oxygen g dry wt⁻¹ hr⁻¹ / $\mu\text{mol s}^{-1} \text{m}^{-2}$.

Photosynthesis / irradiance curves of *Synechococcus* 1479/5 incubated with ASM (pH 7.0) and phosphate buffer (pH 7.0) are shown in Figure 76. Higher photosynthetic rates were measured in cells incubated in the presence of ASM as opposed to those incubated with phosphate buffer. Table 19 presents the photosynthetic parameters calculated from Figure 76. It can be seen that the value of α increased from 0.453 to 0.617 mg oxygen g dry wt⁻¹ hr⁻¹ / $\mu\text{mol s}^{-1} \text{m}^{-2}$ when cells were incubated phosphate buffer as opposed to ASM. As was found for eukaryotic green micro-algae, P_{\max} was considerably higher when cells were incubated in ASM. Phosphate buffer was not found to affect either respiration or light enhanced dark respiration rates. The value of I_k was, however, double for cells incubated in the presence of ASM compared to those in phosphate buffer. Cells of *Synechococcus* 1479/5 showed indications of photoinhibition; the value of β was -0.0526 mg oxygen g dry wt⁻¹ hr⁻¹ / $\mu\text{mol s}^{-1} \text{m}^{-2}$.

Figure 77 shows the effects of phosphate buffer on the photosynthesis / irradiance response curves of *Ankistrodesmus antarcticus*. As was found with the other micro-algae, photosynthetic rates were lower when the cells were incubated in phosphate buffer. The effect of phosphate buffer on the photosynthetic parameters determined from Figure 77 are presented in Table 20. The maximum rate of photosynthesis of *Ankistrodesmus antarcticus* incubated in phosphate buffer was 48.34 mg oxygen g dry wt⁻¹ hr⁻¹, which was approximately 2 times less than the P_{\max} measured for cells suspended in ASM (92.13 mg oxygen g dry wt⁻¹ hr⁻¹). The value of α decrease from 0.382 mg oxygen g dry wt⁻¹ hr⁻¹ in ASM to 0.249 mg oxygen g dry wt⁻¹ hr⁻¹ in phosphate buffer. Phosphate buffer did not significantly affect the respiration or light enhanced dark respiration rates. The PFD at which P_{\max} was attained (P_{\max}^{PFD})

Table 20. The effect of phosphate buffer on the photosynthetic parameters of cells of *Ankistrodesmus antarcticus*.

P / I parameter	ASM (pH 7.0)	Phosphate buffer (pH 7.0)
α (mg oxygen g dry wt ⁻¹ hr ⁻¹ / $\mu\text{mol s}^{-1} \text{m}^{-2}$)	0.382	0.249
P_{max} (mg oxygen g dry wt ⁻¹ hr ⁻¹)	92.13	48.34
I_k ($\mu\text{mol s}^{-1} \text{m}^{-2}$)	241.17	194.13
β (mg oxygen g dry wt ⁻¹ hr ⁻¹ / $\mu\text{mol s}^{-1} \text{m}^{-2}$)	no data	no data
I_β ($\mu\text{mol s}^{-1} \text{m}^{-2}$)	no data	no data
$P_{\text{max}}^{\text{PPFD}}$ ($\mu\text{mol s}^{-1} \text{m}^{-2}$)	100	200-300
Initial dark respiration (mg oxygen g dry wt ⁻¹ hr ⁻¹)	22.63 ± 1.7	24.9 ± 3.8
LED _R (mg oxygen g dry wt ⁻¹ hr ⁻¹)	63.75 ± 3.7	73.4 ± 6.5

Table 21. The effect of nitrate on the photosynthesis / irradiance curves of cells of *Scenedesmus sp.*

P / I parameter	ASM with nitrate	ASM minus nitrate
α (mg oxygen g dry wt ⁻¹ hr ⁻¹ / $\mu\text{mol s}^{-1} \text{m}^{-2}$)	2.63	2.21
P_{max} (mg oxygen g dry wt ⁻¹ hr ⁻¹)	110.06	102.2
I_k ($\mu\text{mol s}^{-1} \text{m}^{-2}$)	41.84	46.24
β (mg oxygen g dry wt ⁻¹ hr ⁻¹ / $\mu\text{mol s}^{-1} \text{m}^{-2}$)	no data	-0.158
I_β ($\mu\text{mol s}^{-1} \text{m}^{-2}$)	no data	646.83
$P_{\text{max}}^{\text{PPFD}}$ ($\mu\text{mol s}^{-1} \text{m}^{-2}$)	100	100
Initial dark respiration (mg oxygen g dry wt ⁻¹ hr ⁻¹)	11.2 ± 3.15	7.86 ± 1.25
LED _R (mg oxygen g dry wt ⁻¹ hr ⁻¹)	38.187 ± 2.13	30.32 ± 1.69

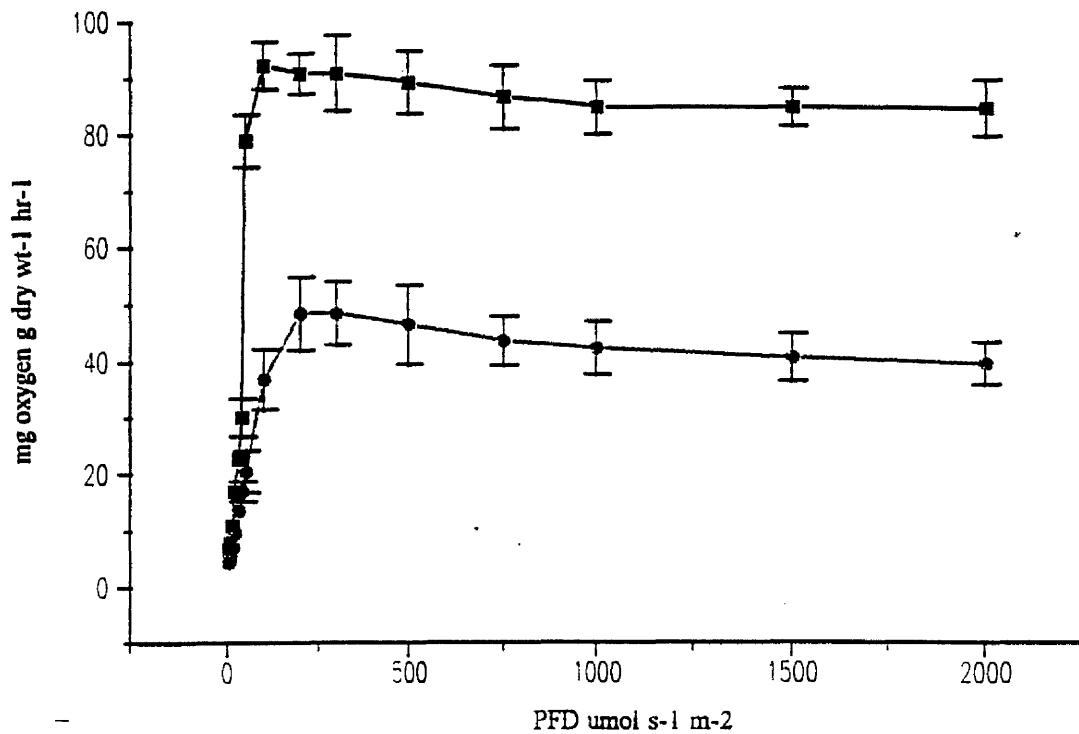


Figure 77. The effect of measuring photosynthesis / irradiance response curves from cells of *Ankistrodesmus antarcticus* incubated in phosphate buffer (pH 7.0) against ASM (pH 7.0) , ●—● phosphate buffer. ■—■ ASM.

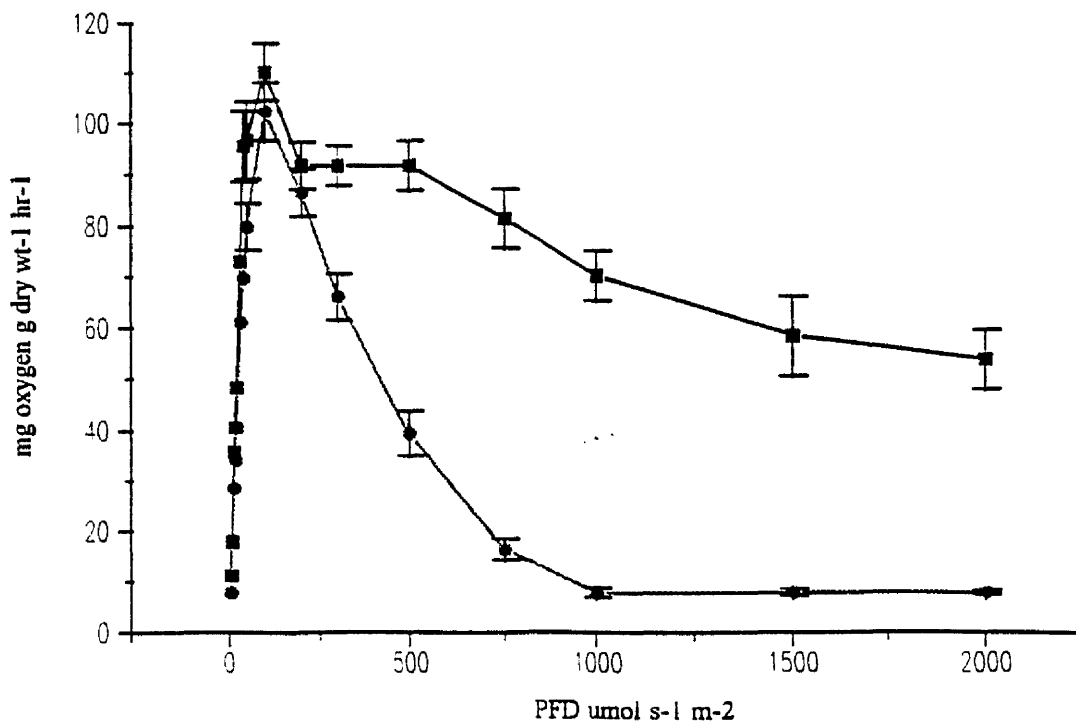


Figure 78. The effect of nitrate absence / presence on the photosynthesis / irradiance response curves of *Scenedesmus sp.*, ●—● nitrate absent, ■—■ nitrate present.

increased from $100\mu\text{mol s}^{-1} \text{ m}^{-2}$ in ASM to $200\text{-}300\mu\text{mol s}^{-1} \text{ m}^{-2}$ in phosphate buffer.

3.3.3 The effect of the presence and absence of nitrate on the measurement of photosynthesis / irradiance curves.

Figure 78 shows the effect of the presence or absence of nitrate on the photosynthesis / irradiance curves of *Scenedesmus sp.* It can be seen that there was a sharp contrast between the two curves shown in Figure 78. The cells incubated in the presence of nitrate appeared to tolerate high light levels better than those without nitrate. Table 21 shows the photosynthetic parameters calculated from Figure 78. It can be seen that the presence of nitrate had no significant effect on the values of P_{max} , I_K , P_{max}^{PFD} or α . However nitrate had an effect on the onset of photoinhibition. Cells of *Scenedesmus sp.* incubated in the presence of nitrate (Figure 78), had higher rates of photosynthesis at PFDs above P_{max} . In contrast, the photosynthetic rates of cells in ASM without nitrate decreased sharply at PFDs above P_{max} (β being equal to -0.158).

Figure 79 shows the effect of nitrate on the photosynthesis / irradiance curves of *Ankistrodesmus antarcticus*. Unlike the photosynthesis / irradiance curves of *Scenedesmus sp.* cells of *Ankistrodesmus antarcticus* did not show an obvious difference in curves measured with and without nitrate. The values of α were almost identical (4.09 and $4.097 \text{ mg oxygen g dry wt}^{-1} \text{ hr}^{-1} / \mu\text{mol s}^{-1} \text{ m}^{-2}$) with each set of cells regardless of the presence of nitrate. In contrast, the maximum rate of photosynthesis P_{max} , was found to be higher (Table 22), with cells incubated in the presence of nitrate ($151.38 \text{ mg oxygen g dry wt}^{-1} \text{ hr}^{-1}$) than those incubated in the absence of nitrate ($112.58 \text{ mg oxygen g dry wt}^{-1} \text{ hr}^{-1}$). As cells of *Ankistrodesmus antarcticus* did not exhibit significant reductions in photosynthesis at high light intensities, the value of β could not be determined. Similar to that observed for *Scenedesmus sp.* the LEDR of cells in the presence of nitrate ($98.22 \text{ mg oxygen g dry wt}^{-1} \text{ hr}^{-1}$) was significantly higher than that of cells measured in the absence of nitrate ($67.89 \text{ mg oxygen g dry wt}^{-1} \text{ hr}^{-1}$).

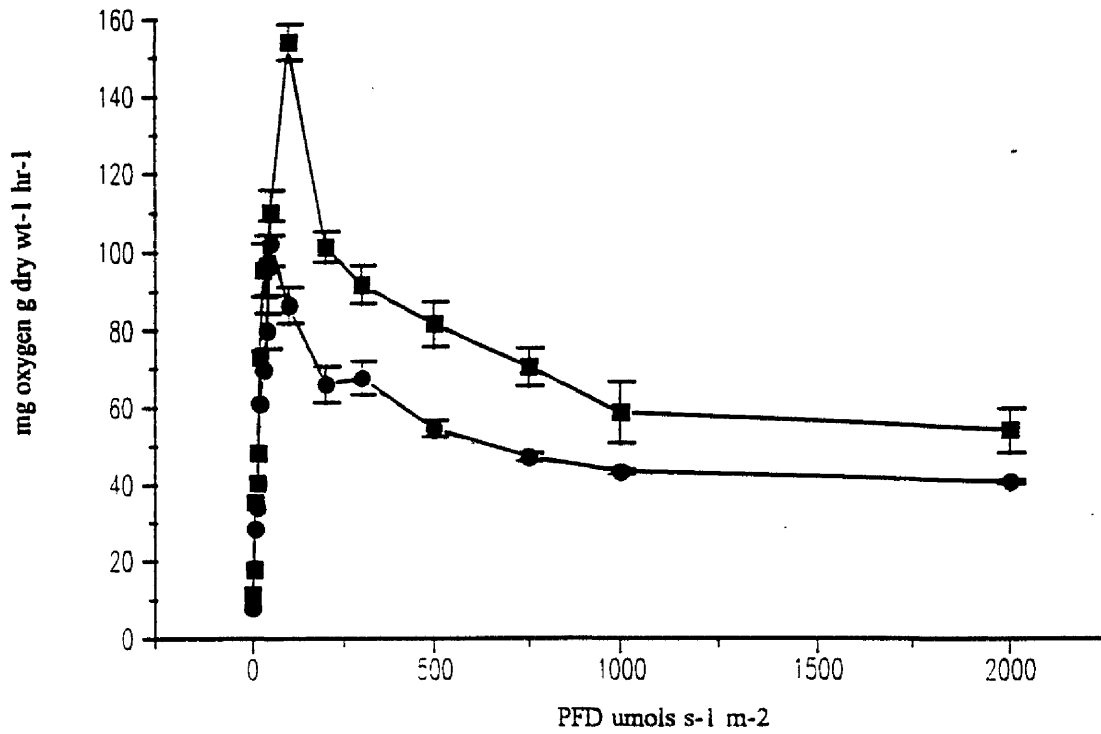


Figure 79. The effect of nitrate absence / presence on the photosynthesis / irradiance response curves of *Ankistrodesmus antarcticus*, ●—● nitrate absent, ■—■ nitrate present.

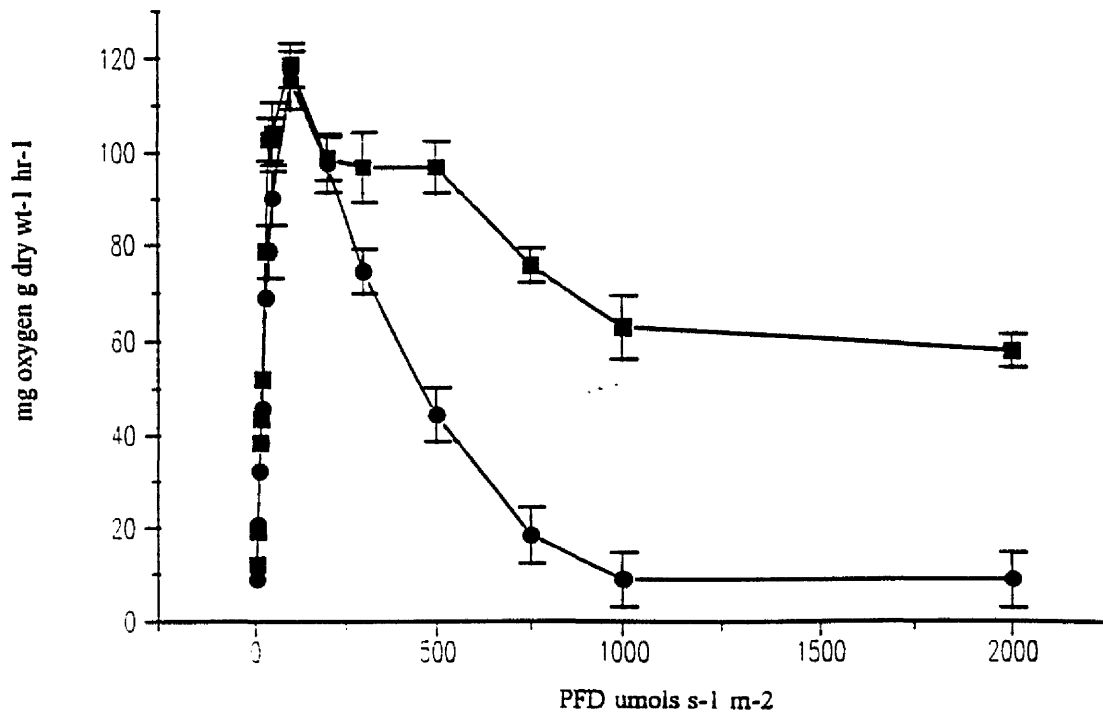


Figure 80. The effect of nitrate absence / presence on the photosynthesis / irradiance response curves of *Synechococcus sp.*, ●—● nitrate absent, ■—■ nitrate present.

Table 22. The effect of nitrate on the photosynthesis / irradiance curves of cells of *Ankistrodesmus antarcticus*.

P / I parameter	ASM with nitrate	ASM minus nitrate
α (mg oxygen g dry wt ⁻¹ hr ⁻¹ / $\mu\text{mol s}^{-1} \text{m}^{-2}$)	4.09	4.097
P_{max} (mg oxygen g dry wt ⁻¹ hr ⁻¹)	151.38	112.58
I_k ($\mu\text{mol s}^{-1} \text{m}^{-2}$)	37.01	27.47
β (mg oxygen g dry wt ⁻¹ hr ⁻¹ / $\mu\text{mol s}^{-1} \text{m}^{-2}$)	no data	no data
I_β ($\mu\text{mol s}^{-1} \text{m}^{-2}$)	no data	no data
$P_{\text{max}}^{\text{PPFD}}$ ($\mu\text{mol s}^{-1} \text{m}^{-2}$)	100	100
Initial dark respiration (mg oxygen g dry wt ⁻¹ hr ⁻¹)	55.24 ± 4.6	52.18 ± 5.9
LEDR (mg oxygen g dry wt ⁻¹ hr ⁻¹)	98.22 ± 8.5	67.89 ± 4.9

Table 23. The effect of nitrate on the photosynthesis / irradiance curves of *Synechococcus* 1479/5.

P / I parameter	ASM with nitrate	ASM minus nitrate
α (mg oxygen g dry wt ⁻¹ hr ⁻¹ / $\mu\text{mol s}^{-1} \text{m}^{-2}$)	2.83	2.01
P_{max} (mg oxygen g dry wt ⁻¹ hr ⁻¹)	118.53	101.446
I_k ($\mu\text{mol s}^{-1} \text{m}^{-2}$)	41.88	50.47
β (mg oxygen g dry wt ⁻¹ hr ⁻¹ / $\mu\text{mol s}^{-1} \text{m}^{-2}$)	no data	-0.15
I_β ($\mu\text{mol s}^{-1} \text{m}^{-2}$)	no data	676.3
$P_{\text{max}}^{\text{PPFD}}$ ($\mu\text{mol s}^{-1} \text{m}^{-2}$)	100	200
Initial dark respiration (mg oxygen g dry wt ⁻¹ hr ⁻¹)	12.095 ± 1.8	10.52 ± 2.33
LEDR (mg oxygen g dry wt ⁻¹ hr ⁻¹)	27.21 ± 3.11	19.65 ± 2.06

The effect of nitrate on the photosynthesis / irradiance curves of *Synechococcus* 1479/5 and *Synechococcus sp.* are shown in Figures 81 and 80 respectively. The photosynthetic parameters for *Synechococcus* 1479/5 and *Synechococcus sp.* determined from the photosynthesis / irradiance curves are presented in Tables 23 and 24 respectively. It can be seen (Table 24) that the presence of nitrate in the suspending medium had little effect on the values of α and I_k . A small increase in P_{max} (118.53 - 101.446 mg oxygen g dry wt⁻¹ hr⁻¹) occurred with cells in ASM without nitrate. However as was found with *Scenedesmus sp.*, cells of *Synechococcus* 1479/5 showed sharp a decrease in photosynthetic rates at PFDs above that of P_{max} (Figure 80). The LEDR values of cells in ASM with nitrate were significantly higher than cells in the absence of nitrate.

Cells of *Synechococcus* 1479/5 showed a similar response as *Synechococcus sp.* in the presence of nitrate. The photosynthetic parameters determined for *Synechococcus* 1479/5 in the presence and absence of nitrate are given in Table 24. It was found that the value of I_k was not significantly affected by the presence or absence of nitrate. However, the maximum rate of photosynthesis was higher for cells incubated with nitrate (115.39 mg oxygen g dry wt⁻¹ hr⁻¹) compared to cells incubated in the absence of nitrate (93.07 mg oxygen g dry wt⁻¹ hr⁻¹). The value of α decreased in cells incubated in the absence of nitrate. Although an increase in LEDR was noted in cells incubated with nitrate, the value was not significantly different to cells incubated in the absence of nitrate. It can be seen (Figure 81) that the cells showed a large reduction in photosynthetic rate due to photoinhibition in the absence of nitrate.

The decrease in the rates of photosynthesis at high light intensities may be due to nitrate limitation leading to a reduction in cellular protein synthesis. This may ultimately lead to a reduction in cell repair enzymes which help prevent cellular photodamage from occurring. However the presence of nitrate was found to increase the light enhanced dark respiration rate determined after photosynthesis / irradiance measurements had been carried out. This would seem to support the above suggestion that the presence of nitrate was required for protein synthesis. However the increase in respiration due to the presence of nitrate may also be a direct result of there being a greater concentration of photosynthetic substrate formed by cells able to continue photosynthesising at high rates at the higher light intensities.

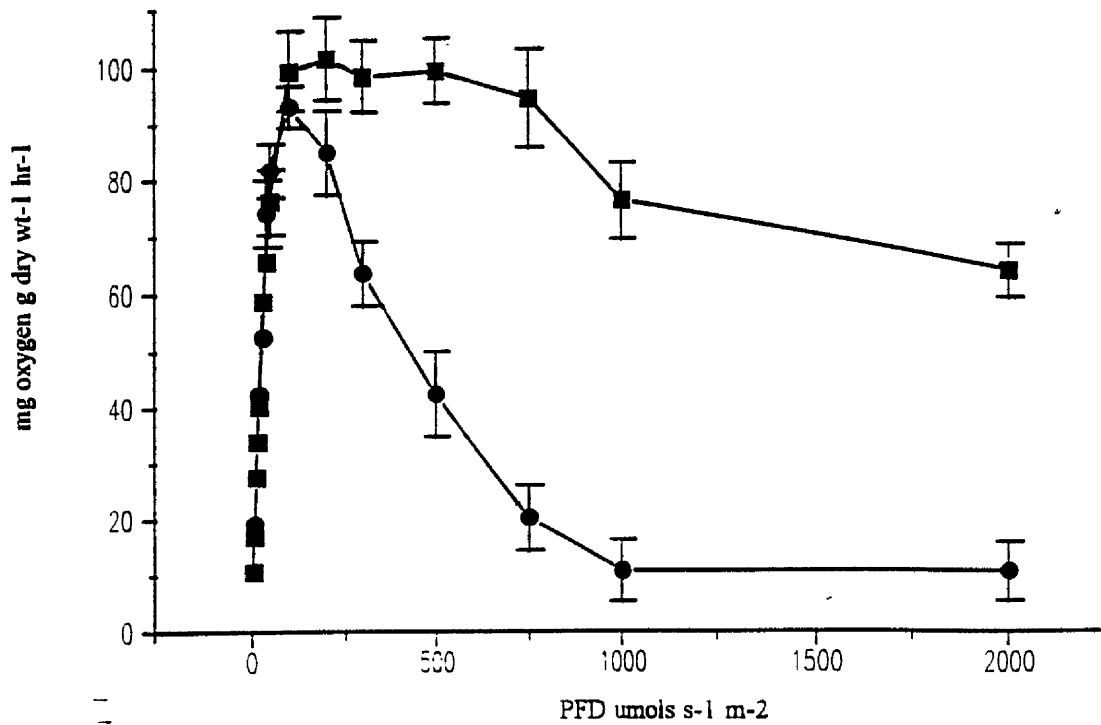


Figure 81. The effect of nitrate absence / presence on the photosynthesis / irradiance response curves of *Synechococcus* 1479/5, ●—● nitrate absent, ■—■ nitrate present.

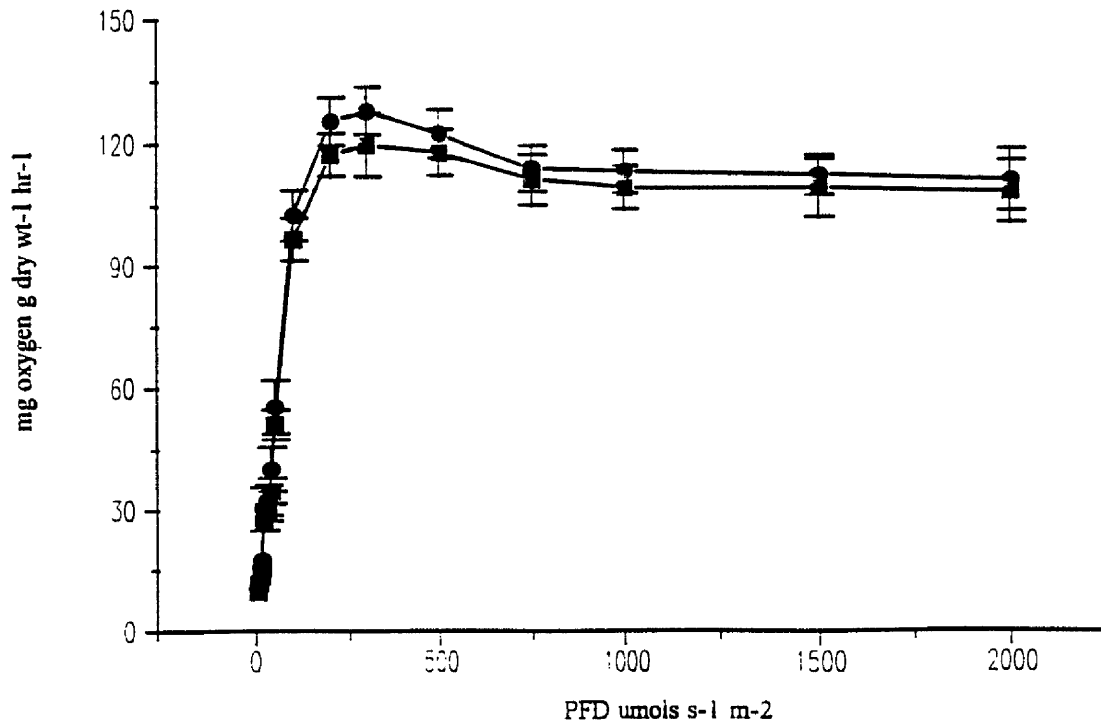


Figure 82. The effect of trace element absence / presence on the photosynthesis / irradiance response curves of *Chlorella vulgaris* 211/11c, ●—● trace elements absent, ■—■ trace elements present.

Table 24. The effect of nitrate on the photosynthesis / irradiance curves of *Synechococcus* sp.

P / I parameter	ASM with nitrate	ASM minus nitrate
α (mg oxygen g dry wt ⁻¹ hr ⁻¹ / $\mu\text{mol s}^{-1} \text{m}^{-2}$)	2.5	1.95
P_{max} (mg oxygen g dry wt ⁻¹ hr ⁻¹)	115.39	93.07
I_k ($\mu\text{mol s}^{-1} \text{m}^{-2}$)	46.156	47.7
β (mg oxygen g dry wt ⁻¹ hr ⁻¹ / $\mu\text{mol s}^{-1} \text{m}^{-2}$)	no data	-0.115
I_β ($\mu\text{mol s}^{-1} \text{m}^{-2}$)	no data	809.3
$P_{\text{max}}^{\text{PFD}}$ ($\mu\text{mol s}^{-1} \text{m}^{-2}$)	100	100
Initial dark respiration (mg oxygen g dry wt ⁻¹ hr ⁻¹)	8.87 ± 2.8	10.65 ± 1.22
LED R (mg oxygen g dry wt ⁻¹ hr ⁻¹)	46.28 ± 6.6	32.46 ± 6.9

Table 25. The effect of trace elements on the photosynthesis / irradiance curves of *Chlorella vulgaris* 211/11c.

P / I parameter	ASM with trace elements	ASM minus trace elements
α (mg oxygen g dry wt ⁻¹ hr ⁻¹ / $\mu\text{mol s}^{-1} \text{m}^{-2}$)	0.6	0.59
P_{max} (mg oxygen g dry wt ⁻¹ hr ⁻¹)	127.82 ± 5.62	119.51 ± 7.68
I_k ($\mu\text{mol s}^{-1} \text{m}^{-2}$)	213.03	202.5
$P_{\text{max}}^{\text{PFD}}$ ($\mu\text{mol s}^{-1} \text{m}^{-2}$)	300	300
Initial dark respiration (mg oxygen g dry wt ⁻¹ hr ⁻¹)	31.25 ± 4.7	33.79 ± 6.4
LED R (mg oxygen g dry wt ⁻¹ hr ⁻¹)	78.4 ± 6.3	83.71 ± 5.7

3.3.4 The effect of trace elements on the measurement of photosynthesis irradiance response curves.

The effect of trace elements upon the photosynthesis / irradiance curves of *Chlorella vulgaris* 211/11c and *Scenedesmus sp.* are shown in Figures 82 and 83 respectively.

Table 25 shows the photosynthetic parameters determined from Figure 82. It can be seen that the presence of trace elements in the incubating medium of cells of *Chlorella vulgaris* 211/11c had virtually no significant effect on the values of I_k , P_{max} or respiration rates.

The photosynthetic parameters of *Scenedesmus sp.* calculated from the data presented in Figure 83 are given in Table 26. As can be seen from Figure 83 cells of *Scenedesmus sp.* showed almost identical photosynthesis / irradiance curves when incubated in the presence or the absence of trace elements. Similarly the presence / absence of trace elements in ASM had no effect on either the photosynthetic, respiration or light enhanced dark respiration rates.

3.3.5 The effect of centrifugation on the measurement of photosynthesis / irradiance response curve.

The effect of centrifugation on the photosynthesis / irradiance curves of *Chlorella vulgaris* 211/11c, *Synechococcus* 1479/5 and *Scenedesmus sp.* are shown in Figures 84, 85 and 86 respectively.

Figure 84 displays the photosynthesis / irradiance curves of *Chlorella vulgaris* 211/11c, measured from cells which had been centrifuged prior to dilution (O.D 560nm 0.15) with ASM and from cells which had just been diluted to O.D 560nm 0.15. The photosynthetic parameters determined from Figure 84 are presented in Table 27. It can be seen (Table 27) that centrifugation had a very pronounced effect on the initial dark respiration rate of *Chlorella vulgaris* 211/11c. The respiration rate of centrifuged cells was almost double that of uncentrifuged cells. The large increase in respiration rate was then included in the determination of the overall photosynthetic rates, hence the P_{max} for centrifuged cells was $142 \text{ mg oxygen g dry wt}^{-1} \text{ hr}^{-1}$

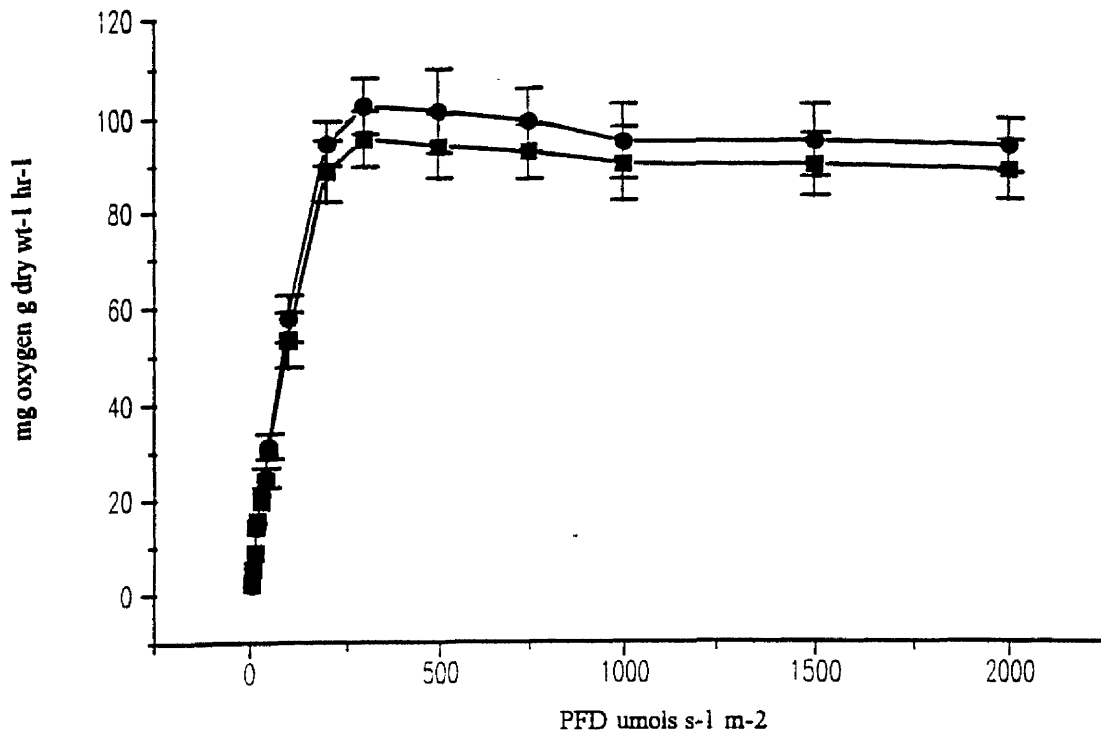


Figure 83. The effect of trace element absence / presence on the photosynthesis / irradiance response curves of *Scenedesmus sp.*, ●—● trace elements absent, ■—■ trace elements present.

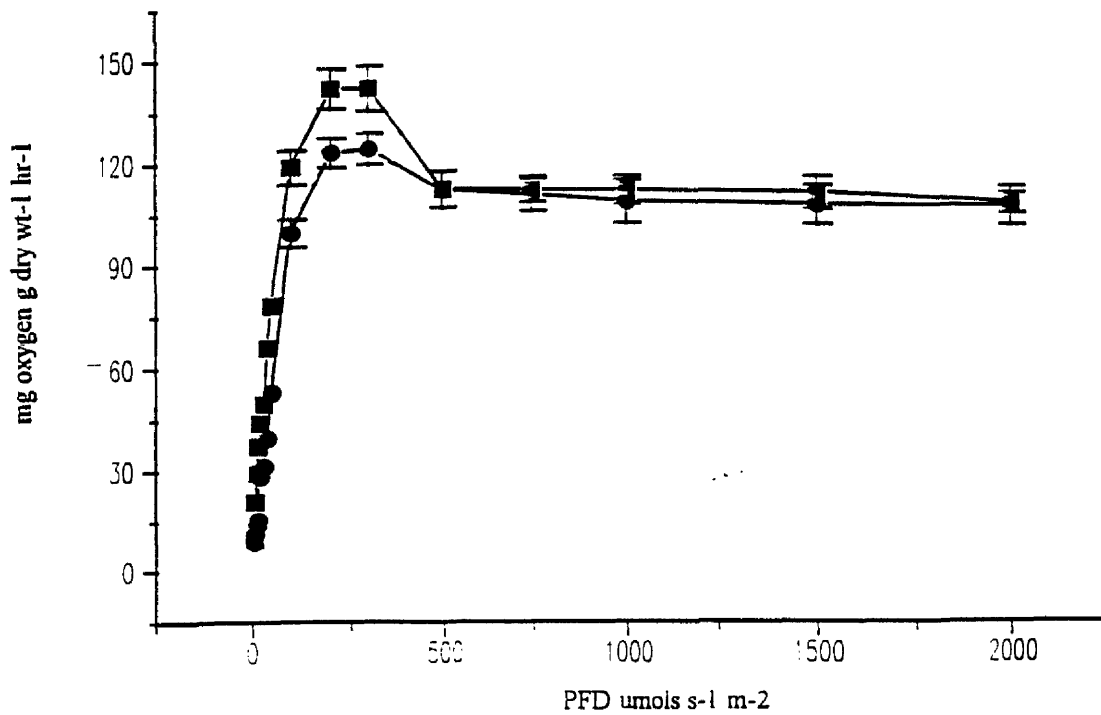


Figure 84. The effect of centrifuging cells of *Chlorella vulgaris* 211/11c prior to photosynthesis / irradiance response measurements, ■—■ centrifuged cells, ●—● uncentrifuged cells.

Table 26. The effect of trace elements on the photosynthesis / irradiance curves of *Scenedesmus sp.*

P / I parameter	ASM with trace elements	ASM minus trace elements
α (mg oxygen g dry wt ⁻¹ hr ⁻¹ / $\mu\text{mol s}^{-1} \text{m}^{-2}$)	0.988	0.987
P_{max} (mg oxygen g dry wt ⁻¹ hr ⁻¹)	102.17 \pm 3.12	95.41 \pm 7.13
I_k ($\mu\text{mol s}^{-1} \text{m}^{-2}$)	103.41	96.667
$P_{\text{max}}^{\text{PPFD}}$ ($\mu\text{mol s}^{-1} \text{m}^{-2}$)	300	300
Initial dark respiration (mg oxygen g dry wt ⁻¹ hr ⁻¹)	15.41 \pm 2.1	16.71 \pm 2.3
LEDR (mg oxygen g dry wt ⁻¹ hr ⁻¹)	68.35 \pm 4.8	65.22 \pm 3.19

Table 27. The effect of centrifugation on the photosynthesis / irradiance curves of *Chlorella vulgaris* 211/11c.

P / I parameter	ASM with centrifugation (2000g 10min)	ASM (no centrifugation)
α (mg oxygen g dry wt ⁻¹ hr ⁻¹ / $\mu\text{mol s}^{-1} \text{m}^{-2}$)	2.29	0.55
P_{max} (mg oxygen g dry wt ⁻¹ hr ⁻¹)	142.01	124.39
I_k ($\mu\text{mol s}^{-1} \text{m}^{-2}$)	62	226.16
$P_{\text{max}}^{\text{PPFD}}$ ($\mu\text{mol s}^{-1} \text{m}^{-2}$)	300	300
Light compensation point ($\mu\text{mol s}^{-1} \text{m}^{-2}$)	30-40	20
Initial dark respiration (mg oxygen g dry wt ⁻¹ hr ⁻¹)	56.34	29.82
LEDR (mg oxygen g dry wt ⁻¹ hr ⁻¹)	132.14	81

compared to 124.19 mg oxygen g dry wt⁻¹ hr⁻¹ for uncentrifuged cells. The value of α for centrifuged cells was over 4 times that measured for uncentrifuged cells. This difference in the value of α caused a large difference in the value of I_k . The I_k for uncentrifuged cells was found to be approximately 4 times higher (226.16 $\mu\text{mol s}^{-1} \text{m}^{-2}$) as that measured for centrifuged cells (62 $\mu\text{mol s}^{-1} \text{m}^{-2}$). The effect of centrifuging *Chlorella vulgaris* 211/11c was most apparent on the cellular light compensation point; centrifuged cells had a significantly higher light compensation point (30-40 $\mu\text{mol s}^{-1} \text{m}^{-2}$) than uncentrifuged cells (20 $\mu\text{mol s}^{-1} \text{m}^{-2}$).

The effects of centrifugation on the photosynthesis / irradiance curves of *Synechococcus* 1479/5 are shown in Figure 85. It can be seen that there was little apparent difference between the response curves of centrifuged cells and uncentrifuged cells in direct contrast to the photosynthesis / irradiance curve for *Chlorella vulgaris* 211/11c. The photosynthetic parameters determined from Figure 86 are presented in Table 29. The maximum rate of photosynthesis (P_{max}) of centrifuged cells (Table 30) was slightly less than that of uncentrifuged cells (91.82 compared to 99.54 mg oxygen g dry wt⁻¹ hr⁻¹). However the dark respiration rate of centrifuged cells was found to be almost twice that measured from uncentrifuged cells. The value of α for uncentrifuged cells was 3 fold less (0.419 mg oxygen g dry wt⁻¹ hr⁻¹ / $\mu\text{mol s}^{-1} \text{m}^{-2}$) than that obtained for

The effects of centrifugation on the photosynthesis / irradiance curves of *Scenedesmus* sp. are shown in Figure 86. It can be seen that centrifuged cells had increased photosynthetic rates compared to uncentrifuged cells. The photosynthetic parameters determined from Figure 86 are presented in Table 28. The cells of *Scenedesmus* sp. showed a similar pattern to that observed for *Chlorella vulgaris* 21/11c. The greatest effect of centrifugation was on cellular respiration. Cells centrifuged prior to photosynthesis / irradiance measurement had respiration rates approximately 3 times higher than uncentrifuged cells. The maximum rate of photosynthesis of centrifuged cells was 126.59 mg oxygen g dry wt⁻¹ hr⁻¹ compared to 102.47 mg oxygen g dry wt⁻¹ hr⁻¹ in uncentrifuged cells. The value of α of uncentrifuged cells was half that of centrifuged cells (1.00 compared to 1.95 mg oxygen g dry wt⁻¹ hr⁻¹ / $\mu\text{mol s}^{-1} \text{m}^{-2}$). Similar to *Chlorella vulgaris* 211/11c, centrifuged cells of *Scenedesmus* sp. showed a light compensation point twice that of uncentrifuged cells (40 compared to 20 $\mu\text{mol s}^{-1} \text{m}^{-2}$).

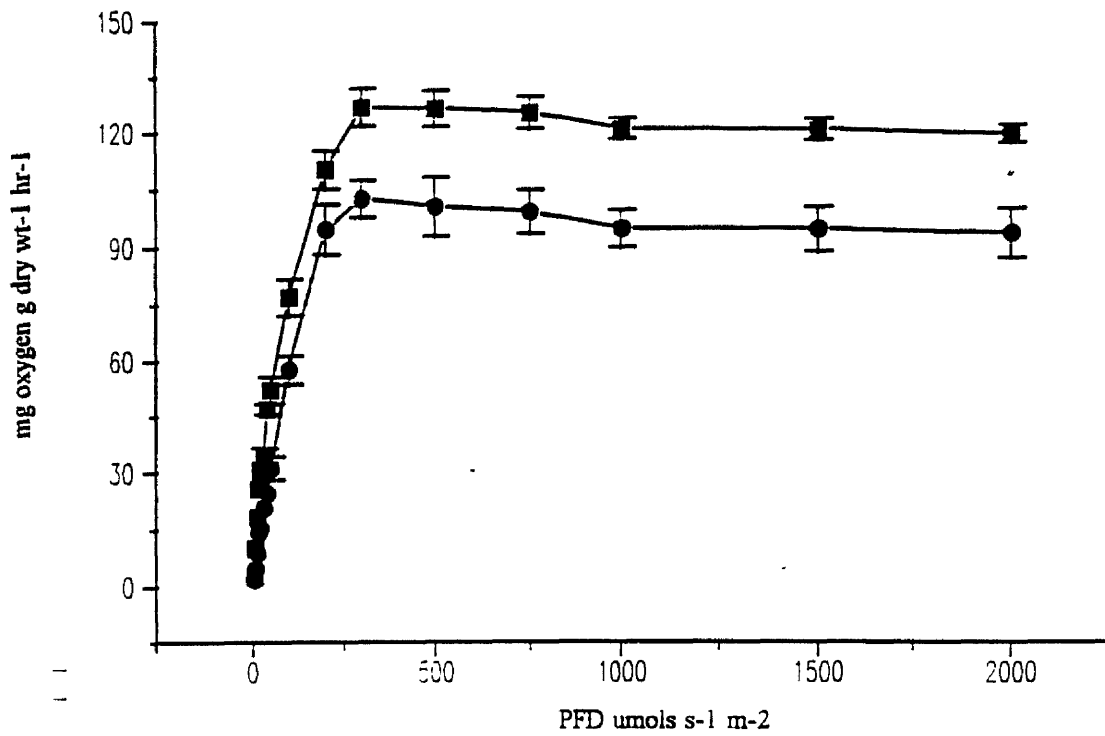


Figure 85. The effect of centrifuging cells of *Synechococcus* 1479/5 prior to photosynthesis / irradiance response measurements. ■—■ centrifuged cells, ●—● uncentrifuged cells.

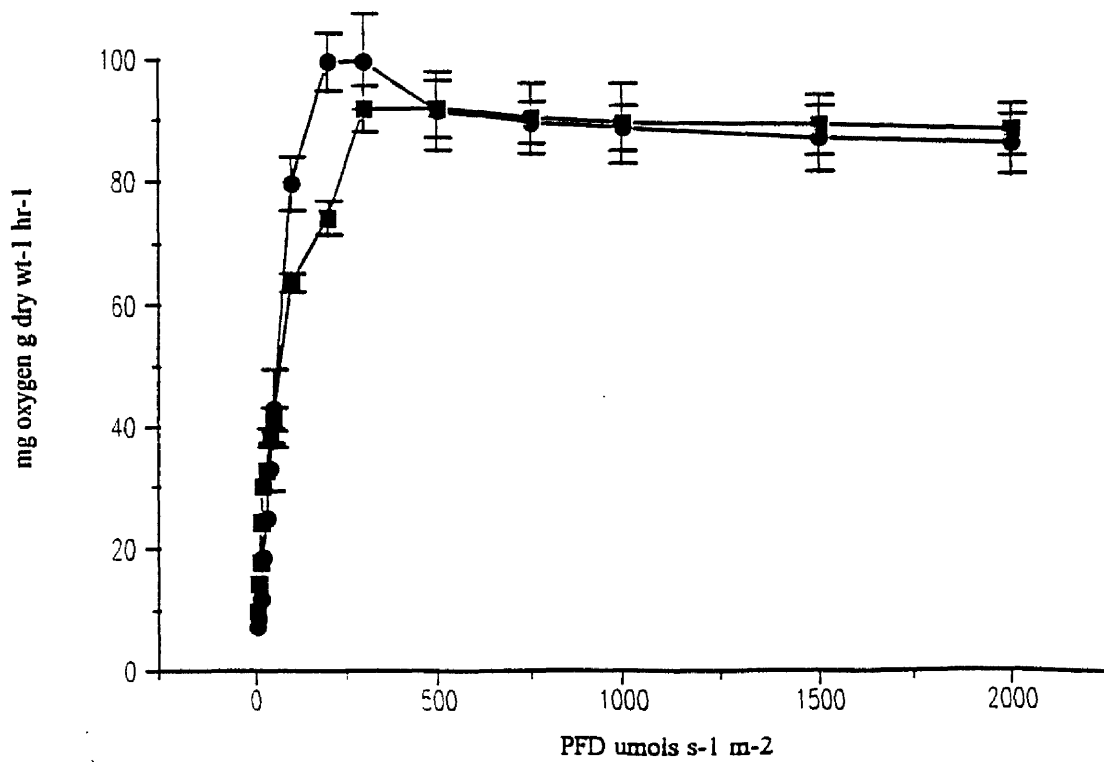


Figure 86. The effect of centrifuging cells of *Scenedesmus* sp. prior to photosynthesis / irradiance response measurements. ■—■ centrifuged cells, ●—● uncentrifuged cells.

Table 28. The effect of centrifugation on the photosynthesis / irradiance curves of *Scenedesmus sp.*

P / I parameter	ASM with centrifugation (2000g 10min)	ASM (no centrifugation)
α (mg oxygen g dry wt ⁻¹ hr ⁻¹ / $\mu\text{mol s}^{-1} \text{m}^{-2}$)	1.95	1.00
P_{max} (mg oxygen g dry wt ⁻¹ hr ⁻¹)	126.59	102.47
I_k ($\mu\text{mol s}^{-1} \text{m}^{-2}$)	64.91	102.47
$P_{\text{max}}^{\text{PPFD}}$ ($\mu\text{mol s}^{-1} \text{m}^{-2}$)	300	300
Light compensation point ($\mu\text{mol s}^{-1} \text{m}^{-2}$)	40	20
Initial dark respiration (mg oxygen g dry wt ⁻¹ hr ⁻¹)	41.33 \pm 2.39	15.411 \pm 1.67
LEDR (mg oxygen g dry wt ⁻¹ hr ⁻¹)	78.91 \pm 4.1	68.35 \pm 3.5

Table 29. The effect of centrifugation on the photosynthesis / irradiance curves of *Synechococcus 1479/5*.

P / I parameter	ASM with centrifugation (2000g 10min)	ASM (no centrifugation)
α (mg oxygen g dry wt ⁻¹ hr ⁻¹ / $\mu\text{mol s}^{-1} \text{m}^{-2}$)	1.164	0.419
P_{max} (mg oxygen g dry wt ⁻¹ hr ⁻¹)	91.82	99.54
I_k ($\mu\text{mol s}^{-1} \text{m}^{-2}$)	78.88	237.56
$P_{\text{max}}^{\text{PPFD}}$ ($\mu\text{mol s}^{-1} \text{m}^{-2}$)	300	300
Light compensation point ($\mu\text{mol s}^{-1} \text{m}^{-2}$)	50-100	30
Initial dark respiration (mg oxygen g dry wt ⁻¹ hr ⁻¹)	46.61 \pm 3.59	24.86 \pm 2.88
LEDR (mg oxygen g dry wt ⁻¹ hr ⁻¹)	76.37 \pm 6.48	76.00 \pm 7.19

centrifuged cells ($1.164 \text{ mg oxygen g dry wt}^{-1} \text{ hr}^{-1} / \mu\text{mol s}^{-1} \text{ m}^{-2}$). As was found with cells of *Chlorella vulgaris* 211/11c and *Scenedesmus sp.* centrifuged cells of *Synechococcus* 1479/5 showed a higher light compensation point of $50\text{-}100 \mu\text{mol s}^{-1} \text{ m}^{-2}$ than uncentrifuged cells ($30 \mu\text{mol s}^{-1} \text{ m}^{-2}$). Unlike that observed with *Chlorella vulgaris* 211/11c and *Scenedesmus sp.* the LEDR rates of centrifuged and uncentrifuged cells were almost identical at $76 \text{ mg oxygen g dry wt}^{-1} \text{ hr}^{-1}$.

Micro-algae are capable of transporting inorganic carbon in the form of HCO_3^- across the cell membrane for photosynthesis (Beardall and Raven, 1989). Green micro-algae and cyanobacteria have been reported to have a high affinity for dissolved inorganic carbon when cultured in environments low in carbon availability (Sültemeyer *et al.*, 1989). The cells of micro-algae and cyanobacteria used in the above experiments were cultured using atmospheric carbon dioxide i.e. very low carbon availability. To examine the role of carbon on the rates of photosynthesis, carbon was supplied in the form of NaHCO_3 during photosynthesis / irradiance measurements. It has been reported (Berry *et al.*, 1976; Badger *et al.*, 1980; Beardall and Raven, 1990) that cells of micro-algae possess an inorganic carbon concentrating mechanism which raises the level of carbon dioxide within the cell. A high carbon dioxide to oxygen ratio within the cell leads to a suppression of the activity of Rubisco (Beardall and Raven, 1990). The suppression of Rubisco prevents the process of photorespiration. The proposed carbon concentrating mechanism (' HCO_3^- pump') apparently functions more efficiently at the higher pH (Sültemeyer *et al.*, 1989). Using the marine cyanobacterium *Synechococcus sp.* they found that low carbon dioxide grown cells achieved a higher P_{max} than high carbon dioxide grown cells. However it was observed that high carbon dioxide grown cells had a much higher initial dark respiration rates. Results – reported here did not show an increase in the initial rate of oxygen uptake in cells of *Chlorella vulgaris* 211/11c, *Scenedesmus sp.* or *Synechococcus* 1479/5 (Tables 14, 15 and 16 respectively). Although, the presence of HCO_3^- in the suspending medium did significantly increase the LEDR rate of *Scenedesmus sp.* (Table 15). Sültemeyer *et al.*, (1989) also observed that the values of α were higher in high carbon dioxide grown cells compared to low carbon dioxide grown cells. The experiments found that low carbon dioxide grown cells had a much higher affinity for inorganic carbon ($K_{1/2} = 6\text{-}8 \mu\text{M} [\text{CO}_2 + \text{HCO}_3^-]$) than high carbon dioxide grown cells ($130 \mu\text{M} [[\text{CO}_2 + \text{HCO}_3^-]]$). The affinity for carbon dioxide was found to be extremely high in cells

grown in atmospheric carbon ($K_{1/2} = 56\text{-}74\text{nM } [\text{CO}_2]$). Although *Chlorella vulgaris* 211/11c (Fig 71) showed a slight increase in P_{max} , *Scenedesmus sp.* and *Synechococcus* 1479/5 (Figures 72 and 73 respectively) had significant increases in their maximum rates of photosynthesis when HCO_3^- was present in the incubating media. *Synechococcus* 1479/5 was the only organism in which there was a large increase in α when incubated in the presence of HCO_3^- (0.492 to 0.909 mg oxygen g dry wt⁻¹ hr⁻¹ / $\mu\text{mol s}^{-1} \text{m}^{-2}$). Sültemeyer *et al.*, 1989 displayed that cells of the marine cyanobacterium *Synechococcus sp.* had high affinities for both HCO_3^- and carbon dioxide. They concluded though that in the presence of both carbon substrates, HCO_3^- would be preferentially taken-up by the cells.

Common experiments are reported where cells of micro-algae and cyanobacteria are cultured in different media to that in which photosynthesis / irradiance response curves are determined. Whilst examining the mechanism for HCO_3^- transport, Miller and Colman, (1980), worked with cells of *Coccochloris peniocyctis* cultured in an enriched media according to that of Miller *et al.*, (1971), however, when photosynthesis / irradiance curves were measured, the cells were incubated in 20mM K_2HPO_4 . Espie and Kandasmy, (1992) when examining the effect of sodium ion on the transport and accumulation of dissolved inorganic carbon, grew cells of *Synechococcus* UTEX 625 in unbuffered Allen's medium (Espie and Canvin, 1987) and then measured photosynthesis response curves whilst incubating the cells in BTP-HCl (pH 8.0) buffer. Cells of *Chlorella vulgaris* 211/11c, *Scenedesmus sp.*, *Ankistrodesmus antarcticus* and *Synechococcus* 1479/5 incubated in phosphate buffer as opposed to ASM, all had significantly lower maximum rates of photosynthesis. It was also found that the presence of nitrate in ASM delayed the onset of photoinhibition at light intensities above P_{max} .

Cells of micro-algae and cyanobacteria are frequently harvested by centrifugation (prior to oxygen electrode measurements) at g forces up to 6000g (Miller and Colman, 1980), 5000g (Badger *et al.*, 1985) and 2000g (Sültemeyer *et al.*, 1986). As can be seen from Tables 27, 28 and 29, the centrifugation of cells of *Chlorella vulgaris* 211/11c, *Scenedesmus sp.* and *Synechococcus* 1479/5, showed a significant increase in the rate of oxygen consumption measured immediately after cells had been centrifuged.

Since in the measurement of standard photosynthesis / irradiance curves, the initial dark respiration rate was added to the net photosynthetic rates, the maximum photosynthetic rate was higher than that determined from uncentrifuged cells. The increase in respiration rate (LEDR), of cells which had been centrifuged, increased at a greater rate when the cells were irradiated during photosynthesis / irradiance measurements.

The LEDR rate of centrifuged cells was approximately 3 times the initial dark respiration rate for *Chlorella vulgaris* 211/11c and twice the initial rate for *Scenedesmus sp.* and *Synechococcus* 1479/5. If the process of LEDR in the light is higher than that measured initially in the dark, and the rate subsequently increases with increasing light intensity and duration, then the process of centrifugation will have a much more profound influence on the measurement of photosynthesis response curves in cells of micro-algae and cyanobacteria.

Further indications of the effect of centrifugation on cellular photosynthesis came from the measurement of the light compensation point. It was observed that the light compensation point of *Chlorella vulgaris* 211/11c, *Scenedesmus sp.* and *Synechococcus* 1479/5, was increased for each alga by a factor of 2. An increase in the light compensation clearly affects a cellular response to light of a given irradiance and spectral quality, thus affecting the resulting interpretation of the photosynthesis / irradiance curve. The results imply that the process of centrifugation is creating stress on the organisms and in doing so changing the interpretation of the measured photosynthesis / irradiance response curve.

3.3.6 The effect of LEDR on the measurement of photosynthesis / irradiance response curves.

Figure 87 shows the photosynthesis / irradiance curve of *Chlorella vulgaris* 211/11c. The net photosynthesis plot was calculated using the initial dark respiration rate measured at the start of the photosynthesis / irradiance measurement. The photosynthetic parameters determined from this curve are shown in Table 30.

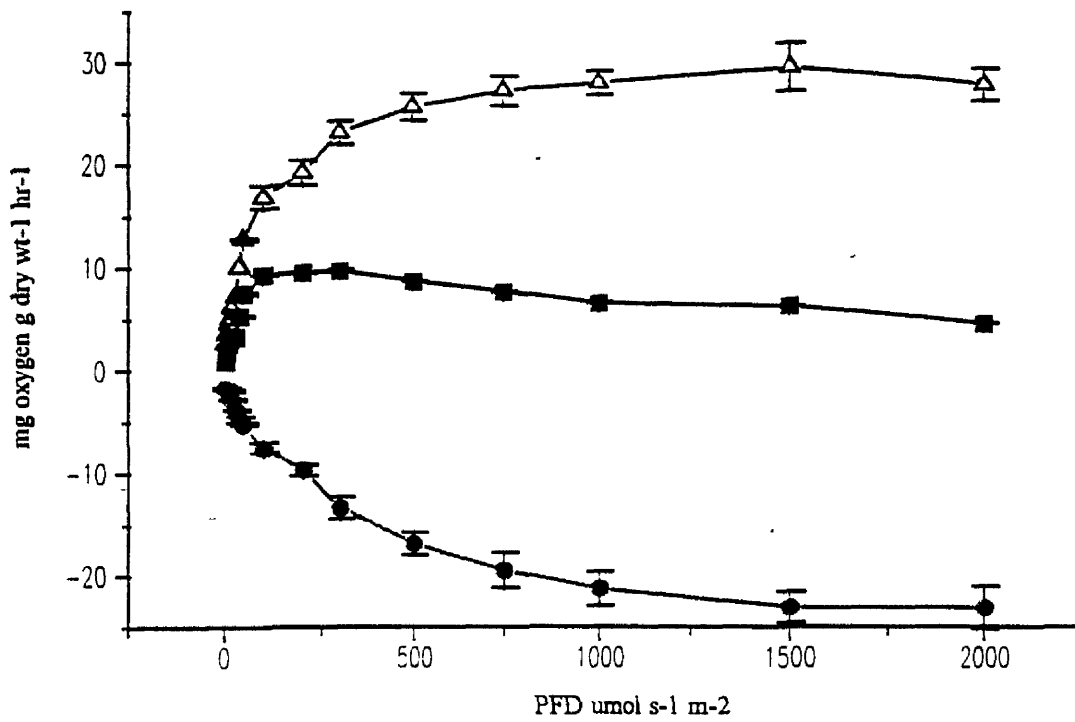


Figure 87. The effect of irradiance on the light enhanced dark respiration of *Chlorella vulgaris* 211/11c and the subsequent effect on a photosynthesis / irradiance curve, ■—■ photosynthesis / irradiance response curve calculated using the initial dark respiration as a constant. ●—● light enhanced dark respiration. Δ—Δ photosynthesis / irradiance response curve calculated using light enhanced dark respiration rate.

Table 30. The effect of increasing dark respiration on the measured photosynthetic parameters of *Chlorella vulgaris* 211/11c.

Photosynthetic parameter	P / I (DR)	P / I (LEDR)
α (mg oxygen g dry wt ⁻¹ hr ⁻¹ / $\mu\text{mol s}^{-1} \text{m}^{-2}$)	0.188	0.206
P_{max} (mg oxygen g dry wt ⁻¹ hr ⁻¹)	9.71	29.33
P_{max}^{PPFD} ($\mu\text{mol s}^{-1} \text{m}^{-2}$)	300	1500
β (mg oxygen g dry wt ⁻¹ hr ⁻¹ / $\mu\text{mol s}^{-1} \text{m}^{-2}$)	----	----
I_{β} ($\mu\text{mol s}^{-1} \text{m}^{-2}$)	----	----
I_k ($\mu\text{mol s}^{-1} \text{m}^{-2}$)	51.64	142.37

Table 31. The effect of increasing dark respiration on the measured photosynthetic parameters of *Scenedesmus* sp.

Photosynthetic parameter	P / I (DR)	P / I (LEDR)
α (mg oxygen g dry wt ⁻¹ hr ⁻¹ / $\mu\text{mol s}^{-1} \text{m}^{-2}$)	0.78	0.81
P_{max} (mg oxygen g dry wt ⁻¹ hr ⁻¹)	41.6	86.29
P_{max}^{PPFD} ($\mu\text{mol s}^{-1} \text{m}^{-2}$)	200	2000
β (mg oxygen g dry wt ⁻¹ hr ⁻¹ / $\mu\text{mol s}^{-1} \text{m}^{-2}$)	no data	no data
I_{β} ($\mu\text{mol s}^{-1} \text{m}^{-2}$)	no data	no data
I_k ($\mu\text{mol s}^{-1} \text{m}^{-2}$)	53.37	107.3

The change in respiration rate with increasing light intensity, termed light enhanced dark respiration (LEDR), was monitored and shown in Figure 87. The photosynthesis / irradiance curve obtained when the subsequent increase in dark respiration was added in place of the initial dark respiration rate is presented in Figure 87. The resultant curve can be seen to have different characteristics compared to the original calculated using the initial dark respiration rate (Table 30). From Table 30, it can be seen that if dark respiration was assumed to be a constant, based solely on the original oxygen consumption rate the P_{\max} for *Chlorella vulgaris* 211/11c of 9.71 mg oxygen g dry wt⁻¹ hr⁻¹. If, however, the change in dark respiration was added to the gross photosynthesis, the new P_{\max} was 29.33 mg oxygen g dry wt⁻¹ hr⁻¹. Table 30 also shows the differences in I_k when dark respiration was assumed to be constant and calculated from the LEDR rate. Assuming a constant dark respiration, I_k was 51.64 $\mu\text{mol s}^{-1} \text{m}^{-2}$, however when the LEDR rate was taken into the calculation, I_k was found to be approximately 3 times higher at 142.37 $\mu\text{mol s}^{-1} \text{m}^{-2}$. *Chlorella vulgaris* 211/11c did not exhibit indications of photoinhibition, hence β could not be determined. The increased oxygen uptake by respiration began when the light intensity reached an equivalent to $\frac{1}{2}P_{\max}$ (20-30 $\mu\text{mol s}^{-1} \text{m}^{-2}$). The increase in the rate of respiration was associated with very high photon flux densities; those at which photoinhibition is known to occur.

Figure 88 shows the photosynthesis / irradiance response curves of *Scenedesmus sp.* The plot of Figure 88 also shows the change in LEDR with increasing irradiance and the subsequent effect that a changing respiration rate has on the photosynthesis / irradiance response curve. The photosynthetic parameters of the curve determined using the initial dark respiration and LEDR rate are shown in Table 31. The curve derived using the initial dark respiration rate had a light limited slope α of 0.729 mg oxygen g dry wt⁻¹ hr⁻¹ / $\mu\text{mol s}^{-1} \text{m}^{-2}$ which was virtually no different to the α of 0.731 mg oxygen g dry wt⁻¹ hr⁻¹ / $\mu\text{mol s}^{-1} \text{m}^{-2}$ determined from the curve calculated using LEDR. The main difference between the two curves was in the maximum rates of photosynthesis. The curve calculated with initial dark respiration was 50% lower than the P_{\max} determined from the curve calculated using LEDR.

Figure 89 shows the photosynthesis / irradiance curves of *Synechococcus* 1479/5. From the curve calculated using the initial dark respiration rate it can be seen that

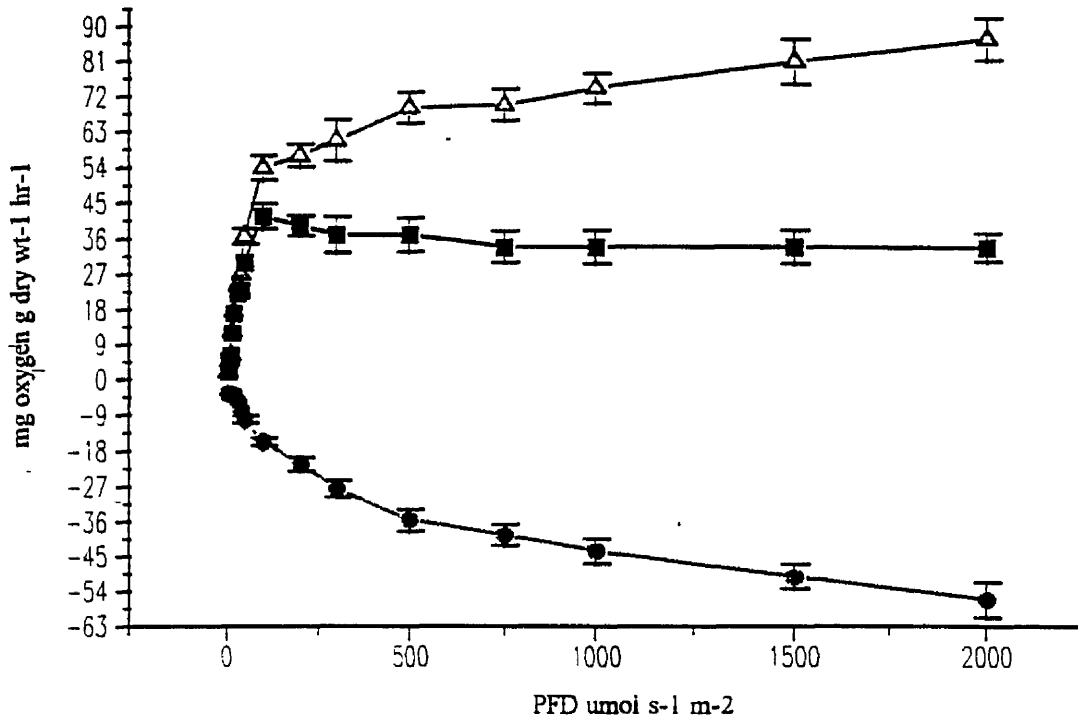


Figure 88. The effect of irradiance on the light enhanced dark respiration of *Scenedesmus sp.* and the subsequent effect on a photosynthesis / irradiance curve, ■—■ photosynthesis / irradiance response curve calculated using the initial dark respiration as a constant, ●—● light enhanced dark respiration, Δ—Δ photosynthesis / irradiance response curve calculated using light enhanced dark respiration rate.

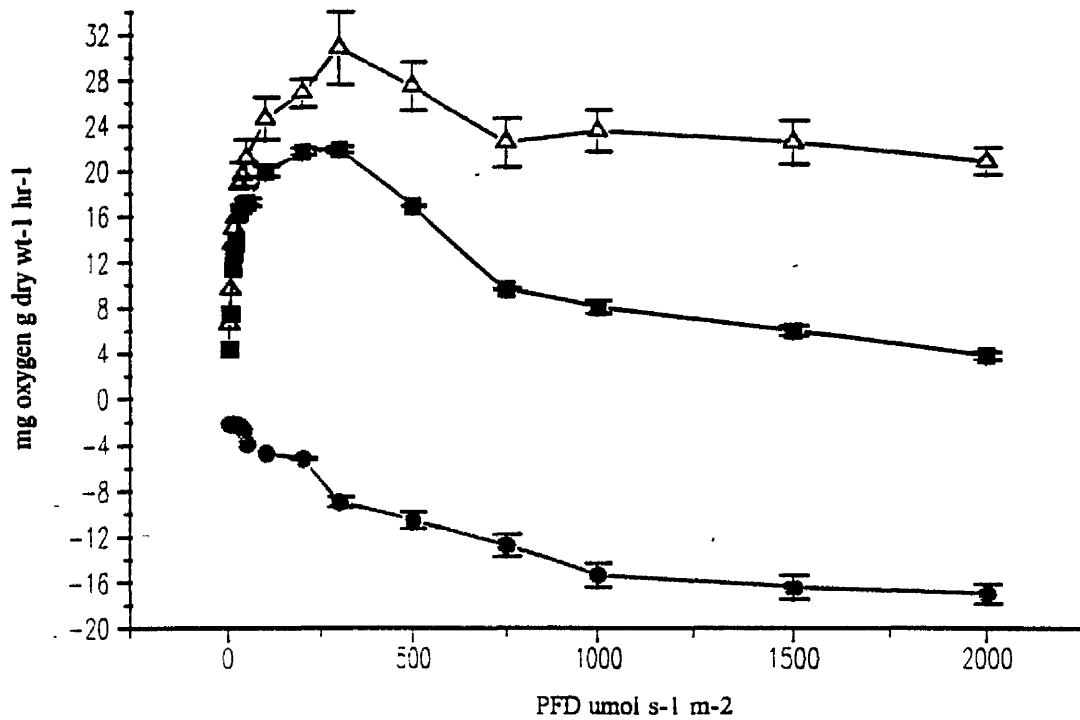


Figure 89. The effect of irradiance on the light enhanced dark respiration of *Synechococcus* 1479/5 and the subsequent effect on a photosynthesis / irradiance curve, ■—■ photosynthesis / irradiance response curve calculated using the initial dark respiration as a constant, ●—● light enhanced dark respiration, Δ—Δ photosynthesis / irradiance response curve calculated using light enhanced dark respiration rate.

Synechococcus 1479/5 displayed a P_{\max} of 21.8 mg oxygen g dry wt⁻¹ hr⁻¹, whereas if the LEDR rate was used in the calculation the value of P_{\max} was 30.74 mg oxygen g dry wt⁻¹ hr⁻¹, a 50% increase compared to that calculated using the initial constant dark respiration rate (Table 32). The value of LEDR approached 50-100% that of P_{\max} when cells were irradiated at 1000 $\mu\text{mol s}^{-1} \text{m}^{-2}$ for 6 minutes. There was virtually no change found in the value of α , β , however, increased approximately 7 fold to -0.186 mg oxygen g dry wt⁻¹ hr⁻¹ / $\mu\text{mol s}^{-1} \text{m}^{-2}$ and there was an approximate 5 fold decrease in I_B to 165.26 $\mu\text{mol s}^{-1} \text{m}^{-2}$. Similar to that observed with *Chlorella vulgaris* 211/11c the rate of LEDR started to significantly increase at irradiances equivalent to $\frac{1}{2}P_{\max}$ (16-30 $\mu\text{mol s}^{-1} \text{m}^{-2}$).

These differences in photosynthetic parameters determined from photosynthesis / irradiance curves measured from the same organism, display the requirement for a better understanding and interpretation of what the measured data actually means. It is suggested that where possible, each photosynthesis / irradiance curve should be accompanied with either measured changes in dark respiration or that the curve is plotted from gross photosynthesis rates accompanied by the initial dark and final respiration rates. The few researchers who have used this method include Takahashi *et al.*, (1971); Raven, (1984); Ferris and Christian, (1991). One of the major problems in determining the level of productivity in phytoplankton lies in the measurement of respiration during photosynthesis. Oxygen consumption has long been considered to be a constant, but the data presented here and from Heichel, (1972); Glidewell and Raven, (1975); Stone and Ganf, (1981); Falkowski *et al.*, (1985); Peltier and Thibault, (1985); Reddy *et al.*, (1991) show that this is probably not the case. Stone and Ganf, (1981) measured enhanced respiration rates of between 400-600% the initial dark respiration rate in both freshwater green micro-algae and cyanobacteria after exposure to light at a PFD of 550 $\mu\text{mol s}^{-1} \text{m}^{-2}$ for 7.5 hours. Although the reason for the changes in respiration remains unclear, it is likely to be due an increased maintenance requirement brought about by cellular photodamage (Raven, 1984). Since the measurement of photosynthesis / irradiance response curves is carried in order to determine the photosynthetic and metabolic status of a cell, it is clear that the change in cellular respiration should be monitored more closely. If the process of LEDR does indeed occur in the light and is increased by increasing PFD, then it would have severe implications on our understanding and interpretation of photosynthesis measurements (Beardall and Raven, 1990).

Table 32. The effect of increasing dark respiration on the measured photosynthetic parameters of *Synechococcus* 1479/5.

Photosynthetic parameter	P / I (DR)	P / I (LEDR)
α (mg oxygen g dry wt ⁻¹ hr ⁻¹ / $\mu\text{mol s}^{-1} \text{m}^{-2}$)	0.729	0.731
P_{max} (mg oxygen g dry wt ⁻¹ hr ⁻¹)	21.8	30.74
$P_{\text{max}}^{\text{PFD}}$ ($\mu\text{mol s}^{-1} \text{m}^{-2}$)	300	300
β (mg oxygen g dry wt ⁻¹ hr ⁻¹ / $\mu\text{mol s}^{-1} \text{m}^{-2}$)	-0.027	-0.186
I_{β} ($\mu\text{mol s}^{-1} \text{m}^{-2}$)	807.77	165.26
I_k ($\mu\text{mol s}^{-1} \text{m}^{-2}$)	29.9	42.1

3.4 The effect of culture temperature and P/I incubation temperature on the Photosynthetic Kinetics of Micro-algae and Cyanobacteria.

The effects of temperature on the respiration and photosynthetic parameters of four unicellular green micro-algae (*Chlorella vulgaris* 211/11c, *Nannochloris atomus*, *Scenedesmus sp.* and *Ankistrodesmus antarcticus*) and two cyanobacteria (*Synechococcus sp.* and *Synechococcus* 1479/5) were examined. Cells of each organism were cultured at 4 temperatures (15, 23, 30 and 35°C respectively). At each culture temperature, photosynthesis / irradiance curves were measured at both the culture temperature and at the other three alternate culture temperatures. The species of micro-algae (*Chlorella vulgaris* 211/11c, *Scenedesmus sp.* and *Ankistrodesmus antarcticus*) were chosen since they were the main photosynthetic organisms found in the high rate algal ponds based at the Scottish Agricultural College, Auchincruive. *Nannochloris atomus* and *Synechococcus sp.* are not frequently found in the HRAPs.

3.4.1 The effect of culture temperature and P/I incubation temperature on cells of micro-algae and cyanobacteria grown at a PFD of $100\mu\text{mol s}^{-1}\text{m}^{-2}$.

The first number before the colon refers to the temperature at which the cells of that particular organism were cultured at. The second number after the colon refers to the photosynthesis / irradiance temperature which the cells were measured at.

P_{max}^x is the maximum rate of photosynthesis ($\text{mg oxygen g dry wt}^{-1}\text{ hr}^{-1}$) measured at a culture temperature x (15, 23, 30 and 35°C). T is any incubation temperature between 15 and 35°C

The photosynthesis / irradiance response curves for *Chlorella vulgaris* 211/11c cultured at 15°C and 23°C measured at the four temperatures of 15, 23, 30 and 35°C are shown in Figure 90 and 91 respectively. It can be seen from Figures 90 and 91 that the P/I measured at an incubation temperature of 35°C gave the highest maximum rates of photosynthesis (P_{max}) of 386.6 and 209.7 $\text{mg oxygen g dry wt}^{-1}\text{ hr}^{-1}$ respectively. The inverse was true for cultures grown at higher temperatures when P/Is were measured at 15 and 23°C, (Fig 92 and 93).

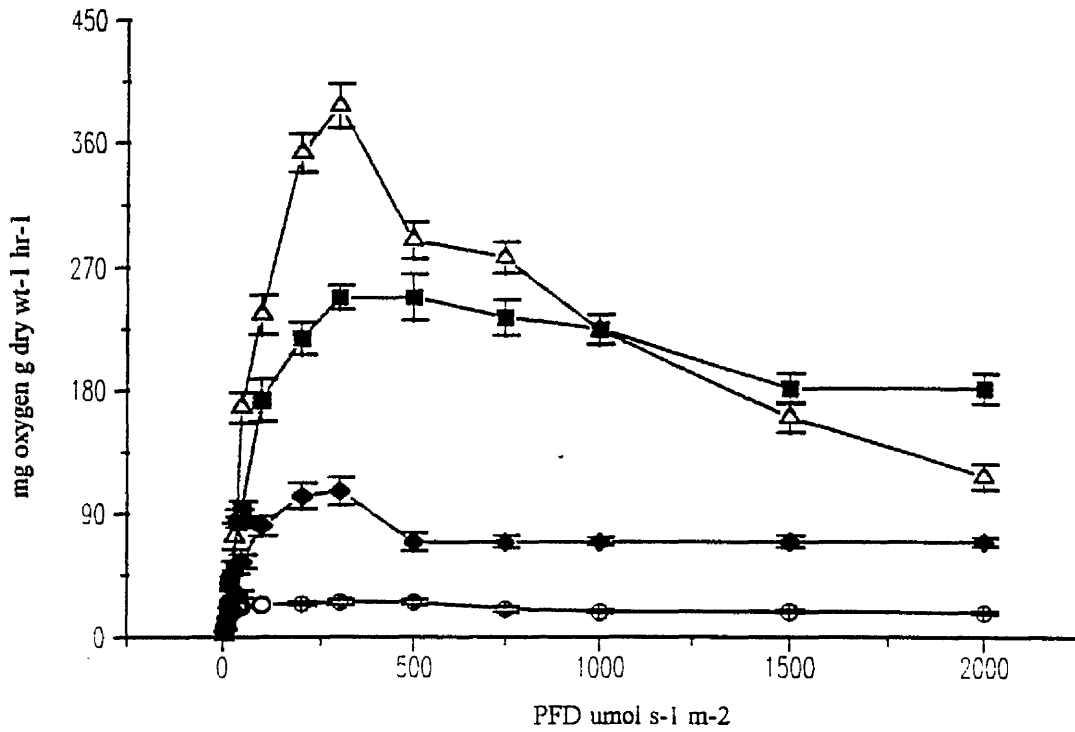


Figure 90. The effect of P/I incubation temperature on the photosynthesis / irradiance response curves of *Chlorella vulgaris* 211/11c cultured at 15°C, ○—○ 15°C, ◆—◆ 23°C, ■—■ 30°C, △—△ 35°C.

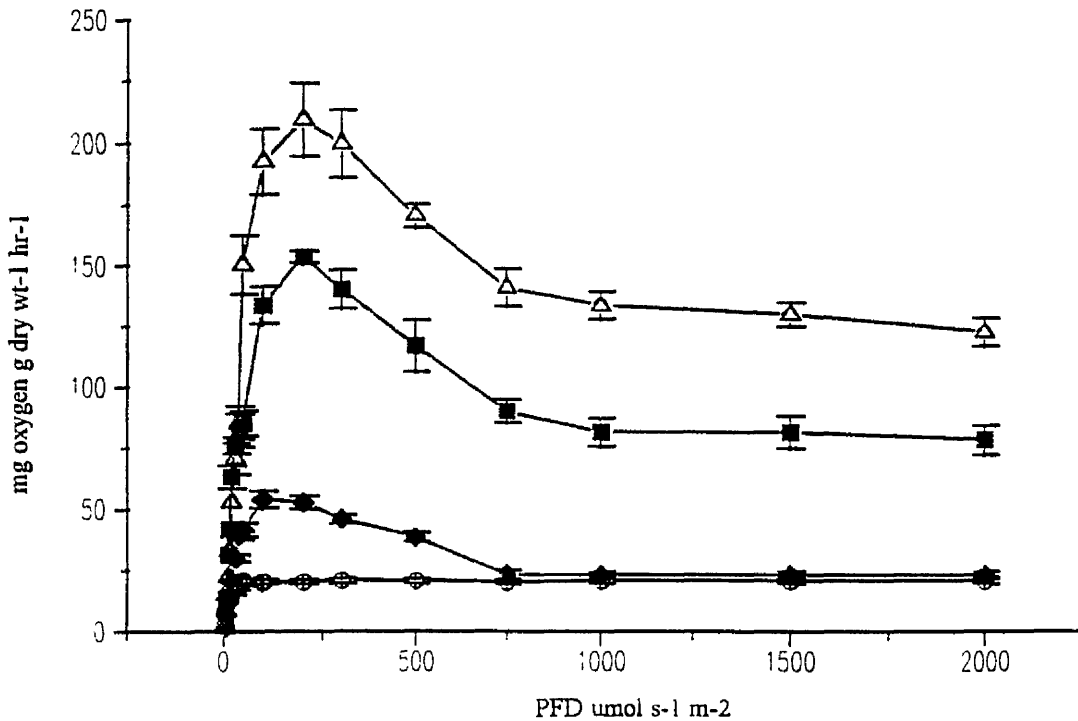


Figure 91. The effect of P/I incubation temperature on the photosynthesis / irradiance response curves of *Chlorella vulgaris* 211/11c cultured at 23°C, ○—○ 15°C, ◆—◆ 23°C, ■—■ 30°C, △—△ 35°C.

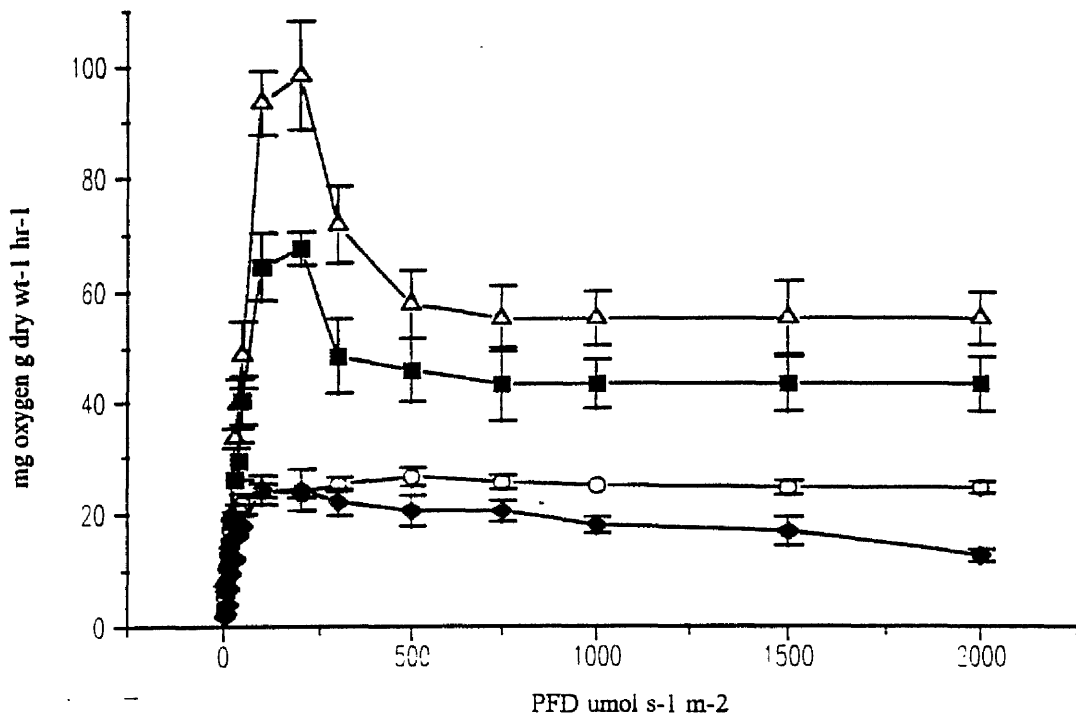


Figure 92 . The effect of P/I incubation temperature on the photosynthesis / irradiance response curves of *Chlorella vulgaris* 211/11c cultured at 30°C, O—O 15°C, ◆—◆ 23°C, ■—■ 30°C, Δ—Δ 35°C.

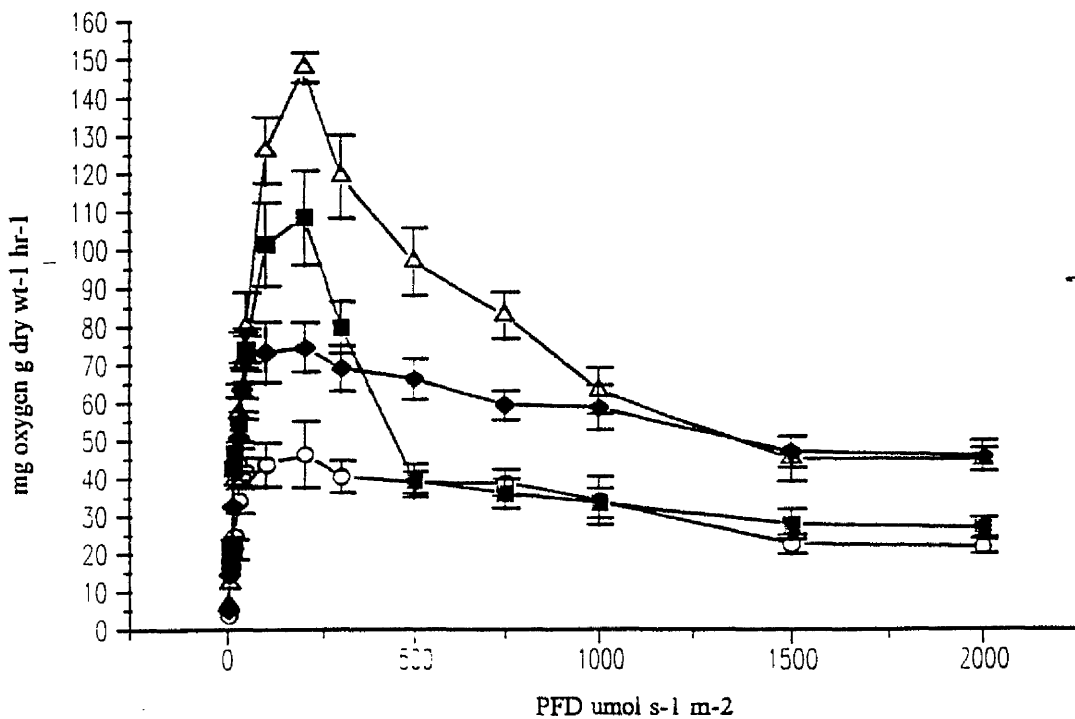


Figure 93 . The effect of P/I incubation temperature on the photosynthesis / irradiance response curves of *Chlorella vulgaris* 211/11c cultured at 35°C, O—O 15°C, ◆—◆ 23°C, ■—■ 30°C, Δ—Δ 35°C.

The relationship between temperature and P_{\max} was a power fit curve for the culture temperatures of 15, 23, 30 and 35°C (Equations 22, 23, 24 and 25 respectively).

15°C

$$P_{\max}^{15} = 0.004136 \times T^{3.228} \quad (\text{Sig } P=0.001) \quad (22)$$

23°C

$$P_{\max}^{23} = 0.008483 \times T^{2.847} \quad (\text{Sig } P=0.001) \quad (23)$$

30°C

$$P_{\max}^{30} = 0.2696 \times T^{1.601} \quad (\text{Sig } P=0.01) \quad (24)$$

35°C

$$P_{\max}^{35} = 1.183 \times T^{1.341} \quad (\text{Sig } P=0.001) \quad (25)$$

Where T was any temperature between 15 and 35°C.

Tables 33, 34, 35 and 36 show that there was an overall increase in both α and I_k (the PFD at which the onset of light saturation is observed) with increasing P/I temperature, at all culture temperatures. Cells cultured at 15°C and then measured at a P/I incubation temperature of 35°C displayed a 15 fold increase in P_{\max} from 25.47mg oxygen mg dry wt⁻¹ hr⁻¹ (measured at a P/I incubation of 15°C) to 386.63mg oxygen mg dry wt⁻¹ hr⁻¹ (measured at a P/I incubation of 35°C). The value of β (an indication of the degree of the photoinhibitive slope) generally increased with increasing P/I temperature. This was supported by the observation that the PFD at which P_{\max} occurred decreased with increasing measurement / incubation temperature. This supports previous evidence (Kirk, 1983., Kirk, 1989) that the higher the incubation temperature, the more rapidly the onset of photoinhibition

Table 33. The effect of temperature on the photosynthetic parameters of *Chlorella vulgaris* 211/11c cultured at 15°C.

Culture temperature °C	P/I temperature °C	α (mg oxygen g dry wt ⁻¹ hr ⁻¹ / μ mol s ⁻¹ m ⁻²)	I_k (μ mol s ⁻¹ m ⁻²)	β (mg oxygen g dry wt ⁻¹ hr ⁻¹ / μ mol s ⁻¹ m ⁻²)	P_{max}^{PFD} (μ mol s ⁻¹ m ⁻²)	P_{max} (mg oxygen g dry wt ⁻¹ hr ⁻¹)
15	15	0.47	54.0	-0.013	300	25.4
15	23	0.87	122.5	-0.079	300	106.6
15	30	1.83	135.7	-0.047	300	248.4
15	35	2.9	133.3	-0.236	300	386.6

Table 34. The effect of temperature on the photosynthetic parameters of *Chlorella vulgaris* 211/11c cultured at 23°C.

Culture temperature °C	P/I temperature °C	α (mg oxygen g dry wt ⁻¹ hr ⁻¹ / μ mol s ⁻¹ m ⁻²)	I_k (μ mol s ⁻¹ m ⁻²)	β (mg oxygen g dry wt ⁻¹ hr ⁻¹ / μ mol s ⁻¹ m ⁻²)	P_{max}^{PFD} (μ mol s ⁻¹ m ⁻²)	P_{max} (mg oxygen g dry wt ⁻¹ hr ⁻¹)
23	15	0.70	28.8	no data	200	20.2
23	23	1.10	49.0	-0.04	200	53.9
23	30	2.55	60.2	-0.11	200	153.6
23	35	3.26	64.3	-0.09	300	209.7

Table 35. The effect of temperature on the photosynthetic parameters of *Chlorella vulgaris* 211/11c cultured at 30°C.

Culture temperature °C	P/I temperature °C	α (mg oxygen g dry wt ⁻¹ hr ⁻¹ / μ mol s ⁻¹ m ⁻²)	I_k (μ mol s ⁻¹ m ⁻²)	β (mg oxygen g dry wt ⁻¹ hr ⁻¹ / μ mol s ⁻¹ m ⁻²)	P_{max}^{PFD} (μ mol s ⁻¹ m ⁻²)	P_{max} (mg oxygen g dry wt ⁻¹ hr ⁻¹)
30	15	0.41	64.3	no data	300	26.4
30	23	0.61	56.0	-0.01	200	34.1
30	30	0.94	72.1	-0.06	200	67.5
30	35	0.81	121.1	-0.12	200	98.2

Table 36. The effect of temperature on the photosynthetic parameters of *Chlorella vulgaris* 211/11c cultured at 35°C.

Culture temperature °C	P/I temperature °C	α (mg oxygen g dry wt ⁻¹ hr ⁻¹ / μ mol s ⁻¹ m ⁻²)	I_k (μ mol s ⁻¹ m ⁻²)	β (mg oxygen g dry wt ⁻¹ hr ⁻¹ / μ mol s ⁻¹ m ⁻²)	P_{max}^{PFD} (μ mol s ⁻¹ m ⁻²)	P_{max} (mg oxygen g dry wt ⁻¹ hr ⁻¹)
35	15	1.35	34.2	-0.022	200	46.2
35	23	1.39	53.6	-0.026	200	74.5
35	30	1.97	55.0	-0.225	200	108.4
35	35	2.26	65.3	-0.161	200	147.7

occurs and the higher the culture temperature, the lower the PFD required to initiate photoinhibition and photodamage.

Figures 94, 95, 96 and 97 show the effect of culture temperature and P/I incubation temperature on the initial dark respiration and light enhanced dark respiration rates of *Chlorella vulgaris* 211/11c. It was found that at the lower culture temperatures (15 and 23°C), an increase in incubation temperature to 30 and 35°C resulted in a large increase (5.5 fold) in the initial measured dark respiration rate. Cells cultured at temperature of 35°C, however, showed very little change in dark respiration when measured at P/I incubation temperatures of 15 and 23°C. It can be seen that there was a general decrease (2.6 fold decrease) in the respiration rate measured at the lower P/I incubation temperature of 15°C. The initial dark respiration rate was measured at the beginning of each experiment, the light enhanced dark respiration (LED R) was determined at the end of a photosynthesis / irradiance measurement. Dark respiration, however, increased 5.5 fold from 16mg oxygen mg dry wt⁻¹ hr⁻¹ (15:15) to 88mg oxygen mg dry wt⁻¹ hr⁻¹ (15:35). The maximum LED R rate of oxygen consumption was 255 mg oxygen mg dry wt⁻¹ hr⁻¹ at a culture temperature of 15°C and a P/I incubation temperature of 35°C.

The following equations determine the initial dark respiration rates of cells at constant temperatures of 15, 23, 30 and 35°C. *T* is the change in temperature from 15 to 35°C. 15°C

$$R_{initial}^{15} = \frac{1}{(-0.1011 + (2.744 \times 10^{-3} \times T))} \quad (\text{Sig } P=0.001) \quad (26)$$

23°C

$$R_{initial}^{23} = \frac{1}{(-0.1665 + (4.482 \times 10^{-3} \times T))} \quad (\text{Sig } P=0.001) \quad (27)$$

30°C

$$R_{initial}^{30} = \frac{1}{(-0.5143 + (1.466 \times 10^{-2} \times T))} \quad (\text{Sig } P=0.001) \quad (28)$$

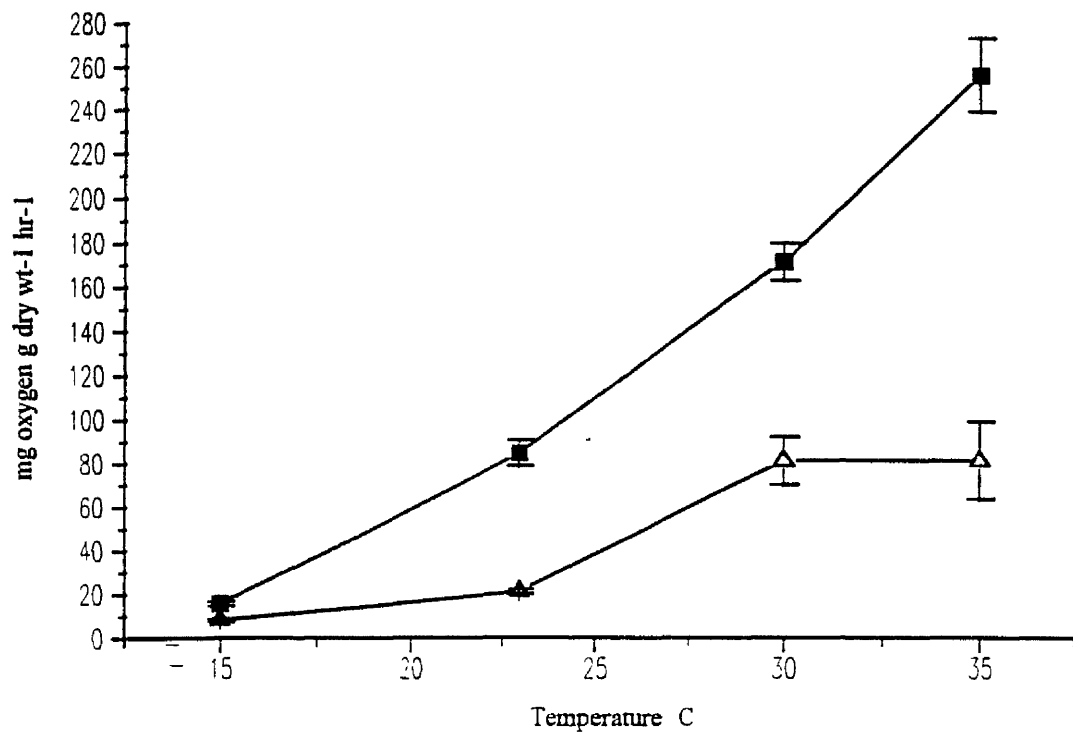


Figure 94. The effect of P/I incubation temperature on the dark respiration Δ — Δ and light enhanced dark respiration \blacksquare — \blacksquare of *Chlorella vulgaris* 211/11c cultured at 15°C.

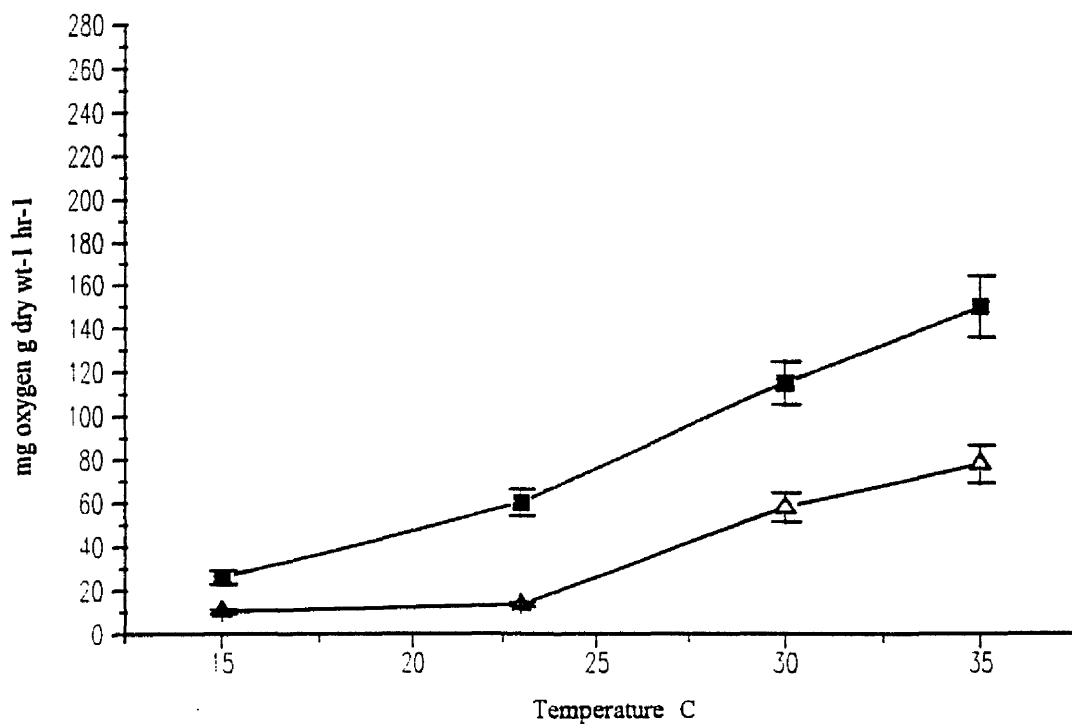


Figure 95. The effect of P/I incubation temperature on the dark respiration Δ — Δ and light enhanced dark respiration \blacksquare — \blacksquare of *Chlorella vulgaris* 211/11c cultured at 23°C.

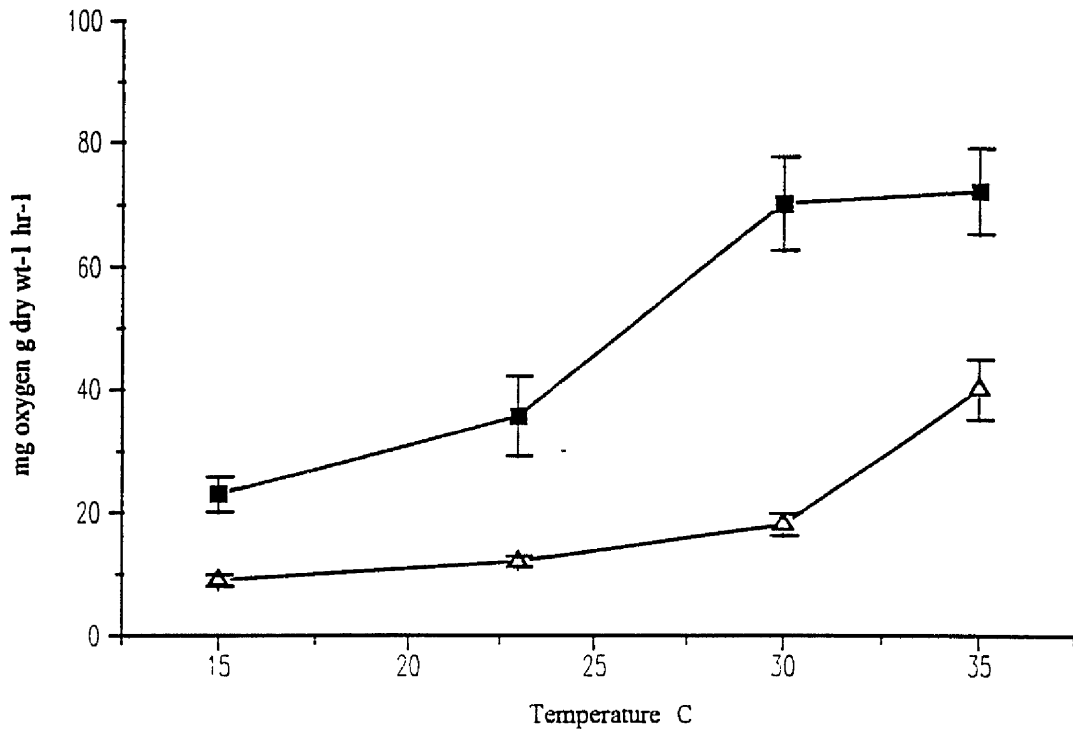


Figure 96. The effect of P/I incubation temperature on the dark respiration Δ — Δ and light enhanced dark respiration \blacksquare — \blacksquare of *Chlorella vulgaris* 211/11c cultured at 30°C.

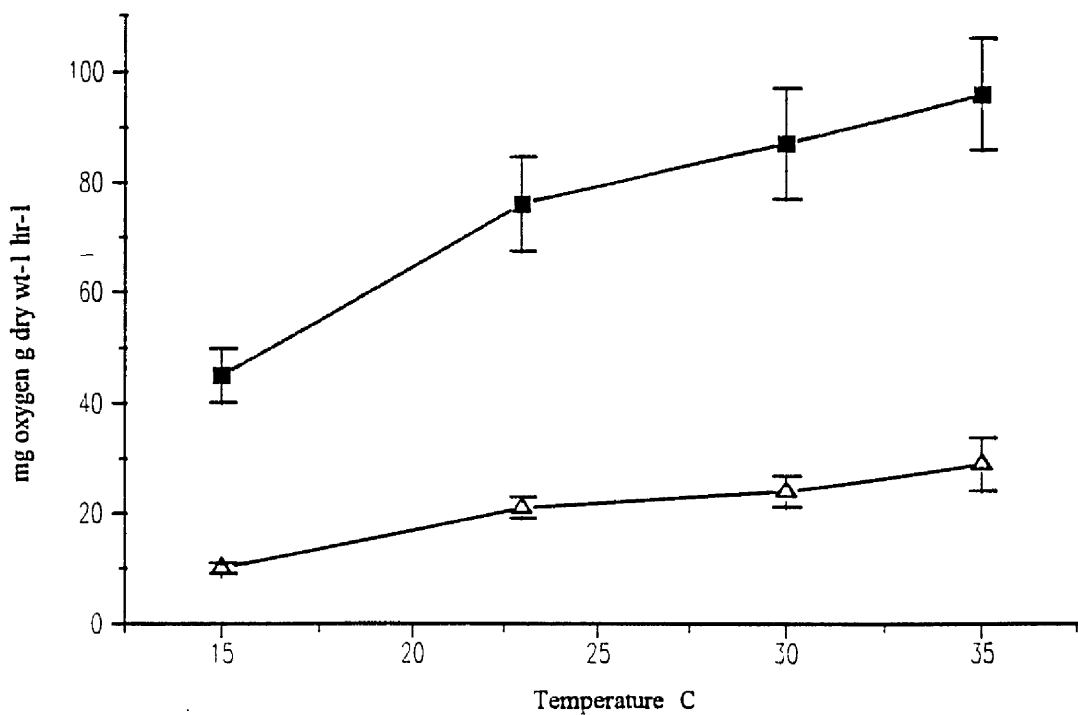


Figure 97. The effect of P/I incubation temperature on the dark respiration Δ — Δ and light enhanced dark respiration \blacksquare — \blacksquare of *Chlorella vulgaris* 211/11c cultured at 35°C.

35°C

$$R_{initial}^{35} = -36.76 + 17.73 \times \ln(T) \quad (\text{Sig } P=0.001) \quad (29)$$

$R_{initial}^{15}$ was the initial respiration rate in mg oxygen mg dry wt⁻¹ hr⁻¹ of cells cultured at the temperature associated with R.

T was any temperature between 15 and 35°C.

It was found that at the lower culture temperatures of 15, 23 and 30°C, cells showed a hyperbolic relationship between initial respiration and temperature (equations 26, 27 and 28 respectively). The cells culture at the higher temperature of 35°C, however, displayed a log based relationship (equation 29).

The following equations predicted the change in respiration (LEDR) after a full photosynthesis / irradiance measurement had been determined from cells cultured at a constant initial temperature of 15 to 35°C but different P/I incubation temperature 15 to 35°C.

15°C

$$LEDR_{final}^{15} = 6.28 \times 10^{-3} \times T^{2.998} \quad (\text{Sig } P=0.001) \quad (30)$$

23°C

$$LEDR_{final}^{23} = 0.1006 \times T^{2.0501} \quad (\text{Sig } P=0.001) \quad (31)$$

30°C

$$LEDR_{final}^{30} = 0.2847 \times T^{1.574} \quad (\text{Sig } P=0.001) \quad (32)$$

35°C

$$LEDR_{final}^{35} = 5.84 \times T^{0.76} \quad (\text{Sig } P=0.01) \quad (33)$$

It was found that cells cultured at the lower temperatures of 15, 23 and 30°C displayed a power fit relationship between LEDR and temperature.

The following equations relate the value of alpha to P/I incubation temperature for cells of *Chlorella vulgaris* 211/11c.

$$\alpha_{15} = 1.815 + (-0.179 \times T) + (6.023 \times 10^{-3} \times T^2) \quad (\text{Sig P}=0.001) \quad (34)$$

$$\alpha_{23} = 1.121 + (-0.102 \times T) + (4.76 \times 10^{-3} \times T^2) \quad (\text{Sig P}=0.001) \quad (35)$$

$$\alpha_{30} = 3.389 \times 10^{-2} \times T^{0.928} \quad (\text{Sig P}=0.01) \quad (36)$$

$$\alpha_{35} = 1.95 + (-8.02 \times 10^{-2} \times T) + (2.58 \times 10^{-3} \times T^2) (\text{Sig P}=0.001) \quad (37)$$

α is the light limited slope (mg oxygen g dry wt⁻¹ hr⁻¹ / $\mu\text{mol s}^{-1} \text{m}^{-2}$).

For equations 34, 35 and 36 the relationship between α and P/I incubation temperature (15 to 35°C) described by a polynomial regression (2 degrees)

Figures 98, 99, 100 and 101 show the arhenius plots for *Chlorella vulgaris* 211/11c of the natural logarithm of photosynthetic rates (mg oxygen g dry wt⁻¹ hr⁻¹), measured at a PFD of 100 $\mu\text{mol s}^{-1} \text{m}^{-2}$ against the reciprocal of P/I incubation temperature (Kelvin) for culture temperatures of 15, 23, 30 and 35°C respectively. It can be seen (Figure 98), that cells of *Chlorella vulgaris* 211/11c cultured at 15°C showed non linearity at the P/I incubation of 35°C.

Nannochloris atomus showed a similar pattern to *Chlorella vulgaris* 211/11c.

Nannochloris atomus cultured at temperature 15 and 23°C showed large increases in P_{max} with increasing P/I incubation temperature of 30 and 35°C (Figures 102 and 103). Cells of *Nannochloris atomus* cultured at the higher temperatures of 30°C and 35°C, however, showed small changes in P_{max} at the lower temperature incubations of 15 and 23°C (Figures 104 and 105). The relationship between temperature and P_{max} for *Nannochloris atomus* cultured at four temperatures was described by the following equations;

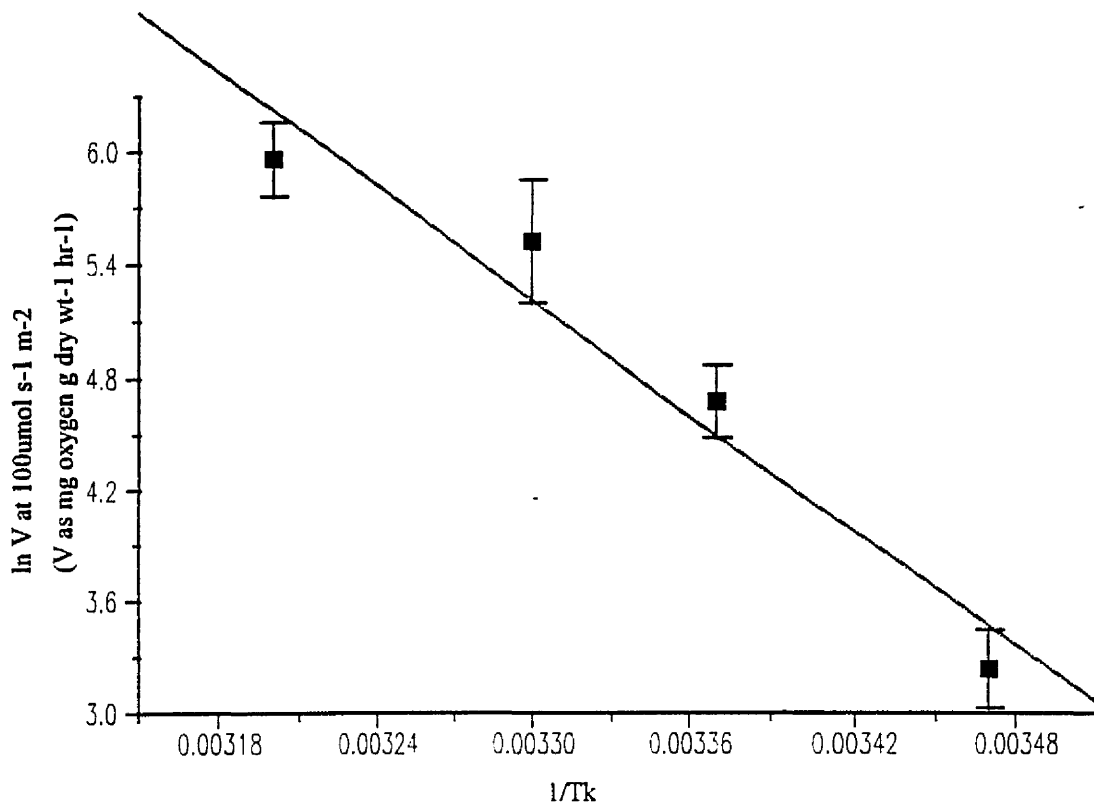


Figure 98. Arrhenius plot of ln photosynthetic rate at a PFD of $100\mu\text{mol s}^{-1} \text{m}^{-2}$ against increasing P/I incubation temperature for *Chlorella vulgaris* 211/11c cultured at a temperature of 15°C.

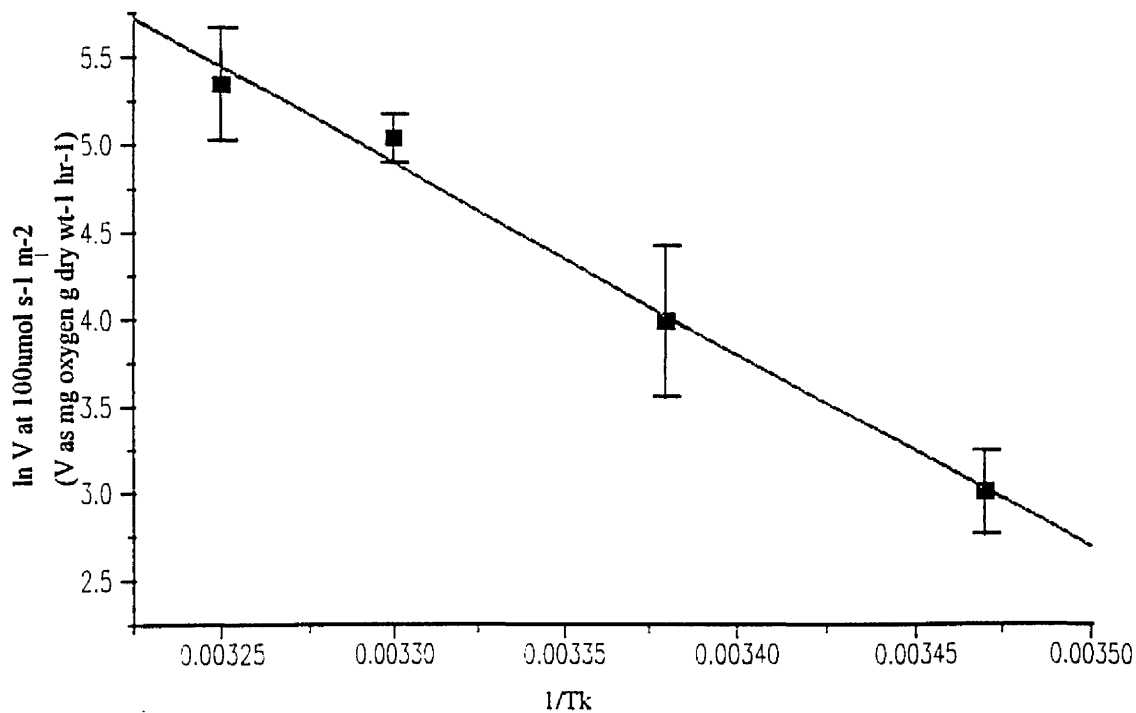


Figure 99. Arrhenius plot of ln photosynthetic rate at a PFD of $100\mu\text{mol s}^{-1} \text{m}^{-2}$ against increasing P/I incubation temperature for *Chlorella vulgaris* 211/11c cultured at a temperature of 23°C.

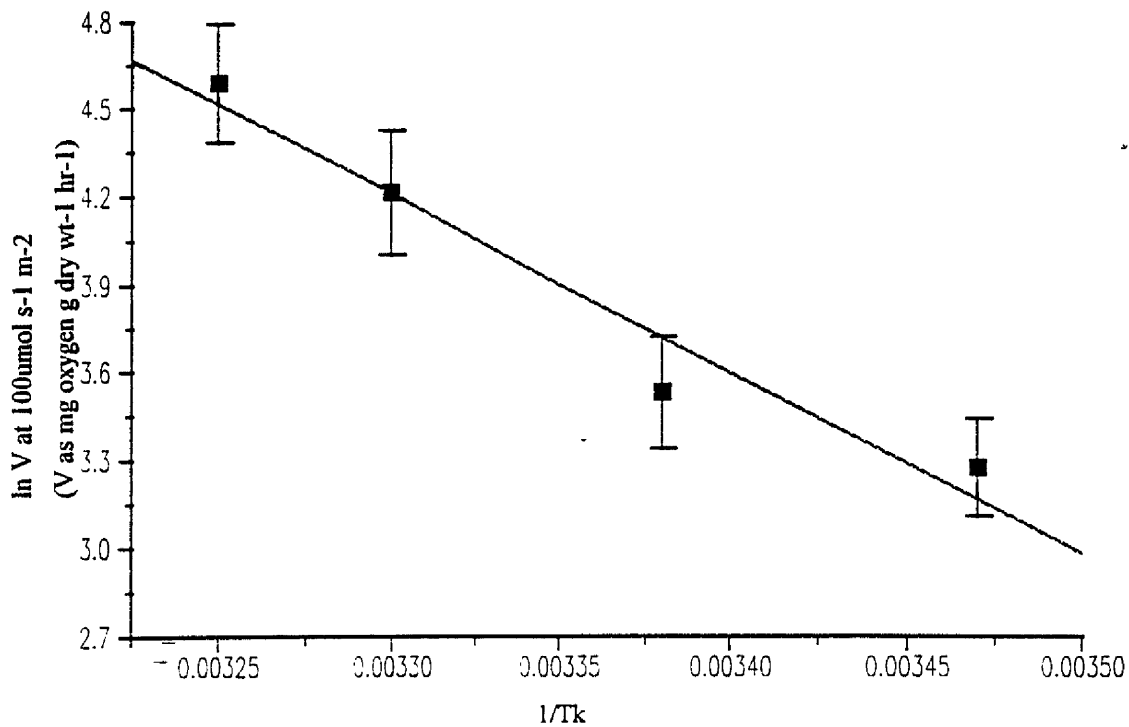


Figure 100. Arrhenius plot of ln photosynthetic rate at a PFD of $100\mu\text{mol s}^{-1} \text{m}^{-2}$ against increasing P/I incubation temperature for *Chlorella vulgaris* 211/11c cultured at a temperature of 30°C.

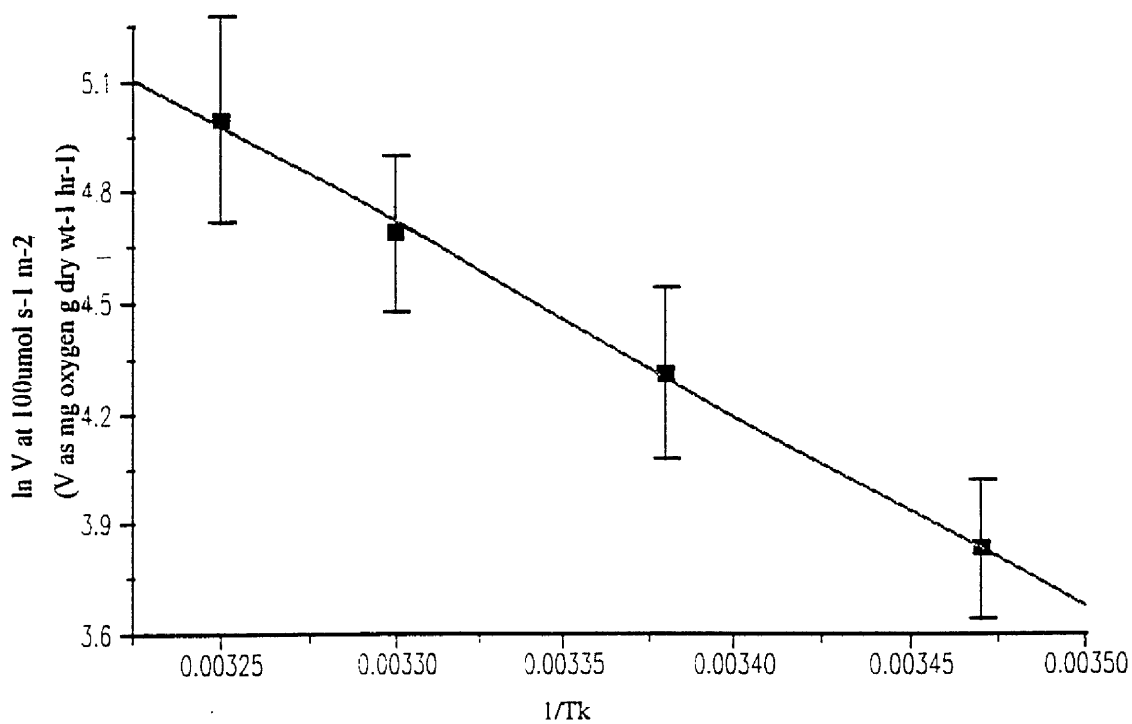


Figure 101. Arrhenius plot of ln photosynthetic rate at a PFD of $100\mu\text{mol s}^{-1} \text{m}^{-2}$ against increasing P/I incubation temperature for *Chlorella vulgaris* 211/11c cultured at a temperature of 35°C.

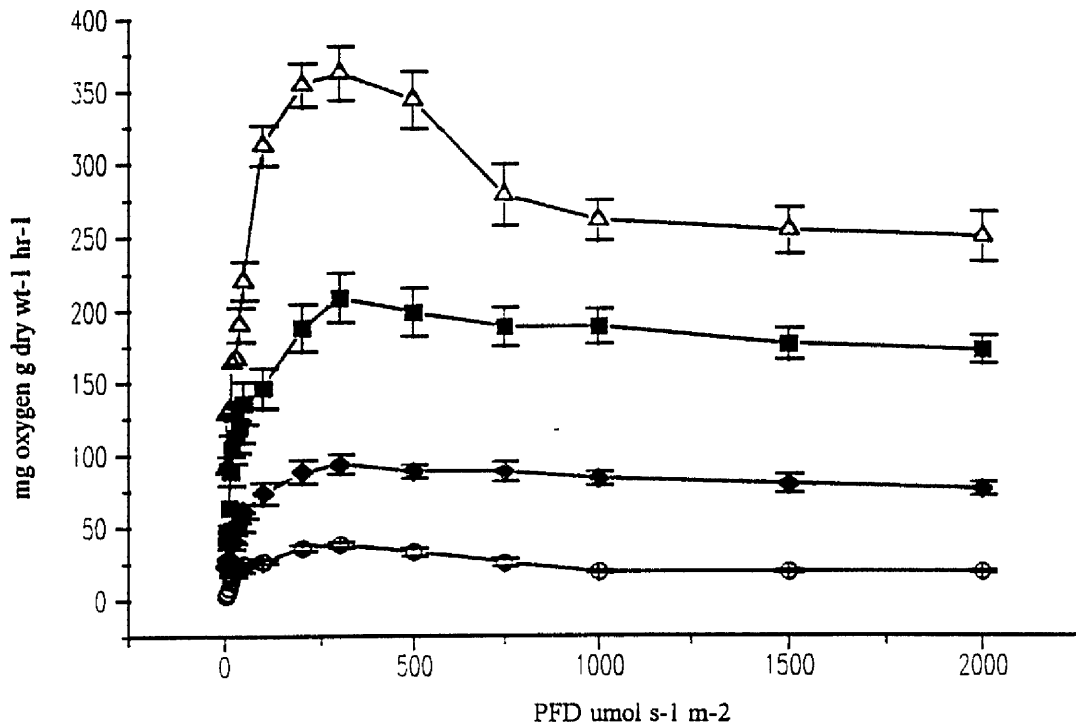


Figure 102. The effect of P/I incubation temperature on the photosynthesis / irradiance response curves of *Nannochloris atomus* cultured at 15°C, ○—○ 15°C, ◆—◆ 23°C, ■—■ 30°C, △—△ 35°C.

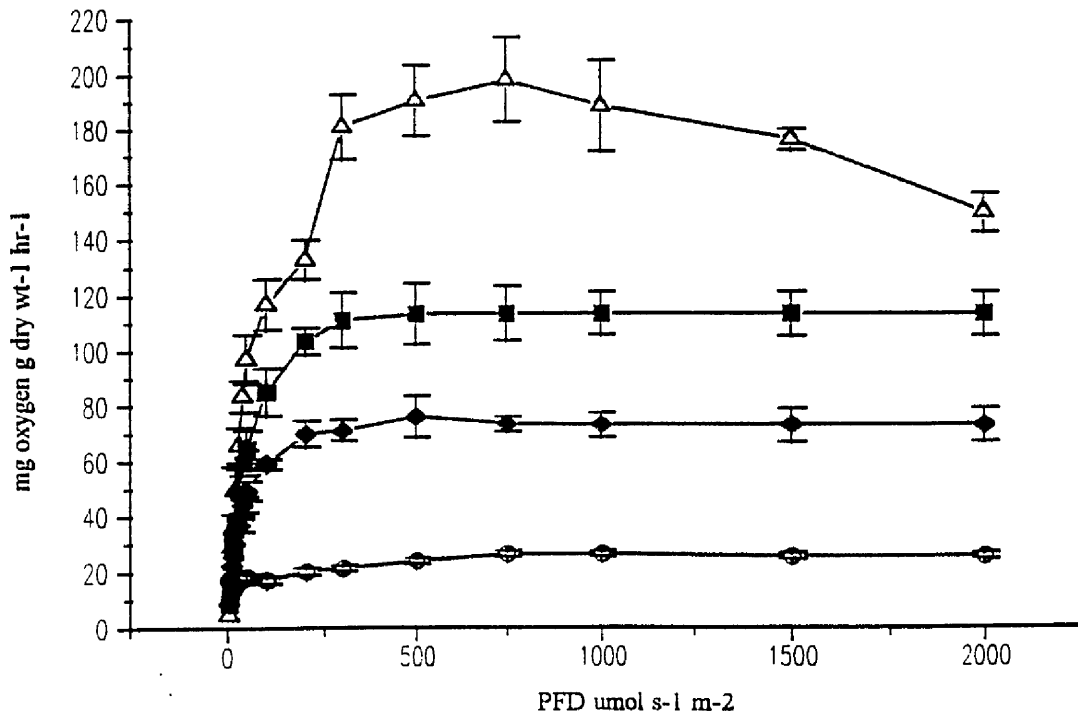


Figure 103. The effect of P/I incubation temperature on the photosynthesis / irradiance response curves of *Nannochloris atomus* cultured at 23°C, ○—○ 15°C, ◆—◆ 23°C, ■—■ 30°C, △—△ 35°C.

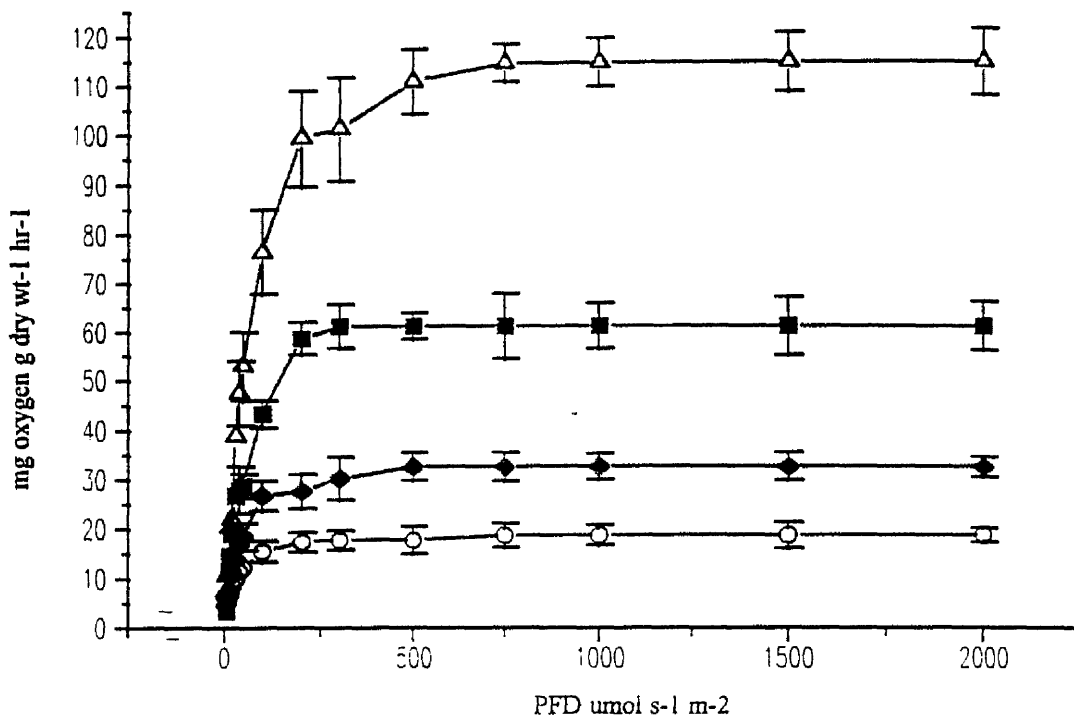


Figure 104. The effect of P/I incubation temperature on the photosynthesis / irradiance response curves of *Nannochloris atomus* cultured at 30°C, ○—○ 15°C, ◆—◆ 23°C, ■—■ 30°C, Δ—Δ 35°C.

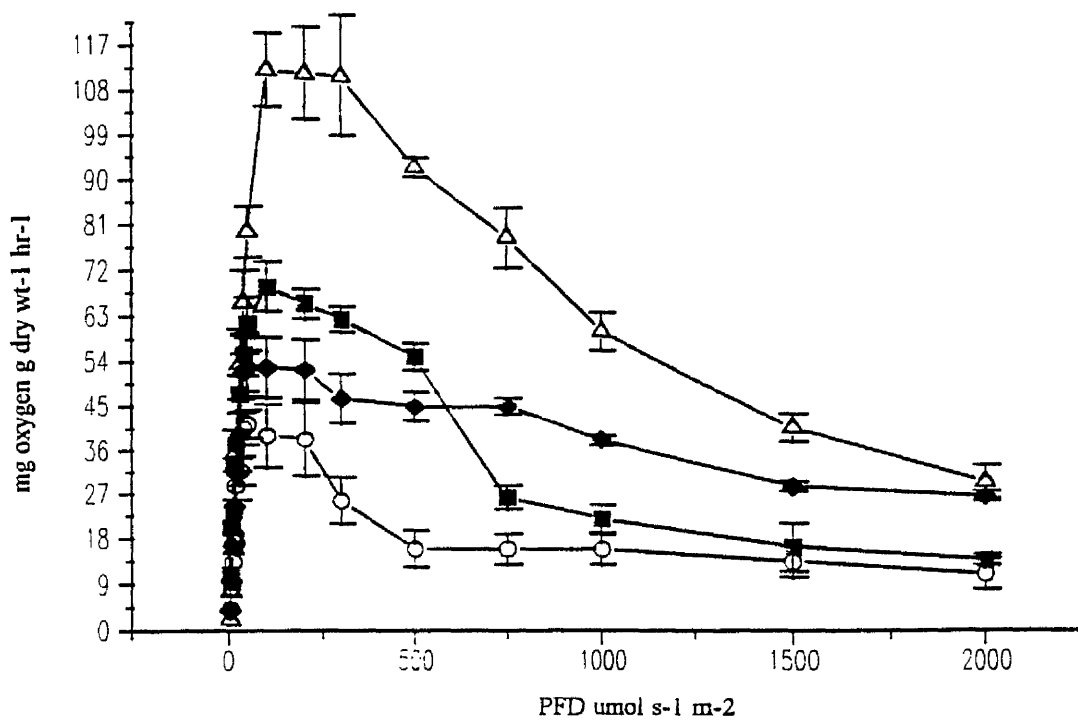


Figure 105. The effect of P/I incubation temperature on the photosynthesis / irradiance response curves of *Nannochloris atomus* cultured at 35°C, ○—○ 15°C, ◆—◆ 23°C, ■—■ 30°C, Δ—Δ 35°C.

15°C

$$P_{\max}^{15} = 0.0275 \times T^{2.638} \quad (\text{Sig } P=0.001) \quad (38)$$

23°C

$$P_{\max}^{23} = 0.05532 \times T^{2.28} \quad (\text{Sig } P=0.001) \quad (39)$$

30°C

$$P_{\max}^{30} = 0.06452 \times T^{2.049} \quad (\text{Sig } P=0.001) \quad (40)$$

35°C

$$P_{\max}^{35} = 1.524 \times T^{1.162} \quad (\text{Sig } P=0.001) \quad (41)$$

It was found that the relationship between the maximum rate of photosynthesis and temperature was a power fit (equations 38, 39, 40 and 41). This was the same type of relationship that was observed with cells of *Chlorella vulgaris* 211/11c.

From Tables 37 and 40, it can be seen that beta was found to increase with increasing P/I incubation temperature in *Nannochloris atomus*. Tables 38 and 39 did not show values for beta since they did not show photoinhibition on the photosynthesis / irradiance response curve. From Tables 37, 38, 39 and 40 it can be seen that the value of I_K displayed an overall increase with increasing P/I incubation temperature. The highest value for P_{\max} of 321 mg oxygen g dry wt⁻¹ hr⁻¹ was measured from cells cultured at a temperature of 15°C and incubated at a P/I temperature of 35°C (Table 37). Cells cultured at a temperature of 35°C (Table 40) had the lowest P_{\max}^{PFD} of 100 μmol s⁻¹ m⁻².

It was found that increasing the P/I incubation temperature resulted in large increase in the rate of respiration (Figures 106, 107 and 108). Cells cultured at 35°C, however, displayed little variation in initial respiration rates with changing P/I incubation temperature (Figure 109).

Table 37. The effect of temperature on the photosynthetic parameters of *Nannochloris atomus* cultured at 15°C.

Culture temperature °C	P/I temperature °C	α (mg oxygen g dry wt ⁻¹ hr ⁻¹ / μ mol s ⁻¹ m ⁻²)	I_k (μ mol s ⁻¹ m ⁻²)	β (mg oxygen g dry wt ⁻¹ hr ⁻¹ / μ mol s ⁻¹ m ⁻²)	P_{max}^{PFD} (μ mol s ⁻¹ m ⁻²)	P_{max} (mg oxygen g dry wt ⁻¹ hr ⁻¹)
15	15	0.82	46.0	-0.026	300	37.7
15	23	1.15	80.9	-0.031	300	93.1
15	30	3.18	65.6	-0.045	300	208.5
15	35	3.89	93.1	-0.19	300	321

Table 38. The effect of temperature on the photosynthetic parameters of *Nannochloris atomus* cultured at 23°C.

Culture temperature °C	P/I temperature °C	α (mg oxygen g dry wt ⁻¹ hr ⁻¹ / μ mol s ⁻¹ m ⁻²)	I_k (μ mol s ⁻¹ m ⁻²)	β (mg oxygen g dry wt ⁻¹ hr ⁻¹ / μ mol s ⁻¹ m ⁻²)	P_{max}^{PFD} (μ mol s ⁻¹ m ⁻²)	P_{max} (mg oxygen g dry wt ⁻¹ hr ⁻¹)
23	15	0.46	57.2	no data	750	26.3
23	23	1.39	54.6	no data	500	75.9
23	30	1.95	58.0	no data	500	113.1
23	35	2.42	81.6	no data	750	197.7

Table 39. The effect of temperature on the photosynthetic parameters of *Nannochloris atomus* cultured at 30°C.

Culture temperature °C	P/I temperature °C	α (mg oxygen g dry wt ⁻¹ hr ⁻¹ / μ mol s ⁻¹ m ⁻²)	I_k (μ mol s ⁻¹ m ⁻²)	β (mg oxygen g dry wt ⁻¹ hr ⁻¹ / μ mol s ⁻¹ m ⁻²)	P_{max}^{PFD} (μ mol s ⁻¹ m ⁻²)	P_{max} (mg oxygen g dry wt ⁻¹ hr ⁻¹)
30	15	0.35	53.5	no data	750	18.7
30	23	0.53	61.5	no data	500	32.6
30	30	0.95	64.3	no data	300	61.1
30	35	1.31	87.5	no data	300	114.6

Table 40. The effect of temperature on the photosynthetic parameters of *Nannochloris atomus* cultured at 35°C.

Culture temperature °C	P/I temperature °C	α (mg oxygen g dry wt ⁻¹ hr ⁻¹ / μ mol s ⁻¹ m ⁻²)	I_k (μ mol s ⁻¹ m ⁻²)	β (mg oxygen g dry wt ⁻¹ hr ⁻¹ / μ mol s ⁻¹ m ⁻²)	P_{max}^{PFD} (μ mol s ⁻¹ m ⁻²)	P_{max} (mg oxygen g dry wt ⁻¹ hr ⁻¹)
35	15	1.21	43.6	-0.022	200	52.8
35	23	1.39	41.87	-0.032	200	58.2
35	30	1.70	40.48	-0.061	100	68.8
35	35	1.72	65.16	-0.070	100	112.1

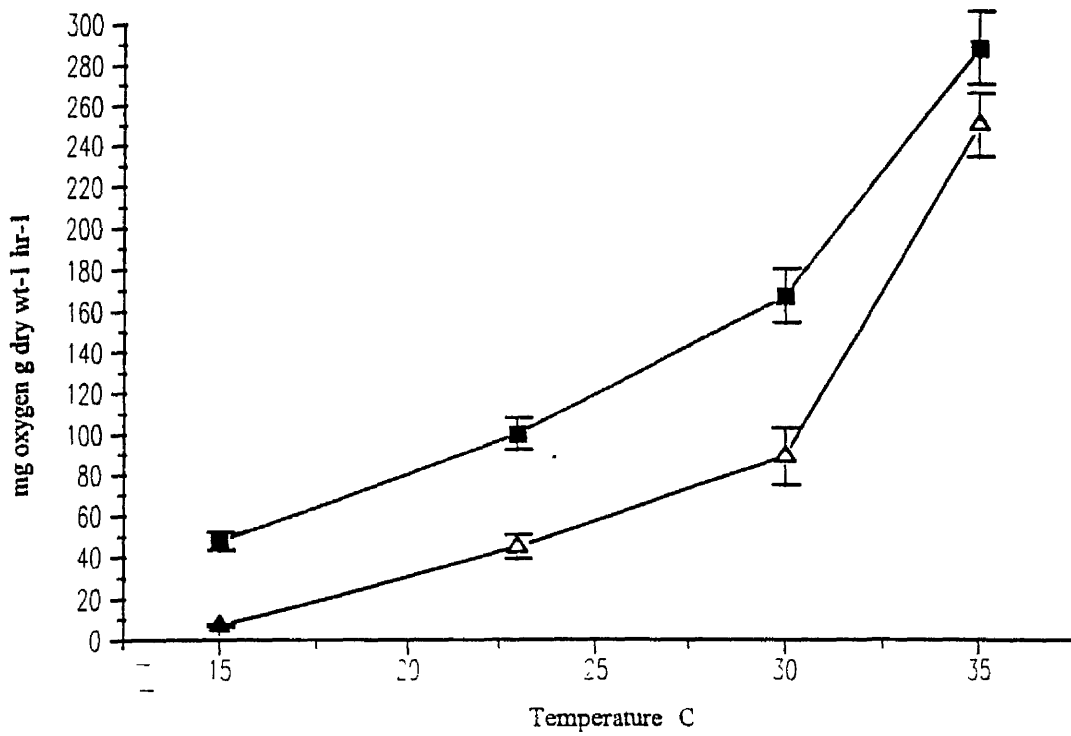


Figure 106. The effect of P/I incubation temperature on the dark respiration Δ — Δ and light enhanced dark respiration \blacksquare — \blacksquare of *Nannochloris atomus* cultured at 15°C.

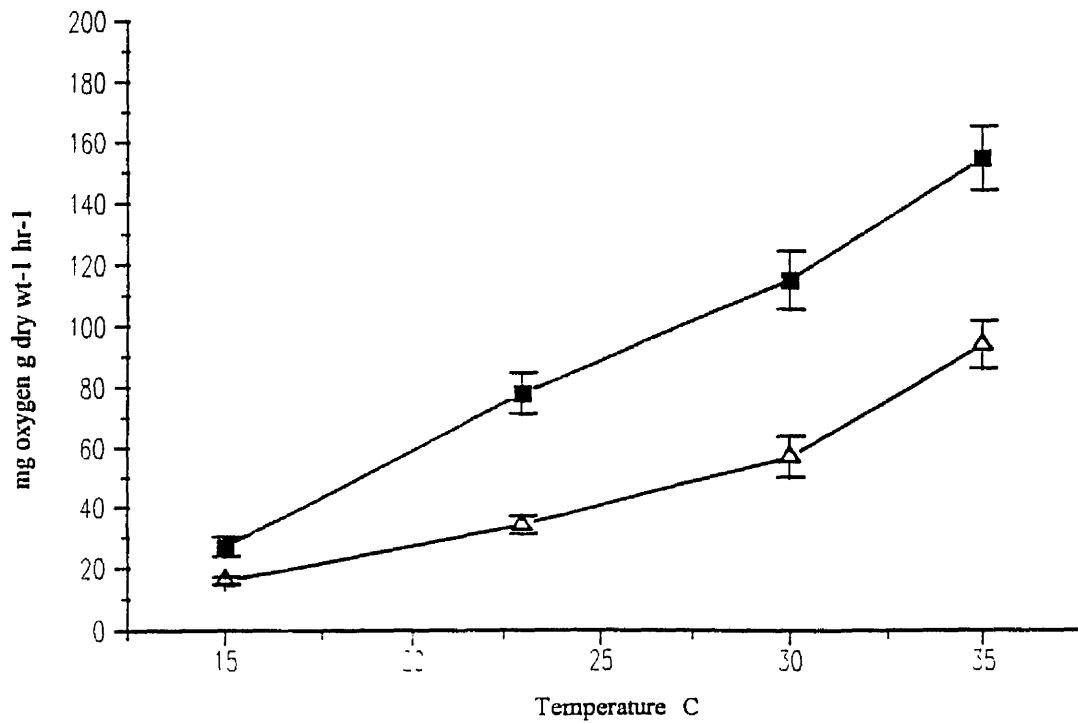


Figure 107. The effect of P/I incubation temperature on the dark respiration Δ — Δ and light enhanced dark respiration \blacksquare — \blacksquare of *Nannochloris atomus* cultured at 23°C.

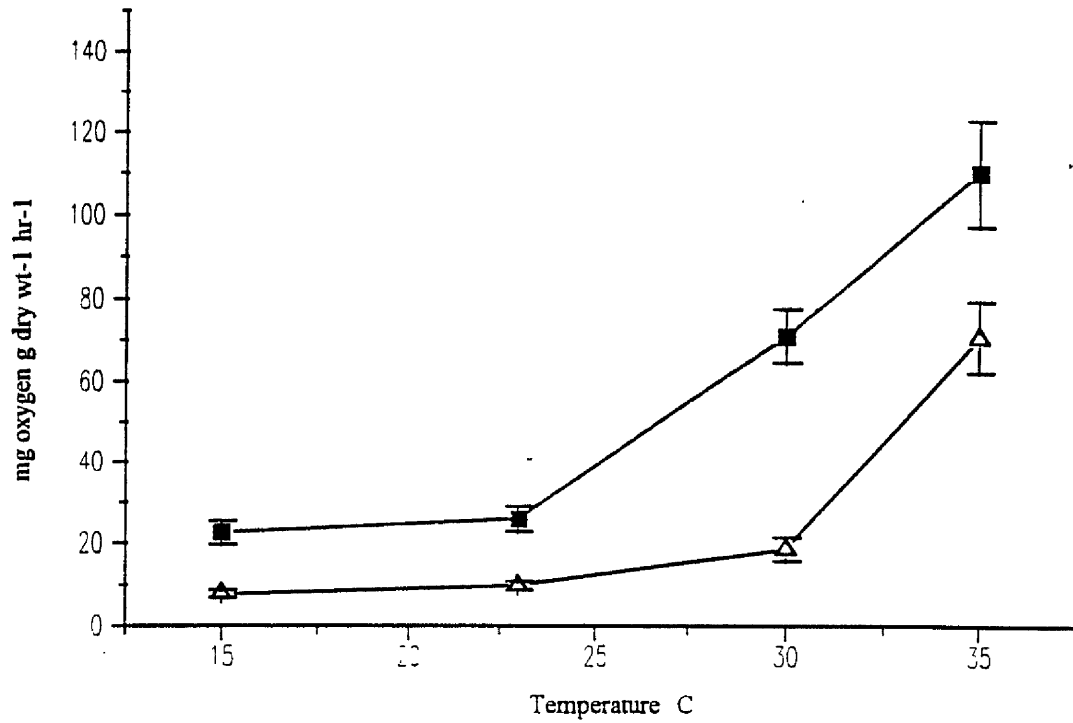


Figure 108. The effect of P/I incubation temperature on the dark respiration Δ — Δ and light enhanced dark respiration \blacksquare — \blacksquare of *Nannochloris atomus* cultured at 35°C.

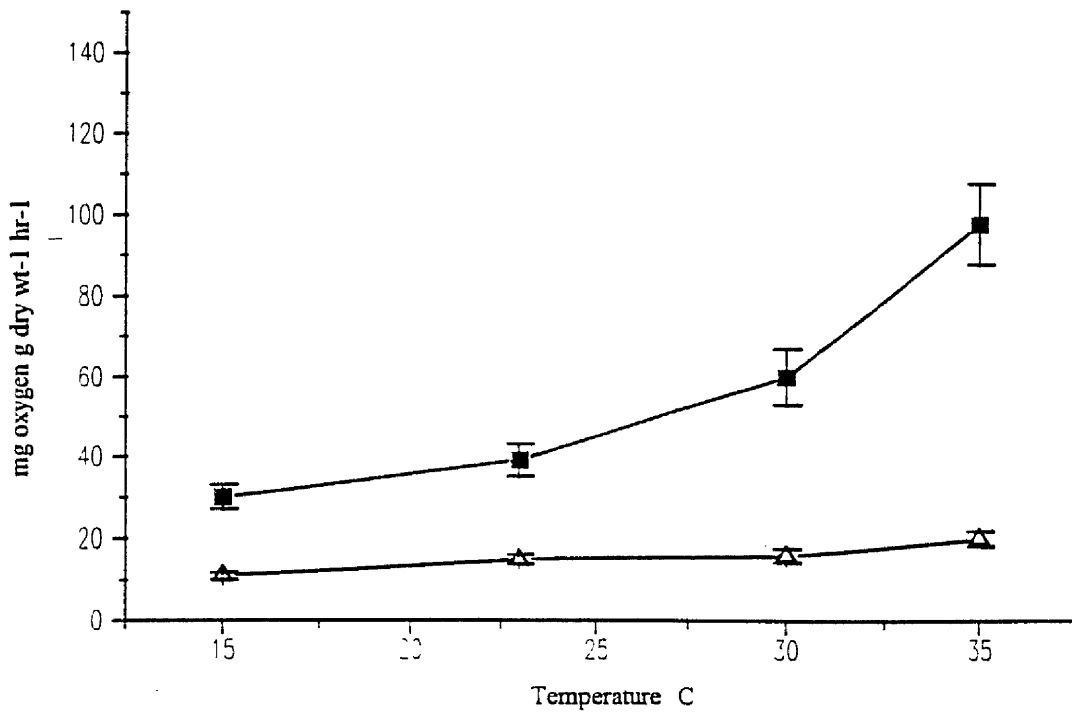


Figure 109. The effect of P/I incubation temperature on the dark respiration Δ — Δ and light enhanced dark respiration \blacksquare — \blacksquare of *Nannochloris atomus* cultured at 30°C.

The following equations were determined for the relationship between temperature and initial dark respiration.

15°C

$$R_{initial}^{15} = 1.442 \times 10^{-3} + (3.327 \times T) \quad (\text{Sig P}=0.001) \quad (42)$$

23°C

$$R_{initial}^{23} = 4.09 \times 10^{-2} + (2.17 \times T) \quad (\text{Sig P}=0.001) \quad (43)$$

30°C

$$R_{initial}^{30} = \frac{1}{0.366 + (-1.008 \times 10^{-2} \times T)} \quad (\text{Sig P}=0.001) \quad (44)$$

35°C

$$R_{initial}^{35} = \frac{1}{9.73 \times 10^{-2} + (-1.37 \times 10^{-3} \times T)} \quad (\text{Sig P}=0.001) \quad (45)$$

From equations 42 and 43, it was found that cells of *Nannochloris atomus* displayed a straight line relationship for the initial dark respiration and temperatures 15 and 23°C. However at the culture temperatures of 30 and 35°C, this relationship was found to be of a hyperbolic nature.

The following equations describe the relationship between temperature and the LEDR of *Nannochloris atomus*.

15°C

$$LEDR_{final}^{15} = 0.1474 \times T^{2.096} \quad (\text{Sig P}=0.001) \quad (46)$$

23°C

$$LEDR_{final}^{23} = 9.575 \times 10^{-2} \times T^{2.069} \quad (\text{Sig P}=0.001) \quad (47)$$

30°C

$$LEDR_{final}^{30} = \frac{1}{5.196 \times 10^{-2} + (-1.164 \times 10^{-3} \times T)} \quad (\text{Sig P}=0.001) \quad (48)$$

35°C

$$LEDR_{final}^{35} = \frac{1}{5.196 \times 10^{-2} + (-1.164 \times 10^{-3} \times T)} \quad (\text{Sig P}=0.001) \quad (49)$$

Equations 46 and 47 show that the LEDR of cells of *Nannochloris atomus* was power related to temperature for cultures grown at 15 and 23°C. At the higher culture temperatures of 30 and 35°C, this relationship was found to be a hyperbolic function (equations 48 and 49).

The following equations relate the value of alpha to P/I incubation temperature for each of the culture temperatures.

$$\alpha_{15} = 1.48 + (-0.143 \times T) + (6.20 \times 10^{-3} \times T^2) \quad (\text{Sig at P}=0.01) \quad (50)$$

$$\alpha_{23} = -1.567 + (0.152 \times T) + (-1.13 \times 10^{-3} \times T^2) \quad (\text{Sig P}=0.01) \quad (51)$$

$$\alpha_{30} = 0.644 + (-4.93 \times 10^{-2} \times T) + (1.96 \times 10^{-3} \times T^2) \quad (\text{Sig P}=0.001) \quad (52)$$

$$\alpha_{35} = 0.35 \times T^{0.446} \quad (\text{Sig P}=0.01) \quad (53)$$

Equations 50, 51 and 52 were calculated using a polynomial regression (2 degrees of freedom).

Figures 110, 111, 112 and 113 show the arhenius plots for *Nannochloris atomus* of the natural logarithm of photosynthetic rates (mg oxygen g dry wt⁻¹ hr⁻¹), measured at a PFD of 100μmol s⁻¹ m⁻² against the reciprocal of P/I incubation temperature (Kelvin) for culture temperatures of 15, 23, 30 and 35°C respectively.

Photosynthesis / irradiance response curves (Figures 114, 115, 116 and 117) were obtained from cells of *Scenedesmus sp.* and support the observations reported for *Chlorella vulgaris* 211/11c and *Nannochloris atomus*. The cells cultured at 15 , 23, 30 and 35°C showed large increase in P_{max} with increasing temperature .It was also found that the value of P_{max} determined at the P/I incubation temperature of 35°C for each culture temperature, decreased with increasing temperature.

The following equations were determined from the maximum rates of photosynthesis and temperature.

15°C

$$P_{\max}^{15} = 7.828 \times e^{(0.102 \times T)} \quad (\text{Sig P}=0.001) \quad (54)$$

23°C

$$P_{\max}^{23} = 4.267 \times e^{(9.68 \times 10^{-2} \times T)} \quad (\text{Sig P}=0.001) \quad (55)$$

30°C

$$P_{\max}^{30} = \frac{1}{4.32 \times 10^{-2} + (-1.04 \times 10^{-3} \times T)} \quad (\text{Sig P}=0.001) \quad (56)$$

35°C

$$P_{\max}^{35} = 0.687 \times T^{1.34} \quad (\text{Sig P}=0.001) \quad (57)$$

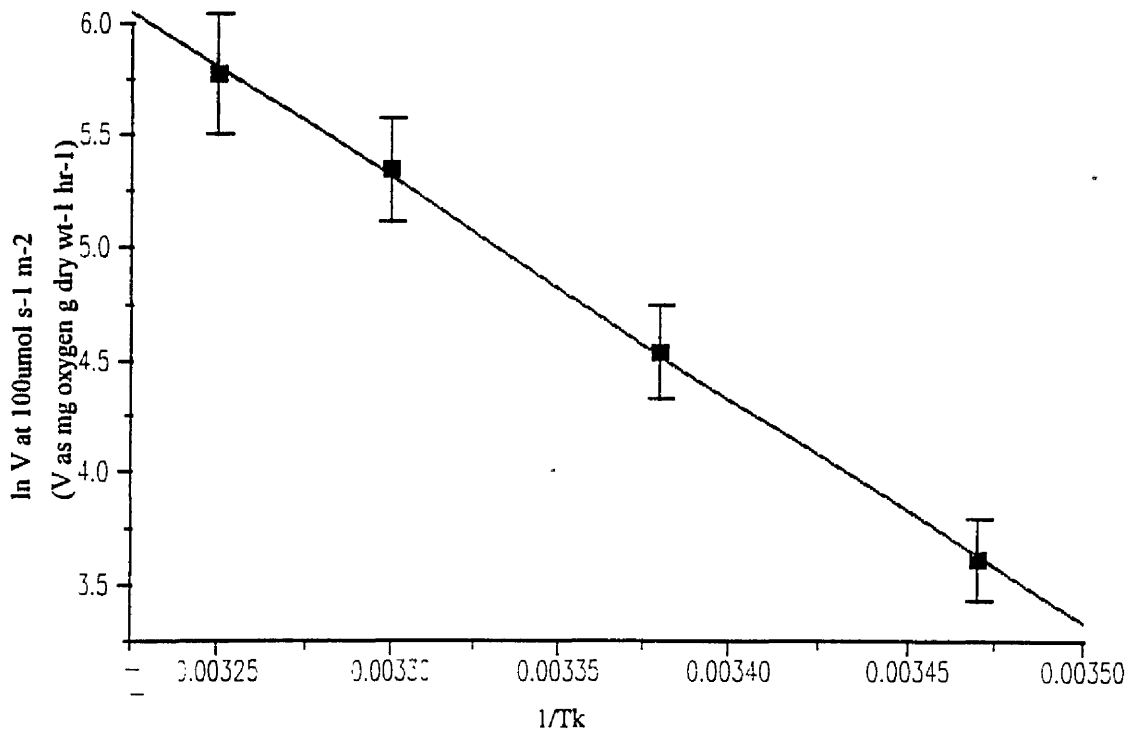


Figure 110. Arrhenius plot of ln photosynthetic rate at a PFD of $100\mu\text{mol s}^{-1} \text{m}^{-2}$ against increasing P/I incubation temperature for *Nannochloris atomus* cultured at a temperature of 15°C .

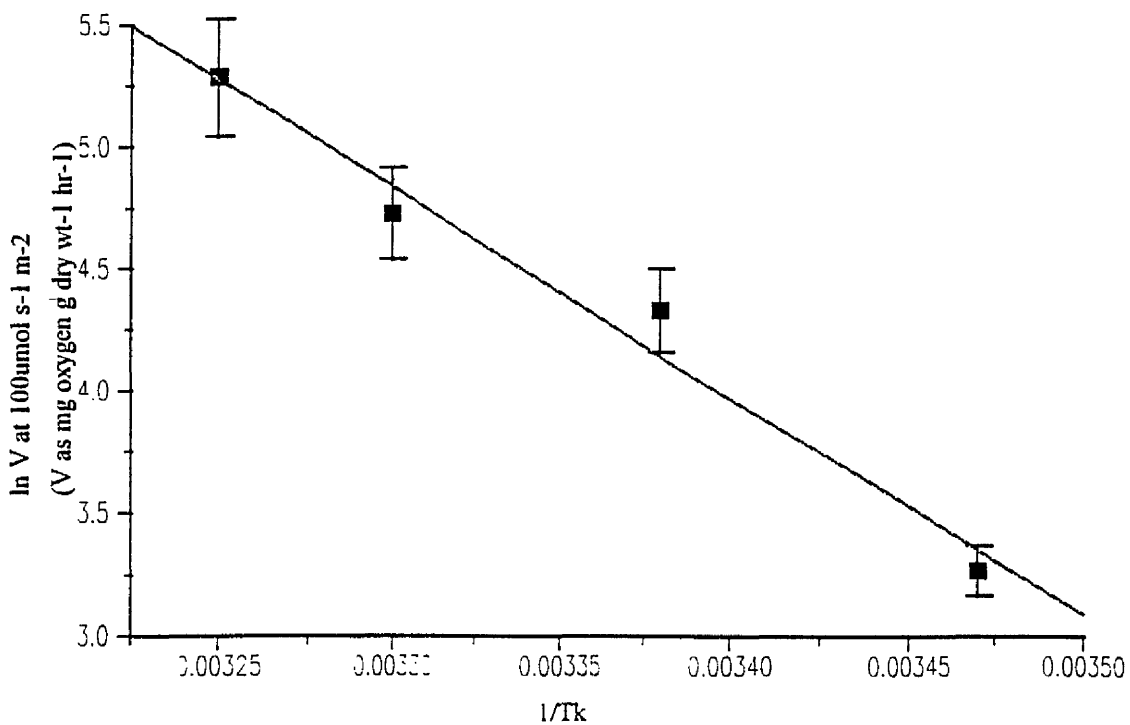


Figure 111. Arrhenius plot of ln photosynthetic rate at a PFD of $100\mu\text{mol s}^{-1} \text{m}^{-2}$ against increasing P/I incubation temperature for *Nannochloris atomus* cultured at a temperature of 23°C .

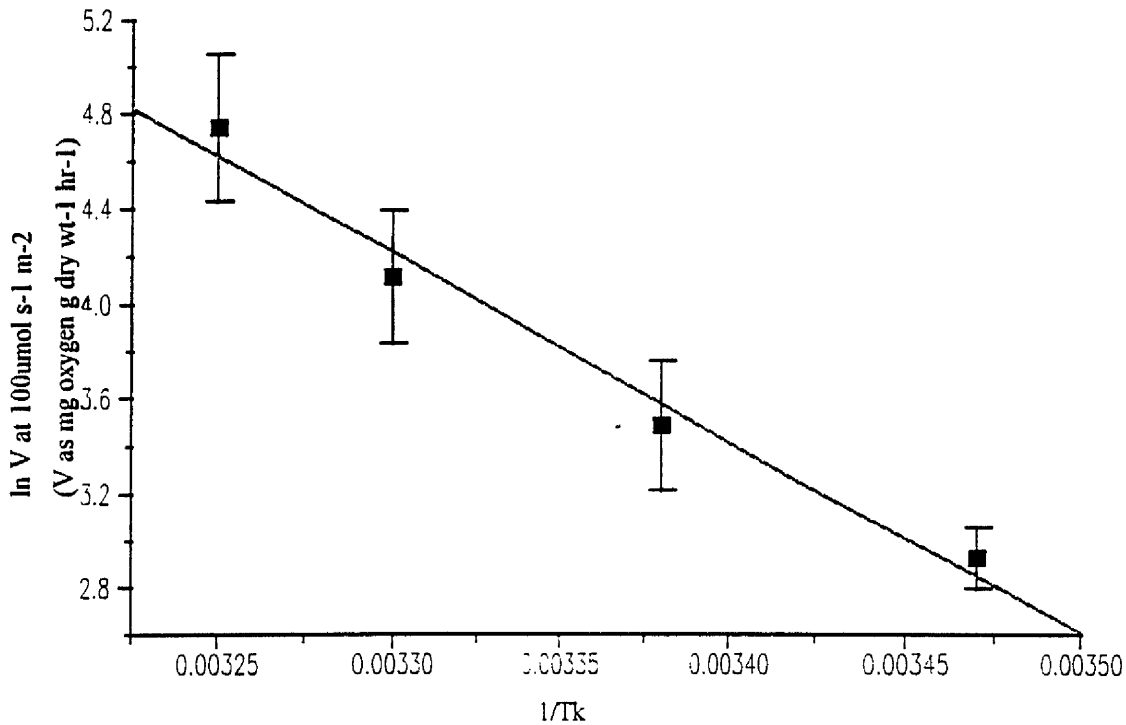


Figure 112. Arrhenius plot of ln photosynthetic rate at a PFD of $100\mu\text{mol s}^{-1} \text{m}^{-2}$ against increasing P/I incubation temperature for *Nannochloris atomus* cultured at a temperature of 30°C .

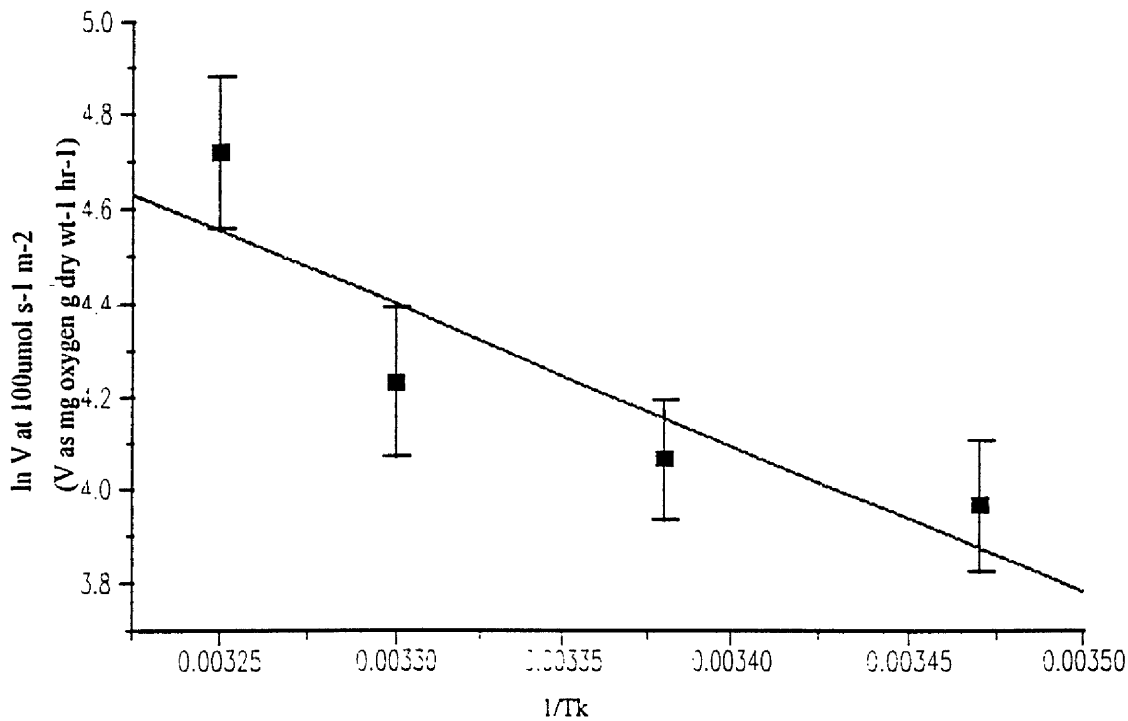


Figure 113. Arrhenius plot of ln photosynthetic rate at a PFD of $100\mu\text{mol s}^{-1} \text{m}^{-2}$ against increasing P/I incubation temperature for *Nannochloris atomus* cultured at a temperature of 35°C .

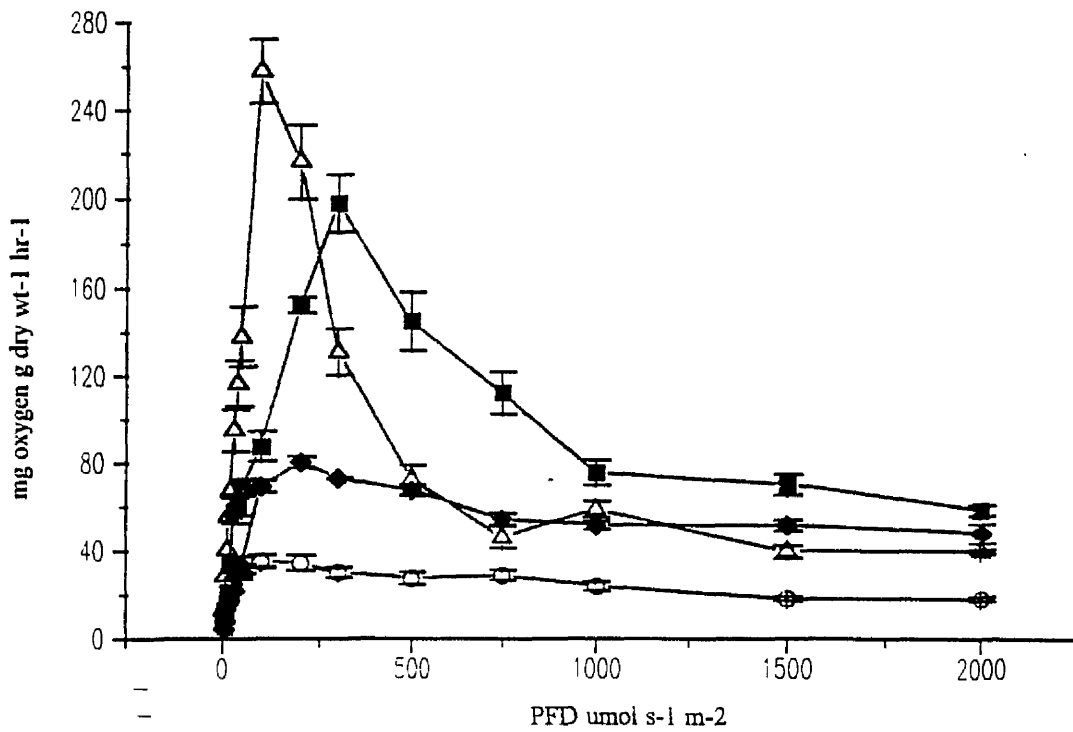


Figure 114. The effect of P/I incubation temperature on the photosynthesis / irradiance response curves of *Scenedesmus sp.* cultured at 15°C, ○—○ 15°C, ◆—◆ 23°C, ■—■ 30°C, △—△ 35°C.

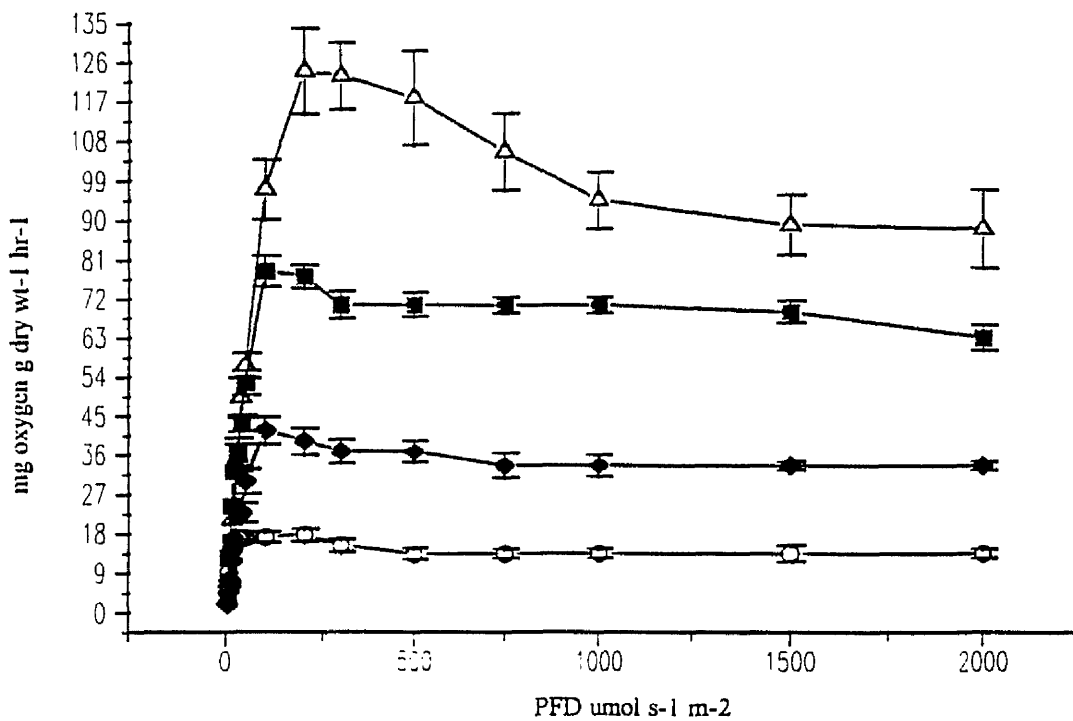


Figure 115. The effect of P/I incubation temperature on the photosynthesis / irradiance response curves of *Scenedesmus sp.* cultured at 23°C, ○—○ 15°C, ◆—◆ 23°C, ■—■ 30°C, △—△ 35°C.

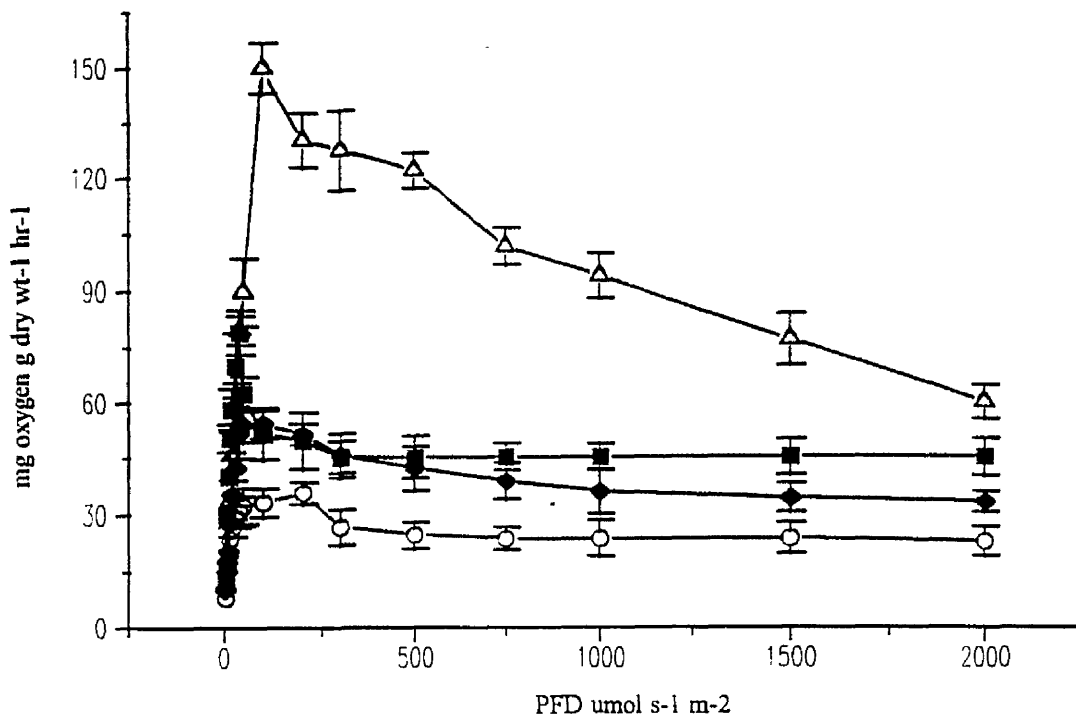


Figure 116. The effect of P/I incubation temperature on the photosynthesis / irradiance response curves of *Scenedesmus sp.* cultured at 30°C, ○—○ 15°C, ◆—◆ 23°C, ■—■ 30°C, △—△ 35°C.

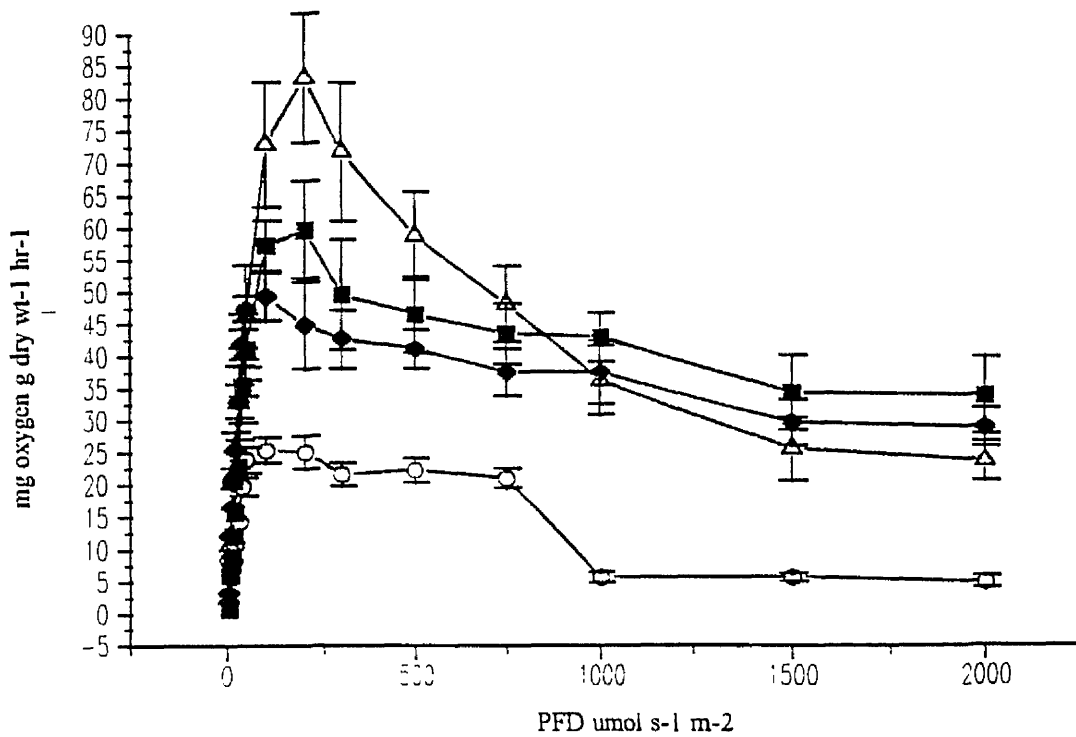


Figure 117. The effect of P/I incubation temperature on the photosynthesis / irradiance response curves of *Scenedesmus sp.* cultured at 35°C, ○—○ 15°C, ◆—◆ 23°C, ■—■ 30°C, △—△ 35°C.

From equations 54 and 55, it was found that P_{\max} was related to temperature by an exponential curve fit. However the higher culture temperatures of 30 and 35°C showed hyperbolic and power relationships respectively (equations 56 and 57)

Tables 41, 42, 43 and 44 show the various photosynthetic parameters determined from the photosynthesis / irradiance curves of *Scenedesmus sp.* For all culture temperatures, the value of beta was found to increase with increasing P/I incubation temperature, whilst the value of I_k was observed to follow a small but gradual increase (with the exception of the 35°C cultured cells). It was found that there was a general increase in alpha with increasing temperature. The highest recorded value for P_{\max} (257.7 mg oxygen g dry wt⁻¹ hr⁻¹) was from cells cultured at 15°C and incubated at a P/I temperature of 35°C.

Figures 118, 119, 120 and 121 show the effect of P/I incubation temperature on cellular respiration. It was found that cells cultured at 15 and 23°C (Fig 118 and 119) showed a large increase in respiration when incubated at increasing P/I incubation temperatures of 30 and 35°C. This pattern was observed with all the unicellular green micro-algae. As the culture temperature was increased to 35°C (Figure 121), the cellular respiration varied little with decreasing incubation temperature.

It was found that the following equations described the relationship between respiration and P/I incubation temperature at the four culture temperatures of 15, 23, 30 and 35°C.

15°C

$$R_{initial}^{15} = 1.62 \times 10^{-2} \times T^{2.037} \quad (\text{Sig P}=0.001) \quad (58)$$

23°C

$$R_{initial}^{23} = 0.3405 \times e^{0.145 \times T} \quad (\text{Sig P}=0.001) \quad (59)$$

30°C

$$R_{initial}^{30} = 1.656 \times e^{8.328 \times 10^{-2} \times T} \quad (\text{Sig P}=0.001) \quad (60)$$

Table 41. The effect of temperature on the photosynthetic parameters of *Scenedesmus sp.* cultured at 15°C.

Culture temperature °C	P/I temperature °C	α (mg oxygen g dry wt ⁻¹ hr ⁻¹ / $\mu\text{mol s}^{-1} \text{m}^{-2}$)	I_k ($\mu\text{mol s}^{-1} \text{m}^{-2}$)	β (mg oxygen g dry wt ⁻¹ hr ⁻¹ / $\mu\text{mol s}^{-1} \text{m}^{-2}$)	$P_{\text{max}}^{\text{PFD}}$ ($\mu\text{mol s}^{-1} \text{m}^{-2}$)	P_{max} (mg oxygen g dry wt ⁻¹ hr ⁻¹)
15	15	0.65	54.2	-0.024	100	35.2
15	23	1.28	62.6	-0.040	200	80.2
15	30	1.47	134.5	-0.188	300	197.8
15	35	3.48	74.1	-0.633	100	257.7

Table 42. The effect of temperature on the photosynthetic parameters of *Scenedesmus sp.* cultured at 23°C.

Culture temperature °C	P/I temperature °C	α (mg oxygen g dry wt ⁻¹ hr ⁻¹ / $\mu\text{mol s}^{-1} \text{m}^{-2}$)	I_k ($\mu\text{mol s}^{-1} \text{m}^{-2}$)	β (mg oxygen g dry wt ⁻¹ hr ⁻¹ / $\mu\text{mol s}^{-1} \text{m}^{-2}$)	$P_{\text{max}}^{\text{PFD}}$ ($\mu\text{mol s}^{-1} \text{m}^{-2}$)	P_{max} (mg oxygen g dry wt ⁻¹ hr ⁻¹)
23	15	0.60	29.51	no data	100	17.7
23	23	0.78	53.33	-0.020	100	41.6
23	30	1.38	56.77	-0.024	100	78.4
23	35	1.62	76.49	-0.038	200	123.9

Table 43. The effect of temperature on the photosynthetic parameters of *Scenedesmus sp.* cultured at 30°C.

Culture temperature °C	P/I temperature °C	α (mg oxygen g dry wt ⁻¹ hr ⁻¹ / μ mol s ⁻¹ m ⁻²)	I_k (μ mol s ⁻¹ l m ⁻²)	β (mg oxygen g dry wt ⁻¹ hr ⁻¹ / μ mol s ⁻¹ m ⁻²)	P_{max}^{PFD} (μ mol s ⁻¹ m ⁻²)	P_{max} (mg oxygen g dry wt ⁻¹ hr ⁻¹)
30	15	1.25	28.6	-0.033	200	35.7
30	23	1.47	36.8	-0.042	100	54.1
30	30	1.88	41.9	-0.378	100	78.9
30	35	3.05	49.1	-0.112	100	149.8

Table 44. The effect of temperature on the photosynthetic parameters of *Scenedesmus sp.* cultured at 35°C.

Culture temperature °C	P/I temperature °C	α (mg oxygen g dry wt ⁻¹ hr ⁻¹ / μ mol s ⁻¹ m ⁻²)	I_k (μ mol s ⁻¹ l m ⁻²)	β (mg oxygen g dry wt ⁻¹ hr ⁻¹ / μ mol s ⁻¹ m ⁻²)	P_{max}^{PFD} (μ mol s ⁻¹ m ⁻²)	P_{max} (mg oxygen g dry wt ⁻¹ hr ⁻¹)
35	15	0.22	115.4	-0.019	100	25.5
35	23	0.93	53.1	-0.033	100	49.4
35	30	1.40	42.7	-0.040	200	59.8
35	35	1.86	44.8	-0.079	200	83.3

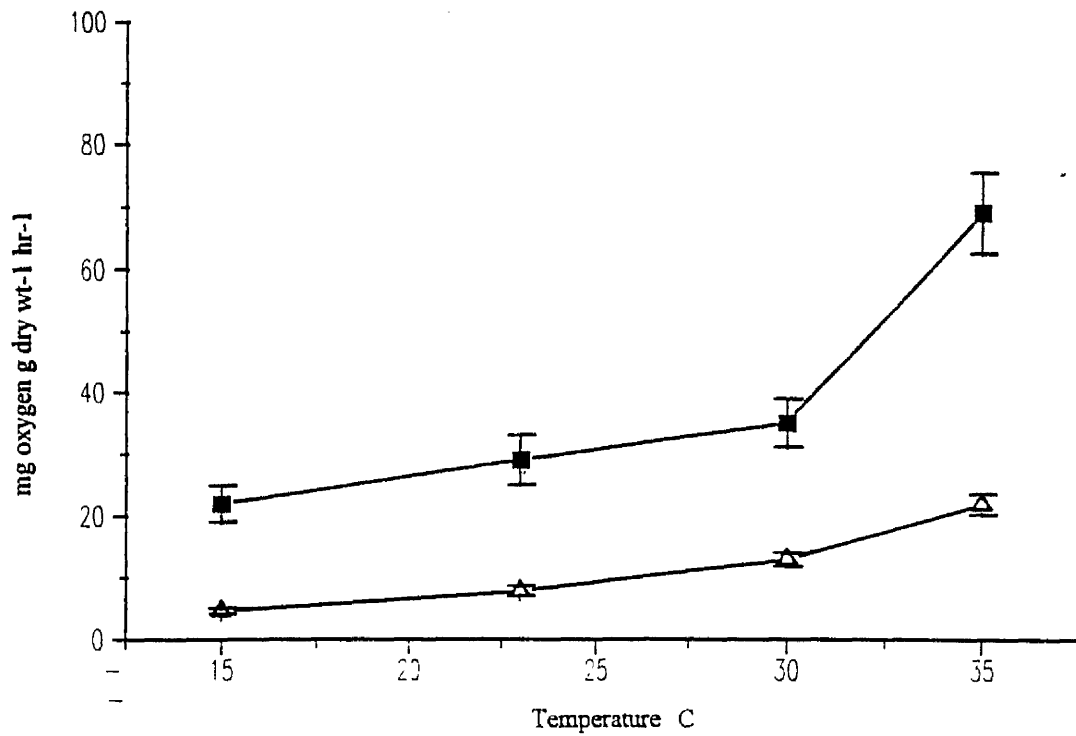


Figure 118. The effect of P/I incubation temperature on the dark respiration Δ — Δ and light enhanced dark respiration \blacksquare — \blacksquare of *Scenedesmus sp.* cultured at 15°C.

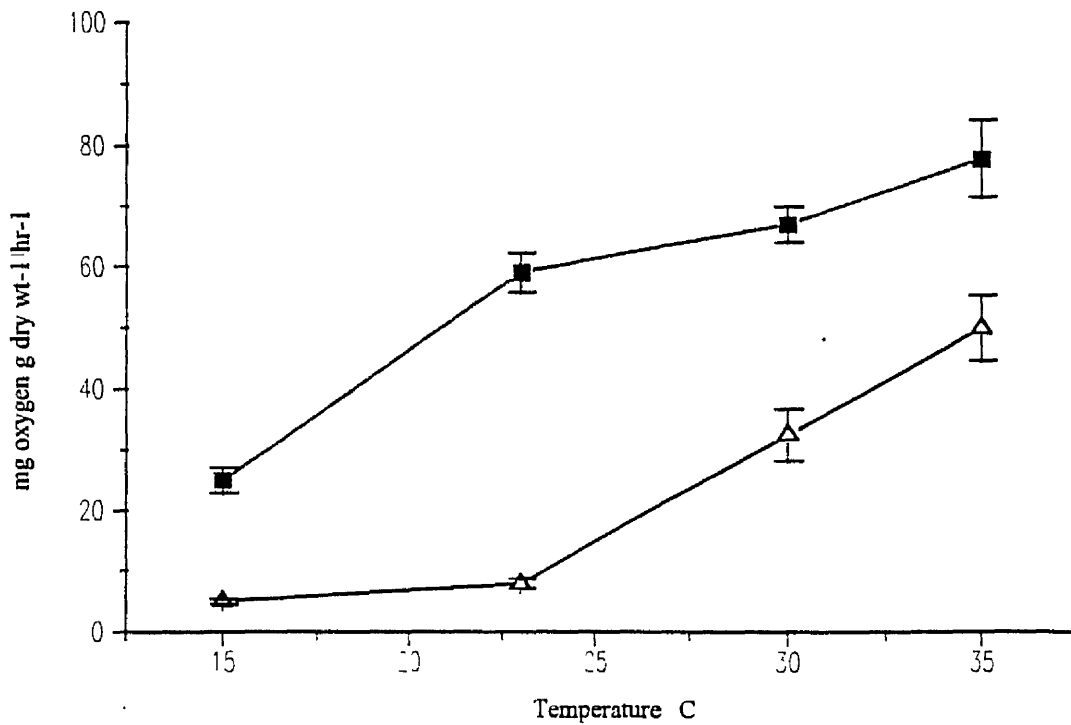


Figure 119. The effect of P/I incubation temperature on the dark respiration Δ — Δ and light enhanced dark respiration \blacksquare — \blacksquare of *Scenedesmus sp.* cultured at 23°C.

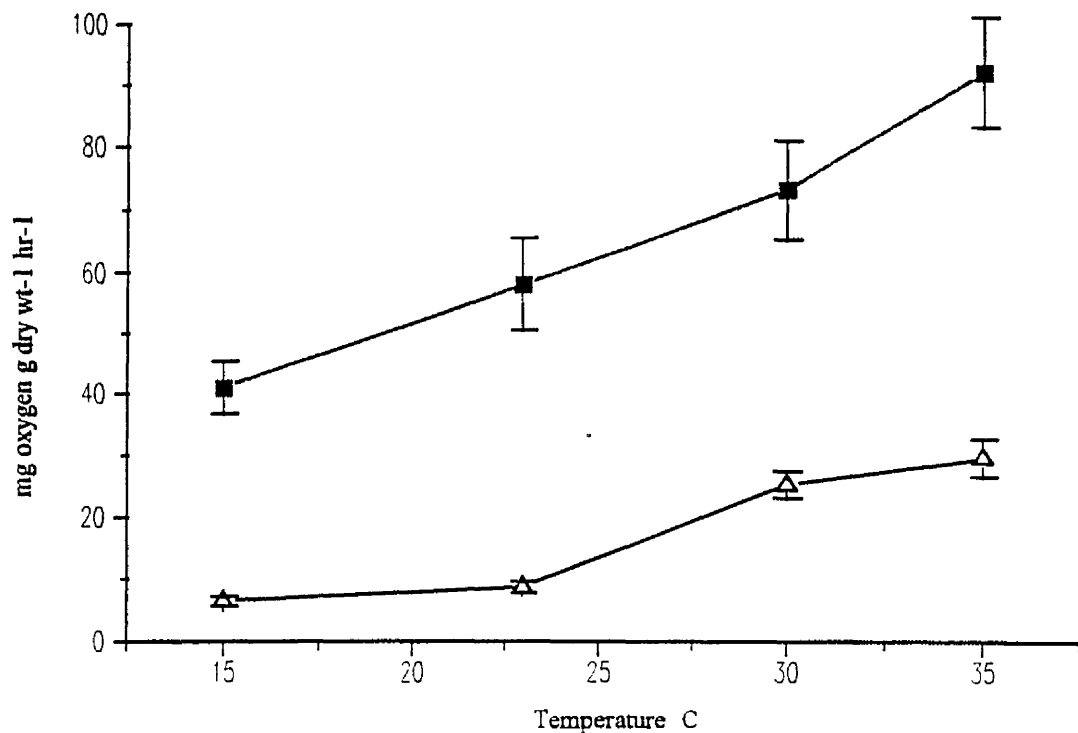


Figure 120. The effect of P/I incubation temperature on the dark respiration Δ — Δ and light enhanced dark respiration \blacksquare — \blacksquare of *Scenedesmus sp.* cultured at 30°C.

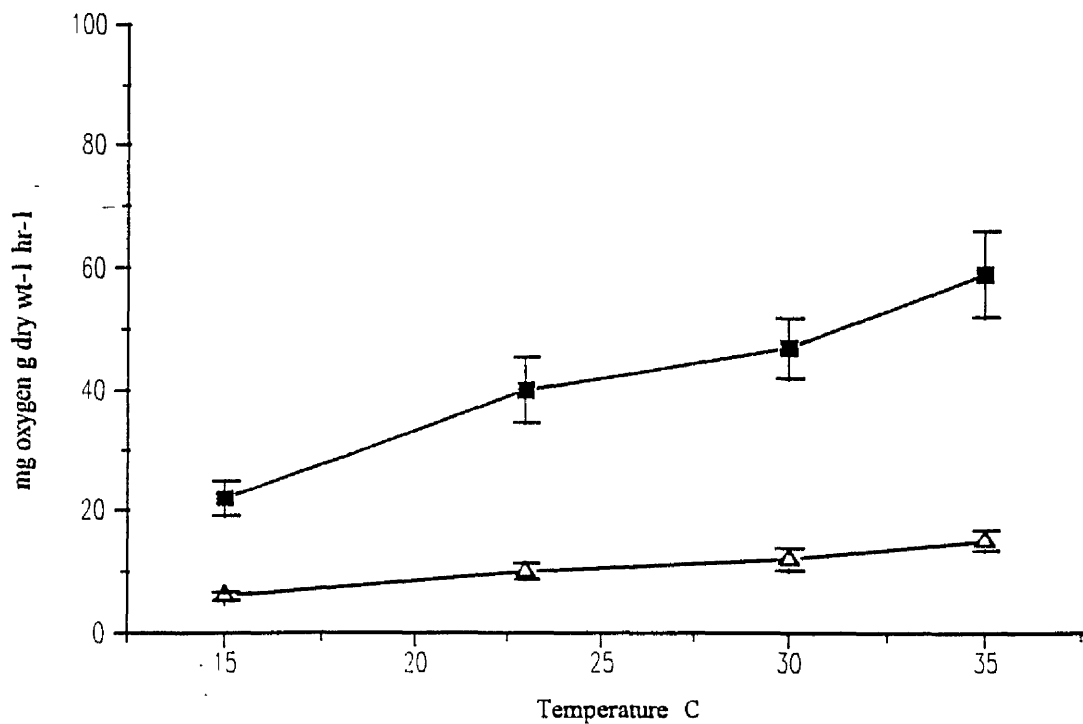


Figure 121. The effect of P/I incubation temperature on the dark respiration Δ — Δ and light enhanced dark respiration \blacksquare — \blacksquare of *Scenedesmus sp.* cultured at 35°C.

35°C

$$R_{initial}^{35} = 0.1533 \times T^{1.295} \quad (\text{Sig P}=0.001) \quad (61)$$

From equations 58 and 61, it can be seen that the relationship between oxygen consumption and temperature was a power fit, however, at the culture temperatures of 23 and 30°C (equations 59 and 60) the relationship was an exponential fit.

The following equations describe the relationship between LEDR and P/I incubation temperature for each of the four culture temperatures.

15°C

$$LEDR_{final}^{15} = \frac{1}{5.69 \times 10^{-2} + (-1.098 \times 10^{-3} \times T)} \quad (\text{Sig P}=0.001) \quad (62)$$

23°C

$$LEDR_{final}^{23} = 0.99 \times T^{1.23} \quad (\text{Sig P}=0.01) \quad (63)$$

30°C

$$LEDR_{final}^{30} = \frac{1}{3.259 \times 10^{-2} + (-6.188 \times 10^{-4} \times T)} \quad (\text{Sig P}=0.001) \quad (64)$$

35°C

$$LEDR_{final}^{35} = 4.02 \times T^{0.704} \quad (\text{Sig P}=0.05) \quad (65)$$

From equations 62 and 64 it can be seen that the relationship between the LEDR oxygen consumption and temperature was a hyperbolic fit, however, at the culture temperatures of 23 and 35°C (equations 63 and 65) the relationship was a power fit.

The rate of LEDR decreased when 35°C cultured cells were incubated at P/I temperatures of 30 and 35°C (Figure 121). This may be due to a high degree of photodamage and photoinhibition caused by the high temperature and light combination.

The following equations best describe the relationship between the value of alpha and the P/I incubation temperature at the 4 culture temperatures of 15, 23, 30 and 35°C.

$$\alpha_{15} = 0.205 \times e^{(7.55 \times 10^{-2} \times T)} \quad (\text{Sig P}=0.01) \quad (66)$$

$$\alpha_{23} = 0.586 + (-2.42 \times 10^{-2} \times T) + (1.57 \times 10^{-3} \times T^2) \quad (\text{Sig P}=0.01) \quad (67)$$

$$\alpha_{30} = 0.609 \times e^{(4.207 \times 10^{-2} \times T)} \quad (\text{Sig P}=0.01) \quad (68)$$

$$\alpha_{35} = 2.74 \times 10^{-4} \times T^{2.513} \quad (\text{Sig P}=0.01) \quad (69)$$

Figures 122, 123, 124 and 125 show the arhenius plots for *Scenedesmus sp.* of the natural logarithm of photosynthetic rates (mg oxygen g dry wt⁻¹ hr⁻¹), measured at a PFD of 100µmol s⁻¹ m⁻² against the reciprocal of P/I incubation temperature (Kelvin) for culture temperatures of 15, 23, 30 and 35°C respectively. A very good relationship was obtained for the changes in oxygen evolution measured at a PFD of 100µmol s⁻¹ m⁻² with increasing temperature.

Ankistrodesmus antarcticus was the final eukaryotic micro-alga to be used in this analysis. Like the other unicellular green micro-algae, cells of *Ankistrodesmus antarcticus* showed the general pattern of increases in P_{max} with increasing temperature (Figures 126, 127, 128 and 129). P_{max}, however, decreased when the cells cultured at 15°C were incubated at a P/I temperature of 35°C (Figure 126). It is suggested that this may be due to the fact that *Ankistrodesmus antarcticus* as its name implies was a unicellular green isolated from the Antarctic. It was observed that organism had an optimum growth rate at the lower temperature of 15°C. However the combined effect of high light intensity during photosynthetic response measurements

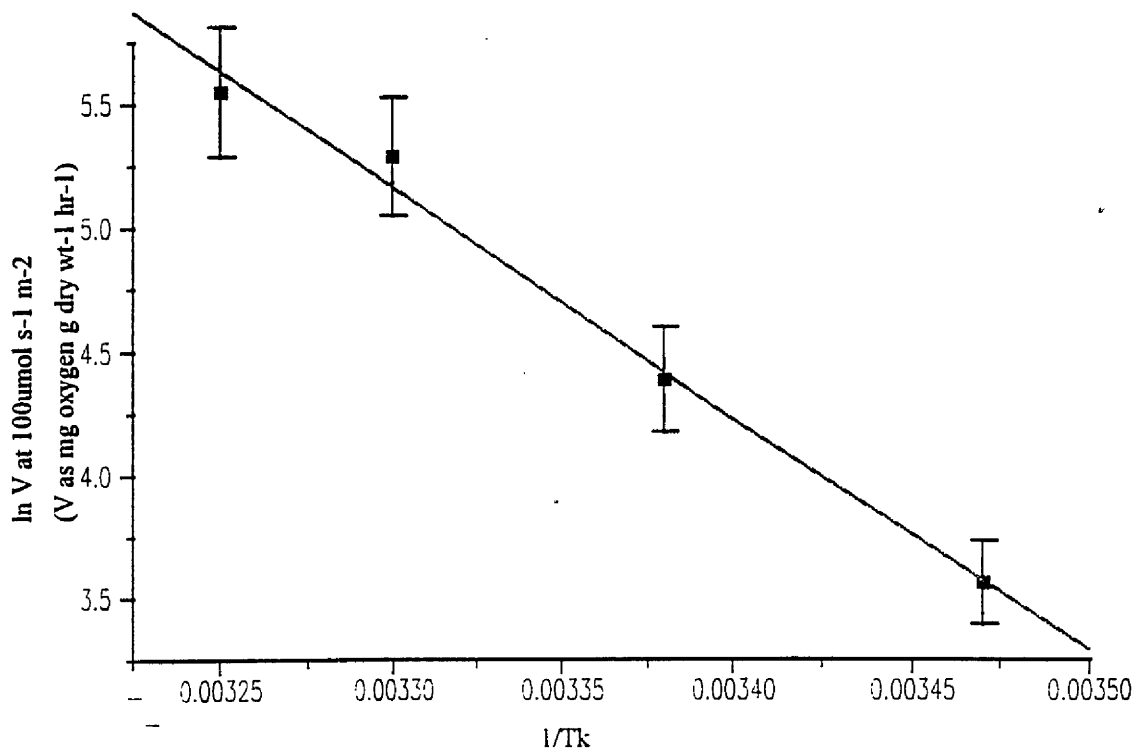


Figure 122. Arrhenius plot of ln photosynthetic rate at a PFD of $100\mu\text{mol s}^{-1} \text{m}^{-2}$ against increasing P/I incubation temperature for *Scenedesmus sp.* cultured at a temperature of 15°C .

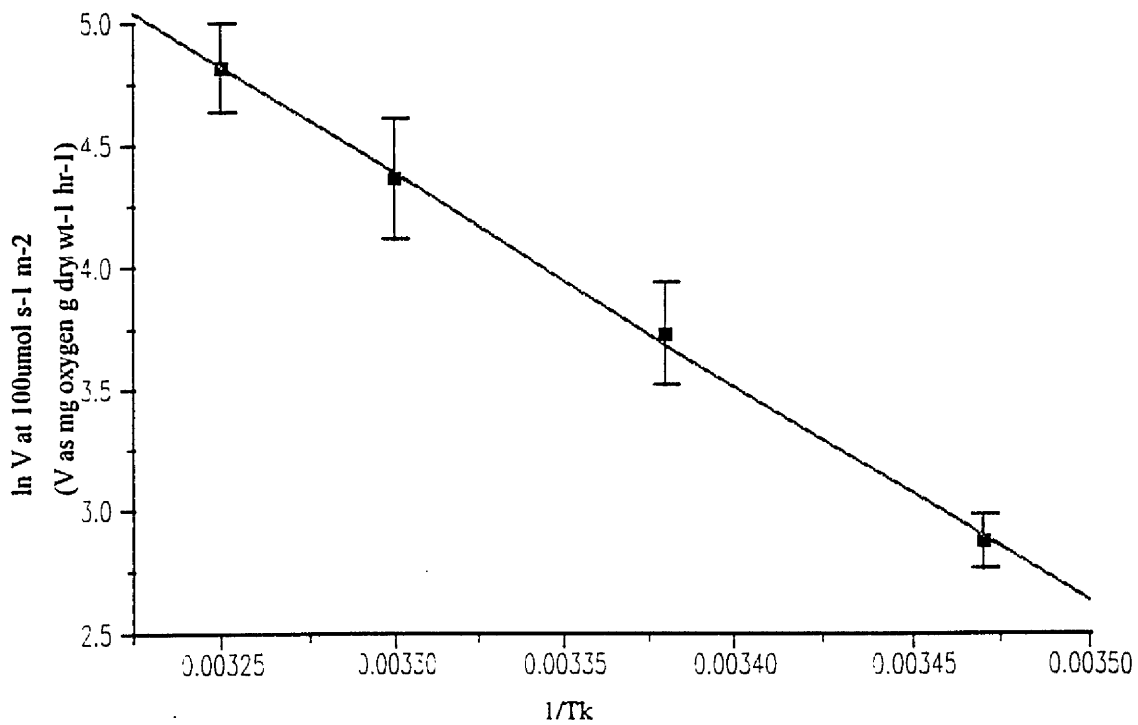


Figure 123. Arrhenius plot of ln photosynthetic rate at a PFD of $100\mu\text{mol s}^{-1} \text{m}^{-2}$ against increasing P/I incubation temperature for *Scenedesmus sp.* cultured at a temperature of 23°C .

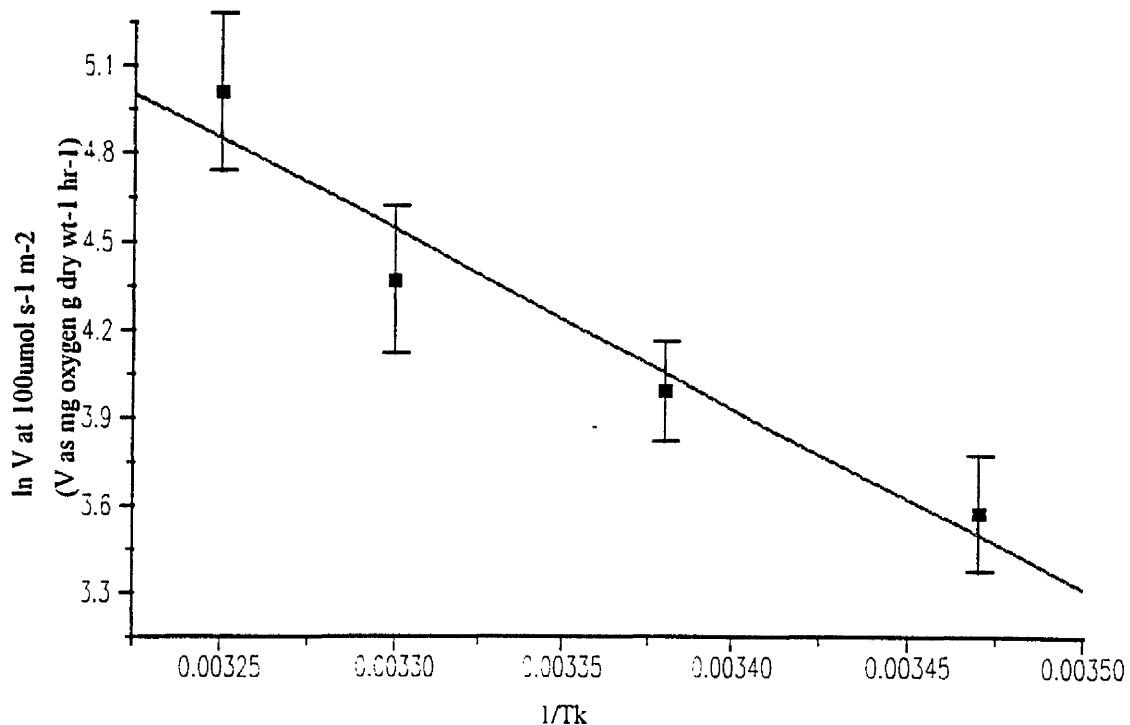


Figure 124. Arrhenius plot of ln photosynthetic rate at a PFD of $100\mu\text{mol s}^{-1} \text{m}^{-2}$ against increasing P/I incubation temperature for *Scenedesmus sp.* cultured at a temperature of 30°C .

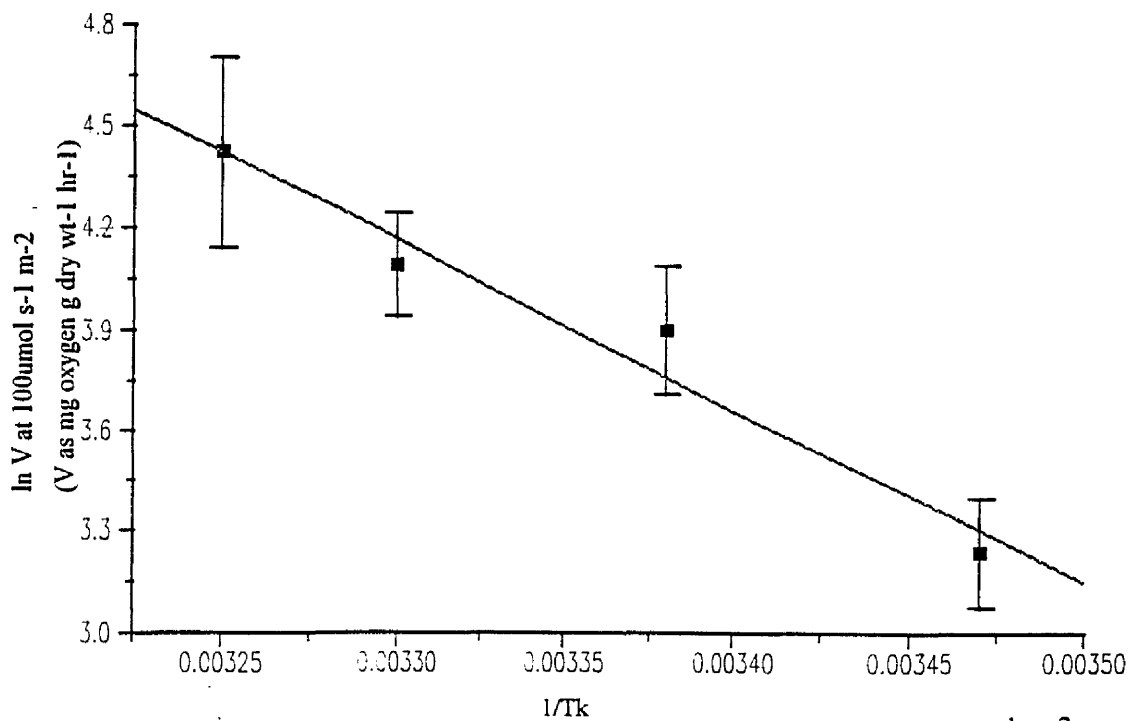


Figure 125. Arrhenius plot of ln photosynthetic rate at a PFD of $100\mu\text{mol s}^{-1} \text{m}^{-2}$ against increasing P/I incubation temperature for *Scenedesmus sp.* cultured at a temperature of 35°C .

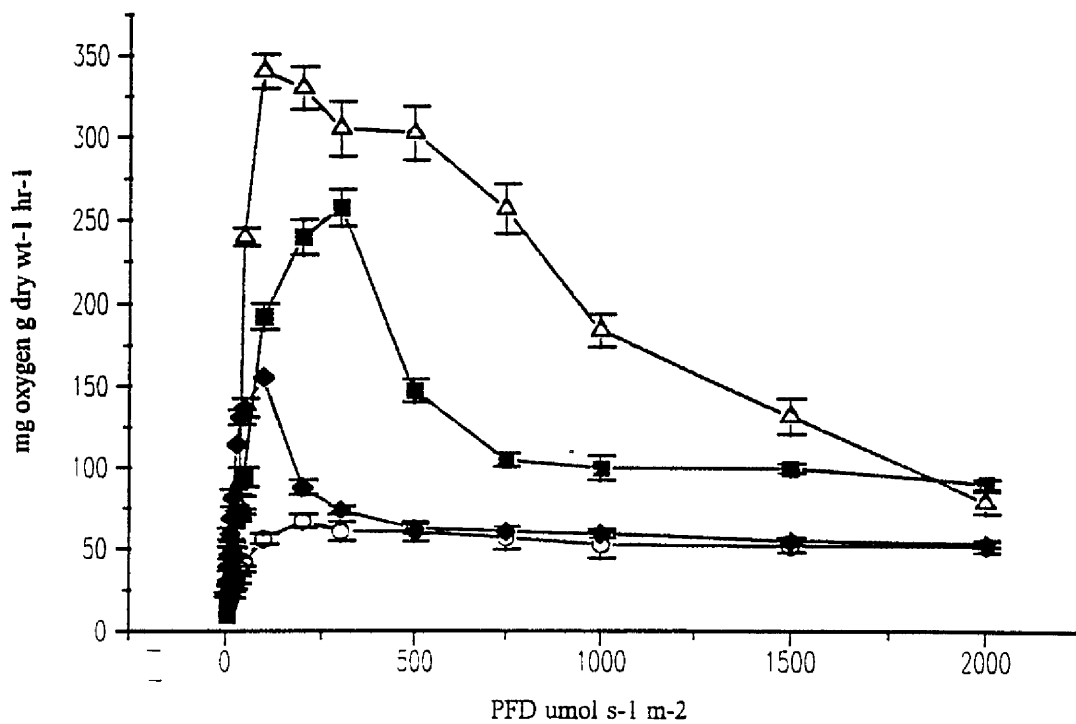


Figure 126. The effect of P/I incubation temperature on the photosynthesis / irradiance response curves of *Ankistrodesmus antarcticus* cultured at 15°C, ○—○ 15°C, ◆—◆ 23°C, ■—■ 30°C, Δ—Δ 35°C.

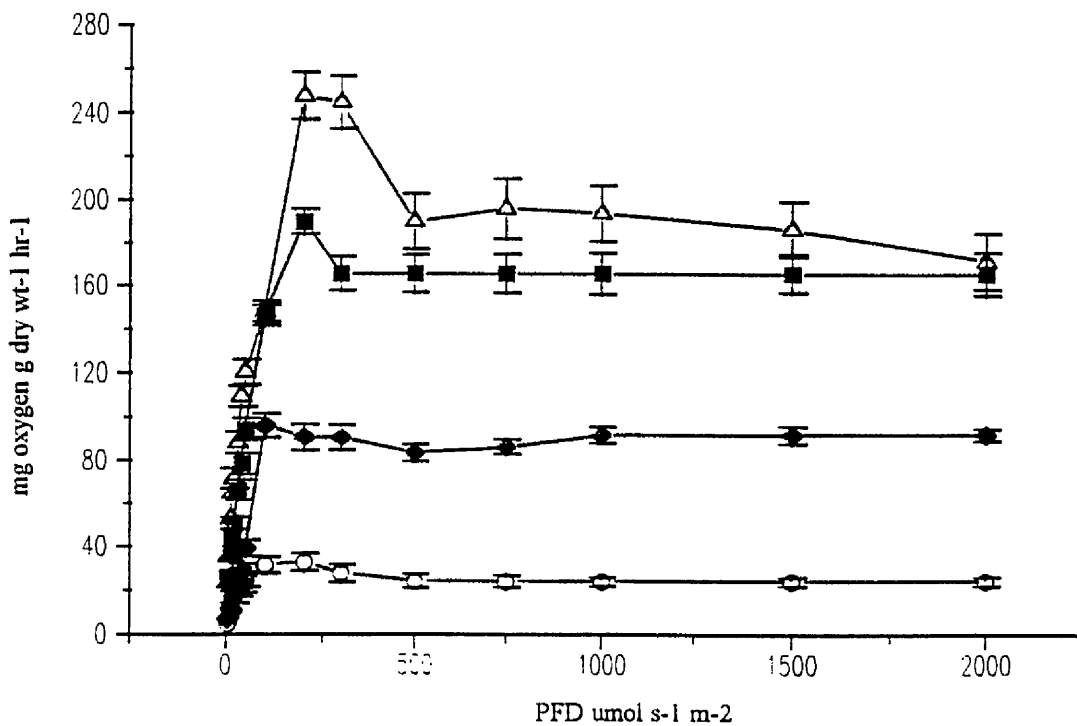


Figure 127. The effect of P/I incubation temperature on the photosynthesis / irradiance response curves of *Ankistrodesmus antarcticus* cultured at 23°C, ○—○ 15°C, ◆—◆ 23°C, ■—■ 30°C, Δ—Δ 35°C.

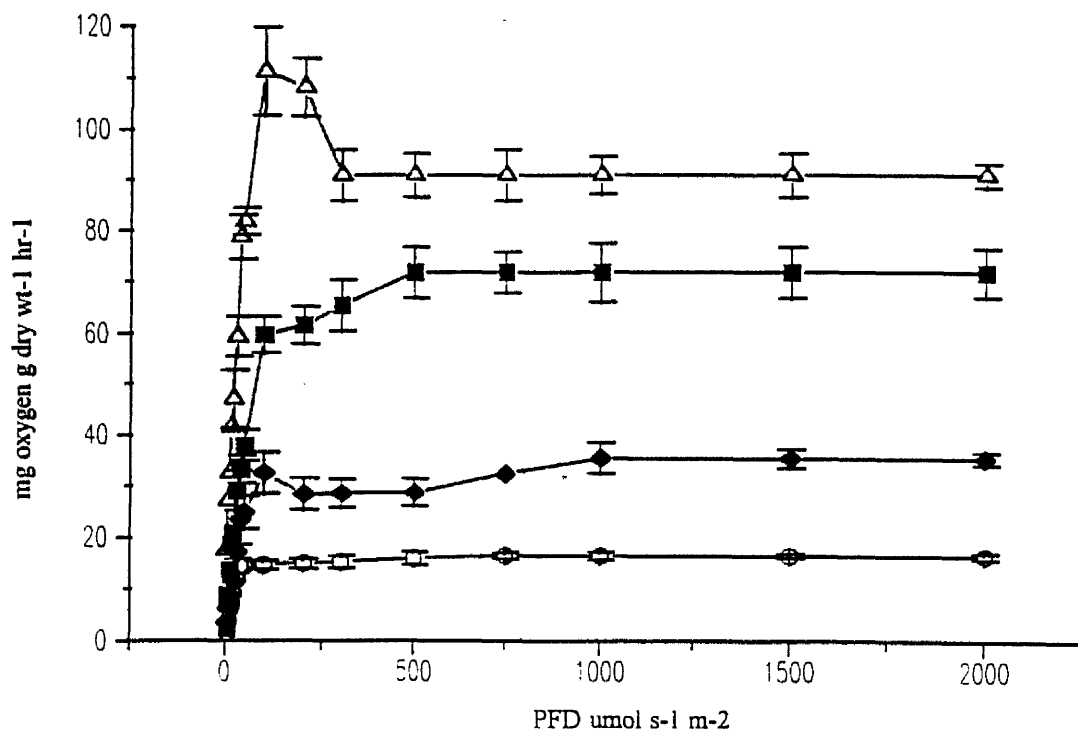


Figure 128. The effect of P/I incubation temperature on the photosynthesis / irradiance response curves of *Ankistrodesmus antarcticus* cultured at 30°C, ○—○ 15°C, ◆—◆ 23°C, ■—■ 30°C, △—△ 35°C.

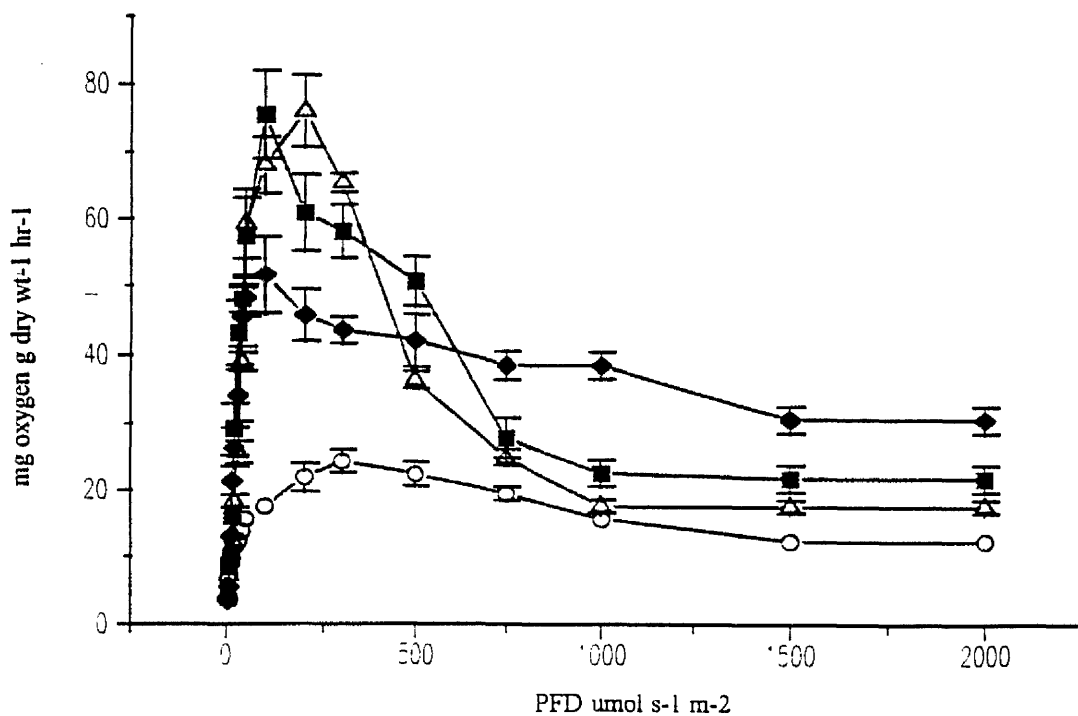


Figure 129. The effect of P/I incubation temperature on the photosynthesis / irradiance response curves of *Ankistrodesmus antarcticus* cultured at 35°C, ○—○ 15°C, ◆—◆ 23°C, ■—■ 30°C, △—△ 35°C.

and the increase in temperature of the surrounding medium to 35°C caused a severe reduction in photosynthetic oxygen evolution.

The following equations were determined from the relationship between P_{\max} and temperature.

15°C

$$P_{\max}^{15} = 0.104 \times T^{2.418} \quad (\text{Sig P}=0.001) \quad (70)$$

23°C

$$P_{\max}^{23} = 4.669 \times 10^{-2} \times T^{2.427} \quad (\text{Sig P}=0.001) \quad (71)$$

30°C

$$P_{\max}^{30} = 3.45 \times e^{9.888 \times 10^{-2} \times T} \quad (\text{Sig P}=0.001) \quad (72)$$

35°C

$$P_{\max}^{35} = 0.547 \times T^{1.42} \quad (\text{Sig P}=0.001) \quad (73)$$

It can be seen from equations 70, 71 and 73 that the relationship between P_{\max} and temperature was a power curve. Equation 72 shows that an exponential fit was best to describe this same relationship.

Table 45, 46, 47 and 48 show the photosynthetic parameters of *Ankistrodesmus antarcticus*. At culture temperatures of 15, 23 and 30°C, (Tables 45, 46 and 47) the value of alpha was observed to increase with increasing P/I incubation temperature. At the culture temperature of 35°C (Table 48), alpha increased with increasing P/I incubation temperature from 15-30°C, after which increasing the P/I incubation temperature to 35°C resulted in a decrease in alpha. From Tables 45, 46 and 48 it can be seen that the value for beta increased with increasing temperature. Figure 47 does not display any values for beta since it was not possible to measure it from the data

Table 45. The effect of temperature on the photosynthetic parameters of *Ankistrodesmus antarcticus* cultured at 15°C.

Culture temperature °C	P/I temperature °C	α (mg oxygen g dry wt ⁻¹ hr ⁻¹ / μ mol s ⁻¹ m ⁻²)	I_k (μ mol s ⁻¹ m ⁻²)	β (mg oxygen g dry wt ⁻¹ hr ⁻¹ / μ mol s ⁻¹ m ⁻²)	P_{max}^{PFD} (μ mol s ⁻¹ m ⁻²)	P_{max} (mg oxygen g dry wt ⁻¹ hr ⁻¹)
15	15	0.96	69.8	no data	200	67.0
15	23	1.68	153.1	-0.17	300	155.3
15	30	2.50	136.0	-0.33	100	257.3
15	35	4.03	38.5	-0.41	100	340.1

Table 46. The effect of temperature on the photosynthetic parameters of *Ankistrodesmus antarcticus* cultured at 23°C.

Culture temperature °C	P/I temperature °C	α (mg oxygen g dry wt ⁻¹ hr ⁻¹ / μ mol s ⁻¹ m ⁻²)	I_k (μ mol s ⁻¹ m ⁻²)	β (mg oxygen g dry wt ⁻¹ hr ⁻¹ / μ mol s ⁻¹ m ⁻²)	P_{max}^{PFD} (μ mol s ⁻¹ m ⁻²)	P_{max} (mg oxygen g dry wt ⁻¹ hr ⁻¹)
23	15	0.38	86.2	-0.027	200	32.8
23	23	0.92	104.5	-0.029	100	96.1
23	30	1.65	114.9	-0.069	200	189.6
23	35	3.50	70.7	-0.205	200	247.7

Table 47. The effect of temperature on the photosynthetic parameters of *Ankistrodesmus antarcticus* cultured at 30°C.

Culture temperature °C	P/I temperature °C	α (mg oxygen g dry wt ⁻¹ hr ⁻¹ / μ mol s ⁻¹ m ⁻²)	I_k (μ mol s ⁻¹ m ⁻²)	β (mg oxygen g dry wt ⁻¹ hr ⁻¹ / μ mol s ⁻¹ m ⁻²)	P_{max}^{PFD} (μ mol s ⁻¹ m ⁻²)	P_{max} (mg oxygen g dry wt ⁻¹ hr ⁻¹)
30	15	0.49	33.4	no data	750	16.4
30	23	0.41	69.9	no data	500	28.7
30	30	1.35	53.1	no data	500	71.7
30	35	1.92	57.9	-0.102	100	111.2

Table 48. The effect of temperature on the photosynthetic parameters of *Ankistrodesmus antarcticus* cultured at 35°C.

Culture temperature °C	P/I temperature °C	α (mg oxygen g dry wt ⁻¹ hr ⁻¹ / μ mol s ⁻¹ m ⁻²)	I_k (μ mol s ⁻¹ m ⁻²)	β (mg oxygen g dry wt ⁻¹ hr ⁻¹ / μ mol s ⁻¹ m ⁻²)	P_{max}^{PFD} (μ mol s ⁻¹ m ⁻²)	P_{max} (mg oxygen g dry wt ⁻¹ hr ⁻¹)
35	15	0.59	41.1	-0.01	300	24.2
35	23	0.73	70.6	-0.04	100	51.6
35	30	1.52	49.6	-0.08	100	75.5
35	35	0.94	80.9	-0.13	200	76.1

obtained during the photosynthesis / irradiance measurements. At the lower culture temperatures of 15 and 23°C (Table 45 and 46) the value of I_k was found to increase initially and then fall with increasing P/I incubation temperature. However with the higher culture temperatures of 30 and 35°C (Tables 47 and 48) the value of I_k had no relationship with increasing temperature.

Apart from the anomalous data obtained (in duplicate) at the 15:35 photosynthesis / irradiance curve (Figure 130), *Ankistrodesmus antarcticus* showed increasing respiration with increasing temperature (Figures 130, 131, 132 and 133). The sharp increases in respiration and LEDR, however were not observed in Figure 133, compared to Figures 130, 131 and 132. The following equations were found to relate initial dark respiration to temperature:

15°C

$$R_{initial}^{15} = 5.47 \times 10^{-2} \times T^{2.146} \quad (\text{Sig P}=0.001) \quad (74)$$

23°C

$$R_{initial}^{23} = \frac{1}{0.1286 + (-3.59 \times 10^{-3} \times T)} \quad (\text{Sig P}=0.001) \quad (75)$$

30°C

$$R_{initial}^{30} = \frac{1}{0.563 + (-1.652 \times 10^{-2} \times T)} \quad (\text{Sig P}=0.001) \quad (76)$$

35°C

$$R_{initial}^{35} = 0.1533 \times T^{1.295} \quad (\text{Sig P}=0.001) \quad (77)$$

From equations 74 and 77, it can be seen that the relationship between oxygen consumption and temperature was a power fit, however, at the culture temperatures of 23 and 30°C (equations 75 and 76) the relationship was an exponential fit.

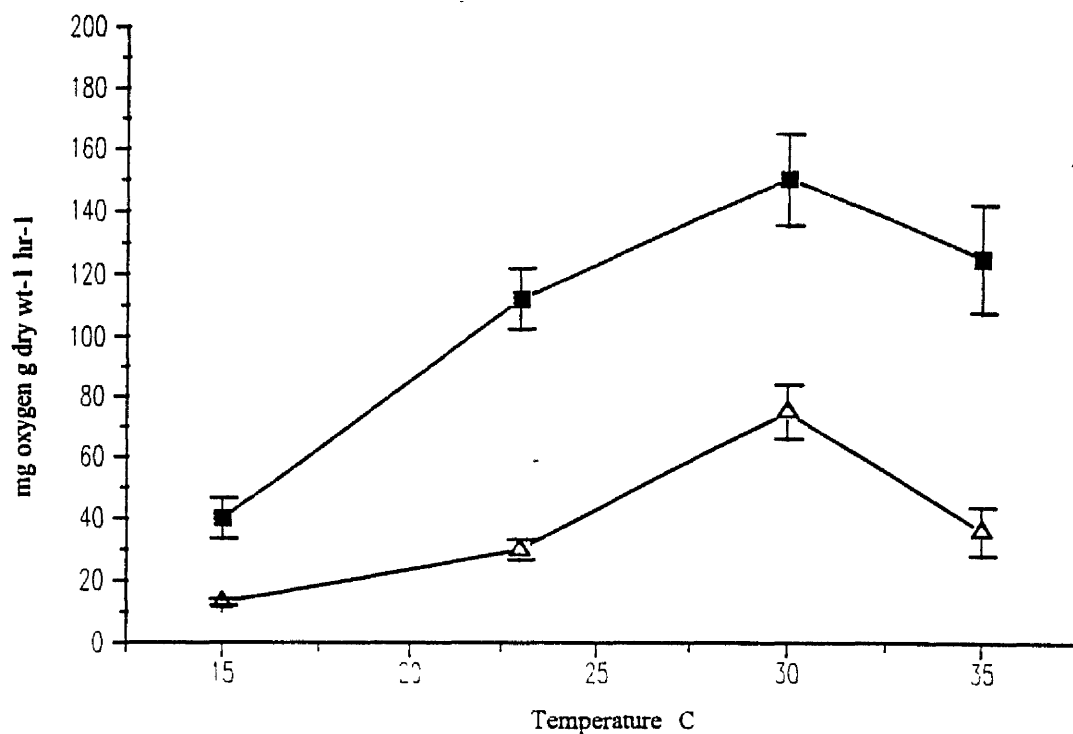


Figure 130. The effect of P/I incubation temperature on the dark respiration Δ — Δ and light enhanced dark respiration \blacksquare — \blacksquare of *Ankistrodesmus antarcticus* cultured at 15°C.

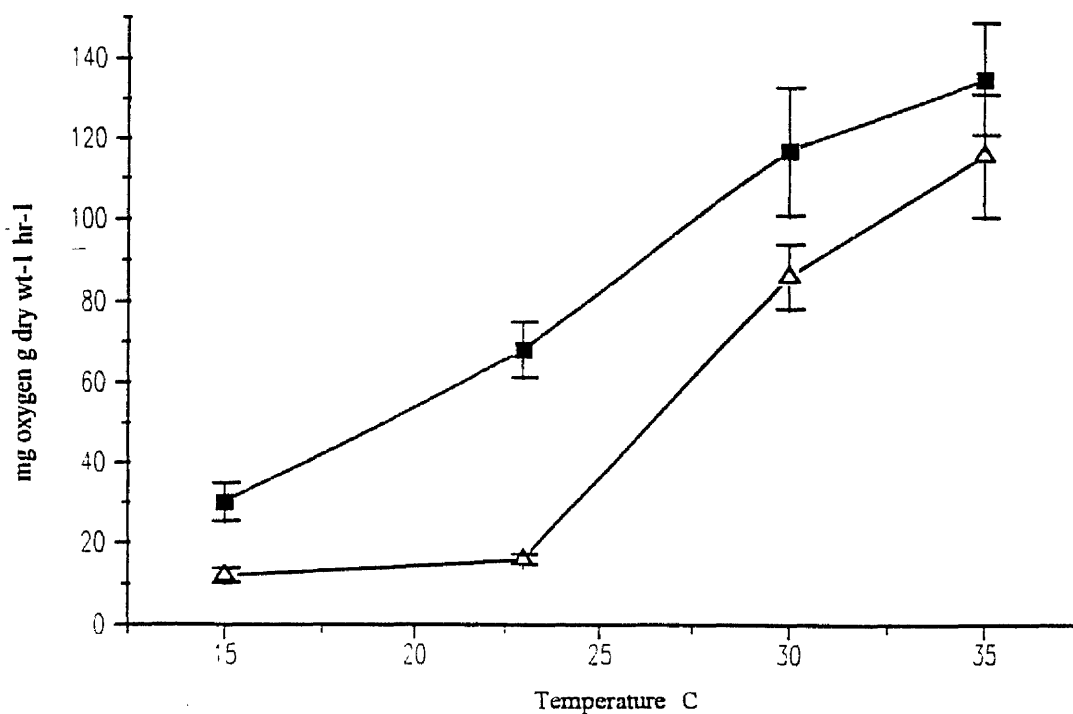


Figure 131. The effect of P/I incubation temperature on the dark respiration Δ — Δ and light enhanced dark respiration \blacksquare — \blacksquare of *Ankistrodesmus antarcticus* cultured at 23°C.

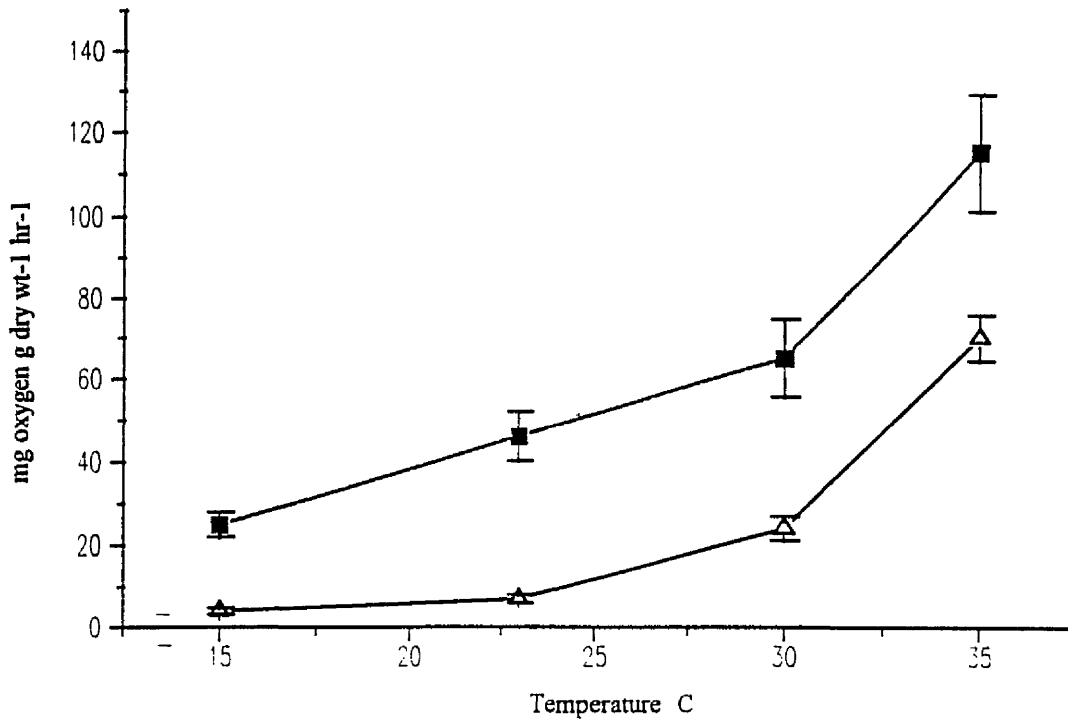


Figure 132. The effect of P/I incubation temperature on the dark respiration Δ — Δ and light enhanced dark respiration \blacksquare — \blacksquare of *Ankistrodesmus antarcticus* cultured at 30°C.

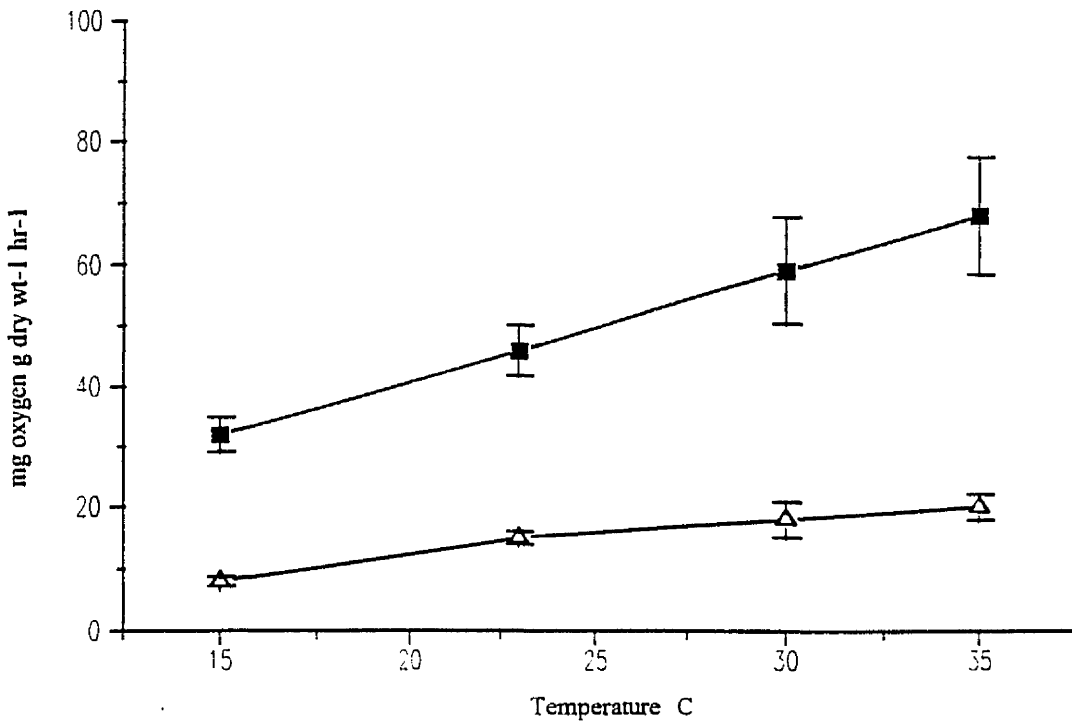


Figure 133. The effect of P/I incubation temperature on the dark respiration Δ — Δ and light enhanced dark respiration \blacksquare — \blacksquare of *Ankistrodesmus antarcticus* cultured at 35°C.

The following equations describe the relationship between LEDR and P/I incubation temperature for each of the four culture temperatures.

15°C

$$LEDR_{final}^{15} = \frac{1}{5.69 \times 10^{-2} + (-1.098 \times 10^{-3} \times T)} \quad (\text{Sig P}=0.001) \quad (78)$$

23°C

$$LEDR_{final}^{23} = 0.99 \times T^{1.23} \quad (\text{Sig P}=0.01) \quad (79)$$

30°C

$$LEDR_{final}^{30} = \frac{1}{3.259 \times 10^{-2} + (-6.188 \times 10^{-4} \times T)} \quad (\text{Sig P}=0.001) \quad (80)$$

35°C

$$LEDR_{final}^{35} = 4.02 \times T^{-0.704} \quad (\text{Sig P}=0.05) \quad (81)$$

From equations 78 and 80 it can be seen that the relationship between the LEDR oxygen consumption and temperature was a hyperbolic fit, however, at the culture temperatures of 23 and 35°C (equations 79 and 81) the relationship was a power fit. The rate of LEDR decreased when 35°C cultured cells were incubated at P/I temperatures of 30 and 35°C (Figure 133). This may be due to a high degree of photodamage and photoinhibition caused by the high temperature and light combination.

The following equations best describe the relationship between the value of alpha and the P/I incubation temperature at the 4 culture temperatures of 15, 23, 30 and 35°C.

$$\alpha_{15} = 0.205 \times e^{(7.55 \times 10^{-2} \times T)} \quad (\text{Sig P}=0.01) \quad (82)$$

$$\alpha_{23} = 0.586 + (-2.42 \times 10^{-2} \times T) + (1.57 \times 10^{-3} \times T^2) \quad (\text{Sig } P=0.01) \quad (83)$$

$$\alpha_{30} = 0.609 \times e^{(4.207 \times 10^{-2} \times T)} \quad (\text{Sig } P=0.01) \quad (84)$$

$$\alpha_{35} = 2.74 \times 10^{-4} \times T^{2.513} \quad (\text{Sig } P=0.01) \quad (85)$$

Figures 134, 135, 136 and 137 show the arhenius plots for *Ankistrodesmus antarcticus* of the natural logarithm of photosynthetic rates (mg oxygen g dry wt⁻¹ hr⁻¹), measured at a PFD of 100μmol s⁻¹ m⁻² against the reciprocal of P/I incubation temperature (Kelvin) for culture temperatures of 15, 23, 30 and 35°C respectively. Figure 134 showed a decrease in the rate of oxygen evolution at the P/I incubation temperature of 35°C.

Figures 138, 139, 140 and 141 show the photosynthesis / irradiance curves measured at various temperatures using cultured cells of *Synechococcus* 1479/5. As was found with the green micro-algae, cells of *Synechococcus* 1479/5 showed an increase in the values of P_{max} with increasing P/I incubation temperature. The very low oxygen evolution by cells cultured at 15 and 23°C, indicated that the cells were being grown at a temperature well below their optimum growth temperature, which may be 35°C

It was found that the following equations described the relationship between the maximum rate of photosynthesis and the variation in temperature.

15°C

$$P_{\max}^{15} = 2.269 \times 10^{-2} \times T^{2.57} \quad (\text{Sig } P=0.001) \quad (86)$$

23°C

$$P_{\max}^{23} = 1.263 \times 10^{-2} \times T^{2.61} \quad (\text{Sig } P=0.001) \quad (87)$$

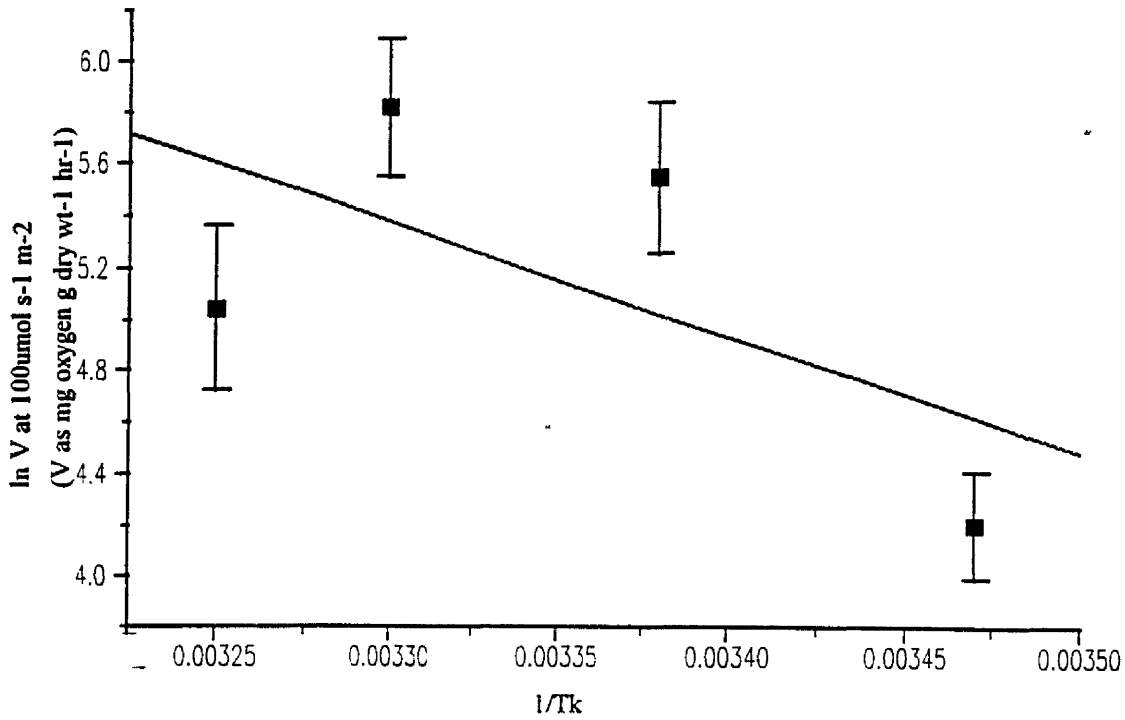


Figure 134. Arrhenius plot of ln photosynthetic rate at a PFD of $100\mu\text{mol s}^{-1} \text{m}^{-2}$ against increasing P/I incubation temperature for *Ankistrodesmus antarcticus* cultured at a temperature of 15°C .

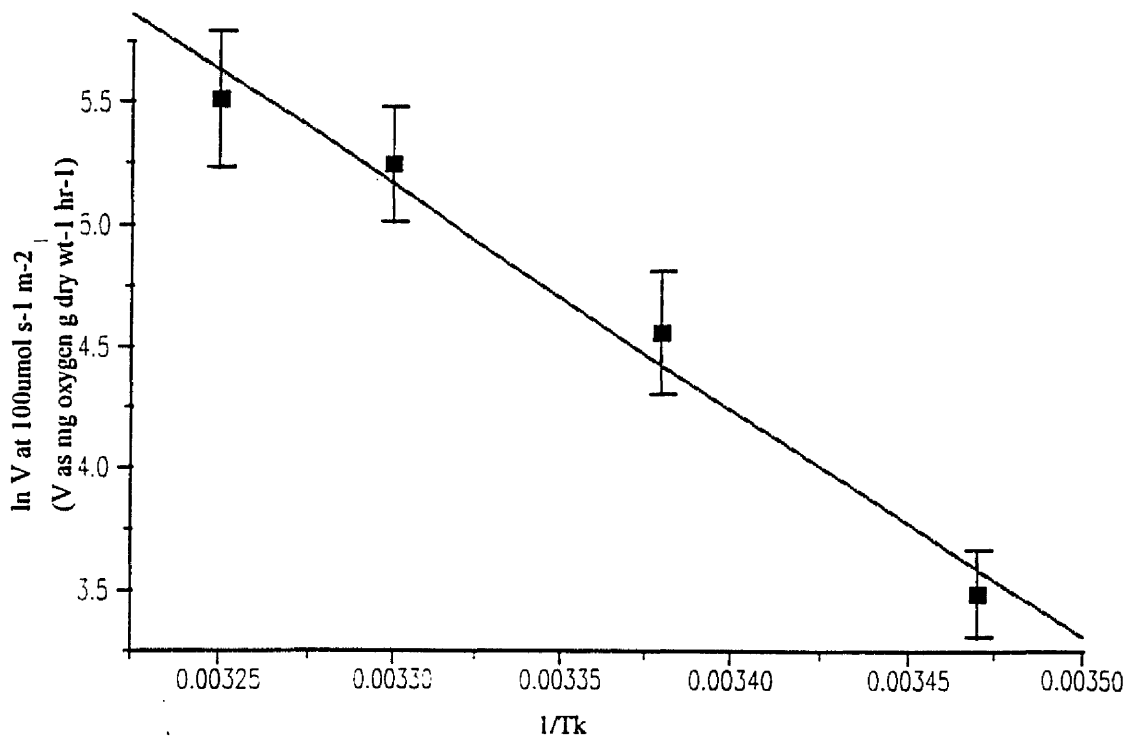


Figure 135. Arrhenius plot of ln photosynthetic rate at a PFD of $100\mu\text{mol s}^{-1} \text{m}^{-2}$ against increasing P/I incubation temperature for *Ankistrodesmus antarcticus* cultured at a temperature of 23°C .

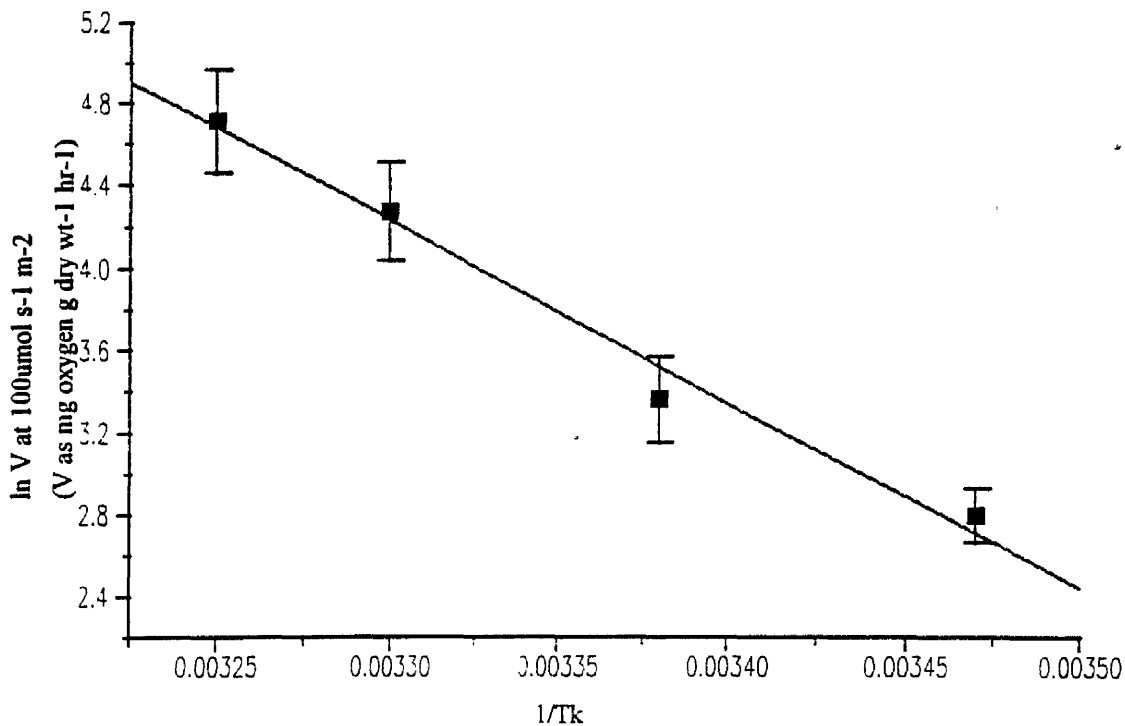


Figure 136. Arrhenius plot of ln photosynthetic rate at a PFD of $100\mu\text{mol s}^{-1} \text{m}^{-2}$ against increasing P/I incubation temperature for *Ankistrodesmus antarcticus* cultured at a temperature of 30°C .

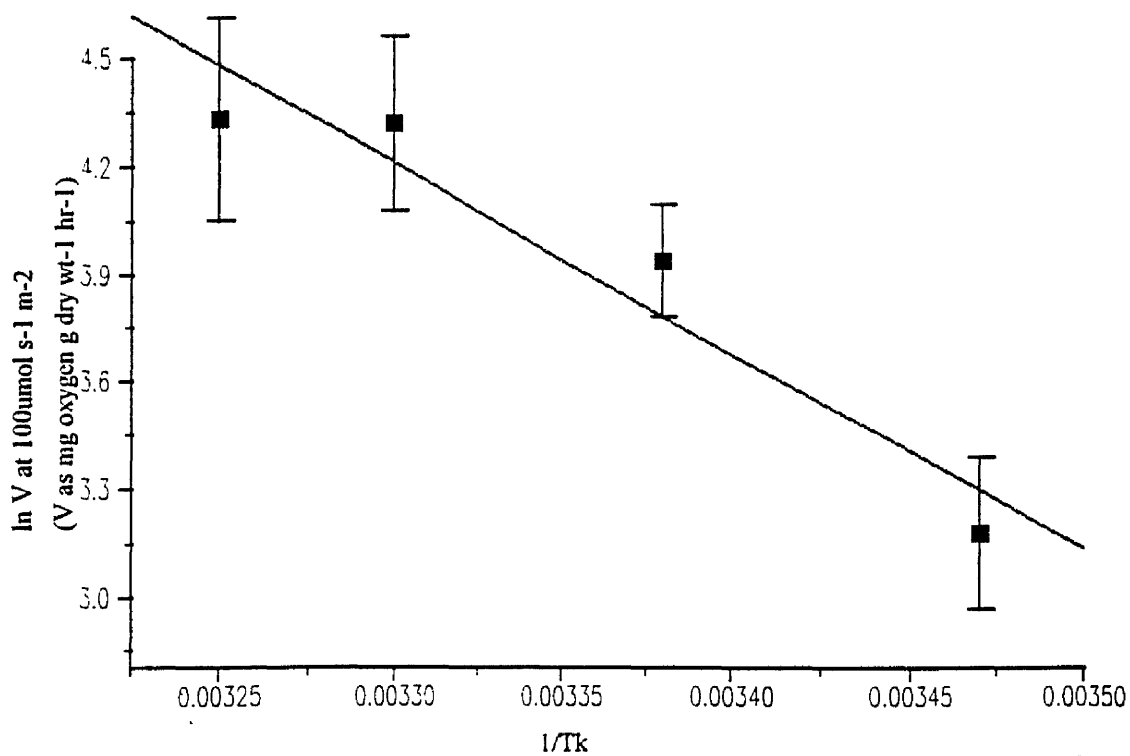


Figure 137. Arrhenius plot of ln photosynthetic rate at a PFD of $100\mu\text{mol s}^{-1} \text{m}^{-2}$ against increasing P/I incubation temperature for *Ankistrodesmus antarcticus* cultured at a temperature of 35°C .

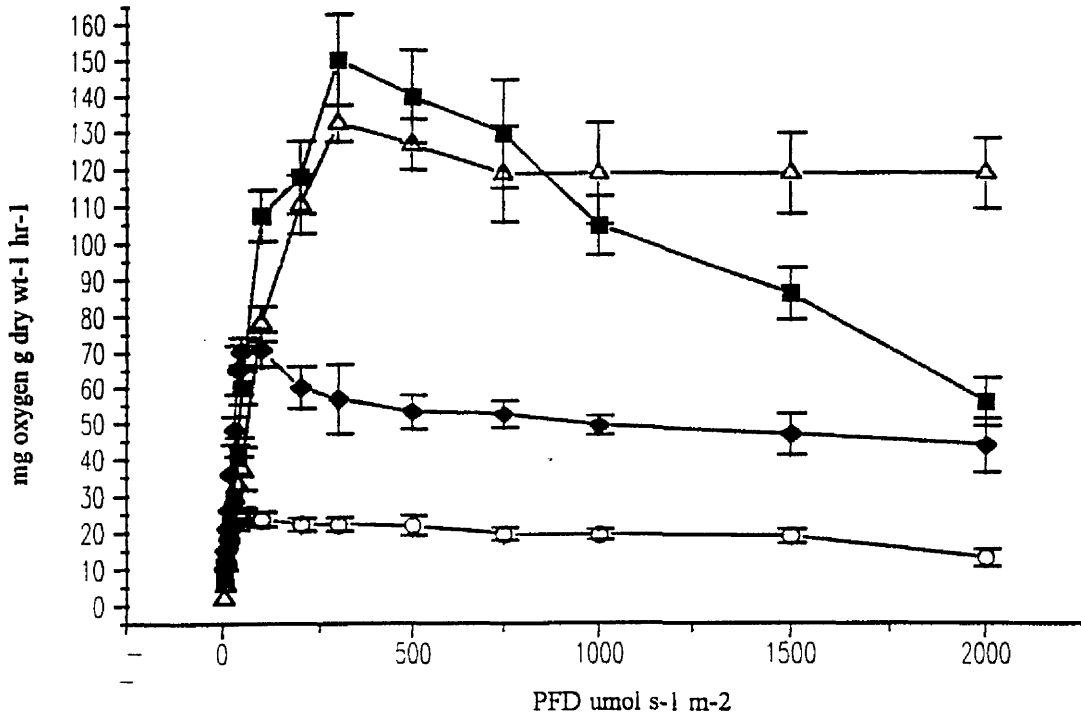


Figure 138. The effect of P/I incubation temperature on the photosynthesis / irradiance response curves of *Synechococcus* 1479/5 cultured at 15°C, ○—○ 15°C, ◆—◆ 23°C, ■—■ 30°C, △—△ 35°C.

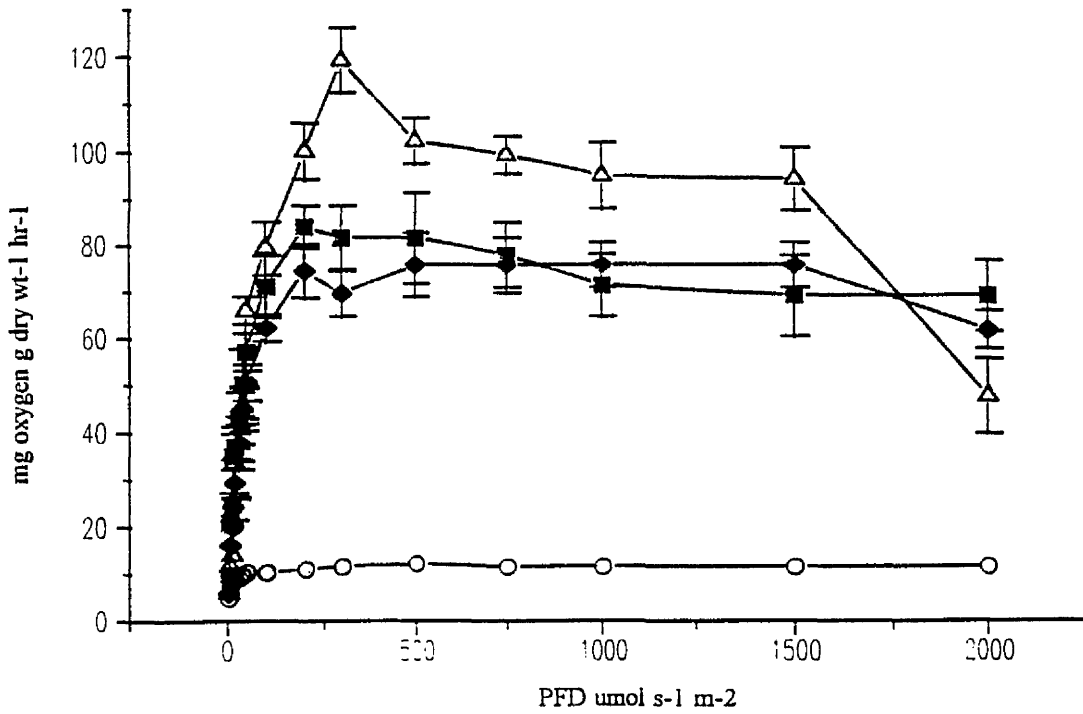


Figure 139. The effect of P/I incubation temperature on the photosynthesis / irradiance response curves of *Synechococcus* 1479/5 cultured at 23°C, ○—○ 15°C, ◆—◆ 23°C, ■—■ 30°C, △—△ 35°C.

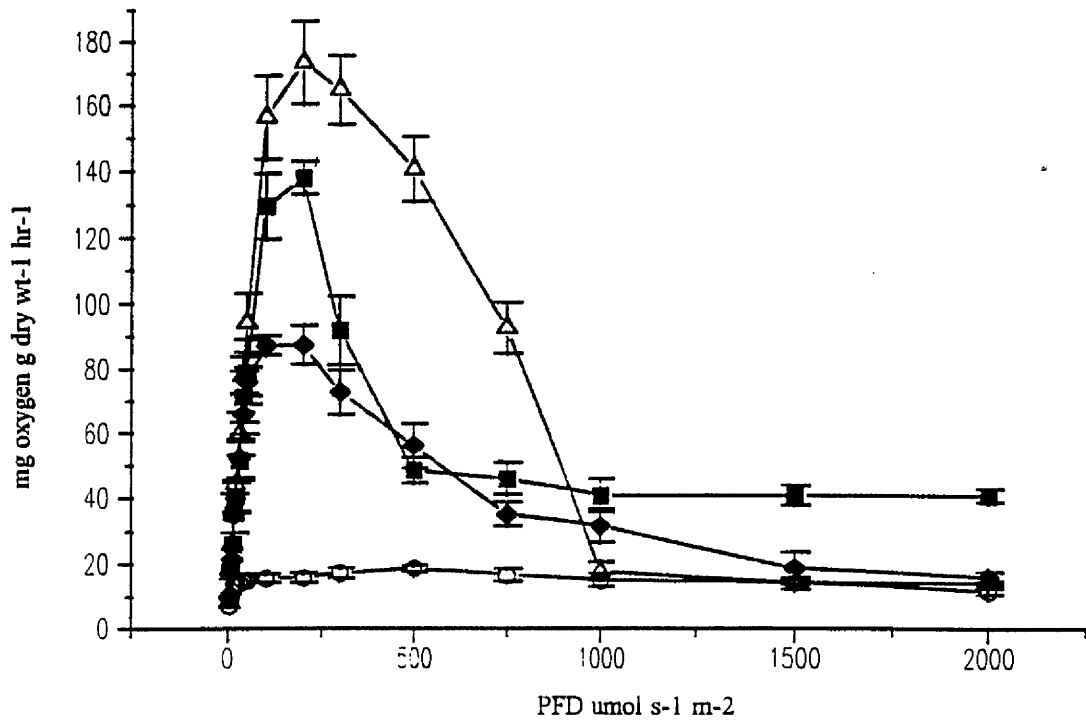


Figure 140. The effect of P/I incubation temperature on the photosynthesis / irradiance response curves of *Synechococcus* 1479/5 cultured at 30°C, ○—○ 15°C, ◆—◆ 23°C, ■—■ 30°C, △—△ 35°C.

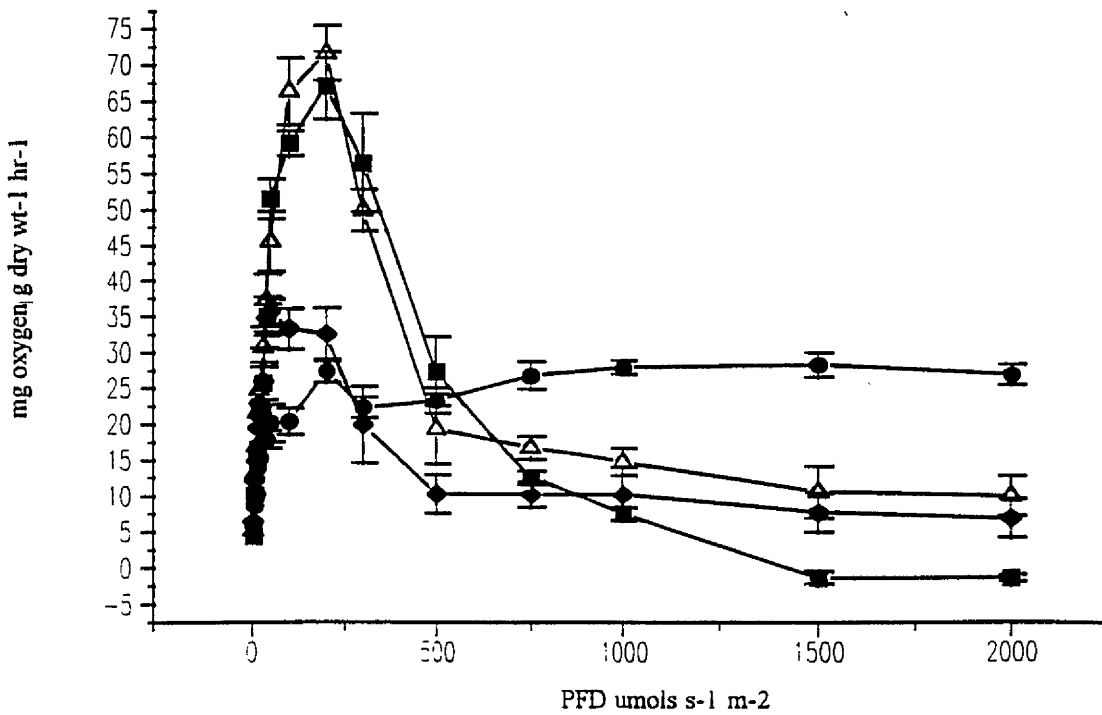


Figure 141. The effect of P/I incubation temperature on the photosynthesis / irradiance response curves of *Synechococcus* 1479/5 cultured at 35°C, ○—○ 15°C, ◆—◆ 23°C, ■—■ 30°C, △—△ 35°C.

30°C

$$P_{\max}^{30} = \frac{1}{5.512 \times 10^{-2} + (-1.228 \times 10^{-3} \times T)} \quad (\text{Sig } P=0.001) \quad (88)$$

35°C

$$P_{\max}^{35} = 1.617 \times 10^{-2} \times T^{2.65} \quad (\text{Sig } P=0.001) \quad (89)$$

From equations 86, 87 and 89, it was found that the maximum rate of photosynthesis was related to temperature by a power fit. However cells cultured at 30°C were found to exhibit a hyperbolic relationship between P_{\max} and temperature (equation 88).

The photosynthetic parameters calculated from Figures 138, 139, 140 and 141 are presented in Tables 49, 50, 51 and 52 respectively. Similar to the unicellular green micro-algae the cells of *Synechococcus* 1479/5 showed an overall increase in alpha with increasing temperature. Where measurement was possible the value of beta increased with increasing temperature (Table 49, 51 and 52). At the lower culture temperature of 15°C (Table 49) the value of beta increased from -0.017 to 0.07 mg oxygen g dry wt⁻¹ hr⁻¹ / μmol s⁻¹ m⁻² with increasing P/I incubation temperature (15 to 30°C), before decreasing at the higher P/I incubation temperature of 35°C to -0.031 mg oxygen g dry wt⁻¹ hr⁻¹ / μmol s⁻¹ m⁻².

Increasing P/I incubation temperature generally resulted in an overall increase in the value of I_k (Tables 49, 50 and 52). Figure 51 showed no correlation between I_k and P/I incubation temperature. Unlike the results obtained from *Chlorella vulgaris* 211/11c, *Nannochloris atomus*, *Scenedesmus* sp. and *Ankistrodesmus antarcticus*, the highest value for P_{\max} was 173.3 mg oxygen g dry wt⁻¹ hr⁻¹ recorded from *Synechococcus* 1479/5 that had been cultured at 30°C and measured at a P/I incubation temperature of 35°C.

It was found that cells of *Synechococcus* 1479/5 showed increases in respiration rates with increasing P/I incubation temperature (Figures 142, 143, 144 and 145).

Table 49. The effect of temperature on the photosynthetic parameters of *Synechococcus* 1479/5 cultured at 15°C

Culture temperature °C	P/I temperature °C	α (mg oxygen g dry wt ⁻¹ hr ⁻¹ / μ mol s ⁻¹ m ⁻²)	I_k (μ mol s ⁻¹ m ⁻²)	β (mg oxygen g dry wt ⁻¹ hr ⁻¹ / μ mol s ⁻¹ m ⁻²)	P_{max}^{PFD} (μ mol s ⁻¹ m ⁻²)	P_{max} (mg oxygen g dry wt ⁻¹ hr ⁻¹)
15	15	0.43	57.8	-0.017	100	24.8
15	23	1.04	68.0	-0.045	100	70.7
15	30	1.34	111.8	-0.070	300	149.9
15	35	1.47	90	-0.031	300	132.3

Table 50. The effect of temperature on the photosynthetic parameters of *Synechococcus* 1479/5 cultured at 23°C

Culture temperature °C	P/I temperature °C	α (mg oxygen g dry wt ⁻¹ hr ⁻¹ / μ mol s ⁻¹ m ⁻²)	I_k (μ mol s ⁻¹ m ⁻²)	β (mg oxygen g dry wt ⁻¹ hr ⁻¹ / μ mol s ⁻¹ m ⁻²)	P_{max}^{PFD} (μ mol s ⁻¹ m ⁻²)	P_{max} (mg oxygen g dry wt ⁻¹ hr ⁻¹)
23	15	0.29	40.8	no data	500	12.2
23	23	1.47	50.65	no data	200	74.5
23	30	1.97	42.64	no data	200	84.0
23	35	1.20	99.22	-0.042	300	119.1

Table 51. The effect of temperature on the photosynthetic parameters of *Synechococcus* 1479/5 cultured at 30°C

Culture temperature °C	P/I temperature °C	α (mg oxygen g dry wt ⁻¹ hr ⁻¹ / μ mol s ⁻¹ m ⁻²)	I_k (μ mol s ⁻¹ m ⁻²)	β (mg oxygen g dry wt ⁻¹ hr ⁻¹ / μ mol s ⁻¹ m ⁻²)	P_{max}^{PFD} (μ mol s ⁻¹ m ⁻²)	P_{max} (mg oxygen g dry wt ⁻¹ hr ⁻¹)
30	15	0.52	35.7	no data	500	18.6
30	23	1.99	43.8	-0.101	200	87.3
30	30	2.20	62.4	-0.113	200	137.8
30	35	2.26	76.7	-0.286	200	173.3

Table 52. The effect of temperature on the photosynthetic parameters of *Synechococcus* 1479/5 cultured at 35°C

Culture temperature °C	P/I temperature °C	α (mg oxygen g dry wt ⁻¹ hr ⁻¹ / μ mol s ⁻¹ m ⁻²)	I_k (μ mol s ⁻¹ m ⁻²)	β (mg oxygen g dry wt ⁻¹ hr ⁻¹ / μ mol s ⁻¹ m ⁻²)	P_{max}^{PFD} (μ mol s ⁻¹ m ⁻²)	P_{max} (mg oxygen g dry wt ⁻¹ hr ⁻¹)
35	15	0.85	42.1	no data	200	27.4
35	23	1.05	33.9	-0.019	200	35.6
35	30	1.33	53.8	-0.134	200	71.6
35	35	1.03	65.1	-0.171	200	67.1

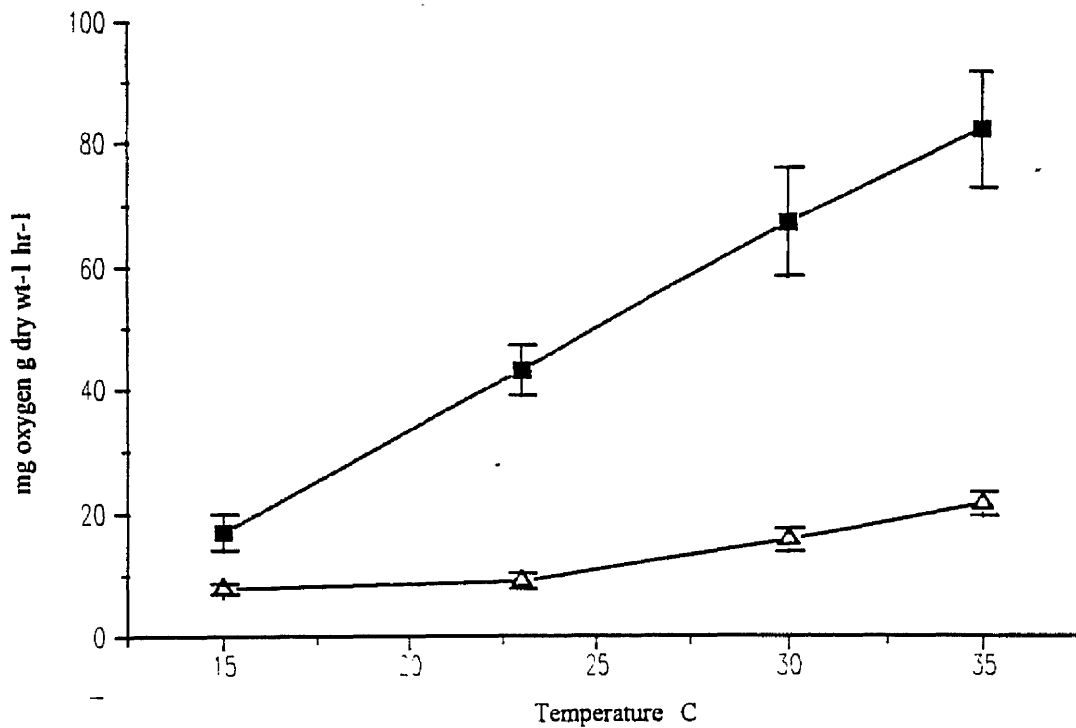


Figure 142. The effect of P/I incubation temperature on the dark respiration Δ — Δ and light enhanced dark respiration \blacksquare — \blacksquare of *Synechococcus* 1479/5 cultured at 15°C.

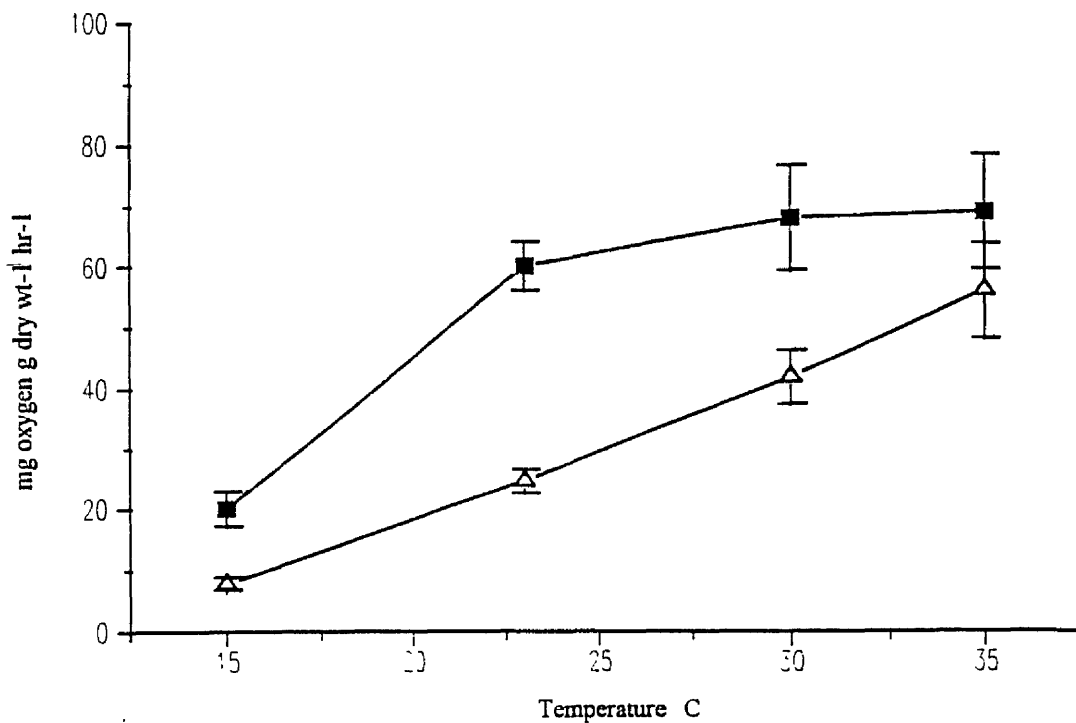


Figure 143. The effect of P/I incubation temperature on the dark respiration Δ — Δ and light enhanced dark respiration \blacksquare — \blacksquare of *Synechococcus* 1479/5 cultured at 23°C.

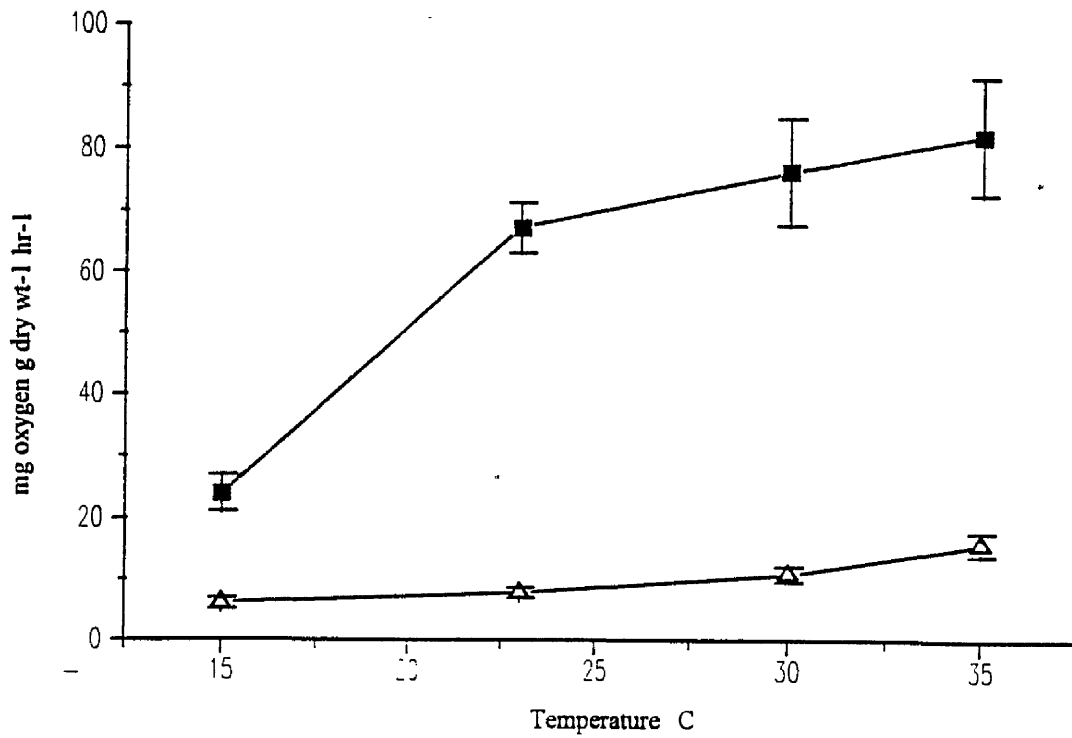


Figure 144. The effect of P/I incubation temperature on the dark respiration Δ — Δ and light enhanced dark respiration \blacksquare — \blacksquare of *Synechococcus* 1479/5 cultured at 30°C.

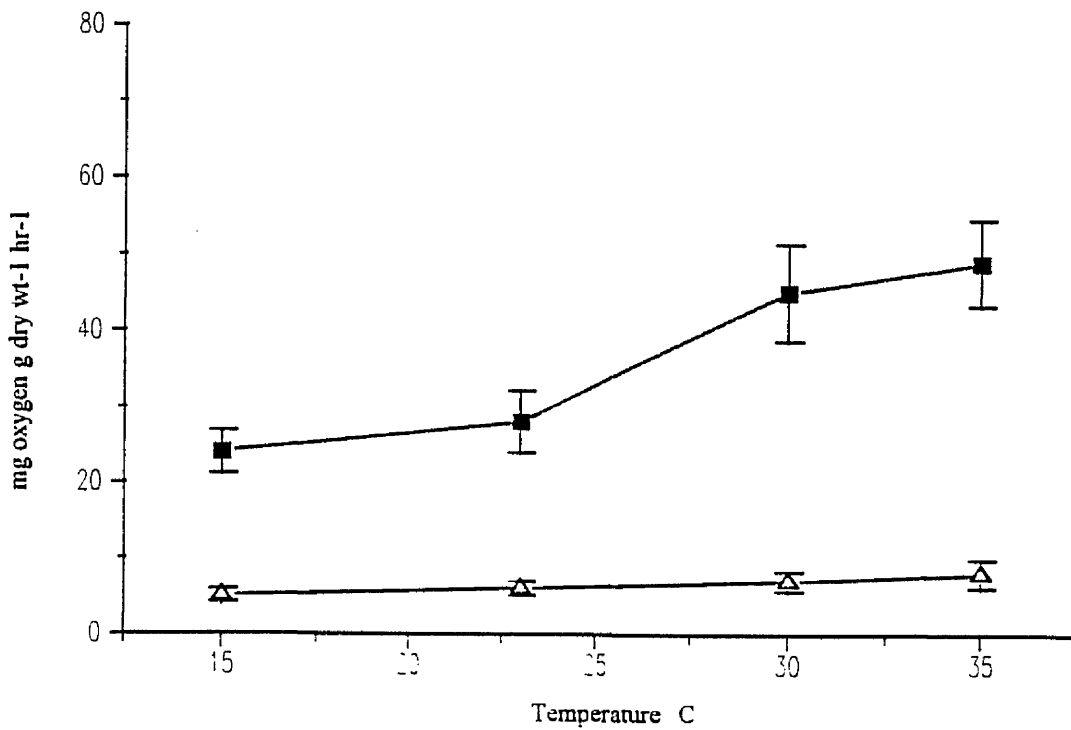


Figure 145. The effect of P/I incubation temperature on the dark respiration Δ — Δ and light enhanced dark respiration \blacksquare — \blacksquare of *Synechococcus* 1479/5 cultured at 35°C.

Figures 144 and 145 show, however, that respiration changes were only slight when the cells were incubated at temperatures below the culture temperature.

The following equations were found to relate temperature to the initial dark respiration rate.

15°C

$$R_{initial}^{15} = 3.8188 \times e^{5.82 \times 10^{-2} \times T} \quad (\text{Sig } P=0.001) \quad (89)$$

23°C

$$R_{initial}^{23} = 1.96 \times 10^{-2} \times T^{2.21} \quad (\text{Sig } P=0.001) \quad (90)$$

30°C

$$R_{initial}^{30} = -7.045 + 0.681 \times T \quad (\text{Sig } P=0.001) \quad (91)$$

35°C

$$R_{initial}^{35} = 2.2635 + 0.1256 \times T \quad (\text{Sig } P=0.01) \quad (92)$$

It was found that cells cultured at the higher temperatures of 30 and 35°C (equations 91 and 92) showed a straight line relationship between respiration rate and changes in incubation temperature. Cells cultured at 15 and 23°C were described by exponential and power relationships respectively.

The following equations were determined from the relationship between light enhanced dark respiration and temperature.

15°C

$$LEDR_{final}^{15} = 0.135 \times T^{1.804} \quad (\text{Sig } P=0.001) \quad (93)$$

23°C

$$LEDR_{final}^{23} = 0.3247 \times T^{1.545} \quad (\text{Sig P}=0.001) \quad (94)$$

30°C

$$LEDR_{final}^{30} = -159.49 + 68.98 \times \ln(T) \quad (\text{Sig P}=0.001) \quad (95)$$

35°C

$$LEDR_{final}^{35} = -48.44 + 25.606 \times \ln(T) \quad (\text{Sig P}=0.01) \quad (96)$$

From equations 93 and 94 it was found that at the lower temperatures of 15 and 23°C, LEDR was related to temperature via a power fit. At the higher culture temperatures of 30 and 35°C, however, a logarithm based relationship between LEDR and temperature was obtained.

Equations 97, 98 and 99 show the relationship between α and P/I incubation temperature for cell cultured at 15, 23 and 30°C respectively.

$$\alpha_{15} = -1.35 + (0.148 \times T) + (-0.0019 \times T^2) \quad (\text{Sig P}=0.001) \quad (97)$$

$$\alpha_{23} = -5.77 + (0.551 \times T) + (-9.99 \times 10^{-3} \times T^2) \quad (\text{Sig P}=0.01) \quad (98)$$

$$-\alpha_{30} = -10.29 + (1.22 \times T) + (-3.99 \times 10^{-2} \times T^2) + (4.37 \times 10^{-4} \times T^3) \\ (\text{Sig P}=0.001) \quad (99)$$

The relationship between alpha and P/I incubation temperature was best described by a polynomial regression fit (equations 97, 98 and 99 for cells of *Synechococcus* 1479/5 cultured at temperatures of 15, 23 and 30°C respectively). No significant relationship was calculated for cells cultured at 35°C.

Figures 146, 147, 148 and 149 show the arhenius plots *Synechococcus* 1479/5 of the natural logarithm of photosynthetic rates (mg oxygen g dry wt⁻¹ hr⁻¹), measured at a

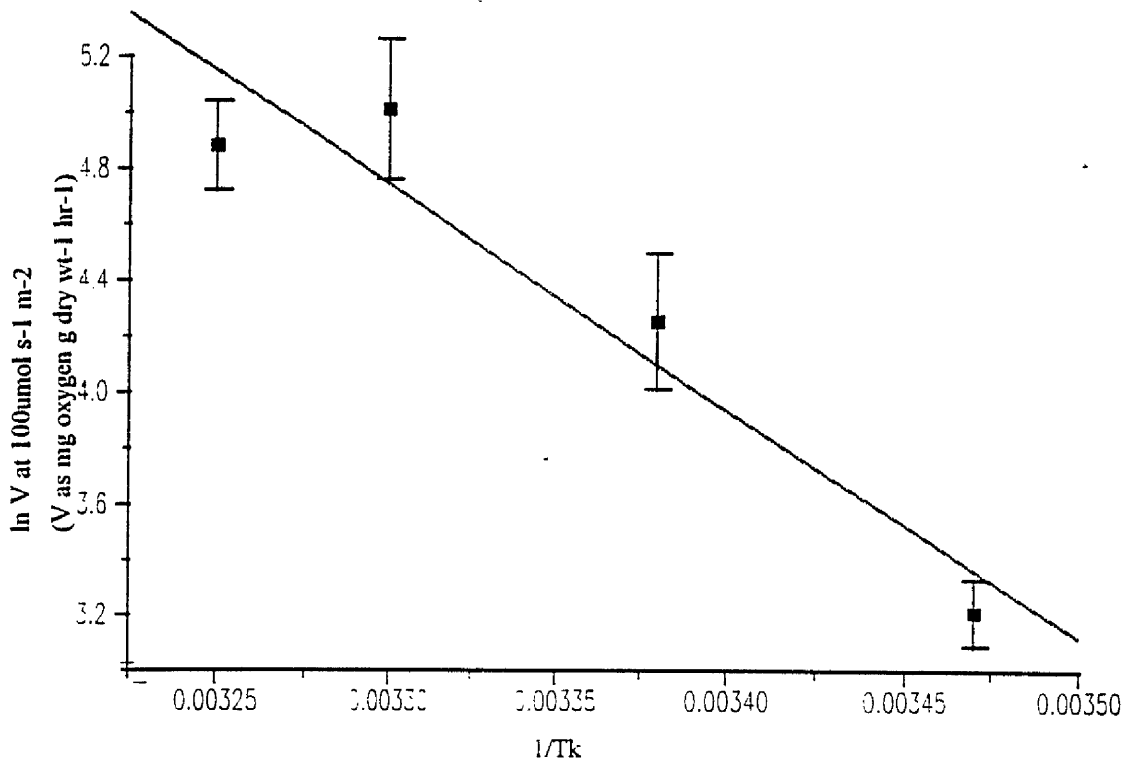


Figure 146. Arrhenius plot of ln photosynthetic rate at a PFD of $100\mu\text{mol s}^{-1} \text{m}^{-2}$ against increasing P/I incubation temperature for *Synechococcus* 1479/5 cultured at a temperature of 15°C .

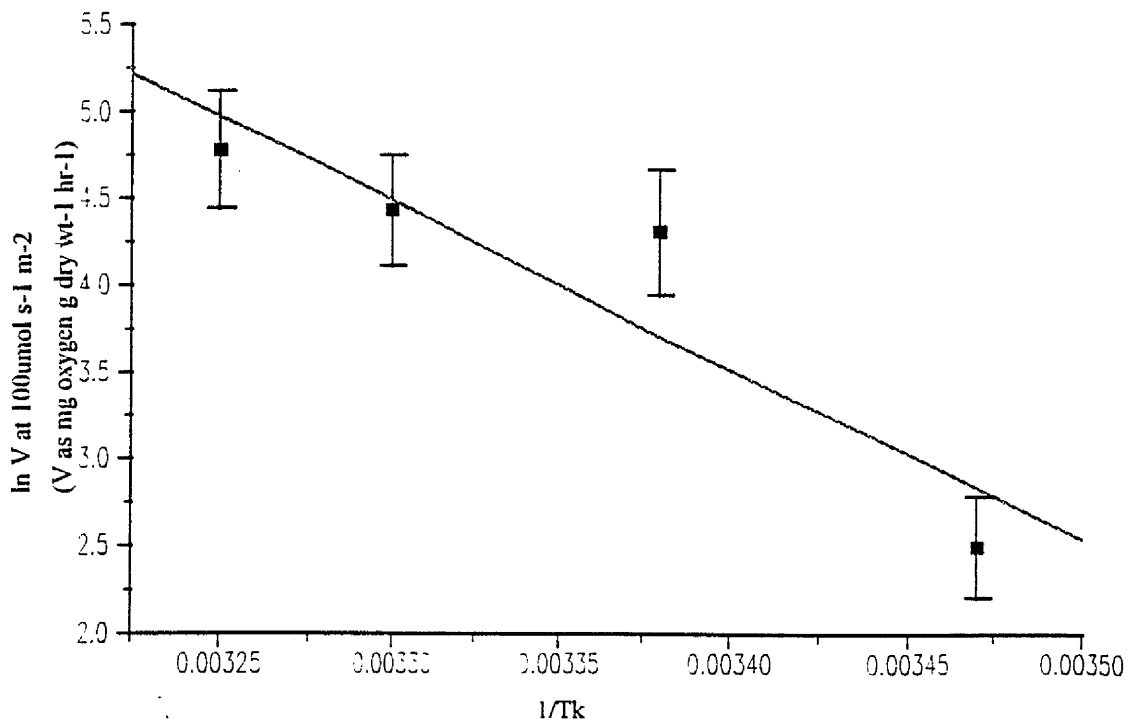


Figure 147. Arrhenius plot of ln photosynthetic rate at a PFD of $100\mu\text{mol s}^{-1} \text{m}^{-2}$ against increasing P/I incubation temperature for *Synechococcus* 1479/5 cultured at a temperature of 23°C .

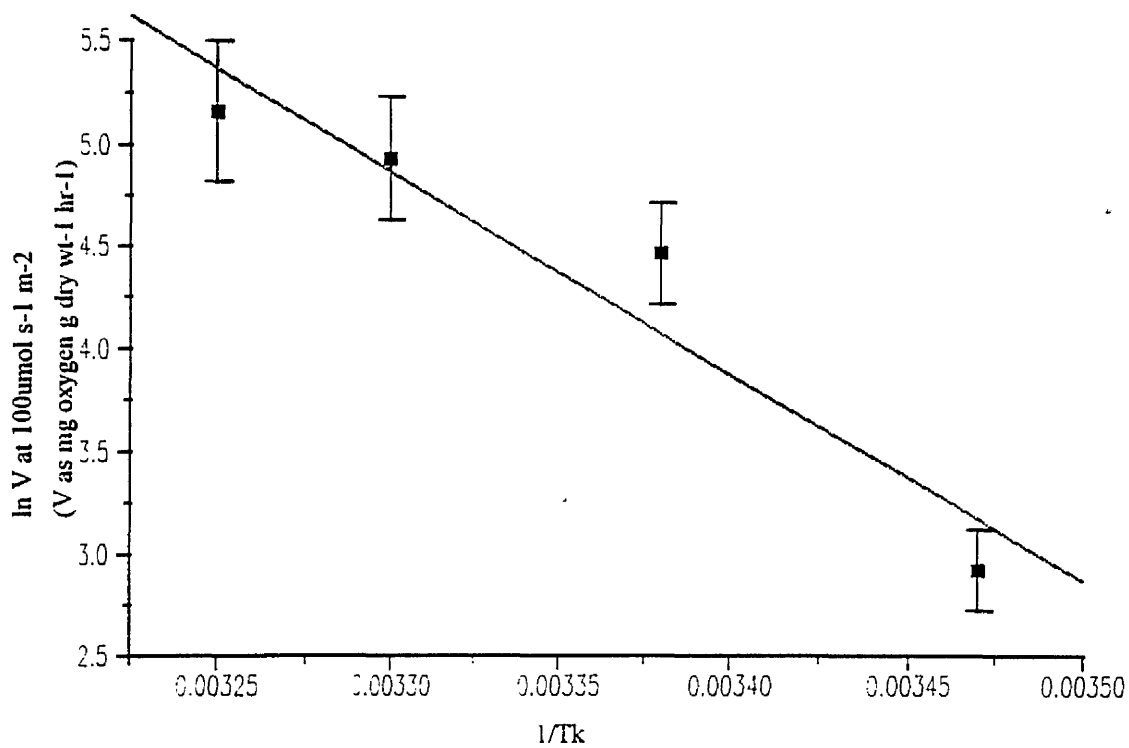


Figure 148. Arrhenius plot of ln photosynthetic rate at a PFD of $100\mu\text{mol s}^{-1} \text{m}^{-2}$ against increasing P/I incubation temperature for *Synechococcus* 1479/5 cultured at a temperature of 30°C.

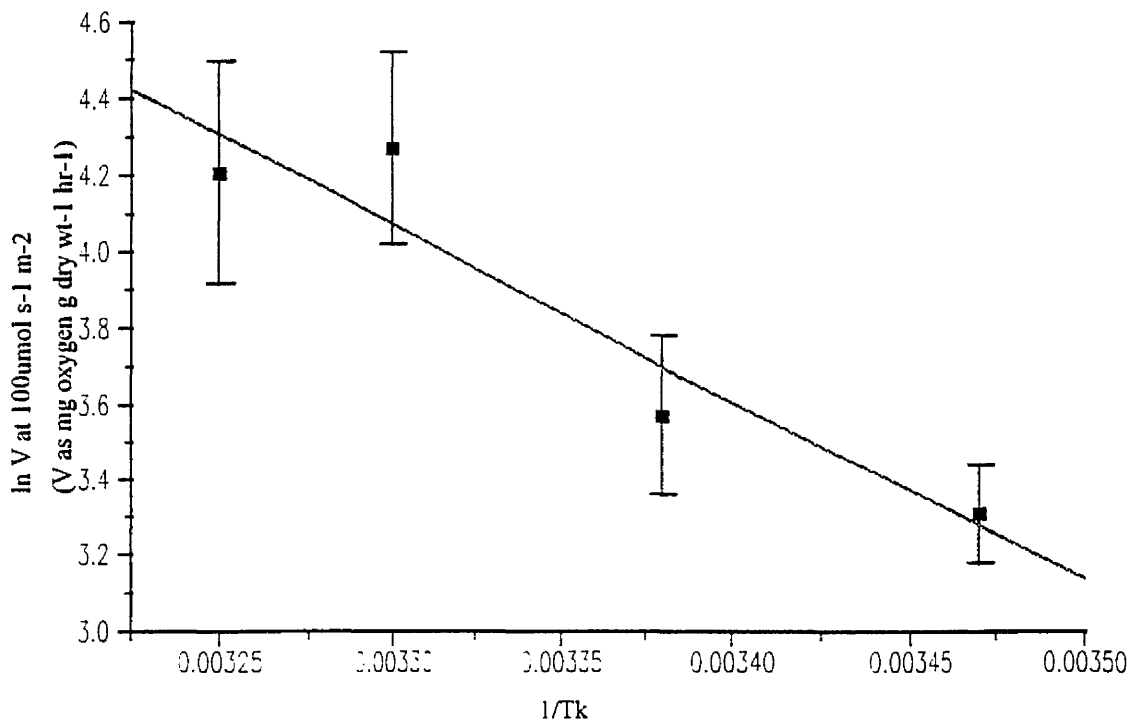


Figure 149. Arrhenius plot of ln photosynthetic rate at a PFD of $100\mu\text{mol s}^{-1} \text{m}^{-2}$ against increasing P/I incubation temperature for *Synechococcus* 1479/5 cultured at a temperature of 35°C.

PFD of $100\mu\text{mol s}^{-1} \text{m}^{-2}$ against the reciprocal of P/I incubation temperature (Kelvin) for culture temperatures of 15, 23, 30 and 35°C respectively.

Cells of the cyanobacterium isolate *Synechococcus sp.* were found to display a similar pattern to that of the unicellular greens. From Figures 150, 151, 152 and 153 it was found that the cells displayed an increase in P_{max} with increasing P/I incubation temperature. However unlike the cells of *Synechococcus* 1479/5 *Synechococcus sp.* appeared to have an optimum temperature (based on maximum rates of photosynthesis studies) of 30°C.

The following equations were found to relate P_{max} to the culture temperatures of 15, 23, 30 and 35°C.

15°C

$$P_{\text{max}}^{15} = 2.815 \times e^{(0.139 \times T)} \quad (\text{Sig } P=0.001) \quad (100)$$

23°C

$$P_{\text{max}}^{23} = -292.71 + 114.26 \times \ln(T) \quad (\text{Sig } P=0.001) \quad (101)$$

30°C

$$P_{\text{max}}^{30} = \frac{1}{6.879 \times 10^{-2} + (-1.89 \times 10^{-3} \times T)} \quad (\text{Sig } P=0.01) \quad (102)$$

35°C

$$P_{\text{max}}^{35} = \frac{1}{8.56 \times 10^{-2} + (-2.07 \times 10^{-3} \times T)} \quad (\text{Sig } P=0.01) \quad (103)$$

From equations 101 and 102 it can be seen that at the higher culture temperatures of 30 and 35°C, cells of *Synechococcus sp.* displayed a hyperbolic relationship between the maximum rate of photosynthesis and temperature. However at the lower culture

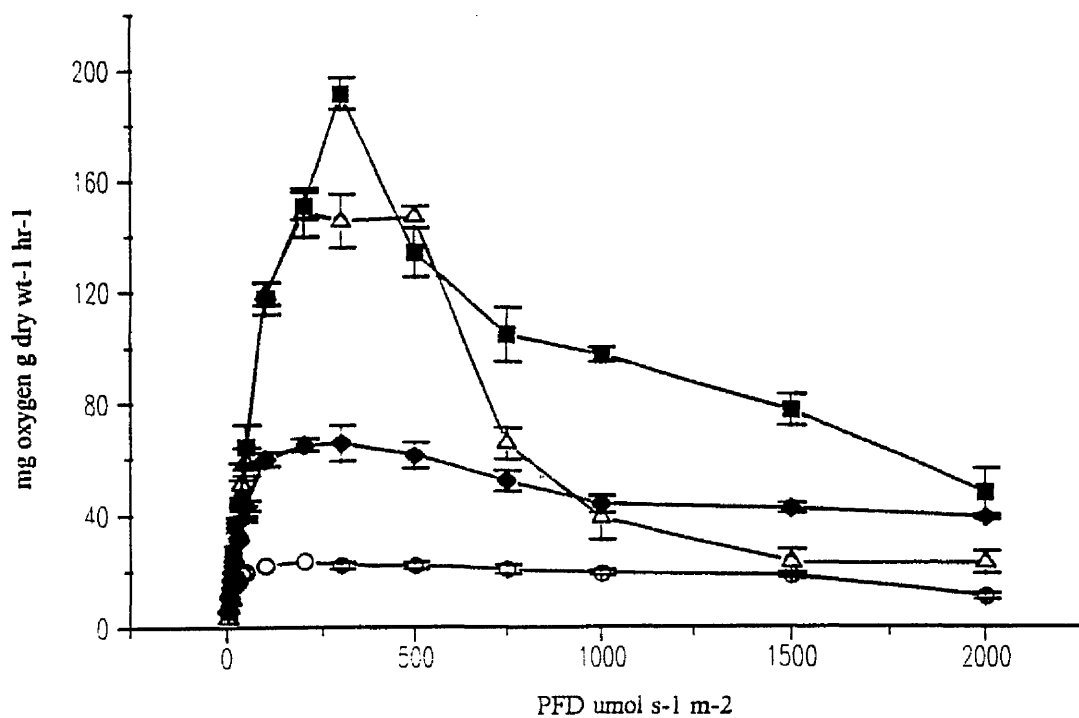


Figure 150. The effect of P/I incubation temperature on the photosynthesis / irradiance response curves of *Synechococcus sp.* cultured at 15°C, ○—○ 15°C, ◆—◆ 23°C, ■—■ 30°C, △—△ 35°C.

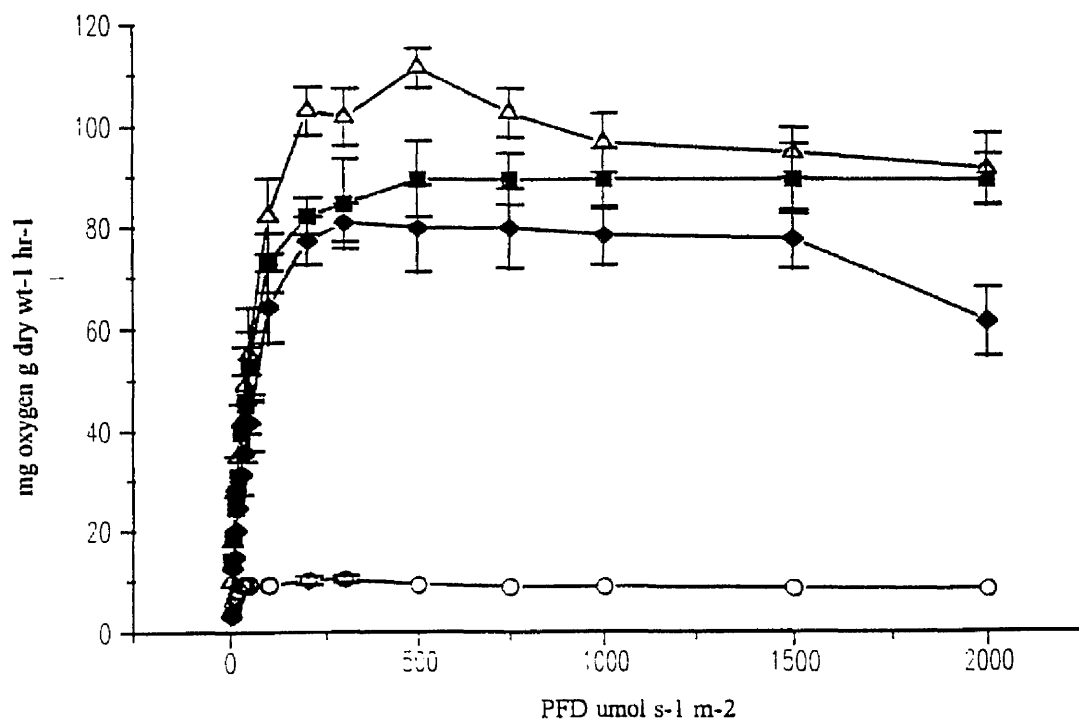


Figure 151. The effect of P/I incubation temperature on the photosynthesis / irradiance response curves of *Synechococcus sp.* cultured at 23°C, ○—○ 15°C, ◆—◆ 23°C, ■—■ 30°C, △—△ 35°C.

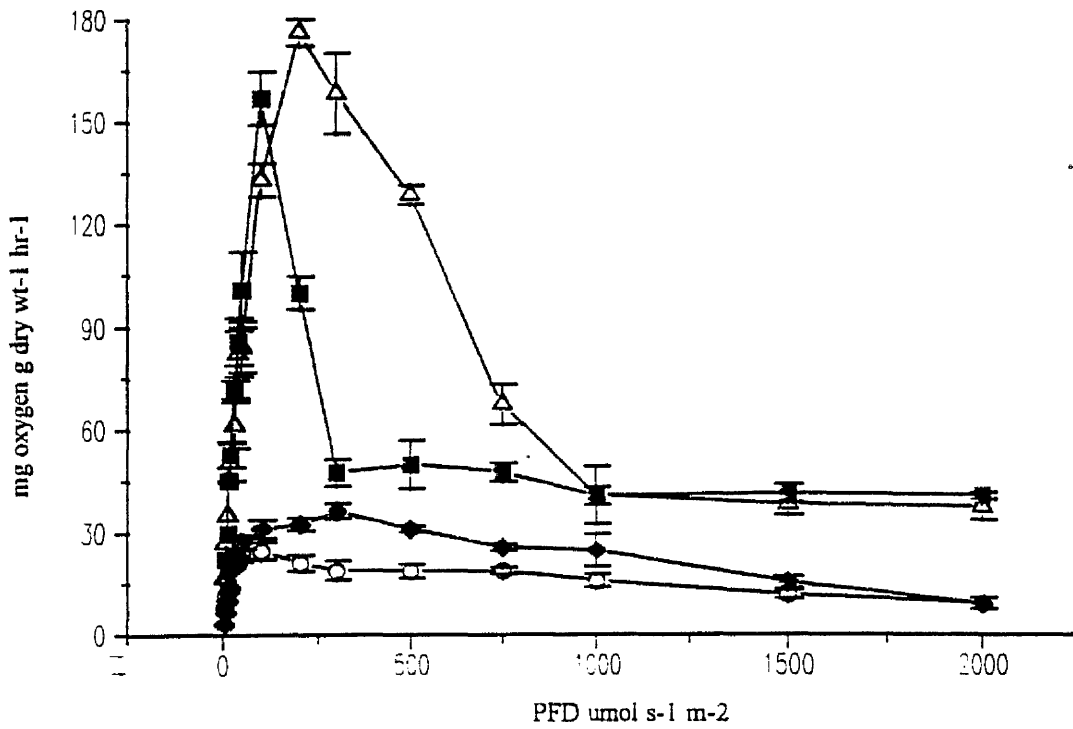


Figure 152. The effect of P/I incubation temperature on the photosynthesis / irradiance response curves of *Synechococcus sp.* cultured at 30°C, ○—○ 15°C, ◆—◆ 23°C, ■—■ 30°C, Δ—Δ 35°C.

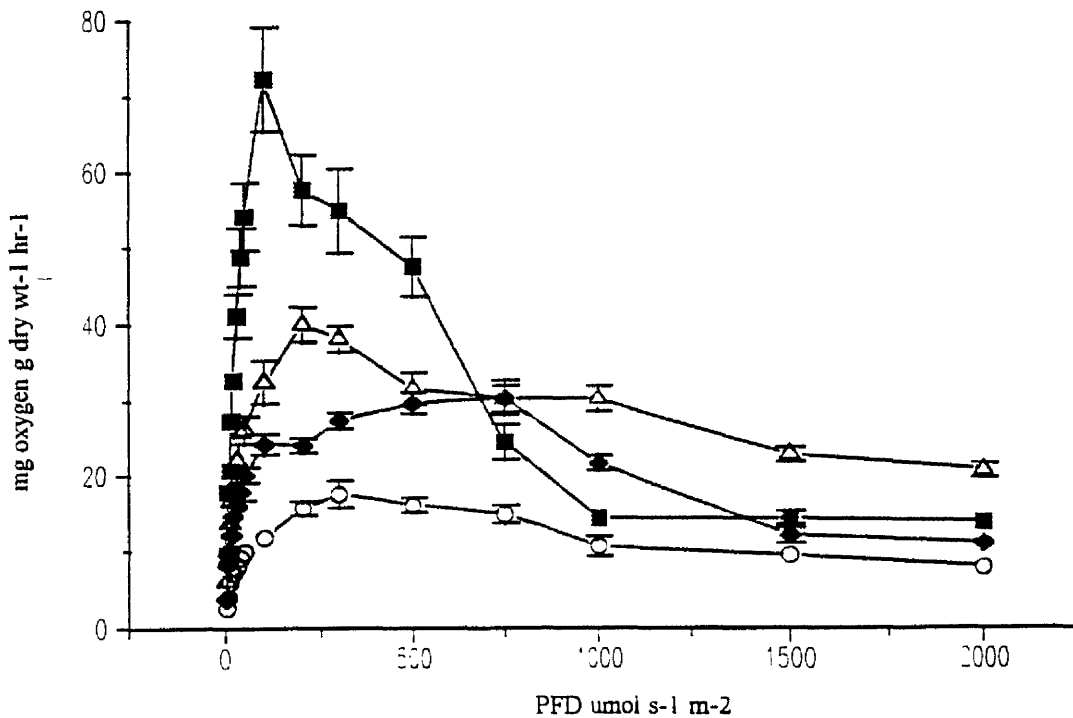


Figure 153. The effect of P/I incubation temperature on the photosynthesis / irradiance response curves of *Synechococcus sp.* cultured at 35°C, ○—○ 15°C, ◆—◆ 23°C, ■—■ 30°C, Δ—Δ 35°C.

temperatures of 15 and 23°C the relationship was determined to be exponential and logarithmic respectively. The photosynthetic parameters of Figures 150, 151, 152 and 153 are presented in Tables 53, 54, 55 and 56 respectively. At culture temperatures of 15, 23 and 30°C, beta was found to increase with increasing P/I incubation temperature from 15 to 30°C. It was determined from Tables 53, 54, 55 and 56 that as P_{max} increased the value of alpha also observed to increase. The value of alpha generally increased with an increase in P/I incubation temperature. As the value of I_k was inversely proportional to the light limited slope, the PFD prior to the onset of light saturation was found to change very little at the culture temperatures of 23, 30 and 35°C (Figures 151, 152 and 153). At the culture temperature of 15°C (Table 53), however, I_k increased with increasing P/I incubation temperature.

Figures 154, 155, 156 and 157 show that the respiration rate increased with increasing temperature (as was observed with all previous micro-algae and cyanobacteria). However from the high temperature cultures of 30 and 35°C (Figures 156 and 157) very little change in respiration was measured with decreasing temperature.

The following equations were found to relate culture temperature to the respiration rates of cells of *Synechococcus sp.*

15°C

$$R_{initial}^{15} = 2.28 \times 10^{-2} \times T^{1.932} \quad (\text{Sig } P=0.01) \quad (104)$$

23°C

$$R_{initial}^{23} = 1.48 \times 10^{-2} \times T^{2.34} \quad (\text{Sig } P=0.001) \quad (105)$$

30°C

$$R_{initial}^{30} = 0.429 \times e^{0.124 \times T} \quad (\text{Sig } P=0.001) \quad (106)$$

35°C

$$R_{initial}^{35} = 0.13 \times T^{1.29} \quad (\text{Sig } P=0.01) \quad (107)$$

Table 53. The effect of temperature on the photosynthetic parameters of *Synechococcus sp.* cultured at 15°C

Culture temperature °C	P/I temperature °C	α (mg oxygen g dry wt ⁻¹ hr ⁻¹ / μ mol s ⁻¹ m ⁻²)	I_k (μ mol s ⁻¹ m ⁻²)	β (mg oxygen g dry wt ⁻¹ hr ⁻¹ / μ mol s ⁻¹ m ⁻²)	P_{max}^{PFD} (μ mol s ⁻¹ m ⁻²)	P_{max} (mg oxygen g dry wt ⁻¹ hr ⁻¹)
15	15	0.32	73.3	no data	200	23.5
15	23	1.2	54.6	-0.031	300	65.5
15	30	1.8	106.1	-0.189	300	191.1
15	35	0.9	164.7	-1.400	200	148.2

Table 54. The effect of temperature on the photosynthetic parameters of *Synechococcus sp.* cultured at 23°C

Culture temperature °C	P/I temperature °C	α (mg oxygen g dry wt ⁻¹ hr ⁻¹ / μ mol s ⁻¹ m ⁻²)	I_k (μ mol s ⁻¹ m ⁻²)	β (mg oxygen g dry wt ⁻¹ hr ⁻¹ / μ mol s ⁻¹ m ⁻²)	P_{max}^{PFD} (μ mol s ⁻¹ m ⁻²)	P_{max} (mg oxygen g dry wt ⁻¹ hr ⁻¹)
23	15	0.31	33.4	no data	300	10.4
23	23	1.16	77.0	no data	300	89.4
23	30	1.31	69.2	no data	300	90.7
23	35	1.67	66.6	-0.029	300	111.2

Table 55. The effect of temperature on the photosynthetic parameters of *Synechococcus sp.* cultured at 30°C

Culture temperature °C	P/I temperature °C	α (mg oxygen g dry wt ⁻¹ hr ⁻¹ / μ mol s ⁻¹ m ⁻²)	I_k (μ mol s ⁻¹ m ⁻²)	β (mg oxygen g dry wt ⁻¹ hr ⁻¹ / μ mol s ⁻¹ m ⁻²)	P_{max}^{PFD} (μ mol s ⁻¹ m ⁻²)	P_{max} (mg oxygen g dry wt ⁻¹ hr ⁻¹)
30	15	0.83	29.8	-0.023	300	24.79
30	23	0.89	40.7	-0.029	200	36.3
30	30	2.37	66.1	-0.546	100	156.81
30	35	2.54	69.3	-0.157	100	176.11

Table 56. The effect of temperature on the photosynthetic parameters of *Synechococcus sp.* cultured at 35°C

Culture temperature °C	P/I temperature °C	α (mg oxygen g dry wt ⁻¹ hr ⁻¹ / μ mol s ⁻¹ m ⁻²)	I_k (μ mol s ⁻¹ m ⁻²)	β (mg oxygen g dry wt ⁻¹ hr ⁻¹ / μ mol s ⁻¹ m ⁻²)	P_{max}^{PFD} (μ mol s ⁻¹ m ⁻²)	P_{max} (mg oxygen g dry wt ⁻¹ hr ⁻¹)
35	15	0.44	39.7	-0.005	300	17.5
35	23	0.66	46.1	-0.013	200	30.4
35	30	1.4	51.6	-0.056	200	72.2
35	35	0.87	45.9	-0.028	100	40.1

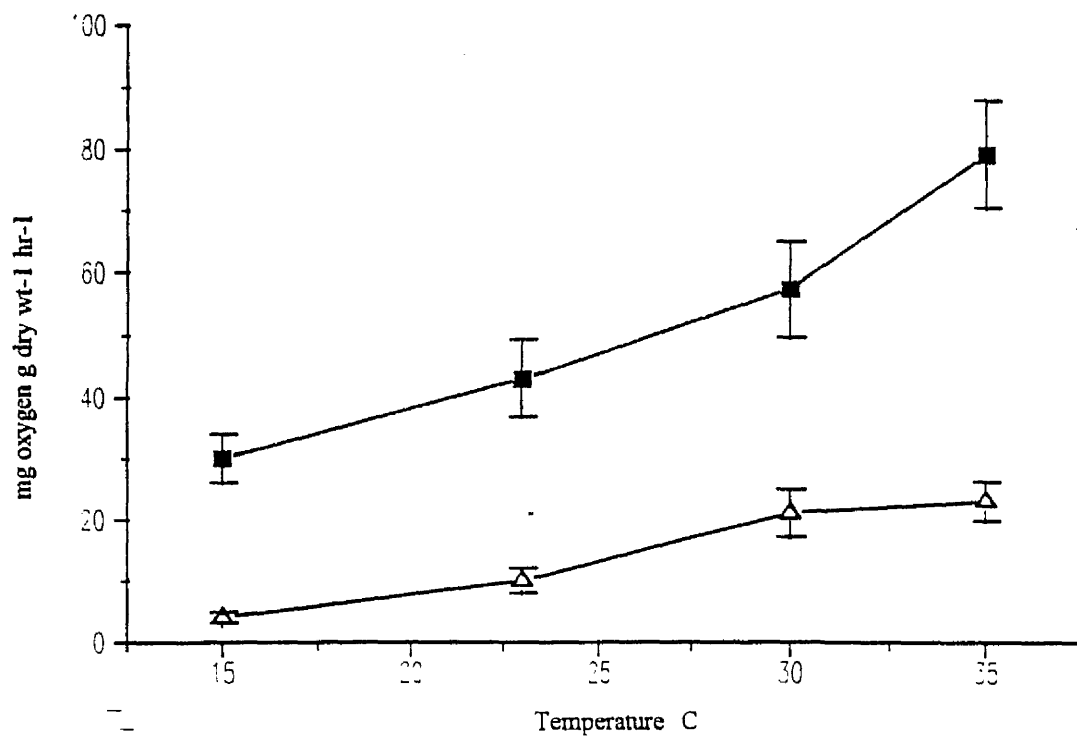


Figure 154. The effect of P/I incubation temperature on the dark respiration Δ — Δ and light enhanced dark respiration \blacksquare — \blacksquare of *Synechococcus* sp. cultured at 15°C.

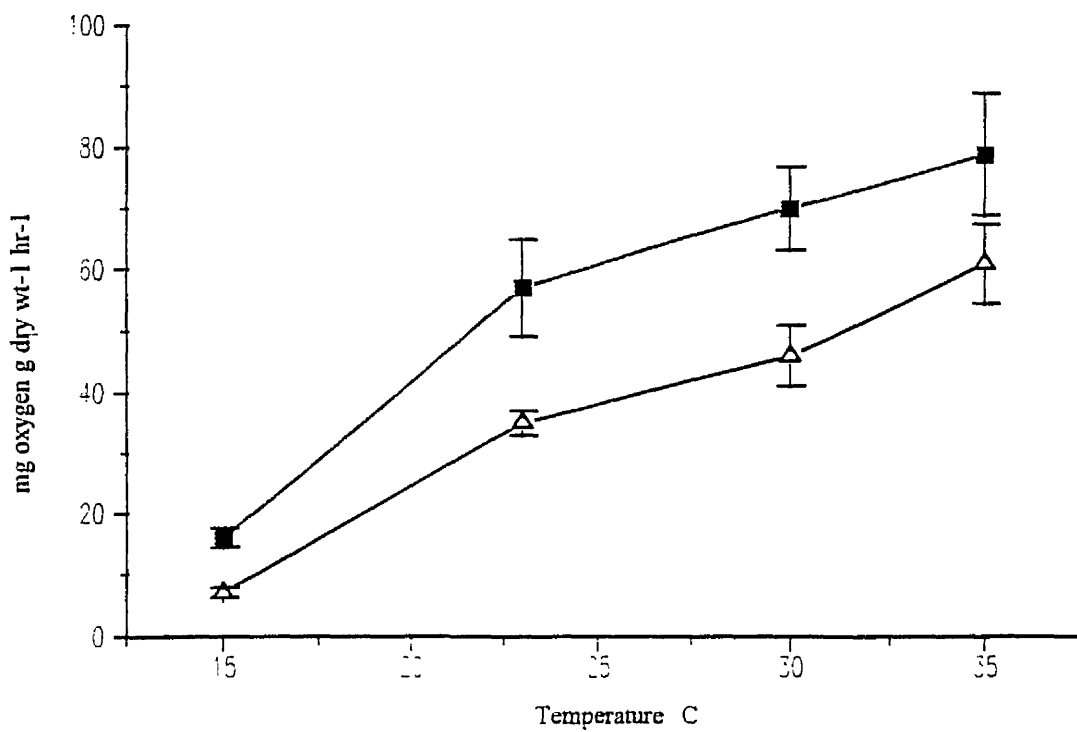


Figure 155. The effect of P/I incubation temperature on the dark respiration Δ — Δ and light enhanced dark respiration \blacksquare — \blacksquare of *Synechococcus* sp. cultured at 23°C.

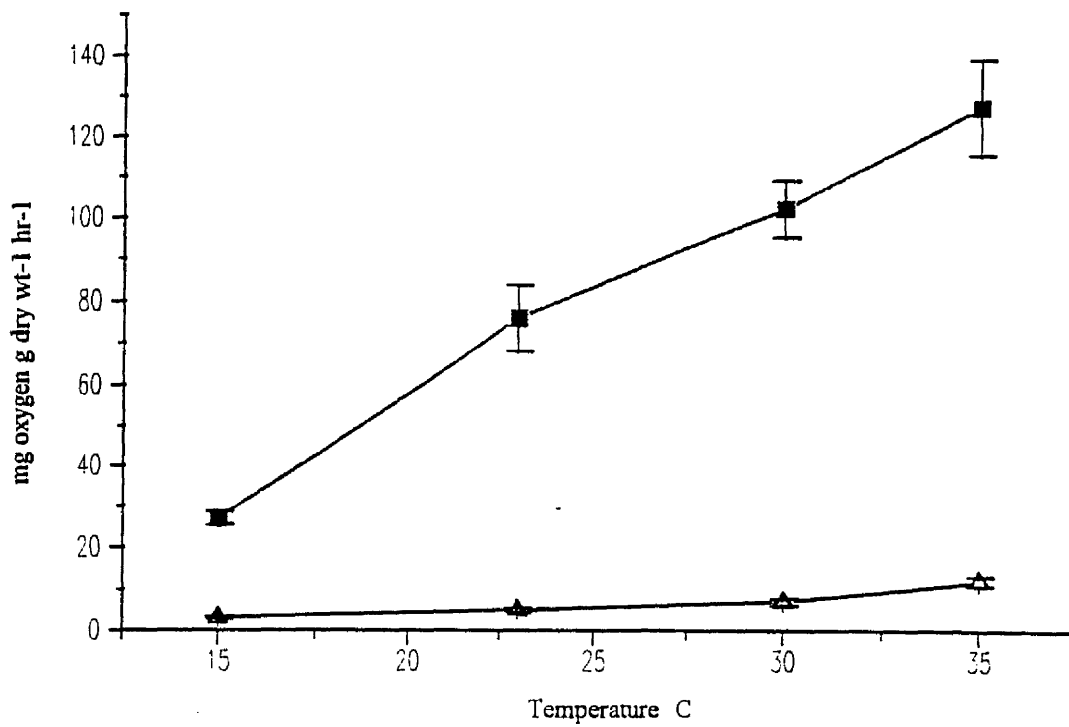


Figure 156. The effect of P/I incubation temperature on the dark respiration Δ — Δ and light enhanced dark respiration \blacksquare — \blacksquare of *Synechococcus sp.* cultured at 30°C.

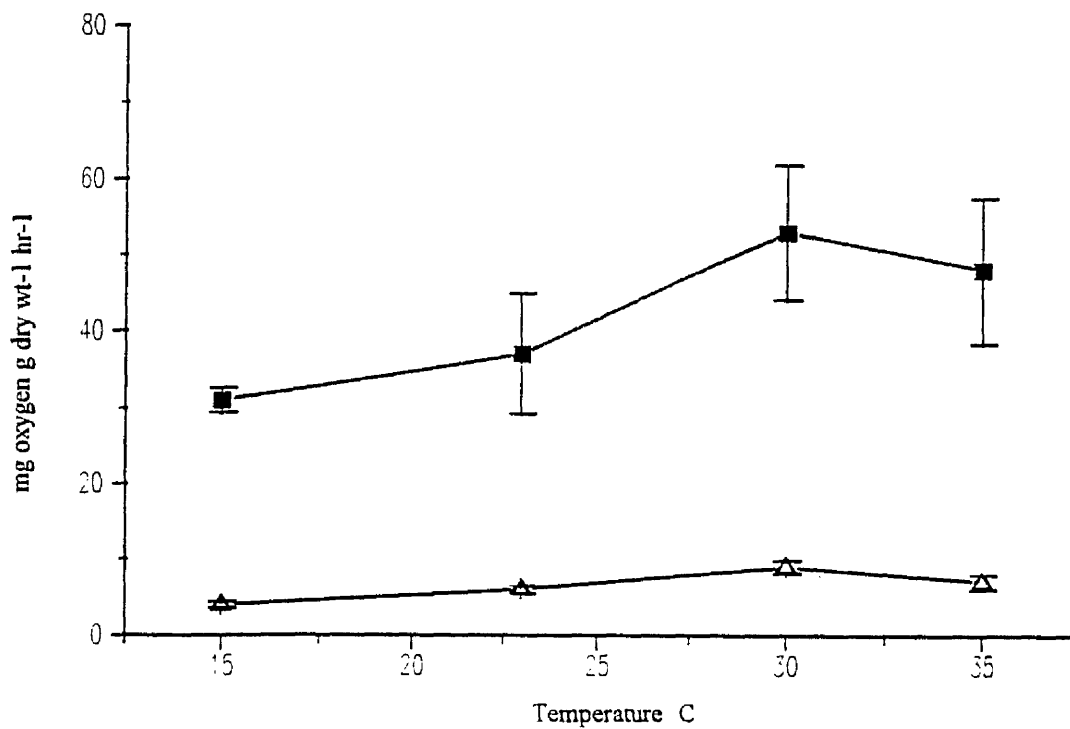


Figure 157. The effect of P/I incubation temperature on the dark respiration Δ — Δ and light enhanced dark respiration \blacksquare — \blacksquare of *Synechococcus sp.* cultured at 35°C.

From equations 104, 105 and 107 (culture temperatures 15, 23 and 35°C respectively) it was found that the cellular respiration was related to temperature by a power fit. At the culture temperature of 30°C, however relationship was best described by exponential curve fit..

The following equations relate the LEDR rate of cells of *Synechococcus sp.* to temperature.

15°C

$$LEDR_{final}^{15} = 14.622 \times e^{4.67 \times 10^{-2} \times T} \quad (\text{Sig P}=0.001) \quad (108)$$

23°C

$$LEDR_{final}^{23} = 7.22 \times 10^{-2} \times T^{2.005} \quad (\text{Sig P}=0.001) \quad (109)$$

30°C

$$LEDR_{final}^{30} = 0.1897 \times T^{1.78} \quad (\text{Sig P}=0.01) \quad (110)$$

35°C

$$LEDR_{final}^{35} = \frac{1}{5.15 \times 10^{-2} + (-9.13 \times 10^{-4} \times T)} \quad (\text{Sig P}=0.05) \quad (111)$$

The cells cultured at 23 and 30°C had a power fit relationship between LEDR and temperature (equations 109 and 110). However the lower culture temperature of 15°C was found to be an exponential fit. Although the hyperbolic function of equation 72 was significant, the unusual points measured at 15 and 30°C (Figure 157) reduced the level at the P=0.05. Cells cultured at 15°C were found to have an exponential relationship between LEDR and temperature (equation 108)

Equations 112 to 114 show the relationship between alpha and P/I incubation temperature.

$$\alpha_{15} = 8.72 + (-1.35 \times T) + (0.068 \times T^2) + (-1.02 \times 10^{-3} \times T^3) \quad \text{Sig P=0.01} \quad (112)$$

$$\alpha_{23} = 1.865 \times 10^{-3} \times T^{1.94} \quad \text{Sig P=0.001} \quad (113)$$

$$\alpha_{30} = 1.049 + (-7.15 \times 10^{-2} \times T) + (3.4 \times 10^{-3} \times T^2) \quad \text{Sig P=0.01} \quad (114)$$

The relationship between alpha and P/I incubation temperature for cells of *Synechococcus sp.* cultured at 15 and 30°C was best described by a polynomial regression fit, whereas cells cultured at 23°C were best described by a power fit. No significant relationship between alpha and P/I incubation temperature was calculated for cells cultured at 35°C.

Figures 158, 159, 160 and 161 show the arhenius plots for *Synechococcus sp.* of the natural logarithm of photosynthetic rates (mg oxygen g dry wt⁻¹ hr⁻¹), measured at a PFD of 100 μmol s⁻¹ m⁻² against the reciprocal of P/I incubation temperature (Kelvin) for culture temperatures of 15, 23, 30 and 35°C respectively. Similar to that of *Synechococcus* 1479/5, cells of *Synechococcus sp.* cultured at 15 and 35°C showed decreases in the rates of oxygen evolution when measured at a P/I incubation temperature of 35°C.

Equations 115 and 116 describe the combined relationship between alpha and P/I incubation temperature for *Chlorella vulgaris* 211/11c, *Nannochloris atomus*, *Scenedesmus sp.* and *Ankistrodesmus antarcticus* cultured at 15 and 23°C respectively.

$$\alpha_{15} = -1.078 + (0.243 \times T) + (-1.202 \times 10^{-2} \times T^2) + (2.53 \times 10^{-4} \times T^3) \quad \text{(Sig P=0.01)} \quad (115)$$

$$\alpha_{23} = 3.003 \times 10^{-3} \times T^{1.88} \quad \text{(Sig P=0.01)} \quad (116)$$

Where α is the light limited slope of the photosynthesis / irradiance response curves

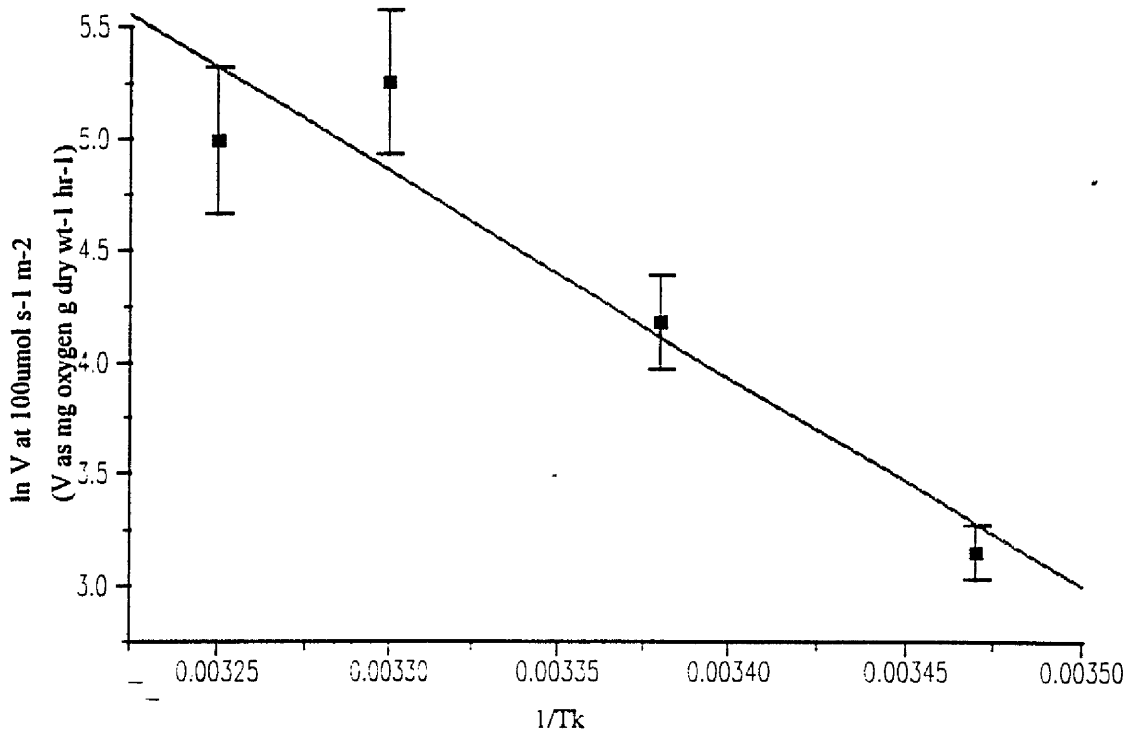


Figure 158. Arrhenius plot of ln photosynthetic rate at a PFD of $100\mu\text{mol s}^{-1} \text{m}^{-2}$ against increasing P/I incubation temperature for *Synechococcus sp.* cultured at a temperature of 15°C.

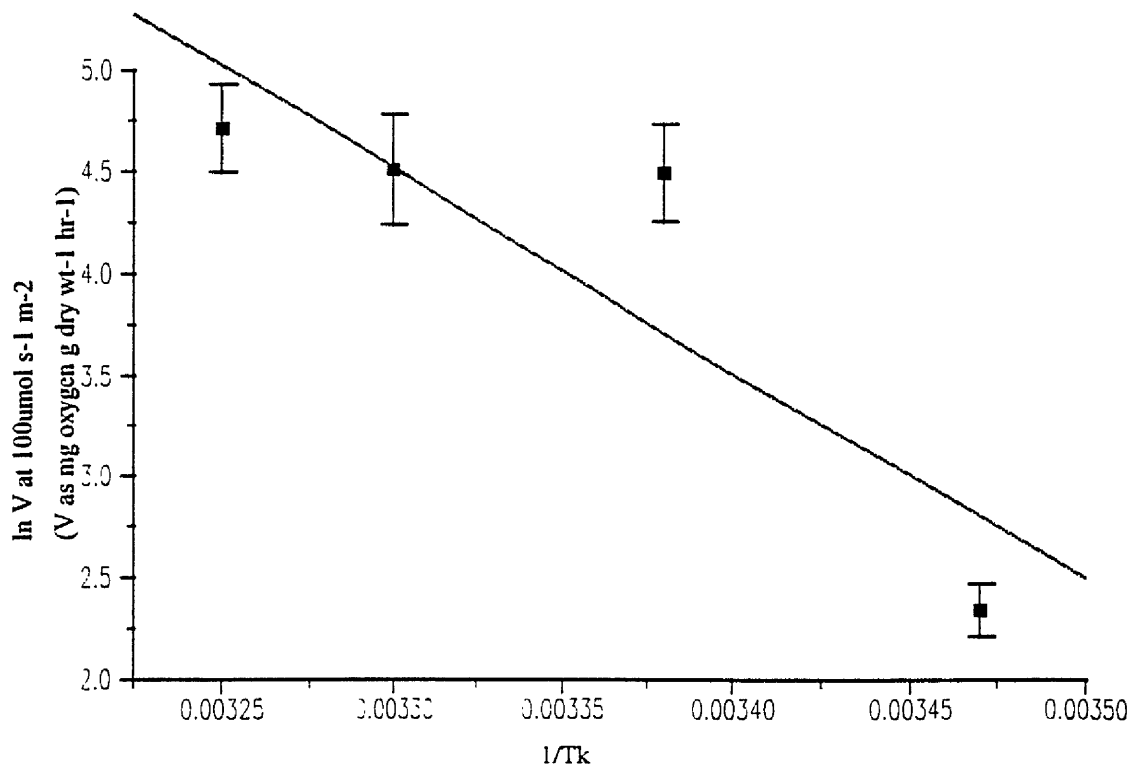


Figure 159. Arrhenius plot of ln photosynthetic rate at a PFD of $100\mu\text{mol s}^{-1} \text{m}^{-2}$ against increasing P/I incubation temperature for *Synechococcus sp.* cultured at a temperature of 23°C.

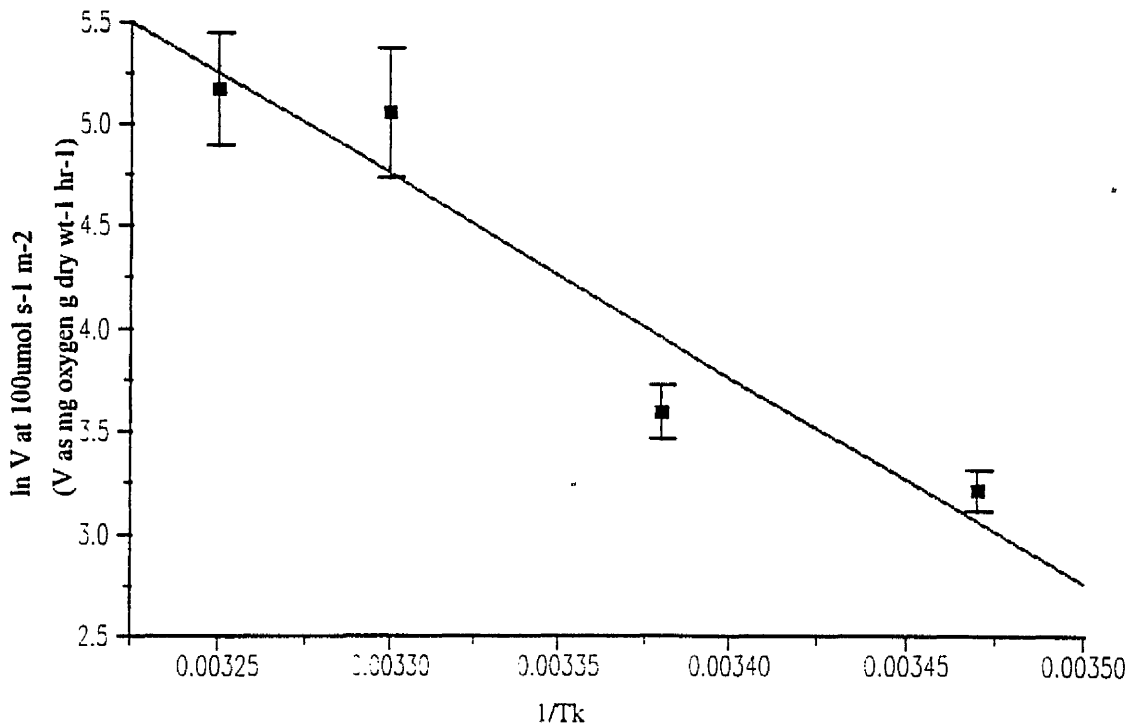


Figure 160. Arrhenius plot of ln photosynthetic rate at a PFD of $100\mu\text{mol s}^{-1} \text{m}^{-2}$ against increasing P/I incubation temperature for *Synechococcus sp.* cultured at a temperature of 30°C .

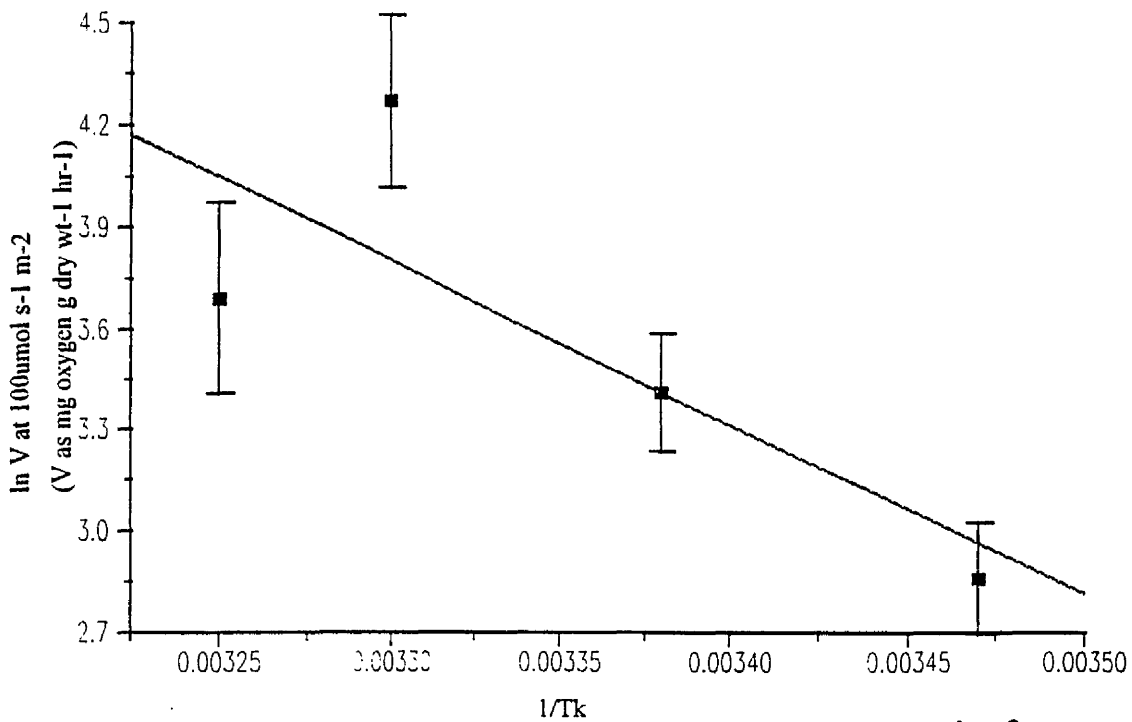


Figure 161. Arrhenius plot of ln photosynthetic rate at a PFD of $100\mu\text{mol s}^{-1} \text{m}^{-2}$ against increasing P/I incubation temperature for *Synechococcus sp.* cultured at a temperature of 35°C .

measured in (mg oxygen g dry wt⁻¹ hr⁻¹ / $\mu\text{mol s}^{-1} \text{m}^{-2}$).

The variation in the maximum rate of photosynthesis / dark respiration rate ratio of *Chlorella vulgaris* 211/11c, *Nannochloris atomus*, *Scenedesmus sp.*, *Ankistrodesmus antarcticus*, *Synechococcus* 1479/5 and *Synechococcus sp.* is presented Tables 57, 58, 59, 60, 61, 62 and 63 respectively.

Table 57 shows the $P_{\text{max}} : \text{DR}$ ratio for cells of *Chlorella vulgaris* 211/11c. It can be seen that the dark respiration rate was approximately 20 to 50% that of P_{max} for all culture temperatures and P/I incubation temperatures. The maximum $P_{\text{max}} : \text{DR}$ ratio of 5.91 was measured from cells cultured at a 35°C and P/I incubated at 35°C. The lowest $P_{\text{max}} : \text{DR}$ ratio of 2.02 was observed at a culture temperature of 23°C and a P/I incubation temperature of 15°C.

The $P_{\text{max}} : \text{DR}$ ratio from cells of *Nannochloris atomus* are presented in Table 58. The maximum $P_{\text{max}} : \text{DR}$ ratio of 7.08 was measured from cells cultured at 30°C and P/I incubated at 23°C. The minimum $P_{\text{max}} : \text{DR}$ ratio of 1.56 was observed at a culture temperature of 15°C and a P/I incubation temperature of 35°C.

Table 59 shows the variation in the ratios of $P_{\text{max}} : \text{DR}$ of *Scenedesmus sp.* The maximum $P_{\text{max}} : \text{DR}$ ratio of 13.36 was measured at a culture temperature of 15°C and a P/I incubation temperature of 30°C. The minimum $P_{\text{max}} : \text{DR}$ ratio of 2.45 was measured at a culture temperature of 23°C and a P/I incubation temperature of 30°C. The $P_{\text{max}} : \text{DR}$ ratio from cells cultured at 35°C increased (4.17-6.94) with increasing P/I incubation temperature (15-35°C).

The $P_{\text{max}} : \text{DR}$ ratio from cells of *Ankistrodesmus antarcticus* are presented in Table 60. The maximum $P_{\text{max}} : \text{DR}$ ratio of 7.14 was measured from cells cultured at temperature of 15°C and P/I incubated at 23°C. The minimum $P_{\text{max}} : \text{DR}$ ratio of 1.63 was measured from cells cultured at 30°C and P/I incubated at 35°C.

Table 61 presents the $P_{\text{max}} : \text{DR}$ ratio of *Synechococcus* 1479/5. The maximum $P_{\text{max}} : \text{DR}$ ratio of 15.75 was measured from cells cultured at 30°C and P/I incubated at 35°C. The minimum $P_{\text{max}} : \text{DR}$ ratio of 2.03 was measured from cells cultured at 23°C and P/I incubated at 15°C. Cells of *Synechococcus* 1479/5 cultured at a temperature

Table 57. Maximum rate of photosynthesis / dark respiration rate ratio of *Chlorella vulgaris* 211/11c.

Culture temp °C	Incubation temp °C			
	15	23	30	35
15	2.49	4.84	2.98	4.8
23	2.02	4.9	2.95	2.62
30	2.83	3.47	5.48	2.50
35	4.48	3.45	4.67	5.91

Table 58. Maximum rate of photosynthesis / dark respiration rate ratio of *Nannochloris atomus*.

Culture temp °C	Incubation temp °C			
	15	23	30	35
15	3.69	3.10	2.30	1.52
23	2.19	2.48	1.98	2.1
30	4.41	7.08	3.10	1.56
35	4.40	4.47	4.9	5.33

Table 59. Maximum rate of photosynthesis / dark respiration rate ratio of *Scenedesmus sp.*

Culture temp °C	Incubation temp °C			
	15	23	30	35
15	7.62	8.9	13.36	12.88
23	3.93	6.11	2.45	2.58
30	5.95	6.76	3.58	7.11
35	4.17	5.74	5.84	6.94

Table 60. Maximum rate of photosynthesis / dark respiration rate ratio of *Ankistrodesmus antarcticus*.

Culture temp °C	Incubation temp °C			
	15	23	30	35
15	5.58	7.14	4.53	5.97
23	2.73	4.81	2.36	2.33
30	4.10	5.74	3.58	1.63
35	3.02	3.44	5.03	4.75

Table 61. Maximum rate of photosynthesis / dark respiration rate ratio of *Synechococcus* 1479/5.

Culture temp °C	Incubation temp °C			
	15	23	30	35
15	3.10	5.89	9.36	6.30
23	2.03	3.10	2.10	2.97
30	5.16	12.47	9.84	15.75
35	5.48	5.93	14.32	14.58

Table 62. Maximum rate of photosynthesis / dark respiration rate ratio of *Synechococcus* sp.

Culture temp °C	Incubation temp °C			
	15	23	30	35
15	5.11	6.82	9.55	8.71
23	1.48	2.55	2.59	2.02
30	8.26	6.05	7.4	6.78
35	4.37	5.06	5.15	4.48

of 35°C displayed increasing P_{\max} : DR ratios (5.48-14.58) with increasing P/I incubation temperature (15-35°C).

The P_{\max} : DR ratios of *Synechococcus sp.* are presented in Table 62. The maximum P_{\max} : DR ratio of 9.55 was measured from cells cultured at 15°C and P/I incubated at 35°C. The minimum P_{\max} : DR ratio of 1.48 was determined from cells cultured at a temperature of 23°C and P/I incubated at 15°C.

The LEDR / DR ratios of *Chlorella vulgaris* 211/11c, *Nannochloris atomus*, *Scenedesmus sp.*, *Ankistrodesmus antarcticus*, *Synechococcus* 1479/5 and *Synechococcus sp.* are shown in Tables 63, 64, 65, 66, 67 and 68 respectively.

The results of the measured LEDR / DR ratios of cells of *Chlorella vulgaris* 211/11c are presented in Table 63. It can be seen that the overall LEDR / DR ratio was found to be approximately 3. The highest LEDR / DR ratio (5.46) was determined from the 30°C culture incubated at 30°C.

Table 64 displays the variation in LEDR / DR ratio of cells of *Nannochloris atomus* with changing temperature. It can be seen that the LEDR / DR ratio was very low at the lower culture temperatures. Increasing the culture temperature to 30 and 35°C generally increased the LEDR / DR ratio to 3-4.5.

Table 65 displays the LEDR / DR ratios of cells of *Scenedesmus sp.* The LEDR / DR ratios on the whole were very high compared to the other unicellular green micro-algae *Chlorella vulgaris* 211/11c, *Ankistrodesmus antarcticus* and *Nannochloris atomus*. Cells of *Scenedesmus sp.* displayed the highest LEDR / DR ratio of 10.53. Similar to the other micro-algae, it was found that the highest LEDR / DR ratios occurred from cells which had been cultured at 15, 23, 30 and 35°C and then subsequently incubated at a temperature of 15°C.

Table 66 displays the changes in the ratio of LEDR / DR at the different culture and incubation temperatures of cells of *Ankistrodesmus antarcticus*. It can be seen that the ratio of LEDR / DR was generally of the order of 2:1 (with minor exceptions at the higher culture temperature of 30 and 35°C). It was found that the LEDR / DR ratio was particularly high (6.25) during the 30°C culture experiments where cells were

incubated at the lower temperature of 15°C. The ratio of LEDR / DR for cultures at 30°C decreased from 6.25 to 1.63 with increasing P/I incubation temperatures of 15 to 35°C.

Table 67 displays the LEDR / DR ratios obtained from cells of *Synechococcus* 1479/5. Unusually (compared to the cells of the other micro-algae and cyanobacteria) the cells of *Synechococcus* 1479/5 exhibited higher LEDR / DR ratios at the higher incubation temperatures of 30 and 35°C. The highest LEDR / DR ratio of 9.61 was measured from cells cultured and incubated at 35°C.

Table 68 displays the LEDR / DR ratios measured from cells of *Synechococcus* sp. It can be seen that the LEDR / DR ratios were of a much higher order (4-9). It was found that the very high LEDR / DR ratios occurred in cells that had been cultured at that had been cultured at 15, 23, 30 and 35°C and then incubated at 15°C. These incubations gave rise to LEDR / DR ratios of 7.34 (15:15), 1.83 (23:15), 9.97 (30:15) and 7.22 (35:15).

Figures 162 to 167 show the variation with temperature in the calculated Q_{10} values of *Chlorella vulgaris* 211/11c, *Nannochloris atomus*, *Scenedesmus* sp., *Ankistrodesmus antarcticus*, *Synechococcus* 1479/5 and *Synechococcus* sp. respectively. These were calculated on the photosynthetic rates measured at a PFD of $200\mu\text{mol s}^{-1} \text{m}^{-2}$.

Figure 162 shows that the Q_{10} for cells of *Chlorella vulgaris* 211/11c, decreased with increasing culture temperature from 4.05 at 15°C to 1.86 at 35°C. The cell optimum at which a change in temperature produced a large degree of change in photosynthesis lay between 15 and 23°C.

In contrast to that of *Chlorella vulgaris* 211/11c (Figure 162), *Nannochloris atomus* (Figure 163) showed an increase in Q_{10} (2.34 to 2.94) upon increasing the culture temperature from 15 to 23°C. Increasing the culture temperature above 23°C resulted in a fall in Q_{10} to a value of 1.49 at a temperature of 35°C.

Scenedesmus sp. showed a slight increase in the value of Q_{10} (Figure 164) from 3.12 to 3.15 upon increasing the culture temperature from 15 to 23°C. Increasing the

Table 63: The effect of temperature on the LEDR / DR ratio of *Chlorella vulgaris* 211/11c.

Culture temperature °C	Photosynthesis irradiance temperature °C	Ratio LEDR / DR
15	15	1.25
15	23	3.09
15	30	1.81
15	35	2.89
23	15	2.5
23	23	4.59
23	30	2.06
23	35	1.78
30	15	2.3
30	23	2.78
30	30	5.46
30	35	1.75
35	15	4.34
35	23	3.35
35	30	2.89
35	35	3.64

Table 64: The effect of temperature on the LEDR / DR ratio of *Nannochloris atomus*.

Culture temperature °C	Photosynthesis irradiance temperature °C	Ratio LEDR / DR
15	15	3.57
15	23	2
15	30	1.61
15	35	1.29
23	15	1.68
23	23	1.9
23	30	1.72
23	35	1.47
30	15	4.64
30	23	3.91
30	30	3.13
30	35	1.42
35	15	2.28
35	23	2.31
35	30	3.59
35	35	4.37

Table 65: The effect of temperature on the LEDR / DR ratio of *Scenedesmus sp.*

Culture temperature °C	Photosynthesis irradiance temperature °C	Ratio LEDR / DR
15	15	6.28
15	23	2.89
15	30	2.22
15	35	2.9
23	15	2.79
23	23	4.21
23	30	2.22
23	35	1.34
30	15	10.53
30	23	4.55
30	30	2.16
30	35	3.42
35	15	4.13
35	23	4.5
35	30	3.74
35	35	2.97

Table 66: The effect of temperature on the LEDR / DR ratio of *Ankistrodesmus antarcticus*

Culture temperature °C	Photosynthesis irradiance temperature °C	Ratio LEDR / DR
15	15	2.08
15	23	2.96
15	30	1.99
15	35	2.71
23	15	2.02
23	23	2.81
23	30	1.39
23	35	1.21
30	15	6.25
30	23	4.88
30	30	2.32
30	35	1.63
35	15	4.3
35	23	2.87
35	30	2.99
35	35	4.45

Table 67: The effect of temperature on the LEDR / DR ratio of *Synechococcus* 1479/5.

Culture temperature °C	Photosynthesis irradiance temperature °C	Ratio LEDR / DR
15	15	1.85
15	23	2.61
15	30	2.88
15	35	2.83
23	15	2.5
23	23	2.42
23	30	1.6
23	35	1.37
30	15	5.66
30	23	9.21
30	30	3.99
30	35	6.11
35	15	4.19
35	23	3.15
35	30	6.47
35	35	9.61

Table 68: The effect of temperature on the LEDR / DR ratio of *Synechococcus* sp.

Culture temperature °C	Photosynthesis irradiance temperature °C	Ratio LEDR / DR
15	15	7.34
15	23	3.97
15	30	2.66
15	35	4.38
23	15	1.83
23	23	1.8
23	30	1.65
23	35	1.34
30	15	9.97
30	23	4.79
30	30	4.26
30	35	3.96
35	15	7.22
35	23	3.05
35	30	4.69
35	35	4.37

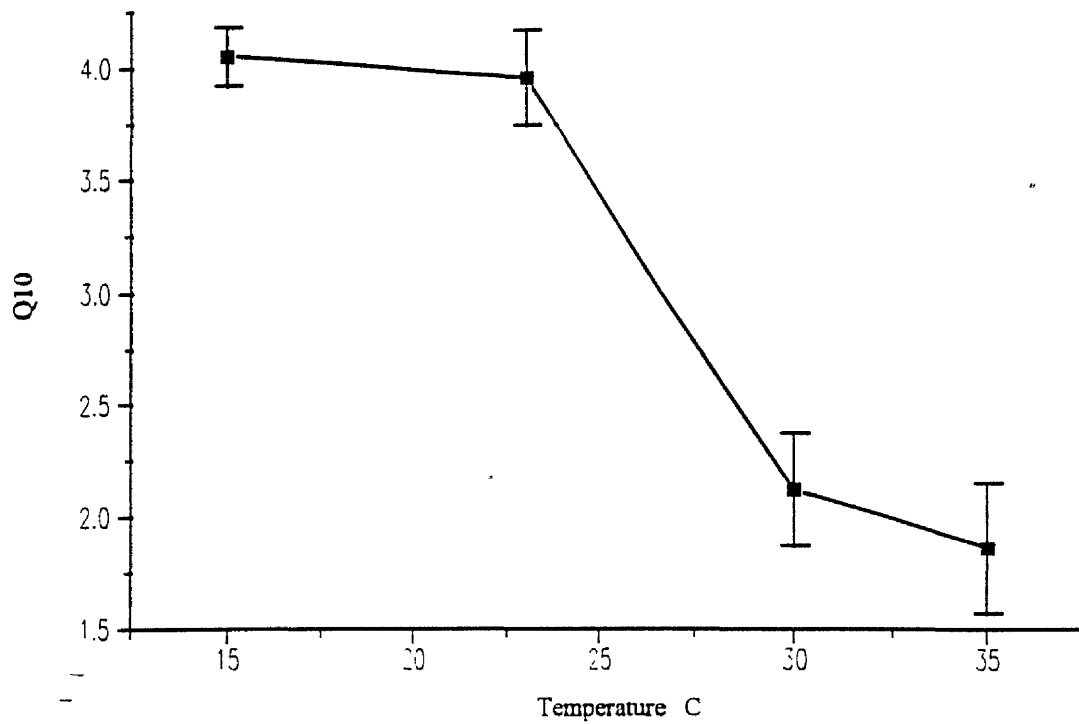


Figure 162. Variation in the Q_{10} values with increasing temperature for *Chlorella vulgaris* 211/11c.

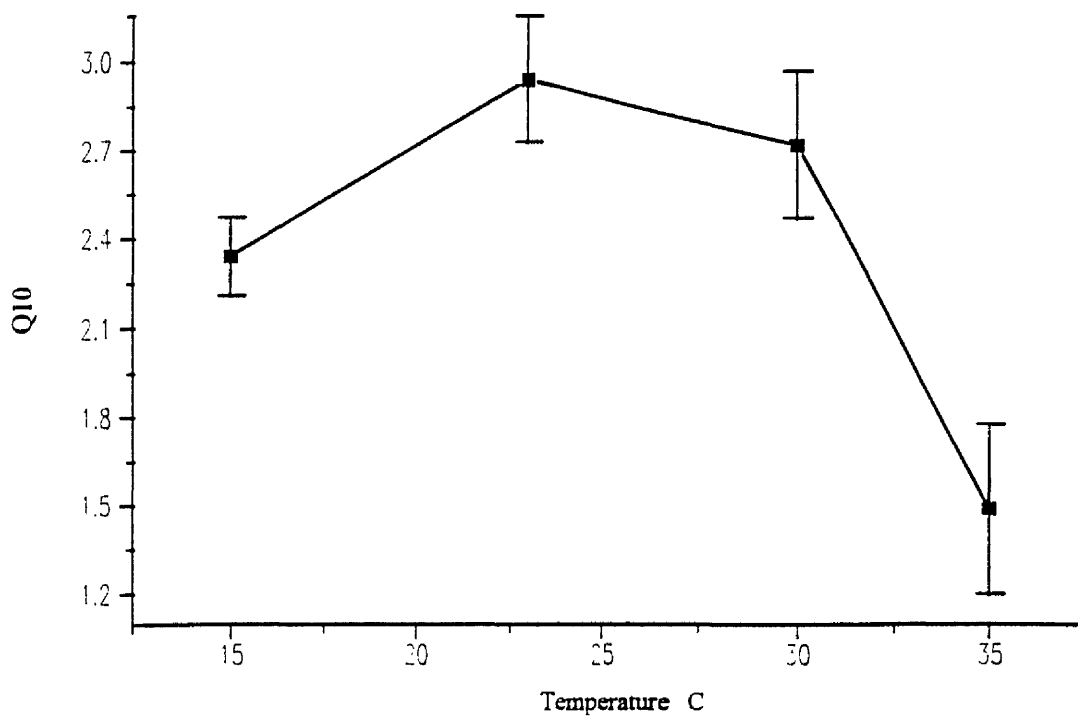


Figure 163. Variation in the Q_{10} values with increasing temperature for *Nannochloris atomus*.

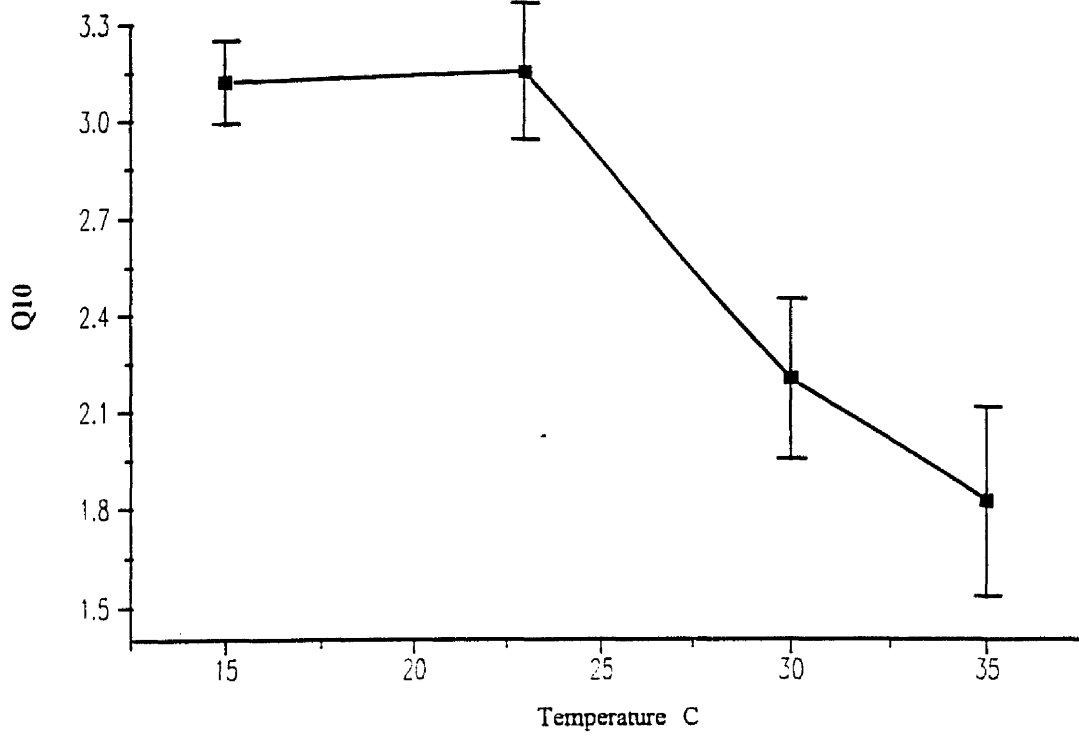


Figure 164. Variation in the Q₁₀ values with increasing temperature for *Scenedesmus sp.*

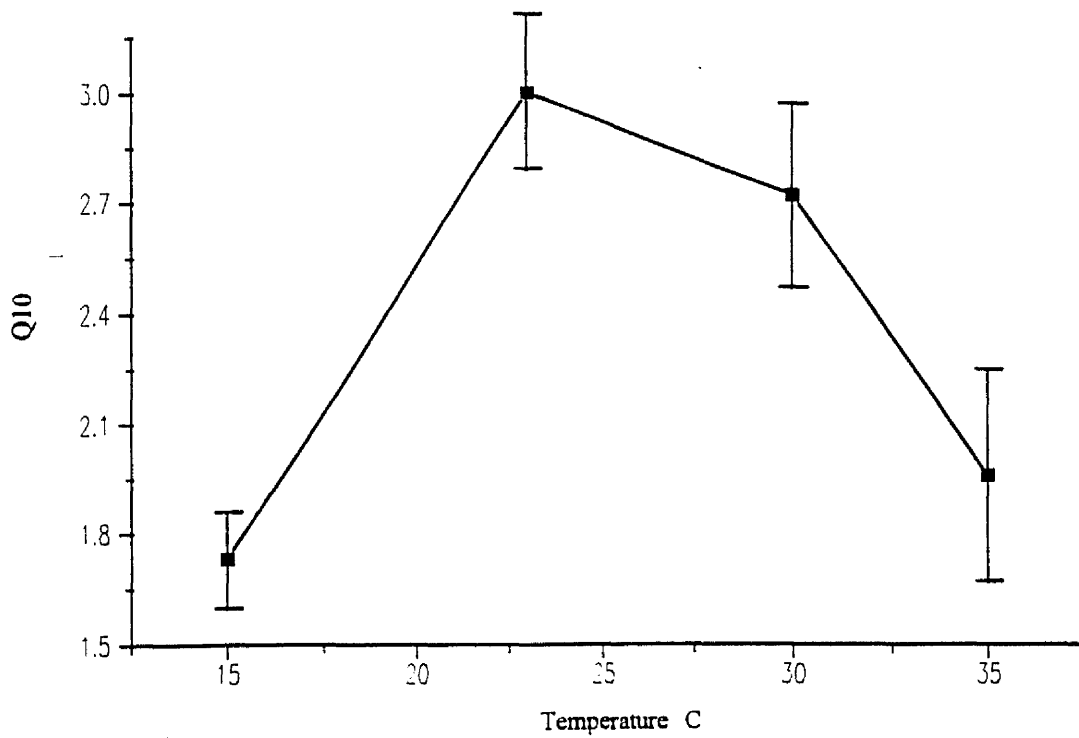


Figure 165. Variation in the Q₁₀ values with increasing temperature for *Ankistrodesmus antarcticus*.

culture temperature above 23°C resulted in a decrease in Q_{10} . At a culture temperature of 35°C the Q_{10} has fallen to 1.82.

Similar to that observed with *Nannochloris atomus*, cells of *Ankistrodesmus antarcticus* (Figure 165) showed an increase in Q_{10} from 1.73 to 3.00 upon increasing the culture temperature from 15 to 23°C. The Q_{10} decreased to 1.96 when the culture temperature was increased to 35°C.

Similar to that observed with both *Nannochloris atomus* and *Ankistrodesmus antarcticus*, *Synechococcus* 1479/5 showed an increase in Q_{10} (Figure 166) with increasing the culture temperature from 15 to 23°C. The Q_{10} decreased when the culture temperature was increased above 23°C.

As was observed with *Synechococcus* 1479/5, cells of *Synechococcus sp.* showed an increase in Q_{10} (Figure 167) upon increasing the culture temperature from 15 to 23°C. Increasing the culture temperature to 35°C resulted in a decrease in Q_{10} to 1.82.

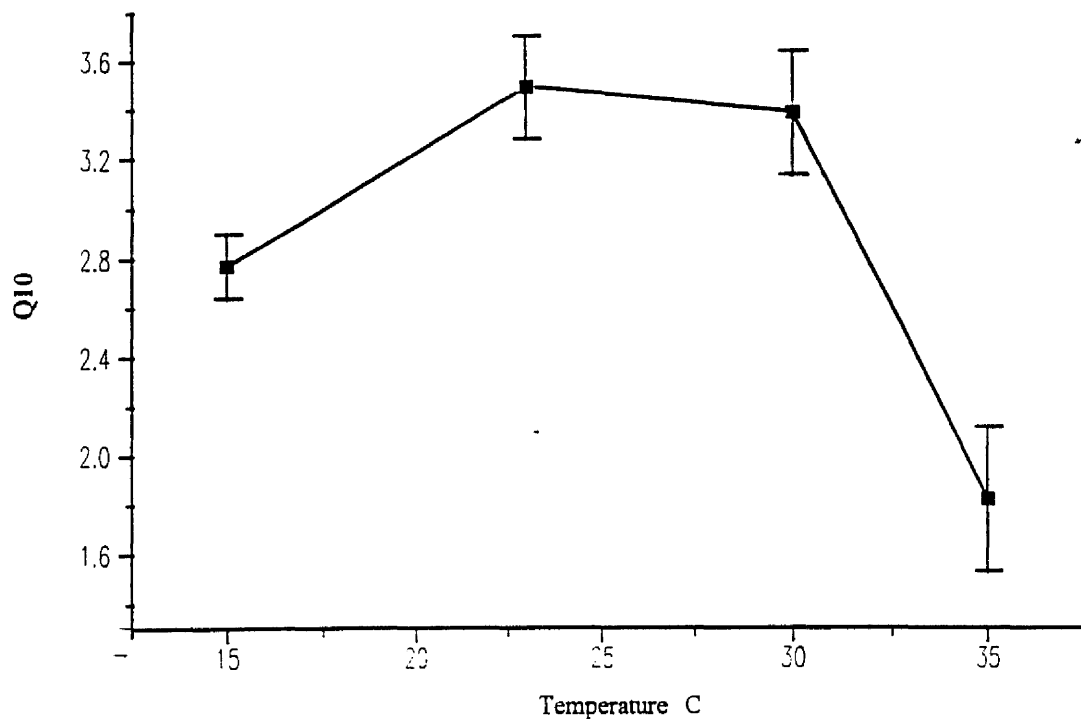


Figure 166. Variation in the Q₁₀ values with increasing temperature for *Synechococcus* 1479/5.

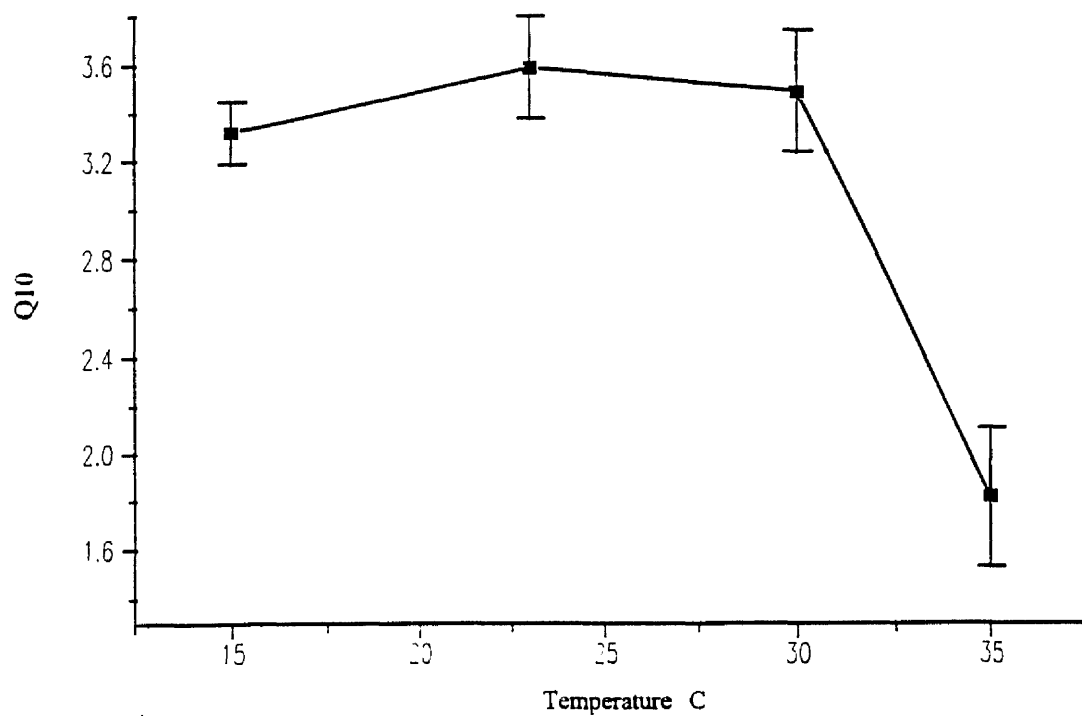


Figure 167. Variation in the Q₁₀ values with increasing temperature for *Synechococcus* sp.

3.4.2 The effect of culture temperature and P/I incubation temperature on the cells of micro-algae and cyanobacteria grown at a PFD of $200\mu\text{mol s}^{-1} \text{ m}^{-2}$.

Cells of *Chlorella vulgaris* 211/11c, *Synechococcus* 1479/5 and *Scenedesmus* sp. were cultured at temperatures of 15, 23, 30 and 35°C at a PFD of $200\mu\text{mol s}^{-1} \text{ m}^{-2}$, using 2 500W Quartz Halogen Lamps to examine the effect of culture temperature and changes in incubation temperature on the photosynthesis, respiration and light enhanced dark respiration rates.

The photosynthesis / irradiance response curves of *Chlorella vulgaris* 211/11c cultured at a temperature of 15°C are shown in Figure 168. Table 69 shows the photosynthetic parameters calculated from Figure 168. It can be seen (Table 69) that the maximum rate of photosynthesis P_{max} increased with increasing incubation temperature. The lowest P_{max} ($48.7\text{mg oxygen g dry wt}^{-1} \text{ hr}^{-1}$) was recorded at a temperature of 15°C (the temperature at which the cells had been cultured). On increasing the temperature to 35°C, the value of P_{max} increased by a factor of 8.25 to $402.7\text{mg oxygen g dry wt}^{-1} \text{ hr}^{-1}$. The value I_k and α generally increased with increasing incubation temperature (15 to 35°C). The initial dark respiration rate (DR) increased with increasing temperature. A 4 fold increase in respiration was measured when cells were incubated at 35°C compared to 15°C. The rate of light enhanced dark respiration increased nearly 10 fold when cells were incubated at 35°C compared to 15°C.

The results of culturing *Chlorella vulgaris* 211/11c at a temperature of 23°C are shown in Figure 169 and the effect on photosynthetic parameters is shown in Table 70. Similar to cells cultured at 15°C, cells culture at 23°C showed an increase in P_{max} with increasing incubation temperature. The maximum value for P_{max} of $225.34 \text{ mg oxygen g dry wt}^{-1} \text{ hr}^{-1}$ was recorded at a temperature of 35°C. This was nearly half that measured of cells cultured at 15°C whilst incubated at 35°C. The values of I_k , α , DR, and LEDR all increased with increasing incubation temperature.

The results of culturing *Chlorella vulgaris* 211/11c cells at a temperature of 30°C are shown in Figure 170 and the variation in photosynthetic parameters are presented in Table 71. The values of P_{max} , α , and LEDR all increased with increasing incubation

Table 69. The effect of temperature on the photosynthesis / irradiance curves of *Chlorella vulgaris* 211/11c cultured at 15°C.

Photosynthetic parameter	Culture temperature °C : photosynthetic / irradiance measurement temperature °C.			
	15:15	15:23	15:30	15:35
P_{max} (mg oxygen g dry wt ⁻¹ hr ⁻¹)	48.7	187.5	267.8	402.7
P_{max}^{PFD} ($\mu\text{mol s}^{-1} \text{m}^{-2}$)	200	200	300	300
I_k ($\mu\text{mol s}^{-1} \text{m}^{-2}$)	39.0	124.1	97.6	153.3
Dark respiration (mg oxygen g dry wt ⁻¹ hr ⁻¹)	17.8	26.3	85.7	86.5
LEDR (mg oxygen g dry wt ⁻¹ hr ⁻¹)	34.2	95.3	201.3	278.4
α (mg oxygen g dry wt-1 hr-1 / $\mu\text{mol s}^{-1} \text{m}^{-2}$)	1.2	1.5	2.7	2.6

Table 70. The effect of temperature on the photosynthesis / irradiance curves of *Chlorella vulgaris* 211/11c cultured at 23°C.

Photosynthetic parameter	Culture temperature °C : photosynthetic / irradiance measurement temperature °C.			
	23:15	23:23	23:30	23:35
P_{max} (mg oxygen g dry wt ⁻¹ hr ⁻¹)	48.8	75.9	170.0	225.3
P_{max}^{PFD} ($\mu\text{mol s}^{-1} \text{m}^{-2}$)	300	200	300	300
I_k ($\mu\text{mol s}^{-1} \text{m}^{-2}$)	45.8	51.4	53.8	62.7
Dark respiration (mg oxygen g dry wt ⁻¹ hr ⁻¹)	12.5	15.3	57.9	78.9
LEDR (mg oxygen g dry wt ⁻¹ hr ⁻¹)	35.3	78.6	124.2	166.2
α (mg oxygen g dry wt-1 hr-1 / $\mu\text{mol s}^{-1} \text{m}^{-2}$)	1.1	1.5	3.2	3.5

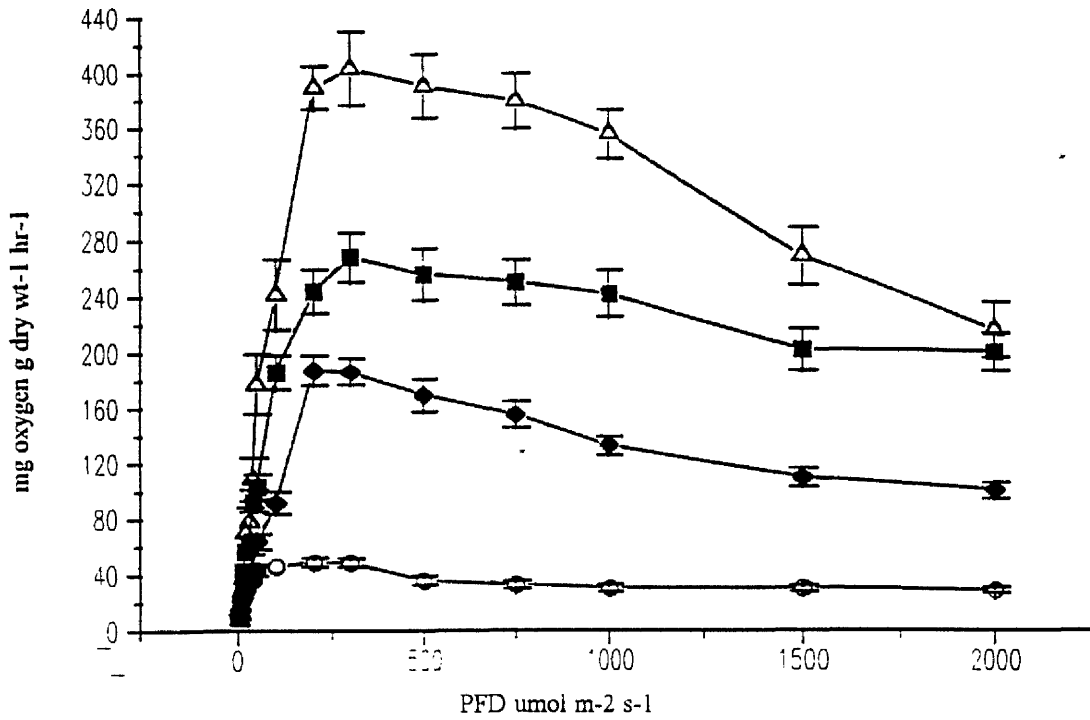


Figure 168. The effect of P/I incubation temperature on the photosynthesis / irradiance response curves of *Chlorella vulgaris* 211/11c cultured at 15°C, ○—○ 15°C, ◆—◆ 23°C, ■—■ 30°C, △—△ 35°C.

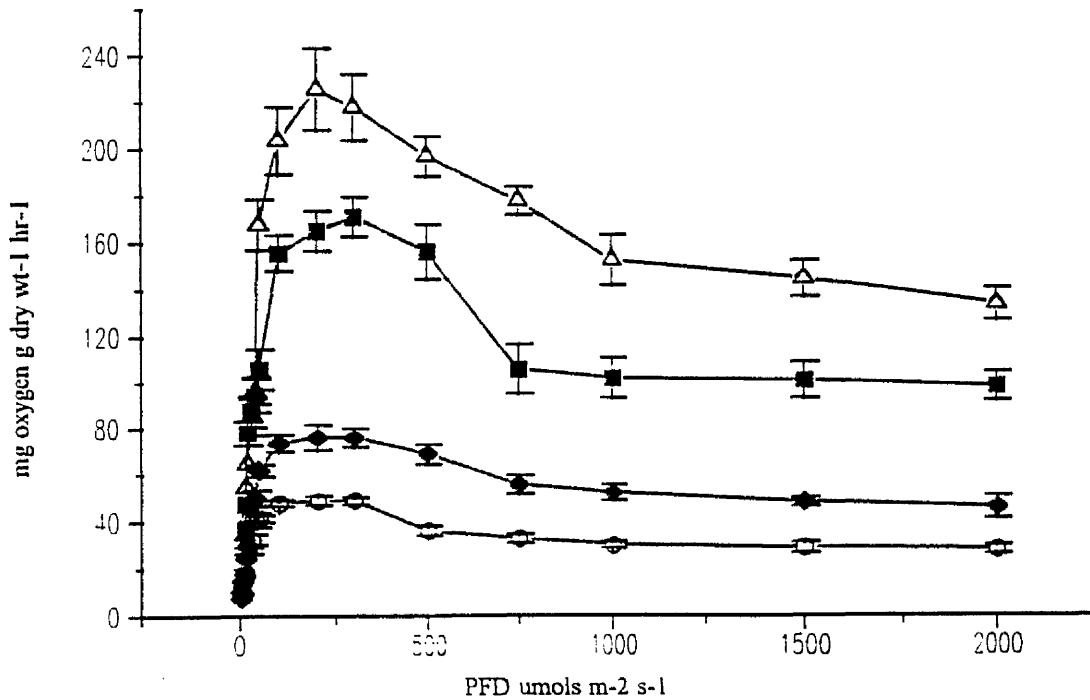


Figure 169. The effect of P/I incubation temperature on the photosynthesis / irradiance response curves of *Chlorella vulgaris* 211/11c cultured at 23°C, ○—○ 15°C, ◆—◆ 23°C, ■—■ 30°C, △—△ 35°C.

Table 71. The effect of temperature on the photosynthesis / irradiance curves of *Chlorella vulgaris* 211/11c cultured at 30°C.

Photosynthetic parameter	Culture temperature °C : photosynthetic / irradiance measurement temperature °C.			
	30:15	30:23	30:30	30:35
P _{max} (mg oxygen g dry wt ⁻¹ hr ⁻¹)	33.2	61.9	87.5	127.9
P _{max} ^{PFD} (μmol s ⁻¹ m ⁻²)	200	200	200	200
I _k (μmol s ⁻¹ m ⁻²)	44.8	69.6	91.0	88.0
Dark respiration (mg oxygen g dry wt ⁻¹ hr ⁻¹)	10.3	12.7	15.8	33.5
LEDR (mg oxygen g dry wt ⁻¹ hr ⁻¹)	32.8	45.8	108.5	118.4
α (mg oxygen g dry wt ⁻¹ hr ⁻¹ / μmol s ⁻¹ m ⁻²)	0.7	0.9	1.0	1.4

Table 72. The effect of temperature on the photosynthesis / irradiance curves of *Chlorella vulgaris* 211/11c cultured at 35°C.

Photosynthetic parameter	Culture temperature °C : photosynthetic / irradiance measurement temperature °C.			
	35:15	35:23	35:30	35:35
P _{max} (mg oxygen g dry wt ⁻¹ hr ⁻¹)	56.3	97.8	128.8	155.5
P _{max} ^{PFD} (μmol s ⁻¹ m ⁻²)	200	200	200	200
I _k (μmol s ⁻¹ m ⁻²)	40.1	41.2	49.9	58.8
Dark respiration (mg oxygen g dry wt ⁻¹ hr ⁻¹)	13.6	18.7	24.7	27.9
LEDR (mg oxygen g dry wt ⁻¹ hr ⁻¹)	56.4	84.2	94.4	107.7
α (mg oxygen g dry wt ⁻¹ hr ⁻¹ / μmol s ⁻¹ m ⁻²)	1.4	2.4	2.6	2.7

temperature. Dark respiration and I_k both increased with increasing temperature up to and including 30°C.

The effect of culturing *Chlorella vulgaris* 211/11c at a temperature of 35°C is shown in Figure 171 and the photosynthetic parameters are presented in Table 72. Similar to all previous culture temperatures (15, 23 and 30°C), P_{max} , I_k , α , DR and LEDR all increased with increasing incubation temperature.

Equations 117, 118, 119 and 120 show the relationships between the maximum rates of photosynthesis at different culture temperatures.

$$P_{max}^{15} = 13.76 \times e^{(8.04 \times 10^{-2} \times T)} \quad \text{sig } P=0.01 \quad (117)$$

$$P_{max}^{23} = 13.76 \times e^{(8.04 \times 10^{-2} \times T)} \quad \text{sig } P=0.001 \quad (118)$$

$$P_{max}^{30} = 12.79 \times e^{(6.56 \times 10^{-2} \times T)} \quad \text{sig } P=0.001 \quad (119)$$

$$P_{max}^{35} = -16.6 + 4.9 \times T \quad \text{sig } P=0.001 \quad (120)$$

Where P_{max}^x is the maximum rate of photosynthesis (mg oxygen g dry wt⁻¹ hr⁻¹) measured at a culture temperature x (15, 23, 30 and 35°C). T is any incubation temperature between 15 and 35°C

Equations 121, 122, 123 and 124 show the relationship between dark respiration and temperature.

$$R_{initial}^{15} = 4.19 \times e^{(9.03 \times 10^{-2} \times T)} \quad \text{sig } P=0.01 \quad (121)$$

$$R_{initial}^{23} = 56.04 + (-5.84 \times T) + (0.188 \times T^2) \quad \text{sig } P=0.001 \quad (122)$$

$$R_{initial}^{30} = 57.33 + (-4.9 \times T) + (0.122 \times T^2) \quad \text{sig } P=0.001 \quad (123)$$

$$R_{initial}^{35} = 2.45 + 0.73 \times T \quad \text{sig } P=0.01 \quad (124)$$

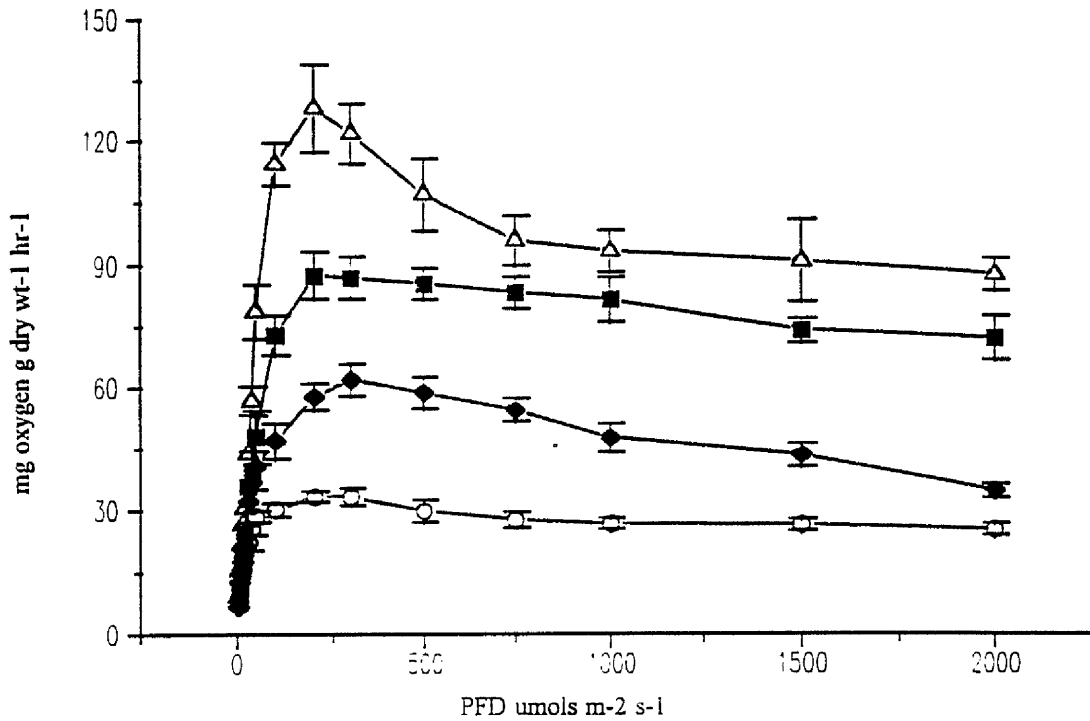


Figure 170 . The effect of P/I incubation temperature on the photosynthesis / irradiance response curves of *Chlorella vulgaris* 211/11c cultured at 30°C, ○—○ 15°C, ◆—◆ 23°C, ■—■ 30°C, △—△ 35°C.

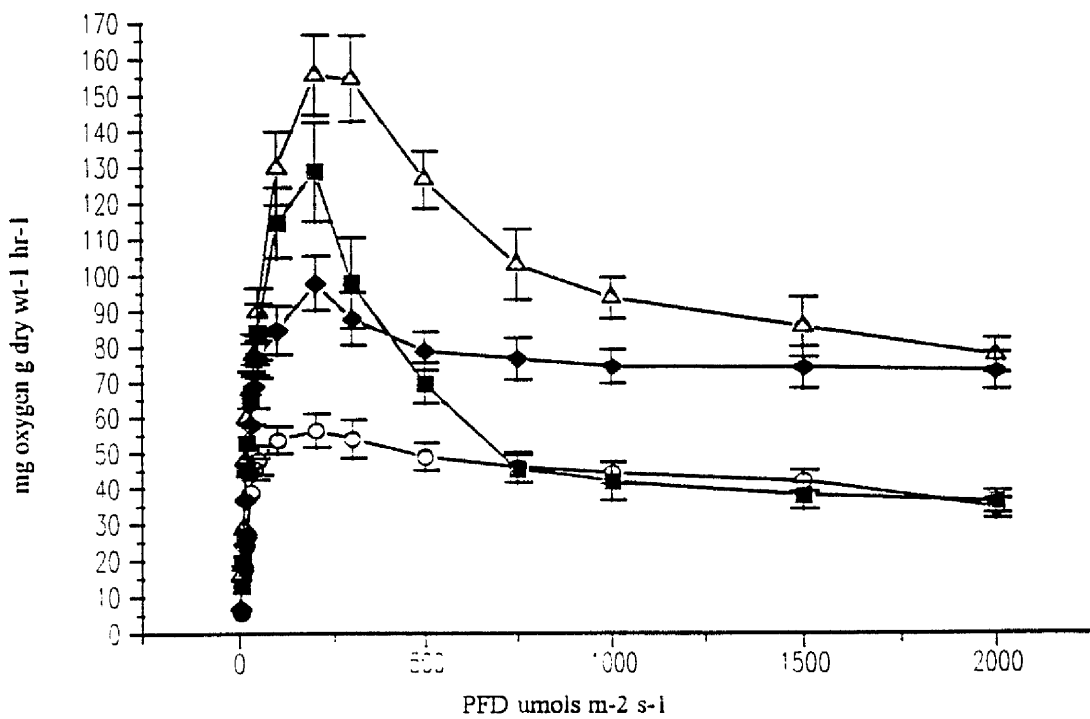


Figure 171 . The effect of P/I incubation temperature on the photosynthesis / irradiance response curves of *Chlorella vulgaris* 211/11c cultured at 35°C, ○—○ 15°C, ◆—◆ 23°C, ■—■ 30°C, △—△ 35°C.

R is the dark respiration rate (mg oxygen g dry wt⁻¹ hr⁻¹) of cells cultured at specified temperature (15, 23, 30 and 35°C). T is any P/I incubation temperature between 15 and 35°C.

Equations 125, 126, 127 and 128 show the relationship between light enhanced dark respiration and temperature.

$$LEDR_{final}^{15} = 3.82 \times 10^{-2} \times T^{2.506} \quad \text{sig P}=0.01 \quad (125)$$

$$LEDR_{final}^{23} = 0.25 \times T^{1.81} \quad \text{sig P}=0.001 \quad (126)$$

$$LEDR_{final}^{30} = 10.75 \times e^{(7.06 \times 10^{-2} \times T)} \quad \text{sig P}=0.001 \quad (127)$$

$$LEDR_{final}^{35} = 7.72 \times T^{0.743} \quad \text{sig P}=0.01 \quad (128)$$

$LEDR$ is the light enhanced dark respiration rate (mg oxygen g dry wt⁻¹ hr⁻¹) measured after the determination of a full photosynthesis / irradiance response curve.

The eukaryotic unicellular green micro-algal isolate *Scenedesmus sp.* was used to examine the effects of culture irradiance and temperature on photosynthesis / irradiance response curves.

The photosynthesis / irradiance response curves of *Scenedesmus sp.* grown at a temperature of 15°C are shown in Figure 172. The photosynthetic parameters are presented in Table 73 . The values of P_{max} , α , DR, and LEDR all increased with increasing incubation temperature (15-35°C). I_k increased from 56.43 to 90.9 $\mu\text{mol s}^{-1} \text{m}^{-2}$ upon increasing the temperature 15-30°C, however, it decreased to 69.1 $\mu\text{mol s}^{-1} \text{m}^{-2}$ when the temperature was further increased to 35°C.

The effect of culturing cells at a temperature of 23°C (Figure 173) on the photosynthetic parameters of *Scenedesmus sp.* are shown in Table 74. The maximum rate of photosynthesis increased with increasing temperature. There was a 5 fold increase in P_{max} when cells were incubated at 35°C compared to 15°C.

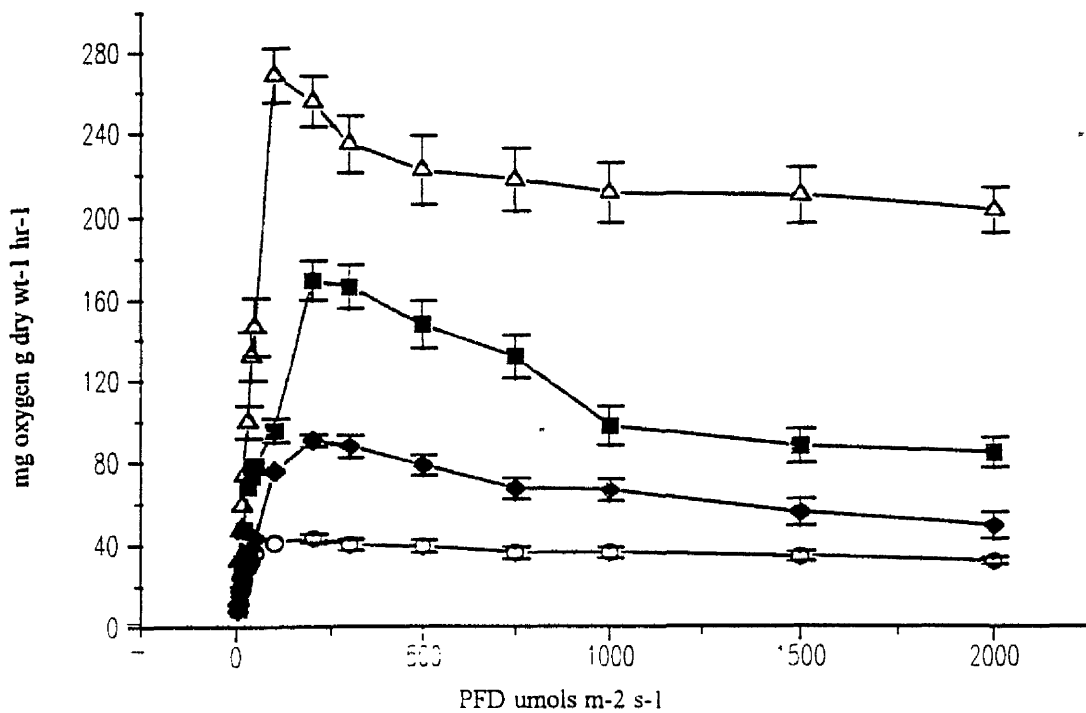


Figure 172. The effect of P/I incubation temperature on the photosynthesis / irradiance response curves of *Scenedesmus sp.* cultured at 15°C, ○—○ 15°C, ◆—◆ 23°C, ■—■ 30°C, △—△ 35°C.

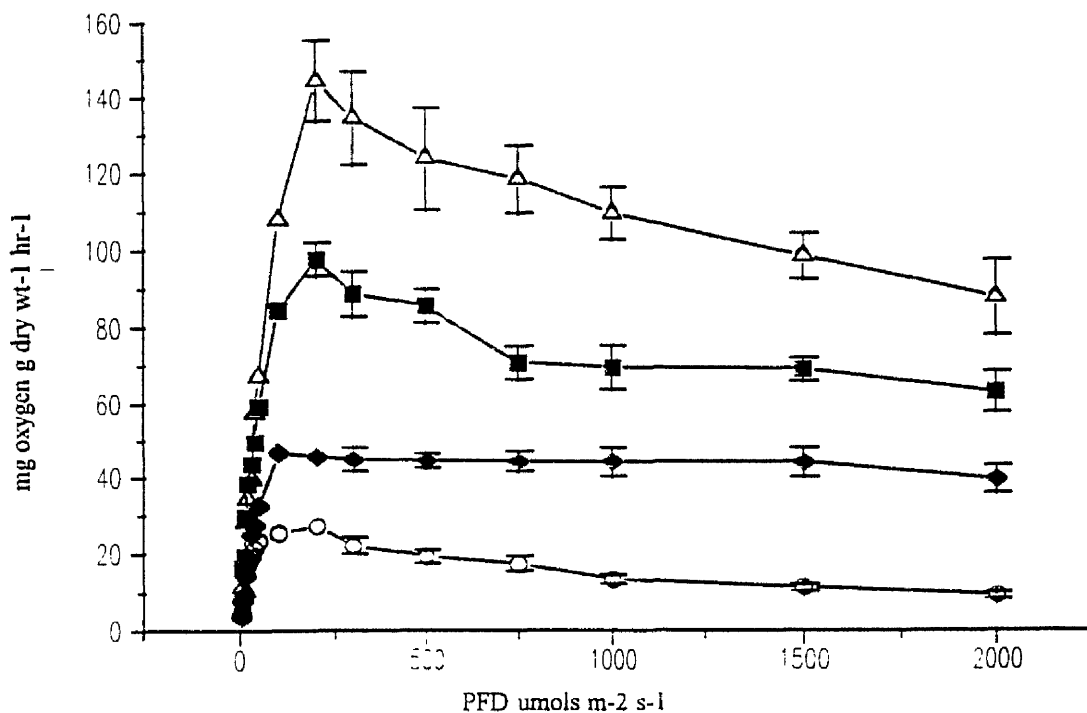


Figure 173. The effect of P/I incubation temperature on the photosynthesis / irradiance response curves of *Scenedesmus sp.* cultured at 23°C, ○—○ 15°C, ◆—◆ 23°C, ■—■ 30°C, △—△ 35°C.

Figure 174 shows photosynthesis / irradiance response curves of *Scenedesmus sp.* cells cultured at a temperature of 30°C. The photosynthetic parameters calculated from Figure 174 are presented in Table 75. The difference in P_{\max} between cells cultured at 35 and 15°C was a factor of 3 (170.67 compared to 45.58 mg oxygen g dry wt⁻¹ hr⁻¹). Dark respiration, LEDR both increased with increasing temperature. The value of α increased with increasing temperature from 15-30°C, however, it then decreased when the temperature was increased to 35°C.

The photosynthesis / irradiance curves of *Scenedesmus sp.* cultured at 35°C are shown in Figure 175. Table 76 presents the photosynthetic parameters. Similar to the other results presented in Tables 73, 74 and 75, the value of P_{\max} increased with increasing incubation temperature from 30.45 to 94.5mg oxygen g dry wt⁻¹ hr⁻¹ (temperature 15 and 35°C respectively). The values of DR and LEDR both increased with increasing incubation temperature. No relationship was determined between either I_k and temperature or α and temperature. The maximum rates of photosynthesis measured at the same growth temperature and P/I temperature were seen to increase with increasing growth temperature.

Equation 129, 130, 131 and 132 show the relationship between the maximum rates of photosynthesis and temperature.

$$P_{\max}^{15} = 11.17 \times e^{(9.07 \times 10^{-2} \times T)} \quad \text{sig } P=0.001 \quad (129)$$

$$P_{\max}^{23} = 7.14 \times e^{(8.56 \times 10^{-2} \times T)} \quad \text{sig } P=0.001 \quad (130)$$

$$P_{\max}^{30} = 108.4 + (-8.52 \times T) + (0.29 \times T^2) \quad \text{sig } P=0.001 \quad (131)$$

$$P_{\max}^{35} = 0.989 \times T^{1.116} \quad \text{sig } P=0.001 \quad (132)$$

P_{\max}^x is the maximum rate of photosynthesis (mg oxygen g dry wt⁻¹ hr⁻¹) measured at a culture temperature (15, 23, 30 and 35°C). T is any incubation temperature between 15 and 35°C. Equations 133, 134, 135 and 136 show the relationship between dark respiration and temperature.

$$R_{\text{initial}}^{15} = 1.94 \times e^{(7.93 \times 10^{-2} \times T)} \quad \text{sig } P=0.01 \quad (133)$$

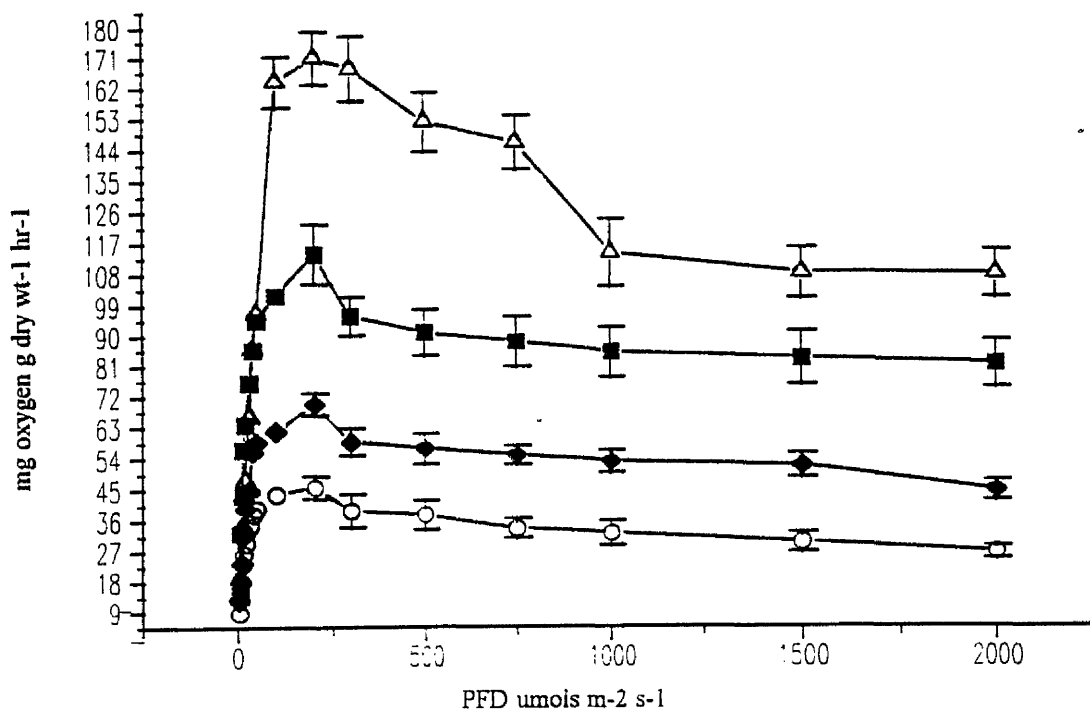


Figure 174 . The effect of P/I incubation temperature on the photosynthesis / irradiance response curves of *Scenedesmus sp.* cultured at 30°C, ○—○ 15°C, ◆—◆ 23°C, ■—■ 30°C, △—△ 35°C.

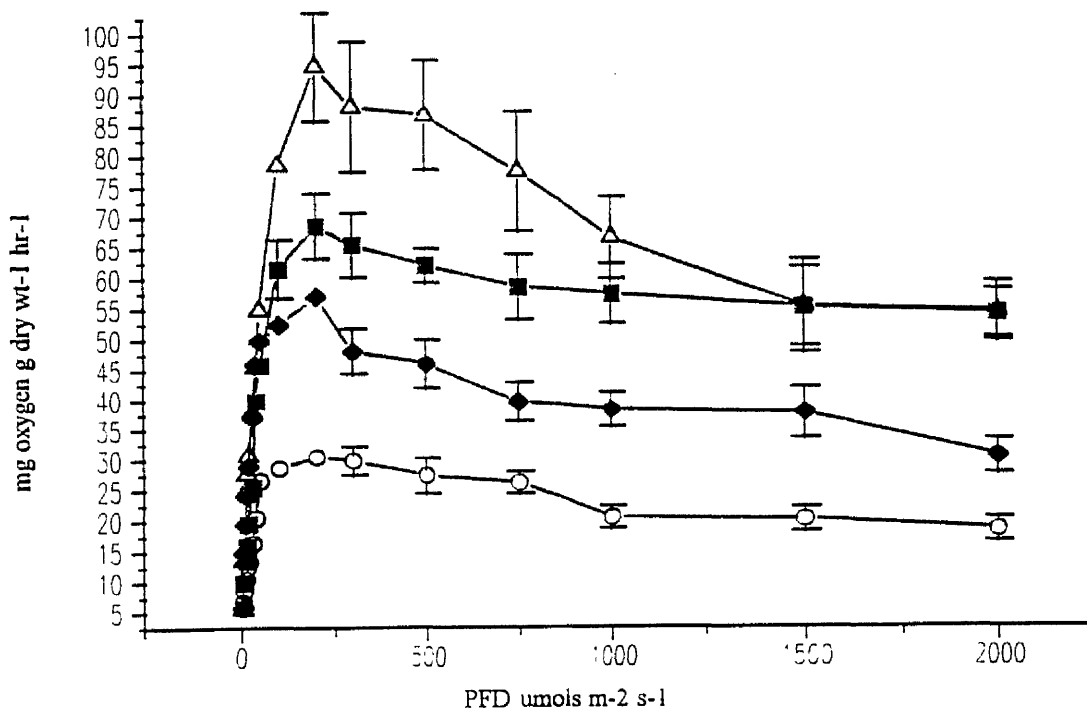


Figure 175 . The effect of P/I incubation temperature on the photosynthesis / irradiance response curves of *Scenedesmus sp.* cultured at 35°C, ○—○ 15°C, ◆—◆ 23°C, ■—■ 30°C, △—△ 35°C.

Table 73. The effect of temperature on the photosynthesis / irradiance curves of *Scenedesmus sp.* cultured at 15°C.

Photosynthetic parameter	Culture temperature °C : photosynthetic / irradiance measurement temperature °C.			
	15:15	15:23	15:30	15:35
P _{max} (mg oxygen g dry wt ⁻¹ hr ⁻¹)	43.6	90.5	169.5	268.6
P _{max} ^{PFD} (μmol s ⁻¹ m ⁻²)	300	300	300	200
I _k (μmol s ⁻¹ m ⁻²)	56.4	63.2	90.9	69.2
Dark respiration (mg oxygen g dry wt ⁻¹ hr ⁻¹)	6.5	12.2	19.6	32.9
LEDR (mg oxygen g dry wt ⁻¹ hr ⁻¹)	32.9	44.3	54.3	77.6
α (mg oxygen g dry wt ⁻¹ hr ⁻¹ / μmol s ⁻¹ m ⁻²)	0.7	1.4	1.8	3.9

Table 74. The effect of temperature on the photosynthesis / irradiance curves of *Scenedesmus sp.* cultured at 23°C.

Photosynthetic parameter	Culture temperature °C : photosynthetic / irradiance measurement temperature °C.			
	23:15	23:23	23:30	23:35
P _{max} (mg oxygen g dry wt ⁻¹ hr ⁻¹)	27.1	46.5	97.6	144.6
P _{max} ^{PFD} (μmol s ⁻¹ m ⁻²)	200	200	200	200
I _k (μmol s ⁻¹ m ⁻²)	39.3	51.2	52.3	78.2
Dark respiration (mg oxygen g dry wt ⁻¹ hr ⁻¹)	7.9	8.9	37.9	46.7
LEDR (mg oxygen g dry wt ⁻¹ hr ⁻¹)	43.2	67.9	88.9	96.9
α (mg oxygen g dry wt ⁻¹ hr ⁻¹ / μmol s ⁻¹ m ⁻²)	0.7	0.8	1.8	1.9

Table 75. The effect of temperature on the photosynthesis / irradiance curves of *Scenedesmus sp.* cultured at 30°C.

Photosynthetic parameter	Culture temperature °C : photosynthetic / irradiance measurement temperature °C.			
	30:15	30:23	30:30	30:35
P_{max} (mg oxygen g dry wt ⁻¹ hr ⁻¹)	45.6	69.6	113.7	170.7
P_{max}^{PFD} ($\mu\text{mol s}^{-1} \text{m}^{-2}$)	200	200	200	200
I_k ($\mu\text{mol s}^{-1} \text{m}^{-2}$)	31.7	43.8	33.9	65.9
Dark respiration (mg oxygen g dry wt ⁻¹ hr ⁻¹)	8.6	9.7	29.5	23.8
LEDR (mg oxygen g dry wt ⁻¹ hr ⁻¹)	35.7	48.9	107.6	113.6
α (mg oxygen g dry wt ⁻¹ hr ⁻¹ / $\mu\text{mol s}^{-1} \text{m}^{-2}$)	1.4	1.6	3.3	2.6

Table 76. The effect of temperature on the photosynthesis / irradiance curves of *Scenedesmus sp.* cultured at 35°C.

Photosynthetic parameter	Culture temperature °C : photosynthetic / irradiance measurement temperature °C.			
	35:15	35:23	35:30	35:35
P_{max} (mg oxygen g dry wt ⁻¹ hr ⁻¹)	30.5	56.9	68.5	94.6
P_{max}^{PFD} ($\mu\text{mol s}^{-1} \text{m}^{-2}$)	200	200	200	200
I_k ($\mu\text{mol s}^{-1} \text{m}^{-2}$)	64.1	38.5	81.2	49.0
Dark respiration (mg oxygen g dry wt ⁻¹ hr ⁻¹)	4.8	15.7	17.8	23.2
LEDR (mg oxygen g dry wt ⁻¹ hr ⁻¹)	34.9	67.4	73.4	94.3
α (mg oxygen g dry wt ⁻¹ hr ⁻¹ / $\mu\text{mol s}^{-1} \text{m}^{-2}$)	0.4	1.5	1.8	1.9

$$R_{initial}^{23} = 26.75 + (-2.84 \times T) + (0.10 \times T^2) \quad \text{sig P}=0.01 \quad (134)$$

$$R_{initial}^{30} = 15.63 + (-1.38 \times T) + (5.61 \times 10^{-2} \times T^2) \quad \text{sig P}=0.001 \quad (135)$$

$$R_{initial}^{35} = -6.92 + 0.865 \times T \quad \text{sig P}=0.001 \quad (136)$$

R is the dark respiration rate (mg oxygen g dry wt⁻¹ hr⁻¹). T is any incubation temperature between 15 and 35°C.

Equations 137, 138, 139 and 140 describe the relationship between LEDR and temperature.

$$LEDR_{final}^{15} = 17.41 \times e^{(4.07 \times 10^{-2} \times T)} \quad \text{sig P}=0.01 \quad (137)$$

$$LEDR_{final}^{23} = 3.13 \times T^{0.975} \quad \text{sig P}=0.001 \quad (138)$$

$$LEDR_{final}^{30} = 13.01 \times e^{(6.41 \times 10^{-2} \times T)} \quad \text{sig P}=0.001 \quad (139)$$

$$LEDR_{final}^{35} = 1.78 \times T^{1.116} \quad \text{sig P}=0.01 \quad (140)$$

LEDR is the light enhanced dark respiration rate (mg oxygen g dry wt⁻¹ hr⁻¹). T is any temperature between 15 and 35°C.

The photosynthesis / irradiance curves of *Synechococcus* 1479/5 cultured at a temperature of 15°C are presented in Figure 176. Table 77 shows the photosynthetic parameters calculated from Figure 176. Similar to the results obtained for *Chlorella vulgaris* 211/11c and *Scenedesmus* sp. the value P_{max} increased with increasing temperature. The values of DR, LEDR and α also increased with increasing incubation temperature.

The photosynthesis / irradiance response curves of *Synechococcus* 1479/5 cultured at a temperature of 23°C are shown in Figure 177. The photosynthetic parameters of

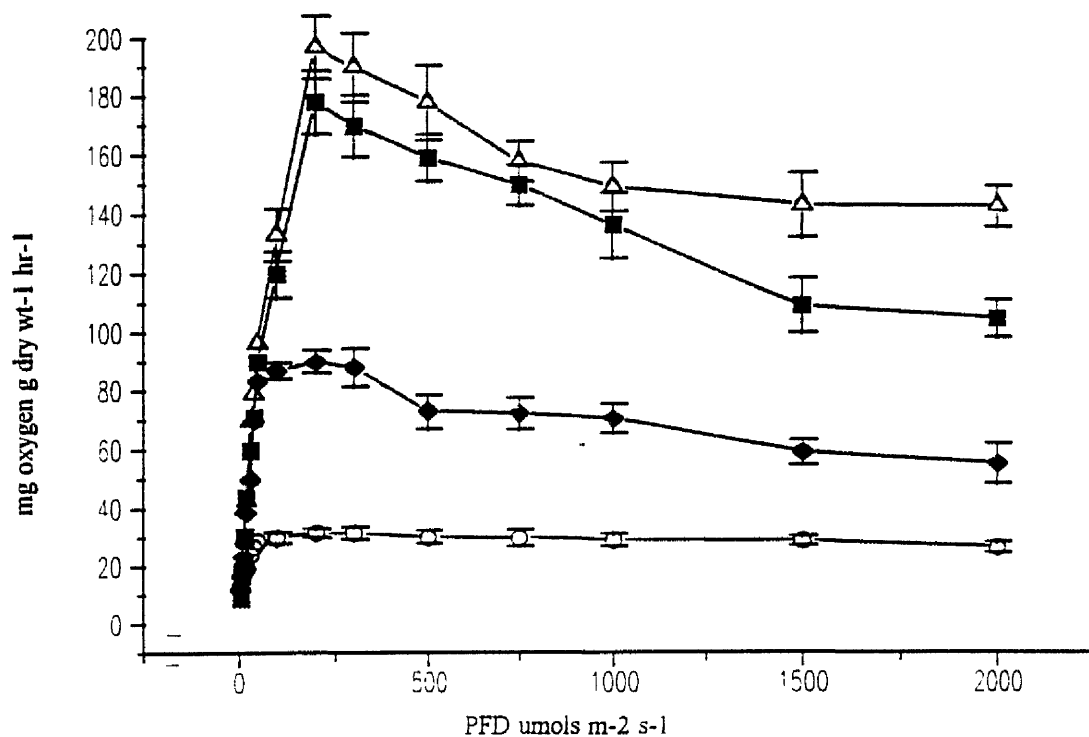


Figure 176. The effect of P/I incubation temperature on the photosynthesis / irradiance response curves of *Synechococcus* 1479/5 cultured at 15°C, ○—○ 15°C, ◆—◆ 23°C, ■—■ 30°C, △—△ 35°C.

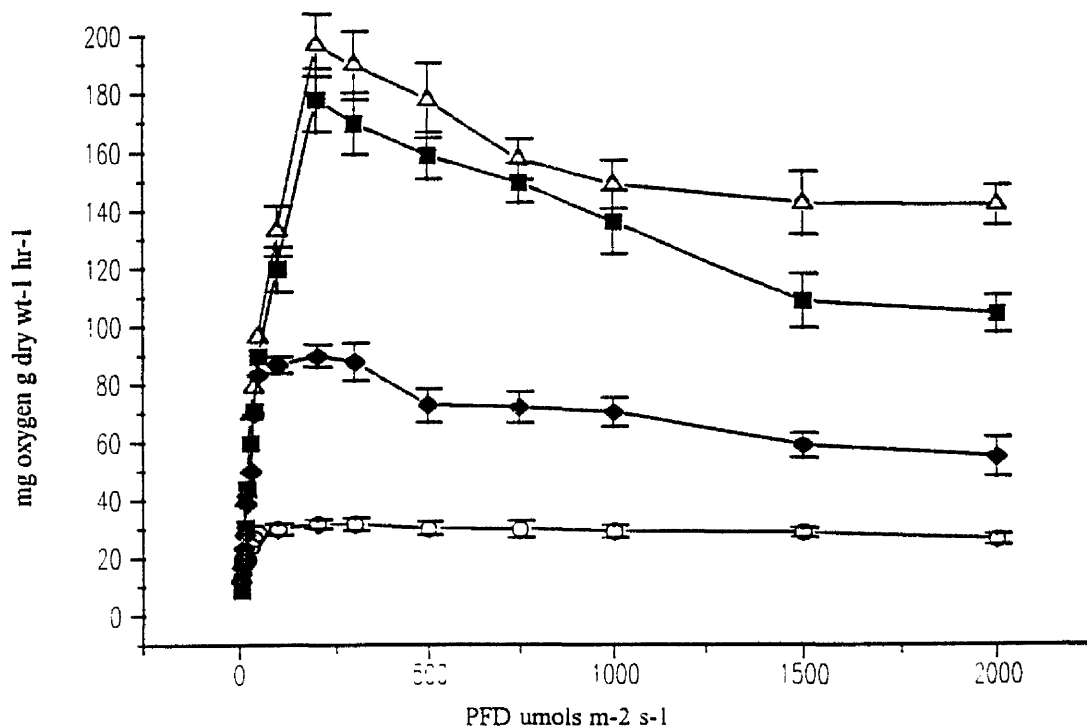


Figure 177. The effect of P/I incubation temperature on the photosynthesis / irradiance response curves of *Synechococcus* 1479/5 cultured at 23°C, ○—○ 15°C, ◆—◆ 23°C, ■—■ 30°C, △—△ 35°C.

Figure 177 are shown in Table 78. The values of P_{\max} , DR, LEDR and α increased with increasing temperature. The value of α increased from 0.5mg oxygen g dry wt-1 hr-1 / $\mu\text{mol s}^{-1} \text{m}^{-2}$ measured at 15°C to 3.2mg oxygen g dry wt-1 hr-1 / $\mu\text{mol s}^{-1} \text{m}^{-2}$ measured at 35°C. The value of I_k showed no relationship with temperature.

The photosynthesis / irradiance response curves of *Synechococcus* 1479/5 cultured at a temperature of 30°C are shown in Figure 178. Table 79 shows the photosynthetic parameters. Similar to all previous data recorded from *Synechococcus* 1479/5 cells cultured at temperature of 15 and 23°C, the values of P_{\max} , DR, LEDR and α all increased with increasing temperature. The value I_k also increased with increasing temperature from 38.5 $\mu\text{mol s}^{-1} \text{m}^{-2}$ at 15°C to 63.8 $\mu\text{mol s}^{-1} \text{m}^{-2}$ at 35°C.

The photosynthesis /irradiance response curves of *Synechococcus* 1479/5 cultured at a temperature of 35°C are shown in Figure 179. The photosynthetic parameters calculated from Figure 179 are shown in Table 80. The value of P_{\max} , I_k , DR and LEDR all increased with increasing incubation temperature, however, α showed no such relationship.

Equations 141, 142, 143 and 144 show the relationship between the maximum rates of photosynthesis and culture temperature.

$$P_{\max}^{15} = 7.42 \times 10^{-2} \times T^{2.25} \quad \text{sig } P=0.01 \quad (141)$$

$$P_{\max}^{23} = 0.186 \times T^{1.87} \quad \text{sig } P=0.01 \quad (142)$$

$$P_{\max}^{30} = -92.97 + 8.23 \times T \quad \text{sig } P=0.01 \quad (143)$$

$$P_{\max}^{35} = 13.04 + e^{(5.61 \times 10^{-2} \times T)} \quad \text{sig } P=0.01 \quad (144)$$

The maximum rate of photosynthesis measured at 15:15 to 30:30 increased with increasing growth temperature but decreased when 35°C cultured cells were measured at a P/I incubation temperature of 35°C (Tables 77 to 80).

Equations 145, 146, 147 and 148 show the relationship between dark respiration and temperature.

$$R_{\text{initial}}^{15} = 38.59 + (-3.07 \times T) + (8.41 \times 10^{-2} \times T^2) \quad \text{sig } P=0.001 \quad (145)$$

Table 77. The effect of temperature on the photosynthesis / irradiance curves of *Synechococcus* 1479/5 cultured at 15°C.

Photosynthetic parameter	Culture temperature °C : photosynthetic / irradiance measurement temperature °C.			
	15:15	15:23	15:30	15:35
P _{max} (mg oxygen g dry wt ⁻¹ hr ⁻¹)	31.6	89.8	177.7	196.5
P _{max} ^{PF_D} (μmol s ⁻¹ m ⁻²)	200	200	200	200
I _k (μmol s ⁻¹ m ⁻²)	74	65.8	102.3	95.3
Dark respiration (mg oxygen g dry wt ⁻¹ hr ⁻¹)	10.8	13.8	19.8	34.7
LEDR (mg oxygen g dry wt ⁻¹ hr ⁻¹)	25.7	47.8	78.9	103.7
α (mg oxygen g dry wt ⁻¹ hr ⁻¹ / μmol s ⁻¹ m ⁻²)	0.4	1.4	1.7	2.0

Table 78. The effect of temperature on the photosynthesis / irradiance curves of *Synechococcus* 1479/5 cultured at 23°C.

Photosynthetic parameter	Culture temperature °C : photosynthetic / irradiance measurement temperature °C.			
	23:15	23:23	23:30	23:35
P _{max} (mg oxygen g dry wt ⁻¹ hr ⁻¹)	26.4	86.9	96.8	138.6
P _{max} ^{PF_D} (μmol s ⁻¹ m ⁻²)	200	200	200	200
I _k (μmol s ⁻¹ m ⁻²)	51.5	48.1	34.7	43.2
Dark respiration (mg oxygen g dry wt ⁻¹ hr ⁻¹)	8.9	17.9	47.8	57.6
LEDR (mg oxygen g dry wt ⁻¹ hr ⁻¹)	24.1	75.3	89.7	93.2
α (mg oxygen g dry wt ⁻¹ hr ⁻¹ / μmol s ⁻¹ m ⁻²)	0.5	1.8	2.8	3.2

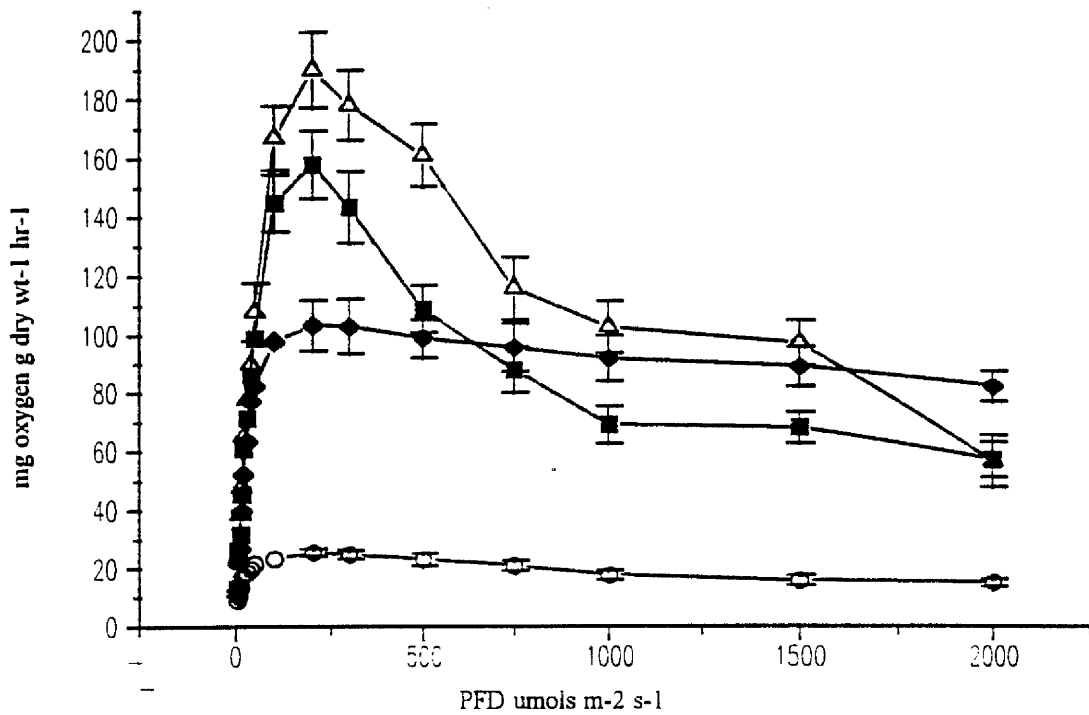


Figure 178. The effect of P/I incubation temperature on the photosynthesis / irradiance response curves of *Synechococcus* 1479/5 cultured at 30°C, ○—○ 15°C, ◆—◆ 23°C, ■—■ 30°C, △—△ 35°C.

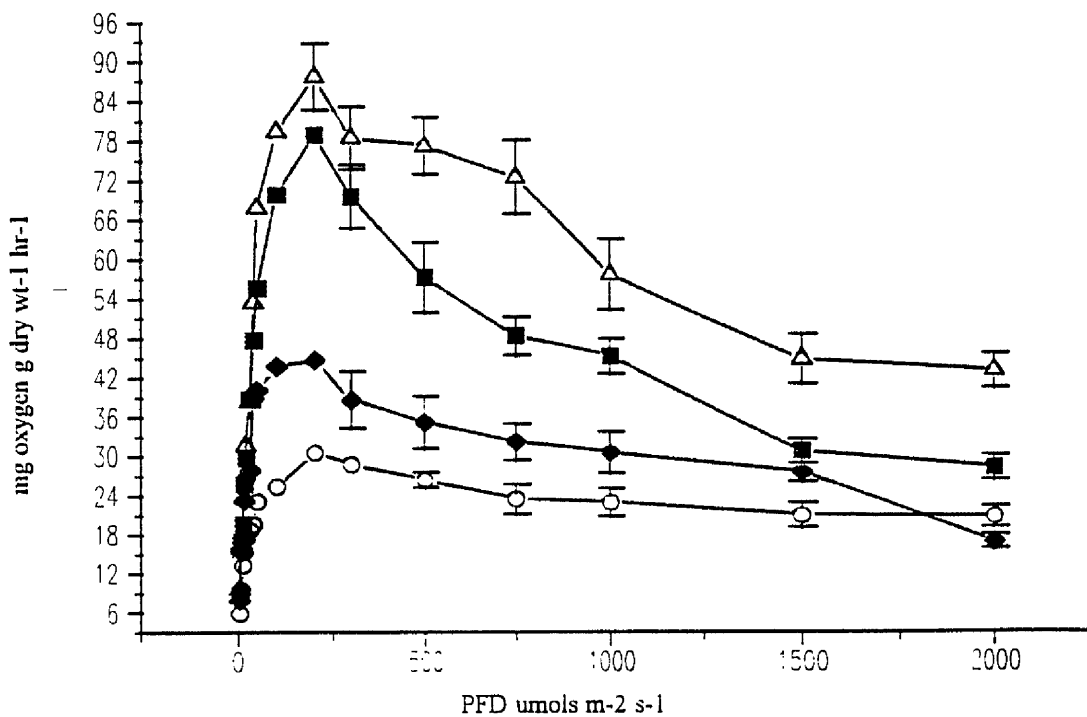


Figure 179. The effect of P/I incubation temperature on the photosynthesis / irradiance response curves of *Synechococcus* 1479/5 cultured at 35°C, ○—○ 15°C, ◆—◆ 23°C, ■—■ 30°C, △—△ 35°C.

Table 79. The effect of temperature on the photosynthesis / irradiance curves of *Synechococcus* 1479/5 cultured at 30°C.

Photosynthetic parameter	Culture temperature °C : photosynthetic / irradiance measurement temperature °C.			
	30:15	30:23	30:30	30:35
P_{max} (mg oxygen g dry wt ⁻¹ hr ⁻¹)	25.5	103.2	157.8	189.8
P_{max}^{PFD} ($\mu\text{mol s}^{-1} \text{m}^{-2}$)	200	200	200	200
I_k ($\mu\text{mol s}^{-1} \text{m}^{-2}$)	38.5	44.8	62.1	63.8
Dark respiration (mg oxygen g dry wt ⁻¹ hr ⁻¹)	5.8	8.7	24.7	28.7
LEDR (mg oxygen g dry wt ⁻¹ hr ⁻¹)	33.2	78.7	83.2	94.9
α (mg oxygen g dry wt ⁻¹ hr ⁻¹ / $\mu\text{mol s}^{-1} \text{m}^{-2}$)	0.7	2.3	2.5	2.9

Table 80. The effect of temperature on the photosynthesis / irradiance curves of *Synechococcus* 1479/5 cultured at 35°C.

Photosynthetic parameter	Culture temperature °C : photosynthetic / irradiance measurement temperature °C.			
	35:15	35:23	35:30	35:35
P_{max} (mg oxygen g dry wt ⁻¹ hr ⁻¹)	30.5	44.6	78.9	87.6
P_{max}^{PFD} ($\mu\text{mol s}^{-1} \text{m}^{-2}$)	200	200	200	200
I_k ($\mu\text{mol s}^{-1} \text{m}^{-2}$)	37.9	36.9	57.6	79.1
Dark respiration (mg oxygen g dry wt ⁻¹ hr ⁻¹)	7.0	44.8	67.8	84.7
LEDR (mg oxygen g dry wt ⁻¹ hr ⁻¹)	39.6	44.8	67.8	84.8
α (mg oxygen g dry wt ⁻¹ hr ⁻¹ / $\mu\text{mol s}^{-1} \text{m}^{-2}$)	0.8	1.2	1.4	1.1

$$R_{initial}^{23} = 1.99 \times e^{(9.92 \times 10^{-2} \times T)} \quad \text{sig P}=0.01 \quad (146)$$

$$R_{initial}^{30} = 1.48 \times e^{(8.66 \times 10^{-2} \times T)} \quad \text{sig P}=0.01 \quad (147)$$

$$R_{initial}^{35} = 9.47 + (-0.305 \times T) + (8.84 \times 10^{-3} \times T^2) \quad \text{sig P}=0.001 \quad (148)$$

R is the dark respiration (mg oxygen g dry wt⁻¹ hr⁻¹). T is any temperature between 15 and 35°C.

Equations 149, 150, 151 and 152 relate the LEDR rate to incubation temperature.

$$LEDR_{final}^{15} = 9.23 \times e^{(0.07 \times T)} \quad \text{sig P}=0.01 \quad (149)$$

$$LEDR_{final}^{23} = -144.72 + (14.68 \times T) + (-0.226 \times T^2) \quad \text{sig P}=0.001 \quad (150)$$

$$LEDR_{final}^{30} = -94.6 + (11.09 \times T) + (-0.16 \times T^2) \quad \text{sig P}=0.001 \quad (151)$$

$$LEDR_{final}^{35} = 64.45 + (-3.42 \times T) + (0.115 \times T^2) \quad \text{sig P}=0.001 \quad (152)$$

LEDR is the light enhanced dark respiration rate (mg oxygen g dry wt⁻¹ hr⁻¹). T is any temperature between 15 and 35°C.

Table 81, 82 and 83 show the ratio of the maximum rates of photosynthesis to the dark respiration rates for *Chlorella vulgaris* 211/11c, *Scenedesmus sp.* and *Synechococcus* 1479/5 respectively. The $P_{max} : DR$ ratios of *Chlorella vulgaris* 211/11c (Table 81) were low when the cells were incubated at a temperature of 15°C regardless of the culture temperature. The $P_{max} : DR$ ratio recorded from cells incubated at 23 and 30°C were the highest at 5-7 compared to 2-4 for cultures incubated at 15 and 35°C. Other than the cells cultured at 15°C, all other cultures had the highest $P_{max} : DR$ ratios recorded at the same incubation temperature as that which they had been grown at (23, 30 and 35°C). The maximum $P_{max} : DR$ ratio of 7.12 was recorded at a culture temperature of 15°C with an incubation temperature of 23°C.

Table 81. Maximum rate of photosynthesis / dark respiration rate ratio of *Chlorella vulgaris* 211/11c.

Culture temp °C	Incubation temp °C			
	15	23	30	35
15	2.73	7.12	3.12	4.65
23	3.90	4.96	2.9	2.85
30	3.22	4.87	5.50	3.80
35	4.13	5.22	5.21	5.50

Table 82. Maximum rate of photosynthesis / dark respiration rate ratio of *Scenedesmus* sp.

Culture temp °C	Incubation temp °C			
	15	23	30	35
15	6.70	7.40	8.60	8.16
23	3.43	5.22	2.57	3.09
30	5.3	7.17	3.85	7.17
35	6.34	3.62	3.84	4.07

Table 83. Maximum rate of photosynthesis / dark respiration rate ratio of *Synechococcus* 1479/5.

Culture temp °C	Incubation temp °C			
	15	23	30	35
15	2.92	6.50	8.90	5.67
23	2.96	4.85	2.02	2.40
30	4.40	11.86	6.38	6.61
35	4.35	0.99	1.16	1.03

The $P_{\max} : DR$ ratio for cells of *Scenedesmus sp.* are shown in Table 82. Unlike those results recorded with *Chlorella vulgaris* 211/11c and *Synechococcus* 1479/5, the $P_{\max} : DR$ ratios of *Scenedesmus sp.* were high in all culture / incubation temperatures. The maximum $P_{\max} : DR$ ratio of 8.6 was recorded from cells cultured at 15°C and incubated at 30°C.

The $P_{\max} : DR$ ratio from cells of *Synechococcus* 1479/5 are presented in Table 83. Similar to the observations recorded from *Chlorella vulgaris* 211/11c, the $P_{\max} : DR$ ratios were much higher from cells incubated at 23°C regardless of culture temperature, with the exception of cells cultured at 35°C. Cells cultured at 35°C were recorded to have higher $P_{\max} : DR$ ratios (1.03, 1.16, 0.99) when the incubation temperature was decreased from 35 to 15°C. The maximum $P_{\max} : DR$ ratio of 11.86 was recorded from cells cultured at 30°C and incubated at 23°C. Very low $P_{\max} : DR$ ratios (0.99, 1.16 and 1.03) were obtained from cells cultured at 35°C and incubated at 23, 30 and 35°C respectively.

The LEDR : DR ratios of *Chlorella vulgaris* 211/11c, *Scenedesmus sp.* and *Synechococcus* 1479/5 and are presented in Tables 84, 85 and 86 respectively.

Table 84 shows the LEDR : DR ratio for cells of *Chlorella vulgaris* 211/11c measured at four culture and P/I incubation temperatures of 15, 23, 30 and 35°C. The minimum LEDR : DR ratio was measured to be 1.92 for cells cultured at 15°C and P/I incubated at 15°C. The maximum LEDR : DR ratio was determined to be 6.86 from cells cultured at 30°C and P/I incubated at 30°C.

The LEDR : DR ratio of cells of *Scenedesmus sp.* are presented in Table 85. The maximum LEDR : DR ratio of 7.63 was measured from cells cultured at 23°C and incubated at 23°C. Similar to that observed with cells of *Synechococcus* 1479/5 the minimum LEDR : DR ratio (2.07) was measured from cells cultured at 23°C and incubated at 35°C

The LEDR : DR ratios from cells of *Synechococcus* 1479/5 are presented in 86. The maximum LEDR : DR ratio of 9.04 was measured from cells cultured at 30°C and P/I incubated at 23°C. The minimum LEDR : DR ratio of 1.61 was measured from cells cultured at 23°C and P/I incubated at 35°C.

Figures 180, 181, 182 and 183 show the arhenius plots of the natural logarithm of the photosynthetic rate (measured at a PFD of $200\mu\text{mol s}^{-1} \text{m}^{-2}$) vs the reciprocal of P/I incubation temperature (Kelvin) for *Chlorella vulgaris* 211/11c cultured at 15, 23, 30 and 35°C respectively. For normalisation Q_{10} was calculated for the temperature range 20-30°C. A good linear relationship was obtained from the oxygen evolution rate measured at a PFD of $200\mu\text{mol s}^{-1} \text{m}^{-2}$ and increases in temperature.

The arhenius plots of *Scenedesmus sp.* calculated from the photosynthetic rate measured at a PFD of $200\mu\text{mol s}^{-1} \text{m}^{-2}$ are shown in Figures 184, 185, 186 and 187. As was observed with *Chlorella vulgaris* 211/11c a good relationship was obtained between temperature change and oxygen evolution.

Figures 188, 189, 190 and 191 show the arhenius plots for *Synechococcus* 1479/5 (measured at a PFD of $200\mu\text{mol s}^{-1} \text{m}^{-2}$). The results showed a good relationship for culture temperatures 15°C and 35°C. Figure 189 and 190 measured at culture temperatures of 23°C and 30°C, however, showed some deviation from the general trend.

Figures 192, 193 and 194 show the changes in the Q_{10} values with changing culture temperature. It can be seen (Figure 192), that the Q_{10} of *Chlorella vulgaris* 211/11c decreased with increasing culture temperature. At a culture temperature of 15°C the Q_{10} was 3.0, whereas at a temperature of 35°C, the value of Q_{10} had decreased to 2.20. As was found with *Chlorella vulgaris* 211/11c, the Q_{10} of *Scenedesmus sp.* decreased with increasing culture temperature (Figure 193), from 2.85 at 15°C to 1.86 at 35°C. The results showed a similar trend to that observed with both *Chlorella vulgaris* 211/11c and *Scenedesmus sp.* in that the Q_{10} for *Synechococcus* 1479/5 decreased with increasing culture temperature (Figure 194) from 2.88 at 15°C to 1.82 at 35°C.

Table 84: The effect of temperature on the LEDR / DR ratio of *Chlorella vulgaris* 211/11c.

Culture temperature °C	P/I incubation temperature °C	Ratio LEDR / DR
15	15	1.92
15	23	3.62
15	30	2.34
15	35	3.21
23	15	2.84
23	23	5.13
23	30	2.14
23	35	2.11
30	15	3.18
30	23	3.60
30	30	6.86
30	35	3.53
35	15	4.15
35	23	4.50
35	30	3.82
35	35	3.86

Table 85: The effect of temperature on the LEDR / DR ratio of *Scenedesmus* sp.

Culture temperature °C	P/I incubation temperature °C	Ratio LEDR / DR
15	15	5.10
15	23	3.63
15	30	2.77
15	35	2.35
23	15	5.46
23	23	7.63
23	30	2.34
23	35	2.07
30	15	4.15
30	23	5.04
30	30	3.64
30	35	4.77
35	15	7.27
35	23	4.29
35	30	4.12
35	35	4.06

Table 86: The effect of temperature on the LEDR / DR ratio of *Synechococcus* 1479/5.

Culture temperature °C	P/I incubation temperature °C	Ratio LEDR / DR
15	15	2.37
15	23	3.46
15	30	3.98
15	35	2.98
23	15	2.70
23	23	4.20
23	30	1.87
23	35	1.61
30	15	5.71
30	23	9.04
30	30	3.36
30	35	3.30
35	15	5.65
35	23	4.11
35	30	3.62
35	35	4.32

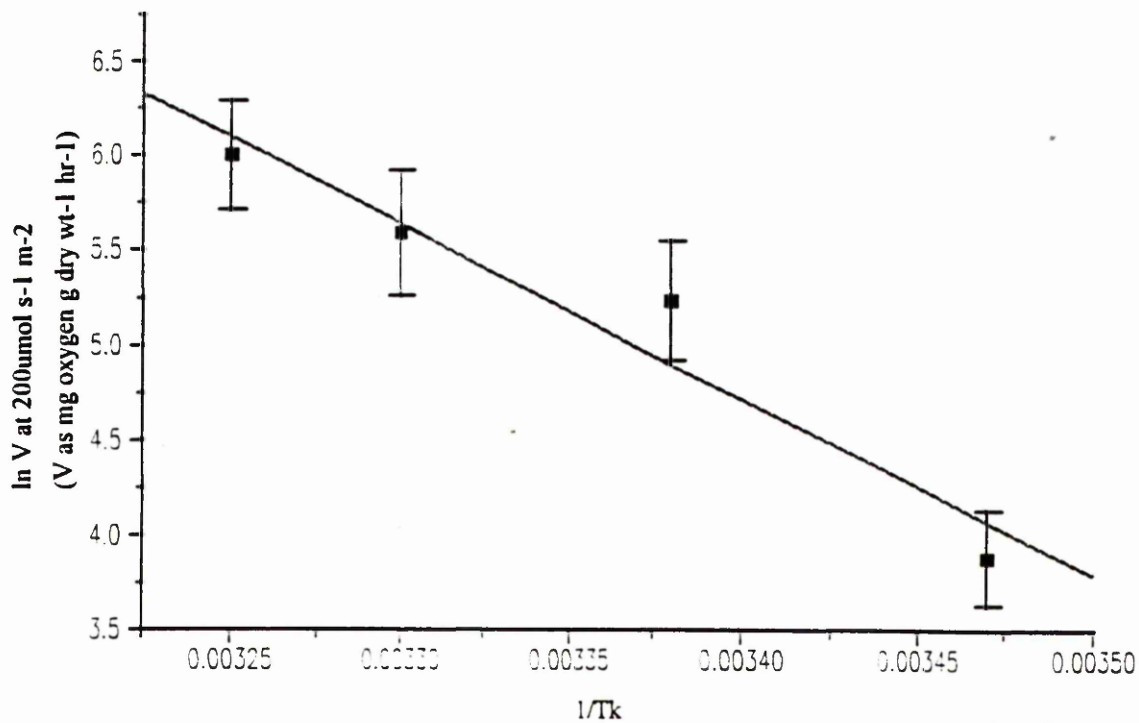


Figure 180. Arrhenius plot of ln photosynthetic rate at a PFD of $200\mu\text{mol s}^{-1} \text{m}^{-2}$ against increasing P/I incubation temperature for *Chlorella vulgaris* 211/11c cultured at a temperature of 15°C.

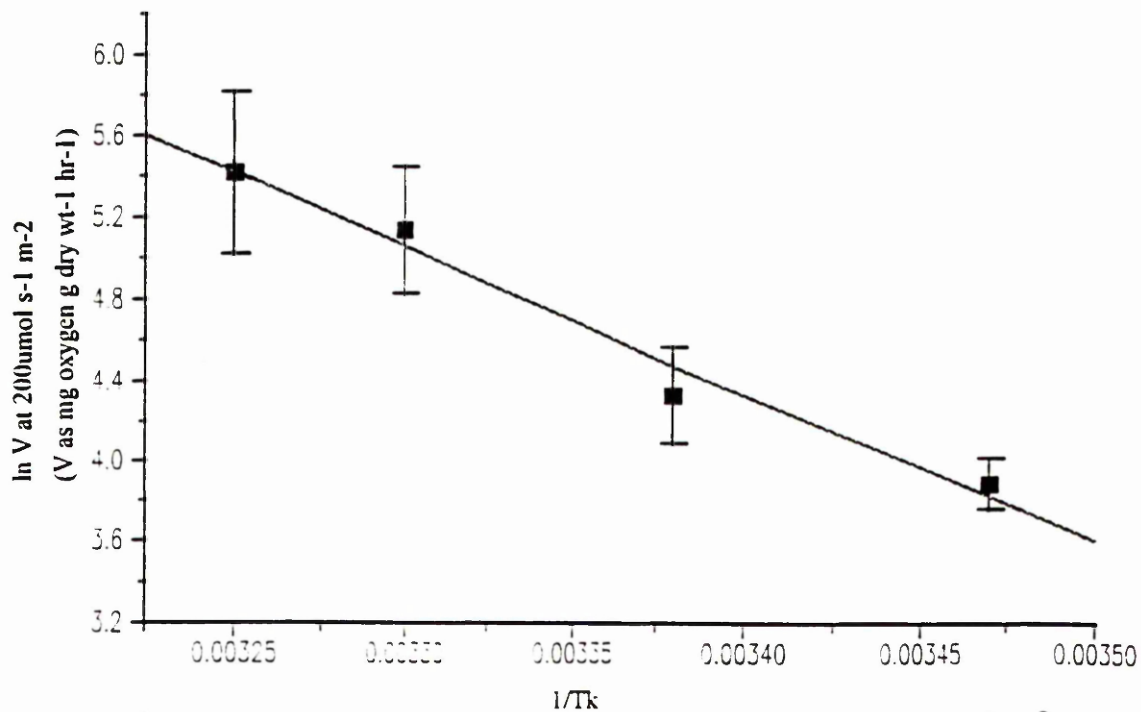


Figure 181. Arrhenius plot of ln photosynthetic rate at a PFD of $200\mu\text{mol s}^{-1} \text{m}^{-2}$ against increasing P/I incubation temperature for *Chlorella vulgaris* 211/11c cultured at a temperature of 23°C.

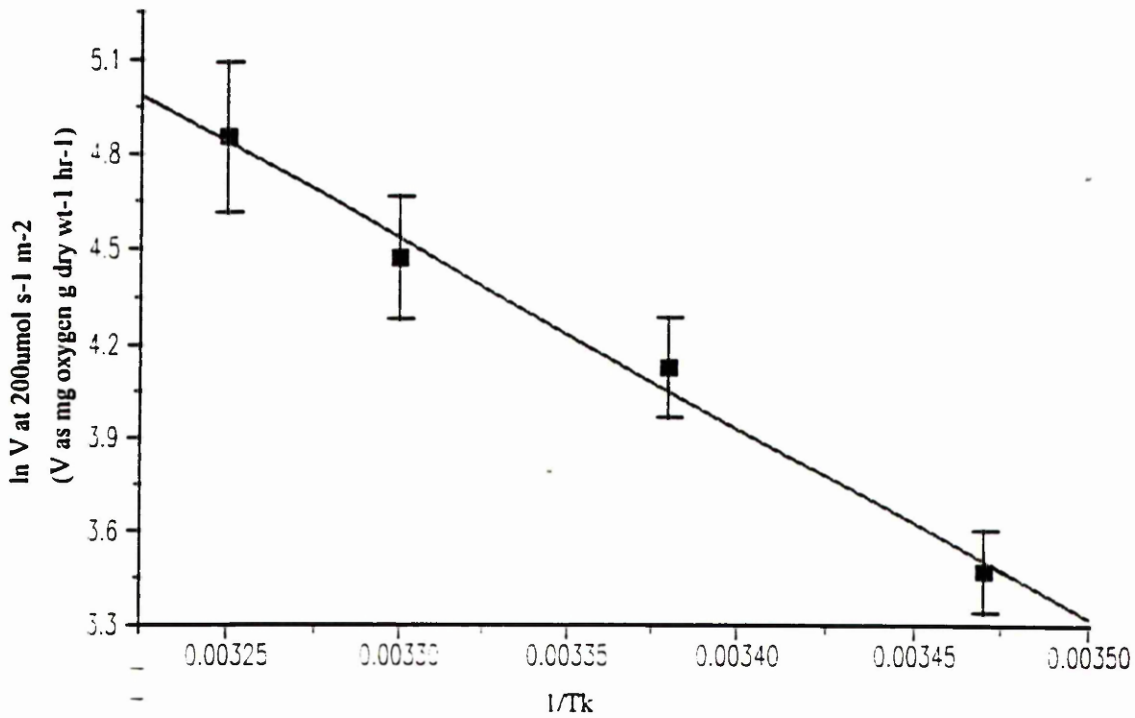


Figure 182. Arrhenius plot of ln photosynthetic rate at a PFD of $200\mu\text{mol s}^{-1} \text{m}^{-2}$ against increasing P/I incubation temperature for *Chlorella vulgaris* 211/11c cultured at a temperature of 30°C.

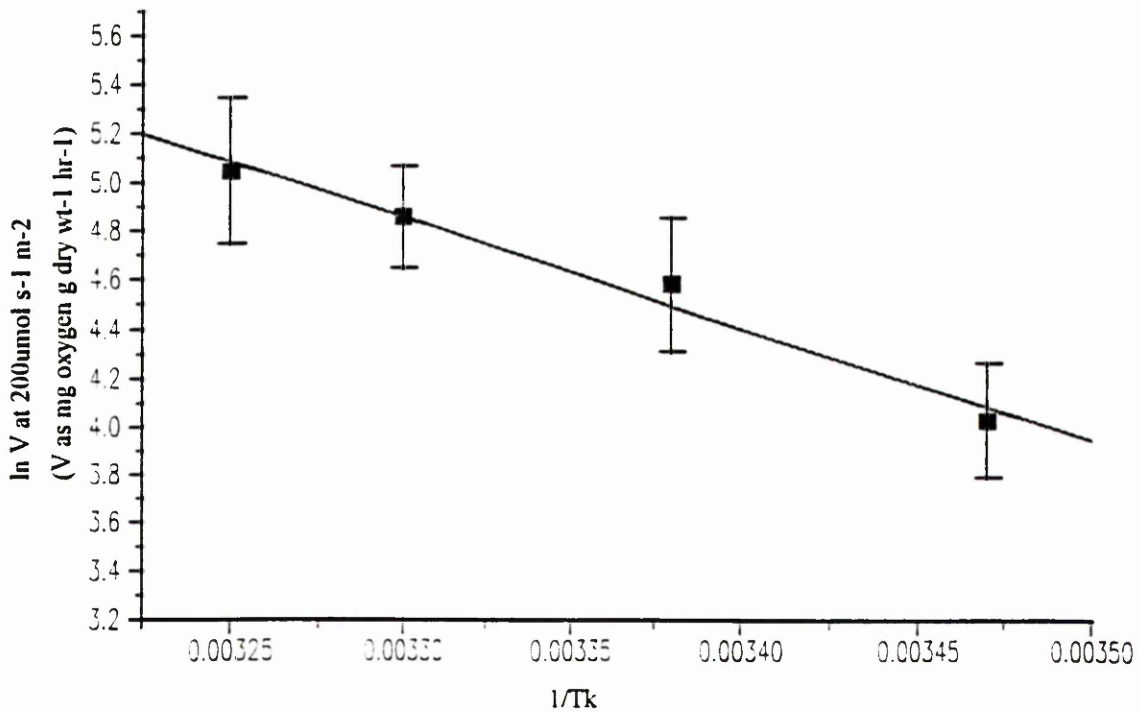


Figure 183. Arrhenius plot of ln photosynthetic rate at a PFD of $200\mu\text{mol s}^{-1} \text{m}^{-2}$ against increasing P/I incubation temperature for *Chlorella vulgaris* 211/11c cultured at a temperature of 35°C.

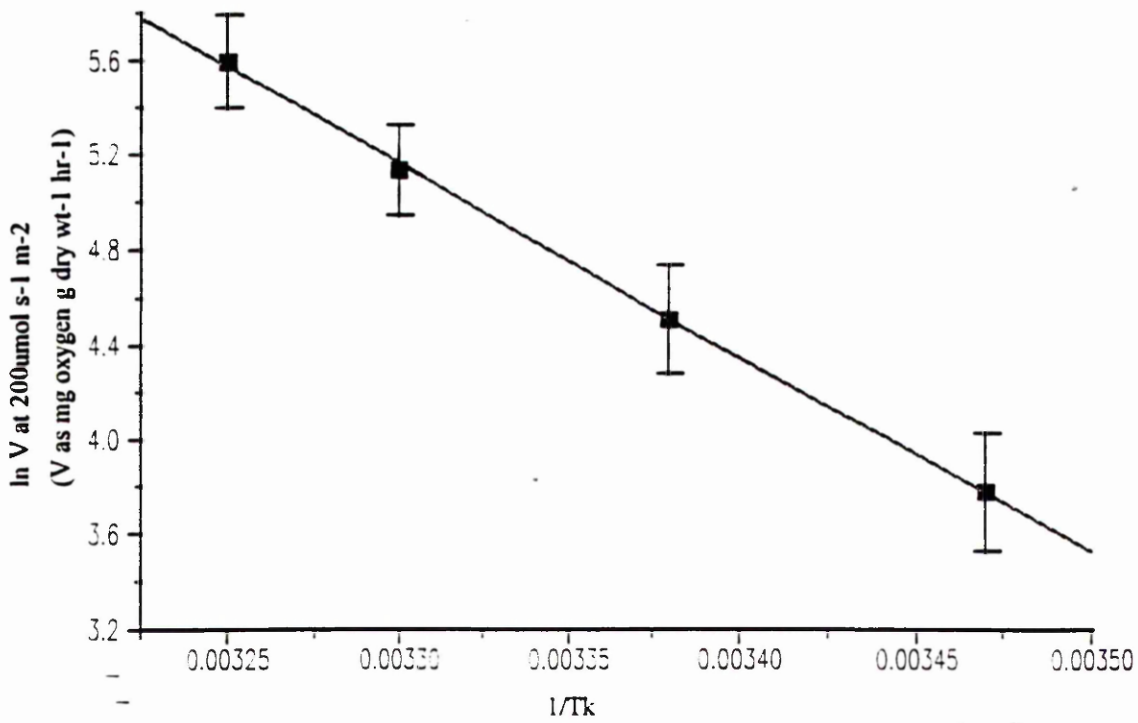


Figure 184. Arrhenius plot of ln photosynthetic rate at a PFD of $200\mu\text{mol s}^{-1} \text{m}^{-2}$ against increasing P/I incubation temperature for *Scenedesmus sp.* cultured at a temperature of 15°C .

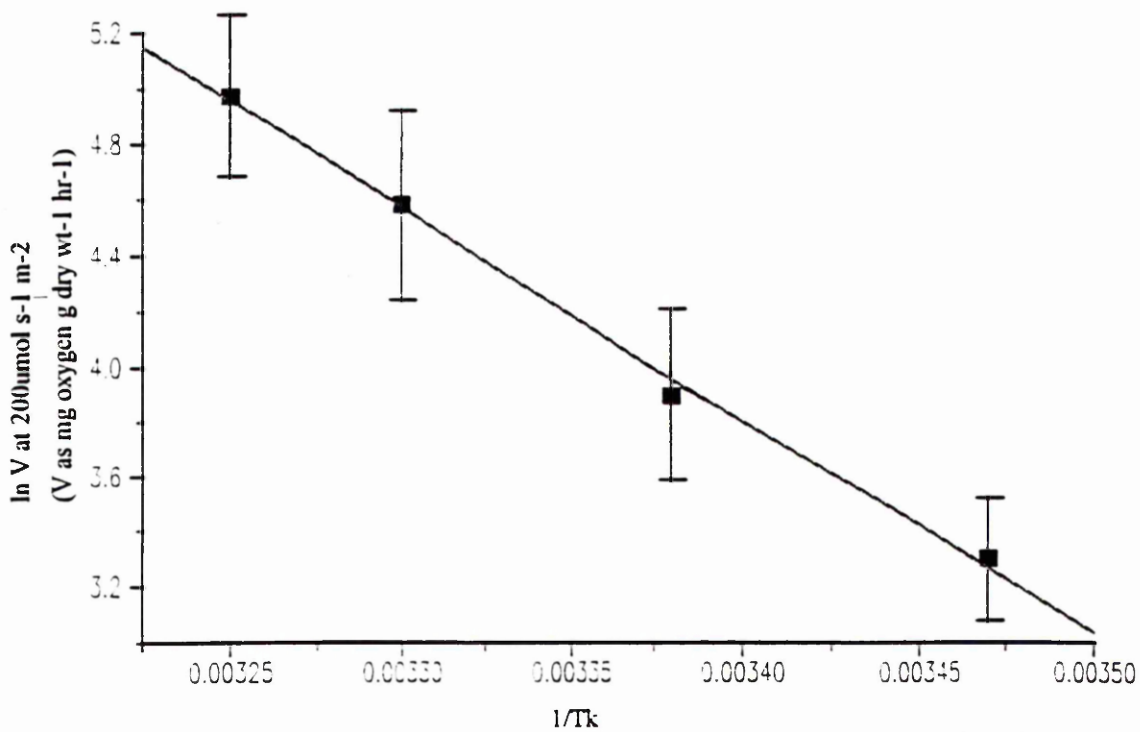


Figure 185. Arrhenius plot of ln photosynthetic rate at a PFD of $200\mu\text{mol s}^{-1} \text{m}^{-2}$ against increasing P/I incubation temperature for *Scenedesmus sp.* cultured at a temperature of 23°C .

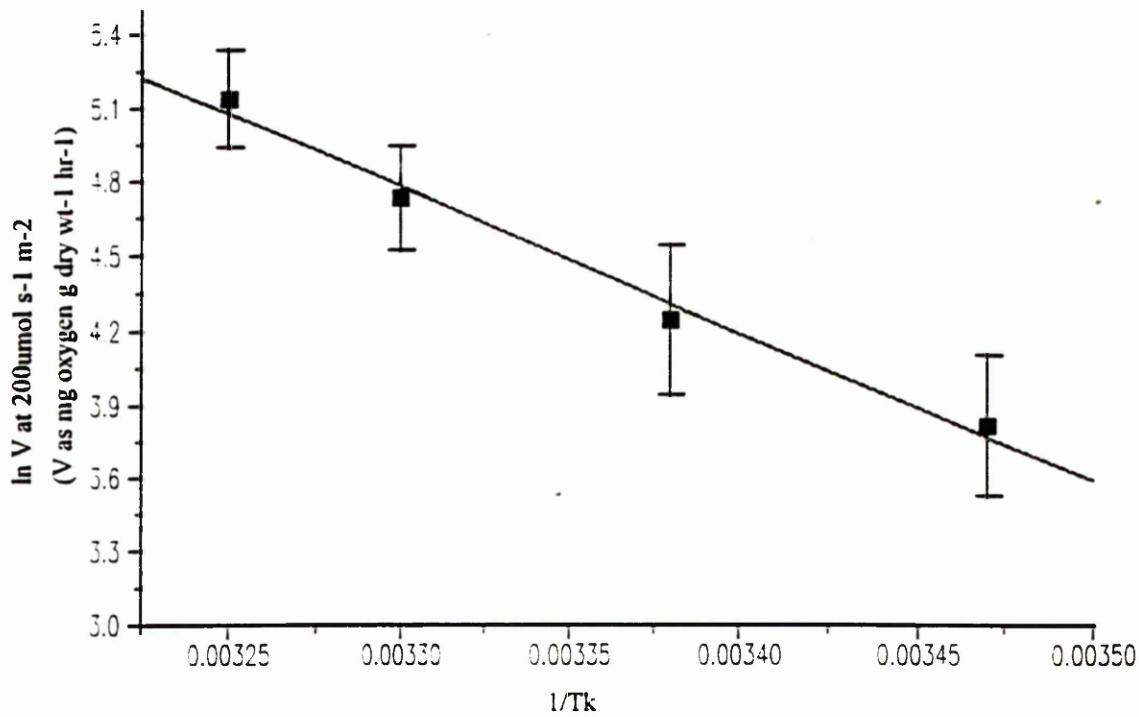


Figure 186. Arrhenius plot of ln photosynthetic rate at a PFD of $200\mu\text{mol s}^{-1} \text{m}^{-2}$ against increasing P/I incubation temperature for *Scenedesmus sp.* cultured at a temperature of 30°C .

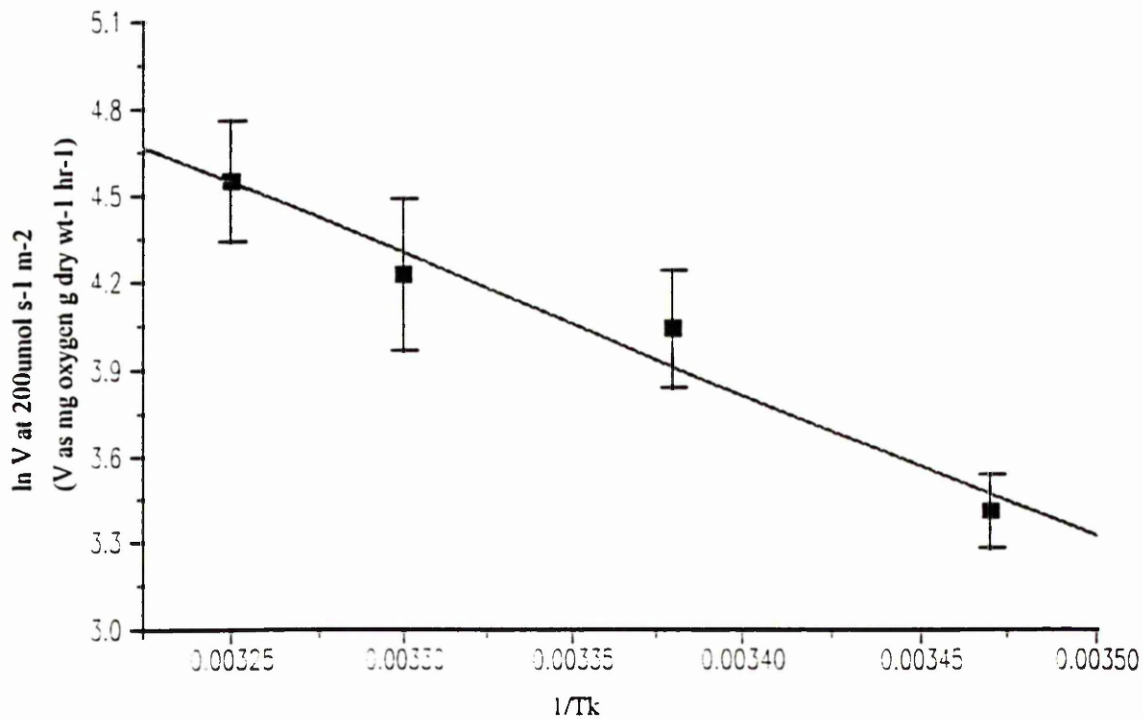


Figure 187. Arrhenius plot of ln photosynthetic rate at a PFD of $200\mu\text{mol s}^{-1} \text{m}^{-2}$ against increasing P/I incubation temperature for *Scenedesmus sp.* cultured at a temperature of 35°C .

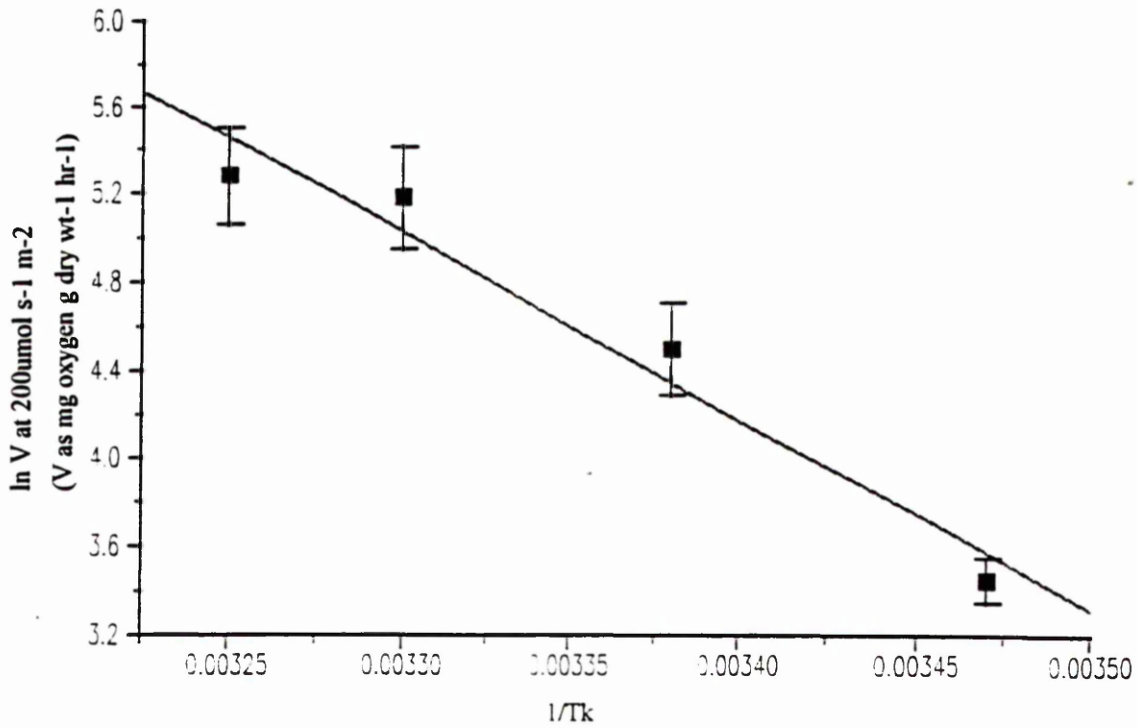


Figure 188. Arrhenius plot of ln photosynthetic rate at a PFD of $200 \mu\text{mol s}^{-1} \text{m}^{-2}$ against increasing P/I incubation temperature for *Synechococcus* 1479/5 cultured at a temperature of 15°C .

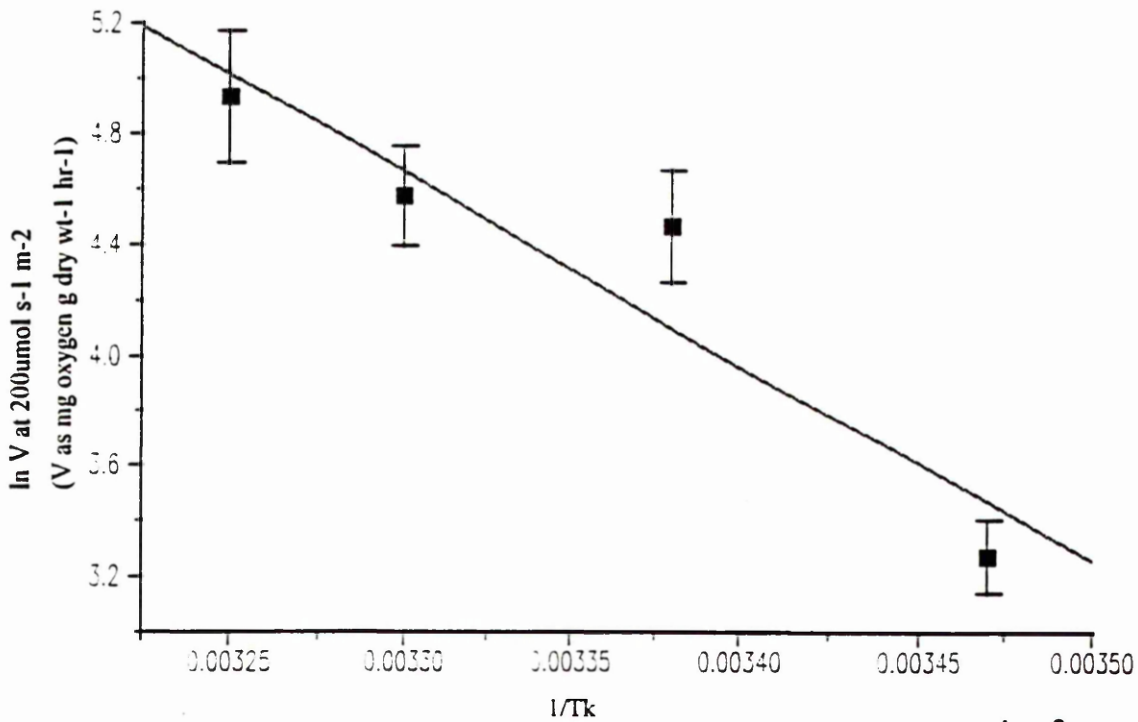


Figure 189. Arrhenius plot of ln photosynthetic rate at a PFD of $200 \mu\text{mol s}^{-1} \text{m}^{-2}$ against increasing P/I incubation temperature for *Synechococcus* 1479/5 cultured at a temperature of 23°C .

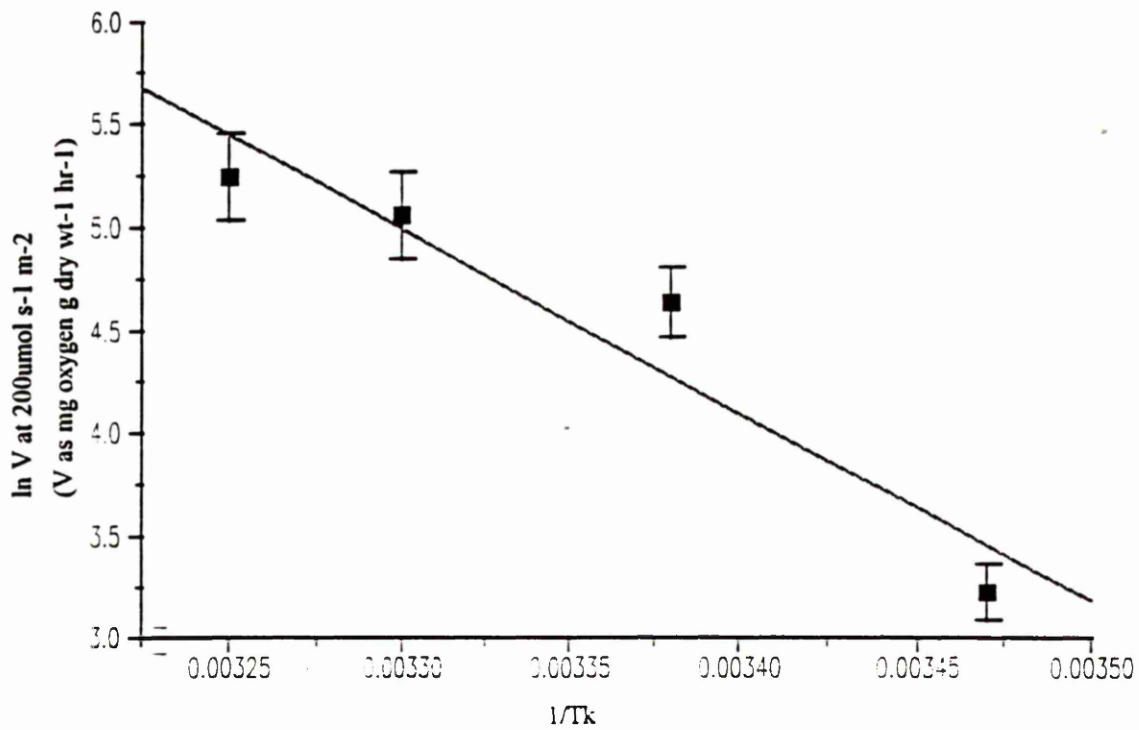


Figure 190. Arrhenius plot of ln photosynthetic rate at a PFD of $200\mu\text{mol s}^{-1} \text{m}^{-2}$ against increasing P/I incubation temperature for *Synechococcus* 1479/5 cultured at a temperature of 30°C .

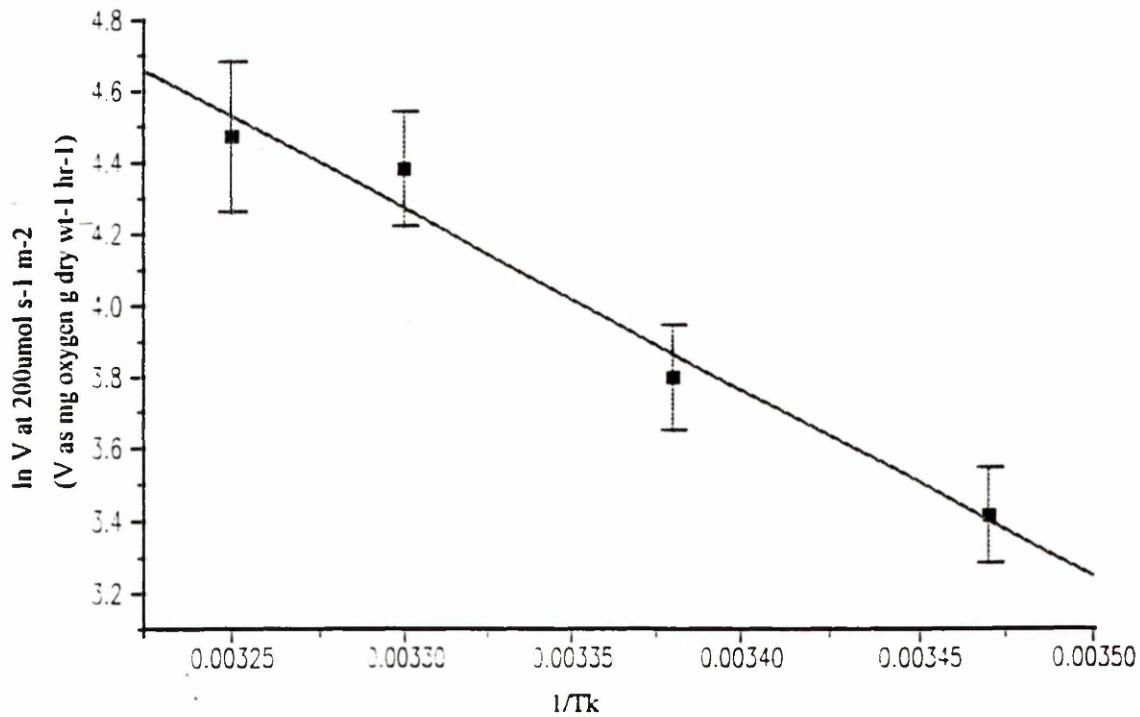


Figure 191. Arrhenius plot of ln photosynthetic rate at a PFD of $200\mu\text{mol s}^{-1} \text{m}^{-2}$ against increasing P/I incubation temperature for *Synechococcus* 1479/5 cultured at a temperature of 35°C .

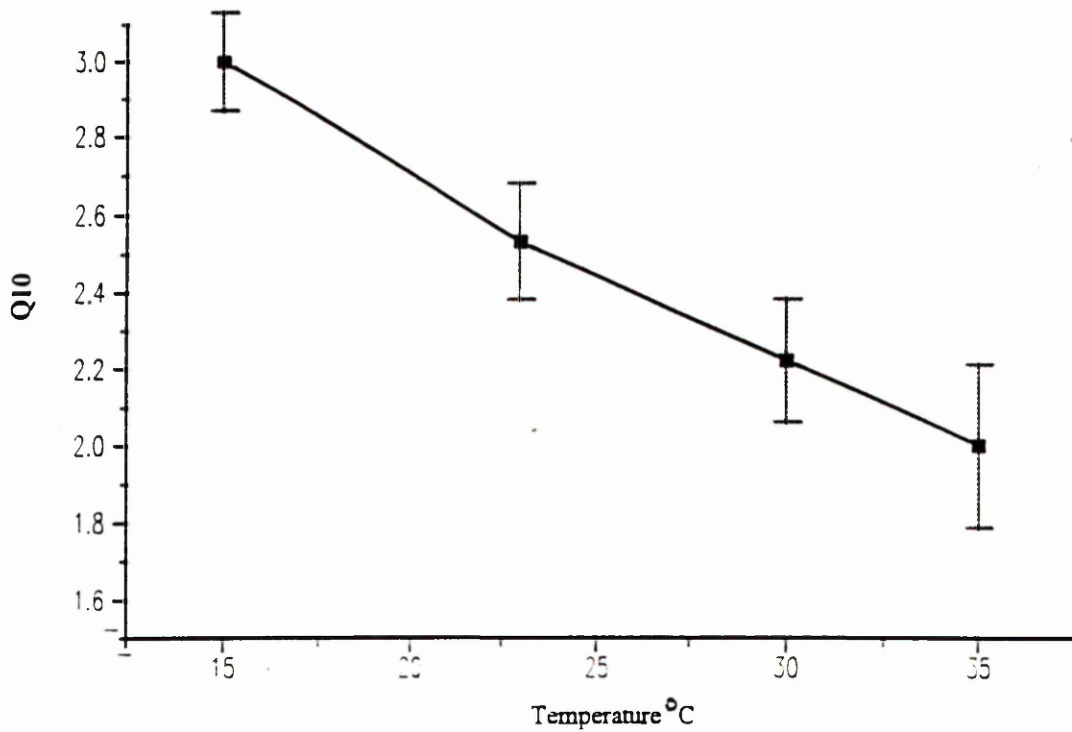


Figure 192. Variation in the Q₁₀ values with increasing temperature for *Chlorella vulgaris* 211/11c.

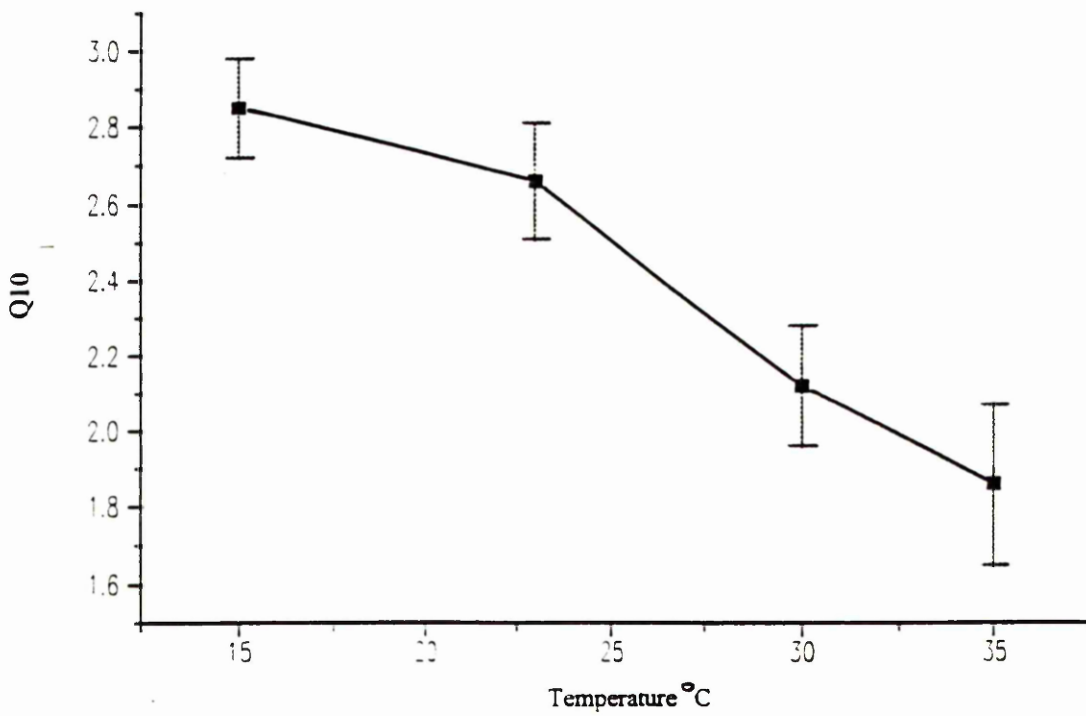


Figure 193. Variation in the Q₁₀ values with increasing temperature for *Scenedesmus* sp.

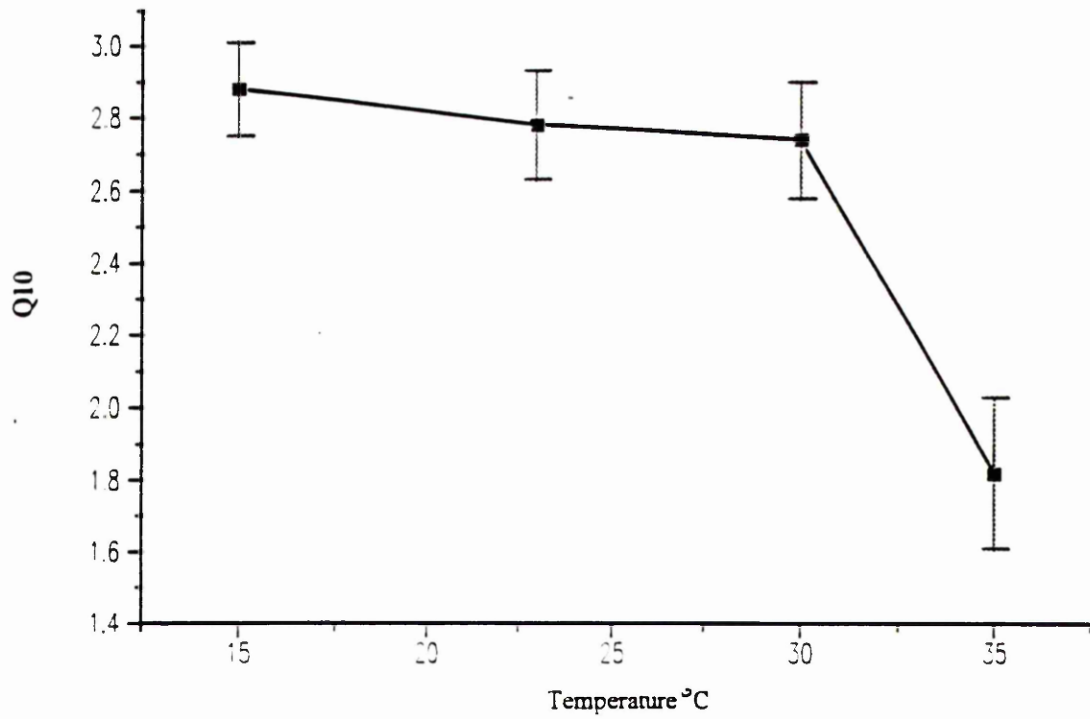


Figure 194. Variation in the Q10 values with increasing temperature for *Synechococcus* 1479/5.

It was generally found that the light limited slope α of the photosynthesis / irradiance curve was higher from cultures of *Chlorella vulgaris* 211/11c grown with a PFD of $200\mu\text{mol s}^{-1} \text{m}^{-2}$ (Tables 69, 70, 71 and 72) compared to cultures grown at a PFD of $100\mu\text{mol s}^{-1} \text{m}^{-2}$ (Tables 33, 34, 35 and 36). The maximum rates of photosynthesis were all higher from cells cultured at a PFD of $200\mu\text{mol s}^{-1} \text{m}^{-2}$ compared to cells cultured at a PFD of $100\mu\text{mol s}^{-1} \text{m}^{-2}$, however, the photosynthetic rates at P/I PFDs below P_{max} were similar from cells cultured at both 100 and $200\mu\text{mol s}^{-1} \text{m}^{-2}$. Although the value of I_k generally increased with increasing P/I incubation temperature, no significant difference existed between those cells cultured at a PFD of $100\mu\text{mol s}^{-1} \text{m}^{-2}$ and those cultured at a PFD of $200\mu\text{mol s}^{-1} \text{m}^{-2}$. Cells cultured with the higher PFD of $200\mu\text{mol s}^{-1} \text{m}^{-2}$ had a higher dark respiration than similar cells cultured at a PFD of $100\mu\text{mol s}^{-1} \text{m}^{-2}$. Cells cultured at a PFD of $200\mu\text{mol s}^{-1} \text{m}^{-2}$ did not display clear indications of photoinhibition shown by an absence of the value beta, compared to cells cultured at a PFD of $100\mu\text{mol s}^{-1} \text{m}^{-2}$. At first sight this suggests the possibility that the cells had in some way become photoadapted to the new irradiance of $200\mu\text{mol s}^{-1} \text{m}^{-2}$. Examination of the LEDR rates, however, suggested that the cells were suffering from photoinhibition but a reduction in oxygen evolution was not apparent. It may also suggest that incubation of cells at higher growth irradiances that are not photoinhibitory may minimise the affect of future photoinhibitory light irradiances. Changes in the rate of LEDR, however, do suggest that the cells were under some form of stress.

Similar to that observed with *Chlorella vulgaris* 211/11c, the values of α and P_{max} for cells of *Scenedesmus sp.* were generally higher in cultures irradiated with a PFD of $200\mu\text{mol s}^{-1} \text{m}^{-2}$ (Tables 73, 74, 75 and 76) compared to similar cells cultured at a PFD of $100\mu\text{mol s}^{-1} \text{m}^{-2}$ (Tables 41, 42, 43 and 44). The photosynthetic rates of cells irradiated at P/I PFDs below P_{max} were similar from cultures grown at 100 and $200\mu\text{mol s}^{-1} \text{m}^{-2}$. The value of I_k increased with increasing temperature with the exception of the 35°C PFD $100\mu\text{mol s}^{-1} \text{m}^{-2}$ irradiated. Like *Chlorella vulgaris* 211/11c, the dark respiration rates were higher from cells cultured at $200\mu\text{mol s}^{-1} \text{m}^{-2}$ compared to $100\mu\text{mol s}^{-1} \text{m}^{-2}$.

Synechococcus 1479/5 showed a similar pattern to that observed with the unicellular green algae *Chlorella vulgaris* 211/11c and *Scenedesmus sp.* in that the values of α and P_{max} were higher from cells cultured at a PFD of $200\mu\text{mol s}^{-1} \text{m}^{-2}$ compared to

100 $\mu\text{mol s}^{-1} \text{ m}^{-2}$ at the same P/I incubation temperature. No significant difference between I_k and culture irradiance was found. As was observed *Chlorella vulgaris* 211/11c and *Scenedesmus sp.* cells of *Synechococcus* 1479/5 showed similar photosynthetic rates at P/I PFDs below P_{max} from cultures grown at 100 and 200 $\mu\text{mol s}^{-1} \text{ m}^{-2}$.

The photosynthetic measurements determined from the photosynthesis / irradiance response curves of *Chlorella vulgaris* 211/11c, *Nannochloris atomus*, *Scenedesmus sp.*, *Ankistrodesmus antarcticus*, *Synechococcus* 1479/5 and *Synechococcus sp.* cultured at PFDs of 100 and 200 $\mu\text{mol s}^{-1} \text{ m}^{-2}$ demonstrated that the values of α and P_{max} increased with increasing P/I incubation temperature (15 to 35°C). These observations are similar to those recorded by other researchers. Steemann Nielsen and Jorgensen, (1968); Steemann Nielsen, (1975) and Talbot *et al.*, (1991). Steemann Nielsen, (1975) higher maximum rates of photosynthesis and I_k values with increasing experimental temperature whilst working with the marine diatom *Skeletonema costatum*. Although considered to have a primary affect of enzyme kinetics, temperature has also been shown to affect cellular carbon uptake (Coleman and Colman, 1980). The effect of temperature on the cells affinity to carbon dioxide was shown to directly affect the overall photosynthetic capacity. This point has already been described and discussed in section 3.2.3.

Talbot *et al.*, (1991) examined the combined effect of temperature and light on both the growth and photosynthesis of *Ankistrodesmus falcatus*, *Phormidium bohneri* and *Oscillatoria agardii*. As was found with the data presented in this section, the results of Talbot *et al.*, (1991) suggested that although temperature increases are usually uniform, it affects different organisms in different ways and is strictly species dependant. The effect of temperature on the photosynthesis / irradiance curves of *Ankistrodesmus falcatus* showed good agreement with that obtained with *Ankistrodesmus antarcticus* presented here. As was found with all the micro-algae and cyanobacteria, no relationship was determined between temperature and the photosynthetic parameter beta (negative slope of the photosynthesis / irradiance curve; the magnitude of which is indicative of photoinhibition). This observation was also apparently lacking from the results of Talbot *et al.*, (1991).

It is well documented that micro-algal and cyanobacterial cells respond to increasing light by a reduction in their pigment content, (Steemann Nielsen and Jorgensen, 1968; Sheridan, 1972b; Prezelin, 1976). Myers, (1970) suggested that light limited photosynthesis was primarily a function of the efficiency of a cells pigments in absorbing light energy. The data showed that the chlorophyll a specific value α_{chl} was independent of the irradiance at which the cells were grown but that the dry weight specific value α_{dw} was dependent and decreased at decreasing irradiances. The data presented here agrees with the above observations based solely on dry weight determinations, since the values of α were lower in cells cultured at a PFD of $100\mu\text{mol s}^{-1}\text{ m}^{-2}$ compared to $200\mu\text{mol s}^{-1}\text{ m}^{-2}$ for all the micro-algae and cyanobacteria used in the research. Foy and Gibson, (1982a) observed small changes (both increases and decreases) in the value of α_{chl} in response to increase in irradiance whilst working with 20 strains of planktonic blue-green cyanobacteria. Myers, (1970) also reported that the chlorophyll specific value P_{\max}^{chl} decreased at decreasing irradiances, whereas, the dry weight specific value P_{\max}^{dw} did not. The data presented here does not support this as dry weight specific values of P_{\max} increased with increasing PFD (100 to $200\mu\text{mol s}^{-1}\text{ m}^{-2}$), however, it was noted that the photosynthetic rates at P/I PFDs below P_{\max} were similar in cells cultured at 100 and $200\mu\text{mol s}^{-1}\text{ m}^{-2}$.

Increases in the rate of P_{\max}^{dw} with increasing irradiance has been recorded in *Chlorella vulgaris* 211/11h (Steemann Nielsen *et al.*, 1962) grown under light at 50 and $525\mu\text{mol s}^{-1}\text{ m}^{-2}$ whereas the value of α was found to increase with decreasing irradiance. Yentsch and Lee, (1966) observed similar increases in P_{\max}^{dw} with increasing irradiance supporting the observations presented here whilst working with the unicellular green micro-algae *Nannochloris atomus*. The differences in photosynthetic response to varying culture irradiance is thought to be more complicated than merely pigment / cell mass can explain (Geider and Osborne, 1992). Myers and Graham, (1971) found that a linear relationship existed between the cellular chlorophyll content and the size of the photosynthetic unit whilst working with *Chlorella pyrenoidosa*. It was also concluded that when the culture irradiance was reduced, cellular pigment content increased up to 5 times, whereas, the photosynthetic unit increased by only 1-1.5 times. Other work examining the effect of decreasing irradiances on the pigment content of *Dunaliella tertiolecta* (Falkowski and Owens, 1980) showed that upon decreasing the growth irradiance from 600 to $30\mu\text{mol s}^{-1}\text{ m}^{-2}$, the pigment content

increased five fold. This degree of change in pigment content is strictly species specific since the marine diatom *Skeletonema costatum* showed a fractional increase in pigment content when the growth irradiance was reduced from 130 to 20 $\mu\text{mol s}^{-1} \text{m}^{-2}$. These results were unresponsive for the proposal that pigment content was directly responsible for changes in the maximum rate of photosynthesis. Similar increases in the value of P_{max}^{dw} with increasing irradiance has been recorded in the marine diatom *Skeletonema costatum* and *Dunaliella tertiolecta* (Falkowski and Owens, 1980), however no such change occurred was recorded in α_{dw} . They found that a reduction in the value of α_{chl} occurred when the irradiance was decreased. This behaviour pattern is similar to the model of Ramus, 1981 where cells of micro-algae can alter the size and orientation of the photosynthetic single unit in direct response to changes in the light environment.

It has been argued that since the maximum rate of photosynthesis is dependent upon enzymic activity, there should be no adaptation to culture irradiance and a cells P/I response should be governed primarily by temperature and nutrient availability (Jensen and Knutsen, 1993). It has been recorded that the photosynthetic parameters determined from P/I response curves are greatly influenced by the nutrient state of the cell population, especially in environments which are stressful to a cell (Prezelin and Matlick, 1983; Prezelin *et al.*, 1986). The effect of nitrate and phosphate is discussed in sections 3.2.5 and 3.3.3. One major factor that is not usually included in photosynthesis / irradiance curves and its effect on the measurement of photosynthetic parameters (P_{max} , α and I_k) is the change in dark respiration with increasing light. Tables 63, 65 and 67 show the change in respiration of *Chlorella vulgaris* 211/11c, *Scenedesmus sp.* and *Synechococcus* 1479/5 (cultured at a PFD of 100 $\mu\text{mol s}^{-1} \text{m}^{-2}$) expressed as LEDR to DR ratio. Tables 84, 85 and 86 show the same LEDR to DR ratio for the respective organisms cells cultured at a PFD of 200 $\mu\text{mol s}^{-1} \text{m}^{-2}$. It can be seen that the LEDR / DR ratio for *Chlorella vulgaris* 211/11c was significantly higher in cells cultured at the higher irradiance of 200 $\mu\text{mol s}^{-1} \text{m}^{-2}$ compared to cells cultured at a PFD of 100 $\mu\text{mol s}^{-1} \text{m}^{-2}$. A similar observation (some points of non conformity were apparent at the higher culture temperature of 35°C) was also seen with cells of *Scenedesmus sp.* and *Synechococcus* 1479/5. The higher LEDR rates measured from cells cultured at the higher irradiance of 200 $\mu\text{mol s}^{-1} \text{m}^{-2}$ were significantly higher than LEDR rates measured in cells cultured at a PFD of 100 $\mu\text{mol s}^{-1} \text{m}^{-2}$. This suggests that cells may have photoadapted themselves to the increase in

PFD which changed both the dark respiration rate, LEDR rate and photosynthetic kinetics accordingly. The higher LEDR rates observed in cells of *Chlorella vulgaris* 211/11c, *Scenedesmus sp.* and *Synechococcus* 1479/5 suggests that the changes in dark respiration is dependent mainly on light but is not entirely independent of temperature. Further evidence to support the proposal that LEDR may be dependent on mainly light can be seen in Figures 97, 109, 121, 133, 145 and 157 for *Chlorella vulgaris* 211/11c, *Nannochloris atomus*, *Scenedesmus sp.*, *Ankistrodesmus antarcticus*, *Synechococcus* 1479/5 and *Synechococcus sp.* respectively. Each Figure shows the changes in dark respiration rate and LEDR rate from cells cultured at 35°C measured at different P/I incubation temperatures. It can be seen that the respiration rate changes very slightly with changing temperature, whereas the LEDR rate increases significantly for each organism, suggesting that light was directly responsible for the increase. Gallon *et al.*, (1993) reported similar findings whilst working with the cyanobacterium *Anabaena cylindrica* cultured at 25°C which demonstrated no change in respiration rate when incubated at a temperature of 40°C. It has been suggested that light enhanced dark respiration or post illumination enhanced respiration is chiefly caused by an increase in the availability of respiratory substrates (Beito and Osmond, 1983). This increase in substrate availability requires oxidation, achieved by increasing oxygen consumption by the cell. The increase in LEDR rate, however, can be measured in cells immediately after a relatively short exposure time to the light which suggests that enhances in respiration were primarily linked to the early products of photosynthesis. Although Figures 97, 109, 121, 133, 145 and 157 show that light was the main contributor to changes in LEDR the effect of temperature can not be entirely ruled out. If LEDR is linked to the formation of the early products of photosynthesis, then the formation of such compounds would rely heavily on enzyme controlled reaction rates which is governed to a large extent by temperature. Since the initial dark respiration was found to change very little at the higher P/I incubation temperatures, it would suggest that photodamaging light was the reason for increased oxygen uptake. Further evidence for this comes from the observations that the fact that during photosynthetic / irradiance response curve measurements cells received the same dosage of light, irrespective of growth temperature and growth irradiance. Yet the LEDR / DR ratios of micro-algae as described above, were higher in cells cultured at a PFD of 200 compared to 100 $\mu\text{mol s}^{-1} \text{m}^{-2}$ suggesting that light history plays a major role. Further discussion on the mechanism of LEDR and its role of photosynthesis can be found in section 3.10.

3.5 Light / dark cycling.

Chlorella vulgaris 211/11c and *Synechococcus* 1479/5 were used to study the effects of light / dark cycling on the photosynthesis and respiration of cells when irradiated with light intensities at and beyond P_{max} . In an oxygen electrode, previous studies had determined that a response time of between 7 and 10 seconds was required for the probe to reach within 90-95% of the final measured value. Measurements on specific photosynthetic or respiration rates were only measured when the minimum time spent in either light or dark was no less than 10 seconds. As the relay timer had a maximum delay of 280 seconds, that too was a constraint on the maximum time spent in either the light or the dark. To ensure that the cells did not become nutrient limited additions of 400mg C l^{-1} (NaHCO_3 pH 7.0) every 8 hours dissolved in 100% ASM were made. These additions were made to the chamber using a small sterile hypodermic placed through a needle size hole in the top of the electrode chamber. Oxygen saturation of the incubating medium was between 20 and 50% at the start of each experiment and was never higher than 85% saturation at the end. A time period of twenty four hours was chosen as some cultures were known to approach 100% oxygen saturation at high light to dark ratios and since aquatic pond systems seldom have a constant surface irradiance it was decided for convenience to limit the experiments to this time period.

All experiments carried out in Figures 195-218 were based on monitoring the state of the photosynthetic capacity and/or respiration of cells incubated in light / dark cycles of known duration. Unless stated, all experiments were carried out for 24 hours, although for appearance and to show the variation in the response, all Figures do not show the X axis data up to 24 hours. All experiments were carried out at a temperature of 23°C .

3.5.1 The effect of light / dark cycles of medium frequency on the photosynthesis of *Chlorella vulgaris* 211/11c.

Figure 195 shows the results of incubating cells of *Chlorella vulgaris* 211/11c in various light / dark cycles whilst irradiated at a PFD of $300\mu\text{mol s}^{-1} \text{m}^{-2}$. It can be seen that cells incubated in a light / dark cycle of 30:02 seconds showed a reduction in

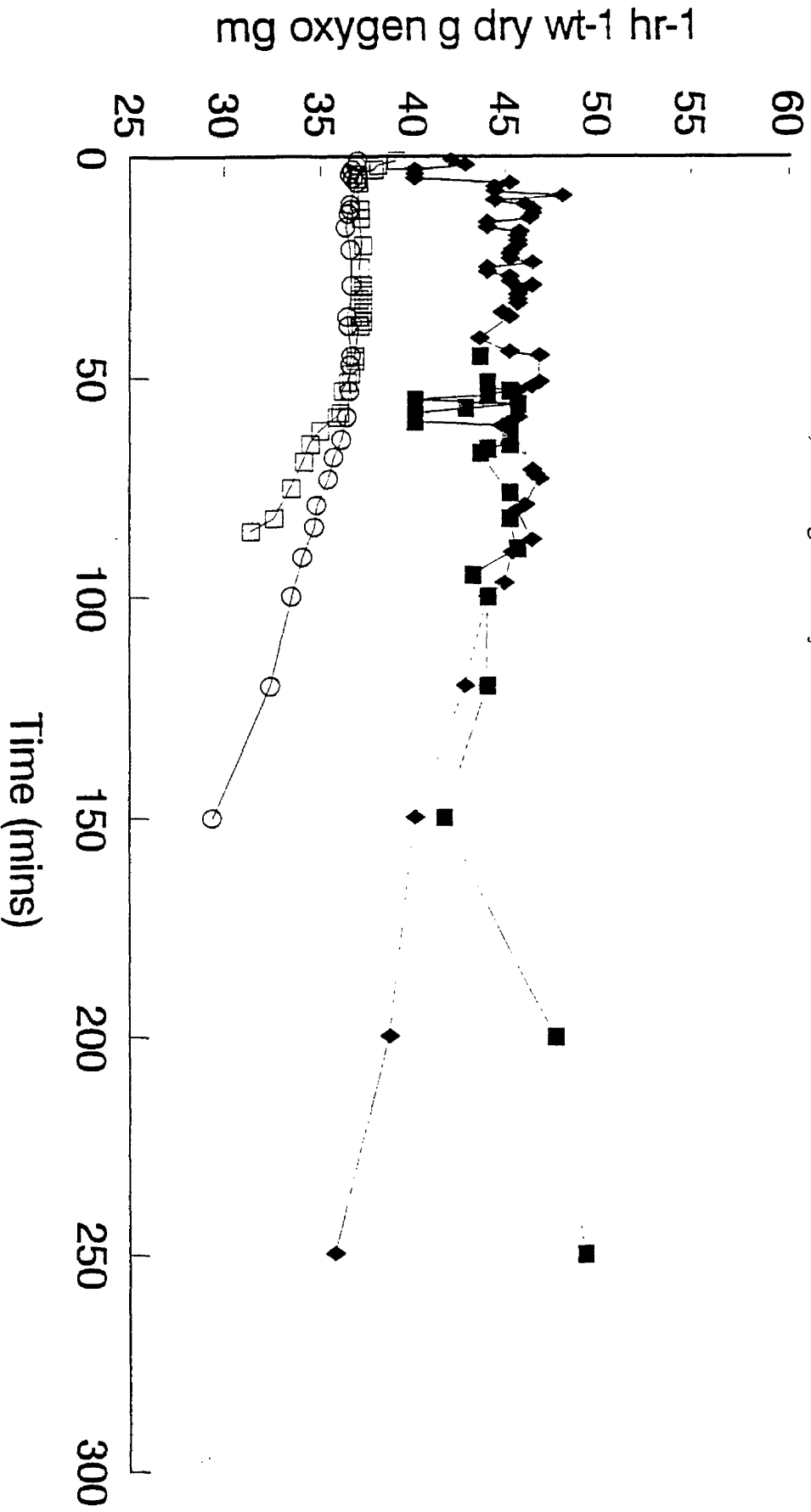


Figure 195. The effect of light / dark cycles at a PFD of $300\mu\text{mol s}^{-1} \text{m}^{-2}$ on the maximum rate of photosynthesis of *Chlorella vulgaris* 211/1c, □—□ light / dark cycle of 30:02 seconds, ○—○ light / dark cycle of 30:05 seconds, ◆—◆ light / dark cycle of 30:10 seconds, ■—■ light / dark cycle of 30:15 seconds.

the photosynthetic rate after 50 minutes. In order to maintain a constant photosynthetic rate for a period of 24 hours, *Chlorella vulgaris* 211/11c required a dark period of 15 seconds (L / D ratio of 2:1).

Figure 195a shows the results of irradiating cells of *Chlorella vulgaris* 211/11c in various light / dark cycles at a PFD of $300\mu\text{mol s}^{-1} \text{m}^{-2}$. Irradiated constantly at this PFD for more than 6 minutes resulted in a decline in the photosynthetic rate. An incubation period of 20 seconds in the dark was necessary for the cells of *Chlorella vulgaris* 211/11c to maintain a constant photosynthetic rate whilst irradiated with a 60 second exposure to light of PFD $300\mu\text{mol s}^{-1} \text{m}^{-2}$. This constant rate was monitored and maintained at a light / dark ratio of 3:1 for 24 hours.

Figure 196 shows the respiration rates of *Chlorella vulgaris* 211/11c measured during the light / dark cycling experiments carried out to obtain the constant rate recorded in Figure 195a. After each exposure to the PFD of $300\mu\text{mol s}^{-1} \text{m}^{-2}$ the respiration oxygen consumption rate was recorded. It can be seen that the dark respiration is relatively constant with time. It is suggested that increases in dark respiration can be indicative of cellular photodamage. Experiments carried out on the effects of light on LEDR displayed that light irradiances of PFDs above $\frac{1}{2}P_{\text{max}}$ begin to cause slight increases oxygen uptake to be observed (Ratchford and Fallowfield unpublished). Irradiances at PFDs at P_{max} can double the oxygen uptake rate whereas the most significant increases in respiration are observed at PFDs at photoinhibitory levels where LEDR can be 10 times the original dark respiration rate (Geider and Osborne, 1992).

The light / dark cycling results of *Chlorella vulgaris* 211/11c irradiated for 80 seconds at a PFD of $300\mu\text{mol s}^{-1} \text{m}^{-2}$ are shown in Figure 197. It was found that the cells required a recovery time of 35 seconds after being irradiated with light at a PFD of $300\mu\text{mol s}^{-1} \text{m}^{-2}$ for 80 seconds.

Figure 198 shows the light / dark cycle data obtained from *Chlorella vulgaris* 211/11c when irradiated at a PFD of $300\mu\text{mol s}^{-1} \text{m}^{-2}$ for 120 seconds. When incubated in a light / dark cycle of 120:20 seconds (6:1 ratio) the photosynthetic rate began to decline after 30-40 minutes. Increasing the duration of the dark cycle to 40 seconds whilst maintaining a constant light duration, giving an overall ratio of 3:1, extended

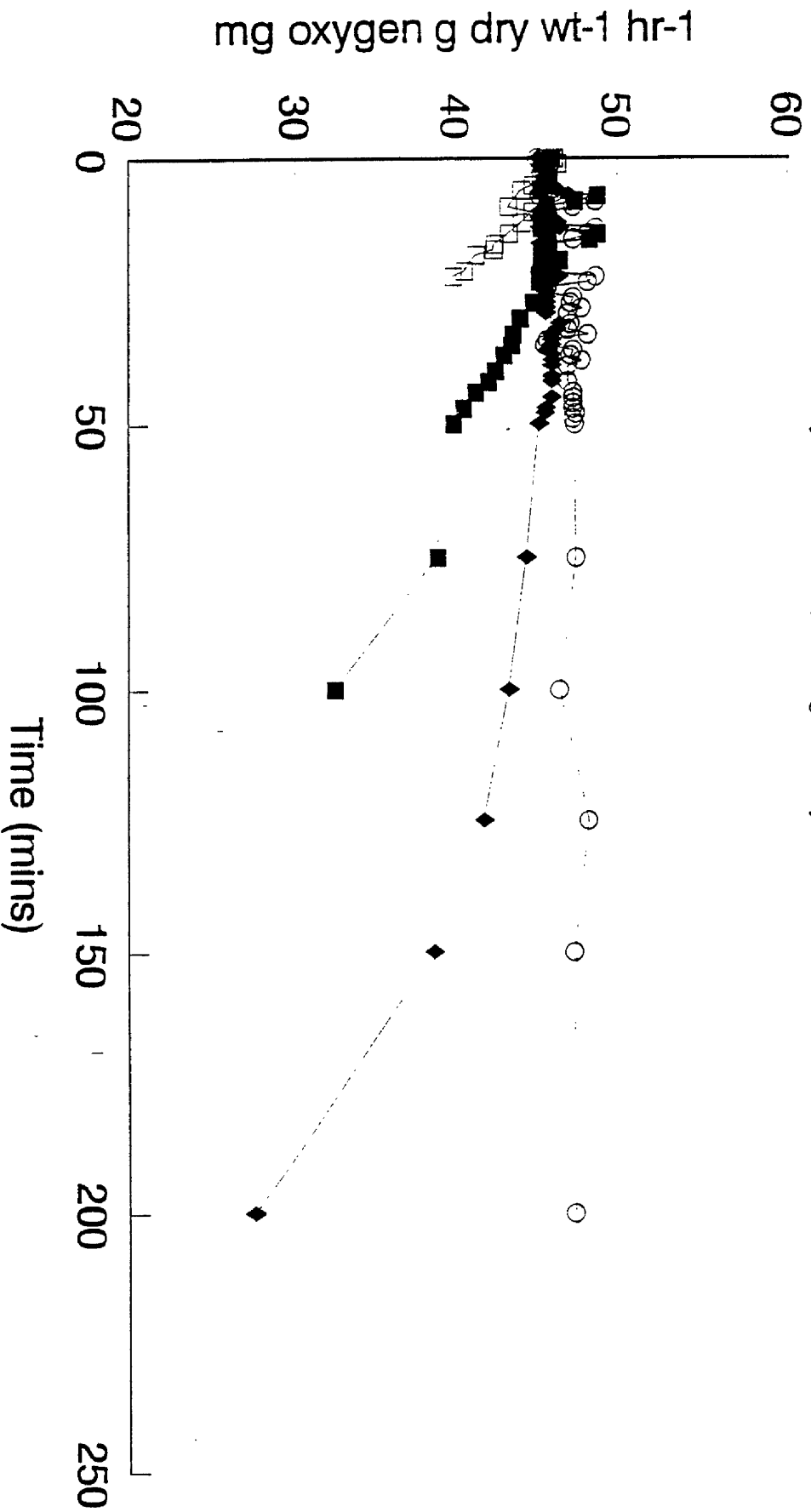


Figure 195a. The effect of light / dark cycles at a PFD of $300\mu\text{mol s}^{-1} \text{m}^{-2}$ on the maximum rate of photosynthesis of *Chlorella vulgaris* 211/11c, \square — \square light of PFD $300\mu\text{mol s}^{-1} \text{m}^{-2}$, \blacksquare — \blacksquare light / dark cycle of 60:10 seconds, \diamond — \diamond continuous light of PFD $300\mu\text{mol s}^{-1} \text{m}^{-2}$, \circ — \circ light / dark cycle 60:15 seconds, \circ — \circ light / dark cycle 60:20 seconds.

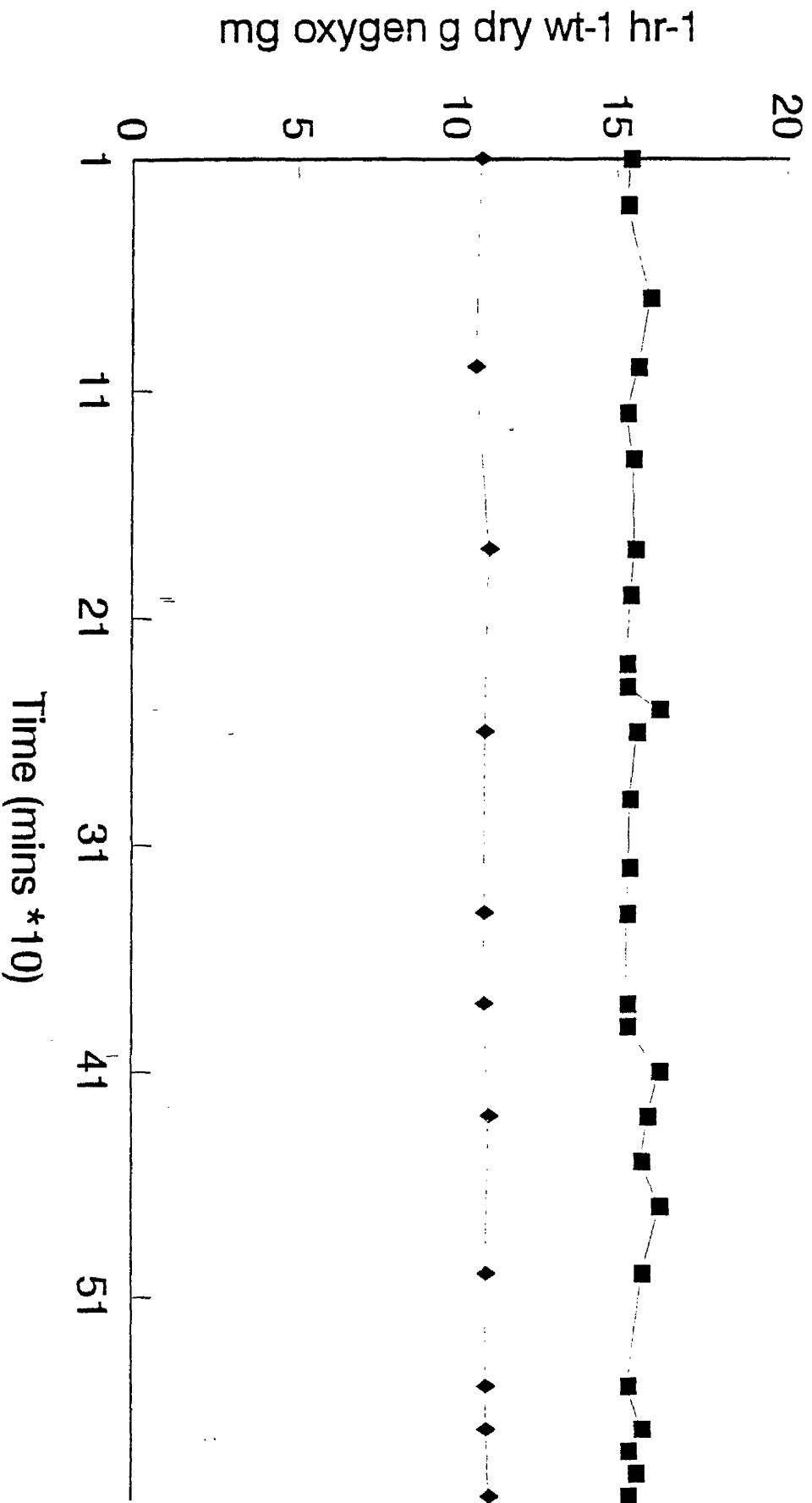


Figure 196. The effect of light / dark cycles of 60:20 seconds at a PFD of 300 $\mu\text{mol s}^{-1} \text{m}^{-2}$ on the photosynthesis and respiration of *Chlorella vulgaris* 211/1c, ■—■ maximum rate of photosynthesis, ◆—◆ respiration rate.

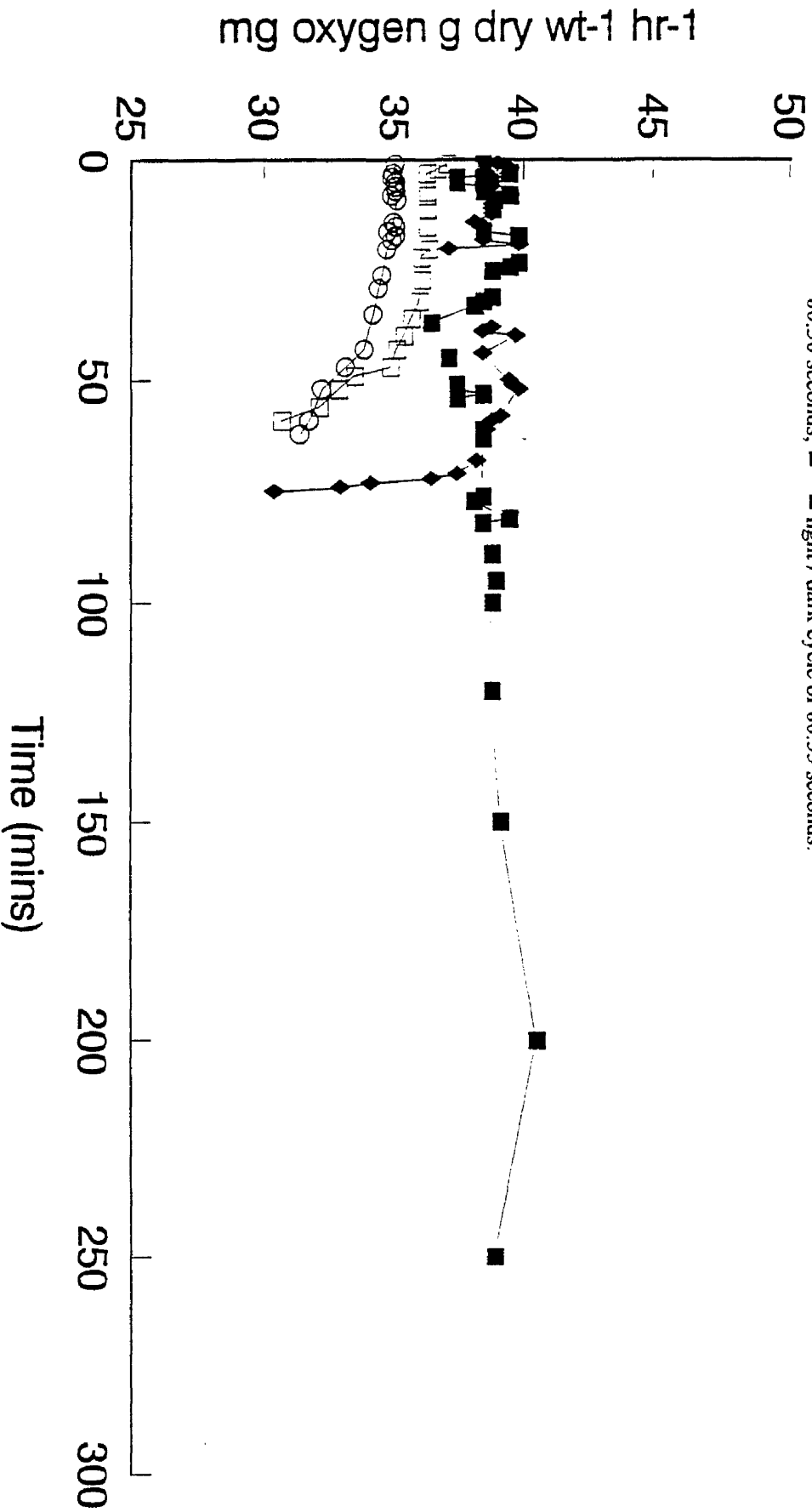
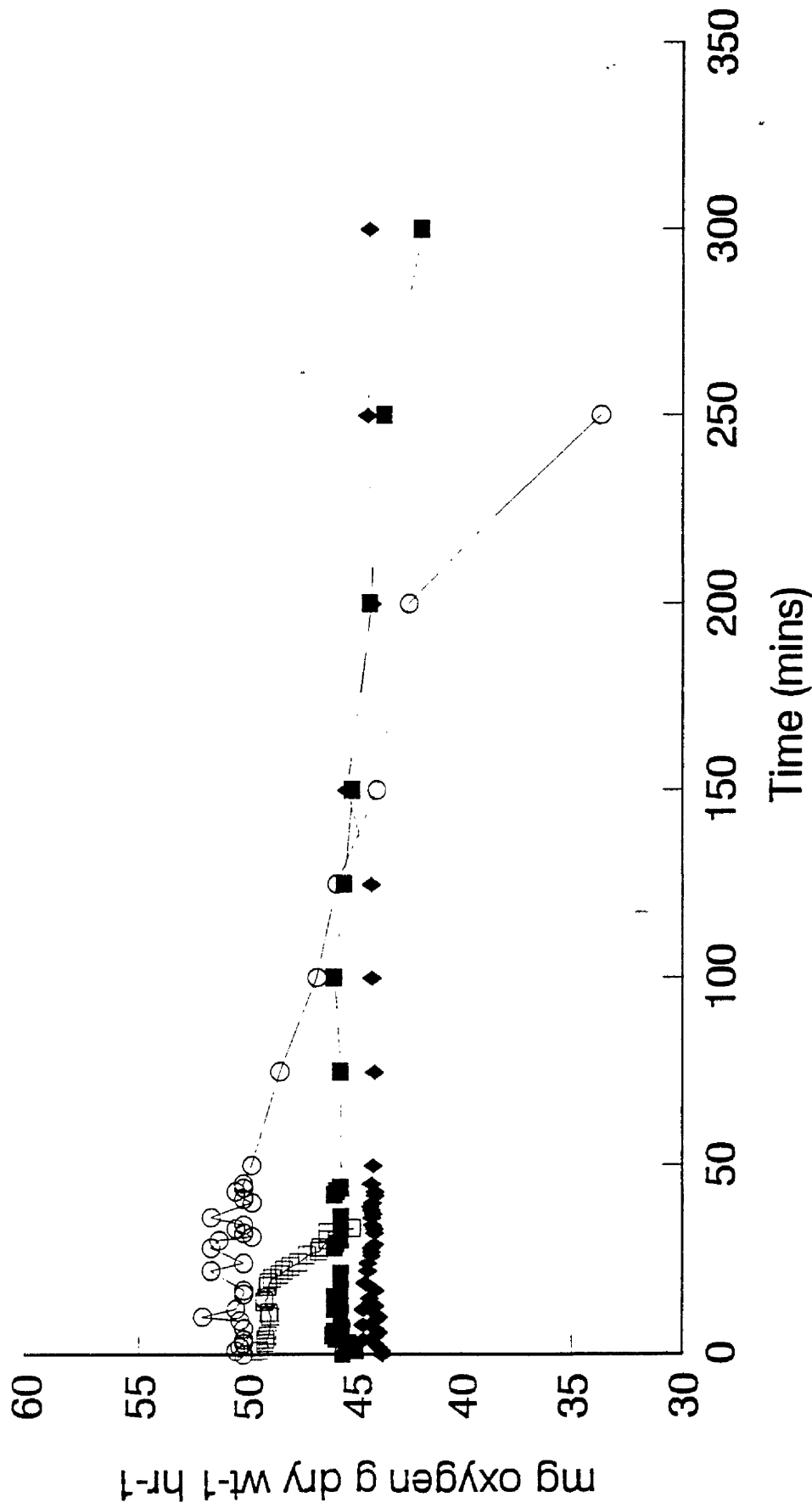


Figure 197. The effect of light / dark cycles at a PFD of 300 μmol s⁻¹ m⁻² on the maximum rate of photosynthesis of *Chlorella vulgaris* 211/1 Ic. O—O light / dark cycle of 80:20 seconds, □—□ light / dark cycle of 80:25 seconds, ◆—◆ light / dark cycle of 80:30 seconds, ■—■ light / dark cycle of 80:35 seconds.

Figure 198. The effect of light / dark cycles at a PFD of $300 \mu\text{mol s}^{-1} \text{m}^{-2}$ on the maximum rate of photosynthesis of *Chlorella vulgaris* 211/11c, \square — \square light / dark cycle 120:20 seconds, \circ — \circ light / dark cycle of 120:30 seconds, \blacksquare — \blacksquare light / dark cycle 120:40 seconds, \blacklozenge — \blacklozenge light / dark cycle 120:50 seconds.



the time period before a decline in photosynthetic rate was observed. This suggested that although in Figure 195 the cells maintained a constant photosynthetic rate at a light / dark cycle ratio of 3:1, doubling the light cycle from 60-120 seconds as in the case of Figure 198 did not necessarily require a doubling of the dark cycle duration. As can be seen a ratio of 2.4:1 (L / D cycle of 120 : 50 seconds) was required to prevent the onset of photoinhibition and photodamage.

Figure 199 shows the results obtained when *Chlorella vulgaris* 211/11c was irradiated at a PFD of $300\mu\text{mol s}^{-1} \text{m}^{-2}$ in a light period of 200 seconds. Various light / dark cycle ratios were employed and it was observed that ratios as low as 2:1 were now insufficient to prevent a decline in the photosynthetic rate. At a light / dark cycle ratio of 200:150 seconds (1.33:1), however, *Chlorella vulgaris* 211/11c maintained a constant photosynthetic rate for a period of 18 hours.

Figure 200 shows the data obtained from incubating *Chlorella vulgaris* 211/11c in light / dark cycles whilst irradiated at a PFD of $500\mu\text{mol s}^{-1} \text{m}^{-2}$. In each experiment the cells were exposed to a 30 second irradiance of light at this PFD. In continuous light of PFD $500\mu\text{mol s}^{-1} \text{m}^{-2}$ cell photosynthetic rates were observed to decline within a few minutes. The effects of this photoinhibitory light, however, were offset by incubating the cells in a light / dark ratio of 30:60 seconds (1:2). In order to fully recover from being irradiated with light at a PFD of $500\mu\text{mol s}^{-1} \text{m}^{-2}$ cells now required a longer period in the dark than in the light. Although no experiments performed in this section were found to give a successful recovery ratio of 1:1, it is suggested that the maximum PFD required for this ratio lay between 300 and $500\mu\text{mol s}^{-1} \text{m}^{-2}$. It should be noted that this was entirely dependent on the length of duration of the initial exposure irradiance.

Figure 201 shows the results of monitoring respiration rates when cells of *Chlorella vulgaris* 211/11c were incubated in light / dark cycles at a PFD of $500\mu\text{mol s}^{-1} \text{m}^{-2}$ (Figure 200). Whereas Figure 200 examined the effects of light / dark cycling on photosynthetic rate Figures 201 shows the effects of the same light / dark cycles on respiration rates. When irradiated with continuous light of PFD $500\mu\text{mol s}^{-1} \text{m}^{-2}$ dark respiration can be seen to increase rapidly for the first 5-10 minutes. There then followed a steady increase at a lower rate than before 10 minutes. This was monitored for a further 15 minutes. A light / dark cycle of 30:60 seconds at this PFD showed an

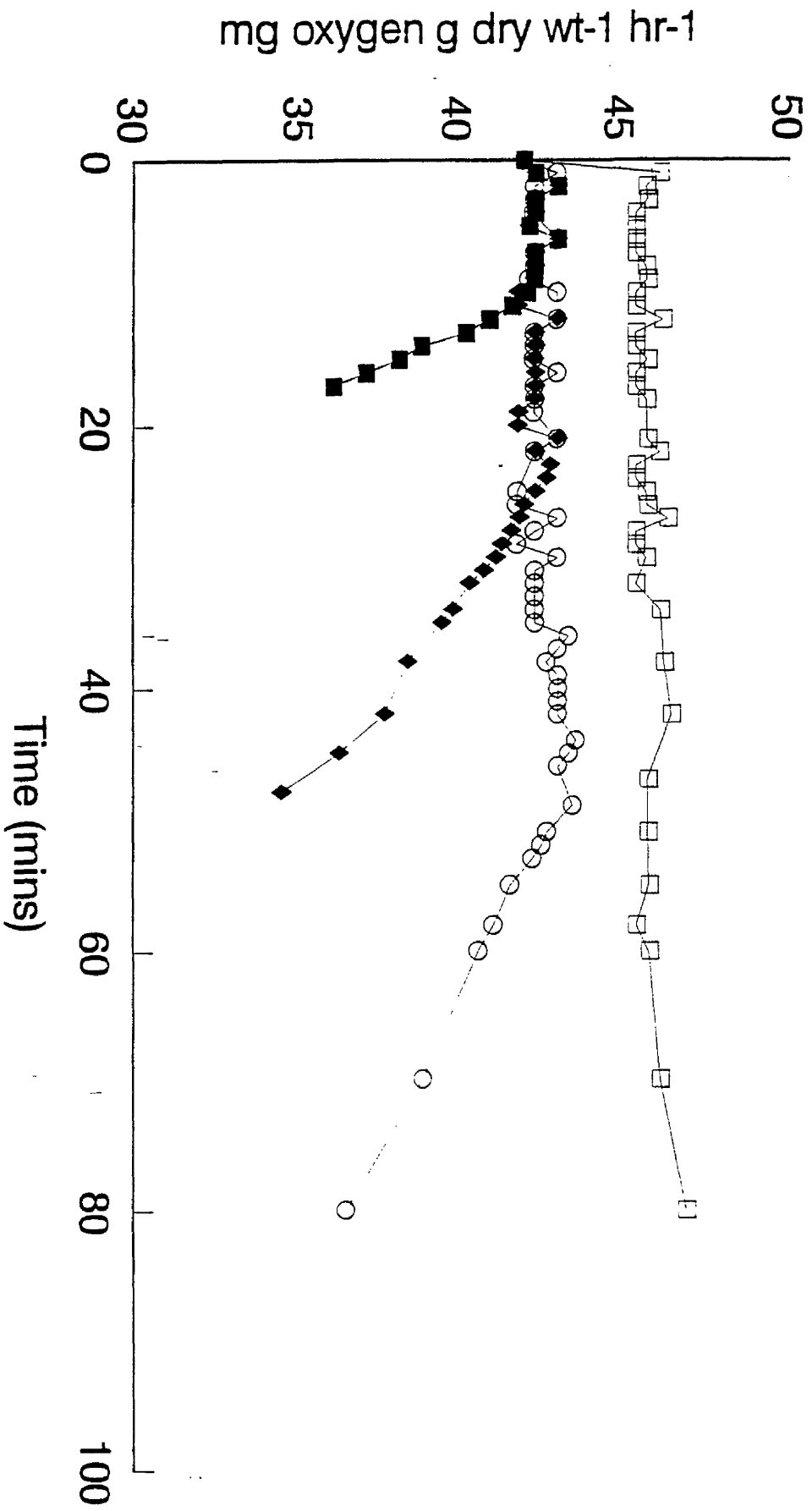


Figure 199. The effect of light / dark cycles at a PFD of 300 $\mu\text{mol s}^{-1} \text{m}^{-2}$ on the maximum rate of photosynthesis of *Chlorella vulgaris* 211/1c, ■—■ light / dark cycle of 200:50 seconds, ◆—◆ light / dark cycle of 200:100 seconds, ○—○ light / dark cycle of 200:120 seconds, □—□ light / dark cycle of 200:150 seconds.

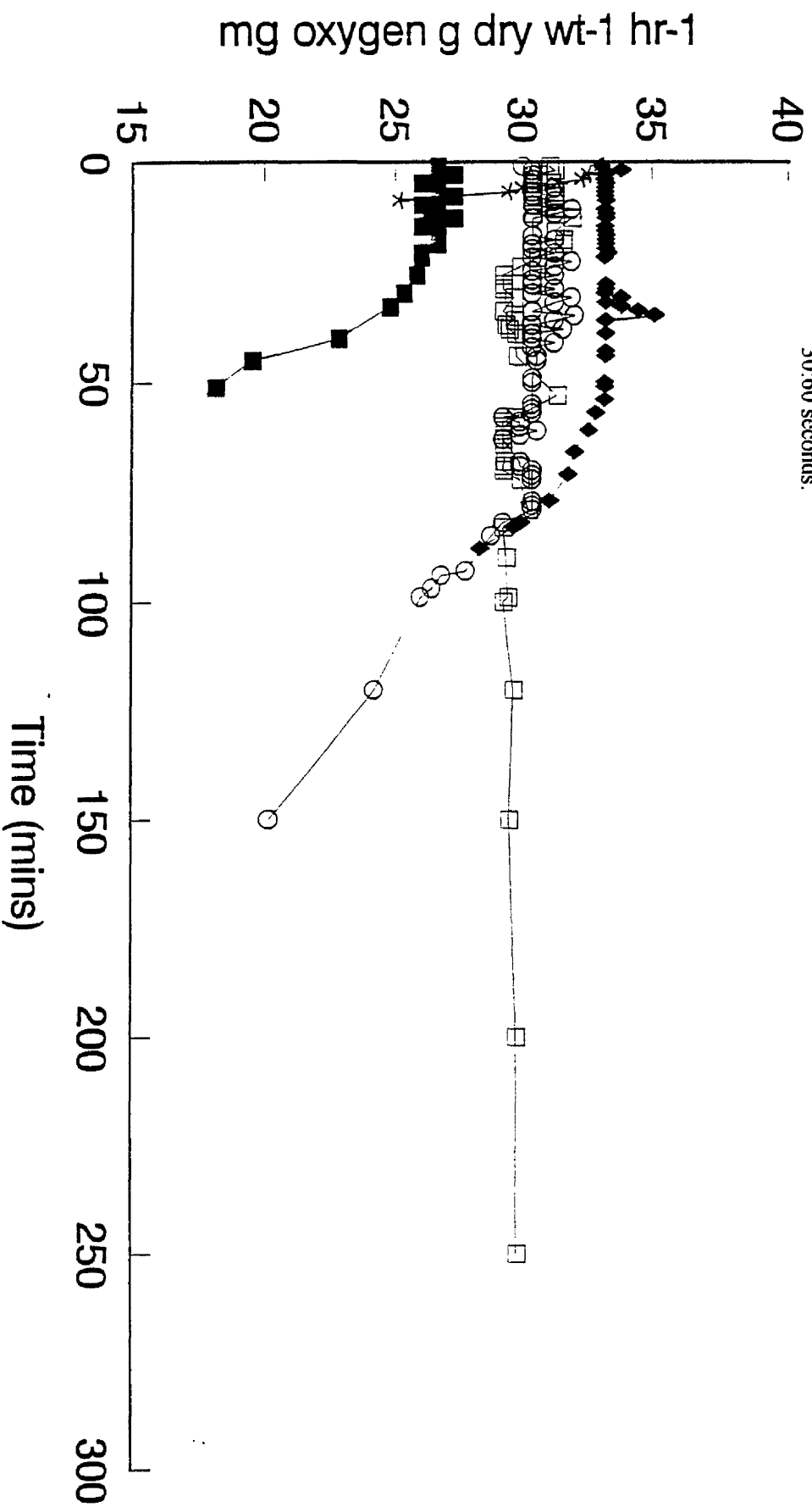


Figure 200. The effect of light / dark cycles at a PFD of 500 $\mu\text{mol s}^{-1} \text{m}^{-2}$ on the maximum rate of photosynthesis of *Chlorella vulgaris* 211/11c, *—* continuous light of 500 $\mu\text{mol s}^{-1} \text{m}^{-2}$, ■—■ light / dark cycle of 30:15 seconds, ◆—◆ light / dark cycle of 30:30 seconds, ○—○ light / dark cycle of 30:45 seconds, □—□ light / dark cycle of 30:60 seconds.

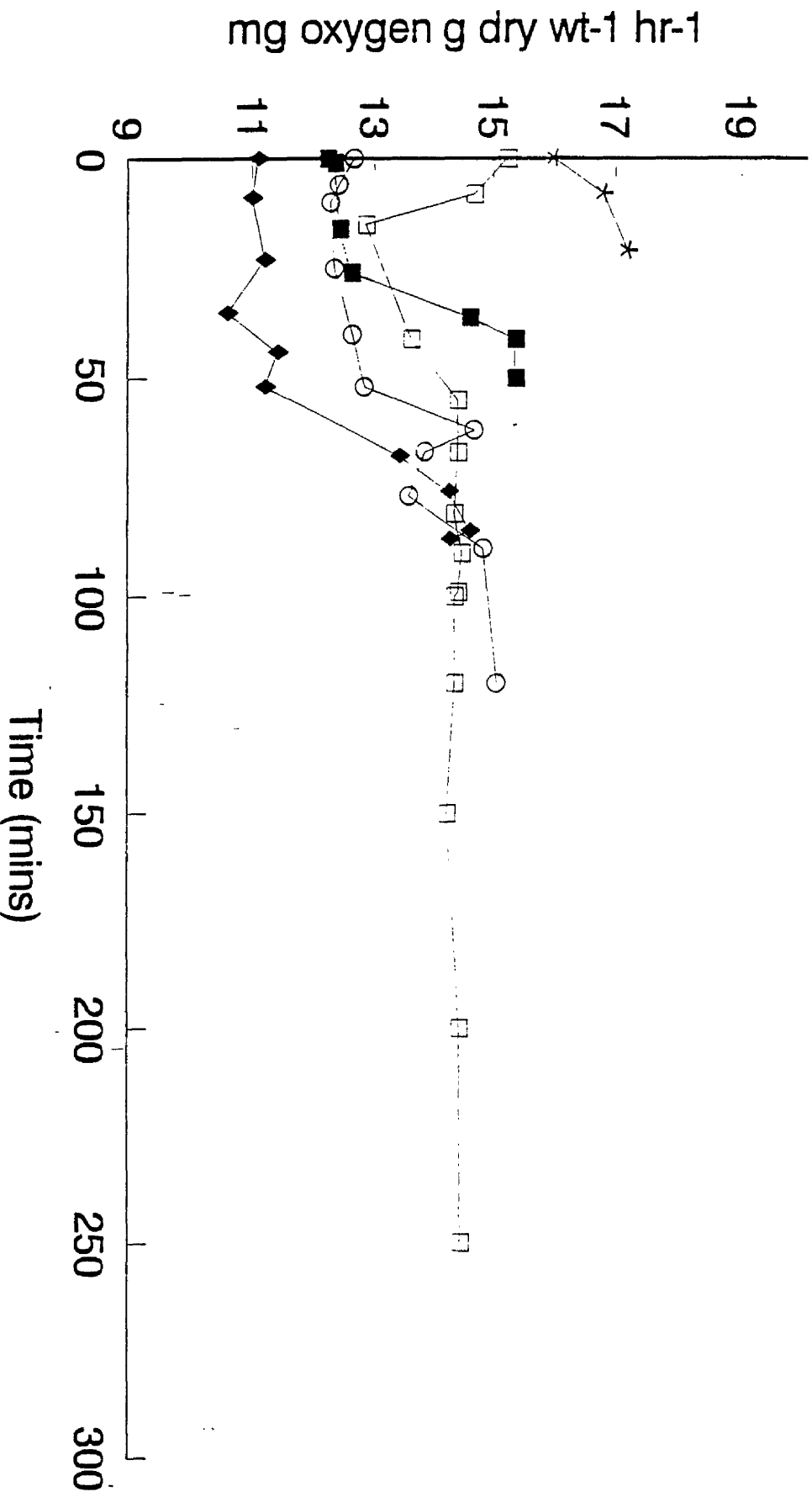


Figure 201. The effect of light / dark cycles of PFD $500 \mu\text{mol s}^{-1} \text{m}^{-2}$ on the respiration of *Chlorella vulgaris* 211/11c, *—* continuous light of $500 \mu\text{mol s}^{-1} \text{m}^{-2}$, ■—■ light / dark cycle of 30:15 seconds, ○—○ light / dark cycle of 30:45 seconds, ◆—◆ light / dark cycle of 30:30 seconds, □—□ light / dark cycle of 30:60 seconds

uneven respiration rate in the early stages of the experiment but soon settled out and was relatively constant throughout the remaining time of the experiment. It was observed that small oxygen bubbles had developed over the electrode membrane during the time in which photosynthesis occurred. These bubbles were removed manually as displayed by the peaks on the plot.

Figure 202 displays the data obtained by incubating *Chlorella vulgaris* 211/11c in light / dark cycles whilst irradiated at a PFD of $500\mu\text{mol s}^{-1} \text{m}^{-2}$ at an increased exposure time of 60 seconds. It was observed that a light / dark ratio of 1:1 was required to prevent a decline in photosynthetic rate. This suggests that there may be a minimum dark respiration duration below which no recovery can take place or photosynthetic rate maintained.

Figure 203 show the data obtained from incubating cells of *Chlorella vulgaris* 211/11c in light / dark cycles at a PFD of $500\mu\text{mol s}^{-1} \text{m}^{-2}$ for 120 seconds. The light / dark ratio required to maintain a constant photosynthetic rate was observed to decrease to 0.6 as the cells required more time in the dark to recover from the effects of a high light intensity exposure. It can also be seen that longer time scales (3-5 hours) were required to find the break down points of photosynthesis as the PFD irradiance increases into the area known to be highly photoinhibitory to cells of *Chlorella vulgaris* 211/11c. At this PFD of $500\mu\text{mol s}^{-1} \text{m}^{-2}$ in a light / dark cycle of 120:200 and 60:120 seconds, the maximum rate of photosynthesis in these cycles was approximately 50% that obtained from the maximum rate of photosynthesis obtained at a PFD of $200\mu\text{mol s}^{-1} \text{m}^{-2}$ at a temperature of 23°C (Figure 91).

Experiments using light /dark cycles of longer duration could not be carried out due to the length of dark time that would be required to offset these irradiances (limited by the relay timer). Figure 204 shows the plots obtained when incubating *Chlorella vulgaris* 211/11c light / dark cycles at a PFD of $750\mu\text{mol s}^{-1} \text{m}^{-2}$ for 60 seconds. Several unsuccessfully low ratios of light to dark were attempted before a ratio of 60:120 seconds (1:2) was determined as the ratio to maintain a constant photosynthetic rate.

Figure 205 shows the results obtained when incubating cells of *Chlorella vulgaris* 211/11 in light / dark cycles at a PFD of $750\mu\text{mol s}^{-1} \text{m}^{-2}$ for 120 seconds. Even with

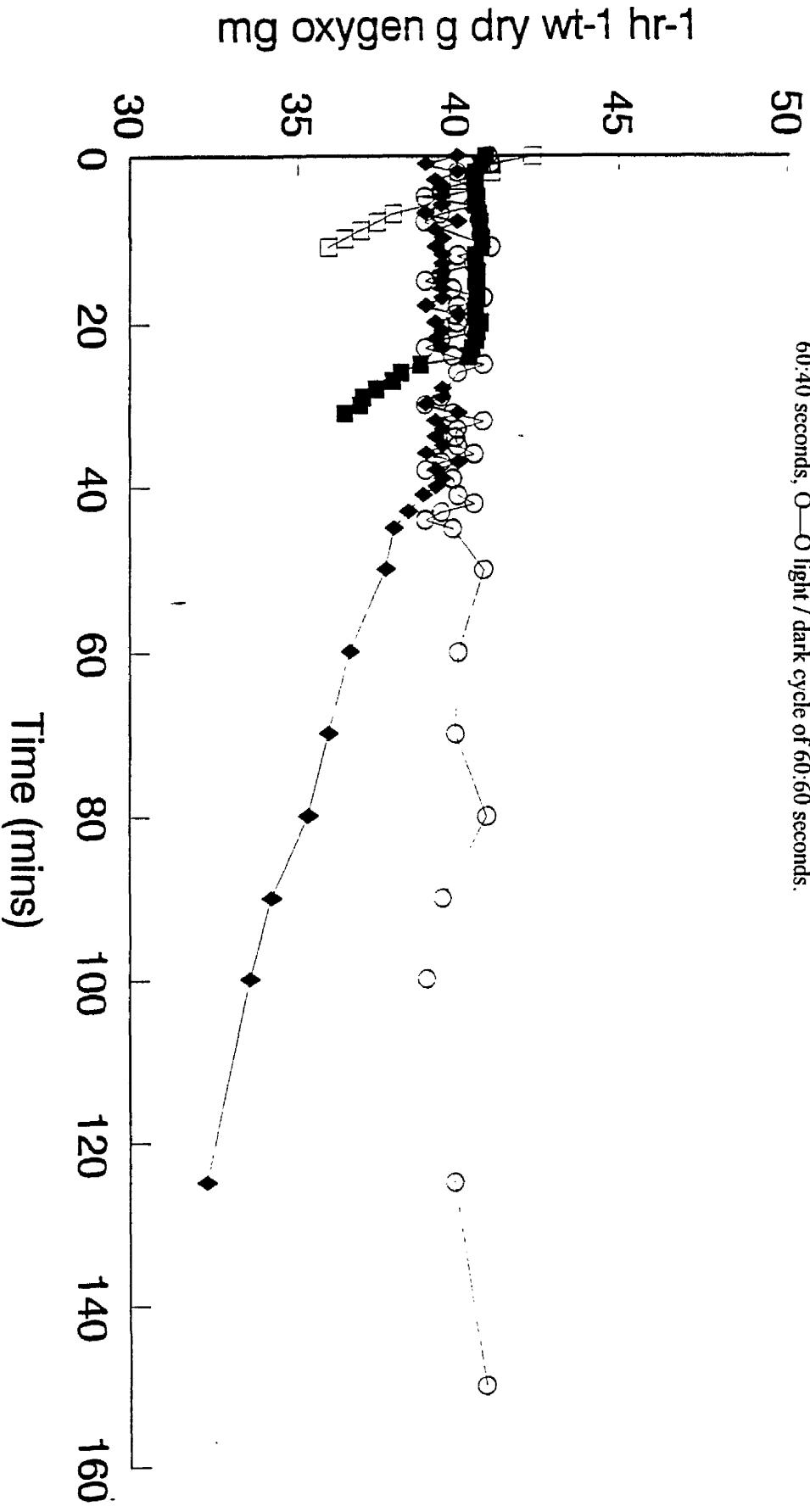


Figure 202. The effect of light / dark cycles at a PFD of 500 $\mu\text{mol s}^{-1} \text{m}^{-2}$ on the maximum rate of photosynthesis of *Chlorella vulgaris* 211/11c, □—□ continuous light of 500 $\mu\text{mol s}^{-1} \text{m}^{-2}$, ■—■ light / dark cycle of 60:30 seconds, ◆—◆ light / dark cycle of 60:40 seconds, ○—○ light / dark cycle of 60:60 seconds.

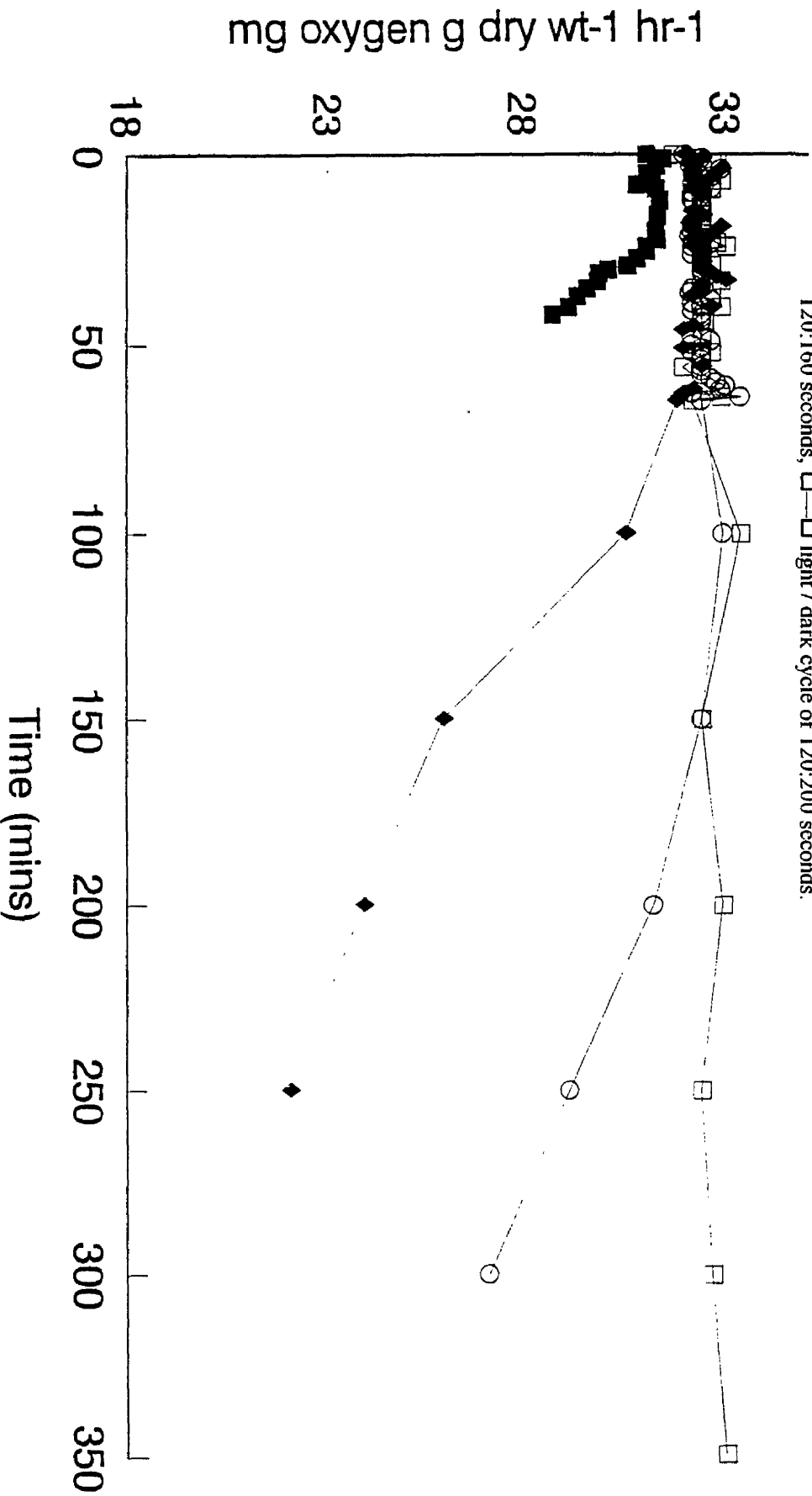


Figure 203. The effect of light / dark cycles at a PFD of $500 \mu\text{mol s}^{-1} \text{m}^{-2}$ on the maximum rate of photosynthesis of *Chlorella vulgaris* 211/11c, ■—■ light / dark cycle of 120:100 seconds, ◆—◆ light / dark cycle of 120:120 seconds, ○—○ light / dark cycle of 120:160 seconds, □—□ light / dark cycle of 120:200 seconds.

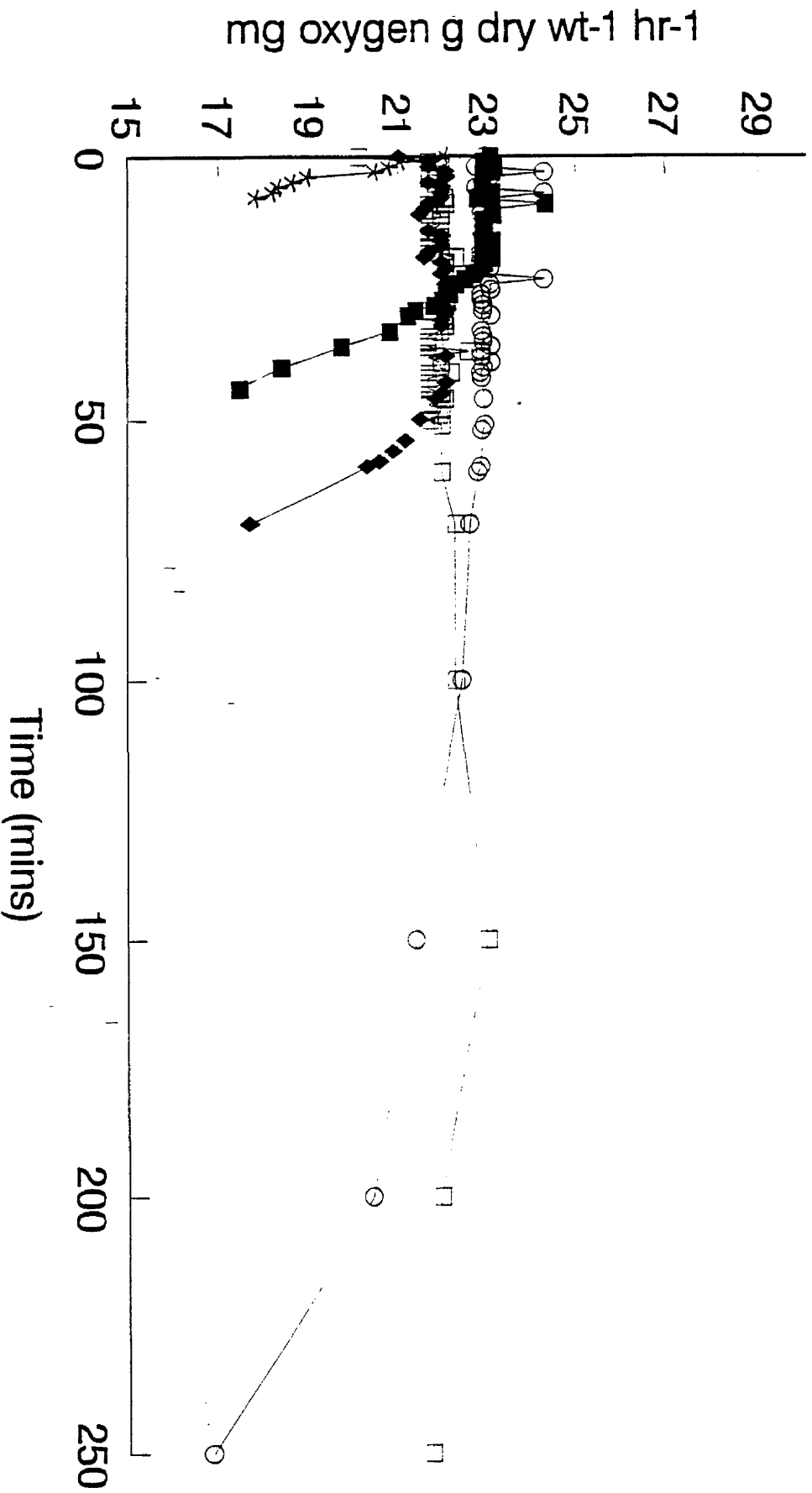


Figure 204. The effect of light / dark cycles at a PFD of $750 \mu\text{mol s}^{-1} \text{m}^{-2}$ on the maximum rate of photosynthesis of *Chlorella vulgaris* 211/11c, *—* continuous light of $750 \mu\text{mol s}^{-1} \text{m}^{-2}$, ■—■ light / dark cycle of 60:30 seconds, ○—○ light / dark cycle of 60:60 seconds, □—□ light / dark cycle of 60:90 seconds, ◆—◆ light / dark cycle of 60:120 seconds.

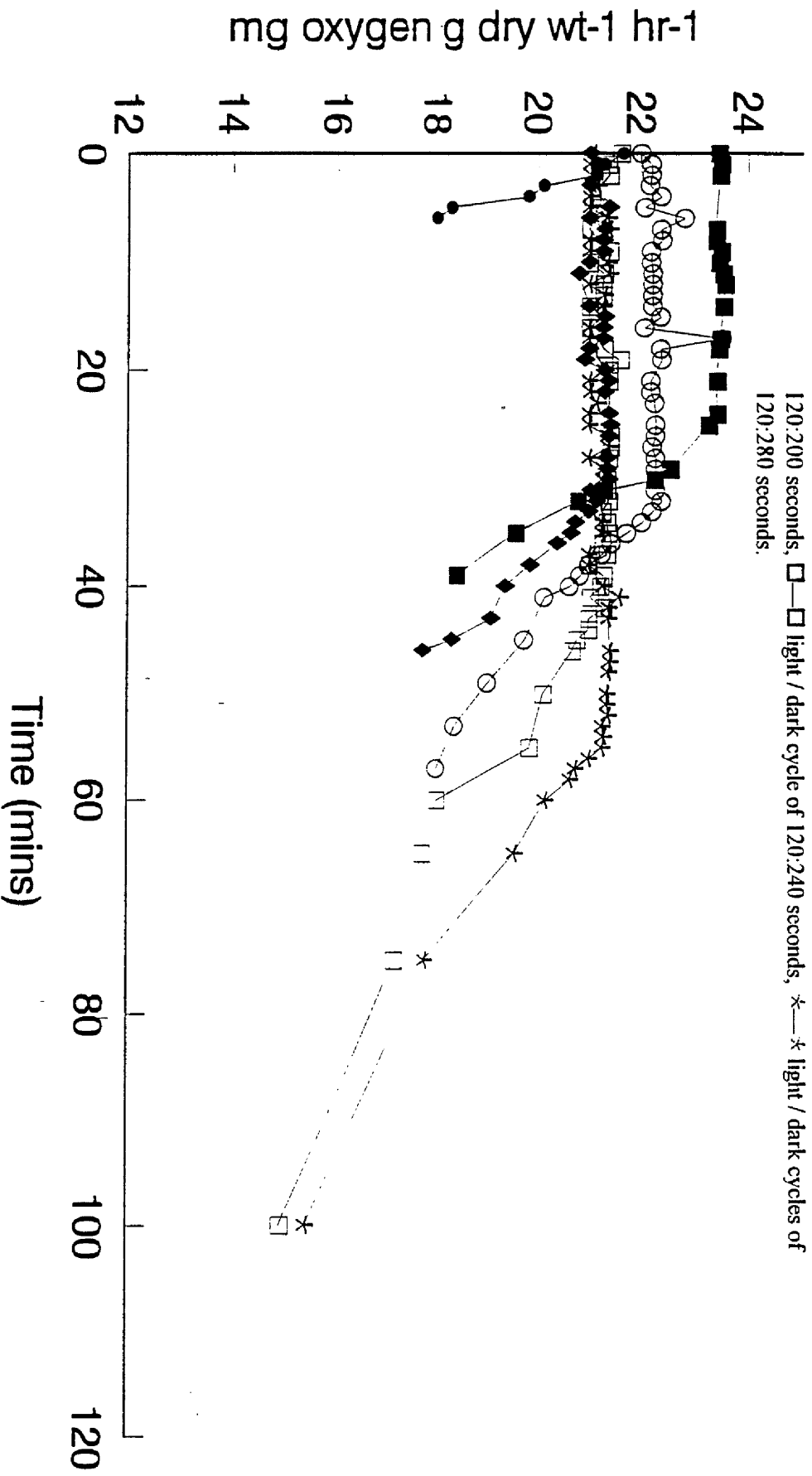


Figure 205. The effect of light / dark cycles at a PFD of 750 μmol s⁻¹ m⁻² on the maximum rate of photosynthesis of *Chlorella vulgaris* 211/1c, ●—● continuous light of 750 μmol s⁻¹ m⁻², ■—■ light / dark cycle of 120:120 seconds, ○—○ light / dark cycle of light / dark cycle of 120:180 seconds, □—□ light / dark cycle of 120:240 seconds, *—* light / dark cycles of 120:280 seconds.

ratios as low as 0.428 the cells still showed signs of photoinhibition after 60 minutes. As the relay timer was unable to go beyond the 280 seconds extended timings were not possible. Hence the light / dark ratio required at this PFD could not be determined.

3.5.2 The effect of light / dark cycles of medium frequency on the photosynthesis of *Synechococcus* 1479/5.

Figure 206 shows similar light / dark cycling experiments to those for *Chlorella vulgaris* 211/11c but performed on the cyanobacteria *Synechococcus* 1479/5. *Synechococcus* 1479/5 displays a P_{\max} value at a PFD of $200\mu\text{mol s}^{-1} \text{m}^{-2}$, however this irradiance PFD is photo inhibitory to the cells if the exposure time is allowed to continue for more than 8 minutes. Figure 206 shows the results of incubating cells of *Synechococcus* 1479/5 at a PFD of $200\mu\text{mol s}^{-1} \text{m}^{-2}$ for a maximum of 205 seconds whilst in different light / dark cycles. It was found that a light / dark cycle of 205:68 seconds (3:1) was required to maintain a steady photosynthetic rate for a period of 22 hours. Higher ratios of 6:1 resulted in severe declines in the photosynthetic rate after about 40 minutes.

Figure 207 shows cells of *Synechococcus* 1479/5 being incubated in light / dark cycles at a PFD of $300\mu\text{mol s}^{-1} \text{m}^{-2}$ for a maximum period of 80 seconds. It can be seen that a light / dark ratio of 2:1 was just insufficient to prevent a reduction in photosynthetic rate observed to decline after 120 minutes. The dark time required for recovery from this PFD was of the order of 50 seconds (a ratio of 1.6:1), however, it should be noted that as in all these plots the figures are approximate since there was no fine tuning to determine the exact figures.

Figure 208 shows the results of incubating cells of *Synechococcus* 1479/5 in light / dark cycles at PFD of $300\mu\text{mol s}^{-1} \text{m}^{-2}$ but for a maximum exposure time of 120 seconds. It was found that time periods for monitoring unsuccessful light / dark cycles on photosynthetic rates were becoming increasingly longer. It was found that a ratio of 2:1 was required to prevent a decline in the rate of photosynthesis at this PFD exposure duration.

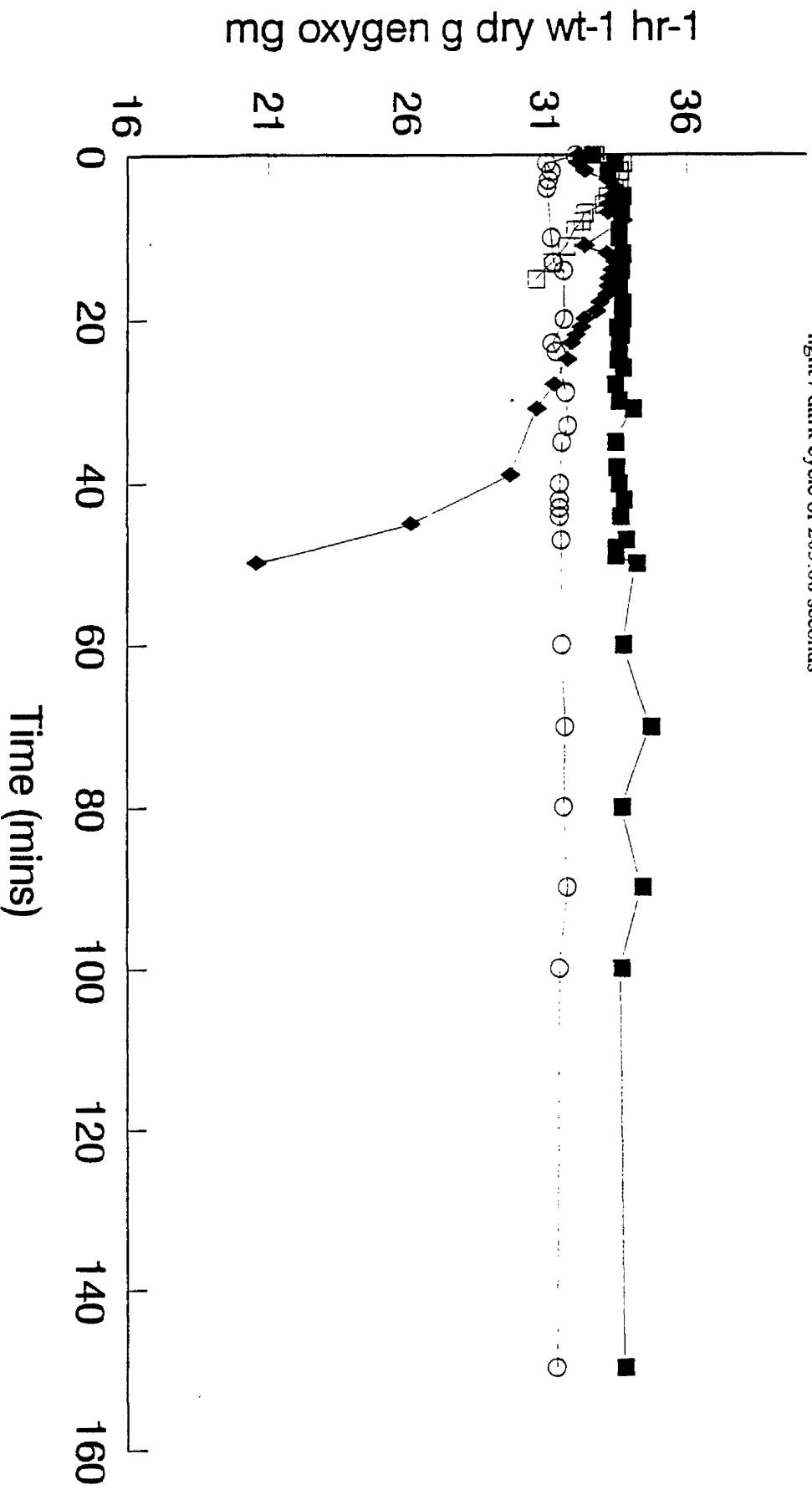


Figure 206. The effect of light / dark cycles of PFD 200 μmol s⁻¹ m⁻² on the photosynthesis of *Synechococcus* 1479/5, □—□ continuous light of 200 μmol s⁻¹ m⁻², ◆—◆ light / dark cycle of 205:34 seconds, ○—○ light / dark cycle of 60:10 seconds, ■—■ light / dark cycle of 205:68 seconds

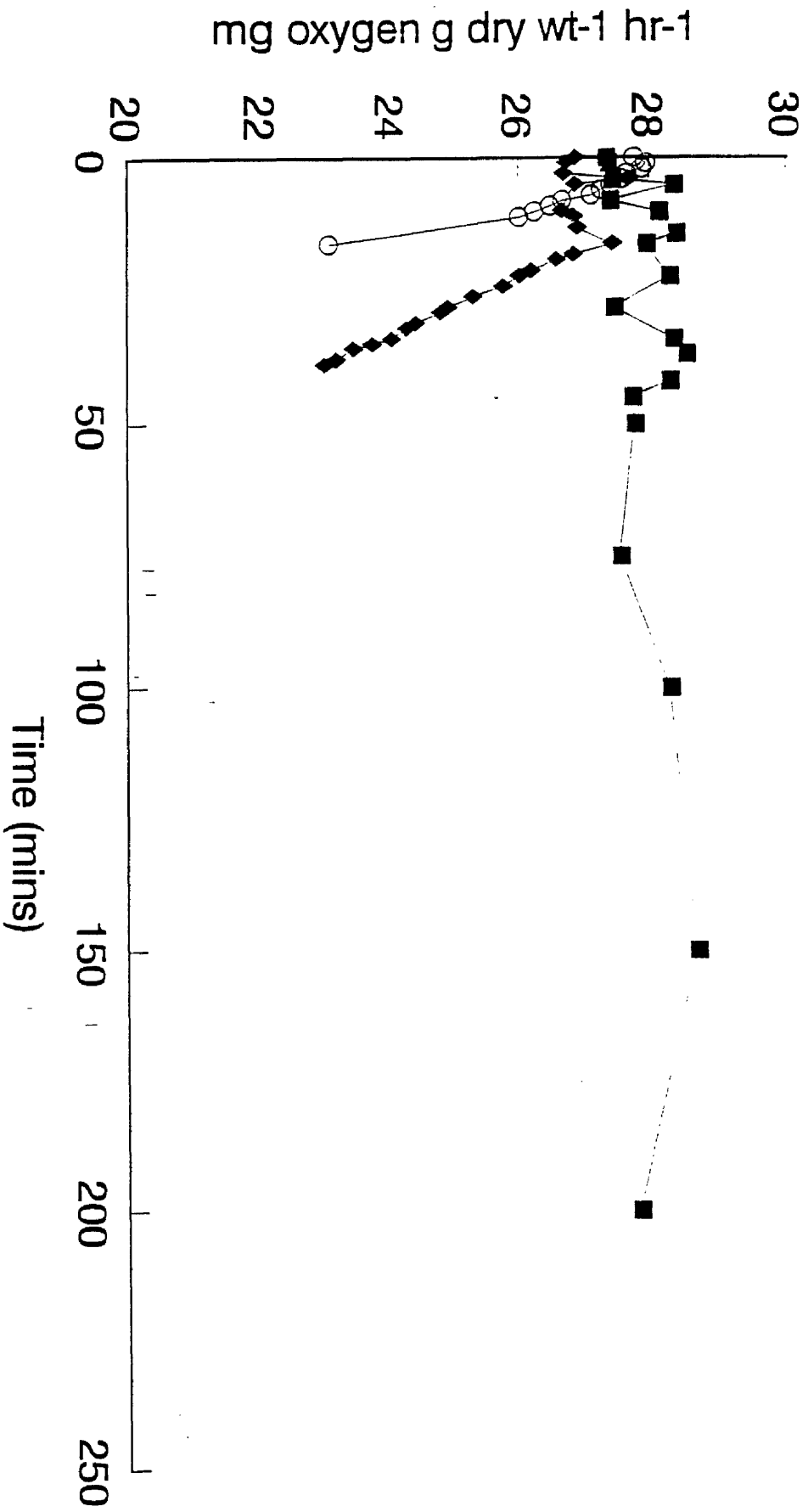


Figure 207. The effect of light / dark cycles of PFD 300 μ mol s⁻¹ m⁻² on the photosynthesis of *Synechococcus* 1479/5, \square — \square light / dark cycle of 60:10 seconds, \circ — \circ light / dark cycle of 80:20 seconds, \blacklozenge — \blacklozenge light / dark cycle of 80:40 seconds, \blacksquare — \blacksquare light / dark cycle of 80:50 seconds.

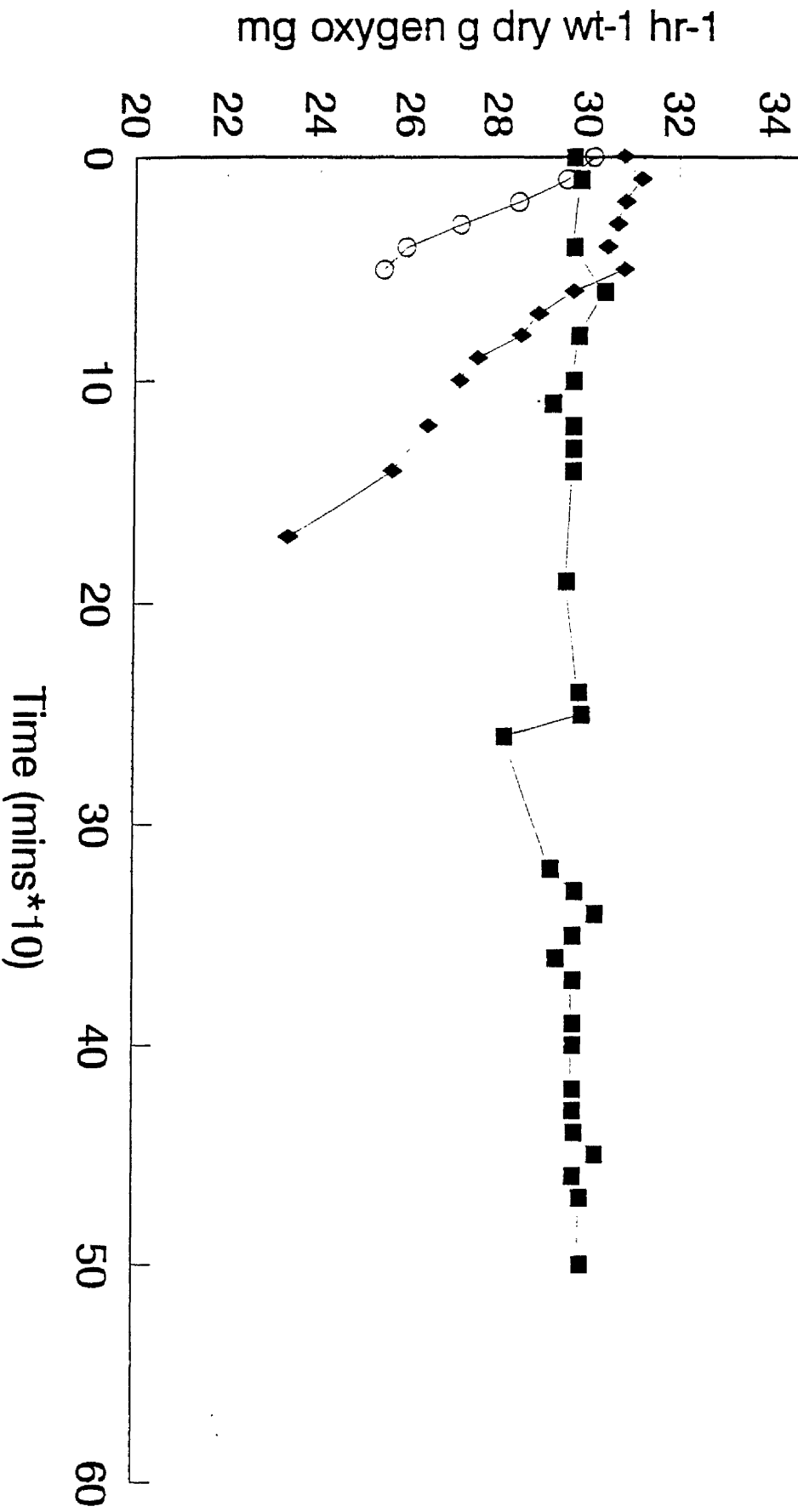


Figure 208. The effect of light / dark cycles of PFD 300μmol s⁻¹ m⁻² on the photosynthesis of *Synechococcus* 1479/5, O—O light / dark cycle of 120:10 seconds, ◆—◆ light / dark cycle of 120:40 seconds, ■—■ light / dark cycle of 120:60 seconds.

Figure 209 shows the results obtained when incubating cells of *Synechococcus* 1479/5 in light / dark cycles at a PFD of $300\mu\text{mol s}^{-1} \text{m}^{-2}$ for a maximum period of 205 seconds. It was found that a ratio of 2:1 similar to the results obtained in Figure 208 was necessary to offset a decline in photosynthetic rate.

Figure 210 shows the results obtained from incubating cells of *Synechococcus* 1479/5 in light / dark cycles at a PFD of $500\mu\text{mol s}^{-1} \text{m}^{-2}$ for a maximum duration of 80 seconds. As with the results obtained from the work involving *Chlorella vulgaris* 211/11c, *Synechococcus* 1479/5 shows a similar pattern in that the light / dark ratio required to recover from cell photodamage was inverted i.e. the cells were observed to require a longer period in the dark to recover from a period in the light at this PFD. In this case a L / D cycle ratio of 1:1.5 was required to ensure no decline in photosynthetic rates during a period of 16 hours.

Figure 211 shows the results from incubating cells of *Synechococcus* 1479/5 in light / dark cycles at a PFD of $500\mu\text{mol s}^{-1} \text{m}^{-2}$ for a maximum light duration of 120 seconds. The length of dark time required to offset an exposure of $500\mu\text{mol s}^{-1} \text{m}^{-2}$ for 120 seconds was 180 seconds, a ratio of 1:1.5.

Figure 212 displays the results of incubating cells of *Synechococcus* 1479/5 in light / dark cycles at a PFD of $500\mu\text{mol s}^{-1} \text{m}^{-2}$ for a time period of 205 seconds. Figure 212 displayed a similar pattern to that of Figure 211 in that cells of *Synechococcus* 1479/5 displayed a requirement recovery ratio of 1:1.36 (light / dark), to maintain a constant photosynthetic rate. Due to Figure 211 displaying the requirement for a dark phase duration of 160 seconds, the result obtained at a light dark cycle of 205:280 seconds on Figure 212 was a maximum dark respiration duration i.e. the dark duration time required by the cells may have been lower since no time duration's between 136 and 280 seconds were performed.

Figure 213 shows the data obtained from cells of *Synechococcus* 1479/5 incubated in light / dark cycles at a PFD $750\mu\text{mol s}^{-1} \text{m}^{-2}$ at exposure times of 82 and 136 seconds respectively. In this experiment the length of dark duration remained constant and the light duration cycle was altered until a constant photosynthetic rate was obtained. It can be seen that a ratio of 1:1.5 was not enough to prevent photoinhibition being observed after approximately 30 minutes. However a much

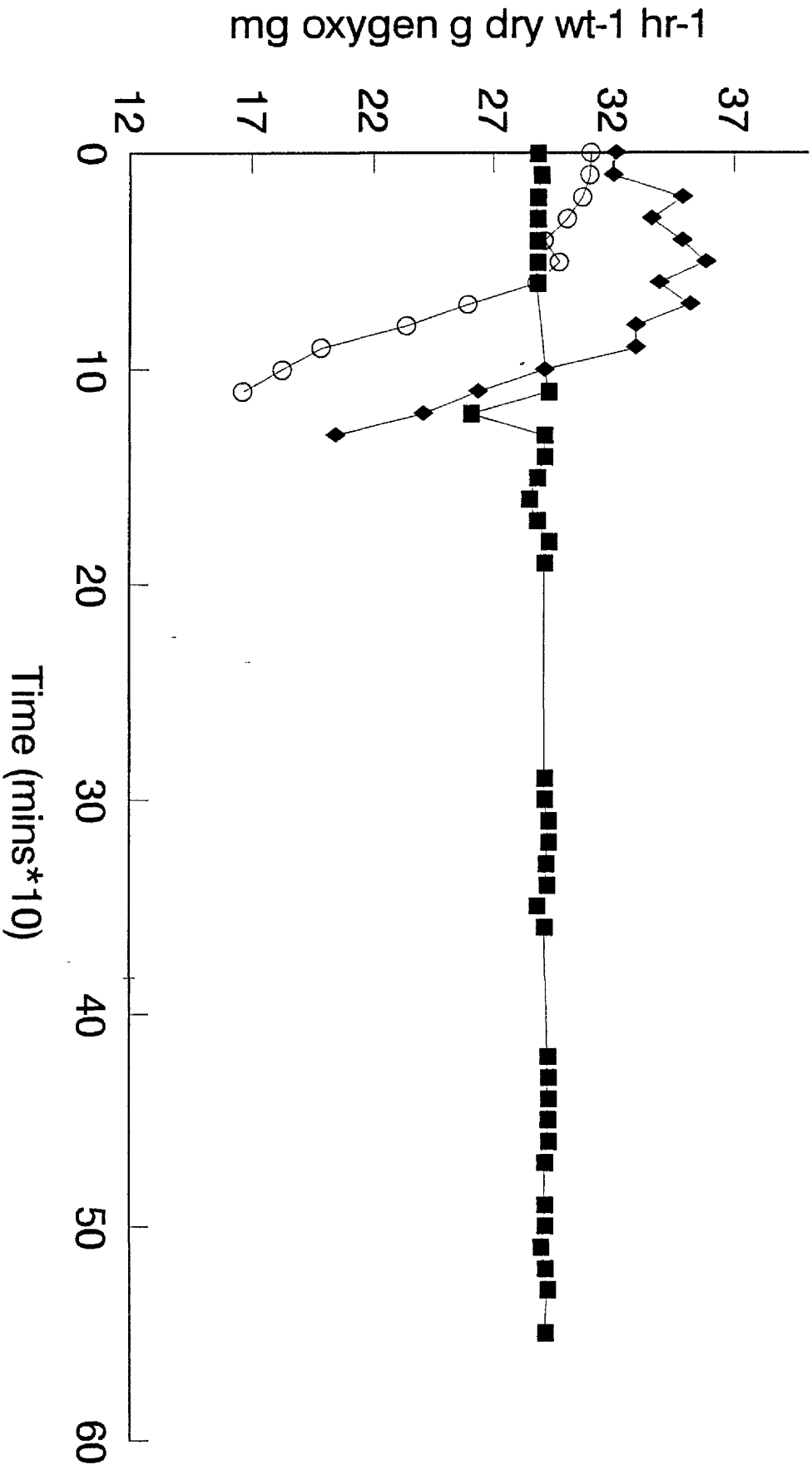


Figure 209. The effect of light / dark cycles of PFD 300 μmol s⁻¹ m⁻² on the photosynthesis of *Synechococcus* 1479/5, O—O continuous light of 300 μmol s⁻¹ m⁻², ◆—◆ light / dark cycle of 205:68 seconds, ■—■ light / dark cycle of 205:102 seconds.

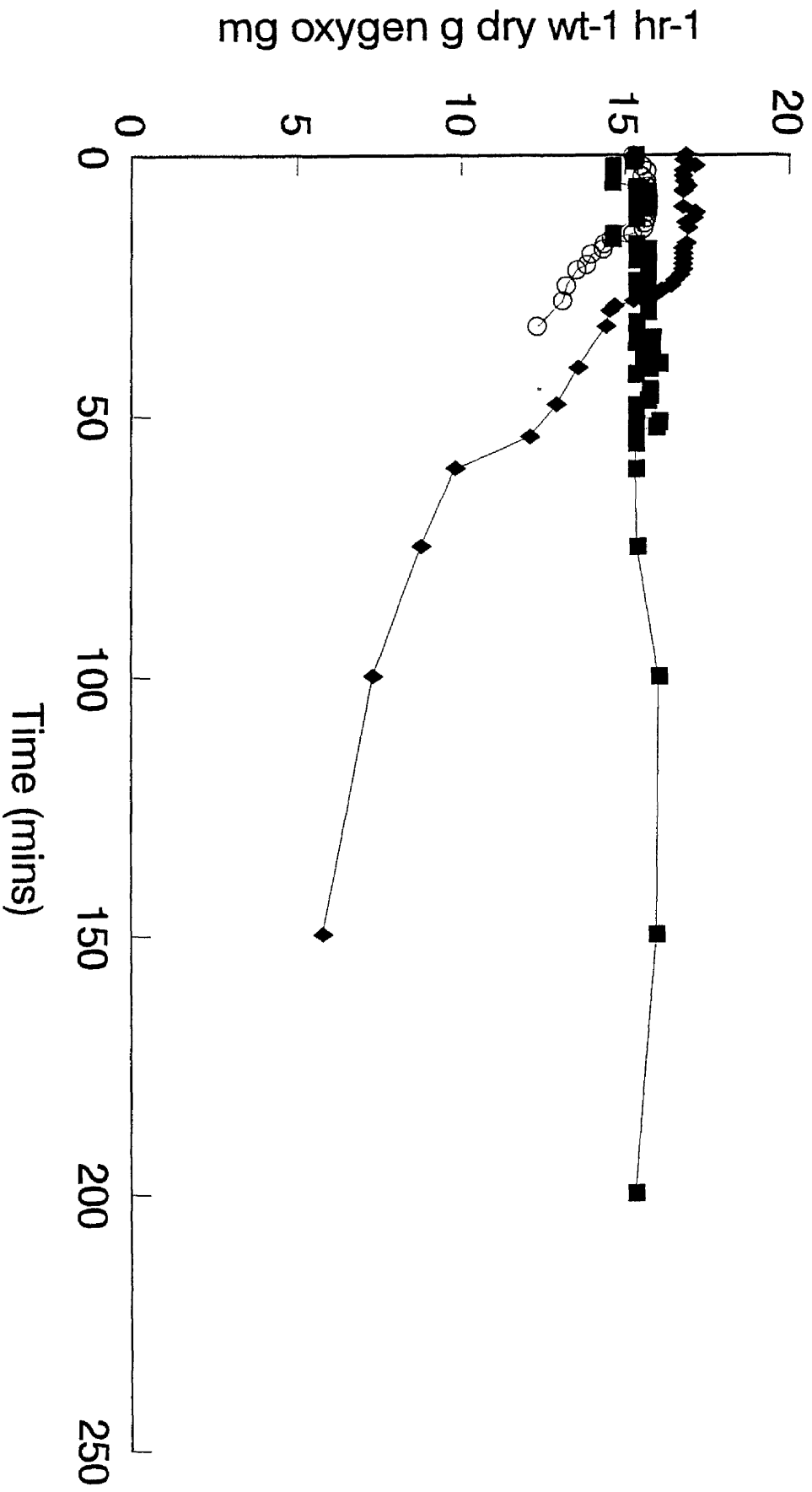


Figure 210. The effect of light / dark cycles of PFD 500μmol s⁻¹ m⁻² on the photosynthesis of *Synecchococcus* 1479/5, ◆—◆ light / dark cycle of 80:40 seconds, O—O light / dark cycle of 80:80 seconds, ■—■ light / dark cycle of 80:120 seconds.

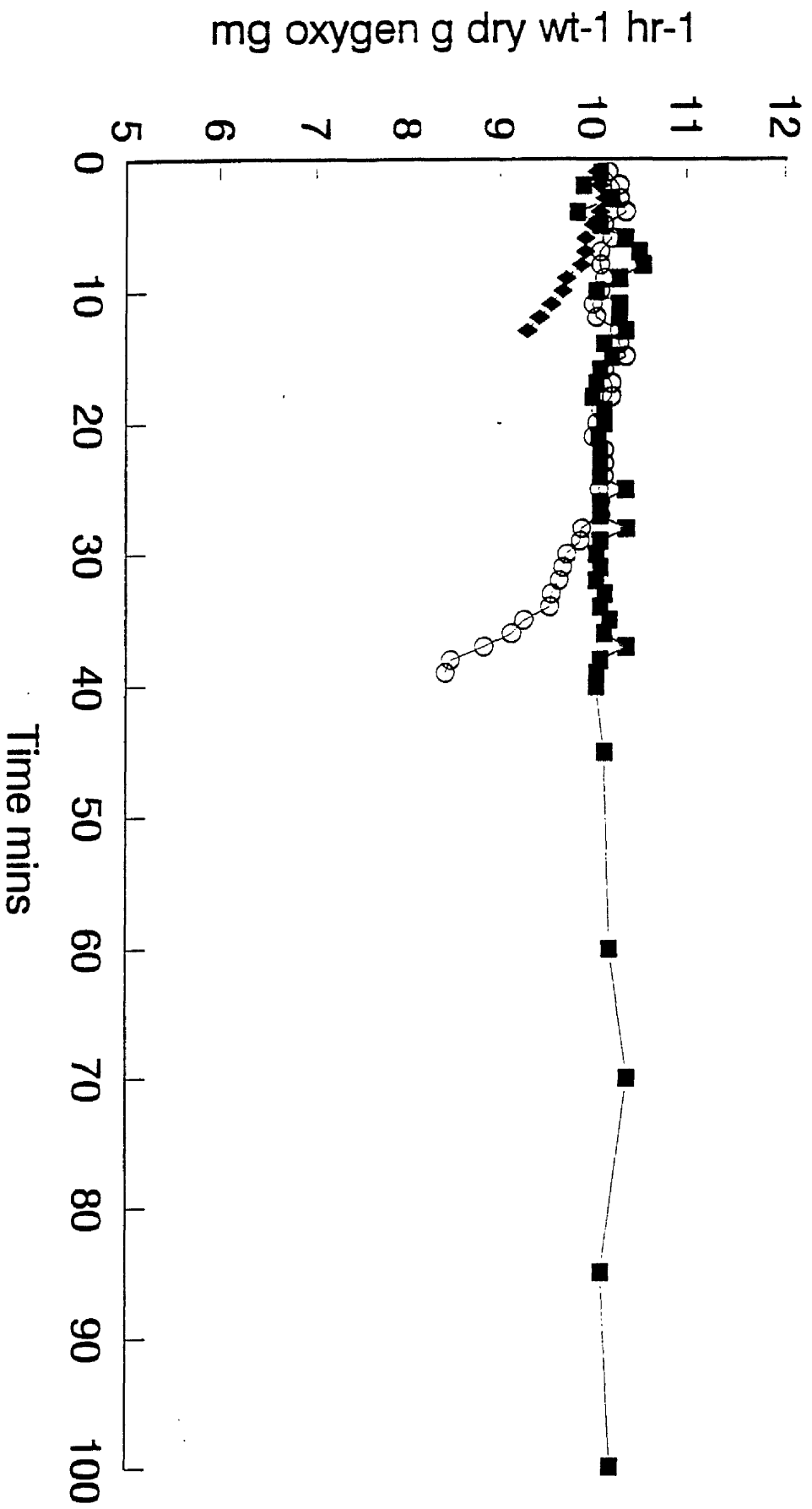


Figure 211. The effect of light / dark cycles of PFD $500\mu\text{mol s}^{-1} \text{m}^{-2}$ on the photosynthesis of *Synechococcus* 1479/5, \blacklozenge — \blacklozenge light / dark cycle 120:60 seconds, \circ — \circ light / dark cycle 120:80 seconds, \blacksquare — \blacksquare light / dark cycle 120:160 seconds.

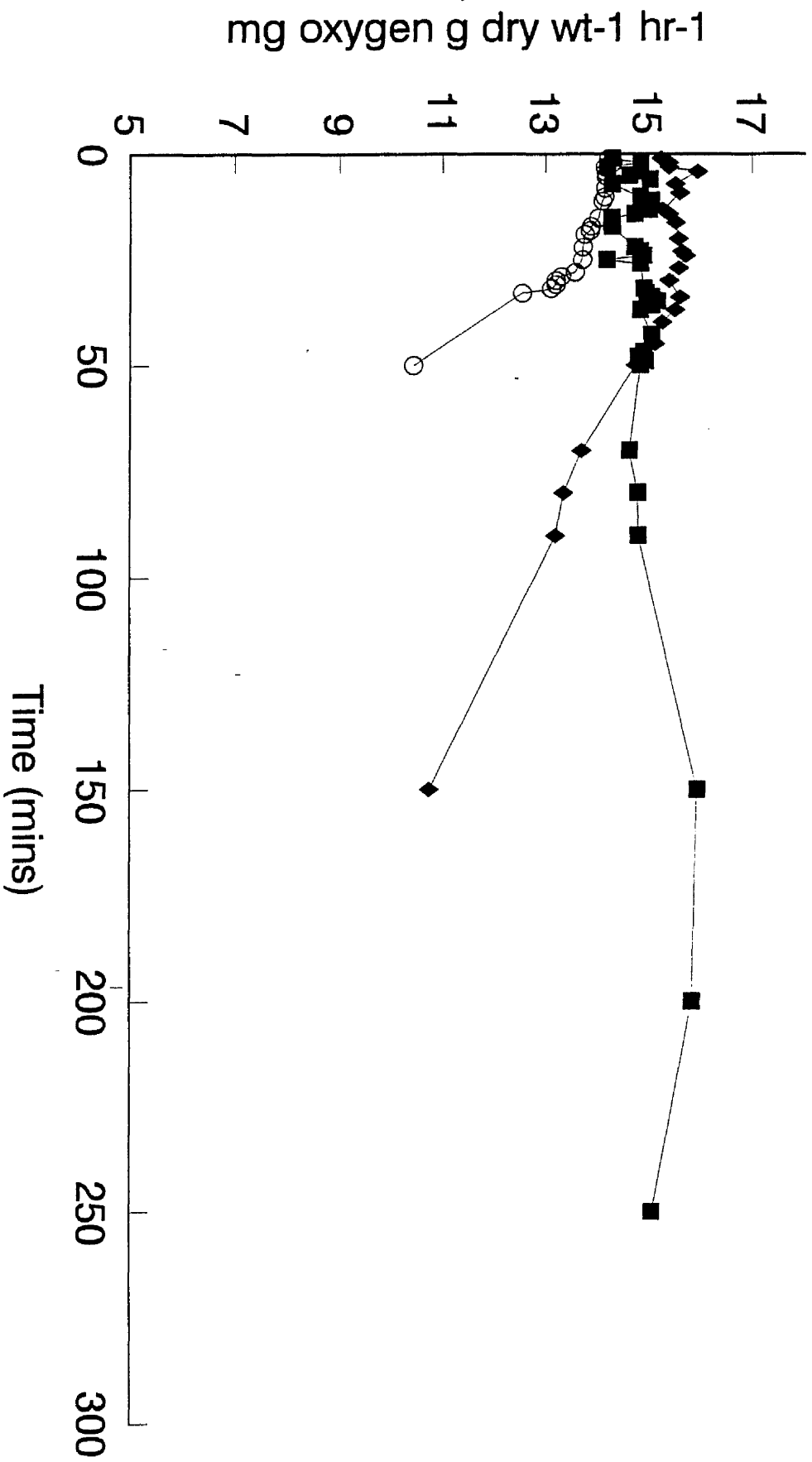


Figure 212. The effect of light / dark cycles of PFD $500 \mu\text{mol s}^{-1} \text{m}^{-2}$ on the photosynthesis of *Synechococcus* 1479/5, O—O light / dark cycle 60:10 seconds, ◆—◆ light / dark cycle 205:136 seconds, ■—■ light / dark cycle 280:280 seconds.

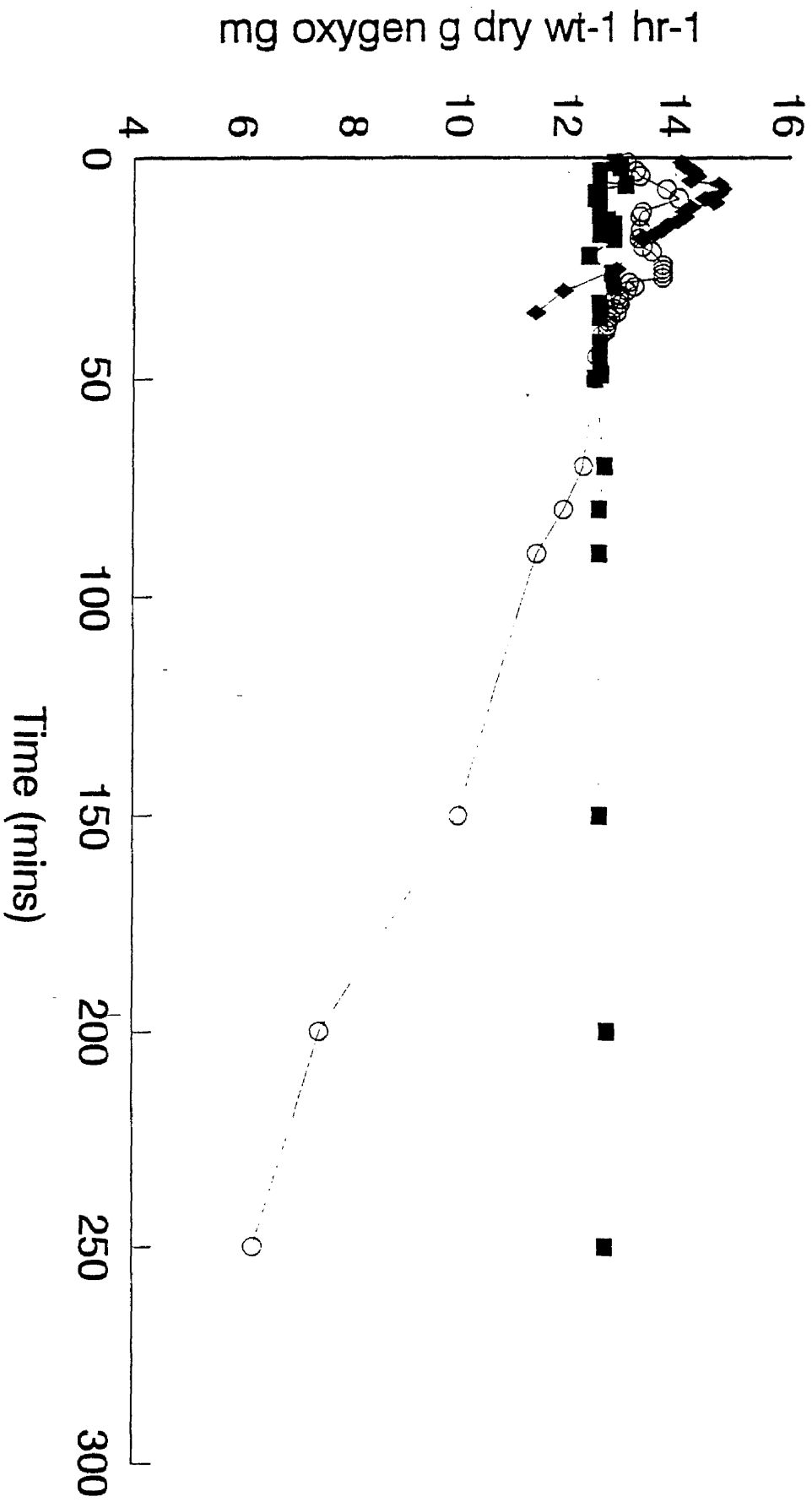


Figure 213. The effect of light / dark cycles of PFD 750 μmol s⁻¹ m⁻² on the photosynthesis of *Synechococcus* 1479/5, ◆ continuous light of 750 μmol s⁻¹ m⁻², ○ light / dark cycle of 136:205 seconds, ■ light / dark cycle of 82:205 seconds.

lower light / dark cycle ratio of 1:2.5 was determined to be sufficient to maintain a constant photosynthetic rate.

Figure 214 shows the results obtained when incubating cells of *Synechococcus*.1479/5 at a PFD $750\mu\text{mol s}^{-1} \text{m}^{-2}$ for a maximum of 120 seconds. It can be seen that a lower ratio of 1:2.33 (greater duration in the dark) was required to offset the effects of photoinhibition.

Figure 215 shows the results of incubating cells of *Synechococcus* 1479/5 in light / dark cycles of 60:10 seconds at PFDs of 750, 1000, 1500 and $2000\mu\text{mol s}^{-1} \text{m}^{-2}$ respectively. The cells display an increased deterioration in their respective photosynthetic rates with increasing PFDs. After each of the experiments where cells displayed a reduction in photosynthetic rates, samples were removed for biochemical analysis to ensure that there were no limiting factors affecting the rates of photosynthesis and cellular metabolism. This was necessary since the work involving the effects of nutrient availability on photosynthesis yielded useful data on the role of nitrate in delaying the onset of photoinhibition. In all experiments, no component of ASM was found to be limiting within the sample chamber throughout the course of the 24 hours.

Figure 216 shows the results of dosage experiments which were carried in a second oxygen electrode system using cells of *Synechococcus* 1479/5. The data shows the results of successful ratios of light to dark, 46:29, 58:17 and 23:52 seconds respectively, at different PFDs of 250, 200 and $500\mu\text{mol s}^{-1} \text{m}^{-2}$ respectively. Each of the three L / D cycles was 75 seconds in duration and therefore had a total dosage equivalent to $11000 \pm 100\mu\text{mol}$.

Figure 217 however shows a different set of dosage experiments in which the cells of *Synechococcus* 1479/5 were exposed to a dosage equivalent of $18000\mu\text{mol s}^{-1} \text{m}^{-2}$ in 75 seconds. It can be observed that the cells at the lower PFD maintain a constant photosynthetic rate until approximately 60 minutes after which the rate begins to fall. However cells exposed to the higher PFD have a near constant photosynthetic rate even after 225 minutes.

Figure 218 shows the combined results obtained from the light / dark cycling experiments carried out on both *Chlorella vulgaris* 211/11c and *Synechococcus*

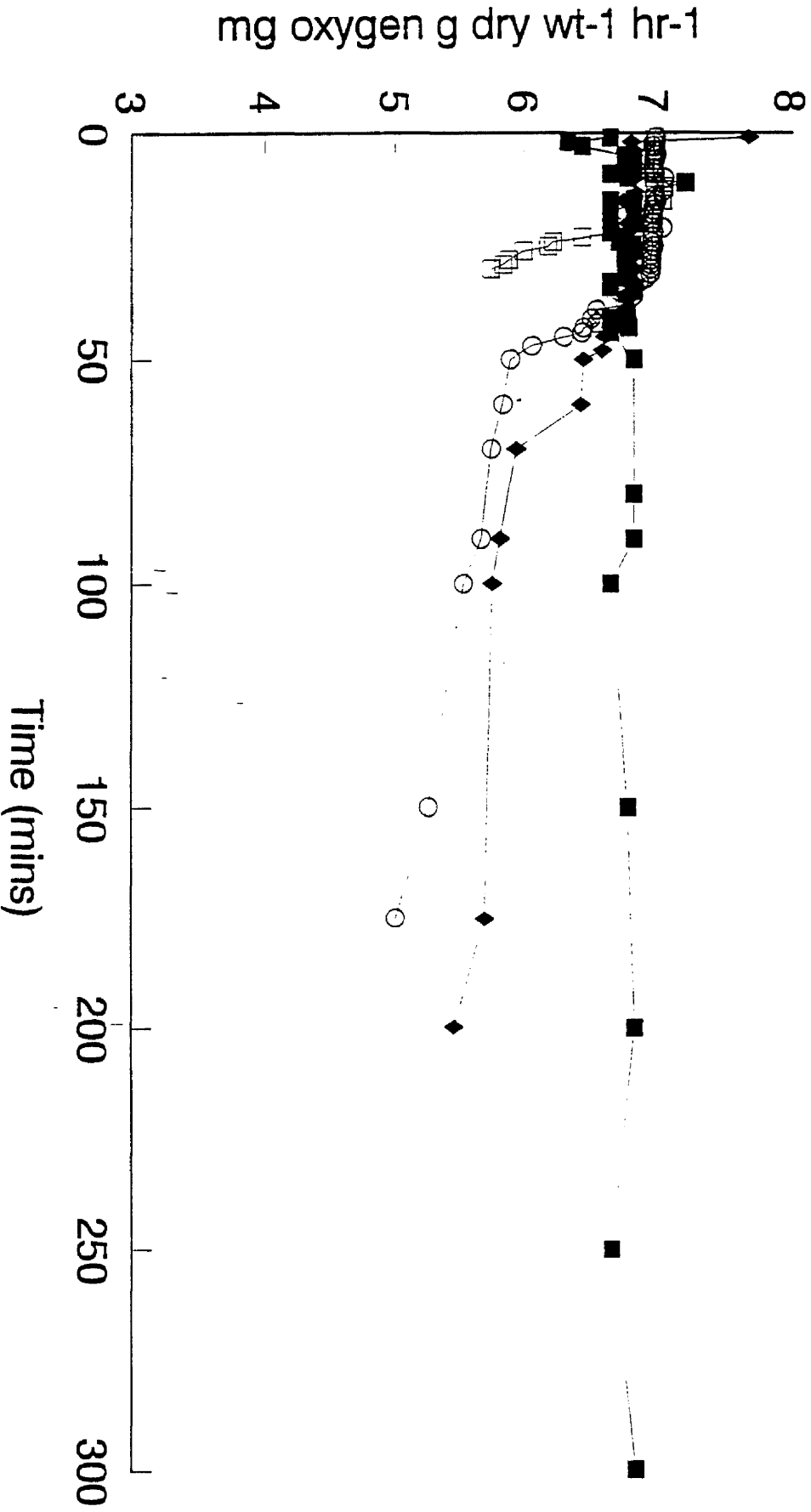


Figure 214. The effect of light / dark cycles of PFD $750\mu\text{mol s}^{-1} \text{m}^{-2}$ on the photosynthesis of *Synechococcus* 1479/5, □—□ light / dark cycle of 120:120 seconds, ○—○ light / dark cycle of 120:160 seconds, ◇—◇ light / dark cycle of 120:200 seconds, ■—■ light / dark cycle of 120:280 seconds.

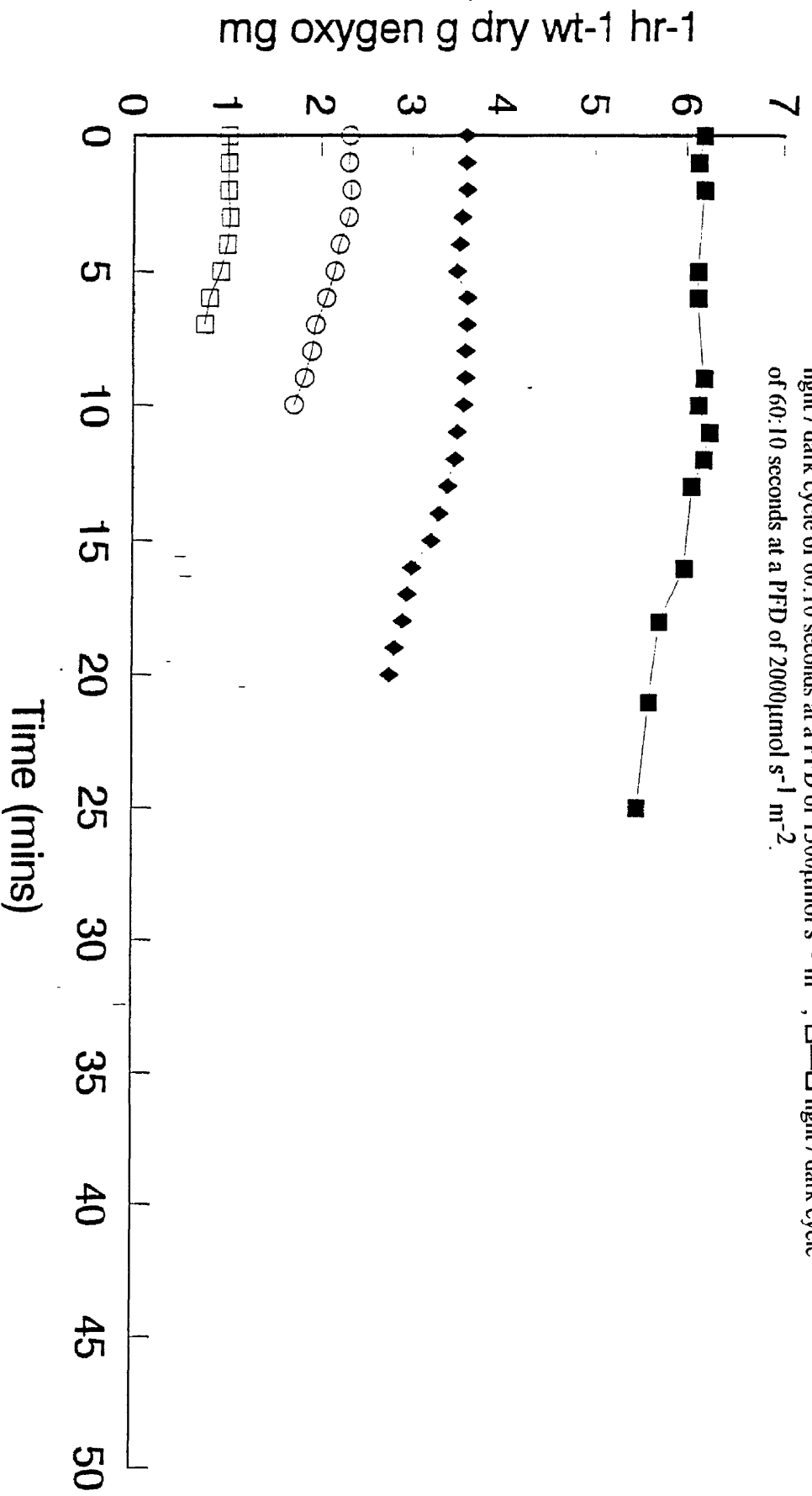


Figure 215. The effect of light / dark cycles of different PFD on the photosynthesis of *Synchococcus* 1479/5, ■—■ light / dark cycle of 60:10 seconds at a PFD of 750 $\mu\text{mol s}^{-1} \text{m}^{-2}$, ◆—◆ light / dark cycle of 60:10 seconds at a PFD of 1000 $\mu\text{mol s}^{-1} \text{m}^{-2}$, O—O light / dark cycle of 60:10 seconds at a PFD of 1500 $\mu\text{mol s}^{-1} \text{m}^{-2}$, □—□ light / dark cycle of 60:10 seconds at a PFD of 2000 $\mu\text{mol s}^{-1} \text{m}^{-2}$.

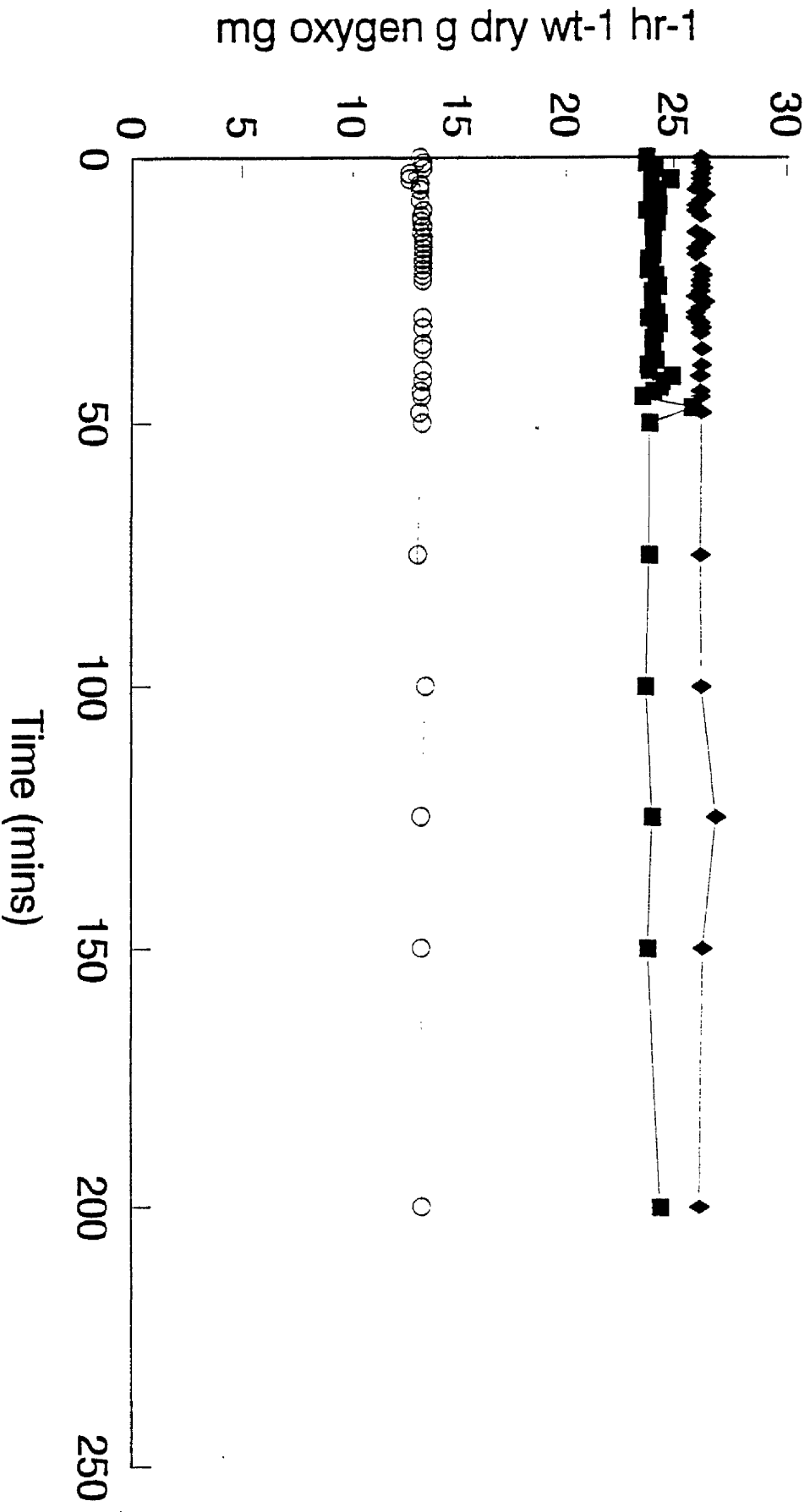


Figure 216. The effect of light dosage and light dark cycles on the photosynthesis of *Synechococcus* 1479/5, ◆—◆ light / dark cycle of 46:29 seconds at a PFD of 250 μmol s⁻¹ m⁻², ■—■ light / dark cycle of 58:17 seconds at a PFD of 200 μmol s⁻¹ m⁻², ○—○ light / dark cycle of 23:52 seconds at a PFD of 500 μmol s⁻¹ m⁻².

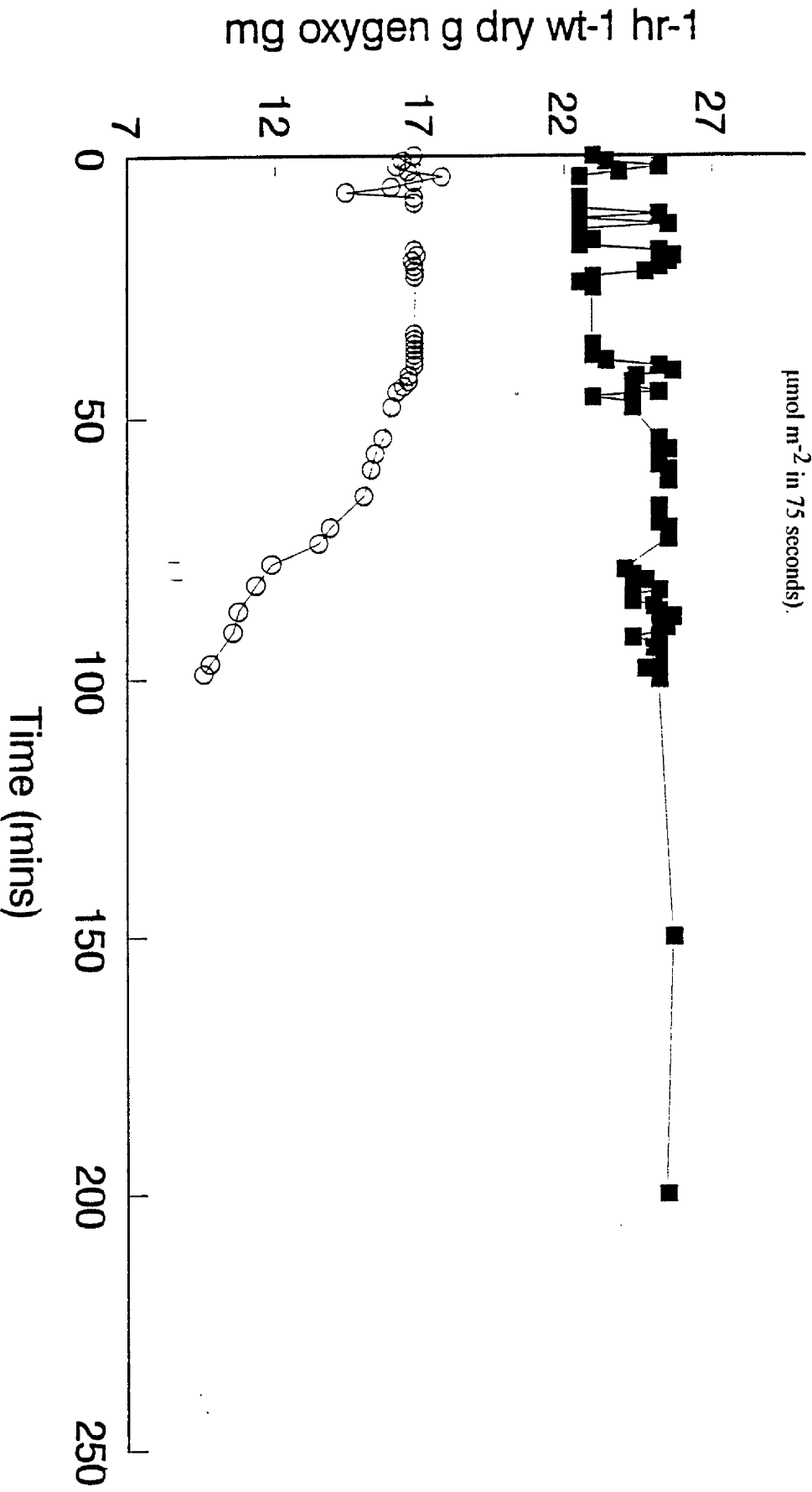


Figure 217. The effect of light dosage and light / dark cycles of PFD 300 $\mu\text{mol s}^{-1} \text{m}^{-2}$ and 600 $\mu\text{mol s}^{-1} \text{m}^{-2}$ on the photosynthesis of *Synechococcus* 1479/5, O—O light / dark cycle of 60:15 seconds PFD 300 $\mu\text{mol s}^{-1} \text{m}^{-2}$ (total light dosage 18000 $\mu\text{mol m}^{-2}$ in 75 seconds), ■—■ light / dark cycle of 30:45 seconds PFD 600 $\mu\text{mol s}^{-1} \text{m}^{-2}$ (total dosage 18000 $\mu\text{mol m}^{-2}$ in 75 seconds).

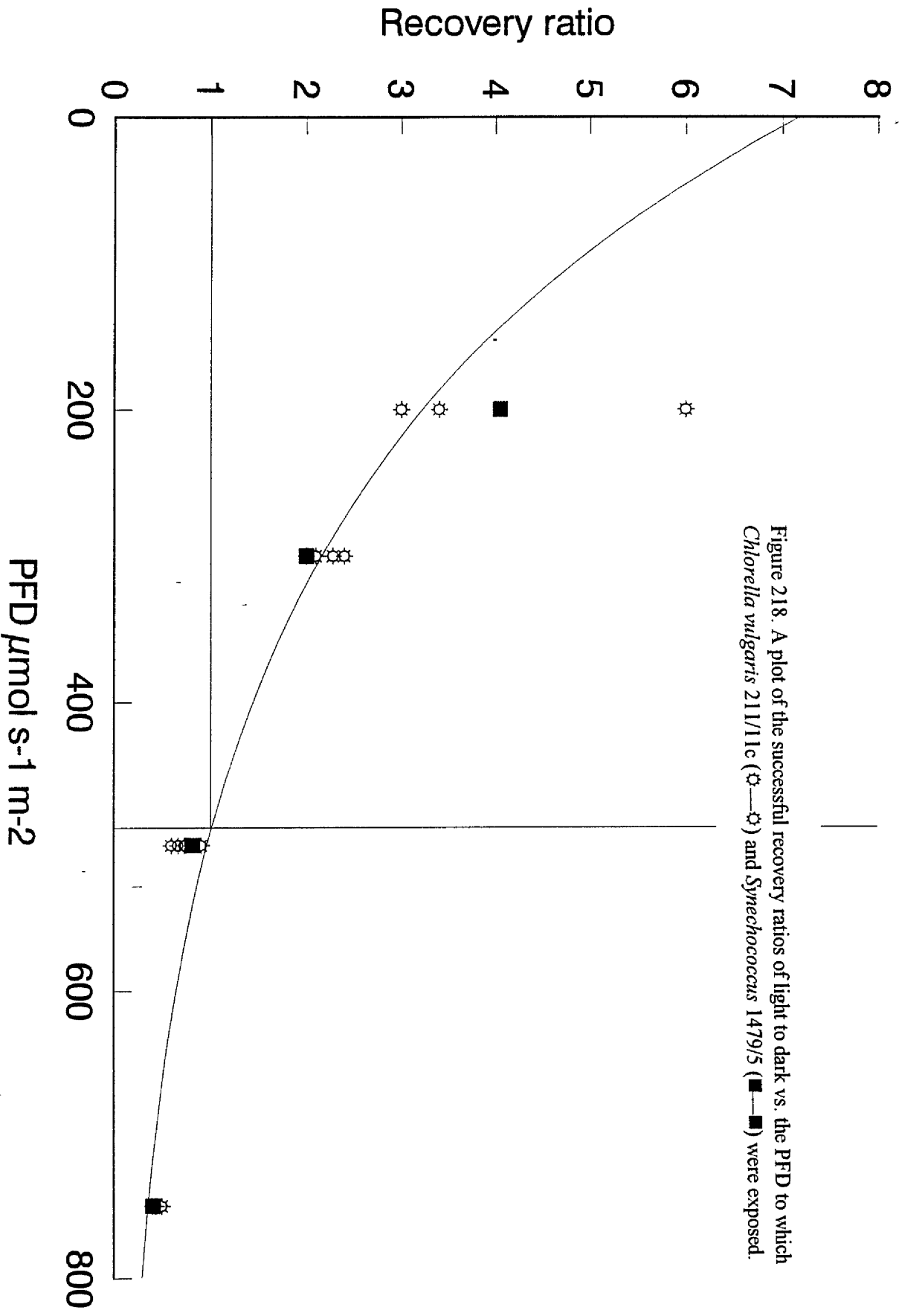


Figure 218. A plot of the successful recovery ratios of light to dark vs. the PFD to which *Chlorella vulgaris* 211/11c (○) and *Synechococcus* 1479/5 (■) were exposed.

1479/5. Figure 218 shows a plot of photon flux density (i.e. the irradiance at which the light / dark cycle was carried out) against recovery ratio (i.e. the ratio of light to dark where a constant photosynthetic rate was maintained at a particular PFD for a minimum of 24 hours). The equation describing Figure 218 is presented below: All data points were plotted regardless of the light duration the experiment was concerned with.

$$R_D^L = 40588.4 \times PFD^{-1.73} \quad (\text{Sig } P=0.01) \quad (153)$$

PFD = photon flux density ($\mu\text{mol s}^{-1} \text{m}^{-2}$)

R_D^L = Light / Dark ratio from which no indication of photoinhibition was obtained.

The vertical line intersecting the power line plot of figure 218 shows the point at which a light / dark cycle of 1:1 ratio is obtained at the corresponding PFD. This point was found to be at an approximate PFD of $470 \mu\text{mol s}^{-1} \text{m}^{-2}$ which is in between the values of those carried out in all of the above experiments. Equation (153) has only been determined from the results of experiments performed using *Chlorella vulgaris* 211/11c and *Synechococcus* 1479/5 in light / dark cycles of 10-280 seconds based on a data sample of 112 experiments. In HRAPs and lakes this time scale is important, however, in sea and ocean water systems the light / dark duration times may well exceed this time scale. It was shown that the effects of light / dark cycles on the photosynthesis of cells of a eukaryotic green micro-algae and a cyanobacterium was determined solely by the duration and magnitude of the light intensity. Although not extensively examined, light dosage did not appear to play a major role in the degree of photoinhibition and subsequent recovery. The data presented in Figures 198 and 199 were obtained from cells of *Chlorella vulgaris* 211/11c irradiated a PFD of $300 \mu\text{mol s}^{-1} \text{m}^{-2}$. It can be seen that at ratios of approximately 2:1 i.e. light / dark cycles of 120 : 50 seconds and 200 : 100 seconds resulted in different cellular responses. At the increased duration of 200 seconds (Figure 199) the cells responded swiftly with a decrease in the rate of photosynthesis as opposed to Figure 198 where the cells showed good stability when irradiated in a 2 : 1 ratio light / dark cycle whilst irradiated for 120 seconds.

Photodamage can be characterised from a photosynthesis / irradiance response curve by the PFD at which photosynthetic capacity is observed to decline. This decline has

been given a term I_b although it can be expressed as an angle β (Platt *et al.*, 1980). Light at photoinhibitory levels causing photodamage is not confined to the visible wavelengths (400-700nm). Jones and Kok, (1966) experimented using isolated spinach chloroplasts and found that a larger degree of photodamage was caused by the ultraviolet wavelengths of 250-300nm. It has been suggested that light of this wavelength affects plastoquinone in the electron transport chain linking photosystems I and II (Kirk, 1983). Cells that are confronted with light of high, photoinhibitive PFDs have to remove the energy they receive in excess of that required for the cell photosynthesis. This energy removal is usually non radiative decay as heat (NRD). The removal of energy of high light intensity light as heat is considered to be an important process in preventing photodamage (Powles, 1984). Other methods of high energy removal from light include the transferring of excitation energy between groups of pigments (Fork and Satoh, 1986). They also suggested that cycling electron flow around photosystem II may help as a method of spreading out light energy absorbed by reaction centres. This would ultimately reduce the energy impact on one photosystem and thus help reduce light saturation of that photosystem and hence reduce cellular photodamage. This should not be confused with the transfer of energy from photosystem II to photosystem I (the spillover theory; Kirk, 1983), as this process is not thought to occur in green micro-algae.

Light / dark cycles similar to those measured in the above experiments (seconds to minutes) are known to occur in lake and pond systems (Gallegos and Platt, 1981; Ferris and Christian, 1991; Prezelin *et al.*, 1991). Light / dark cycles of the order of seconds / minutes have been caused by clouds (Walsh and Legendre, 1983), surface waves; floating macrophytes; edge shadows (Walsh and Legendre, 1983). Other physical changes can create a change in light in the upper layers of a water body e.g. internal breaking waves (minutes to hours) (Denman and Gargett, 1983); Langmuir circulation (20-30 minutes) (Denman and Gargett, 1983). The time scales of these cycles has been shown to affect the productivity of micro-algae (Grobbelaar *et al.*, 1992); the short term continuous exposure to light / dark cycles produced in the above experiments has been shown to affect both the photosynthesis and respiration of micro-algae and cyanobacteria. The rapid response to changes in light / dark cycles suggests that even changes in time scales down to several seconds may determine if a cell will survive when competing for nutrients with other species of cells.

It has been suggested that water movements affect algal cell light / dark cycling to a similar extent as scattered cloud passing (Gallegos and Platt, 1982). However even if this were to be correct, the degree of change in spectral quality would have a more profound effect on photosynthesis and productivity with depth of the water body rather than the surface. The effect of spectral quality is discussed further in Section 3.9.1 and 3.9.2.

Whilst working with Arctic marine populations it has been observed by Gallegos *et al* (1983), that cells which become low light adapted are more prone to damage by light of lower PFD than the same surface population. The results of this work are supported from the observations made in Section 3.4 where cells cultured at a PFD of $200\mu\text{mol s}^{-1} \text{m}^{-2}$ had a higher resistance to the onset of photoinhibition than similar cells cultured at a PFD of $100\mu\text{mol s}^{-1} \text{m}^{-2}$. It is well documented that certain diatoms and brown algae are capable of avoiding photodamage by shifting their orientation to the light source (Kirk, 1983), or by migration and volume change (Kirk, 1983; Powles, 1984). This data presented here would support that cells capable of changing the physical orientation to reduce exposure to light would have a distinct advantage in harsh light regimes compared to non migrating cells.

Light of PFDs as high as $1500\mu\text{mol s}^{-1} \text{m}^{-2}$ has been recorded at the surface of HRAPs based at Auchincruive Ayr. This high light intensity is photoinhibitive to virtually all species of algae and cyanobacteria present within these ponds systems. However the cells may only be exposed to light of high PFDs for only a few seconds or minutes as they continually move throughout the pond depth with varying attenuation. By examining such light / dark cycles that exist in pond systems it is possible to change the mixing conditions in order to manipulate the time spent in certain photoinhibitive PFDs. The data presented for *Chlorella vulgaris* 211/11c would certainly suggest that unicellular cells of green micro-algae would not be affected by photoinhibiting irradiance of PFD as high as $1500\mu\text{mol s}^{-1} \text{m}^{-2}$. Further analysis on the short term effect of light / dark cycles on other typical species of micro-algae found in HRAP would be required to confirm this.

The data obtained from light / dark cycling is extremely useful since very little information is freely available concerning the effects of medium frequency (seconds to minutes) (Grobbelaar, 1989) light / dark cycles on micro-algal and cyanobacterial

photosynthesis and productivity. Richmond *et al.*, (1980) suggested that light / dark cycles ranging from seconds to minutes would enhance the output rate from algal cultures. From the experiments presented here and Section 3.10. light / dark cycling is seen as a means by which cells can recover from the effects of photoinhibitive light. Whether this recovery takes the form of cellular maintenance, resulting in increases in protein synthesis, or takes the form of energy transfer to prevent saturation problems of the photoreaction centres is unclear. Due to the large increases in respiration rates that are accompanied with exposure to high light intensities, it suggests that protein synthesis and cellular maintenance / repair is the likely method.

Very high light intensities can result in a decrease in photosynthetic oxygen production (Jensen and Knutsen 1993), however, the process of photoinhibition is usually accompanied with an increase in the light enhanced dark respiration oxygen uptake rate. It is the duration and intensity of the light that determines a cell's photosynthetic rate and overall survivability in a given circumstance as opposed to the dosage of light. A cell can recover from photoinhibition provided the length of time spent in the dark is sufficient for cell repair mechanisms to deal with photodamage before the next exposure to the same irradiance. It is unclear whether light at a very low intensity actually aids in the cell repair mechanism after exposure to very high light intensities. Further information on the effects of light / dark cycling of medium frequency (seconds to minutes) on photosynthetic enhancement can be found in the results and discussion concerning the growth of micro-algae in light gradients under batch kinetics (section 3.8).

3.6 The growth of Micro-algae and Cyanobacteria in light / dark cycles of medium frequency in the FPALR under continuous kinetics.

A relationship was determined using an oxygen electrode system, between irradiance (photon flux density) and the time required for cellular dark respiration to prevent the onset of photoinhibition. This relationship, however, had been determined in a 24 hour period in a system operating under timed fed batch kinetics. It was therefore necessary to examine the role of light / dark cycles of medium frequency on both the growth / photosynthetic kinetics and in the role preventing the onset of photoinhibition in cells growing under continuous kinetics.

3.6.1 The effect of light / dark cycles of medium frequency on the growth of cells of *Chlorella vulgaris* 211/11c.

Chlorella vulgaris 211/11c was cultured in the FPALR (10 litre volume) under conditions of 4% carbon dioxide, 23°C, Reynolds number 5800 and PFDs of 100, 200, 400 and 750 $\mu\text{mol s}^{-1} \text{m}^{-2}$. At a Reynolds number of 5800, the cells were circulating within the FPALR through a light / dark cycle of 58:26 seconds. The experiment was carried out in duplicate. Where possible cells were only left in a steady state at each photon flux density (PFD) for a maximum of 5 days before changing to the next irradiance to prevent the possibility of photoadaptation to the given irradiance. Since the PFD of the FPALR was increased sequentially such that the culture became an inoculum for the next PFD increase, the prevention of photoadaptation was potentially important. Data from Brand *et al.*, (1981) suggested that between 5 and 20 generations (cell divisions) were required at a given irradiance before cells become fully adapted to that environment.

The FPALR was run under batch kinetics between day 0 and day 5 to allow the cells time to adapt to the higher shear forces that existed in the FPALR, compared to the shaker flasks the cells were grown in prior to inoculation. Data obtained from experiments performed in growing cells of micro-algae and cyanobacteria in the FPALR operating under batch kinetics (section 3.2) showed that the cells remained

approximately 48-70 hours in a lag growth phase. Since during this lag phase of growth, the growth rates were extremely low, the subsequent culturing of cells in the FPALR operating under continuous kinetics would have washed them out of system. After 5 days the FPALR was switched over to continuous operation and growth was monitored via optical density (560nm). Using the growth rate of 1.05 day^{-1} (cell doubling time 15.84 hours) determined from culturing cells of *Chlorella vulgaris* 211/11c in the FPALR operating under batch kinetics (3.2), the dilution rate was set at 0.92 day^{-1} . This was below the maximum growth rate for cells of *Chlorella vulgaris* 211/11c cultured under conditions of 4% carbon dioxide, at a temperature of 23°C and irradiated at a PFD of $100 \mu\text{mol s}^{-1} \text{ m}^{-2}$. However it was necessary to ensure that any reduction in the growth rate of cells did not cause the process of wash out from within the FPALR. At the dilution rate of 0.92 day^{-1} , the residence time in the FPALR was 18.07 hours.

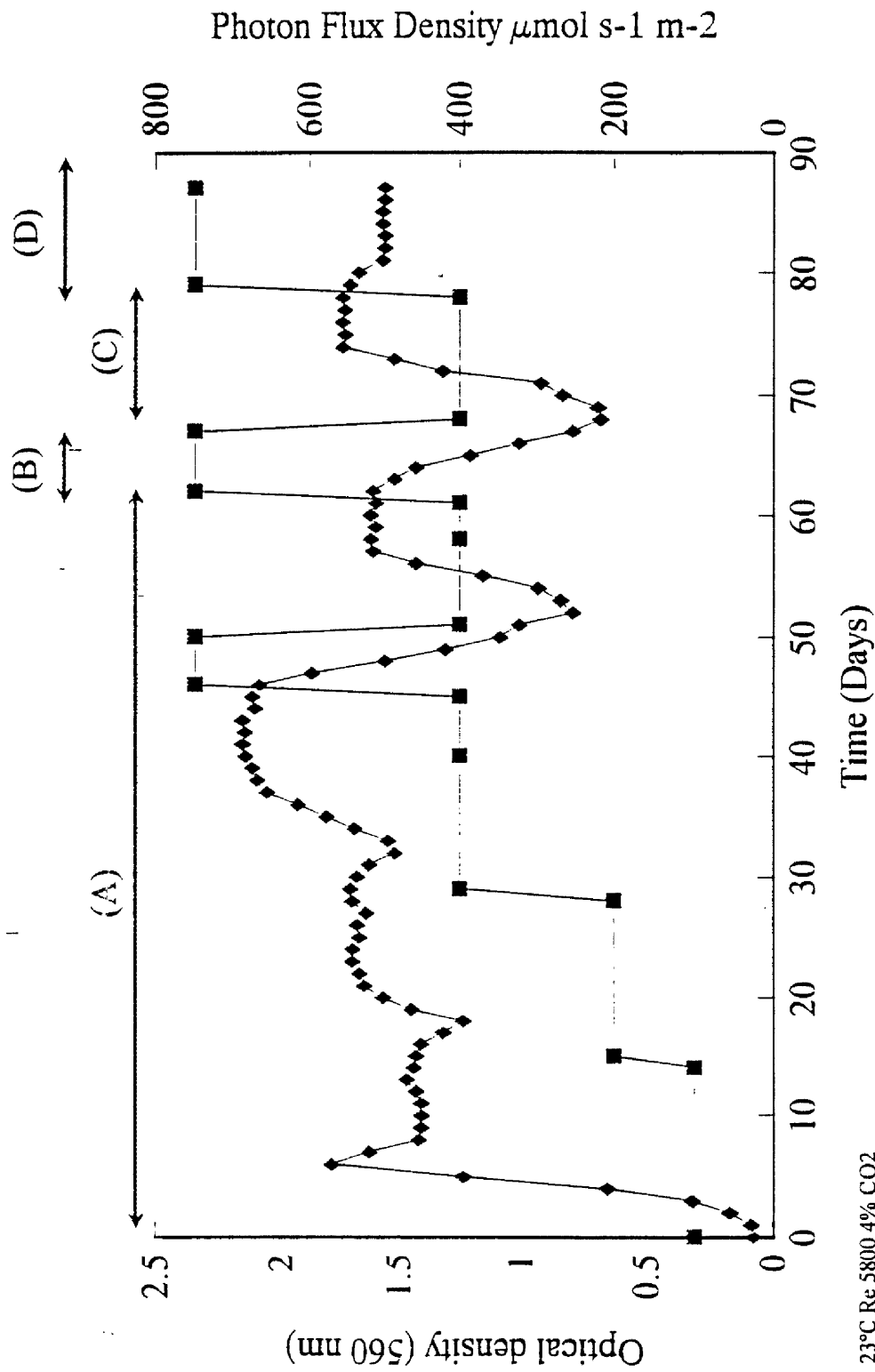
Figure 219 shows the variation in optical density (560nm) with changing PFD. Figure 220 shows the variation in the measured chlorophyll a content whilst Table 87 shows the average chlorophyll a levels with errors obtained over each constant PFD value. At a dilution rate of 0.922 day^{-1} the cells were observed to have reached steady state after 11 days and were maintained under these conditions for a further 4 days after which the PFD was increased to $200 \mu\text{mol s}^{-1} \text{ m}^{-2}$ (Figure 219). The chlorophyll a content of the culture measured at a PFD of $100 \mu\text{mol s}^{-1} \text{ m}^{-2}$ was $16.93 \mu\text{g ml}^{-1}$. The increase in PFD from 100 - $200 \mu\text{mol s}^{-1} \text{ m}^{-2}$ was achieved by exchanging the neutral density field filter with one that had previously been constructed for the higher PFD. The time taken for the exchange of light fields was less than 10 minutes. It was found after increasing the light field to $200 \mu\text{mol s}^{-1} \text{ m}^{-2}$, that there was a decrease in the optical density. This decrease in optical density was later confirmed with equivalent decreases in both chlorophyll a (Table 87) and dry matter content. The decrease was monitored continuously and continued for 2 days after which the optical density increased to reach a new steady state plateau, higher than the one previously observed for cells at a PFD of $100 \mu\text{mol s}^{-1} \text{ m}^{-2}$ (Figure 219). The chlorophyll a content at a PFD of $200 \mu\text{mol s}^{-1} \text{ m}^{-2}$ was $14.71 \mu\text{g ml}^{-1}$. This new steady state was maintained for 5 days until the light field was increased to a PFD $400 \mu\text{mol s}^{-1} \text{ m}^{-2}$. As was recorded previously there was an initial decrease in optical density recorded for 3 days after which the optical density rose to a new steady state. At this new PFD the cells were still in the light / dark cycle ratio of 2.23:1 (58:26 seconds) but at a known

Table 87: The effect of changing PFD on the average cell chlorophyll a content ($\mu\text{g ml}^{-1}$) of *Chlorella vulgaris* 211/11c cultured in the FPALR.

PFD in FPALR $\mu\text{ mol s}^{-1}\text{ m}^{-2}$	Average Chlorophyll a ($\mu\text{g ml}^{-1}$)
100	16.932 \pm 0.326
200	14.71 \pm 0.772
400	10.89 \pm 0.393
750	8.326 \pm 0.701
400	10.403 \pm 0.886
750	7.933 \pm 1.11
400	11.82 \pm 0.913
750	8.786 \pm 0.933

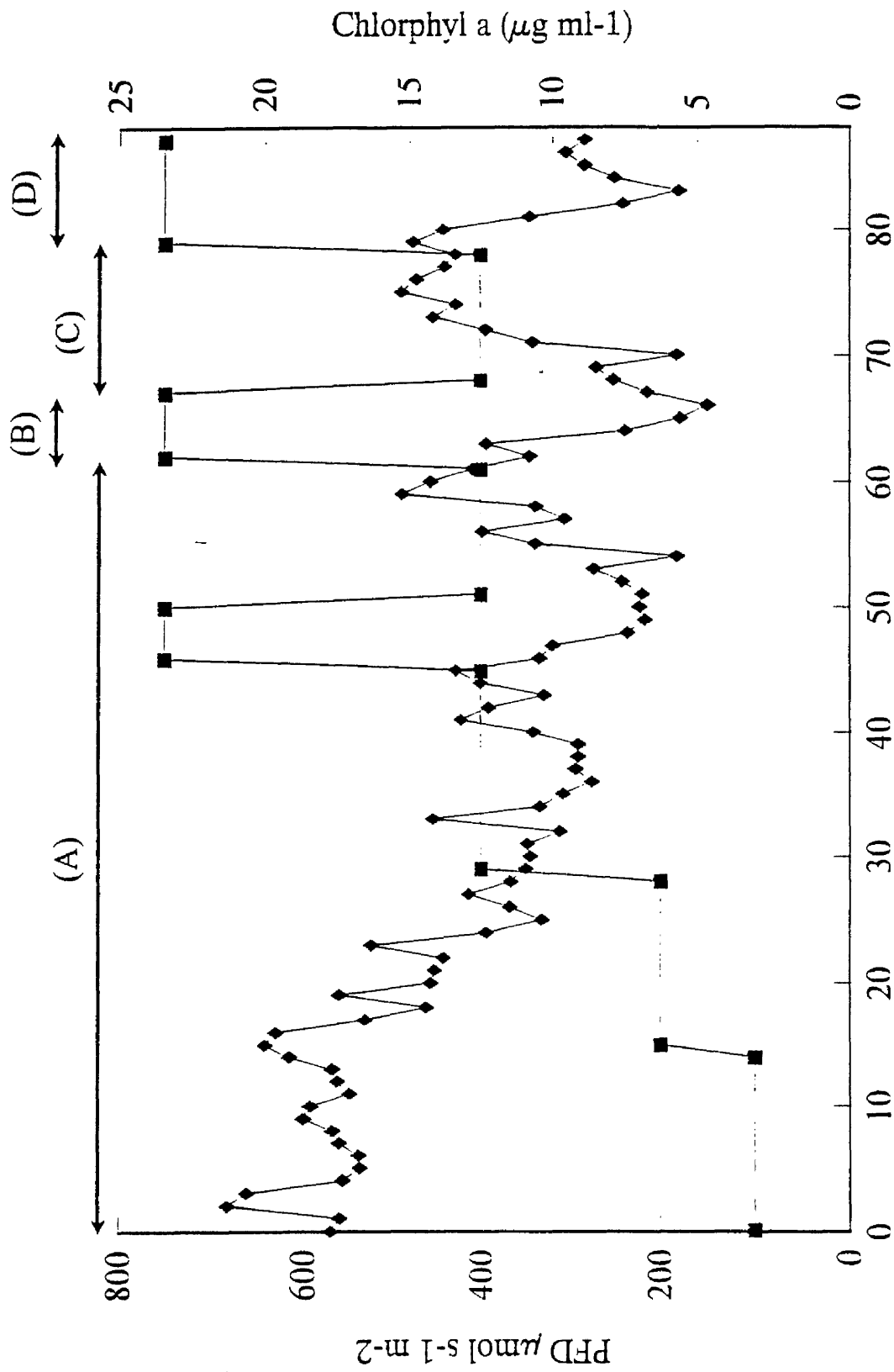
Table 88: The effect of changing PFD on the average cell chlorophyll a content ($\mu\text{g ml}^{-1}$) of *Synechococcus* 1479/5 cultured in the FPALR.

PFD in FPALR $\mu\text{ mol s}^{-1}\text{ m}^{-2}$	Average Chlorophyll a ($\mu\text{g ml}^{-1}$)
100	13.8 \pm 1.06
200	11.21 \pm 0.88
400	8.46 \pm 1.12
750	5.61 \pm 0.57
400	7.1 \pm 1.2
750	4.78 \pm 1.19
400	7.83 \pm 0.77
750	4.02 \pm 2.16
400	7.33 \pm 1.28
750	6.36 \pm 0.65



23°C Re 5800 4% CO₂

Figure 219. The variation in optical density (560nm) of *Chlorella vulgaris* 211/1c with changes in PFD and light / dark cycles, ■— PFD ($\mu\text{mol s}^{-1} \text{m}^{-2}$), ◆— optical density (560nm), (A) light / dark cycle 58:26 seconds, (B) light / dark cycle 29:55 seconds, (C) light / dark cycle 58:26 seconds, (D) light / dark cycle 19:65 seconds.



4% CO₂ 23°C Rey5800

Time (days)

Figure 220. The variation in chlorophyll a concentration of *Chlorella vulgaris* 211/11c with changes in PFD and light / dark cycles, ■—■ PFD ($\mu\text{mol s}^{-1} \text{m}^{-2}$), ◆—◆ chlorophyll a concentration, (A) light / dark cycle 58:26 seconds, (B) light / dark cycle 29:55 seconds, (C) light / dark cycle 58:26 seconds, (D) light / dark cycle 19:65 seconds.

photoinhibitory PFD to cells of *Chlorella vulgaris* 211/11c (Figure 195). The chlorophyll a content of the culture decreased from $14.71\mu\text{g ml}^{-1}$ (measured at a PFD of $200\mu\text{mol s}^{-1} \text{m}^{-2}$) to $10.89\mu\text{g ml}^{-1}$ (determined at a PFD of $400\mu\text{mol s}^{-1} \text{m}^{-2}$). The plot of Figure 218 (displaying light / dark recovery ratio vs. PFD) suggested that in order for cells of *Chlorella vulgaris* 211/11c to maintain photosynthetic rates and productivity at a PFD of $400\mu\text{mol s}^{-1} \text{m}^{-2}$ the ratio of light to dark would have to be of the order 1.2 : 1. As the measured ratio in the FPALR was 2.23:1 (at a PFD of $400\mu\text{mol s}^{-1} \text{m}^{-2}$ in a light dark cycle of 58:26 seconds) it would indicate that the cells in the FPALR were close to the "survival" ratio but the results supported the data obtained with the oxygen electrode that suggested cells would continue to photosynthesise and maintain growth rates.

After a steady state period of approximately 5 days had elapsed, the light field was increased to a PFD of $750\mu\text{mol s}^{-1} \text{m}^{-2}$. The light / dark cycle was maintained at 58:26 seconds (2.23:1). The cells of *Chlorella vulgaris* 211/11c responded rapidly to this new PFD and the optical density decreased sharply. Unlike the previous response to increases in PFD, there was no measured increase in optical density after the initial fall. The chlorophyll a content of the culture at the PFD of $750\mu\text{mol s}^{-1} \text{m}^{-2}$ was $8.32\mu\text{g ml}^{-1}$. This continuous decrease in optical density suggested that the cells were suffering from photoinhibition and possible photodamage. The growth rate was now below the dilution rate and productivity fell as the culture approached wash out from within the FPALR.

Figure 204 suggested that cells of *Chlorella vulgaris* 211/11c irradiated at a PFD of $750\mu\text{mol s}^{-1} \text{m}^{-2}$ for 60 seconds required a dark stage of 120 seconds to recover (1:2 ratio). However the light / dark cycle ratio in the FPALR was 58:26 seconds (2.23:1). The observed decrease in the optical density and chlorophyll content of the culture in the FPALR supports the data recorded in the plot of Figure 204.

After the optical density had fallen to 0.7 it was decided to place the cells back at a PFD $400\mu\text{mol s}^{-1} \text{m}^{-2}$ in a light / dark cycle of 58 : 26 seconds, in an attempt to maintain the culture. At this lower PFD of $400\mu\text{mol s}^{-1} \text{m}^{-2}$ the optical density decreased for a further 2 days, after which it began to increase to a steady state plateau lower than the one previously attained by cells previously irradiated at $400\mu\text{mol s}^{-1} \text{m}^{-2}$ (Figure 219). Although the recovery took place in a similar light regime

the optical characteristics, however, were different to the original in which the cells had been exposed to (i.e. the original cells irradiated at a PFD of $400\mu\text{mol s}^{-1} \text{m}^{-2}$ had originally been irradiated at $200\mu\text{mol s}^{-1} \text{m}^{-2}$ and so had originated from a densely populated mass of cells. The new population of cells growing at a PFD of $400\mu\text{mol s}^{-1} \text{m}^{-2}$ had originated from what was left over after the parent population had been exposed to a photoinhibitory PFD of $750\mu\text{mol s}^{-1} \text{m}^{-2}$. This difference could account for the difference in final steady state plateau between the $400\mu\text{mol s}^{-1} \text{m}^{-2}$ irradiated populations after each of the $750\mu\text{mol s}^{-1} \text{m}^{-2}$ irradiances. The cells were maintained at a steady state for 5 days at a PFD of $400\mu\text{mol s}^{-1} \text{m}^{-2}$ to monitor any subsequent changes in growth pattern. Subsequent measurement of the chlorophyll a content of the culture showed that it had increased from $8.32\mu\text{g ml}^{-1}$ (at a PFD of $750\mu\text{mol s}^{-1} \text{m}^{-2}$) to $10.4\mu\text{g ml}^{-1}$ (at a PFD of $400\mu\text{mol s}^{-1} \text{m}^{-2}$)

Since the cells of *Chlorella vulgaris* 211/11c suffered some degree of photoinhibition / photodamage whilst being irradiated at a PFD of $750\mu\text{mol s}^{-1} \text{m}^{-2}$ in a light / dark cycle of 58:26 seconds, it was necessary to alter the light / dark cycle ratio to examine the effects on cellular growth. Although a change in the dark stage volume was the simplest method to alter the light / dark cycle, this would not have generated the desired new light / dark cycle ratio of 1 : 2.4 (suggested from Figure 204 and equation 154). The top half of the photostage (channels 1-11) of the FPALR was blacked out using a sheet of white card to increase the length of time the culture spent in the dark phase of the cycle from 26 to 55 seconds creating a new light / dark cycle ratio of 29:55 seconds (1:1.89) (Figure 219). At this new light / dark cycle ratio of 29:55 seconds, the PFD was increased to $750\mu\text{mol s}^{-1} \text{m}^{-2}$. Figure 219 shows that the cell response at this PFD was very rapid and that optical density decreased sharply. The chlorophyll a content of the culture decreased to $7.93\mu\text{g ml}^{-1}$. The length of time spent in the dark was clearly not long enough for the cells to recover from the PFD of $750\mu\text{mol s}^{-1} \text{m}^{-2}$. Equation 154 predicted that a ratio of 1 : 2.4 was required for the sustainability of photosynthesis whereas the FPALR was operating at a light / dark cycle ratio of 1 : 1.89. This clearly shows that the equation needs optimising.

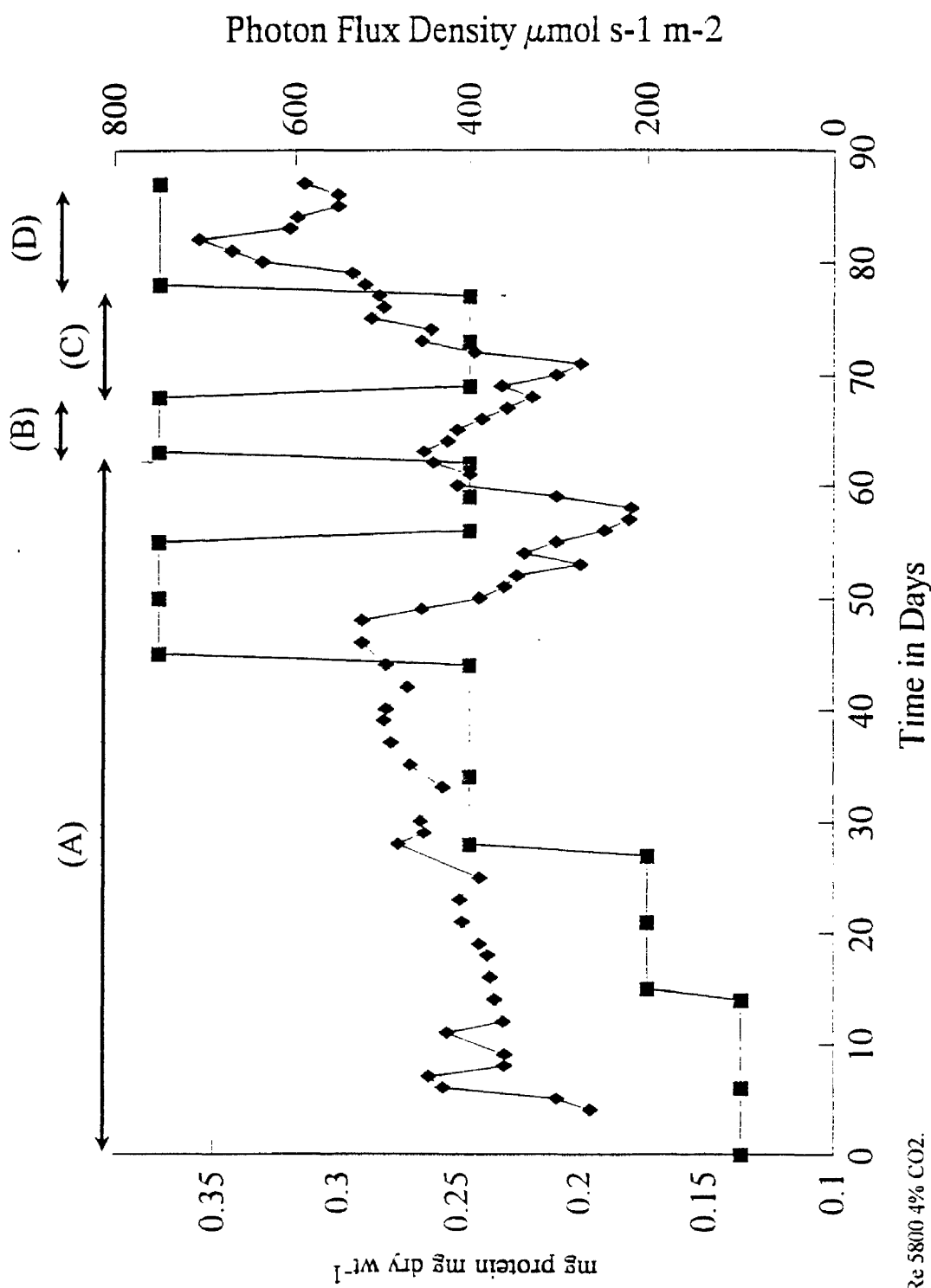
The decrease in optical density continued until the PFD was decreased to $400\mu\text{mol s}^{-1} \text{m}^{-2}$. The white card was removed at this PFD changing the light / dark cycle back to 58:26 seconds (Figure 219). At this decreased PFD of $400\mu\text{mol s}^{-1} \text{m}^{-2}$ the

chlorophyll a content of the culture was $11.82\mu\text{g ml}^{-1}$. The cells were maintained until a steady state plateau was obtained.

Using the white card, 0.66 of the photostage (channels 1-15) of the FPALR was shielded from the light providing a new light / dark cycle of 19:65 seconds (1:3.42) (Figure 219). This light / dark cycle ratio of 19:65 seconds (1:3.42) was above that suggested by Figure 204 for the "survival" of cells of *Chlorella vulgaris* 211/11c at a PFD of $750\mu\text{mol s}^{-1} \text{m}^{-2}$. At this new light / dark cycle ratio the cells were again exposed to a PFD of $750\mu\text{mol s}^{-1} \text{m}^{-2}$. It was observed that at this new light / dark cycle ratio there followed a small decrease in optical density, after which the cells reached a steady state value. No decrease in optical density was observed during this steady state period. The chlorophyll a content of the culture was maintained at approximately $8.78\mu\text{g ml}^{-1}$.

After 8 days at the new steady state problems with the FPALR forced the experiments to terminate abruptly. These problems within the FPALR were a blockage in the carbon dioxide injection system and attached growth of the *Chlorella vulgaris* 211/11c cells possibly associated with the failure to supply carbon dioxide.

Figure 221 shows the variation in protein content per ml of *Chlorella vulgaris* cells with changes in PFD (100, 200, 400, 750 and $400\mu\text{mol s}^{-1} \text{m}^{-2}$) in various light / dark cycle ratios. As the PFD was increased from 100 to $200\mu\text{mol s}^{-1} \text{m}^{-2}$ it was found that the protein content increased and reached a peak of 0.27mg mg^{-1} dry weight as the PFD was increased to $400\mu\text{mol s}^{-1} \text{m}^{-2}$. It is suggested that as the PFD increase and the cell doubling time decreased (higher growth rate), a higher degree of maintenance, repair, replication and enzyme synthesis was required at these new PFDs. As the PFD reached photodamaging levels ($750\mu\text{mol s}^{-1} \text{m}^{-2}$), however, the cell repair mechanism could not prevent or repair the damage efficiently and sufficiently. Hence the protein level decreased rapidly in a similar pattern to that observed with optical density and chlorophyll a. When the PFD was decreased to $400\mu\text{mol s}^{-1} \text{m}^{-2}$, the initial protein concentration continued to decrease for approximately 4 days, after which the concentration increased to 0.26mg mg^{-1} dry weight. When the PFD was again increased to $750\mu\text{mol s}^{-1} \text{m}^{-2}$ but in a light / dark cycle ratio of 29:55 seconds, the protein content decreased at a slower rate to 0.23mg ml^{-1} , after which the cells were returned to a PFD of $400\mu\text{mol s}^{-1} \text{m}^{-2}$ and a light / dark cycle ratio of 58:26 seconds. As was observed previously, the protein content

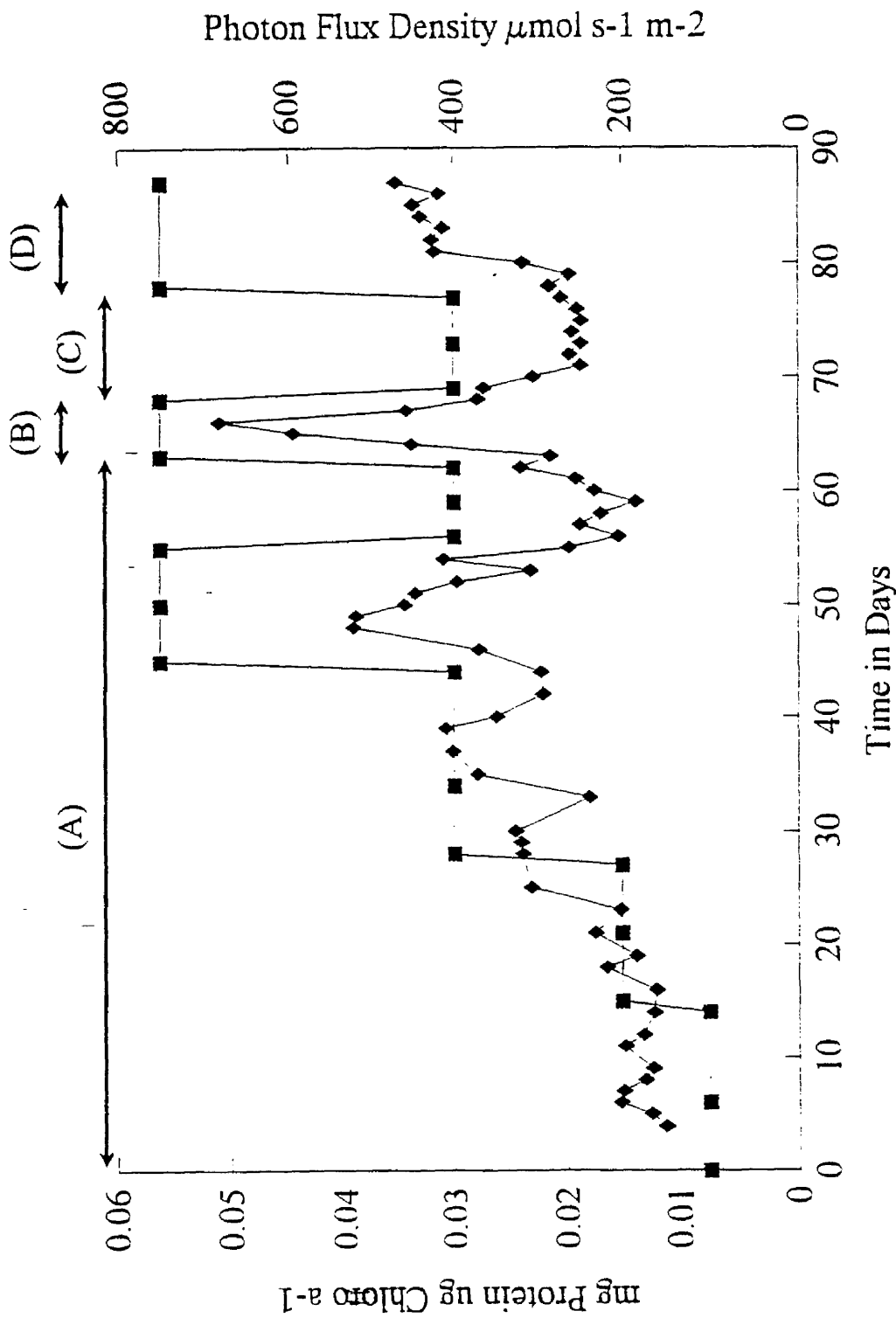


23°C Re 5800 4% CO₂.
 Figure 221. The variation in protein concentration of *Chlorella vulgaris* 211/1c with changes in PFD and light / dark cycles, ■—■ PFD (μmol s⁻¹ m⁻²), ◆—◆ protein content, (A) light / dark cycle 58:26 seconds, (B) light / dark cycle 29:55 seconds, (C) light / dark cycle 19:65 seconds, (D) light / dark cycle 58:26 seconds.

remained unsteady for a period of 3 to 4 days, after which the level increased to approximately 0.28 mg ml^{-1} . When the PFD was increased to $750 \mu\text{mol s}^{-1} \text{ m}^{-2}$ and the light / dark cycle was changed to 19:65 seconds, the protein content increased to 0.35 mg ml^{-1} , however, this steady increase only lasted for 5 days, after which it decreased to a steady value of 0.3 mg ml^{-1} .

Figure 222 shows the protein level per chlorophyll a variation with changing PFD and light / dark cycle. It can be seen that the ratio of protein : chlorophyll increased with increasing PFD until the PFD was increased to $750 \mu\text{mol s}^{-1} \text{ m}^{-2}$. At this PFD the ratio of protein : chlorophyll showed an initial increase to $0.04 \text{ mg protein per } \mu\text{g chlorophyll a}$, after which it decreased rapidly to $0.015 \text{ mg protein per } \mu\text{g chlorophyll a}$. When the PFD was decreased to $400 \mu\text{mol s}^{-1} \text{ m}^{-2}$, the protein : chlorophyll a ratio continued to decrease for a further 5 days, after which it showed a steady increase. During this increase the PFD was increased to $750 \mu\text{mol s}^{-1} \text{ m}^{-2}$ and the light / dark cycle was changed to 29:55 seconds. At this PFD and new light / dark cycle, a burst of protein synthesis was observed to occur at very low levels of chlorophyll a (Figure 220). After the initial increase, there followed a sharp fall in the protein : chlorophyll a ratio to $0.017 \text{ mg protein per } \mu\text{g chlorophyll a}$. The reduction in this ratio continued for 3 days after the cells had been placed in a light field of $400 \mu\text{mol s}^{-1} \text{ m}^{-2}$ at the original light / dark cycle of 58:26 seconds. Little change in the ratio was measured whilst the cells were irradiated at $400 \mu\text{mol s}^{-1} \text{ m}^{-2}$. When the PFD was again increased to $750 \mu\text{mol s}^{-1} \text{ m}^{-2}$ in a new light / dark cycle of 19:65 seconds, the cells showed an increase in the protein : chlorophyll a to $0.032 \text{ mg protein per } \mu\text{g chlorophyll a}$ which remained steady.

Cells of *Chlorella vulgaris* 211/11c were able to continue growing and photosynthesising in the FPALR irradiated for 19 seconds at a PFD of $750 \mu\text{mol s}^{-1} \text{ m}^{-2}$ only when circulated through a dark phase lasting 65 seconds or more. The data from the continuous culturing of *Chlorella vulgaris* 211/11c in the FPALR supports the measurements made Figure 204 on the light / dark cycle experiments involving the oxygen electrode which suggested that cells of *Chlorella vulgaris* 211/11c would "survive" a 60 second exposure to a PFD of $750 \mu\text{mol s}^{-1} \text{ m}^{-2}$ provided recovery could take place for 120 seconds in the dark.



23°C Re-5800 4% CO₂.

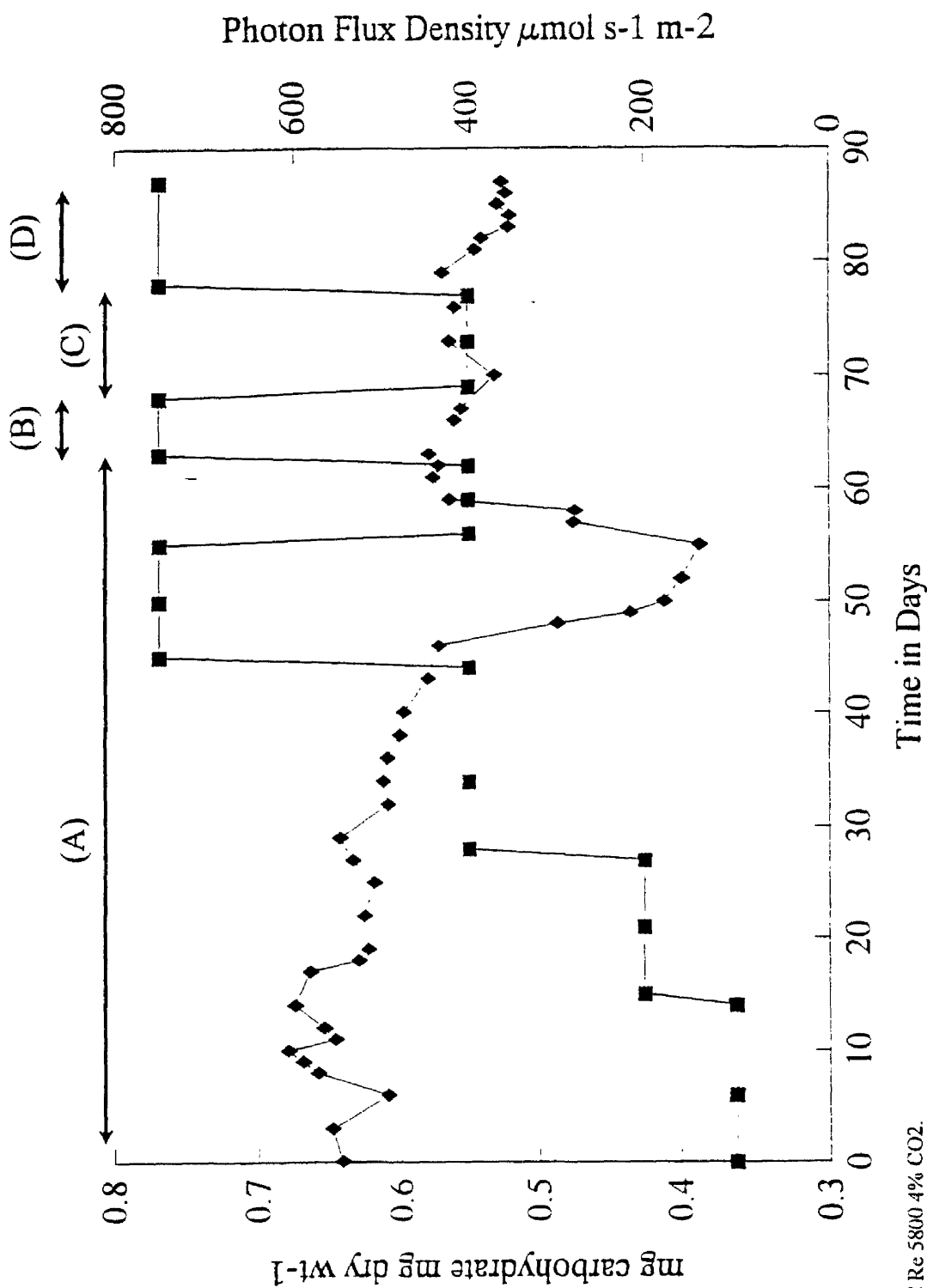
Figure 222. The variation in the protein to chlorophyll a ratio of *Chlorella vulgaris* 211/11c with changes in PFD and light / dark cycles, \blacksquare — \blacksquare PFD ($\mu\text{mol s}^{-1} \text{m}^{-2}$), \blacklozenge — \blacklozenge protein:chlorophyll a ratio, (A) light / dark cycle 58:26 seconds, (B) light / dark cycle 29:55 seconds, (C) light / dark cycle 58:26 seconds, (D) light / dark cycle 19:65 seconds.

Figure 223 shows the variation in the cellular carbohydrate content of *Chlorella vulgaris* 211/11c. It can be seen that the carbohydrate levels fell rapidly during periods of high photoinhibitive light intensity especially when the PFD was at $750 \mu\text{mol s}^{-1} \text{m}^{-2}$ in a light / dark cycle of 58:26 seconds (part A of Figure 223). When the light / dark cycle was changed to 29:55 seconds at a PFD of $750 \mu\text{mol s}^{-1} \text{m}^{-2}$, the carbohydrate did not display any indications of a rapid decrease.

From the above observations, it is clear that the protein per chlorophyll a ratio varied to a large degree when no change was made in the light field. It is unclear why this was the case. It can be seen, however, that the largest changes (decreasing) occurred in the protein per chlorophyll a ratio when the cells were incubated in a light / dark cycle at a high irradiance of $750 \mu\text{mol s}^{-1} \text{m}^{-2}$ (Figure 222). Similar reduction in the protein content of cells when irradiated by light of photoinhibitory intensity has been reported during photooxidation studies (Powles, 1984; Raven and Samuelsson, 1986). High photoinhibitory light may be avoided by decreasing the number of available antenna pigment molecules (Raven, 1989). This, however, does not entirely explain why the protein levels fell so sharply. It has been generally found that the photosynthetic apparatus that is likely to be damaged by photoinhibitory light is the photosystem II protein group (Powles, 1984; Raven, 1989). It is also known that this protein molecule can only be repaired if a new polypeptide chain is resynthesised (Powles, 1984). This would explain why the protein content fell during exposure periods of high light but then increased when the light was reduced to below photoinhibitory levels or the cells were placed in a more favourable light / dark cycle (in which the light fraction was reduced or the dark fraction increased).

3.6.2 The effect of light / dark cycles of medium frequency on the growth of cells of *Synechococcus* 1479/5.

Figure 224 shows the results obtained when culturing *Synechococcus* 1479/5 in the FPALR under the same conditions as previously described above for *Chlorella vulgaris* 211/11c. As with *Chlorella vulgaris* 211/11c the FPALR was operated under batch kinetics for the first 5 days. It can be seen that as the PFD was increased from $100\text{--}400 \mu\text{mol s}^{-1} \text{m}^{-2}$ whilst in a light / dark cycle of 58:26 seconds, the optical density also increased. Unlike *Chlorella vulgaris* 211/11c, however, no decrease in



23°C Re 5800 4% CO₂.

Figure 223. The variation in carbohydrate concentration of *Chlorella vulgaris* 211/11c with changes in PFD and light / dark cycles, ■—■ PFD ($\mu\text{mol s}^{-1} \text{m}^{-2}$), ◆—◆ carbohydrate content, (A) light / dark cycle 58:26 seconds, (B) light / dark cycle 29:55 seconds, (C) light / dark cycle 58:26 seconds, (D) light / dark cycle 19:65 seconds.

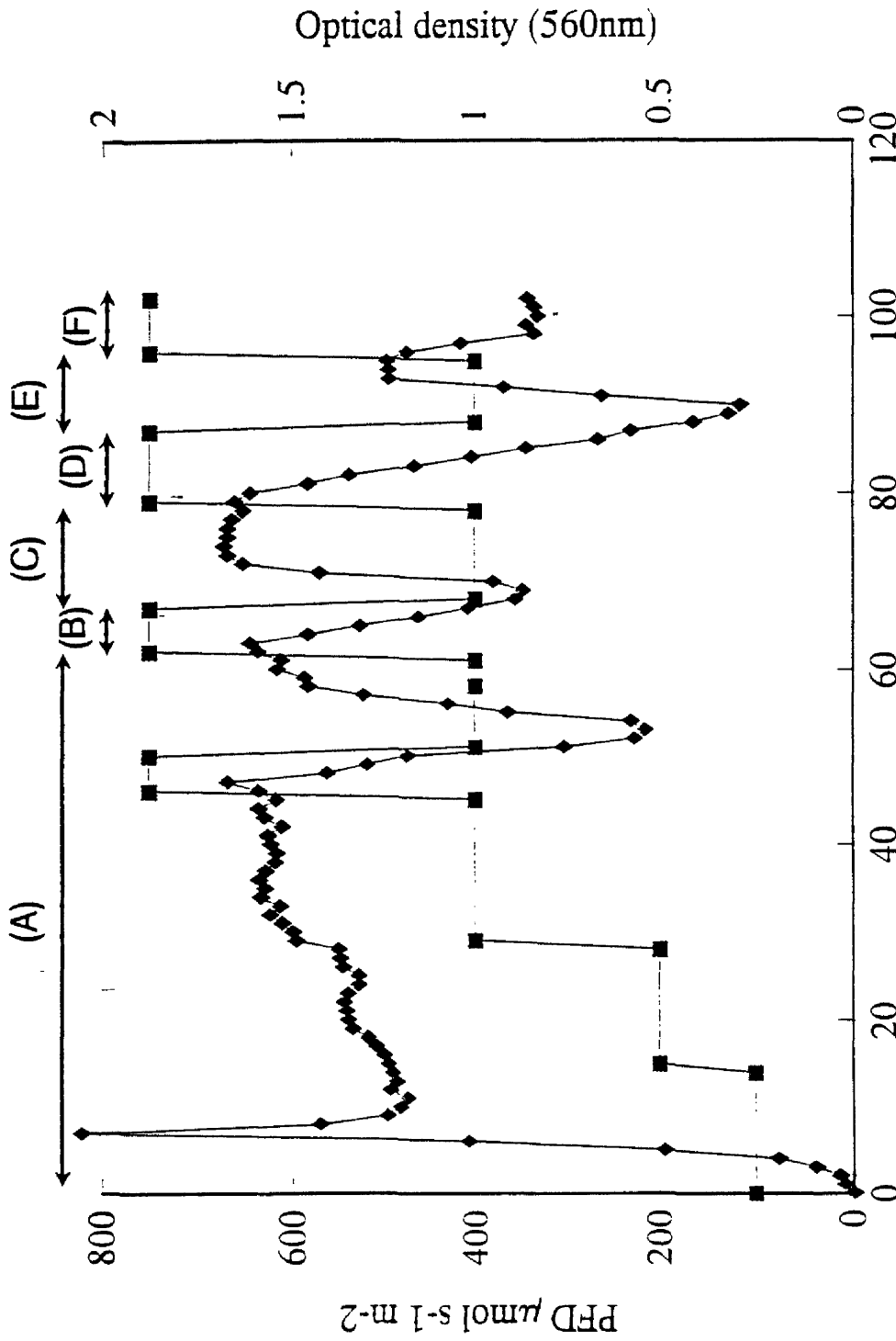


Figure 224. The variation in optical density (560nm) of *Synechococcus* 1479/5 with changes in PFD and light / dark cycles, ■—■ PFD ($\mu\text{mol s}^{-1} \text{m}^{-2}$), ◆—◆ optical density (560nm), (A) light / dark cycle 58:26 seconds, (B) light / dark cycle 29:55 seconds, (C) light / dark cycle 58:26 seconds, (D) light / dark cycle 19:65 seconds (E) light / dark cycle 58:26 seconds, (F) light / dark cycle 14:5:69.5 seconds.

Rey 5800 23°C 4%CO₂

optical density was observed immediately after an increase in PFD (Figure 224 compared to Figure 219). Chlorophyll a was observed to decrease from $13.8\mu\text{g ml}^{-1}$ at a PFD of $100\mu\text{mol s}^{-1} \text{m}^{-2}$ to $11.21\mu\text{g ml}^{-1}$ at a PFD of $200\mu\text{mol s}^{-1} \text{m}^{-2}$ (Figure 225, Table 88). As was found with cells of *Chlorella vulgaris* 211/11c, the chlorophyll a content of the *Synechococcus* 1479/5 culture decreased with each subsequent increase in PFD. When the FPALR was irradiated at a PFD of $400\mu\text{mol s}^{-1} \text{m}^{-2}$ the chlorophyll a content decreased to $8.46\mu\text{g ml}^{-1}$ of culture. At this PFD of $400\mu\text{mol s}^{-1} \text{m}^{-2}$, the cells of *Synechococcus* 1479/5 were in a light / dark cycle of 58:26 seconds. Figure 218 suggested that the light / dark ratio required to prevent the onset of photoinhibition at a PFD of $400\mu\text{mol s}^{-1} \text{m}^{-2}$ was 2:1. The cells of *Synechococcus* 1479/5 were close to the "survival" border and did not show any indications of photoinhibition or photodamage caused by the high light intensity of $400\mu\text{mol s}^{-1} \text{m}^{-2}$.

Increasing the irradiance PFD to $750\mu\text{mol s}^{-1} \text{m}^{-2}$ resulted in decreases in both the optical density and chlorophyll a values (Figures 224 and 225 respectively). The chlorophyll a content of the culture decreased to $5.61\mu\text{g ml}^{-1}$. The cells were only prevented from wash out within the FPALR by decreasing the PFD to $400\mu\text{mol s}^{-1} \text{m}^{-2}$. The chlorophyll a content of the culture irradiated at this reduced PFD of $400\mu\text{mol s}^{-1} \text{m}^{-2}$ increased to $7.1\mu\text{g ml}^{-1}$.

Using the same method adopted for *Chlorella vulgaris* light / dark cycles were changed in the FPALR in an attempt to stabilise the growth of *Synechococcus* 1479/5 cells. Using the white card to cover the top half of the photostage (channels 1-11), a light / dark cycle of 29:55 (1 : 1.89) seconds was created. Figure 214 suggested that cells of *Synechococcus* 1479/5 required a dark period of 280 seconds after being irradiated with light of PFD $750\mu\text{mol s}^{-1} \text{m}^{-2}$ for 120 seconds. This suggested that a light / dark ratio of 1:2.33 was required to prevent the onset of photoinhibition. From Figure 224 it was found the optical density of the culture decreased when the cells were irradiated at a PFD of $750\mu\text{mol s}^{-1} \text{m}^{-2}$ whilst in a light / dark cycle of 29:55 seconds. The chlorophyll a content of the culture decreased to $4.78\mu\text{g ml}^{-1}$ as a result of this increase in PFD (Table 88). The optical density and chlorophyll a content of the culture increased when the PFD was decreased to $400\mu\text{mol s}^{-1} \text{m}^{-2}$ and the light / dark cycle was changed to 58:26 seconds. The chlorophyll a content at this reduced PFD was $7.83\mu\text{g ml}^{-1}$, which was comparable to the previous chlorophyll a content

measured in the culture ($7.1\mu\text{g ml}^{-1}$) previously irradiated at a PFD of $400\mu\text{mol s}^{-1}\text{ m}^{-2}$. By placing the white card over 0.66 of the photostage (channels 1-15) a light / dark of 19:65 seconds was created. Increasing the PFD from 400 to $750\mu\text{mol s}^{-1}\text{ m}^{-2}$ whilst in this new light / dark cycle resulted in a decrease in both optical density and chlorophyll a content (Figure 224 and 225). The chlorophyll a content decreased to $2.02\mu\text{g ml}^{-1}$ (Figure 225). Figure 214 suggested that a light dark cycle ratio of 1:2.33 was sufficient to prevent the onset of photoinhibition, however, a light / dark cycle ratio in the FPALR of 1:3.42 was insufficient to prevent decreases in both optical density and chlorophyll a. It should be noted, however, that Figure 218 requires more experiments performed at and around the values of P_{max} measured at PFDs $300\text{--}750\mu\text{mol s}^{-1}\text{ m}^{-2}$ both in the oxygen electrode in the short term (1-24 hours) and in the FPALR in the long term (5-80 days). It should also be noted that the cells in the oxygen electrode (where the light / dark cycle experiments were performed) were mixed using a magnetic stirrer and not under high stress levels brought about by the high shear forces that exist in the FPALR. These high shearing rates combined with the high light intensity of PFD $750\mu\text{mol s}^{-1}\text{ m}^{-2}$ may account for the explanation why cells of *Synechococcus* 1479/5 failed to maintain its growth rate and photosynthetic capacity in the FPALR in a light dark cycle ratio of 1:3.42. When the *Synechococcus* 1479/5 culture had reached an optical density of 0.5 the PFD was decreased from $750\mu\text{mol s}^{-1}\text{ m}^{-2}$ to $400\mu\text{mol s}^{-1}\text{ m}^{-2}$ (Figure 224 part B). The light / dark cycle was returned to 58:26 seconds (2.23:1). The optical density continued to decrease for a further 2 days. During the 2 days after being irradiated at a PFD of $750\mu\text{mol s}^{-1}\text{ m}^{-2}$ the chlorophyll a content continued to decrease to $1.12\mu\text{g ml}^{-1}$ of culture even though the FPALR was at a PFD of $400\mu\text{mol s}^{-1}\text{ m}^{-2}$. After 2 days, however, the optical density and chlorophyll content of the culture increased. The optical density reached 1.2 (Figure 224) and the chlorophyll a content $6.34\mu\text{g ml}^{-1}$ (Figure 225). Using the white card 0.75 of the photostage (channels 1-17) of the FPALR was shielded from light. The FPALR was now operating at a light dark cycle of 14.5:69.5 seconds (1:4.8 ratio). The PFD of the FPALR was then increased to $750\mu\text{mol s}^{-1}\text{ m}^{-2}$ whilst the culture was in the light / dark cycle of 14.5:69.5 seconds. From Figure 224 it can be seen that the optical density decreased from 1.2 to 0.85 and remained fairly constant at the PFD of $750\mu\text{mol s}^{-1}\text{ m}^{-2}$. The chlorophyll a content of the culture decreased from $6.7\mu\text{g ml}^{-1}$ at a PFD of $400\mu\text{mol s}^{-1}\text{ m}^{-2}$ to $4.6\mu\text{g ml}^{-1}$ at a PFD of $750\mu\text{mol s}^{-1}\text{ m}^{-2}$. The chlorophyll a content remained approximately constant for a further 4 days at the PFD of $750\mu\text{mol s}^{-1}\text{ m}^{-2}$. It was generally found that the data of

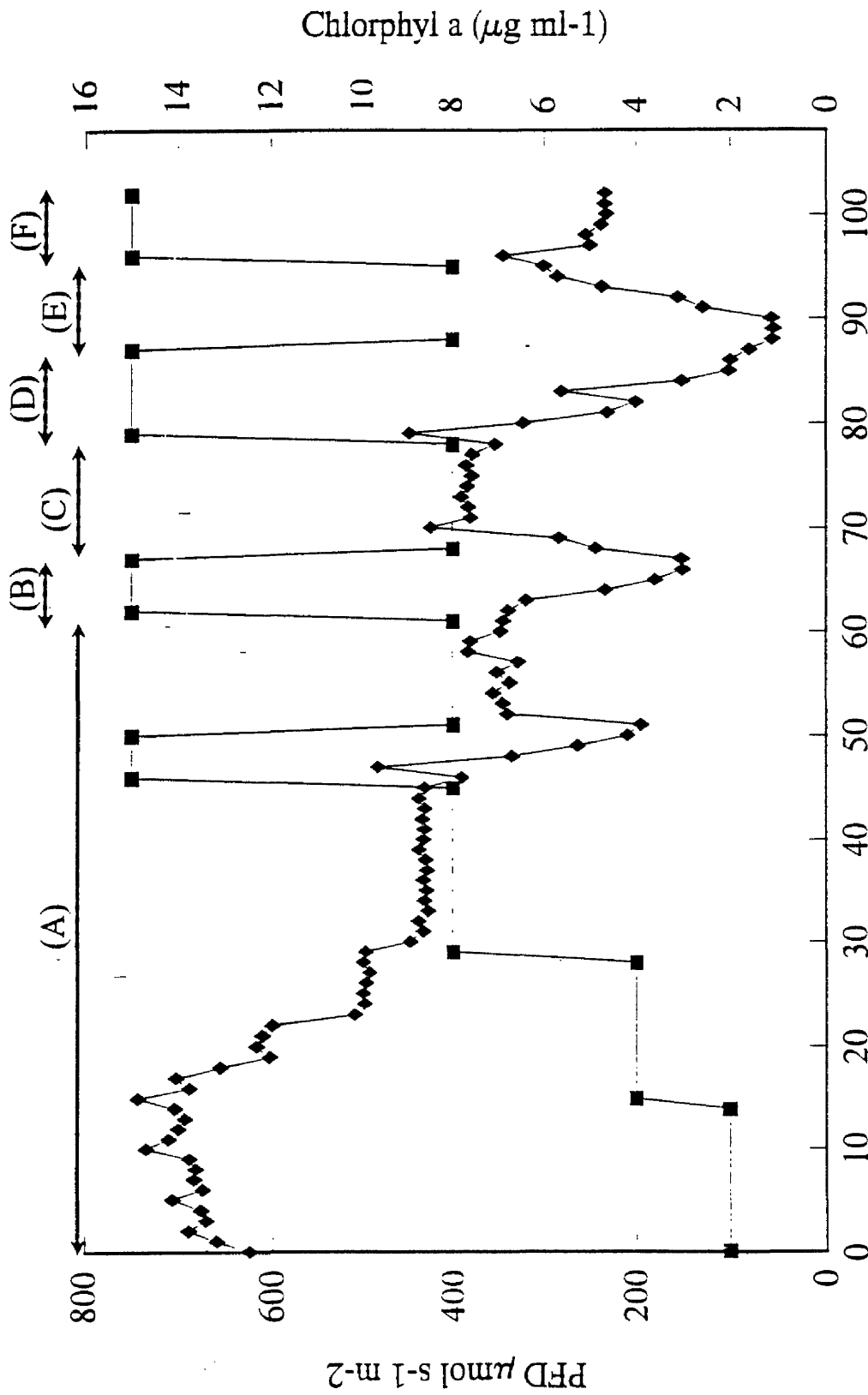
optical density and chlorophyll a measured with *Synechococcus* 1479/5 agreed much better than that observed with *Chlorella vulgaris* 211/11c.

Figure 224 and 225 show that the cells of *Synechococcus* 1479/5 would continue to maintain growth rates and photosynthetic capacities whilst irradiated in the FPALR for 14.5 seconds at a PFD of $750\mu\text{mol s}^{-1} \text{m}^{-2}$ provided a dark phase cycle of 69.5 seconds is available for cellular recovery. The data does not entirely support the findings of the light / dark cycle experiments performed on cells of *Synechococcus* 1479/5 in the oxygen electrode. Figure 213 suggested that a light / dark cycle ratio of 1:2.5 was required for cells to maintain photosynthetic capacity irradiated at a PFD of $750\mu\text{mol s}^{-1} \text{m}^{-2}$ for 82 seconds. However this light / dark ratio was insufficient for cells to maintain photosynthesis and a lower ratio was necessary.

Figure 226 shows the variation in the protein content of cells of *Synechococcus* 1479/5. It can be seen that the protein content increased steadily during the stepped increases in light intensity (100 to $400\mu\text{mol s}^{-1} \text{m}^{-2}$). When the PFD was increased to $750\mu\text{mol s}^{-1} \text{m}^{-2}$, however, the protein content decreased rapidly, following the pattern observed in both dry matter (data not shown) and chlorophyll a. When the PFD was restored to $400\mu\text{mol s}^{-1} \text{m}^{-2}$, however, the protein content increased to a value of approximately $0.46\text{mg protein mg dry wt}^{-1}$. The protein level then followed the familiar pattern of decreasing whenever the PFD was increased to $750\mu\text{mol s}^{-1} \text{m}^{-2}$ and increasing when the PFD was reduced to $400\mu\text{mol s}^{-1} \text{m}^{-2}$. Unlike Figure 226, the carbohydrate content (Figure 227) remained steady throughout the light / dark cycle and PFD changes. The initial high carbohydrate content (approximately $0.7\text{ mg carbohydrate mg dry wt}^{-1}$) decreased with increasing PFD to $0.5\text{ mg carbohydrate mg dry wt}^{-1}$ at a PFD of $400\mu\text{mol s}^{-1} \text{m}^{-2}$. When the PFD was increased to $750\mu\text{mol s}^{-1} \text{m}^{-2}$, the carbohydrate content was reduced to $0.46\text{ mg carbohydrate mg dry wt}^{-1}$ but increased when the PFD was reduced to $400\mu\text{mol s}^{-1} \text{m}^{-2}$.

The changes in the carbohydrate content of both *Chlorella vulgaris* 211/11c and *Synechococcus* 1479/5 were found to be marginal, irrespective of the irradiance PFD. This may have been due to the fact that the bulk of carbohydrate is used as a storage product which may be slower in its response to changes in the growth conditions.

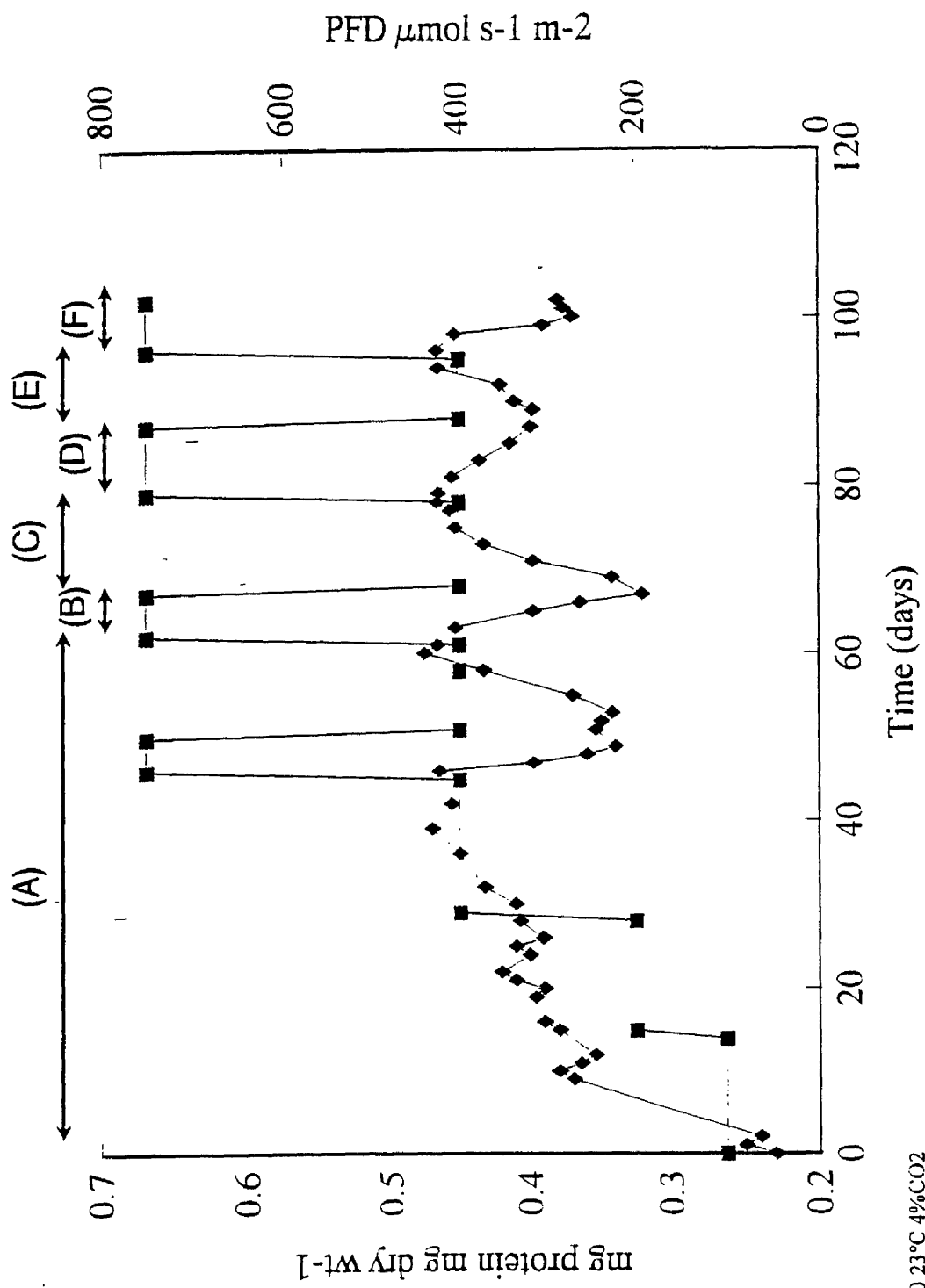
It was observed that the chlorophyll a content of both *Chlorella vulgaris* 211/11c and *Synechococcus* 1479/5 decreased with increasing irradiance (Figures 220 and 225



4% CO₂ 23°C Rey5800

Time (days)

Figure 225. The variation in the chlorophyll a content of *Synechococcus* 1479/5 with changes in PFD and light / dark cycles, \blacksquare —PFD ($\mu\text{mol s}^{-1} \text{m}^{-2}$), \blacklozenge —chlorophyll a content, (A) light / dark cycle 58:26 seconds, (B) light / dark cycle 29:55 seconds, (C) light / dark cycle 58:26 seconds, (D) light / dark cycle 19:65 seconds (E) light / dark cycle 58:26 seconds, (F) light / dark cycle 14.5:69.5 seconds.



Rey 5800 23°C 4%CO₂

Figure 226. The variation in the protein content of *Synechococcus* 1479/5 with changes in PFD and light / dark cycles, ■—■ PFD (μmol s⁻¹ m⁻²), ◆—◆ protein content, (A) light / dark cycle 58:26 seconds, (B) light / dark cycle 29:55 seconds, (C) light / dark cycle 58:26 seconds, (D) light / dark cycle 19:65 seconds (E) light / dark cycle 58:26 seconds, (F) light / dark cycle 14.5:69.5 seconds.

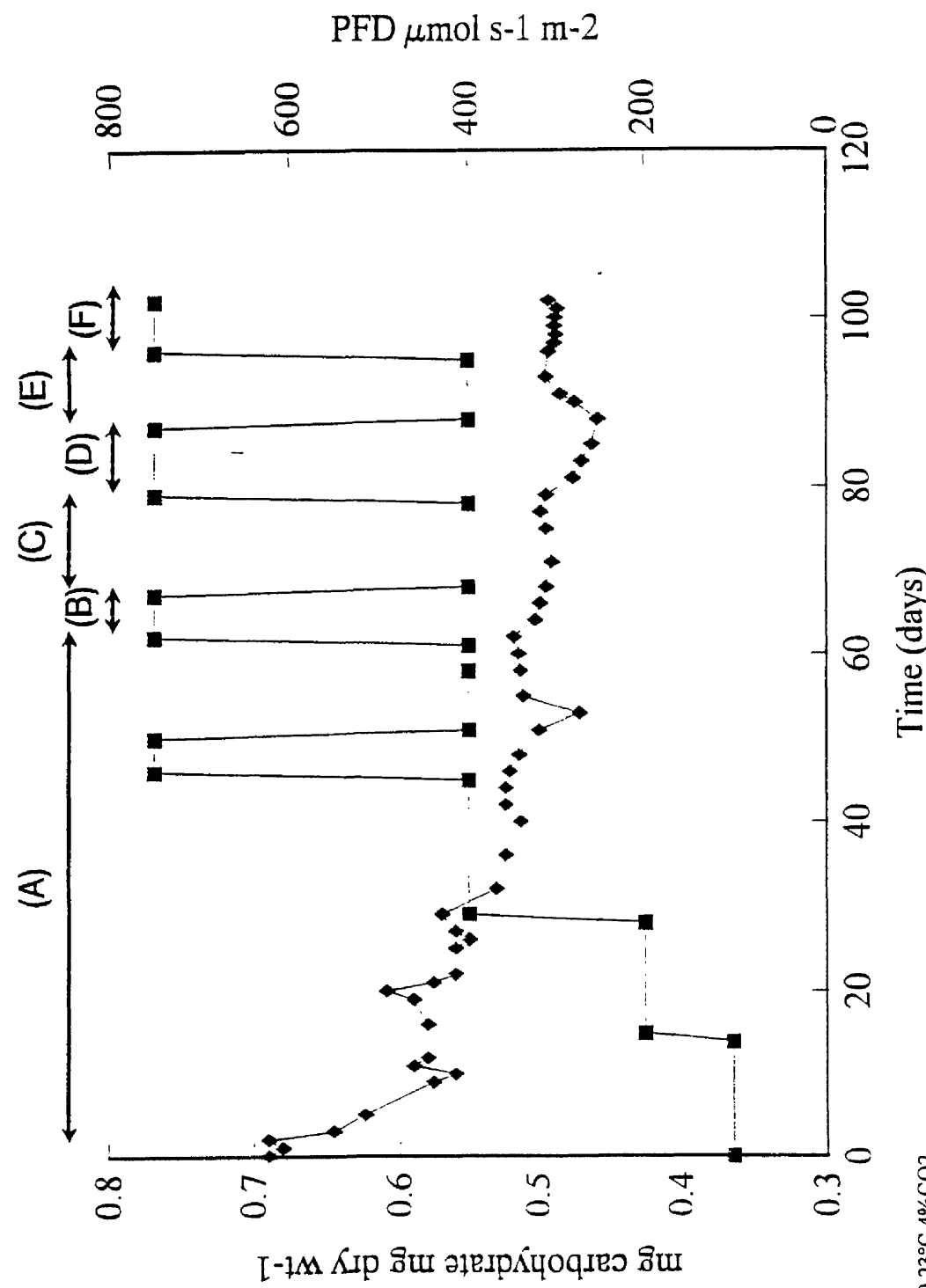


Figure 227. The variation in the carbohydrate content of *Synechococcus* 1479/5 with changes in PFD and light / dark cycles, \blacksquare — \blacksquare PFD ($\mu\text{mol s}^{-1} \text{m}^{-2}$), \blacklozenge — \blacklozenge carbohydrate content, (A) light / dark cycle 58:26 seconds, (B) light / dark cycle 29:55 seconds, (C) light / dark cycle 58:26 seconds, (D) light / dark cycle 19:65 seconds (E) light / dark cycle 58:26 seconds, (F) light / dark cycle 14.5:69.5 seconds.

Rey 5800 23°C 4%CO2

respectively). Increases in the cellular chlorophyll a content with a decrease in light intensity has been observed in *S.costatum* and *D.tertiolecta* (Falkowski and Owens, 1980). Other researchers have also reported decreases in chlorophyll a with increasing PFD whilst working on *Phaodactylum tricorutum* (Geider *et al.*, 1992). Similar stepped increases in PFD has been used by Nielsen *et al.*, (1962) to examine changes in photosynthetic parameters with variations in PFD. Whilst experimenting on *Chlorella vulgaris* it was observed that transferring cells from a 3k lux light environment to one of 30k lux resulted in a decrease in chlorophyll a levels and a subsequent increase in dry matter production. Rapid changes in cell response to changes in PFD has been observed before in other algal species especially in the metabolism of chlorophyll (Grumbach *et al.*, 1978; Owens *et al.*, 1978; Riper *et al.*, 1979; Fallowfield and Osborne, 1989). Other responses include changes in chemical composition and cell dynamics (e.g. volume). It can be seen from Figure 220, Figure 225, Table 87 and Table 88 that as the light intensity increased from 100-750 $\mu\text{mol s}^{-1} \text{m}^{-2}$ the cultures of *Chlorella vulgaris* 211/11c and *Synechococcus* 1479/5 contained less chlorophyll ($\mu\text{g ml}^{-1}$). At the start of the continuous exercise the *Chlorella vulgaris* 211/11c contained approximately 18 μg chlorophyll a ml^{-1} of culture. As the PFD was increased from 100 to 200 to 400 $\mu\text{mol s}^{-1} \text{m}^{-2}$ respectively, the chlorophyll a content of the culture decreased by half to approximately 8.5 $\mu\text{g ml}^{-1}$ of sample. However this was compensated for by an increase in dry matter (results not shown) which caused an overall increase in optical density. After exposure to 750 $\mu\text{mol s}^{-1} \text{m}^{-2}$ the chlorophyll a content reached the minimum values obtained throughout the entire experiment at less than 5 $\mu\text{g ml}^{-1}$. This cellular response to the high light intensity was followed by a noticeable bleaching of the cells. The bleaching of the cells may have reduced the level of self shading that occurred in the FPALR. Continued exposure to light of photoinhibitory levels can result in a loss of chlorophyll caused by photo oxidation with the eventual disruption of the cells (Powles, 1984). The change in optical density with changing irradiance was more severe than the change in chlorophyll a, the cells may have suffered some form of disruption at this PFD of 750 $\mu\text{mol s}^{-1} \text{m}^{-2}$ combined with the high shear forces that existed within the FPALR, the net result of which was a reduction in optical density that did not affect chlorophyll a values to a great extent, since the cells were filtered onto a pad prior to chlorophyll measurement. The problem of self shading has always been difficult to control within reactor vessels. Even a novel reactor such the FPALR does suffer from some minor degree of self shading even in fully turbulent conditions giving rise to increased

chlorophyll a pigment content (Latassa *et al.*, 1992). Since eukaryotic green algal and blue green cyanobacteria growth kinetics are governed primarily by light under conditions of optimum temperature and nutrients, self shading (cells closer to a light source intercepting high levels of photons, reducing the photons that cells further from the light source intercept) has a major influence a cells survival at a given irradiance.

Thus it can be concluded that micro-algal and cyanobacterial cells decrease their chlorophyll a content in a direct response to an increase in irradiance from 100 to 400 $\mu\text{mol s}^{-1} \text{m}^{-2}$. This as previously stated is likely to be due to remove the possibility of photosystem saturation leading to photodamage. However, although the chlorophyll molecules are reduced there is no evidence for chlorophyll metabolism. When the light is increased to that at a photoinhibitory PFD, the cells suffer from severe photodamage and photooxidation due to the damage to the protein core members of photosystem II (Herbert 1990) and the problems of energy removal and so both the chlorophyll a and biomass were seen to decrease. Subsequent incubation in a light field below that responsible for photoinhibition allowed *Chlorella vulgaris* 211/11c and *Synechococcus* 1479/5 to recover from the photodamage. Large bursts in protein synthesis were measured after exposure to photoinhibitory PFDs.

3.7 The effect of light / dark cycles of medium frequency on the photosynthetic parameters, respiration and light enhanced dark respiration of cells of micro-algae cultured in the FPALR under continuous kinetics.

Cells of *Chlorella vulgaris* 211/11c were cultured continuously in the FPALR operated at a Reynolds number of 5800, at a temperature of 23°C and different PFDs of 100, 200, 400 and 750 $\mu\text{mol s}^{-1} \text{m}^{-2}$. Samples were removed from the FPALR every 24 hours for photosynthetic / response curve measurement. When necessary samples were diluted with ASM to an optical density (560nm) of 0.15 prior to analysis with the oxygen electrode. The time interval between removal from the FPALR and the first oxygen measurement in the oxygen electrode was approximately 15 minutes, which included several minutes for the cells to reach a steady state dark

respiration rate. Photosynthesis / irradiance response curves were then determined for each sample.

Photosynthetic parameters of P_{\max} , α , I_k , initial dark respiration and final respiration rates (Figure 10) were determined accordingly.

3.7.1 The effect of light / dark cycles of medium frequency on the photosynthetic kinetics of *Chlorella vulgaris* 211/11c.

The effect of changing PFD on the maximum rate of photosynthesis of cells of *Chlorella vulgaris* 211/11c is shown in Figure 228. Table 89 presents the average rates for P_{\max} calculated for each PFD in the FPALR and includes the P_{\max}^{PFD} values determined as an average of those measured the day prior to and 2 days after a transition stage of changing the FPALR PFD.

It can be seen from Figure 228 that increasing the PFD of the FPALR from 100-200 $\mu\text{mol s}^{-1} \text{m}^{-2}$ resulted in an increase in P_{\max} from 90 to 145 mg oxygen g dry wt⁻¹ hr⁻¹.

The change in cellular P_{\max} was almost instantaneous in response to the increase in PFD. Table 89 transition 1 shows that the average P_{\max} value on the day of the increase in PFD and two days after was higher at 113.12 compared to 100.79 mg oxygen g dry wt⁻¹ hr⁻¹ at the PFD of 100 $\mu\text{mol s}^{-1} \text{m}^{-2}$. the value of P_{\max}^{PFD} was found to have decreased from 300 to 200 $\mu\text{mol s}^{-1} \text{m}^{-2}$.

Increasing the PFD to 400 $\mu\text{mol s}^{-1} \text{m}^{-2}$ resulted in an initial decrease in P_{\max} observed for 4 days, after which P_{\max} increased to approximately 200 mg oxygen g dry wt⁻¹ hr⁻¹. The P_{\max} value measured during transition 2 (Table 89) showed that the maximum rate of photosynthesis had decrease to 97.54 mg oxygen g dry wt⁻¹ hr⁻¹.

This fall in P_{\max} coincided with the falls recorded in optical density and chlorophyll a (Figures 219 and 220 Section 3.6.1). Although the optical density of the culture irradiated in the FPALR at a PFD of 400 $\mu\text{mol s}^{-1} \text{m}^{-2}$ reached a steady state (Figure 219 Section 3.6.1), the P_{\max} of the culture clearly did not (Figure 228). The value of P_{\max}^{PFD} was not changed during the change in PFD from 200 to 400 $\mu\text{mol s}^{-1} \text{m}^{-2}$.

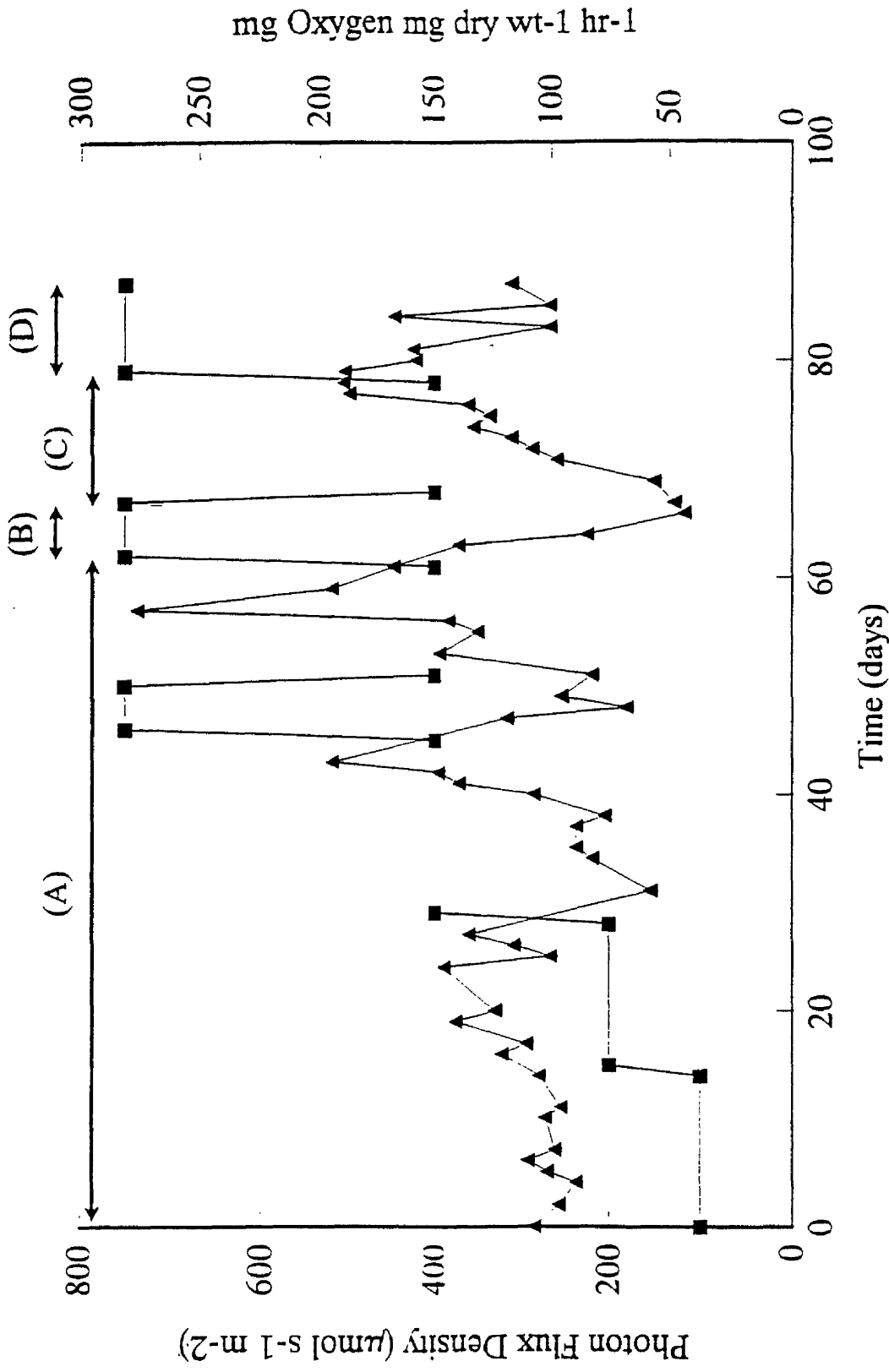


Figure 228. The effect of light / dark cycling in a FPALR on the maximum rate of light saturated photosynthesis of *Chlorella vulgaris* 211/11c. ■—■ PFD ($\mu\text{mol s}^{-1} \text{m}^{-2}$), ▲—▲ change in P_{max} (mg oxygen g dry wt⁻¹ hr⁻¹), (A) light / dark cycle 58:26 seconds, (B) light / dark cycle 29:55 seconds, (C) light / dark cycle 58:26 seconds, (D) light / dark cycle 19:65 seconds.

4% CO₂ 23°C Rey5800

Table 89. The effect of increasing PFD on the P_{\max}^{PFD} of *Chlorella vulgaris* 211/11c cultured in a FPALR operated with continuous kinetics.

PFD $\mu\text{mol s}^{-1} \text{m}^{-2}$	Light / Dark cycle (seconds)	P_{\max}^{PFD} $\mu\text{mol s}^{-1} \text{m}^{-2}$	Average P_{\max} mg oxygen g dry wt ⁻¹ hr ⁻¹ .
100	58:26	300	100.79 ±2.02
100-200 transition 1	58:26	200	113.12 ±5.5
200	58:26	200	124.05 ±5.1
200-400 transition 2	58:26	200	97.54 ±14.83
400	58:26	200	109.36 ±13.58
400-750 transition 3	58:26	200	no data
750	58:26	100	93.9 ±12.16
750-400 transition 4	58:26	100	82.53 ±7.43
400	58:26	200	178.38 ±23.87
400-750 transition 5	29:55	200	153.37 ±10.2
750	29:55	50	58.7 ±10.52
750-400 transition 6	58:26	50	52.1 ±2.96
400	58:26	100	128.9 ±10.13
400-750 transition 7	19:65	300	173.7 ±7.834
750	19:65	200	145.78 ±5.46

Table 89 shows that the average value for P_{\max} measured over the steady state period at a PFD of $400\mu\text{mol s}^{-1} \text{m}^{-2}$ was $109.36 \text{ mg oxygen g dry wt}^{-1} \text{hr}^{-1}$. When the PFD was increased further to $750\mu\text{mol s}^{-1} \text{m}^{-2}$, P_{\max} decreased sharply from approximately 200 to $70 \text{ mg oxygen g dry wt}^{-1} \text{hr}^{-1}$ (Figure 228). No data was obtained for transition 3 (Table 89). The value of P_{\max}^{PFD} however, decreased from 200 to $100\mu\text{mol s}^{-1} \text{m}^{-2}$.

Decreasing the PFD from 750 to $400\mu\text{mol s}^{-1} \text{m}^{-2}$ (Figure 228) resulted in a continual decrease in P_{\max} (Table 89 transition 4) to $82.53 \text{ mg oxygen g dry wt}^{-1} \text{hr}^{-1}$. As the culture was maintained at a PFD of $400\mu\text{mol s}^{-1} \text{m}^{-2}$, however, P_{\max} was observed to increase sharply to $285 \text{ mg oxygen g dry wt}^{-1} \text{hr}^{-1}$. The average value for P_{\max} during the irradiance at a PFD of $400\mu\text{mol s}^{-1} \text{m}^{-2}$ after transition 4 was $178.38 \text{ mg oxygen g dry wt}^{-1} \text{hr}^{-1}$. The irradiance PFD at which P_{\max}^{PFD} was measured increased from 100 to $200\mu\text{mol s}^{-1} \text{m}^{-2}$.

As the PFD of $400\mu\text{mol s}^{-1} \text{m}^{-2}$ was maintained P_{\max} continued to decrease from the maximum rate of 285 to $160 \text{ mg oxygen g dry wt}^{-1} \text{hr}^{-1}$. A sudden increase in P_{\max} was recorded a few days after the PFD had been decreased from 750 to $400\mu\text{mol s}^{-1} \text{m}^{-2}$ (Table 89 transition 4) (Figure 228 B). This was then followed by a gradual reduction in oxygen evolution whilst the PFD remained at $400\mu\text{mol s}^{-1} \text{m}^{-2}$ during which there was a large increase in the protein / chlorophyll a ratio before steadying out (Figure 221 Section 3.6.1).

The light / dark cycle ratio in the FPALR was changed from 58:26 to 29:55 seconds. At this new light / dark cycle the PFD was increased from 400 to $750\mu\text{mol s}^{-1} \text{m}^{-2}$. It was found that P_{\max} decreased sharply from approximately 160 to $50 \text{ mg oxygen g dry wt}^{-1} \text{hr}^{-1}$. Table 89 shows the transition 5 P_{\max} decreasing from 153.37 to $58.7 \text{ mg oxygen g dry wt}^{-1} \text{hr}^{-1}$. The value of P_{\max} continued to decrease whilst at a PFD of $750\mu\text{mol s}^{-1} \text{m}^{-2}$. The P_{\max}^{PFD} decreased to $50\mu\text{mol s}^{-1} \text{m}^{-2}$ whilst at an irradiance of $750\mu\text{mol s}^{-1} \text{m}^{-2}$.

Since Figure 219 (Section 3.6.1) indicated that the culture was approaching wash out the PFD was decreased to $400\mu\text{mol s}^{-1} \text{m}^{-2}$ and the FPALR was operated with a light / dark cycle of 58:26 seconds. During the transitional stage 6 (Table 89), decreasing the PFD from 750 to $400\mu\text{mol s}^{-1} \text{m}^{-2}$ did not immediately reduce the fall of P_{\max} .

Whilst maintained at a constant PFD of $400\mu\text{mol s}^{-1} \text{m}^{-2}$ and in the changed light / dark cycle of 58:26 seconds the value of P_{max} was observed to recover and increased to $128.9\text{mg oxygen g dry wt}^{-1} \text{hr}^{-1}$ (Table 89). The value of $P_{\text{max}}^{\text{PFD}}$ was also found to recover from 50 to $100\mu\text{mol s}^{-1} \text{m}^{-2}$.

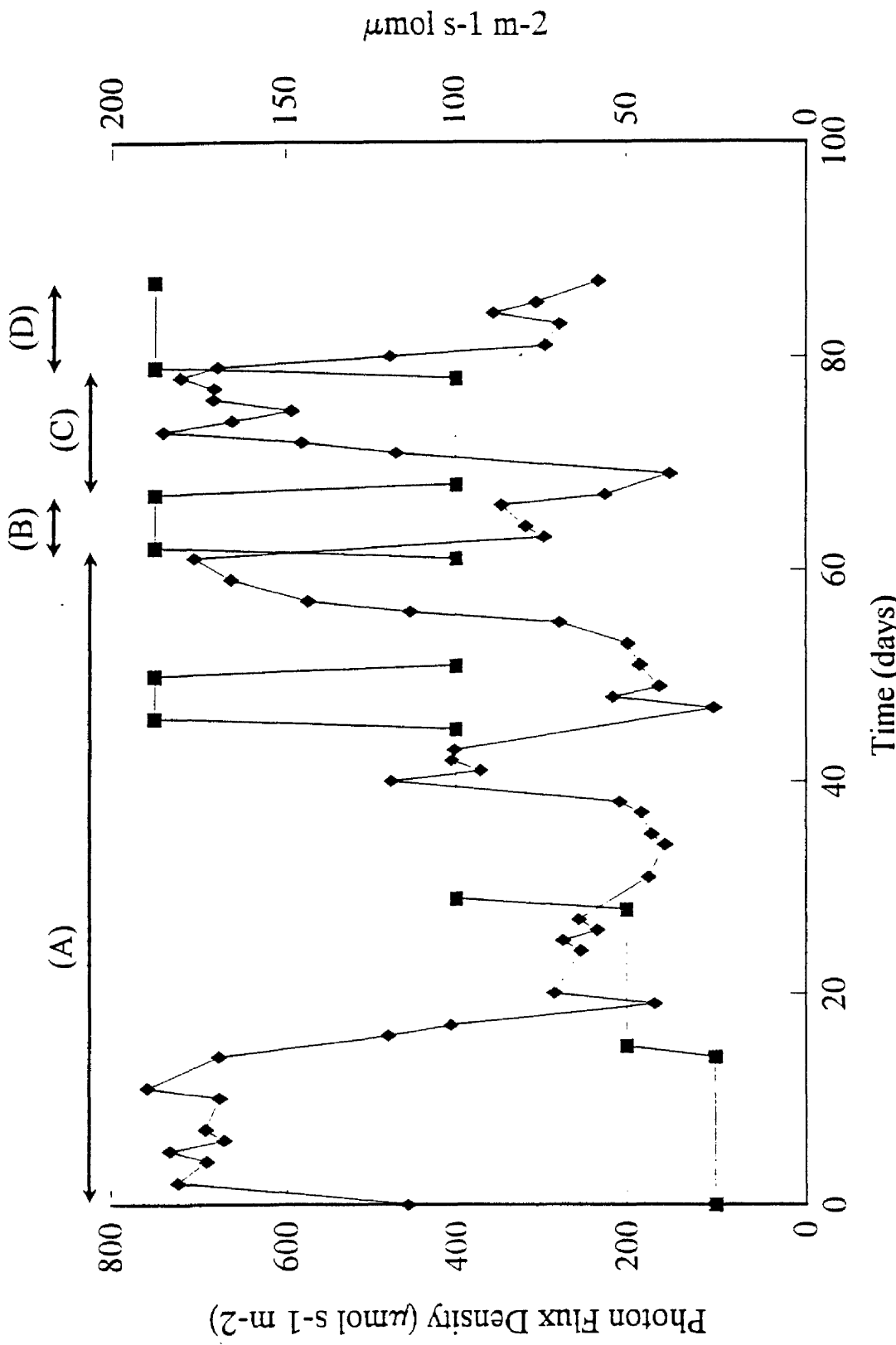
Prior to the immediate increase in PFD from 400 to $750\mu\text{mol s}^{-1} \text{m}^{-2}$ the light dark cycle in the FPALR was changed from 58:26 seconds to 19:65 seconds. When the PFD was increased to $750\mu\text{mol s}^{-1} \text{m}^{-2}$ (Table 89 transition 7) the value of P_{max} increased to $173.7\text{mg oxygen g dry wt}^{-1} \text{hr}^{-1}$ and the value of $P_{\text{max}}^{\text{PFD}}$ increased from 100-300. Whilst the culture was maintained at a PFD of $750\mu\text{mol s}^{-1} \text{m}^{-2}$ the value of P_{max} decreased to $145.78\text{mg oxygen g dry wt}^{-1} \text{hr}^{-1}$ and the value of $P_{\text{max}}^{\text{PFD}}$ decreased from 300 to $200\mu\text{mol s}^{-1} \text{m}^{-2}$ before steadying out at.

Figure 229 shows the relationship between I_k and the PFD in the FPALR.

As the PFD in the FPALR was increased from 100 - $200\mu\text{mol s}^{-1} \text{m}^{-2}$, I_k decreased rapidly from approximately $175\mu\text{mol s}^{-1} \text{m}^{-2}$ to $50\mu\text{mol s}^{-1} \text{m}^{-2}$. Similar decreases in the value of I_k with increasing PFD has been observed during diurnal measurements made in HRAP (Fallowfield unpublished data). This decrease in the I_k value indicated that there had been a decrease in the PFD necessary to bring about the onset of photoinhibition supported by the fall in the value of $P_{\text{max}}^{\text{PFD}}$. Increasing the PFD from 200 to $400\mu\text{mol s}^{-1} \text{m}^{-2}$ resulted in an initial decrease in I_k from around $70\mu\text{mol s}^{-1} \text{m}^{-2}$ to below $40\mu\text{mol s}^{-1} \text{m}^{-2}$. However as the culture was maintained at a PFD of $400\mu\text{mol s}^{-1} \text{m}^{-2}$ the value of I_k was found to increase sharply to $120\mu\text{mol s}^{-1} \text{m}^{-2}$ before steadying out at $100\mu\text{mol s}^{-1} \text{m}^{-2}$. The value of I_k decreased to $30\mu\text{mol s}^{-1} \text{m}^{-2}$ when the PFD was increased from 400 to $750\mu\text{mol s}^{-1} \text{m}^{-2}$. As was found with the value of P_{max} , the value of I_k increased when the PFD was decreased from 750 to $400\mu\text{mol s}^{-1} \text{m}^{-2}$. However the value of I_k increased to a much higher value of $175\mu\text{mol s}^{-1} \text{m}^{-2}$, almost twice that previously measured at a PFD of $400\mu\text{mol s}^{-1} \text{m}^{-2}$.

Changing the light / dark cycle to 29:55 seconds and increasing the PFD from 400 to $750\mu\text{mol s}^{-1} \text{m}^{-2}$ resulted in a sharp decrease in I_k from 175 to $50\mu\text{mol s}^{-1} \text{m}^{-2}$.

However this decrease was stopped when the PFD was decreased from 750 to $400\mu\text{mol s}^{-1} \text{m}^{-2}$ and the light / dark cycle was changed back to 58:26 seconds. Whilst the FPALR was irradiated for the third time at a PFD of $400\mu\text{mol s}^{-1} \text{m}^{-2}$ in a light / dark cycle of 58:26 seconds, the value of I_k increased to $183\mu\text{mol s}^{-1} \text{m}^{-2}$. Increasing the



4% CO₂ 23°C Rey5800
 Figure 229. The effect of light / dark cycling in a FPALR on the photosynthetic parameter I_k of *Chlorella vulgaris* 211/1c. ■—■ PFD ($\mu\text{mol s}^{-1} \text{m}^{-2}$), ◆—◆ change in I_k , (A) light / dark cycle 58:26 seconds, (B) light / dark cycle 29:55 seconds, (C) light / dark cycle 58:26 seconds, (D) light / dark cycle 19:65 seconds.

PFD from 400 to 750 $\mu\text{mol s}^{-1} \text{m}^{-2}$ whilst in a light / dark cycle of 19:65 seconds brought about a decrease in the value of I_k from 176 $\mu\text{mol s}^{-1} \text{m}^{-2}$ to 78 $\mu\text{mol s}^{-1} \text{m}^{-2}$. The value of I_k remained approximately constant at a PFD of 750 $\mu\text{mol s}^{-1} \text{m}^{-2}$ in a light / dark cycle of 19:65 seconds.

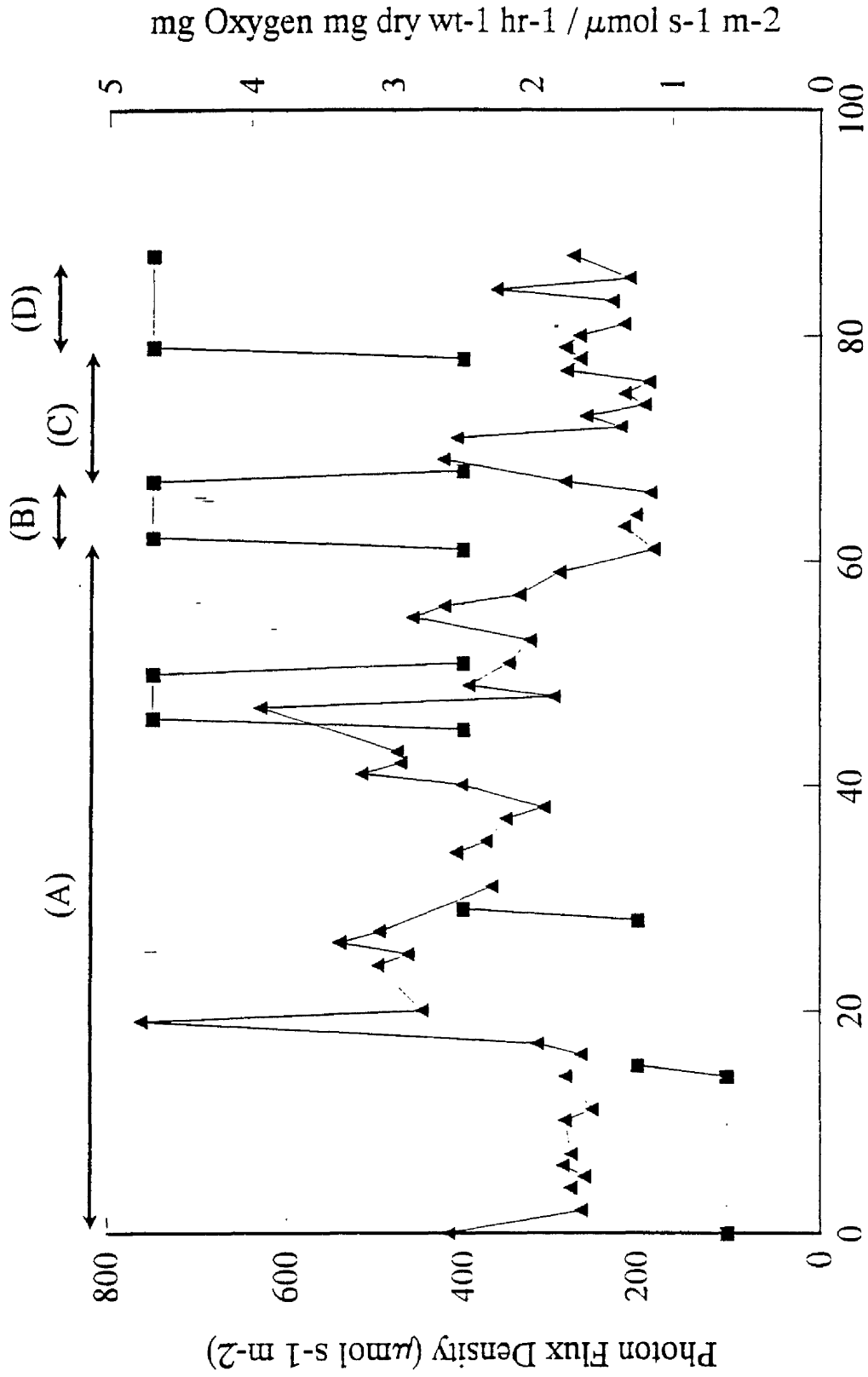
Figure 230 displays the values of α plotted against variations in PFD. The value α was determined as a linear regression of the oxygen evolution rate between 4-20 $\mu\text{mol s}^{-1} \text{m}^{-2}$ i.e. the light limited section of a photosynthesis / irradiance curve. Although α was related to I_k and P_{max} by virtue of equation (154),

$$I_k = \frac{P_{\text{max}}}{\alpha} \quad (154)$$

there appeared to be no correlation between α and variation in PFD. Examination of α on an average basis however, did display that there was a overall general increase in α with increasing PFD from 100 to 400 $\mu\text{mol s}^{-1} \text{m}^{-2}$.

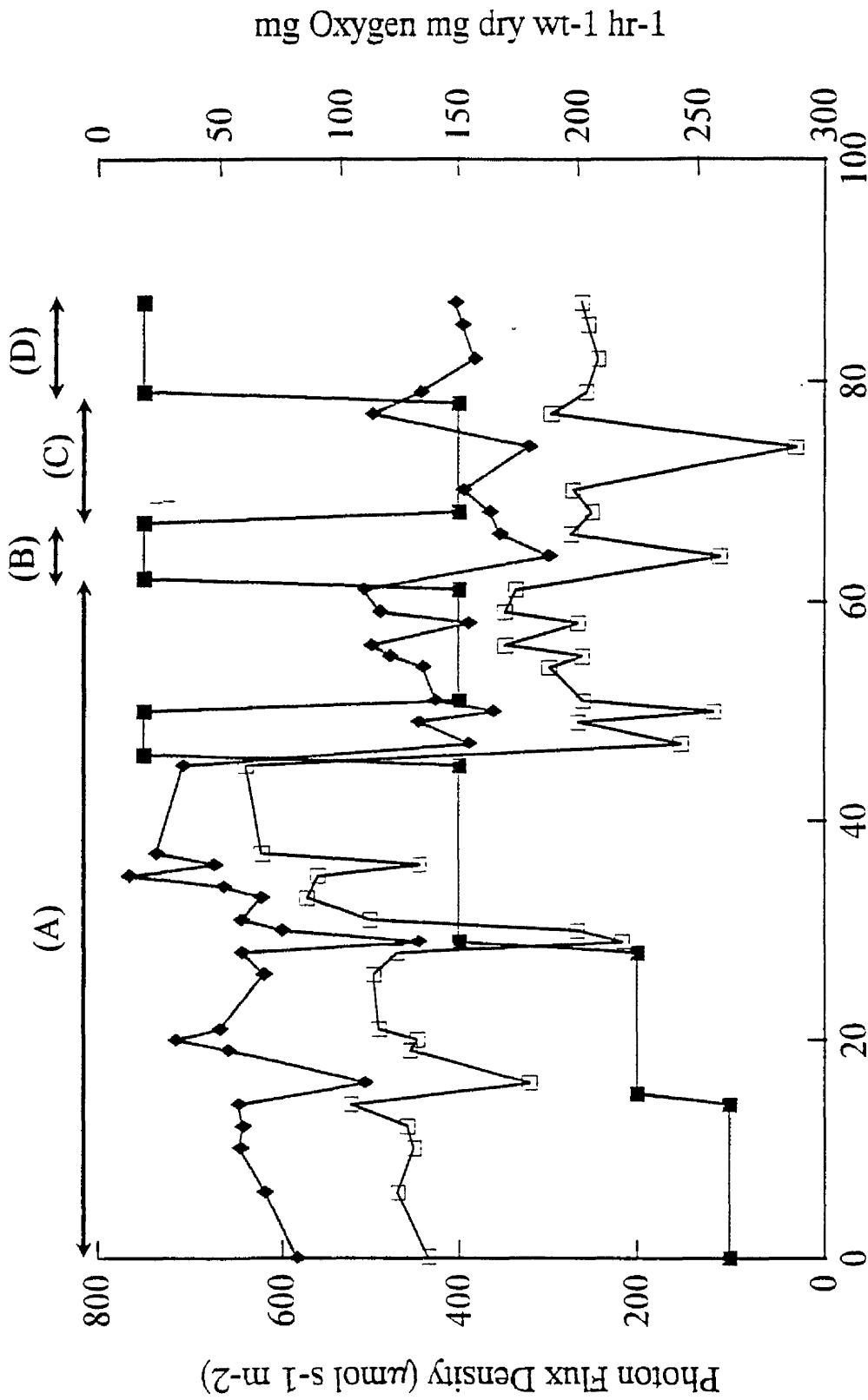
This observation agreed with the results examining the effect of temperature on cells cultured at 80 and 200 $\mu\text{mol s}^{-1} \text{m}^{-2}$ which displayed higher values for alpha and the maximum rate of photosynthesis when cultured at the higher PFD of 200 $\mu\text{mol s}^{-1} \text{m}^{-2}$. PFDs, however, above 400 $\mu\text{mol s}^{-1} \text{m}^{-2}$ resulted in a general decrease in α .

Figure 231 shows the measured changes in dark respiration and light enhanced dark respiration with increasing PFD in the FPALR. At a constant PFD of 100 $\mu\text{mol s}^{-1} \text{m}^{-2}$ the culture had a dark respiration rate of 58 mg oxygen g dry wt⁻¹ hr⁻¹. When the PFD was increased from 100 to 200 $\mu\text{mol s}^{-1} \text{m}^{-2}$, the dark respiration was observed to increase sharply from 50 to 130 mg oxygen g dry wt⁻¹ hr⁻¹. It is suggested that the increase in dark respiration was a direct response to the new light regime of 200 $\mu\text{mol s}^{-1} \text{m}^{-2}$ which may have been attributed to changes in cellular physiology and / or possible mechanisms of photoadaptation. At this new PFD cellular chlorophyll was found to decrease (Figure 220), indicating the possible occurrence of an increase in cellular metabolism of chlorophyll a whilst cell replication was on the increase (Figure 219). It can be seen that Figure 221 and 222 which display changes in the protein content per ml of algae and protein / chlorophyll ratio seems to support this possibility.



4% CO₂ 23°C Rey5800

Figure 230. The effect of light / dark cycling in a FPALR on the photosynthetic parameter α of *Chlorella vulgaris* 211/11c. ■—■ PFD ($\mu\text{mol s}^{-1} \text{m}^{-2}$), ▲—▲ change in α , (A) light / dark cycle 58:26 seconds, (B) light / dark cycle 29:55 seconds, (C) light / dark cycle 58:26 seconds, (D) light / dark cycle 19:65 seconds.



4% CO₂ 23°C Rey5800

Time (days)

Figure 231. The effect of light / dark cycling in a FPALR on the dark respiration and light enhanced dark respiration rates of *Chlorella vulgaris* 211/1c, ■—■ PFD ($\mu\text{mol s}^{-1} \text{m}^{-2}$), ◆—◆ dark respiration rate, □—□ light enhanced dark respiration rate, (A) light / dark cycle 58:26 seconds, (B) light / dark cycle 29:55 seconds, (C) light / dark cycle 58:26 seconds, (D) light / dark cycle 19:65 seconds.

Raven, (1984) suggested that based on the energetics of an organism, cellular respiration should increase with exposure to high PFD in response to level maintenance required to repair photodamage and photooxidation.

The increase in the rate of dark respiration was recorded to occur for only a few days. As the PFD of $200\mu\text{mol s}^{-1} \text{m}^{-2}$ was maintained, the respiration rate decreased to $30\text{mg oxygen g dry wt}^{-1} \text{hr}^{-1}$. The same pattern of sharp increases in the rate of dark respiration was observed when the PFD was increased from 200 to $400\mu\text{mol s}^{-1} \text{m}^{-2}$. However as was measured with the previous increase from 100 to $200\mu\text{mol s}^{-1} \text{m}^{-2}$, the respiration rate decreased back to a very low $20 \text{mg oxygen g}^{-1} \text{dry wt}^{-1}$ soon after the PFD increase had taken place. Respiration rates were seen to reach maximum when the cells were placed in the high light intensity of $750\mu\text{mol s}^{-1} \text{m}^{-2}$. Oxygen consumption at the PFD of $750\mu\text{mol s}^{-1} \text{m}^{-2}$ reached $175 \text{mg oxygen g dry wt}^{-1} \text{hr}^{-1}$ equivalent to 300% of P_{max} (compare with Figure 228). Unlike the previous observations made when soon after a PFD had been increased, the respiration rate was not seen to decrease. The high respiration rate of $150\text{mg oxygen g}^{-1} \text{dry wt}^{-1}$ was maintained until the PFD was decreased from $750\mu\text{mol s}^{-1} \text{m}^{-2}$ to $400\mu\text{mol s}^{-1} \text{m}^{-2}$. When the PFD of the FPALR was reduced to $400\mu\text{mol s}^{-1} \text{m}^{-2}$, the dark respiration rate was observed to fall to approximately $120\text{mg oxygen g dry wt}^{-1} \text{hr}^{-1}$. This respiration rate was maintained as the PFD was maintained at $400\mu\text{mol s}^{-1} \text{m}^{-2}$.

Subsequently returning the cells to an increased PFD of $750\mu\text{mol s}^{-1} \text{m}^{-2}$, although in a new light / dark cycle ratio of 29:55 seconds, resulted in a respiration rate increase of 120 to $185\text{mg oxygen mg dry wt}^{-1} \text{hr}^{-1}$, similar to that observed when the cells were at a PFD of $750\mu\text{mol s}^{-1} \text{m}^{-2}$ but in a light / dark cycle of 58:26 seconds. As previously found, decreasing the PFD from 750- $400\mu\text{mol s}^{-1} \text{m}^{-2}$ and changing the light / dark cycle from 29:55 to 58:26 seconds resulted in a decrease in dark respiration rate to $120\text{mg oxygen g dry wt}^{-1} \text{hr}^{-1}$. This respiration rate was maintained whilst the PFD of $400\mu\text{mol s}^{-1} \text{m}^{-2}$ and light dark cycle of 58:26 seconds was maintained.

Irradiating the cells again at $750\mu\text{mol s}^{-1} \text{m}^{-2}$ whilst in a light / dark cycle of 19:65 seconds resulted in a slight increase in dark respiration rates from 120- 150mg oxygen

g dry wt⁻¹ hr⁻¹. However dark respiration soon decreased back to a steady rate of 140 mg oxygen g dry wt⁻¹ hr⁻¹.

Figure 231 also displays the variations in light enhanced dark respiration rates (LEDR) determined at the end of each photosynthesis / irradiance curve. The measured rates of LEDR were determined 10 minutes after a sample had been placed in the dark following the measurement of a full photosynthesis / irradiance. All photosynthesis / irradiance curve determinations involved the addition of 200mg C l⁻¹ (NaHCO₃ pH 7.0) at the start of each measurement. This was carried out in order to saturate the cells with inorganic carbon which would be concentrated within the cell during photosynthesis and prevent the process of photorespiration (see light enhanced dark respiration 3.10). As was observed with the dark respiration rates, LEDR rates were found to increase with increasing PFD. The LEDR rates were found to follow a similar trend to that of the dark respiration rates.

Figure 232 shows the variation in the nitrate and phosphate composition of the ASM media in the FPALR. The data is expressed as a % of the original contents of 100% ASM (100% ASM containing PO₄^{-P} = 7.4mg l⁻¹, 100% NO₃^{-N} = 303.5mg l⁻¹). It can be seen that in the first 5 days in which the FPALR was operated under batch kinetics, the phosphate level fell rapidly from 100% to 60% ASM, whereas the nitrate level decreased to approximately 80%. However after the FPALR was switched over to continuous mode, the cells continued to remove phosphate and nitrate but at a much lower rate. When the FPALR PFD was increased from 100-200μmol s⁻¹ m⁻² it was found that the rate of removal of phosphate increased. It was found that whilst maintained at a constant PFD of 200μmol s⁻¹ m⁻² the increase in phosphate uptake rate continued to a level of approximately 40% that of ASM. However during the increase in PFD from 100-200μmol s⁻¹ m⁻² it was observed that the nitrate content remained fairly constant within the FPALR at 73% ASM. When the FPALR PFD was increased from 200 to 400μmol s⁻¹ m⁻² it was found that the phosphate content of the ASM decreased for several days. Apart however, for a slight increase in content, the nitrate levels remained relatively unchanged during this change in PFD. Whilst maintained at a PFD of 400μmol s⁻¹ m⁻² phosphate removal rates increased to approximately 50% after 4 days at a constant PFD of 400μmol s⁻¹ m⁻².

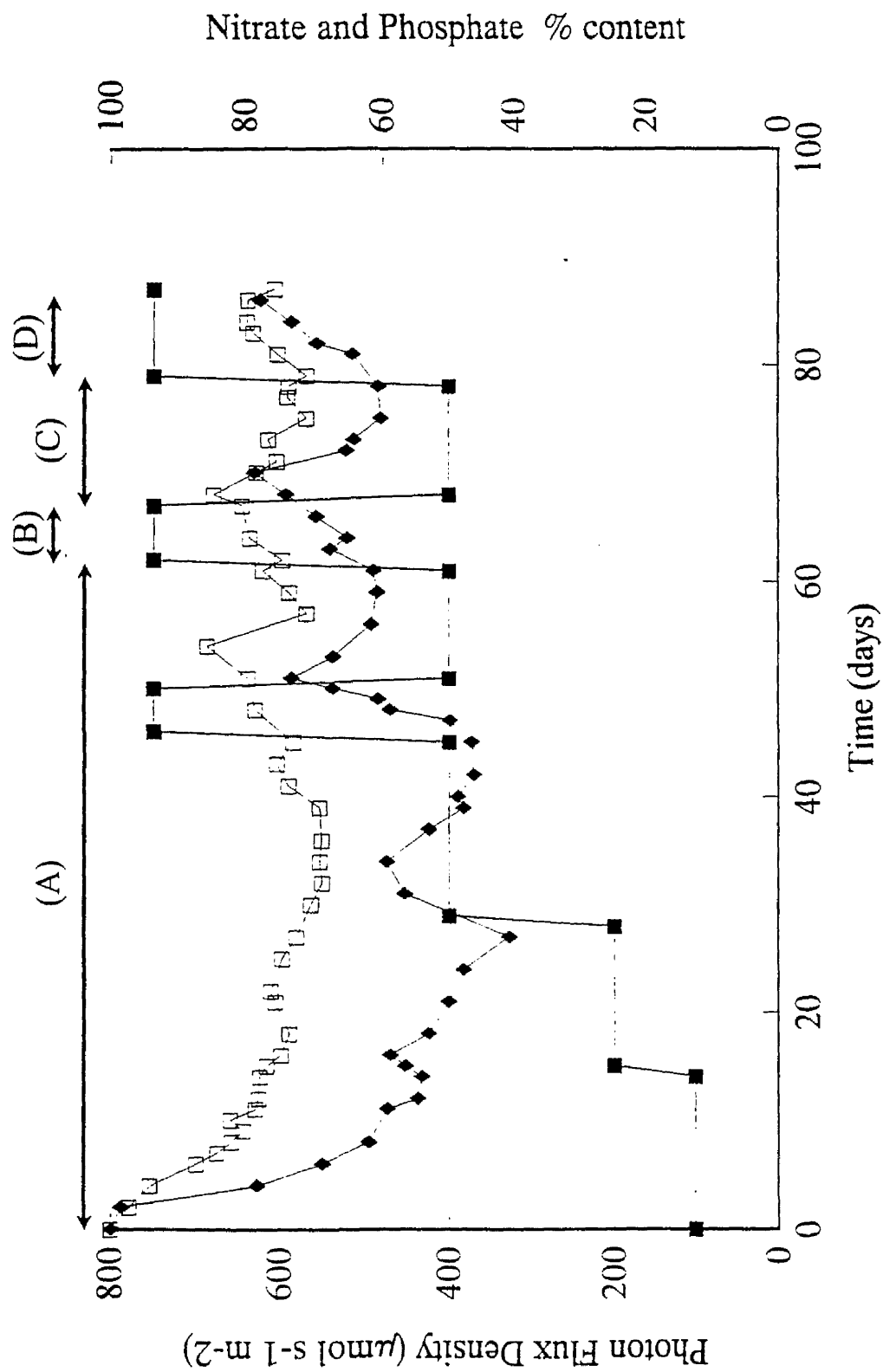


Figure 232. The effect of light / dark cycling in a FPALR on the nitrate and phosphate uptake by *Chlorella vulgaris* 211/11c, ■—■ PFD ($\mu\text{mol s}^{-1} \text{m}^{-2}$), ◆—◆ phosphate content of ASM, □—□ nitrate content of ASM. (A) light / dark cycle 58:26 seconds, (B) light / dark cycle 29:55 seconds, (C) light / dark cycle 58:26 seconds, (D) light / dark cycle 19:65 seconds.

4% CO₂ 23°C Rey5800

Large decreases in both the phosphate and nitrate uptake rates were observed when the PFD was increased to $750\mu\text{mol s}^{-1} \text{m}^{-2}$. At this photoinhibitive PFD the phosphate and nitrate content of ASM increased from 50 and 76% to 77 and 88% respectively. It was only after the PFD had been decreased to $400\mu\text{mol s}^{-1} \text{m}^{-2}$ that the phosphate and nitrate levels of ASM decreased to 65 and 75% respectively as the cells recovered from the photodamaging PFD.

Increasing the PFD from 400 to $750\mu\text{mol s}^{-1} \text{m}^{-2}$ whilst in a light / dark cycle of 29:55 seconds resulted in decline in the cellular uptake phosphate and nitrate. However it was found that the rate of change was not as high as that observed at the same PFD of $750\mu\text{mol s}^{-1} \text{m}^{-2}$ in a light / dark cycle of 58:26 seconds. Following a decrease in PFD to $400\mu\text{mol s}^{-1} \text{m}^{-2}$, cellular uptake of nitrate was found to be extremely rapid. However, there was a noticeable delay of between 2 and 3 days before cellular uptake of phosphate resumed. Whilst at this PFD of $400\mu\text{mol s}^{-1} \text{m}^{-2}$ in a light / dark cycle of 58:26 seconds it was observed that cells of *Chlorella vulgaris* 211/11c had identical uptakes of phosphate and nitrate at day 70 and that the phosphate and nitrate content was approximately 78%.

Increasing the PFD to $750\mu\text{mol s}^{-1} \text{m}^{-2}$, whilst in light / dark cycle of 19:65 seconds was also seen to create a decrease in cellular nitrate and phosphate uptake. However the decrease appeared to be temporary as cells displayed indications of increasing the uptake rate of nitrate whilst irradiated at (day 85).

It can be seen that at and around day 70 (Figure 231), there were large measured increases in cellular dark respiration ($150\text{--}190\text{mg oxygen g dry wt}^{-1} \text{hr}^{-1}$). On the same day large increases in P_{max} (Figure 228), I_K (Figure 229) and α (Figure 230) were recorded respectively. Figures 220 and 221 also showed large increases in chlorophyll a and protein content respectively measured at day 70. It is suggested that at day 70, cellular activity was extremely high, due to the production of pigment protein complexes, enzymes and carriers associated with the electron transport chain, enzymes associated with the carbon reduction pathways and enzymes and building blocks associated with cell repair. The cells of *Chlorella vulgaris* 211/11c had been exposed to a photodamaging PFD of $750\mu\text{mol s}^{-1} \text{m}^{-2}$, but unlike the previous exposure to the same PFD of $750\mu\text{mol s}^{-1} \text{m}^{-2}$ in a light / dark cycle of 58:26 seconds, the cells were in a different light / dark cycle of 29:55 seconds. It is probable

that this new environment was less photodamaging to the cells since the uptake of phosphate and nitrate decreased at a lower rate. Cells were concentrating resources on internal repair and replication, hence the requirement for nitrogen uptake as opposed to phosphate uptake. It is well understood that the enzyme Rubisco is sensitive to high light intensities and it has been determined that 20-30% of total cell nitrogen is in the form of the enzyme Rubisco (Falkowski *et al.*, 1989).

Samples of the media removed from the FPALR, were examined chemically to determine the nutrient status present within culture medium. Since Figure 232 displayed that the cells were not nitrate or phosphate limited, cellular photosynthesis would have been at an optimum under those set conditions. Thus when cellular samples of *Chlorella vulgaris* 211/11c were removed for photosynthesis / irradiance curve measurement, the cells were diluted in 100% ASM. It had already been demonstrated that the presence of nitrate is an important nutrient in delaying the onset of photoinhibition (Section 3.3.3). This was considered to be a satisfactory procedure since the alternative was centrifugation prior to dilution to a low optical density with ASM. It had already been observed that cells which were centrifuged displayed increased respiration rates from controls which were not centrifuged (3.3.5). Since the above continuous FPALR experiments were carried out in order to examine the effects of high photoinhibiting PFDs and light / dark cycles on micro-algal / cyanobacterial growth and photosynthesis, it was decided that increasing the dark respiration rates due to external forces (centrifugation) would lead to an incorrect interpretation of the measured photosynthesis / irradiance curves. This in turn would have lead to different and possibly incorrect conclusions concerning the response of micro-algal / cyanobacterial cells to a given change in their environment.

Myers, (1970), reported that differences between chlorophyll a specific and dry weight specific photosynthesis / irradiance curves of *Chlorella vulgaris* 211/11c cultures adapted to certain PFDs. As was observed in Section 3.4.1 the value of α remained unchanged and the light saturated rates of photosynthesis increased with increasing PFD. This is supported by the results of (Section 3.4.1) which show that the value of α did not change significantly when cells of *Chlorella vulgaris* 211/11c, *Scenedesmus sp.* and *Synechococcus* 1479/5 were cultured at PFDs of 100 or 200 $\mu\text{mol s}^{-1} \text{m}^{-2}$. Further evidence for these observations has been found with the examination of stress levels and adaptation to light. Beardall and Morris, (1976) found

that the chlorophyll a specific maximum rates of photosynthesis decreased in cultures that had become photoadapted to light of low PFD.

Increases in the value of P_{\max} with increasing culture PFD from 100-200 $\mu\text{mol s}^{-1} \text{m}^{-2}$ was opposite to the findings of Cullen and Lewis (1988). Working with the marine diatom *Thalassiosira pseudonana* it was found that the maximum rates of photosynthesis showed little variation and in some cases decreased with increasing PFD. However they did observe a subsequent recovery when decreasing the incident PFD. Although P_{\max} is an indication of the maximum rate of observed photosynthesis, another useful parameter is the PFD value at which the P_{\max} is observed (P_{\max}^{PFD}). It was found that P_{\max}^{PFD} for cells decreased as the PFD in the FPALR was increased (Table 89).

Large increases in the dark respiration rate in response to increasing light intensity has been observed in several species of marine phytoplankton. Falkowski and Owens, (1978) found that oxygen uptake rates were 3 times higher when cells of *Skeletonema costatum*, *Gonyaulax tamarensis* and *Dunaliella tertiolecta* which had been respiring in the dark were irradiated at 1000 $\mu\text{mol s}^{-1} \text{m}^{-2}$. These increase in dark respiration rates were very apparent in the FPALR during transitional stages of increasing PFD (Figure 231). The response to light of very high PFD (750 $\mu\text{mol s}^{-1} \text{m}^{-2}$) was accompanied by a loss of pigment (data not shown). The visible bleaching process within cells of *Chlorella vulgaris* 211/11c has been found to occur during photooxidation studies in *Chlorella pyrenoidosa* (Sironval and Kandler, 1958). Whilst maintained at photoinhibitory light intensities, the reduction in pigment within cells of *Chlorella pyrenoidosa* was found to begin within 2-5 hours. The degree to which the rate of pigment reduction occurred was affected by and increased by the presence of oxygen. Satoh, (1970) found that the photoinactivation of chloroplast isolates from both spinach and higher plants was not a result of photobleaching of the photosynthetic pigments or of the chlorophyll. It was suggested that the bleaching process was a secondary process, occurring after the photosynthetic capacity of the system had been lost. The cells of *Chlorella vulgaris* 211/11c cultured in the FPALR displayed the process of bleaching several hours after being placed at a photoinhibitory PFD of 750 $\mu\text{mol s}^{-1} \text{m}^{-2}$ (Figure 220) in a light / dark cycle of 58:26 seconds. From Figure 220, it can be seen that the decrease in chlorophyll a was accompanied with a sharp decrease in the photosynthetic capacity of the cells at the

same PFD of $750\mu\text{mol s}^{-1} \text{m}^{-2}$ in a light / dark cycle of 58:26 seconds. It was not possible to separate the decreases in both P_{max} and the chlorophyll a, to determine which preceded the other. However, it should be noted that the cells irradiated in the FPALR at a PFD of $750\mu\text{mol s}^{-1} \text{m}^{-2}$ in a light / dark cycle of 16:65 seconds did not display the same degree of both chlorophyll a and P_{max} , which suggests that although the PFD of $750\mu\text{mol s}^{-1} \text{m}^{-2}$ was photoinhibitory to the cells, the length of time in the dark fraction of the cycle offset the mechanism of photooxidation and reduction in photosynthetic capacity. It has been demonstrated that cells maintained in a hostile environment such as being irradiated at high light intensities at photoinhibitory PFDs results in erratic changes in photosynthetic kinetics. When the cells of *Chlorella vulgaris* 211/11c were maintained at a photoinhibitive light intensity of $750\mu\text{mol s}^{-1} \text{m}^{-2}$ but incubated a light / dark cycle of 19 : 65 seconds, the effect on the photosynthetic kinetics of the cell was decreased.

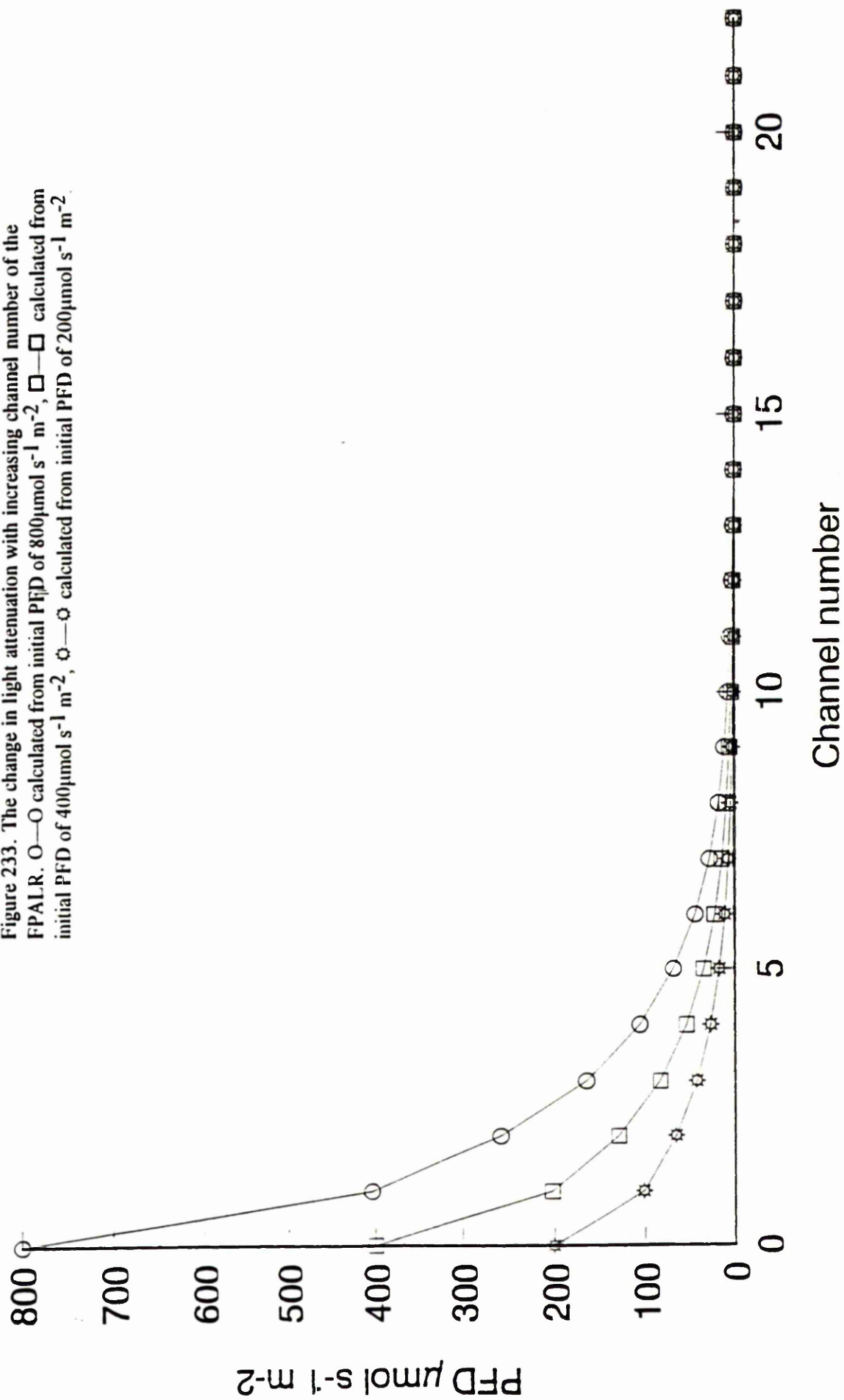
3.8 The effect of light gradients on the growth kinetics of cells of micro-algae and cyanobacteria.

The effect of light / dark cycles of medium frequency had been examined on the photosynthetic kinetics of *Chlorella vulgaris* 211/11c in the FPALR operating under continuous kinetics. Since light varied with depth according to a large number of external parameters determined by the optical properties of the water body, it was necessary to examine the effect of light attenuation on the growth and productivity of micro-algae and cyanobacteria. Due to the problems associated with the time required for continuous kinetic work, all experiments on the effect of light attenuation on growth and productivity were carried out in the FPALR operating under batch kinetics. As the FPALR consisted of a flat plate photostage housing 22 uniform channels, it was possible to manipulate the light field to simulate the changes in light field with depth. The three light gradients of 200, 400 and 800 $\mu\text{mol s}^{-1} \text{m}^{-2}$ were constructed using neutral density filters to ensure that there were no differences in spectral radiant flux which could have an effect on cellular photosynthesis and productivity. With the top channel of the photostage set at the maximum PFD from which the gradients were calculated, cells were circulated through decreasing light gradient. The light gradients calculated from equation 21 were accurately measured and prepared such that even the bottom channel (channel 22) of the photostage allowed the corresponding fraction of light (less than 1 $\mu\text{mol s}^{-1} \text{m}^{-2}$), through the flat plate to the cells. This ensured that cells were not in a true dark stage until they entered the gas riser column which had been wrapped in foil to prevent the entry of stray light. In all experiments the light / dark cycles consisted of the residence times that the cells spent in the photostage and dark stage of the FPALR respectively.

3.8.1 The effect of light gradients on the growth kinetics and productivity of *Chlorella vulgaris* 211/11c and *Synechococcus* 1479/5.

Figures 14, 15, and 16 show the constructed gradients using incident PFDs of 200, 400 and 800 $\mu\text{mol s}^{-1} \text{m}^{-2}$ respectively as the surface (top channel) irradiance PFD. Figure 233 shows the decrease in the PFD with increase channel number. It can be readily seen within a few centimetres of the surface channel, the PFD fell rapidly from

Figure 233. The change in light attenuation with increasing channel number of the FPALR. O—O calculated from initial PFD of $800 \mu\text{mol s}^{-1} \text{m}^{-2}$, □—□ calculated from initial PFD of $400 \mu\text{mol s}^{-1} \text{m}^{-2}$, *—* calculated from initial PFD of $200 \mu\text{mol s}^{-1} \text{m}^{-2}$.



a relatively high photoinhibiting $800\mu\text{mol s}^{-1} \text{m}^{-2}$ to a PFD approaching that where P_{max} is observed. *Chlorella vulgaris* 211/11c and *Synechococcus* 1479/5 were cultured in the FPALR operated under batch kinetics with conditions of 4% v/v carbon dioxide, at a temperature of 23°C , Reynolds number 5800 (unless otherwise stated) and a light / dark cycle of 58:26 seconds (unless otherwise stated). Since the culture was irradiated at a known light intensity of negligible PFD in the lower channels (channel 18-22) of the FPALR (Figure 14, 15 and 16), this was considered to be part of the light cycle, even though the PFD was probably below the light compensation point for photosynthesis.

The growth rates were determined during the mid exponential growth phase of the cells (equation 17) and the maximum stationary phase biomass level was recorded when stated.

Figure 234 shows the growth curves of *Chlorella vulgaris* 211/11c cells cultured in the FPALR in light gradients of 200, 400 and $800\mu\text{mol s}^{-1} \text{m}^{-2}$. The growth rates and maximum stationary phase biomass levels are presented in Table 90. The maximum stationary phase biomass levels were determined at day 10 for each culture light gradient. It can be seen that cells of *Chlorella vulgaris* 211/11c reached a higher stationary phase biomass level (1.62g l^{-1}) when cultured in the $800\mu\text{mol s}^{-1} \text{m}^{-2}$ gradient (Figure 234 and Table 90). The highest cellular growth rate (0.78day^{-1}) was also measured to occur in the $800\mu\text{mol s}^{-1} \text{m}^{-2}$ light gradient. As the gradient PFD was decreased to $200\mu\text{mol s}^{-1} \text{m}^{-2}$ (the PFD at which the maximum rate of photosynthesis was measured for cells of *Chlorella vulgaris* 211/11c) a decline in growth rate (0.54day^{-1}) was observed.

Continuous light above a PFD of $200\mu\text{mol s}^{-1} \text{m}^{-2}$ was photoinhibitory to cells of *Chlorella vulgaris* 211/11c during photosynthesis / irradiance determinations and resulted in a decrease in the photosynthetic capacity (Section 3.4.1) when measured in an oxygen electrode. However, the FPALR was operated at a Reynolds number of 5800, which meant that the cells were moving within the channels of the FPALR at a linear velocity of 33cm s^{-1} . Thus when cultured in the $800\mu\text{mol s}^{-1} \text{m}^{-2}$ gradient the cells were only exposed to light above a PFD of $200\mu\text{mol s}^{-1} \text{m}^{-2}$ for a maximum of 8.6 seconds (Channels 1-4 at PFDs 800, 474, 356 and $267 \mu\text{mol s}^{-1} \text{m}^{-2}$ respectively, including the time taken to turn 180° at the channel ends Figure 16). The cells of *Chlorella vulgaris* 211/11c had higher growth rates and maximum stationary phase

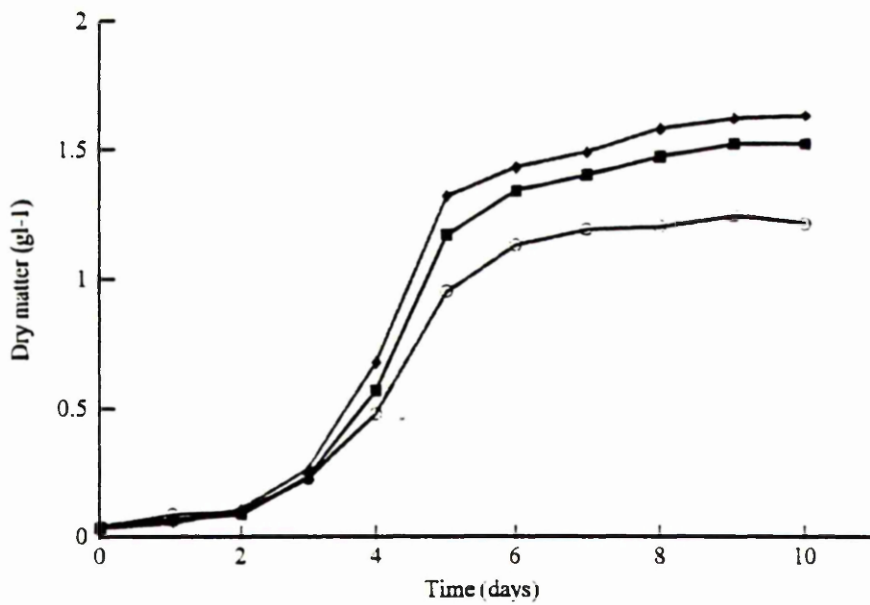


Figure 234. Change in dry weight (g l^{-1}) of *Chlorella vulgaris* 211/11c cultured in the FPALR in a light / dark cycle of 58:26 seconds. $\text{O}-\text{O}$ irradiated in a light gradient of $200\mu\text{mol s}^{-1} \text{m}^{-2}$, $\blacksquare-\blacksquare$ irradiated in a light gradient of $400\mu\text{mol s}^{-1} \text{m}^{-2}$, $\blacklozenge-\blacklozenge$ irradiated in a light gradient of $800\mu\text{mol s}^{-1} \text{m}^{-2}$. FPALR volume = 10.0 litres

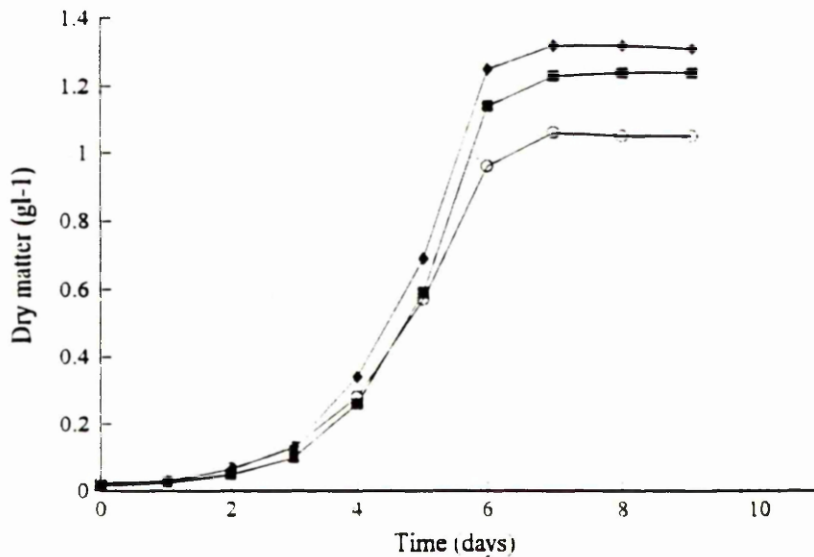


Figure 235. Change in dry weight (g l^{-1}) of *Synechococcus* 1479/5 cultured in the FPALR in a light / dark cycle of 58:26 seconds. $\text{O}-\text{O}$ irradiated in a light gradient of $200\mu\text{mol s}^{-1} \text{m}^{-2}$, $\blacksquare-\blacksquare$ irradiated in a light gradient of $400\mu\text{mol s}^{-1} \text{m}^{-2}$, $\blacklozenge-\blacklozenge$ irradiated in a light gradient of $800\mu\text{mol s}^{-1} \text{m}^{-2}$. FPALR volume = 10.0 litres

Table 90. The effect of light gradients on the growth rates and stationary phase biomass levels of *Chlorella vulgaris* 211/11c cultured in the FPALR.

Light Gradient PFD ($\mu\text{mol s}^{-1} \text{m}^{-2}$) (light / dark cycle ratio 58:26 seconds)	Growth rate (day^{-1})	Maximum stationary phase biomass (gl^{-1})
200	0.54	1.19
400	0.62	1.47
800	0.78	1.62

Table 91. The effect of light gradients on the growth rates and stationary phase biomass levels of *Synechococcus* 1479/5 cultured in the FPALR..

Light Gradient PFD ($\mu\text{mol s}^{-1} \text{m}^{-2}$) (light / dark cycle ratio 58:26 seconds)	Growth rate (day^{-1})	Maximum stationary phase biomass (gl^{-1})
200	0.64	1.07
400	0.73	1.23
800	0.85	1.32

biomass levels when cultured in the FPALR with a $800\mu\text{mol s}^{-1} \text{m}^{-2}$ gradient compared to those obtained in either the 400 or $200\mu\text{mol s}^{-1} \text{m}^{-2}$ gradients.

Although it is accepted that the cells cultured at a PFD of $800\mu\text{mol s}^{-1} \text{m}^{-2}$ saw a greater concentration of light compared to PFDs of 200 and $400\mu\text{mol s}^{-1} \text{m}^{-2}$, it is possible that the cells were displaying an enhanced form of photosynthesis in that the brief exposure to the high light intensity (channels 1-2 and channels 1-4 in the 400 and $800\mu\text{mol s}^{-1} \text{m}^{-2}$ light gradients respectively) completely saturated the intercepting photosystems. The saturation effect was not prolonged and subsequently the onset of photoinhibition was prevented.

Figure 235 shows the growth curves of cells of *Synechococcus* 1479/5 cultured in the FPALR with light gradients of 200 , 400 and $800\mu\text{mol s}^{-1} \text{m}^{-2}$. The growth rates and maximum stationary phase biomass levels (measured at day 9) are presented in Table 91. It was found that the cells of *Synechococcus* 1479/5 produced a similar pattern to that of *Chlorella vulgaris* 211/11c. The highest growth rate of 0.85day^{-1} was recorded during growth in the FPALR in the $800\mu\text{mol s}^{-1} \text{m}^{-2}$ light gradient. Likewise the maximum stationary phase biomass level was also produced by cells cultured in the $800\mu\text{mol s}^{-1} \text{m}^{-2}$ light gradient. As was found with *Chlorella vulgaris* 211/11c, growth rates were observed to fall with decreasing light gradient PFD 800 - 400 - $200\mu\text{mol s}^{-1} \text{m}^{-2}$ respectively.

As well as analysing the effects of light gradients on the growth kinetics of microalgae and cyanobacteria, the frequency of gradient cycles on the growth kinetics was examined on cells of *Chlorella vulgaris* 211/11c. By changing the volume of culture within the FPALR and decreasing the Reynolds number within the flow (achieved by varying the gas input flow rate), it was possible to alter both the period of time spent in the photostage / dark stage and the frequency at which cells were cycled through such time periods.

The FPALR was operated under conditions of 4% v/v carbon dioxide ($2000 \text{cm}^3 \text{min}^{-1}$ air), at a temperature of 23°C and a Reynolds number of 5800 . The FPALR working volume, however, was decreased from 10 to 9.2 litres. Since the design of the FPALR incorporated a dark stage at a higher level than the photostage, decreasing the volume within the FPALR resulted in a reduction in the time taken for the cell

entering the dark stage to re-enter the photostage. The time duration in the photostage remained constant, but the dark stage duration was reduced. The overall frequency of the light / dark cycles over a set period was thus increased. This change in volume in the FPALR resulted in a light / dark cycle ratio of 58:18 seconds (ratio of 3.22 : 1).

Figure 236 shows the results of culturing cells of *Chlorella vulgaris* 211/11c in the FPALR using light gradients of 200, 400 and 800 $\mu\text{mol s}^{-1} \text{m}^{-2}$. The growth rates and maximum stationary phase biomass levels (measured at day 10) are presented in Table 92. It can be observed from Table 92 that the cells of *Chlorella vulgaris* 211/11c had higher growth rates in the FPALR with increasing light gradient PFDs (200, 400 and 800 $\mu\text{mol s}^{-1} \text{m}^{-2}$). The highest maximum stationary phase biomass level occurred in the FPALR irradiated using the 800 $\mu\text{mol s}^{-1} \text{m}^{-2}$ light gradient. The decreasing of the dark stage residence time from 26 seconds (Table 90) to 18 seconds (Table 92) whilst maintaining the light cycle at 58 seconds in the photostage, resulted in higher growth rates but lower maximum stationary phase biomass levels at the respective light gradients of 200, 400 and 800 $\mu\text{mol s}^{-1} \text{m}^{-2}$.

To further examine light / dark cycles on the growth kinetics of cells of *Chlorella vulgaris* 211/11c, the FPALR was operated at a temperature of 23°C and a carbon dioxide concentration of 4% v/v carbon dioxide, however, the air input into the gas riser was decreased to 1750 $\text{cm}^3 \text{min}^{-1}$. The air input into the FPALR was decreased in order to reduce the Reynolds number within the system to 4500. Although being 1300 less than the original 5800, the Reynolds number of 4500 still maintained a fully turbulent flow within the channels of the FPALR. The reduction in the Reynolds number was necessary in order to increase the time period, that the cells spent in the photostage of the FPALR from 58 seconds at a Reynolds number of 5800 to 70 seconds at a Reynolds number of 4500. To maintain the dark period at approximately 18 seconds, it was necessary to reduce the working volume of the FPALR from 10 litres to 9.0 litres. The new light / dark cycle ratio in the FPALR was 70:18 seconds.

Figure 237 shows the growth curves obtained from culturing cells of *Chlorella vulgaris* 211/11c in the FPALR using the 3 light gradients of 200, 400 and 800 $\mu\text{mol s}^{-1} \text{m}^{-2}$ in a light / dark cycle of 70:18 seconds. The growth rates and maximum stationary phase biomass levels (measured at day 10) are presented in Table 93.

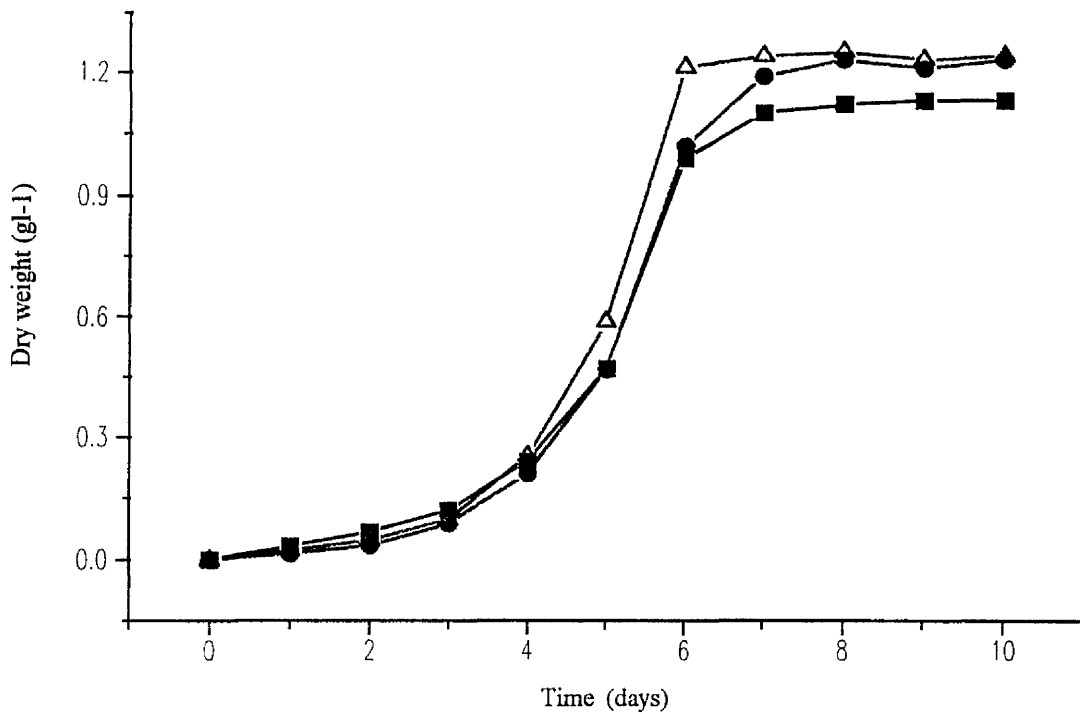


Figure 236. Change in dry weight (g l^{-1}) of *Chlorella vulgaris* 211/11c cultured in the FPALR in a light / dark cycle of 58:18 seconds. ■—■ irradiated in a light gradient of $200 \mu\text{mol s}^{-1} \text{m}^{-2}$, ●—● irradiated in a light gradient of $400 \mu\text{mol s}^{-1} \text{m}^{-2}$, Δ — Δ irradiated in a light gradient of $800 \mu\text{mol s}^{-1} \text{m}^{-2}$. FPALR volume 9.2 litre.

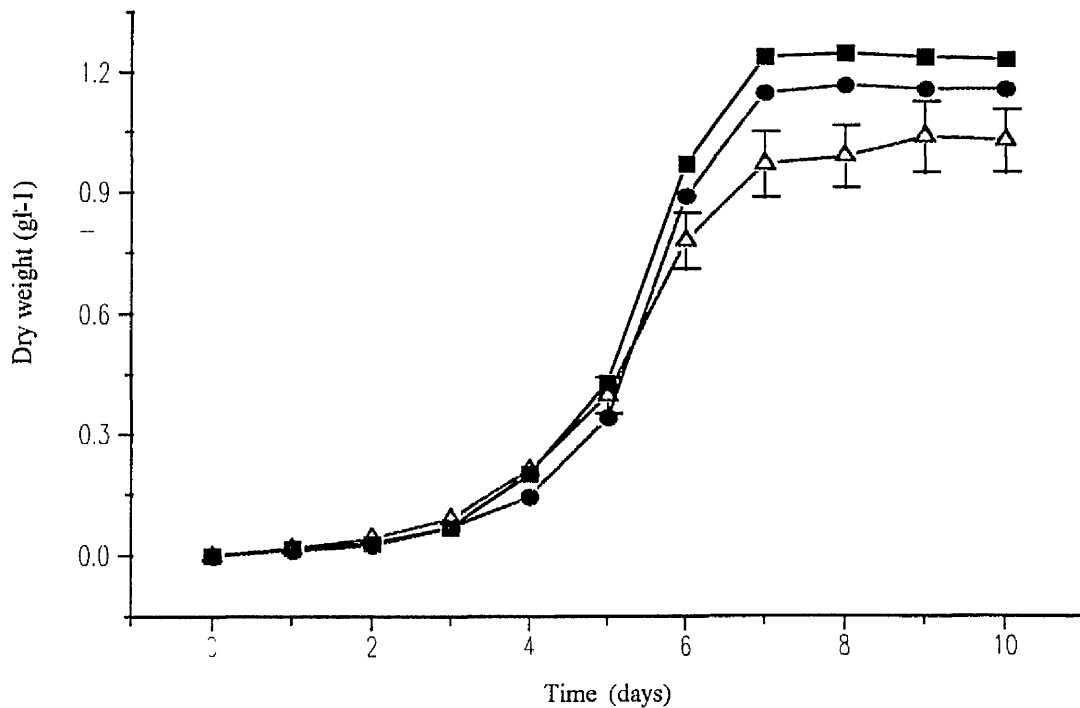


Figure 237. Change in dry weight (g l^{-1}) of *Chlorella vulgaris* 211/11c cultured in the FPALR in a light / dark cycle of 70:17 seconds. ■—■ irradiated in a light gradient of $200 \mu\text{mol s}^{-1} \text{m}^{-2}$, ●—● irradiated in a light gradient of $400 \mu\text{mol s}^{-1} \text{m}^{-2}$, Δ — Δ irradiated in a light gradient of $800 \mu\text{mol s}^{-1} \text{m}^{-2}$. FPALR volume = 9.0 litre.

Table 92. The effect of light gradients (light / dark cycles 58:18 seconds) on the growth rates and stationary phase biomass levels of *Chlorella vulgaris* 211/11c cultured in the FPALR..

Light Gradient PFD ($\mu\text{mol s}^{-1} \text{m}^{-2}$) (light / dark cycle ratio 58:18 seconds)	Growth rate (day^{-1})	Maximum stationary phase biomass (gl^{-1})
200	0.667	1.13
400	0.76	1.23
800	0.81	1.26

Table 93. The effect of light gradients (light / dark cycle 70:18 seconds) on the growth rates and stationary phase biomass levels of *Chlorella vulgaris* 211/11c cultured in the FPALR.

Light Gradient PFD ($\mu\text{mol s}^{-1} \text{m}^{-2}$) (light / dark cycle ratio 70:18 seconds)	Growth rate (day^{-1})	Maximum stationary phase biomass (gl^{-1})
200	0.87	1.24
400	0.82	1.16
800	0.73 ± 0.17	1.04 ± 0.08

It can be seen from Table 93 that the highest growth rate (0.87 day^{-1}) and stationary phase biomass (1.24 g l^{-1}) resulted from the cells cultured in the FPALR with the $200 \mu \text{mol s}^{-1} \text{ m}^{-2}$ light gradient. It was found that both the growth rate and stationary phase biomass level decreased with increasing light gradient ($200, 400$ and $800 \mu \text{mol s}^{-1} \text{ m}^{-2}$).

Since the Reynolds number within the fluid flow had been reduced to 4500, the time period that cells spent in the photoinhibiting 400 and $800 \mu \text{mol s}^{-1} \text{ m}^{-2}$ gradients caused a reduction in both growth rates and stationary phase biomass levels. In all three gradients the measured growth rates were very high. It is suggested that this is probably due to a reduction in cell stress levels caused by reduction in shearing forces brought about by a decrease in Reynolds number.

It was found that reducing the time duration that cells of *Chlorella vulgaris* 211/11c spent in the dark resulted in an increase in cellular growth rates provided the PFD was not at photoinhibitory light intensities. When the photostage duration was increased to 70 seconds only the growth rates in the respective light gradients of 200 and $400 \mu \text{mol s}^{-1} \text{ m}^{-2}$ were recorded to increase. The growth rate of cells cultured in the FPALR in a light / dark cycle of 70:18 seconds in a light gradient of $800 \mu \text{mol s}^{-1} \text{ m}^{-2}$ was found to have decreased to 0.73 day^{-1} . The reduction in the dark stage duration from a light dark cycle of 58:26 to 58:18 seconds resulted in a decrease in the maximum stationary phase biomass levels in the light gradients of 400 and $800 \mu \text{mol s}^{-1} \text{ m}^{-2}$.

Enhancement of cellular growth rates by varying light / dark cycles has been observed in *Spirulina* cells by Richmond and Vonshak, (1978) which supports the enhancement in productivity described in this thesis. It was found that the growth rate of *Spirulina* was significantly increased when the stirring speed of the cultures was doubled. They suggested that the reason for this was the cells being exposed to a more favourable light / dark cycle in which the time interval between each cycle was reduced.

Changes in vortex circulation's from 0.5 to 1 Hz made by the introduction of wing shaped foils was found to increase the productivity in cells of an outdoor mass culture by a factor of 2 (Laws *et al.*, 1983). These observations support the experimental findings described above when culturing cells of *Chlorella vulgaris* 211/11c in the FPALR in light gradients of $200, 400$ and $800 \mu \text{mol s}^{-1} \text{ m}^{-2}$ in the light / dark cycles

of 58:26 and 58:18 seconds (Figures 234 and 236). Over a 24 hour period the cells cultured in the light / dark cycle of 58:26 seconds circulated 1028 complete cycles in the FPALR compared to 1136 cycles by cells cultured in a light / dark cycle of 58:18 seconds. The result was an increase in the growth rates with decreasing duration spent in the dark phase and a constant duration in the photostage. However the maximum stationary phase biomass levels were not found to increase with decrease in the dark stage. Grobbelaar (1989), however, reported no such observations in the growth rate or productivity of *Chlorella sp.* when grown in stationary incubation bottles, but did observe decreased maximum rates of photosynthesis with increasing turbidity. Grobbelaar *et al.*, (1992), however, did suggest that light / dark cycles of medium frequency (seconds to minutes) do affect overall cellular productivity in micro-algae which supports the findings presented here.

The FPALR can simulate the effects of the light attenuation found within lake and HRAP systems. Previous research has concentrated mainly on high frequency light / dark cycles (millisecond) (Myers and Graham, 1971) and low frequency light / dark cycles (hours, Sorokin, 1957) but very little research has been carried out on the effect of medium frequency light / dark cycle (Grobbelaar, 1989) range. Light / dark cycles of seconds to minutes are reported to be similar to those generated by turbulence brought about by wave action (Dera, 1970). Mann *et al.*, (1972) observed that the productivity of macrophytes could be increased by as much as 30% by increasing the turbulence in incubation bottles by rotating them through a light gradient in water. Lee and Pirt, (1981) used a loop reactor to examine the effects of circulating cells of *Chlorella vulgaris* 211/11c through intermittent light of 40 second cycles. It was found that the cells of *Chlorella vulgaris* 211/11c continued to grow in the dark for a maximum duration of 9.2 seconds. It was suggested that cells of micro-algae and cyanobacteria may have the ability maintain growth and photosynthetic rates even after having entered a dark phase.

In conclusion it was recorded that cellular growth rates of *Chlorella vulgaris* 211/11c were increased when either the duration in the dark was reduced or when the duration in the light was increased at a PFD of 200 or 400 $\mu\text{mol s}^{-1} \text{m}^{-2}$. This clearly supports the research and findings of Richmond and Vonshak (1978). This relationship does not entirely hold true when the light is increased to a photoinhibitive PFD of 800 $\mu\text{mol s}^{-1} \text{m}^{-2}$. At the elevated PFD the growth rate was observed to decrease when the dark duration time was increased from 18 to 26 seconds. However, a similar fall in

growth rate was observed when the duration spent in the light was increased from 58 to 70 seconds.

Not only is the time scale of the light / dark cycle of great importance in determining the productivity and photosynthesis of cells of micro-algae and cyanobacteria, but also the response to possible photoadaptation. If the time scale response of the mechanism of photoadaptation is shorter in duration for a known vertical light gradient then the phytoplankton population will have a mixed range of photosynthetic rates at ambient light intensities. If, however, the time scale of circulation through the vertical gradient is shorter than the time scale required for the mechanism of photoadaptation then the photosynthetic properties of the phytoplankton population will be uniform (Cullen and Lewis, 1988). Brand *et al.*, (1981) however, suggested that between 5 and 20 cell divisions were required for photoadaptation to a given light intensity to occur. As the FPALR was operated under batch kinetics in a reduced growth time of 8-10 days, the cell doubling time of which resulted in 15-22 cell generations. It is therefore possible that cellular photoadaptation could have occurred during periods where cell generations exceeded 20 generations. The experiments also suggested that photoadaptation occurred in the FPALR at cell generation times of approximately 7. Hence although the lower limit of 5 generations had been exceeded and that the data may be species specific, the lower and upper limits should be determined individually for each organism instead of relying on previous research data.

Other researchers have found that the time course for photoadaptation under nutrient depleted conditions ranges from hours to several days (Rivkin *et al.*, 1982; Prezelin *et al.*, 1986; Cullen and Lewis, 1988). Prezelin, *et al.*, (1991) suggested that the explanation for the difference in photoadaptation time scales was due to the rate at which cellular growth occurred. From the phosphate and nitrate data shown in Figures 55 and 57, it is unlikely that cells were nitrogen limited. Although phosphate concentration was reduced to almost zero (Figures 55 and 57), further additions of the compound failed to increase the growth rate of the cells, suggesting that it was merely being stored by cells for future use.

Although other research has been carried out on the effects of light / dark cycles on the productivity of micro-algae in continuous culture, these methods have proved inconclusive since micro-algae are not exposed to a constant cycle of on / off lighting

due to the circular geometry of the culture vessels employed (Paasche, 1968; Shifrin and Chisolm, 1981; Rodgers and DePinto, 1981; Laws *et al.*, 1983). Culture vessels based on chemostat design and indeed any vessel based on circular geometry suffer from the main problem of poor light field measurement and light penetration. . Attempts to examine the effect of light / dark cycle without resorting to physically moving a vessel containing algae (Grobbelaar, 1989) through a changing light gradient has been examined using an algal cyclostat with a computer controlled light regime (Kroon *et al.*, 1992a). This system used a typical flat rectangular glass tank in which the cells were incubated and circulated via a sparger. Placed in front of this tank was a venetian blind whose blades could be angled to obtain the desired PFD. Although more flexible than using filters the system is not superior to the FPALR with regards to generating light gradients. The FPALR is superior in its gas mixing, which combined with very high Reynolds numbers, ensures that the cells are in a fully mixed system in an accurately defined light field of known PFD and spectral radiant flux. The experiments of Kroon *et al.*, (1992b) using the algal cyclostat did, however, reveal that the chlorophyll a to chlorophyll b ratio decreased when cells were irradiated in a light / dark cycle of sinusoidal light lasting 8 hours compared to a 1 hour sinusoidal light irradiance with an 8 hour oscillation.

It would have been of value to record not only the changes in growth but also the variation in photosynthetic kinetics as monitored in section 3.7.1. Changes in the maximum rates of photosynthesis may have shown indications of photoadaptation at the different light gradients. Further analysis of these kinetics would have been useful to determine any relationship between dark respiration rate, light enhanced dark respiration rate and carbohydrate synthesis and utilisation. At the high light gradient of $800\mu\text{mol s}^{-1} \text{m}^{-2}$ the saturation of the photoreaction centres (without causing photoinhibition) may have been responsible for high rates of carbohydrate synthesis. Although high rates of polysaccharide synthesis is carried out in the light (Kirk, 1983), the increased photosynthetic substrate will cause high dark respiration rates due to light enhanced dark respiration (Dring and Schmidt, personal communication). Although discussed in section 3.10, the process of LEDR may become vital to a cells survival in a particular light regime. Carbon incorporation into protein synthesis would typically be higher during the light stage of photosynthesis since the major photosynthetic steps and photoreaction centres require enzyme functions. However, once in the dark the carbon incorporation rate into protein synthesis would depend

entirely on the previous light history that the cells had been irradiated with. The cell metabolism would then be controlled by the LEDR rate since this is correlated to both the photosynthetic carbon uptake and polysaccharide synthesis. Carbon loss through respiration has been shown to be of major importance in lakes (Cabecadas and Brogueira, 1987). Due to the variation in light attenuation with depth in high rate algal ponds, this relationship would vary depending on depth. Changes in depth brings a whole new ball game into play since we have to examine the changes in spectral radiant flux which affect the degree to which light energy is absorbed and utilised by cell pigments.

3.9 **The effect of spectral radiant flux on the growth and photosynthesis of micro-algae and cyanobacteria.**

The growth and metabolism of natural populations of phytoplankton is controlled by a complex interaction between many environmental factors. Of these factors, light is the most variable. Although it is often easy to measure the change in attenuation with depth, the change in spectral radiant flux due to wavelengths being selectively filtered out as it penetrates the water column is a more difficult task. It was therefore necessary to examine the role of spectral radiant flux in both the culturing and photosynthesis of micro-algae and cyanobacteria.

3.9.1 The effect of spectral radiant flux on the growth kinetics of micro-algae and cyanobacteria.

Cells of *Chlorella vulgaris* 211/11c, *Scenedesmus sp.* and *Synechococcus* 1479/5 were used to examine the effect of spectral radiant flux (Figures 17 to 22) on their respective growth kinetics.

Figures 17-22 show the spectral characteristics of the various wavelength filters employed in the research. Figure 17 was a dark green (450-600nm) type filter which had wavelength transmissions in two main areas; light below 450nm was removed, as was light of wavelengths between 600-700nm. Peak transmission (65%) was at 525nm. The transmission of light at wavelengths above 700nm increased to approximately 80% at 800nm. Figure 18 was a bright blue (350-575nm) filter with a peak transmission (78%) at 450nm. Wavelengths of light below 350nm and between 575-675nm were removed. Transmission of wavelengths above 675nm increased steadily to 79% at 800nm. Figure 19 was a light red (600-800nm) filter with a very high light transmission (93%) at wavelengths above 575nm. Light below 575nm was completely removed. Figure 20 was a chrome orange (475-800nm) filter with a high transmission (90%) of wavelengths above 475nm. Virtually all wavelengths of light below 475nm were removed. Figure 21 was an orange (550-800nm) type filter which had a high transmission (85%) of wavelengths above 550nm. Virtually all light below 550nm was removed. Figure 22 was a yellow (450-800nm) type filter with a high

(90%) light transmission above 500nm. Virtually all light of wavelengths below 450nm was removed by this filter. All cultures regardless of filter used received light of PFD $50\mu\text{mol s}^{-1} \text{m}^{-2}$ of full spectrum (300-800nm) irradiance.

From Figure 238 and 239 it can be seen that cells of *Chlorella vulgaris* 211/11c grew very poorly with filters red (600-800nm), blue (350-575nm) and green (450-600nm). The growth rates and maximum stationary biomass levels are presented in Table 94. The highest growth rate of 0.647 day^{-1} and stationary phase biomass level of 0.736 g l^{-1} was observed with cells that had been cultured in an orange filter (550-800nm). However the cellular growth in flasks covered with the yellow (450-800nm) and chrome orange (475-800nm) filter also grew with relatively high growth rates of 0.619 day^{-1} and 0.642 respectively. It can be seen that the standard error of the mean of the growth rates of cultures irradiated with yellow (450-800nm), orange (550-800nm) and chrome orange (475-800nm) overlap, suggesting that the addition of wavelengths of filter 475-800nm (allowing the extra wavelengths down to 475nm) and filter 450-800nm (allowing the extra wavelengths down to 450) below those allowed through by filter 550-800nm (i.e. below 550nm) had little effect on cellular growth. However it can be seen there was a significant difference in the stationary phase biomass levels of cultures 450-800nm, 550-800nm and 475-800nm. As flasks grown under yellow (450-800nm) light had a broader spectrum of wavelengths i.e. high transmission of wavelengths above 450nm, it was expected that this culture would have grown at a similar growth rate to the control flask shown in Figure 244 which produced higher growth rates, mean cell doubling times and stationary phase biomass levels (data not shown).

Chlorophyll a has strong absorption peaks at 400-430nm and at 650-665nm (Kirk, 1983). There is virtually no absorption by chlorophyll a above 450nm and below 640nm. Chlorophyll b has strong absorption peaks at 440nm-475nm and 630nm-650nm (Kirk, 1983). There is virtually no absorption of wavelengths in the area between 475nm and 625nm. *Chlorella vulgaris* 211/11c contained relatively high levels of both chlorophyll a and b stored in large chloroplasts within the cell (a typical 7 day old culture contained $14\mu\text{g ml}^{-1}$ chlorophyll a and $5\mu\text{g ml}^{-1}$ chlorophyll b). As the yellow (450-800nm) filter cut out all wavelengths below 450nm (Figure 22), it can

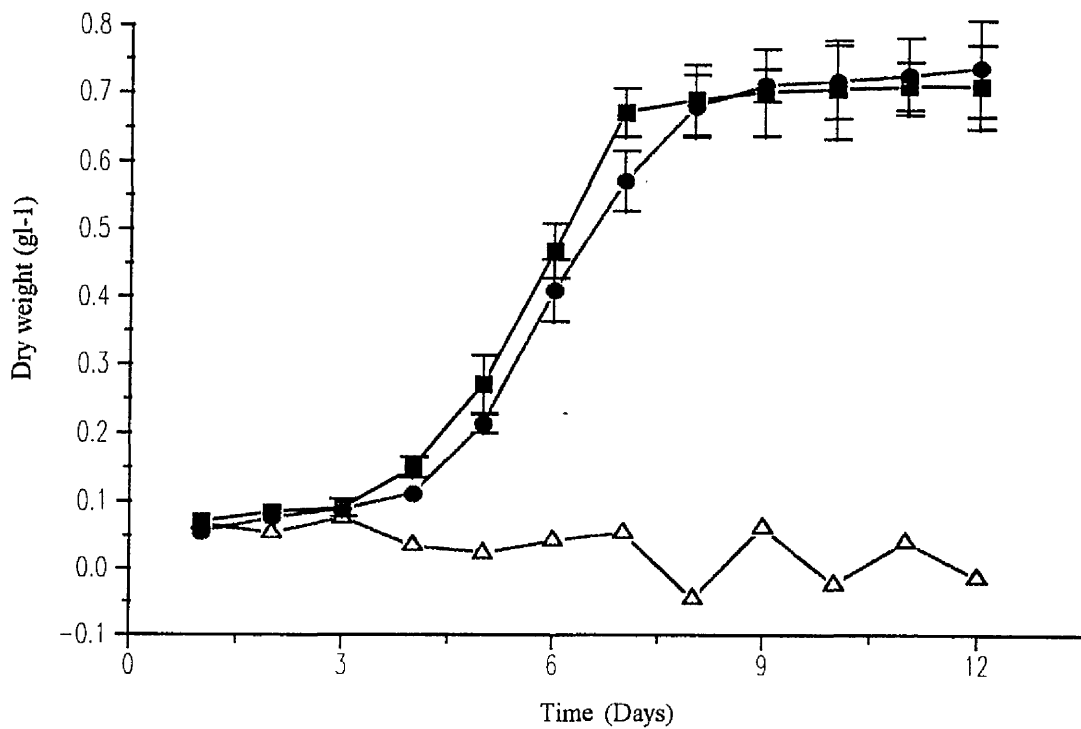


Figure 238. The effect of spectral radiant flux on the growth curves of *Chlorella vulgaris* 211/11c. ■—■ orange light (575-800nm), ●—● yellow light (475-800nm), Δ—Δ green light (450-575nm).

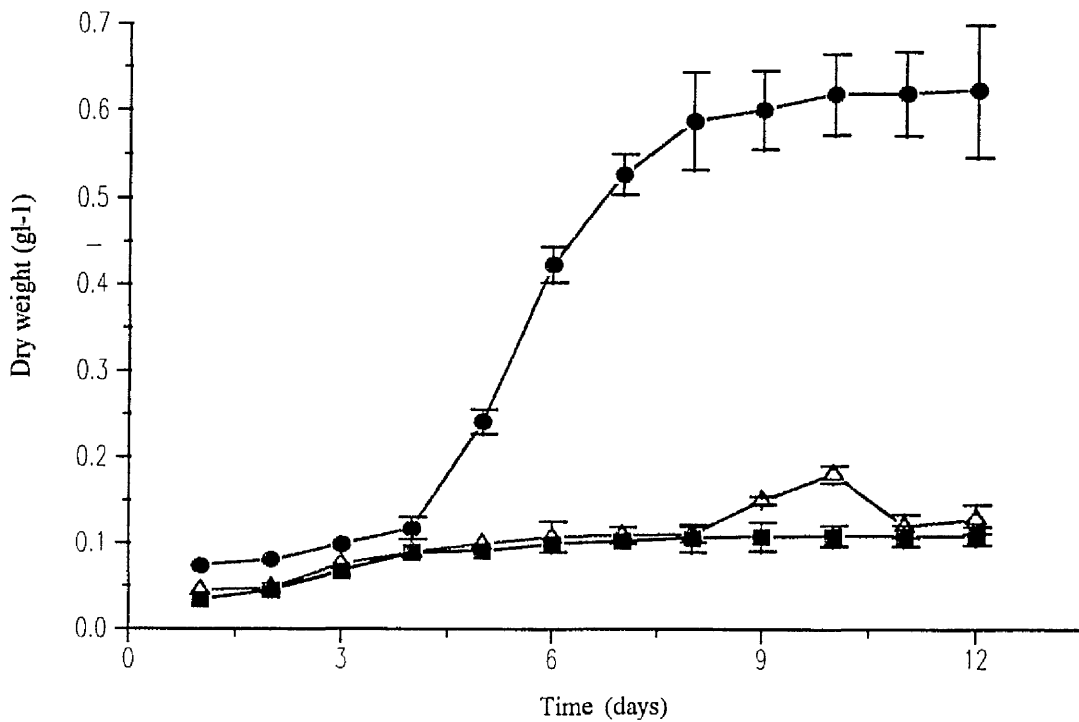


Figure 239. The effect of spectral radiant flux on the growth curves of *Chlorella vulgaris* 211/11c. ■—■ blue light (375-550nm), Δ—Δ red light (600-800nm), ●—● chrome orange light (500-800nm).

Table 94. The effect of wavelength on the growth rates and stationary phase biomass of *Chlorella vulgaris* 211/11c.

<i>Chlorella vulgaris</i> 211/11c							
Filter	None	450-800nm	550-800nm	450-600nm	350-575nm	475-800nm	600-800nm
Growth rate (day ⁻¹)	0.712 ±0.142	0.619 ±0.125	0.647 ±0.19	no data	0.328 ±0.076	0.642 ±0.132	0.319 ±0.033
Chlorophyll a µg ml ⁻¹ (7 day old culture)	10.43	7.56	8.76	no data	4.35	no data	3.12
Maximum stationary phase biomass (g l ⁻¹)	0.835 ±0.117	0.709 ±0.095	0.736 ±0.144	0.062 ±0.004	0.108 ±0.02	0.624 ±0.137	0.18 ±0.046

Table 95. The effect of wavelength on the growth rates and stationary phase biomass of *Scenedesmus* sp.

<i>Scenedesmus</i> sp.							
Filter	None	450-800nm	550-800nm	450-600nm	350-575nm	475-800nm	600-800nm
Growth rate (day ⁻¹)	0.711 ±0.144	0.490 ±0.12	0.478 ±0.077	no data	no data	0.395 ±0.042	0.201 ±0.022
Chlorophyll a µg ml ⁻¹ (7 day old culture)	12.22	11.04	8.93	no data	no data	no data	2.12
Maximum stationary phase biomass (g l ⁻¹)	0.992 ±0.106	0.953 ±0.21	0.625 ±0.095	0.036 ±0.001	0.056 ±0.002	0.761 ±0.010	0.151 ±0.06

be seen from Kirk, (1983), that the major absorbance spectra of chlorophyll a lay below the 450nm cut off point. Thus the cells of *Chlorella vulgaris* 211/11c would have only been able to utilise the wavelengths of light absorbed mainly by chlorophyll b and the high wavelength absorption of chlorophyll a. This alone may explain why the growth rates and stationary phase biomass levels of cells cultured in yellow filter (450-800nm) light were lower than the control flasks.

It is suggested that a similar explanation accounts for the reason why cells cultured in flasks green (450-600nm), blue (350-575nm) and red (600-800nm) grew with very low growth rates of 0.062, 0.328 and 0.319 day⁻¹ respectively. From Figure 17 it can be seen that wavelengths below 450nm and between 600-700nm are completely removed. Figure 18 cuts off all wavelengths in the 600-700nm range. Figure 19 only allows wavelengths of light through above 600nm. Since these wavelengths are those absorbed primarily by chlorophyll a and b, only a small fraction of the light incident on the flasks was available for photosynthesis. Visual examination of all cultures revealed that cells were pale green in colour compared to the control cells. It was found that chlorophyll a levels decrease with decreasing available wavelengths. Cells cultured under red light (600-800nm) contained approximately one third the level of chlorophyll a measured in cells cultured in full spectrum light.

The effect of spectral radiant flux on the growth curves of *Scenedesmus sp.* are presented in Figures 240 and 241. The growth rates and stationary phase biomass levels are presented in Table 95. Cells of *Scenedesmus sp.* showed a similar pattern to that recorded from *Chlorella vulgaris* 211/11c. Low cell growth rates were observed with filters green (450-600nm), blue (350-575nm) and red (600-800nm). The highest growth rate (0.49day⁻¹) and stationary phase biomass level (0.992gl⁻¹) was found with the yellow filter (450-800nm). However high growth rates and stationary phase biomass levels were recorded with filters orange (550-800nm) of 0.478 day⁻¹ and 0.625 gl⁻¹ and chrome orange (475-800nm) of 0.395 day⁻¹ and 0.761 gl⁻¹ respectively. *Scenedesmus sp.*, like *Chlorella vulgaris* 211/11c, is a unicellular eukaryotic green micro-algae and contains similarly high levels of chlorophyll a and b. The control flask of *Scenedesmus sp.* (Figure 244) showed that cells cultured in full spectrum (300-800nm) light had higher growth rates and stationary phase biomass levels than cells cultured in yellow (450-800nm), orange (550-800nm) and chrome (475-800nm) light filters.

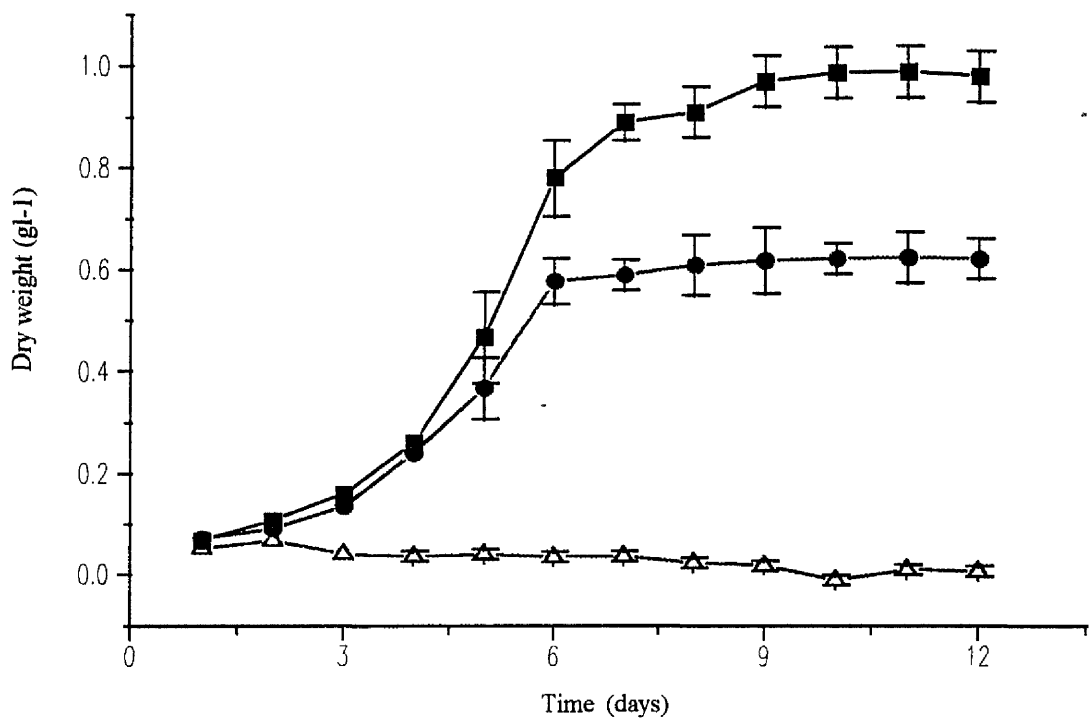


Figure 240. The effect of spectral radiant flux on the growth curves of *Scenedesmus sp.*, ●—● orange light (575-800nm), ■—■ yellow light (475-800nm), △—△ green light (450-575nm).

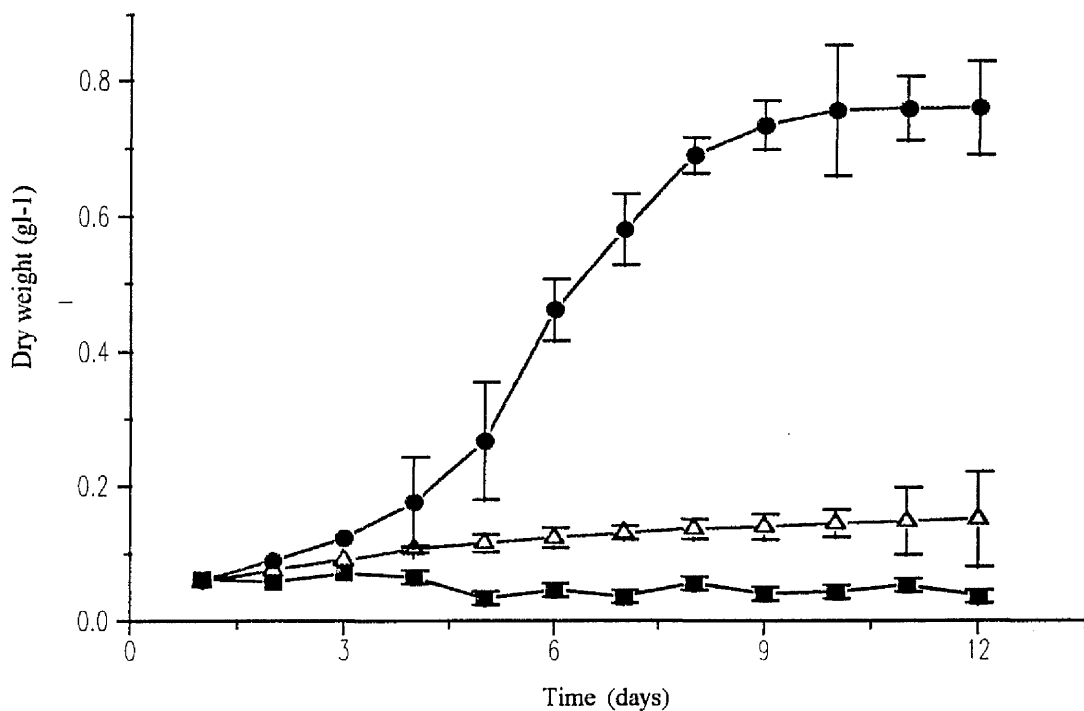


Figure 241. The effect of spectral radiant flux on the growth curves of *Scenedesmus sp.*, ■—■ blue light (375-550nm), △—△ red light (600-800nm), ●—● chrome orange light (500-800nm).

Figures 242 and 243 show the effects of spectral radiant flux on the growth kinetics of *Synechococcus* 1479/5. Growth rates and stationary phase biomass levels are presented in Table 96.

From Figures 242 and 243, it can be seen the cells of *Synechococcus* 1479/5 grew with very low growth rates in filters green (450-600nm) and blue (350-575nm). Although having a very low growth rate in blue light the cells of *Synechococcus* 1479/5 produced 0.121 g l⁻¹ of dry matter. The highest growth rate (0.415 day⁻¹) when using wavelength filters was observed with cells culture in the chrome orange filter (475-800nm). Cells cultured in filter orange (550-800nm), however, produced the highest stationary phase biomass level (0.462gl⁻¹). None of the filter experiments compared with that of the control which grew cells of *Synechococcus* 1479/5 in full spectrum (300-800nm) light (Figure 244) which produced twice as much biomass (0.96 gl⁻¹). Unlike the unicellular eukaryotic green micro-algae, cyanobacteria do not contain chlorophyll b and do not house their pigments in chloroplasts. It is also known that cyanobacteria e.g. *Synechococcus sp.* have relatively lower cell chlorophyll a content compared to the eukaryotic algae (Agusti, 1991a). Data obtained from Agusti and Philips (1992), however, demonstrated that *Synechococcus sp.* had a high cell absorption of light at 400-440nm and 680-700nm. Therefore cells of *Synechococcus* 1479/5 have a large number of other pigments which have maximum absorption coefficients at wavelengths different to those of chlorophyll a.

Although micro-algae can photosynthesise at wavelengths below 400nm and above 700nm, the main bulk of photosynthesis is produced from absorption of light at wavelengths in between 400-700nm. Chlorophyceae such as *Chlorella vulgaris* 211/11c contain both chlorophyll a and b, whereas Cyanophyceae only contain chlorophyll a. Cyanophyceae such as the cyanobacteria *Synechococcus* 1479/5, however, contain a large number of other pigments called phycobiliproteins. Phycoerythrin, phycocyanin and phycoerythrocyanin are the major examples of phycobiliproteins. These pigments have different absorption spectra from those of the chlorophyll's. As was shown by Kirk, (1983), the wavelengths of maximum absorption of chlorophyll a and b are 423, 666 and 453, 647nm respectively. However as the experiments above showed, low growth rates were produced in light absent of these wavelengths. By having different photosynthetic pigments such as the phycobiliproteins, a larger area of the spectrum can become accessible for

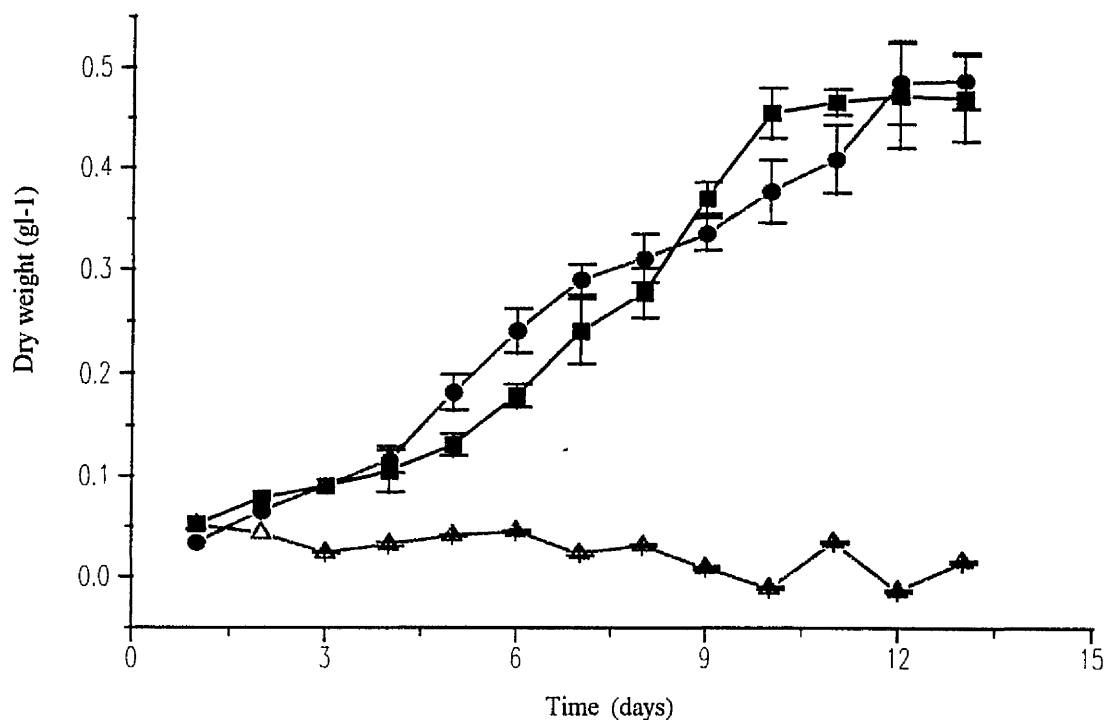


Figure 242. The effect of spectral radiant flux on the growth curves of *Synechococcus* 1479/5, ■—■ orange light (575-800nm), ●—● yellow light (475-800nm), △—△ green light (450-575nm).

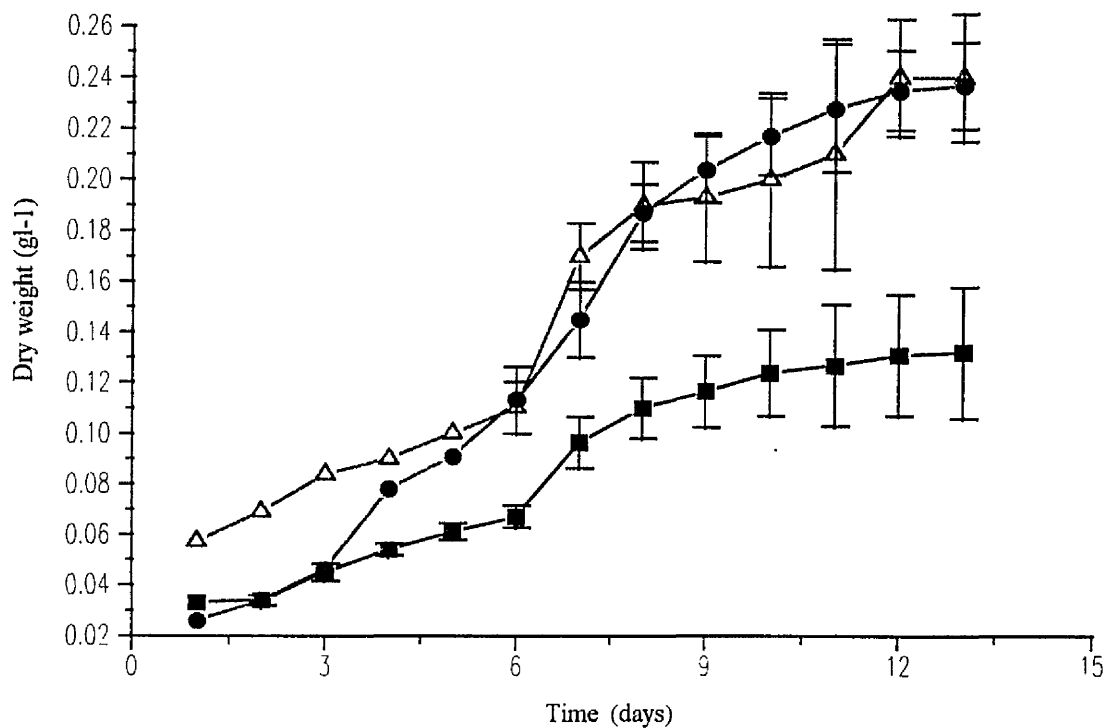


Figure 243. The effect of spectral radiant flux on the growth curves of *Synechococcus* 1479/5, ■—■ blue light (375-550nm), ●—● red light (600-800nm), △—△ chrome orange light (500-800nm).

Table 96. The effect of wavelength on the growth rates and stationary phase biomass of *Synechococcus* 1479/5.

<i>Synechococcus</i> 1479/5							
Filter	None	450- 800nm	550- 800nm	450- 600nm	350- 575nm	475- 800nm	600- 800nm
Growth rate (day ⁻¹)	0.573 ±0.078	0.289 ±0.046	0.365 ±0.072	no data	0.193 ±0.024	0.415 ±0.088	0.132 ±0.021
Chlorophyll a µg ml ⁻¹ (7 day old culture)	6.87	3.65	3.57	no data	0.466	2.45	1.56
Maximum stationary phase biomass (g l ⁻¹)	0.752 ±0.086	0.451 ±0.063	0.462 ±0.054	0.051 ±0.001	0.121 ±0.003	0.306 ±0.007	0.211 ±0.034

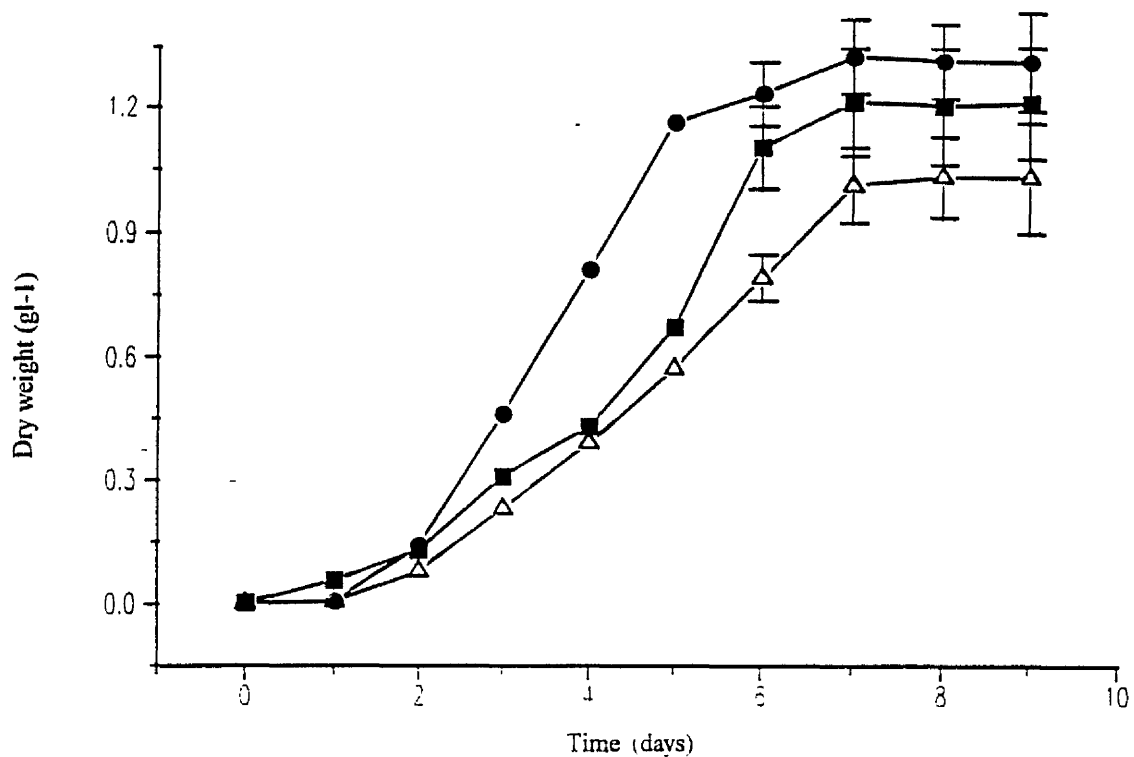


Figure 244. The effect of white light (300-800 nm) at a PFD of $50\mu\text{mol s}^{-1} \text{m}^{-2}$ on the growth curves of microalgae and cyanobacteria. ■—■ (*Chlorella vulgaris* 211/11c, ●—● *Scenedesmus* sp. and Δ—Δ *Synechococcus* 1479/5).

photosynthesis to the cyanobacteria. Several of the phycoerythrin pigments have a strong absorption at wavelengths 492-565 (Myers *et al.*, 1980; Stewart and Farmer, 1984). This may have been the reason why cells of *Synechococcus* 1479/5 grew in blue light.

Olaizola and Duerr, (1990) found that the chlorophyll a content of cells of *Spirulina* cultured under red light was approximately two thirds that measured under white light. It is possible that the phycobiliprotein content of *Synechococcus* 1479/5 aided the cell in obtaining light energy outside the spectrum absorbed by chlorophyll a. The reported findings of Olaizola and Duerr, (1990) showed similar changes in chlorophyll a content of cells cultured in red and green light which supports the findings of the work presented here but contradicts the work of Tandeau de Marsac, (1977), who examined 44 different strains of cyanobacteria, and found no changes in chlorophyll a content.

3.9.2 The effect of spectral radiant flux on the photosynthesis / irradiance curves of micro-algae and cyanobacteria..

Chlorella vulgaris 211/11c, *Scenedesmus* sp. *Synechococcus* sp. and *Synechococcus* 1479/5 were used to study the effects of spectral radiant flux on the photosynthesis / irradiance curves of wavelength adapted cells.

As previously described in Section 3.9.1 cells of the above micro-algae and cyanobacteria were grown in flasks irradiated by red (600-800nm), blue (350-575) and full spectrum light. Photosynthesis / irradiance curves were determined for each culture using red (600-800nm), blue (350-575nm) and full spectrum (300-800nm) light respectively. In each of the presented tables Filter Cul : P.I, refers to the growth of the culture and the conditions under which the photosynthesis / irradiance curve was determined. The first number refers to the wavelength at which the cells were cultured. The second number refers to the wavelength at which the cells were irradiated during the photosynthesis / irradiance response curve measurement. Numbers 118, 182, 101, 179, and 105 refer to the Lee industry standard numbers given to the light filters blue (350-575nm), red (600-800nm), yellow (450-800nm), chrome orange (475-800nm) and orange (550-800nm) respectively.

Figures 245 and 246 show the results of culturing cells of *Chlorella vulgaris* 211/11c in red light (600-800nm) followed by photosynthesis / irradiance measurement with light of varying wavelength. The values for P_{\max} , P_{\max}^{PFD} , alpha and I_k are presented in Table 97. It can be seen that the highest measurement of P_{\max} (37.08mg oxygen g dry wt⁻¹ hr⁻¹) occurred when the photosynthesis / irradiance measurement was carried out using full spectrum light. Although the cells of *Chlorella vulgaris* 211/11c had been adapted to grow in red (600-800nm) light, the photosynthetic apparatus was still functioning at a maximum in light 400-700nm. However it can be seen that the I_k values for the photosynthesis / irradiance curves measured with red (600-800nm) and blue (350-575nm) light were 3 times as high compared to photosynthesis / irradiance curves determined in any of the other filters. These high values for I_k (127.2 (600-800nm), 117.5 $\mu\text{mol s}^{-1} \text{m}^{-2}$ (350-575nm) respectively) were determined from very low alpha values. The alpha values for photosynthesis / irradiance measurements made in red (600-800nm) light and blue (350-575nm) light were 0.146 and 0.215 mg oxygen g dry wt⁻¹ hr⁻¹ / $\mu\text{mol s}^{-1} \text{m}^{-2}$. These values were approximately 4 times lower than alpha values measured for the other filters displaying that the rates of light limited photosynthesis were extremely low.

Figure 247 and 248 show the effect of wavelength on the photosynthesis / irradiance curves of *Chlorella vulgaris* 211/11c cultured in blue (350-575nm) light. Table 98 presents the different photosynthetic parameters determined from the photosynthesis / irradiance curves of Figures 247 and 248. It can be seen from Table 98 that the highest P_{\max} value (52.199 mg oxygen g dry wt⁻¹ hr⁻¹) was measured when cells cultured in blue (350-575nm) light were irradiated with full spectrum light. Cells irradiated with blue (350-575nm) light and full spectrum light has much higher alpha values (1.15 and 2.06 mg oxygen g dry wt⁻¹ hr⁻¹ / $\mu\text{mol s}^{-1} \text{m}^{-2}$ respectively) compared to the other culture flasks. From Table 98, it can also be seen that the value of I_k is higher for the red (600-800nm) irradiated cells compared to other filters.

The effect of wavelength on the photosynthesis / irradiance curves of cells of *Scenedesmus sp.* cultured in red (600-800nm) light can be seen in Figures 249 and 250. The photosynthetic parameters measured from Figures 249 and 250 are presented in Table 99. It can be seen from Figures 249 and 250 that cells of *Scenedesmus sp.* displayed a similar pattern to that observed with *Chlorella vulgaris* 211/11c. Red (600-800nm) light adapted cells displayed a higher P_{\max} rate (36.01 mg

Table 97. the effect of wavelength on the photosynthesis of *Chlorella vulgaris* 211/11c cultured in red (600-800nm) light.

Filter Cul : P.I	600- 800nm :	600- 800nm :	600- 800nm :	600- 800nm :	600- 800nm :	600- 800nm :
	600- 800nm	350- 575nm	Full	450- 800nm	475- 800nm	550- 800nm
P_{max} mg oxygen g dry wt ⁻¹ hr ⁻¹	18.58	25.27	37.08	29.38	23.03	23.16
P_{max}^{PPFD} $\mu\text{mol s}^{-1} \text{m}^{-2}$	500	750	500	300	300	300
α mg oxygen g dry wt ⁻¹ hr ⁻¹	0.146	0.215	0.913	0.724	0.634	0.475
I_k $\mu\text{mol s}^{-1} \text{m}^{-2}$	127.2	117.5	40.6	41.2	36.32	48.75

Table 98. the effect of wavelength on the photosynthesis of *Chlorella vulgaris* 211/11c cultured in blue (350-575nm) light.

Filter Cul : P.I	350- 575nm :	350- 575nm :	350- 575nm :	350- 575nm :	350- 575nm :	350- 575nm :
	350- 575nm	600- 800nm	Full	450- 800nm	475- 800nm	550- 800nm
P_{max} mg oxygen g dry wt ⁻¹ hr ⁻¹	39.89	28.53	52.199	30.96	31.38	28.18
P_{max}^{PPFD} $\mu\text{mol s}^{-1} \text{m}^{-2}$	300	500	500	200	300	300
α mg oxygen g dry wt ⁻¹ hr ⁻¹	1.15	0.468	2.06	0.741	0.676	0.557
I_k $\mu\text{mol s}^{-1} \text{m}^{-2}$	34.68	60.96	25.33	41.78	46.4	50.59

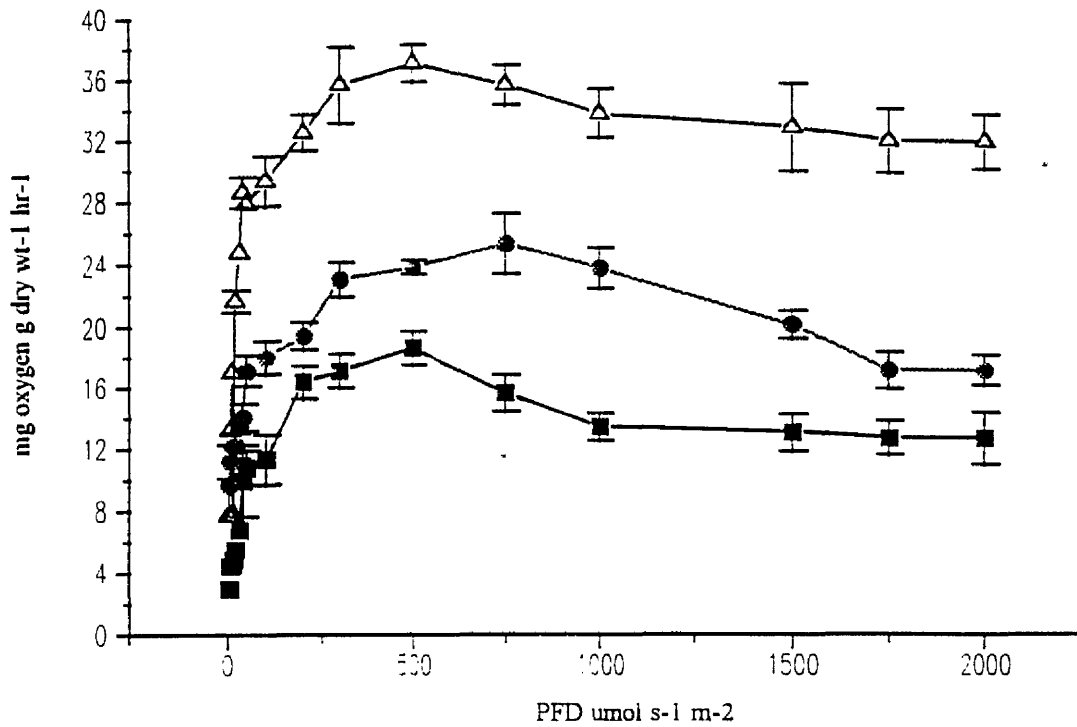


Figure 245. The effect of spectral radiant flux on the photosynthesis / irradiance response curves of *Chlorella vulgaris* 211/11c cultured in red (600-800nm) light, Δ — Δ full spectrum light (300-800nm), \bullet — \bullet blue light (375-550nm), \blacksquare — \blacksquare red light (600-800nm).

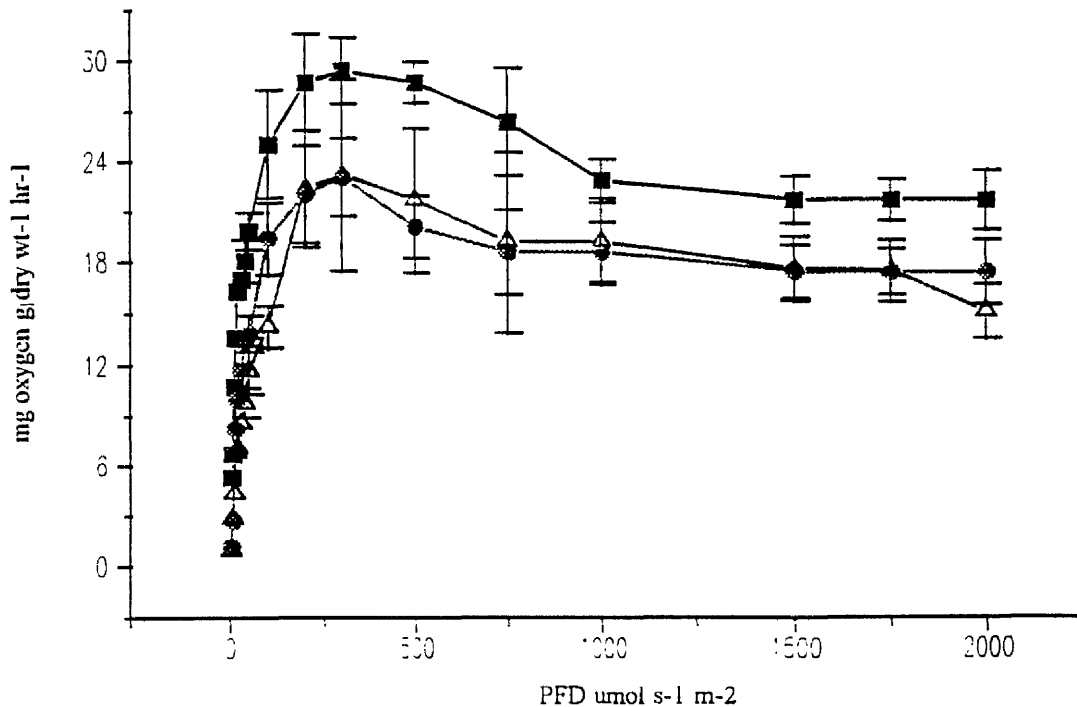


Figure 246. The effect of spectral radiant flux on the photosynthesis / irradiance response curves of *Chlorella vulgaris* 211/11c cultured in red (600-800nm) light, Δ — Δ orange light (575-800nm), \bullet — \bullet chrome orange light (500-800nm), \blacksquare — \blacksquare yellow light (475-800nm).

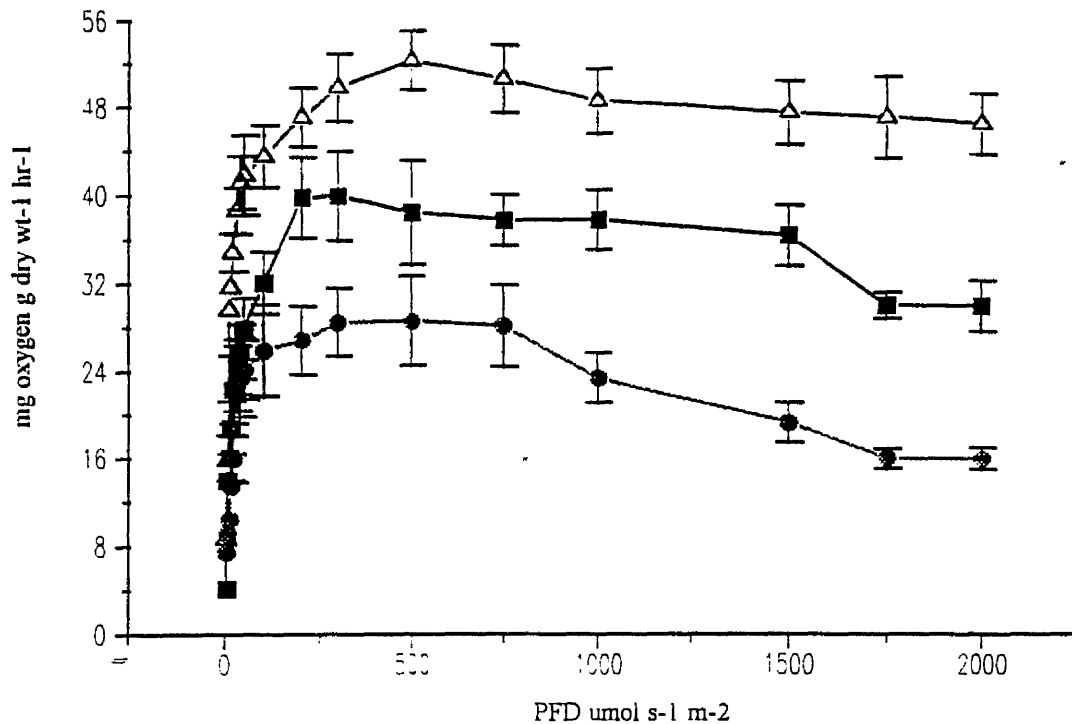


Figure 247. The effect of spectral radiant flux on the photosynthesis / irradiance response curves of *Chlorella vulgaris* 211/11c cultured in blue (375-550nm) light, Δ — Δ full spectrum light (300-800nm), \blacksquare — \blacksquare blue light (375-550nm), \bullet — \bullet red light (600-800nm).

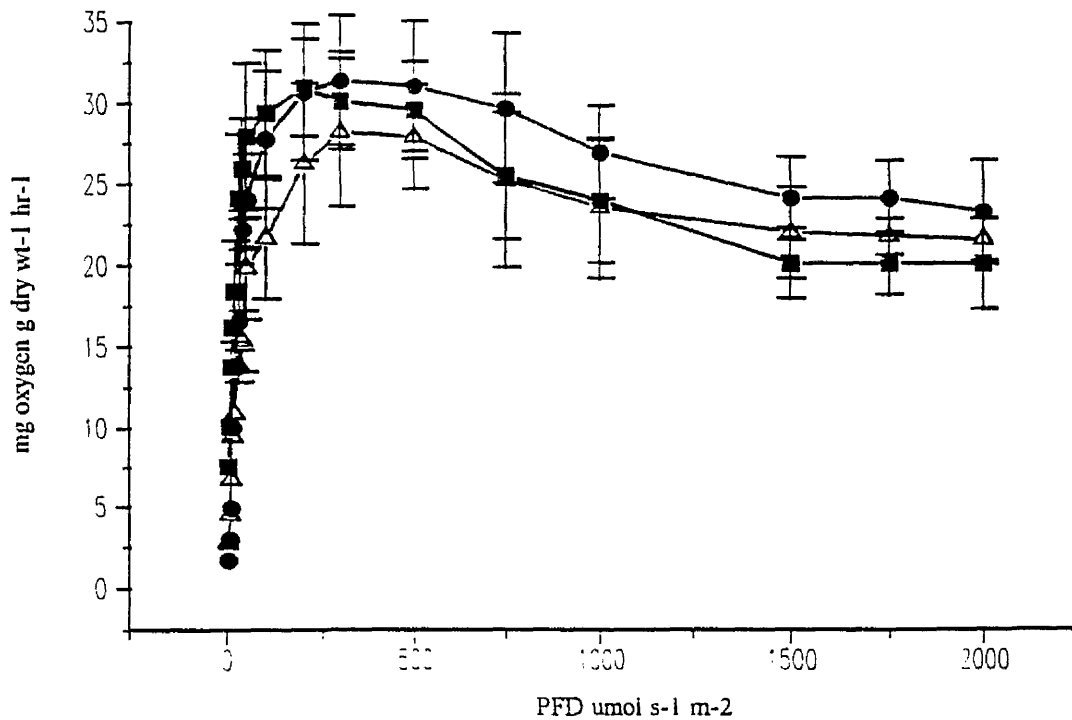


Figure 248. The effect of spectral radiant flux on the photosynthesis / irradiance response curves of *Chlorella vulgaris* 211/11c cultured in blue (375-550nm) light, Δ — Δ orange light (575-800nm), \bullet — \bullet chrome orange light (500-800nm), \blacksquare — \blacksquare yellow light (475-800nm).

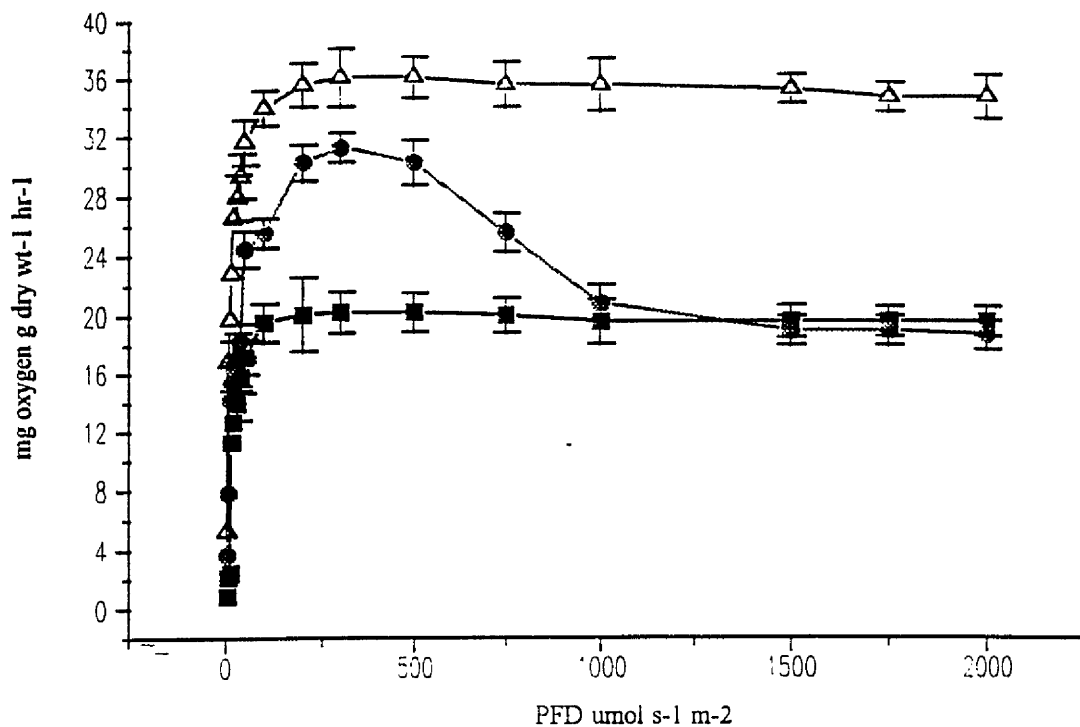


Figure 249. The effect of spectral radiant flux on the photosynthesis / irradiance response curves of *Scenedesmus sp.* cultured in red (600-800nm) light, Δ—Δ full spectrum light (300-800nm), ●—● blue light (375-550nm), ■—■ red light (600-800nm).

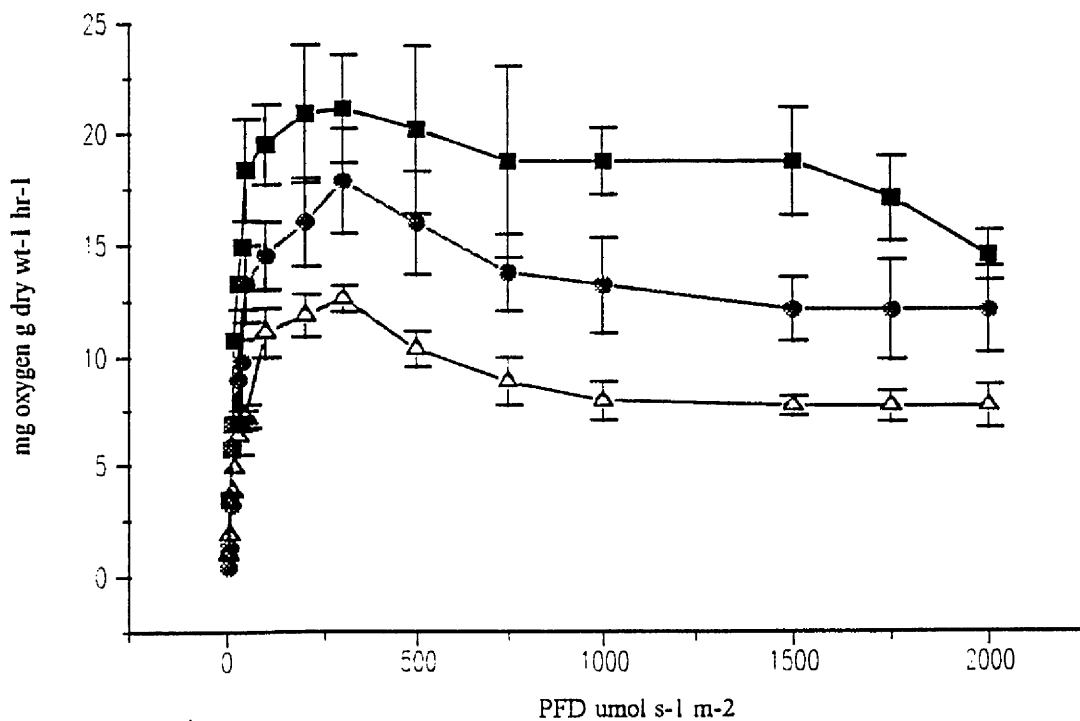


Figure 250. The effect of spectral radiant flux on the photosynthesis / irradiance response curves of *Scenedesmus sp.* cultured in red (600-800nm) light, Δ—Δ orange light (575-800nm), ●—● chrome orange light (500-800nm), ■—■ yellow light (475-800nm).

oxygen g dry wt⁻¹ hr⁻¹) when irradiated with full spectrum light. Blue light (350-575nm) irradiated cells had a higher P_{max} than red irradiated cells (31.24 compared to 20.19 mg oxygen g dry wt⁻¹ hr⁻¹).

The effect of wavelength on the photosynthesis / irradiance curves of cells of *Scenedesmus sp.* cultured in blue (350-575nm) light is shown in Figures 251 and 252. The different photosynthetic parameters of these figures are presented in Table 100. It can be seen that cells of *Scenedesmus sp.* cultured in blue light had a higher P_{max} value (78.46 mg oxygen g dry wt⁻¹ hr⁻¹) when irradiated with full spectrum light. However blue light irradiated cells had a higher alpha value (1.816 mg oxygen g dry wt⁻¹ hr⁻¹) than cells irradiated with full spectrum light (1.494 mg oxygen g dry wt⁻¹ hr⁻¹). Cultures of cells irradiated with light of filter 450-800nm, 550-800nm and 475-800nm displayed almost identical P_{max} values of 45.75, 42.625 and 42.25 mg oxygen g dry wt⁻¹ hr⁻¹ respectively. All flasks displayed similar values for I_k. Cells cultured in light of 450-800nm displayed a higher alpha value than cells irradiated with full spectrum light.

The effect of wavelength on the photosynthesis / irradiance curves of *Synechococcus sp.* cultured in red (600-800nm) light are displayed in Figures 253 and 254 respectively. The photosynthetic parameters determined from the above Figures 253 and 254 are presented in Table 101. It can be seen from Figure 253, that cells of *Synechococcus sp.* displayed a P_{max} value (92.79 mg oxygen g dry wt⁻¹ hr⁻¹) approximately 3 times higher when irradiated with full spectrum light compared to the filters of 450-800nm, 550-800nm, 350-575nm, 450-600nm and 600-800nm. The P_{max}^{PFD} of cells of *Synechococcus sp.* was found to be 500 μmol s⁻¹ m⁻² when irradiated with red (600-800nm) and blue (350-575nm) light. However the P_{max}^{PFD} of each of the remaining filters was found to be 300 μmol s⁻¹ m⁻².

The effect of wavelength on the photosynthesis / irradiance curves of *Synechococcus sp.* cultured in blue (350-575nm) light is presented in Figures 255 and 256. Table 102 shows the various photosynthetic parameters determined from these figures. It can be seen that as was found in all experiments, the cells when irradiated with full spectrum light (300-800nm) displayed a higher P_{max} value (92.79 mg oxygen g dry wt⁻¹ hr⁻¹) than all other filters. The value of alpha was observed to be greater with the full

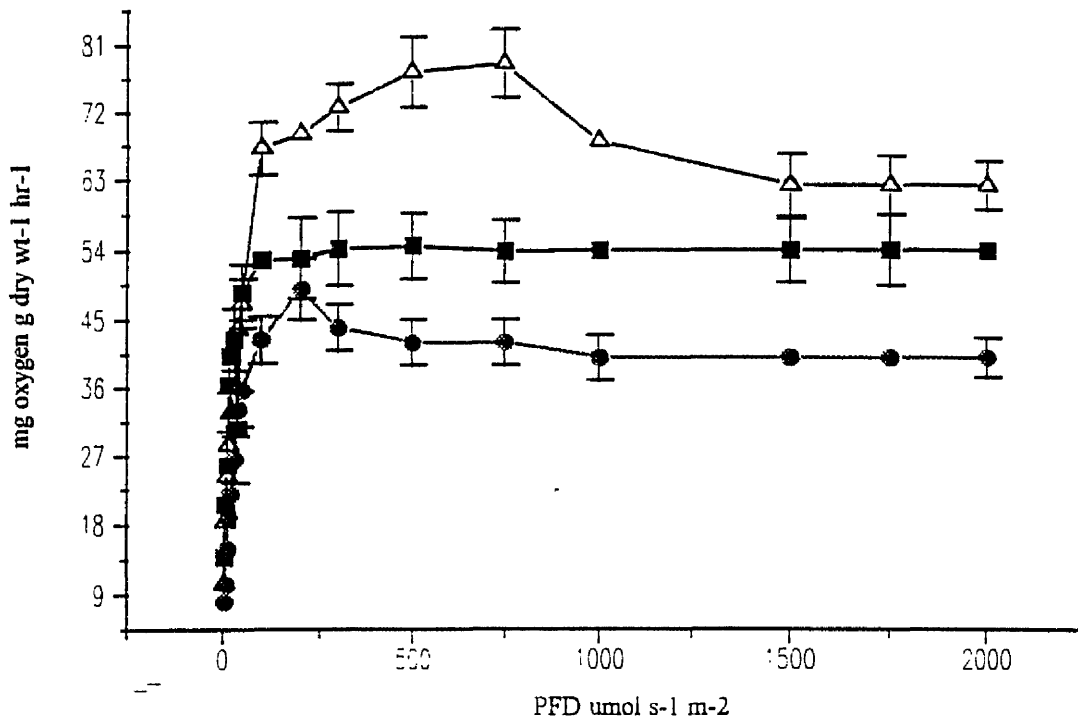


Figure 251. The effect of spectral radiant flux on the photosynthesis / irradiance response curves of *Scenedesmus sp.* cultured in blue (375-550nm) light, Δ — Δ full spectrum light (300-800nm), \blacksquare — \blacksquare blue light (375-550nm), \bullet — \bullet red light (600-800nm).

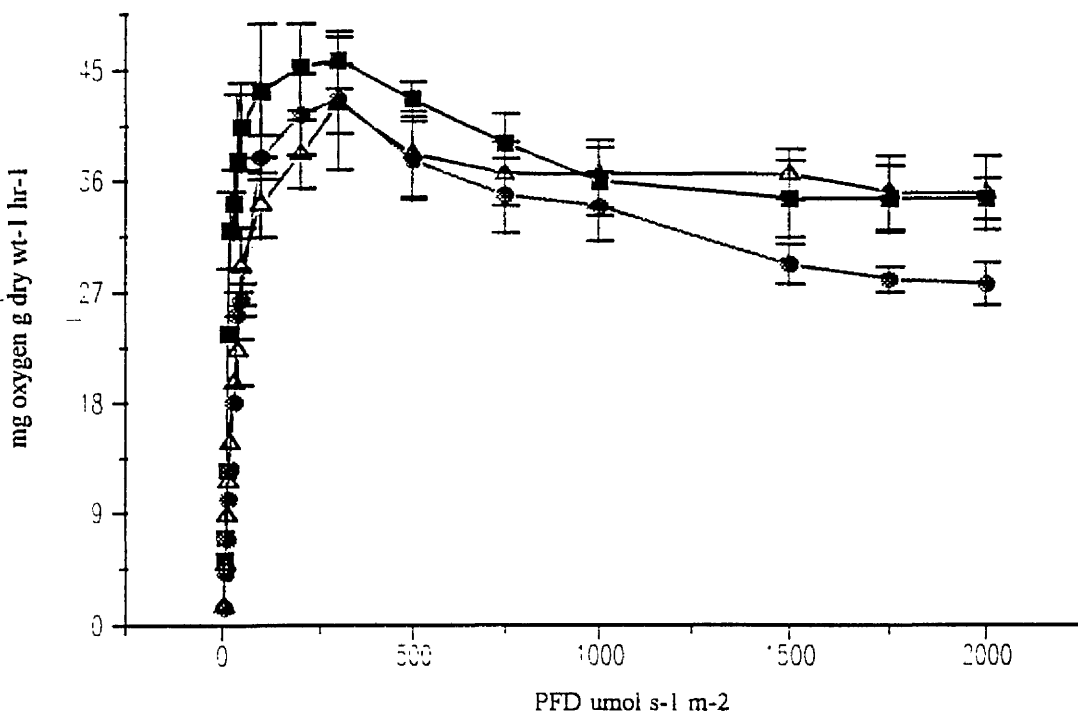


Figure 252. The effect of spectral radiant flux on the photosynthesis / irradiance response curves of *Scenedesmus sp.* cultured in blue (375-550nm) light, Δ — Δ orange light (575-800nm), \bullet — \bullet chrome orange light (500-800nm), \blacksquare — \blacksquare yellow light (475-800nm).

Table 99. The effect of wavelength on the photosynthesis of *Scenedesmus sp.* cultured in red (600-800nm) light.

Filter Cul : P.I	600-800nm : 600-800nm	600-800nm : 350-575nm	600-800nm : Full	600-800nm : 450-800nm	600-800nm : 475-800nm	600-800nm : 550-800nm
P_{max} mg oxygen g dry wt ⁻¹ hr ⁻¹	20.19	31.24	36.01	21.09	17.83	12.61
P_{max}^{PPFD} $\mu\text{mol s}^{-1} \text{m}^{-2}$	300	300	300	300	300	300
α mg oxygen g dry wt ⁻¹ hr ⁻¹	0.78	1.039	1.389	0.485	0.458	0.249
I_k $\mu\text{mol s}^{-1} \text{m}^{-2}$	25.88	30.06	25.92	43.48	38.9	50.64

Table 100. The effect of wavelength on the photosynthesis of *Scenedesmus sp.* cultured in blue (350-575nm) light.

Filter Cul : P.I	350-575nm : 350-575nm	350-575nm : 600-800nm	350-575nm : Full	350-575nm : 450-800nm	350-575nm : 475-800nm	350-575nm : 550-800nm
P_{max} mg oxygen g dry wt ⁻¹ hr ⁻¹	54.58	49	78.46	45.75	42.625	42.25
P_{max}^{PPFD} $\mu\text{mol s}^{-1} \text{m}^{-2}$	500	200	750	300	300	300
α mg oxygen g dry wt ⁻¹ hr ⁻¹	1.816	0.925	1.494	1.523	0.725	0.852
I_k $\mu\text{mol s}^{-1} \text{m}^{-2}$	30.05	52.97	52.51	30.03	58.79	49.54

Table 101. the effect of wavelength on the photosynthesis of *Synechococcus sp.* cultured in red (600-800nm) light.

Filter Cul : P.I	600- 800nm :	600- 800nm :	600- 800nm :	600- 800nm :	600- 800nm :	600- 800nm :
	600- 800nm	350- 575nm	Full	450- 800nm	475- 800nm	550- 800nm
P_{max} mg oxygen g dry wt ⁻¹ hr ⁻¹	35.25	56.48	92.79	34.21	30.39	27.92
P_{max}^{PFD} $\mu\text{mol s}^{-1} \text{m}^{-2}$	500	500	300	300	300	300
α mg oxygen g dry wt ⁻¹ hr ⁻¹	0.83	0.621	1.89	0.607	0.378	50.15
I_k $\mu\text{mol s}^{-1} \text{m}^{-2}$	42.46	90.95	49.09	56.35	80.66	55.67

Table 102. the effect of wavelength on the photosynthesis of *Synechococcus sp.* cultured in blue (350-575nm) light.

Filter Cul : P.I	350- 575nm :	350- 575nm :	350- 575nm :	350- 575nm :	350- 575nm :	350- 575nm :
	350- 575nm	600- 800nm	Full	450- 800nm	475- 800nm	550- 800nm
P_{max} mg oxygen g dry wt ⁻¹ hr ⁻¹	50.54	35.25	92.79	41.83	30.49	28.8
P_{max}^{PFD} $\mu\text{mol s}^{-1} \text{m}^{-2}$	500	500	300	300	500	500
α mg oxygen g dry wt ⁻¹ hr ⁻¹	0.556	0.83	1.89	1.07	0.378	0.423
I_k $\mu\text{mol s}^{-1} \text{m}^{-2}$	90.89	42.46	49.09	39.09	80.66	68.08

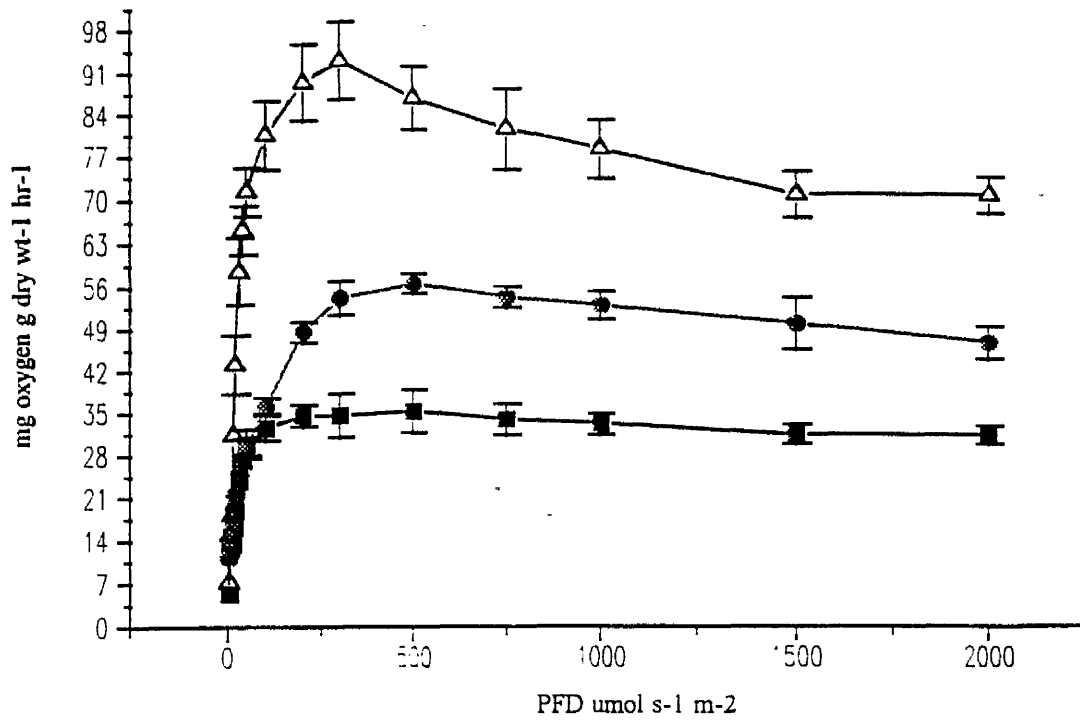


Figure 253. The effect of spectral radiant flux on the photosynthesis / irradiance response curves of *Synechococcus sp.* cultured in red (600-800nm) light, Δ — Δ full spectrum light (300-800nm), \bullet — \bullet blue light (375-550nm), \blacksquare — \blacksquare red light (600-800nm).

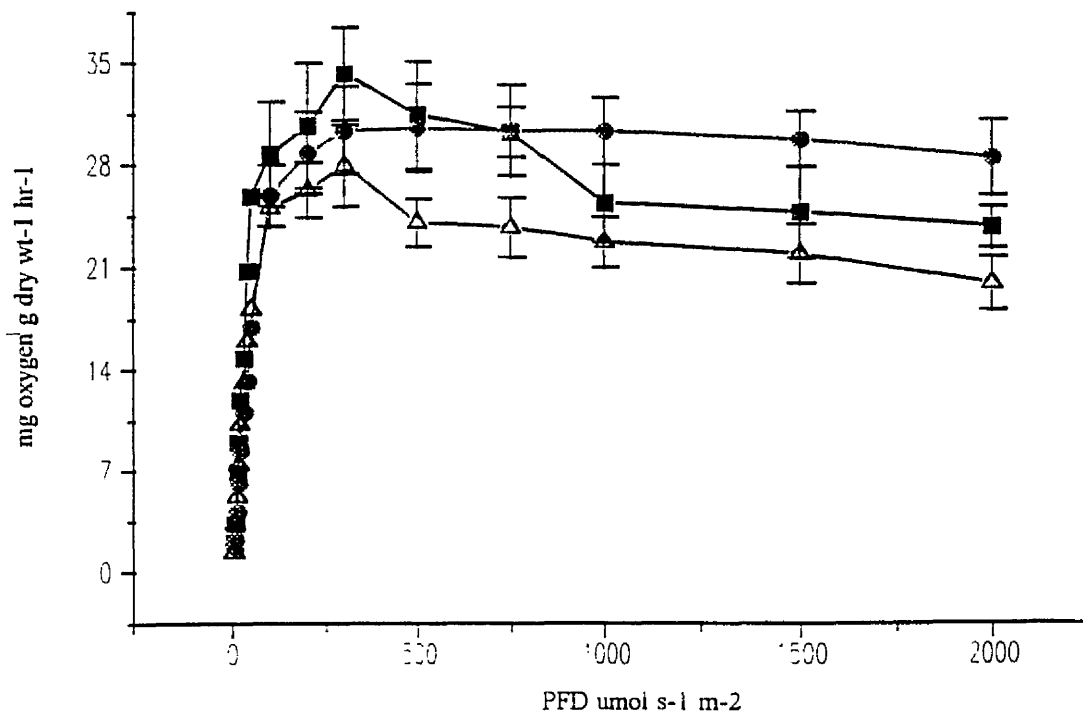


Figure 254. The effect of spectral radiant flux on the photosynthesis / irradiance response curves of *Synechococcus sp.* cultured in red (600-800nm) light, Δ — Δ orange light (575-800nm), \bullet — \bullet chrome orange light (500-800nm), \blacksquare — \blacksquare yellow light (475-800nm).

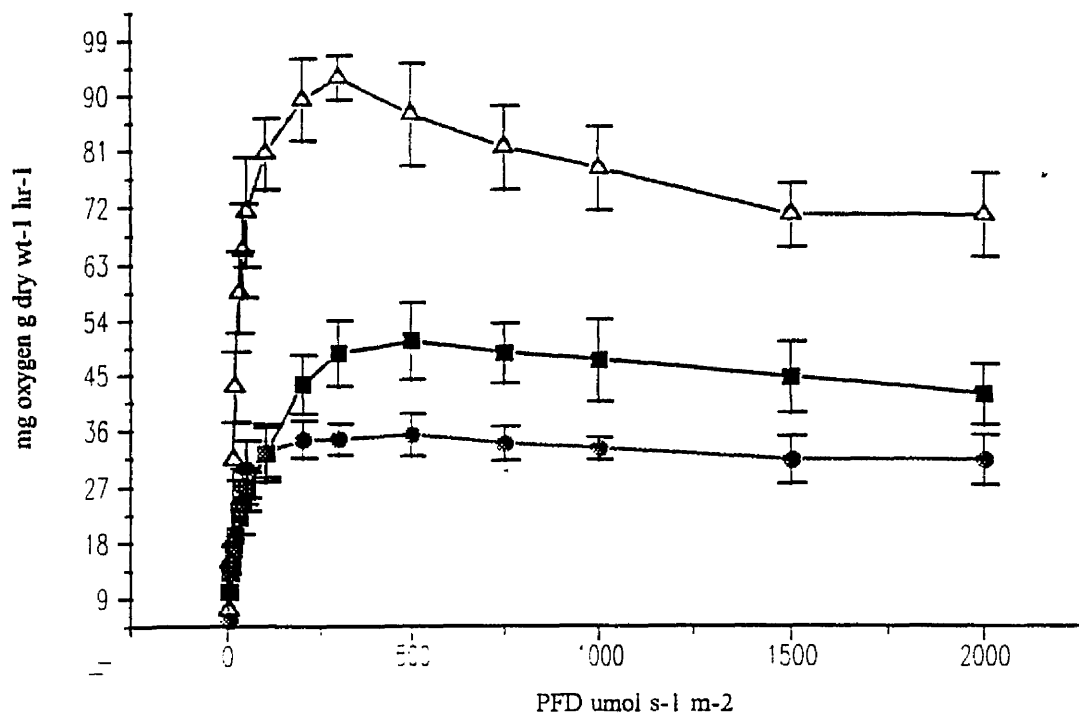


Figure 255. The effect of spectral radiant flux on the photosynthesis / irradiance response curves of *Synechococcus sp.* cultured in blue (375-550nm) light, Δ — Δ full spectrum light (300-800nm), \blacksquare — \blacksquare blue light (375-550nm), \bullet — \bullet red light (600-800nm).

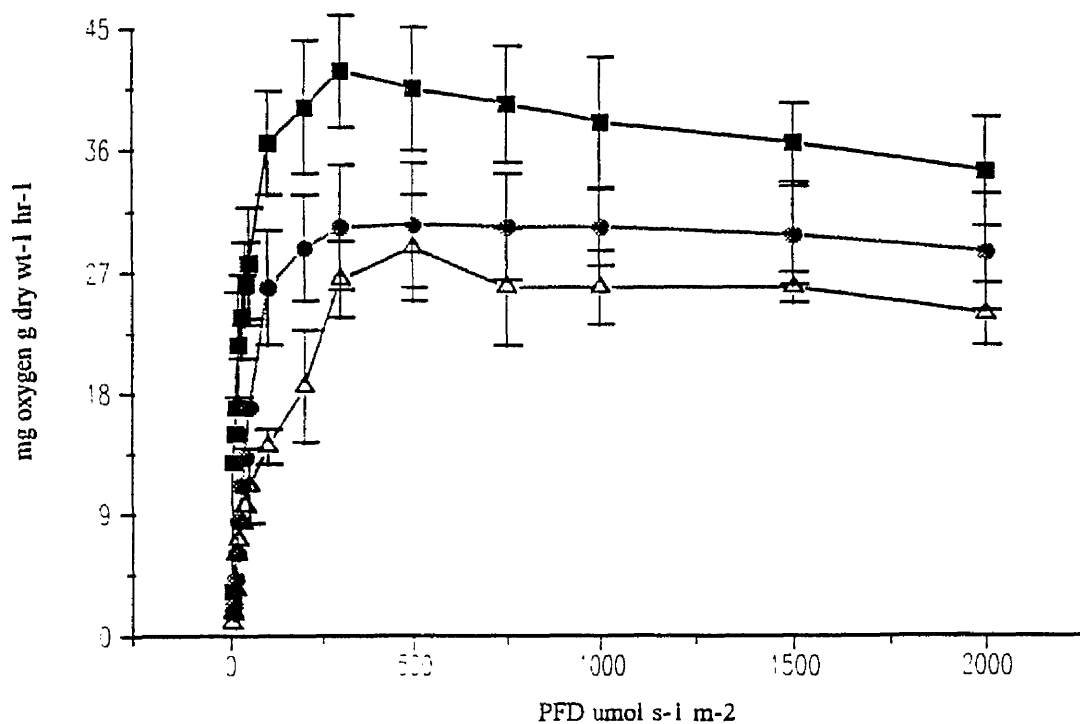


Figure 256. The effect of spectral radiant flux on the photosynthesis / irradiance response curves of *Synechococcus sp.* cultured in blue (375-550nm) light, Δ — Δ orange light (575-800nm), \bullet — \bullet chrome orange light (500-800nm), \blacksquare — \blacksquare yellow light (475-800nm).

spectrum and yellow (450-800nm) filter (1.89 and 1.07 mg oxygen g dry wt⁻¹ hr⁻¹ / μ mol s⁻¹ m⁻² respectively).

Figure 257 shows the photosynthesis / irradiance curves of *Synechococcus* 1479/5, cultured in red (600-800nm) light. Photosynthesis / irradiance curves were only measured from cells irradiated with red (600-800nm), blue (350-575nm) and full spectrum (300-800nm) light. The photosynthetic parameters determined from the above Figure 257 are presented in Table 103. It can be seen from Figure 257 that cells of *Synechococcus* 1479/5 showed a completely different photosynthesis / irradiance curve than that measured for *Synechococcus* sp. When the cells were irradiated with red (600-800nm) light during photosynthesis / irradiance analysis, it was found that P_{max} was measured at lower PFD than that of blue (350-575nm) and full spectrum (300-800) light (Table 103). It can also be seen that the P_{max} measured in red (600-800nm) light (40.76 mg oxygen g dry wt⁻¹ hr⁻¹) was almost identical to that measured in full spectrum light (40.98 mg oxygen g dry wt⁻¹ hr⁻¹). However the measured value of alpha in full spectrum light was 2 times higher than that measured for red (600-800nm) light.

Figure 258 shows the photosynthesis / irradiance curves of cells of *Synechococcus* 1479/5 cultured in blue (350-575nm) light. As was generally observed with *Chlorella vulgaris* 211/11c, *Scenedesmus* sp. and *Synechococcus* sp., cells of *Synechococcus* 1479/5 showed increased oxygen evolution rates when irradiated with blue (350-575nm) light compared to red (600-800nm) light. From Table 104, it can be seen that the highest value for P_{max} (73.87 mg oxygen g dry wt⁻¹ hr⁻¹) and alpha (1.716 mg oxygen g dry wt⁻¹ hr⁻¹ / μ mol s⁻¹ m⁻²) was observed when cells were irradiated with full spectrum light. However the I_k value for cells irradiated with blue (350-575nm) light (74.32 μ mol s⁻¹ m⁻²), was found to be almost 2 times higher than the I_k for cell cultured in either red (600-800nm) or full spectrum light.

Figure 259 shows the variation in spectral radiant flux with increasing depth in Lake Constance (Prezelin *et al.*, 1991). As the increase in depth favours the absorption of light at wavelengths in the blue (375-500nm) and red (625-725) region of the spectrum (Figure 259), the removal of these wavelengths at the surface of a water body has severe implications on the remaining wavelengths that are available for photosynthesis at the lower depths. *Chlorella vulgaris* 211/11c and *Scenedesmus* sp.

Table 103. The effect of wavelength on the photosynthesis / irradiance curves of *Synechococcus* 1479/5 cultured in red (600-800nm) light.

Filter Cul : P.I	600-800nm : 600-800nm	600-800nm : 350-575nm	600-800nm : Full
P_{max} mg oxygen g dry wt ⁻¹ hr ⁻¹	40.76	36.59	52.14
P_{max}^{PPD} $\mu\text{mol s}^{-1} \text{m}^{-2}$	100	200	300
α mg oxygen g dry wt ⁻¹ hr ⁻¹	1.108	0.819	0.8142
I_k $\mu\text{mol s}^{-1} \text{m}^{-2}$	36.78	44.67	64.1

Table 104. The effect of wavelength on the photosynthesis / irradiance curves of *Synechococcus* 1479/5 cultured in blue (350-575nm) light.

Filter Cul : P.I	350-575nm : 350-575nm	350-575nm : 600-800nm	350-575nm : Full
P_{max} mg oxygen g dry wt ⁻¹ hr ⁻¹	44.89	35.12	73.87
P_{max}^{PPD} $\mu\text{mol s}^{-1} \text{m}^{-2}$	300	500	750
α mg oxygen g dry wt ⁻¹ hr ⁻¹	0.604	0.888	1.716
I_k $\mu\text{mol s}^{-1} \text{m}^{-2}$	74.32	39.54	43.04

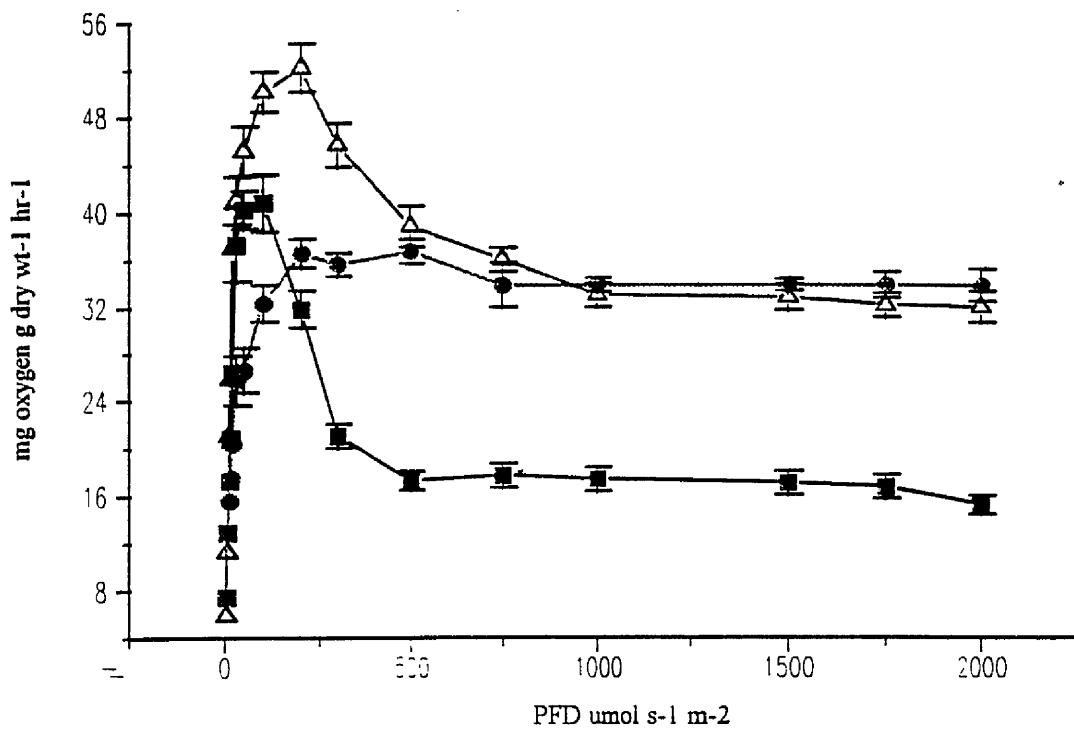


Figure 257. The effect of spectral radiant flux on the photosynthesis / irradiance response curves of *Synechococcus* 1479/5 cultured in red (600-800nm) light, Δ — Δ full spectrum light (300-800nm), \bullet — \bullet blue light (375-550nm), \blacksquare — \blacksquare red light (600-800nm).

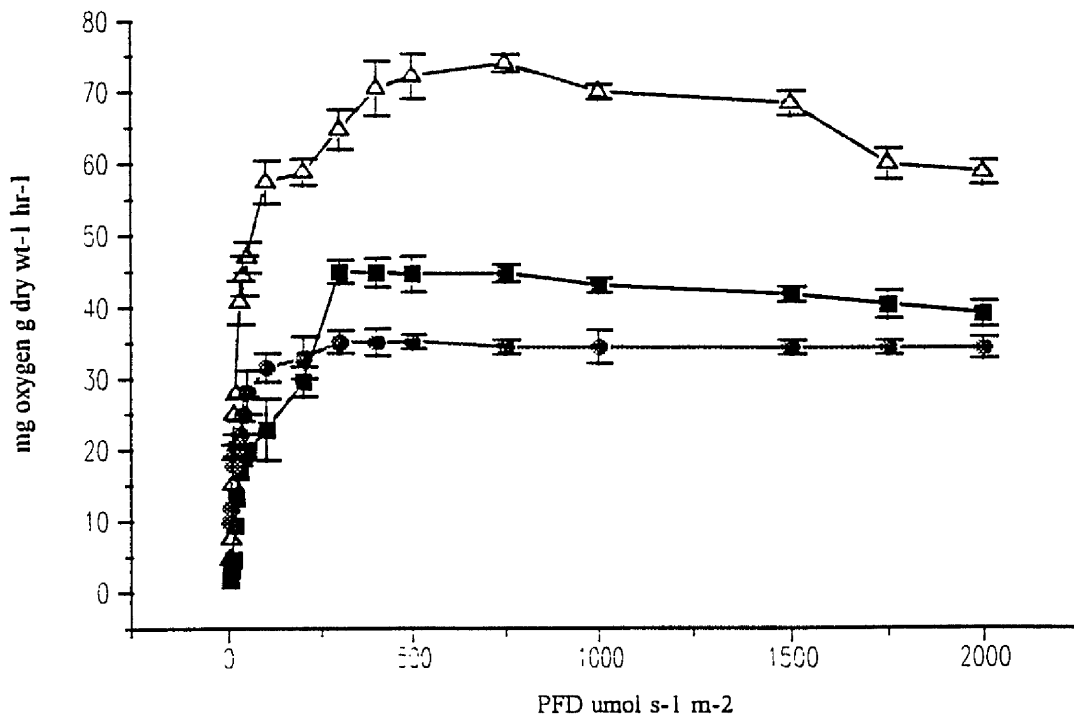
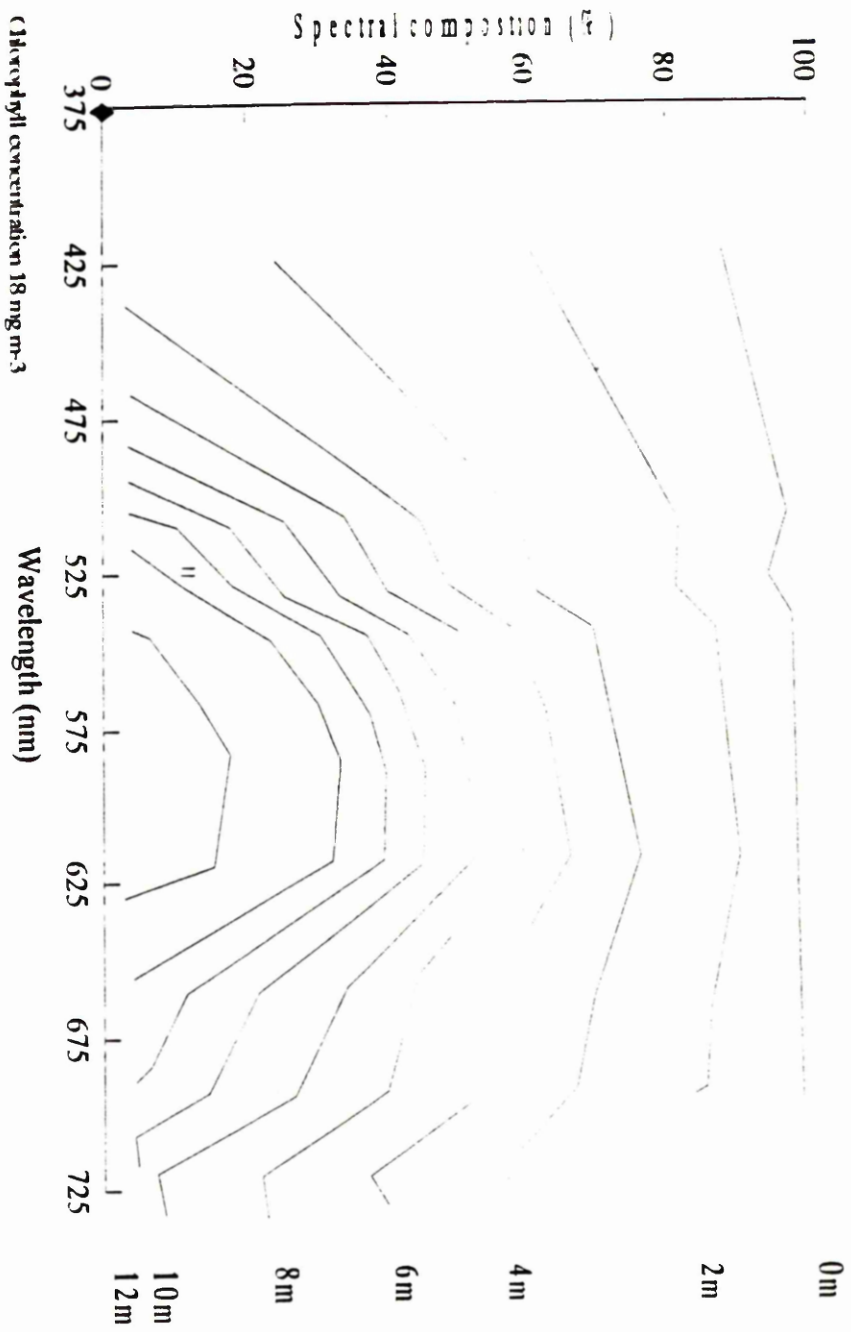


Figure 258. The effect of spectral radiant flux on the photosynthesis / irradiance response curves of *Synechococcus* 1479/5 cultured in blue (375-550nm) light, Δ — Δ full spectrum light (300-800nm), \blacksquare — \blacksquare blue light (375-550nm), \bullet — \bullet red light (600-800nm).

Figure 259. The variation in spectral composition with depth measured at Lake Constance.



both showed higher maximum rates of photosynthesis in full spectrum light (300-800nm) compared to blue light (350-575nm) which in turn yielded higher rates than red light (600-800nm). It can be seen from the control cultures (Figures 260 to 266) that the physiology of the cells cultured in light of different spectral radiant flux was different since the P_{\max} values were all higher for full spectrum light cultured cells that were subsequently P/I irradiated with light devoid of certain wavelengths. From Figure 259, the spectrum region lying between 540 and 620 would be an area of great interest since these wavelengths are not absorbed by cells or to a great extent by the water medium itself. It is possible that unknown types of micro-algae and cyanobacteria may have evolved to exploit these wavelengths.

Ponds and lake systems containing algae, have natural and forced mixing systems. Natural systems take the form of simple rolling motions caused by energy present within winds which creates waves on the surface of water bodies. However in HRAPs, forced mixing is achieved using paddle wheels and air-lift systems (Fallowfield and Garret, 1985). Micro-algae and cyanobacteria move through a gradient of light when growing in these HRAP or lake systems. The attenuation of light with depth is often included in waste treatment models (Martin and Fallowfield unpublished data). However, although PFD is a major factor determining cellular productivity and photosynthesis, ultimately it is the wavelength of light intercepted by the cell which determines the degree of photosynthesis (Kroon *et al.*, 1989).

The spectral characteristics of absorption by pigments and cells of photosynthetic organisms is important in determining primary production, radiative transfer in sea water and in passive remote sensing of phytoplankton (Sathyendranath *et al.*, 1987). Figures 14, 15 and 16 show the changes in photon flux density with increasing depth of a high rate algal pond for 3 surface irradiances of 200, 400 and 800 $\mu\text{mol s}^{-1} \text{m}^{-2}$. Figure 259 shows the change in wavelength with depth in Lake Constance (Prezelin *et al.*, 1991). It can be seen from Figure 259 that the penetration of light at wavelengths blue (400-500nm) and red (600-700nm) decreases with increasing depth. Figure 259 also shows the spectral absorption of a typical algal suspension. It can be seen that the main absorption peaks lie in the blue (400-460nm) and red (640-680nm) wavelength region. Thus the increasing absorption of these wavelengths with increasing depth displays that although the photon flux density of light may still be above the compensation point for an algal species at these increasing depths, the quality of the

light may be of no use if the relevant photosynthetic pigment is incapable of absorbing these wavelengths (500-600nm). However the research reported here is concerned with the effect of wavelength on the photosynthesis and primary productivity of photosynthetic cells. The experiments performed on the effect of culture wavelength on the photosynthesis / irradiance curves of two green unicellular micro-alga and two cyanobacteria, showed that, although the organisms were pre cultured in either red or blue light (36 days and 3 complete growth cycles), the photosynthetic apparatus for the interception and absorption of full spectrum light remained intact (based solely on measured photosynthetic parameters). It was noted that the control cells cultured in full spectrum (300-800nm) light (Figures 260, 261, 262) from which samples were removed for photosynthesis / irradiance response measurement had higher maximum rates of photosynthesis than similar cells cultured in light of different wavelengths. It has been found that pigment formation and structure composition changes with culture wavelength of light. Working on the cyanobacterium *Spirulina platensis*, Babu *et al.*, (1991) found that green light enhanced the synthesis of a phycobiliviolin type chromophore, whereas red or white light had no effect. The spectral quality of light is also known to play a role in the control of nitrate / nitrite uptake of *Monoraphidium braunii* (Aparicio and Quinones, 1991). It was found that cells of *Monoraphidium braunii* containing active levels of nitrate reductase and nitrite reductase and irradiated with strong background red light, only initiated the uptake of oxidised forms of nitrogen when stimulated with blue light. This requirement for blue light for the uptake of nitrate was not affected by carbon dioxide availability. It was also found that when the cells were maintained in a carbon dioxide free environment, cells irradiated with red light (660nm) only evolved oxygen when they were irradiated with blue light. Although a reduction in red (600-800nm) light stimulated oxygen evolution was observed compared to that of full spectrum light (300-800nm), the requirement for blue light in initiating the red light oxygen evolution was not found.

Ratchford and Fallowfield, (1992b) reported that red light cultured cells irradiated with red light had higher light enhanced dark respiration rates than either blue light irradiated or blue light cultured cells. Further results from this work on the effect of wavelength and photon flux density on light enhanced dark respiration can be found in section 3.10.1

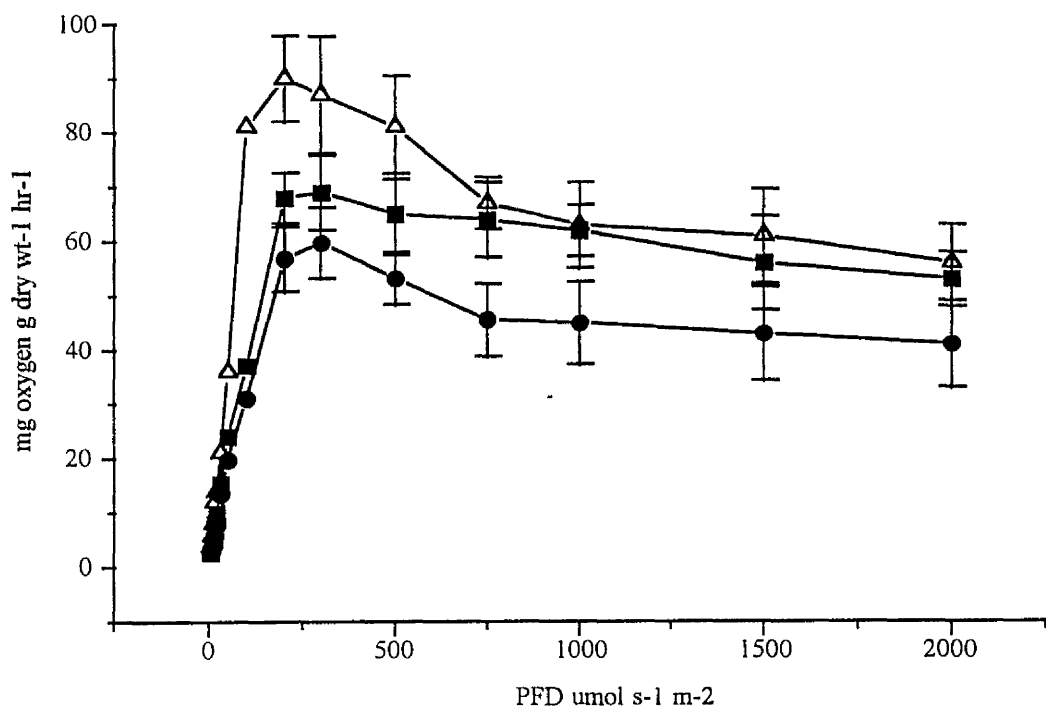


Figure 260. The effect of spectral radiant flux on the photosynthesis / irradiance response curves of *Chlorella vulgaris* 211/11c cultured white light (300-800nm), Δ — Δ full spectrum light (300-800nm), \bullet — \bullet blue light (375-550nm), \blacksquare — \blacksquare red light (600-800nm).

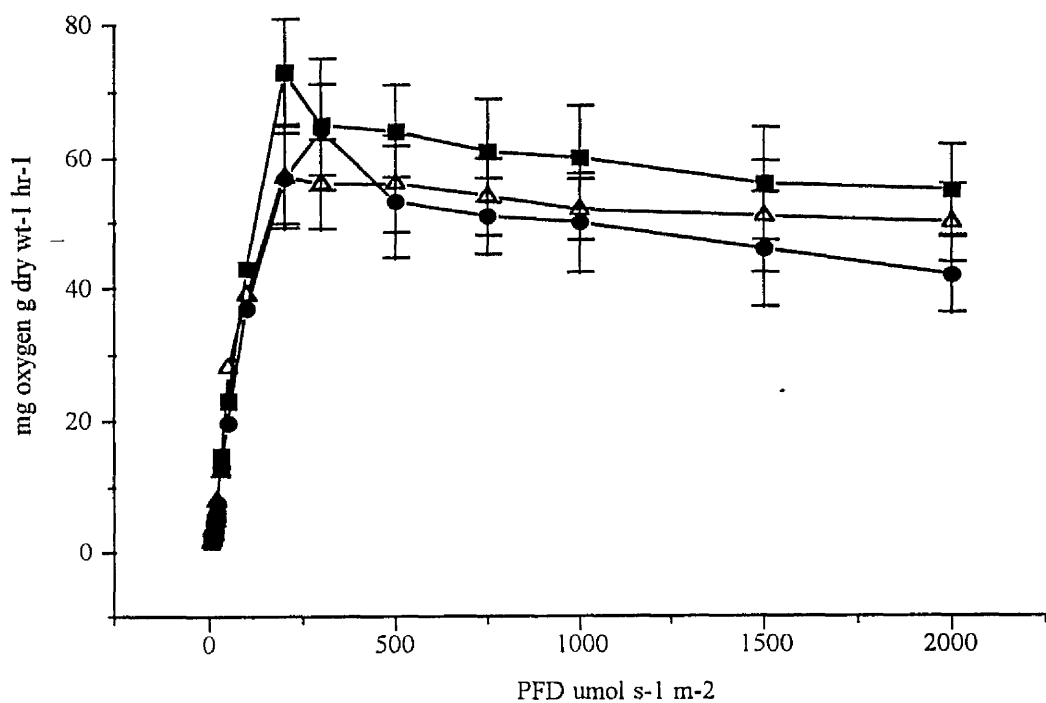


Figure 261. The effect of spectral radiant flux on the photosynthesis / irradiance response curves of *Chlorella vulgaris* 211/11c cultured in white (300-800nm) light, Δ — Δ orange light (575-800nm), \bullet — \bullet chrome orange light (500-800nm), \blacksquare — \blacksquare yellow light (475-800nm).

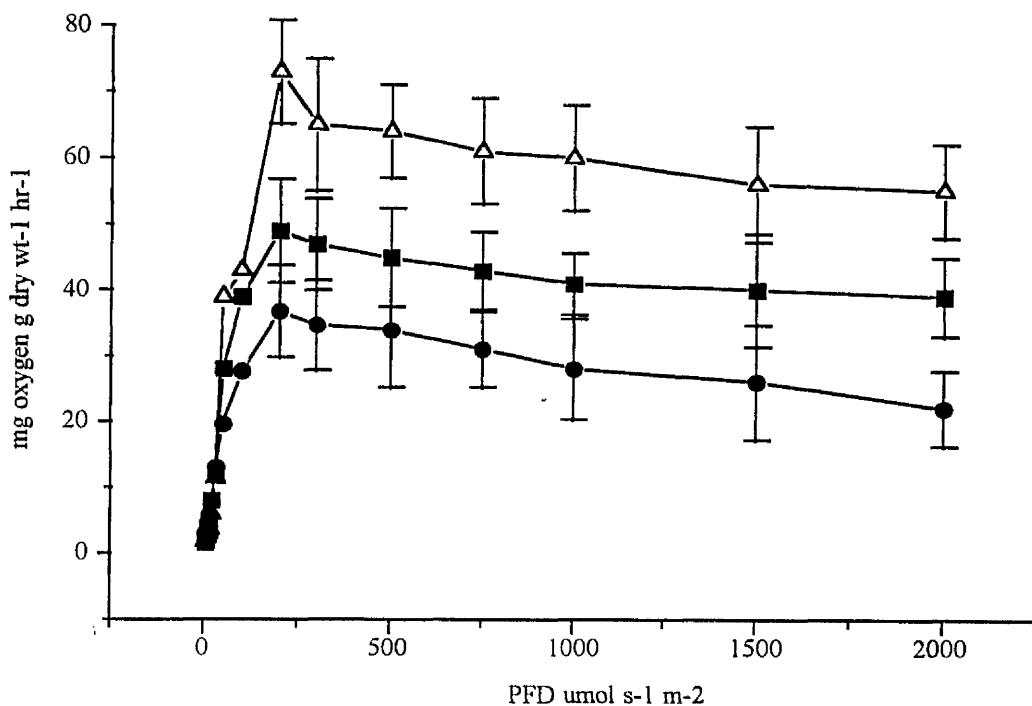


Figure 262. The effect of spectral radiant flux on the photosynthesis / irradiance response curves of *Scenedesmus sp.* cultured in white (300-800nm) light, Δ — Δ full spectrum light (300-800nm), \bullet — \bullet blue light (375-550nm), \blacksquare — \blacksquare red light (600-800nm).

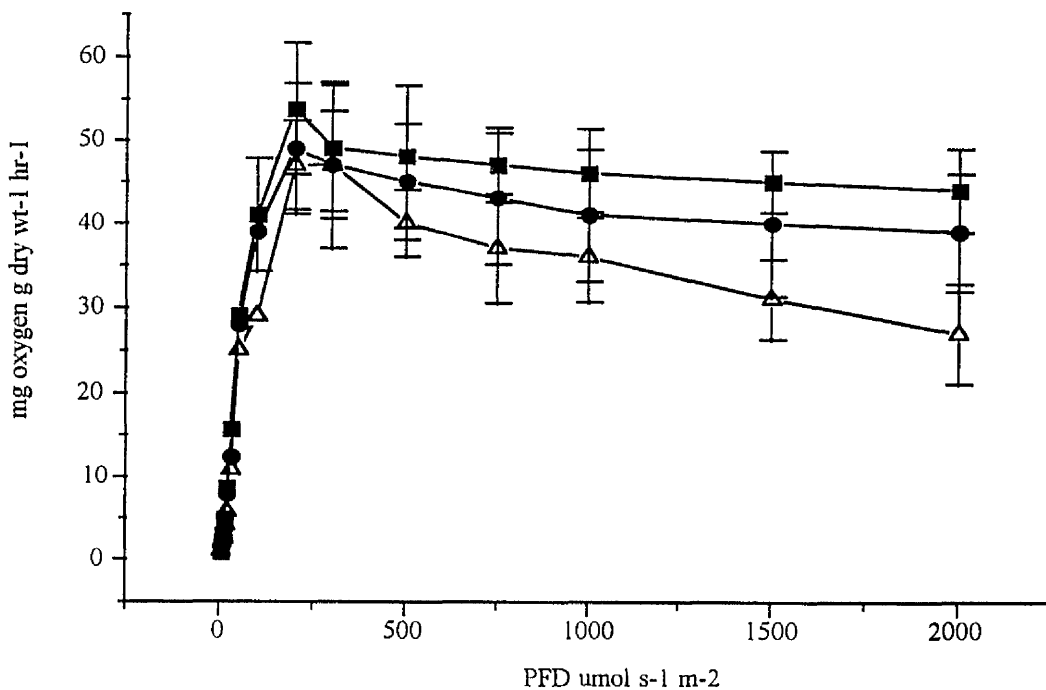


Figure 263. The effect of spectral radiant flux on the photosynthesis / irradiance response curves of *Scenedesmus sp.* cultured in white (300-800nm) light, Δ — Δ orange light (575-800nm), \bullet — \bullet chrome orange light (500-800nm), \blacksquare — \blacksquare yellow light (475-800nm).

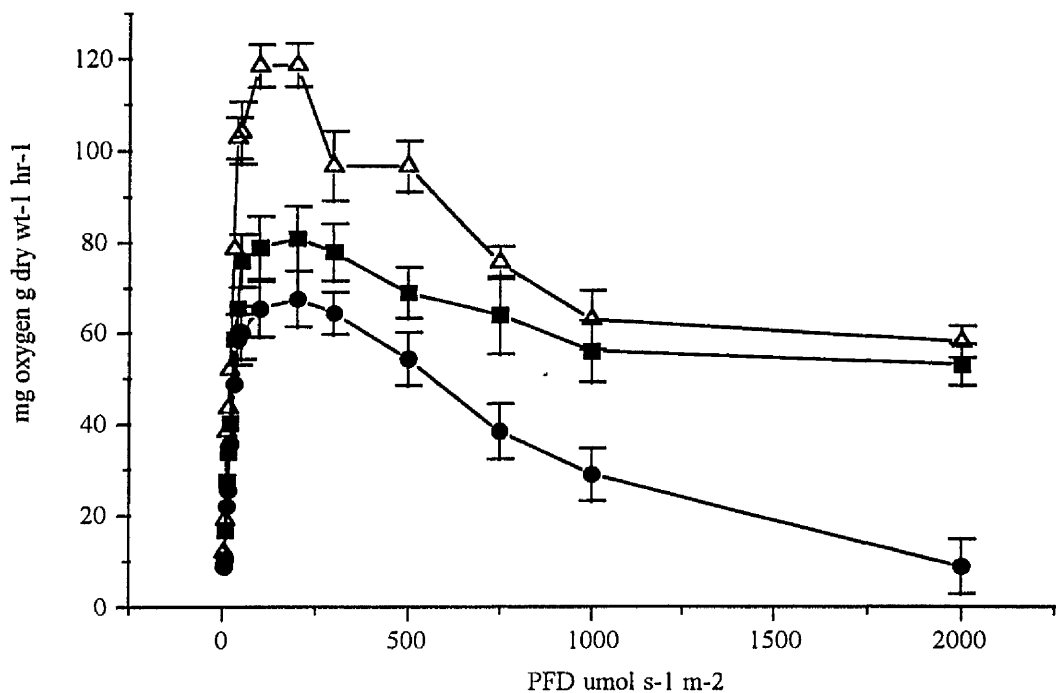


Figure 264. The effect of spectral radiant flux on the photosynthesis / irradiance response curves of *Synechococcus sp.* cultured in white (300-800nm) light, Δ — Δ full spectrum light (300-800nm), \bullet — \bullet blue light (375-550nm), \blacksquare — \blacksquare red light (600-800nm).

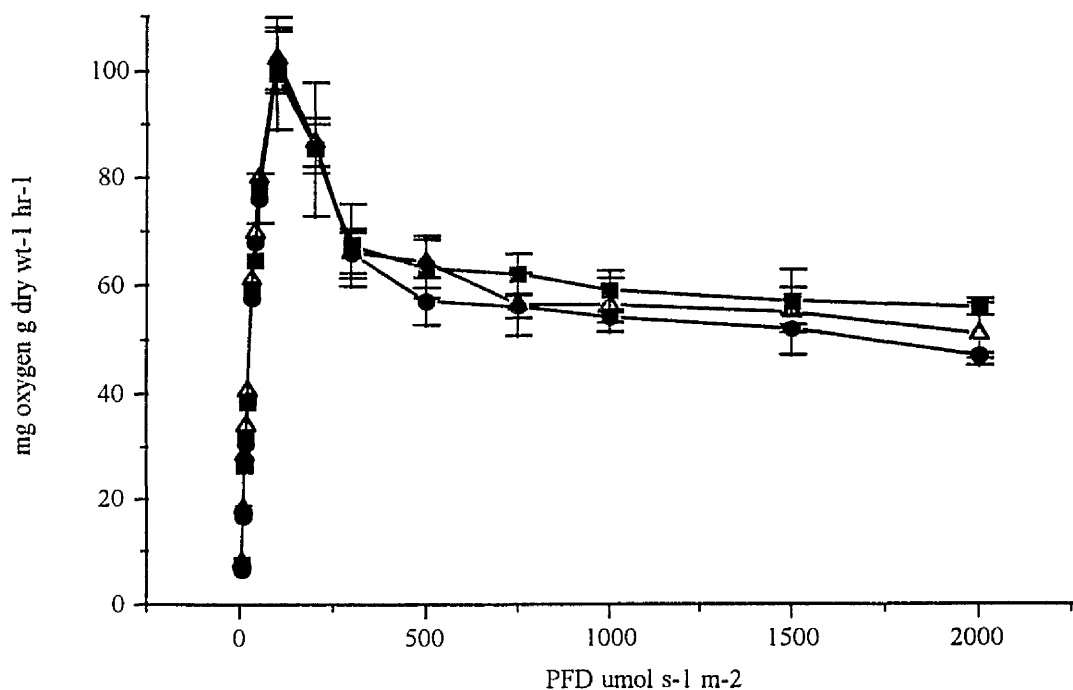


Figure 265. The effect of spectral radiant flux on the photosynthesis / irradiance response curves of *Synechococcus sp.* cultured in white (300-800nm) light, Δ — Δ orange light (575-800nm), \bullet — \bullet chrome orange light (500-800nm), \blacksquare — \blacksquare yellow light (475-800nm).

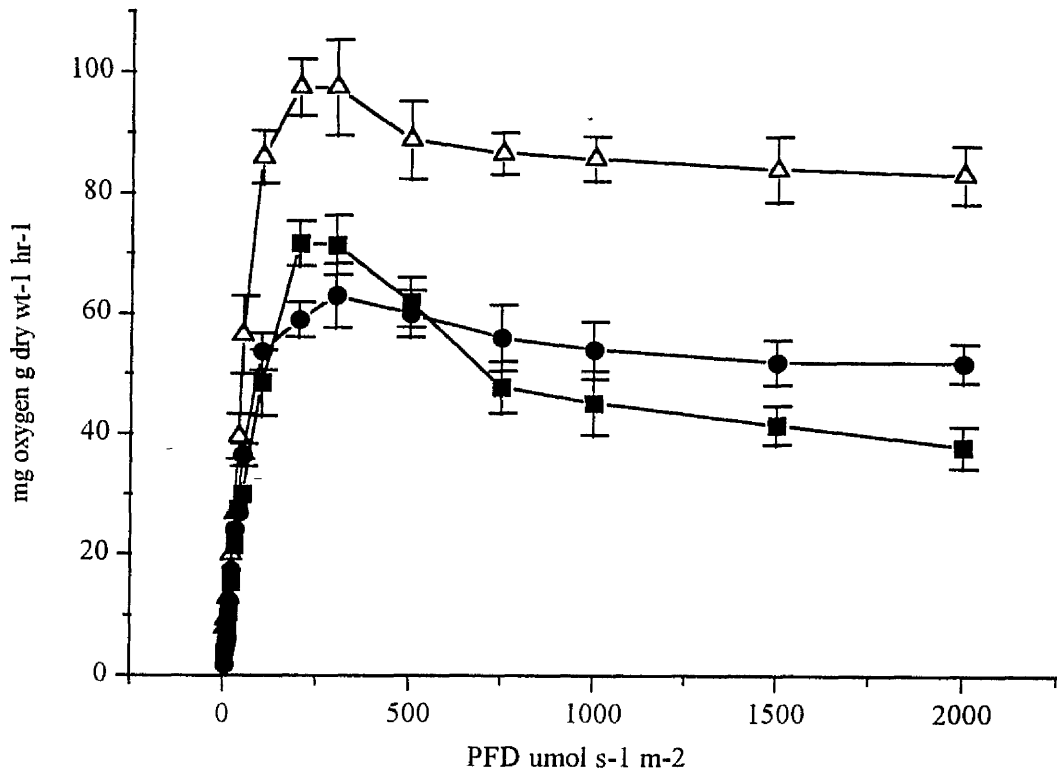


Figure 266. The effect of spectral radiant flux on the photosynthesis / irradiance response curves of *Synechococcus* 1479/5 cultured in white (300-800nm) light, Δ — Δ full spectrum light (300-800nm), \bullet — \bullet blue light (375-550nm), \blacksquare — \blacksquare red light (600-800nm).

It has been reported that the wavelength of light can affect the products of photosynthesis. Early reports on the leaves of sunflowers and tobacco plants indicated that growth in red light resulted in an accumulation of carbohydrates (Voskresenskaya, 1952). However work carried out on *Chlorella* (Cayle and Emerson, 1957) has shown that although the carbon influx rates at wavelengths λ 436nm and λ 644nm were the same, the intermediary products were found to be different. Irradiating the cells of *Chlorella* with a 30 second exposure to blue light, they found that ^{14}C was incorporated into amino acids, glycine, serine and alanine. However when the same cells were irradiated with red light, the levels of ^{14}C found in those amino acids was much lower. Since then blue light has been observed to have links with the formation of aspartic acid, malic acid and glutamic acid (Hauschild *et al.*, 1962). Kowallik and Schätzle, (1980) provided further evidence of the role of blue light in photosynthesis. Using wild-type and mutant cells of *Chlorella* 211/8b they found that in DCMU poisoned cells, the rate of carbohydrate degradation was approximately 1.3 times higher when irradiated with blue light. The stimulation of carbohydrate degradation by blue light is almost certainly linked to the enhancement of respiration by light of the same wavelength. Sargent and Taylor, (1975) suggest that although previous studies indicated that blue light increased the concentration of respiratory substrates, the non operational process of the pentose phosphate pathway, there was no way to direct carbon flux through to glycolysis. They suggested that blue light stimulated RNA synthesis followed by protein translation in the chloroplast, leading to an increase in protein concentration.

The spectral quality of a light source used for the mass culturing of unicellular algae has been shown to affect subsequent growth rates and stationary phase biomass levels in *Chlorella vulgaris* 211/11c and *Scenedesmus acutus* 276/6a (Ratchford and Fallowfield, 1991). It was found that cells of *Chlorella vulgaris* 211/11c had higher growth rates, chlorophyll a and b content and higher stationary phase biomass levels when irradiated with a high pressure sodium lamp compared to quartz-halogen lamps at the same photon flux density (Section 3.2.1). The spectral radiant flux of quartz-halogen lamps has low emissions in the blue energy region of the spectrum. Blue light is known to play a role in the incorporation of carbon into specific amino acids. Ogasawara and Miyachi, (1970), observed that the carbon in $^{14}\text{CO}_2$ was primarily incorporated into aspartic acid, glutamic acid and malic acid when cells of *Chlorella ellipsoidea* were irradiated with blue light (453nm), whereas, ^{14}C was found in P-

esters, free sugars and insoluble material when cells were irradiated with red light (679nm). This ability of micro-algae to change the metabolic pathway of inorganic carbon when irradiated with light of different wavelengths has implications on the prediction of primary productivity from phytoplankton in large deep water bodies, as the wavelength of penetrating light changes rapidly with increasing depth.

Growth of micro-algal or cyanobacterial cells in light of different wavelengths is primarily dependant on the absorption coefficient of the absorbing pigment. In most photosynthetic organisms containing phycobilisomes, virtually all of the chlorophyll a absorption is performed in the lower half of the visible spectrum which is associated with the light harvesting antenna of photosystem I (Ley and Butler, 1980; Myers *et al.*, 1980). These green absorbing phycobiliproteins lie in the 500-600nm wavelength band but appear to be associated with photosystem II (Wang *et al.*, 1977; Clement *et al.*, 1985). The cyanobacterium *Spirulina* contains lipid soluble photo pigments called the carotenes and xanthophylls. which absorb light energy in the 300-500nm range. However carotenoids can serve a dual function in protecting the chlorophyll a molecules from photooxidation and under low light environments, absorb light energy (inside and outside those wavelengths absorbed by chlorophyll a) and transfer it to the chlorophyll a molecules (Siefermann-Harms, 1980).

3.10 Effect of spectral radiant flux on the light enhanced dark respiration of micro-algae and cyanobacteria.

Whilst recording the changes in the photosynthetic kinetics of both micro-algae and cyanobacteria in Section 3.9.2, it was decided to investigate the effect of spectral radiant flux on the respiration and light enhanced dark respiration rate. Using cell samples of *Chlorella vulgaris* 211/11c, *Scenedesmus sp.* and *Synechococcus* 1479/5 cultured in blue (350-550nm) light, red (600-800nm) and full spectrum (300-800nm) light obtained from those cultures used in Section 3.9, experiments were performed to investigate the effect of P/I spectral radiant flux light (blue-350-550nm; red-600-800nm and full spectrum 300-800nm light) on light enhanced dark respiration rates. Unless otherwise stated all light enhanced dark respiration rates were measured after a photosynthesis / irradiance curve had been measured.

3.10.1 The effect of spectral radiant flux on the light enhanced dark respiration of *Chlorella vulgaris* 211/11c, *Scenedesmus sp.* and *Synechococcus* 1479/5.

Figure 247 (Section 3.9.2) shows the photosynthesis / irradiance response curves of *Chlorella vulgaris* 211/11c which had been cultured in blue light. It can be seen that although the cells had been cultured in blue light, increased photosynthetic rates were measured when the cells were P/I irradiated with full spectrum light compared to either blue or red spectrum light. Blue light photosynthetic rates were, however, higher than red light photosynthetic rates. Table 105 shows the initial respiration rates measured before the P/I measurement at time=0 minutes, light enhanced dark respiration rates LEDR₁₀ measured at time=10minutes and LEDR₆₀ measured at time=60minutes, the total time required for the LEDR rate to return to the original dark respiration rate and the LEDR : DR ratio of *Chlorella vulgaris* 211/11c cultured in blue light.. It can be seen that the maximum LEDR : DR ratio of 2.68 was measured from blue light cultured cell that were P/I irradiated with red light. The recovery time for LEDR to return to the original dark respiration rate was also higher with red light at 2 hours and 54 minutes from cells that had been P/I irradiated. The photosynthesis / irradiance response curves of *Chlorella vulgaris* cultured in red (600-800nm) are shown in Figure 245 (section 3.9.2). As was observed in Figure 247,

Table 105. The effect of spectral radiant flux on the light enhanced dark respiration of cells of *Chlorella vulgaris* 211/11c cultured in blue (350-550nm) light.

Photosynthesis / irradiance system	P/I wavelength blue (350-550nm)	P/I wavelength red (600-800nm)	P/I wavelength full (300-800nm)
Initial dark respiration (mg oxygen g dry wt ⁻¹ hr ⁻¹)	16.78	17.44	16.89
LEDR ₁₀ (min) (mg oxygen g dry wt ⁻¹ hr ⁻¹)	25.55±5.1	46.78±7.6	28.76±3.2
LEDR ₆₀ (min) (mg oxygen g dry wt ⁻¹ hr ⁻¹)	20.22±3.22	37.11±2.1	23.12±1.88
Recovery time (hours, mins)	2,05min	2,54min	2,13min
LEDR / DR ratio	1.52	2.68	1.7

Table 106. The effect of spectral radiant flux on the light enhanced dark respiration of cells of *Chlorella vulgaris* 211/11c cultured in red (600-800nm) light.

Photosynthesis / irradiance system	P/I wavelength blue (350-550nm)	P/I wavelength red (600-800nm)	P/I wavelength full (300-800nm)
Initial dark respiration (mg oxygen g dry wt ⁻¹ hr ⁻¹)	12.45	15.34	16.53
LEDR ₁₀ (min) (mg oxygen g dry wt ⁻¹ hr ⁻¹)	37.22±3.24	67.33±6.76	48.45±3.5
LEDR ₆₀ (min) (mg oxygen g dry wt ⁻¹ hr ⁻¹)	27.12±2.9	48.23±4.66	31.33±4.2
Recovery time (hours, mins)	3,15min	3,51min	2,57min
LEDR / DR ratio	2.98	4.38	2.93

cells of *Chlorella vulgaris* 211/11c had higher photosynthetic rates when P/I irradiated with full spectrum light as opposed to blue or red spectrum light. Again, though, blue light photosynthetic rates were higher than red light rates even though the cells had been cultured in red spectrum light. Table 106 shows the respiration and light enhanced dark respiration rates and the changes associated with different photosynthesis / irradiance wavelengths. It can be seen that the red light P/I irradiated cells had a higher LEDR₁₀ rate of 67.33 mg oxygen g dry wt⁻¹ hr⁻¹ compared to 37 and 45 mg oxygen g dry wt⁻¹ hr⁻¹ for blue and full spectrum light. Red light P/I irradiated cells also require a greater recovery time approaching 4 hours and had a higher LEDR : DR ratio of 4.38.

Figure 251 (Section 3.9.2) shows the photosynthetic / irradiance curves of *Scenedesmus sp.* cultured in blue light. It can be seen that photosynthetic rates were higher in cells irradiated with blue light than similar cells irradiated with red light of the same PFD. Cells irradiated with full spectrum light were found to evolve the highest oxygen production rates. The subsequent effect on LEDR rates after being irradiated with red and blue and full spectrum light of high photon flux density is presented in Table 107. The LEDR₁₀ for blue light irradiated cells was approximately 1.5 times lower than either red or full spectrum irradiated cells. Both red and full spectrum P/I irradiance cells required close to 2 hours for a full respiration recovery to be complete.

Figure 249 (Section 3.9.2) shows the photosynthetic / irradiance curves of red (600-800nm) light cultured *Scenedesmus sp.* irradiated with blue, red and full spectrum light. It can be seen that cells irradiated with a P/I light of full spectrum (300-800nm) had higher photosynthetic rates compared to red or blue light. Table 108 shows the light enhanced dark respiration rates associated with differences in P/I light wavelength. Red light P/I irradiated cells had a higher LEDR₆₀ of 41.76 mg oxygen g dry wt⁻¹ hr⁻¹ compared to 32.14 and 27.34mg oxygen g dry wt⁻¹ hr⁻¹ for blue and full spectrum light. The LEDR : DR ratio for all P/I irradiated cells were considerably higher than had been encountered previously (Table 105, 106 and 107).

Figure 258 (Section 3.9.2) shows the photosynthesis / irradiance curves of cells of *Synechococcus* 1479/5 cultured in blue (350-550) light. The effects of red, blue and full spectrum light on the LEDR rates are presented in Table 109. From Figure 258, it

Table 107. The effect of spectral radiant flux on the light enhanced dark respiration rate of cells of *Scenedesmus sp.* cultured in blue (350-550nm) light.

Photosynthesis / irradiance system	P/I wavelength blue (350-550nm)	P/I wavelength red (600-800nm)	P/I wavelength full (300-800nm)
Initial dark respiration mg oxygen g dry wt ⁻¹ hr ⁻¹	12.45	13.49	13.06
LEDR ₁₀ (min) mg oxygen g dry wt ⁻¹ hr ⁻¹	28.44±3.22	39.44±2.1	38.55±3.9
LEDR ₆₀ (min) mg oxygen g dry wt ⁻¹ hr ⁻¹	19.77±3.2	26.34±4.3	25.33±3.1
Recovery time (hours, mins)	1,17min	1,54min	1,31min
LEDR / DR ratio	2.28	2.92	2.95

Table 108. The effect of spectral radiant flux on the light enhanced dark respiration rate of cells of *Scenedesmus sp.* cultured in red (600-800nm) light.

Photosynthesis / irradiance system	P/I wavelength blue (350-550nm)	P/I wavelength red (600-800nm)	P/I wavelength full (300-800nm)
Initial dark respiration mg oxygen g dry wt ⁻¹ hr ⁻¹	10.66	11.84	9.76
LEDR ₁₀ (min) mg oxygen g dry wt ⁻¹ hr ⁻¹	47.45±3.55	59.2±1.09	45.34±3.11
LEDR ₆₀ (min) mg oxygen g dry wt ⁻¹ hr ⁻¹	32.14±2.84	41.76±3.87	27.34±5.2
Recovery time (hours, mins)	2,30min	2,58min	2,13min
LEDR / DR ratio	4.45	5	4.65

can be seen that *Synechococcus* 1479/5 had higher photosynthetic rates when irradiated with blue light as opposed to red light of the same PFD, however, as was found consistently throughout this research, cells irradiated with a P/I of full spectrum light produced the greatest photosynthetic rates. From Table 109 it can be seen that the red light P/I irradiated cells had the highest LEDR₁₀ of 39.64mg oxygen g dry wt⁻¹ hr⁻¹ compared to 25.66 and 30.13mg oxygen g dry wt⁻¹ hr⁻¹ for blue and full spectrum light. The recovery time for red light irradiated cells was also the highest at 2 hour and 38 minutes. The LEDR : DR ratio for all P/I irradiated cultures were between 2 and 3.

Figure 257 shows the photosynthesis / irradiance curves of *Synechococcus* 1479/5 cultured in red (600-800nm) light. From Figure 257 it can be seen that the photosynthetic rates of cells were fairly similar when irradiated with blue or full spectrum light. As was found with *Scenedesmus sp.* and *Chlorella vulgaris* 211/11c, the cells of *Synechococcus* 1479/5 had much lower photosynthetic rates when irradiated with red light. The effects of red, blue and full spectrum light on the LEDR rates are presented in Table 110. The highest LEDR₁₀ rate (67.88 mg oxygen g dry wt⁻¹ hr⁻¹) was measured when cells of *Synechococcus* 1479/5 were irradiated with red spectrum light. The maximum recovery time of 3 hours and 5 minutes for the LEDR rate to return to the initial dark respiration rate occurred when the cells were irradiated with red spectrum light.

Light enhanced dark respiration (LEDR) or enhanced post illumination respiration (EPIR) are the terms given to increased oxygen uptake by micro-algal, cyanobacterial or plant cells. Early observations, however, considered increased oxygen uptake after exposure to light to be that of photorespiration. Photorespiration is the oxygen sensitive loss of carbon dioxide during photosynthesis (Brendan *et al.*, 1982). Although algae are C₃ plants the controversy concerning whether micro-algae exhibit photorespiration still exists. The process of LEDR is believed to be associated with oxidative phosphorylation coupled to a mitochondrial electron transport chain to cytochrome oxidase. This mechanism is supported by observations made by Falkowski *et al.*, (1985) who found a 92% inhibition of LEDR with 100µM CN⁻ in cells of *Thalassiosira weissflogii*. Other oxygen consuming processes have

Table 109. The effect of spectral radiant flux on the light enhanced dark respiration of cells of *Synechococcus* 1479/5 cultured in blue (350-550nm) light.

Photosynthesis / irradiance system	P/I wavelength blue (350-550nm)	P/I wavelength red (600-800nm)	P/I wavelength full (300-800nm)
Initial dark respiration mg oxygen g dry wt ⁻¹ hr ⁻¹	10.75	13.66	13.39
LEDR ₁₀ (min) mg oxygen g dry wt ⁻¹ hr ⁻¹	25.66±3.4	39.64±3.1	30.13±2.1
LEDR ₆₀ (min) mg oxygen g dry wt ⁻¹ hr ⁻¹	15.23±1.9	24.88±4.2	20.13±2.9
Recovery time (hours, mins)	1,45min	2,38min	1,28min
LEDR / DR ratio	2.38	2.90	2.21

Table 110. The effect of spectral radiant flux on the light enhanced dark respiration of cells of *Synechococcus* 1479/5 cultured in red (600-800nm) light.

Photosynthesis / irradiance system	P/I wavelength blue (350-550nm)	P/I wavelength red (600-800nm)	P/I wavelength full (300-800nm)
Initial dark respiration mg oxygen g dry wt ⁻¹ hr ⁻¹	12.44±1.9	13.89±1.6	10.90±3.1
LEDR ₁₀ (min) mg oxygen g dry wt ⁻¹ hr ⁻¹	43.14±3.2	67.88±4.2	49.79±2.9
LEDR ₆₀ (min) mg oxygen g dry wt ⁻¹ hr ⁻¹	27.70±2.8	46.8±3.1	32.14±3.9
Recovery time (hours, mins)	2,34min	3,05min	2,44min
LEDR / DR ratio	3.46	4.88	4.56

been suggested as the cause of LEDR. These include the Mehler reaction, in which oxygen acts as a terminal electron acceptor. Experiments performed by Mehler, (1951), however, suggest that the uptake rate of oxygen consumption in LEDR is much higher (10 times) than that which could be attributed to the Mehler reaction. It has been demonstrated that photorespiration can be suppressed in micro-algae by a carbon concentrating mechanism. This process is known to occur in a range of micro-algae and cyanobacteria including *Chlamydomonas reinhardtii* and *Anabaena variabilis* (Kaplan *et al.*, 1980). The cells actively uptake inorganic carbon in the form of HCO_3^- which as a result of carbon equilibrium means the levels of the carbon dioxide present within the cell are much higher than those acquired by cells passively uptaking carbon dioxide across the plasmalemma. At these elevated ratios of carbon dioxide to oxygen the enzyme system of Rubisco is consequently shut off and hence without this activity photorespiration cannot proceed. The process of light enhanced dark respiration has also been found to occur in some types of plant cells. Using mesophyll protoplasts from leaves of pea, Reddy *et al.*, (1991) found that respiratory oxygen uptake was stimulated 3 fold after 15 minutes at an illumination of $1250 \mu\text{mol s}^{-1} \text{m}^{-2}$ in the presence of 5mM HCO_3^- . It was commented that the mechanism of LEDR is not correlated to the availability of increased respiratory substrate since the sharp increase in respiration within a few minutes of illumination suggests that the early products of photosynthesis may somehow be linked.

Although it has been found that photorespiration can occur in *Chlamydomonas reinhardtii* (Kaplan *et al.*, 1980), Peltier and Thibault, (1985) demonstrated that cells of *Chlamydomonas reinhardtii* which have their glycolate pathway completely inhibited, have the same rate of oxygen uptake in the light and dark and was not inhibited by increased levels of ATP. This observation of similar oxygen uptake rates for *Chlamydomonas reinhardtii* in the light and dark has also been made by (Sueltemeyer *et al.*, 1986). Radmer and Ollinger, (1980), however, observed that the oxygen uptake rate in *Scenedesmus acutus* increased sharply with increasing PFD and suggested that the increase in respiration was due to strong reductants generated by photosystem I leading to a reduction in oxygen by photosystem II. The reports which have recorded the phenomenon of light enhanced dark respiration clearly displays that the process is species dependant. All of the work carried out in this thesis and in similar papers display that the process of LEDR takes place in eukaryotic green micro-algae (Bidwell, 1976; Falkowski *et al.*, 1985; Peltier and Thibault, 1985;),

cyanobacteria (Glidewell and Raven, 1975; Stone and Ganf, 1981; Ratchford and Fallowfield, 1992b) and higher plants (Heichel, 1972; Reddy *et al.*, 1991).

From Tables 106, 108 and 110, it is shown that micro-algal and cyanobacterial cells cultured in red light displayed higher light enhanced dark respiration rates when irradiated with red, blue and full spectrum light than similar cells cultured in blue light. It is well established that high light intensities effect photosystem II to a greater degree than photosystem I. This susceptibility to high intensities is dependent on the duration, PFD and the spectral quality of the light source. It has also been shown (Kyle, 1987) that photosystem II has a repair protein which can reverse the effects of photoinhibition. It has been found that culturing cells of the red alga *Porphyridium cruentum* enhanced the formation of photosystem II (Cunningham *et al.*, 1990).

Whilst growing in red light, cells of *Porphyridium* had 5 times as many photosystem II units per photosystem I. Approximately 39% of chlorophyll in red light cultures was attributed to photosystem II. Since cells of *Chlorella vulgaris* 211/11c, *Scenedesmus sp.* and *Synechococcus* 1479/5 were cultured in red light for 3 successful flask generations, the cells may have had a higher level of photosystem II present. It is suggested that this could explain why the generally cells of each organism irradiated with red light had higher light enhanced dark respiration rates. A second reason for the greater light enhanced dark respiration rates observed in cells irradiated by red light as opposed to full or blue spectrum light, may be due to enzyme activity.

Aparicio and Quinones, (1991) found that light at the lower end of the blue spectrum at wavelengths 450 and 480nm and at the ultra-violet wavelength of 365nm were necessary for the cells of the green alga *Monoraphidium braunii* to take up nitrate and nitrite. Blue light (450 and 480nm) in particular was considered to be responsible for 3 key steps in the process of inorganic metabolism, namely cellular uptake of inorganic nitrogen, nitrate reductase activity and the biosynthesis of nitrite reductase. The work carried out in Section 3.3.3 demonstrated that unicellular green micro-algae and cyanobacteria were more susceptible to the onset of photoinhibition when in conditions of nitrate limitation. Since photosystem II is considered to be the strongest candidate for possible photodamage during exposure to very high light intensities, uptake of inorganic nitrogen to maintain the repair and resynthesis of key photosynthetic apparatus would have been very much reduced in the presence of red light since this had already been shown to create much higher LEDR values.

3.10.2 The effect of inhibitors on the light enhanced dark respiration of *Chlorella vulgaris* 211/11c and *Scenedesmus sp.*

Three chemical agents were employed to examine the effects of light on respiration during photosynthesis. Salicylic hydroxamic acid (SHAM), 3(3,4-Dichloro-phenyl)-1,1-Dimethylurea (DCMU) and Potassium cyanide (KCN) were used in all the experiments. SHAM is an active agent inhibiting the cyclic photophosphorylation pathway (Stuart, 1970). DCMU inhibits the oxygen evolving step of photosynthesis (Bishop, 1958). KCN has an inhibitory site of action associated with the cytochrome oxidase and RuDP carboxylase (Raven, 1969; Sharpless and Burrow, 1970; Raven, 1971) and thus prevents dark respiration oxygen consumption.

In each experiment, the incubating medium was 100% ASM containing 400mg C l⁻¹, in the form of sodium bicarbonate. Photosynthesis / irradiance curves were measured using the standard method previously described in 2.8.1.

Figure 267 shows the results of incubating cells of *Scenedesmus sp.* for 30 mins with various concentrations of 3(3,4-Dichloro-phenyl)-1,1-Dimethylurea (DCMU) prior to photosynthesis / irradiance measurement. Cellular production of oxygen during photosynthesis was completely inhibited in the presence of 50µmol DCMU. With lower concentrations of DCMU < 50µmol, cells produced small quantities of oxygen but did not reach the compensation point where oxygen consumed during respiration equalled that produced by photosynthesis. The effects of DCMU on the light enhanced dark respiration rates of *Scenedesmus sp.* were also examined and the results are presented in Table 111. After the standard photosynthesis / irradiance curve had been determined (without the use of DCMU), cells were placed in the dark to measure LEDR rates. At this point DCMU was injected into the chamber at final concentrations of 1-100µmol. It can be seen that overall DCMU did have some inhibiting effect on LEDR rates (although this was not conclusive), the degree of inhibition generally increased with increasing concentration of DCMU. LEDR rates in the presence of 100µmol were significantly lower than the control experiments suggesting that DCMU had inhibited the process of light enhanced dark respiration. The effect of DCMU was monitored for a further 30

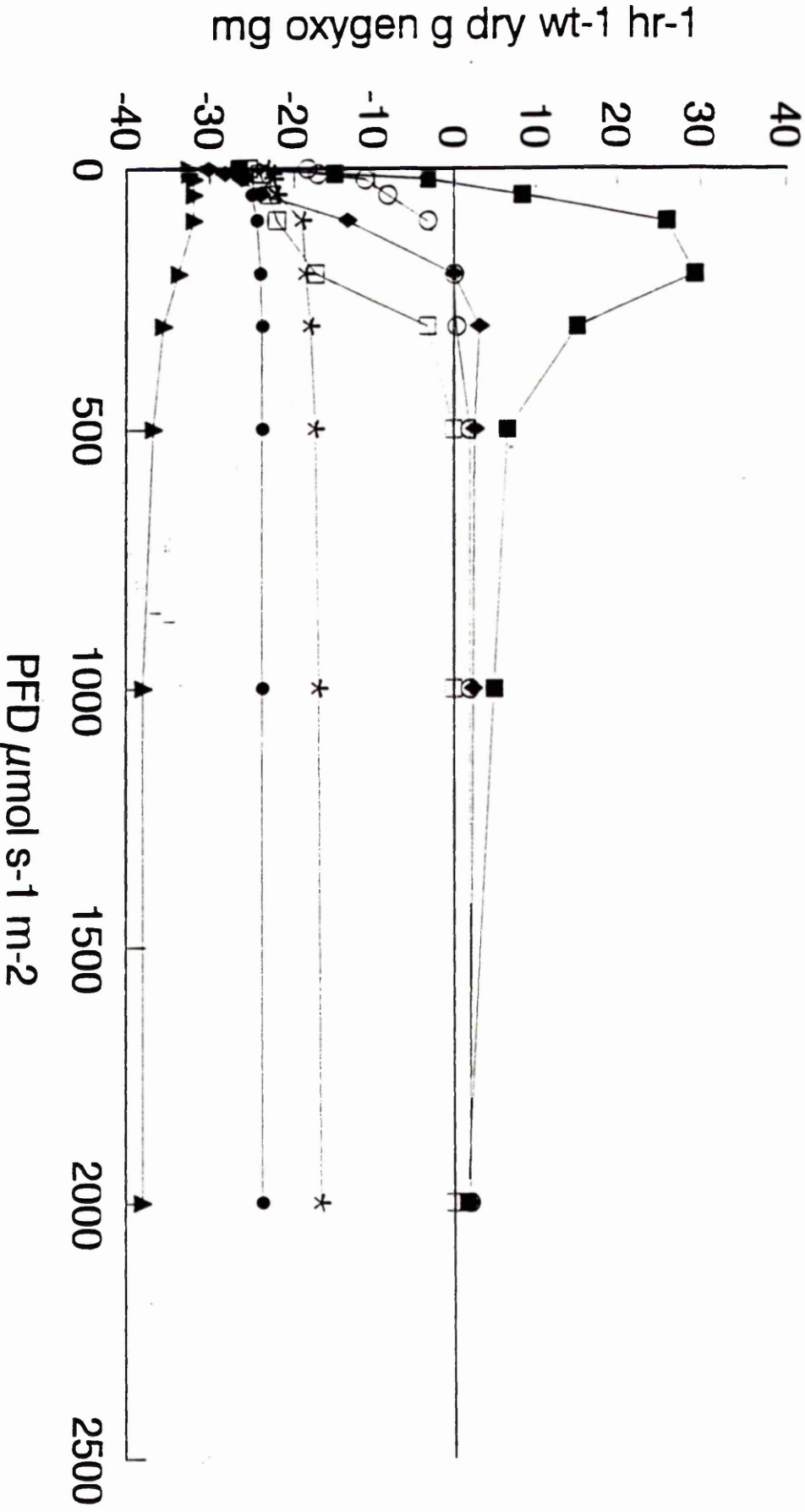


Figure 267. The effect of DCMU on the photosynthesis / irradiance response curves of *Scenedesmus sp.*, ■—■ control (no DCMU), ◆—◆ 1 μmol DCMU, ○—○ 5 μmol DCMU, □—□ 17 μmol DCMU, *—* 50 μmol DCMU, ●—● 85 μmol DCMU, ▲—▲ 100 μmol DCMU.

Table 111. The effect of DCMU concentration on the respiration of *Scenedesmus* sp.

	DCMU concentration (μmol)						
	Control	1	5	17	50	85	100
Initial dark respiration (DR) (mg oxygen g dry wt ⁻¹ hr ⁻¹)	11.74	13.33	12.12	11.21	10.24	11.65	14.39
Light enhanced dark respiration (mg oxygen g dry wt ⁻¹ hr ⁻¹)	19.86	20.39	21.89	24.81	18.54	18.80	24.10
LEDR 10 mins after DCMU injection (mg oxygen g dry wt ⁻¹ hr ⁻¹)	18.88	18.27	18.44	16.59	14.06	13.15	15.09
LEDR 30 mins after DCMU injection (mg oxygen g dry wt ⁻¹ hr ⁻¹)	15.43	14.32	15.65	13.88	13.66	12.05	14.83

Table 112. The effect of KCN concentration on the respiration of *Scenedesmus* sp.

KCN concentration	Control	10 μmol	50 μmol	100 μmol
Initial dark respiration (DR) (mg oxygen g dry wt ⁻¹ hr ⁻¹)	11.71	12.71	13.42	10.33
Light enhanced dark respiration (mg oxygen g dry wt ⁻¹ hr ⁻¹)	21.42	23.31	23.39	23.66
Light enhanced dark respiration (mg oxygen g dry wt ⁻¹ hr ⁻¹) after 10min	21.03	2.57	0.93	0.94
% inhibition	0	89	96	96

minutes (Table 111), where it was found that LEDR rates had almost decreased to the initial cellular dark respiration. Figure 268 shows the effects of KCN on the light enhanced dark respiration of cells of *Scenedesmus sp.* The schematic plot shows that injections of 50-100 $\mu\text{mol CN}^-$ results in 96% inhibition of LEDR rates after a standard photosynthesis / irradiance curve had been measured. From Table 112 it can be seen the use of cyanide at lower concentrations e.g. 10 μmol resulted in a lower inhibition of 89% the LEDR rate. Figure 269 shows the results of incubating cells of *Scenedesmus sp.* in the presence of SHAM after a photosynthesis / irradiance curve had been determined. It can be seen that the presence of SHAM in the incubating medium after introduction via injection had no effect on the LEDR rate.

Figure 270 shows the inhibition of photosynthesis of *Chlorella vulgaris* 211/11c in the presence of various concentrations of DCMU. DCMU was not found to significantly affect the rate of LEDR (Table 114). Figure 271 shows that as with *Scenedesmus sp.*, cellular respiration of *Chlorella vulgaris* 211/11c was in some way inhibited in the presence of 50-100 $\mu\text{mol CN}^-$. However unlike *Scenedesmus sp.* which showed an 89% (Table 112) decrease in the rate of LEDR in the presence of 10 $\mu\text{mol CN}^-$, cells of *Chlorella vulgaris* 211/11c showed a 68% (Table 115) decrease in the rate of LEDR. Incubation of *Chlorella vulgaris* 211/11c cells with SHAM had no effect on the LEDR rates (Figure 272). Table 116 shows the initial dark respiration values, LEDR and recovery times in the presence of the various inhibitors.

Cells of *Chlorella vulgaris* 211/11c and *Scenedesmus sp.* inhibited by 50 $\mu\text{mol KCN}^-$ were washed (3 times) and then placed in a light field of 20 $\mu\text{mol s}^{-1}\text{m}^{-2}$ in an attempt to reverse the effects of the CN^- inhibition. The results of the comparison between washed and unwashed cells are presented in Table 117 and are expressed as a percentage of the oxygen evolution produced by control cells irradiated at a PFD of 2020 $\mu\text{mol s}^{-1}\text{m}^{-2}$ which had not been exposed to cyanide. It was found that even after 6 hours in 100% ASM the washed cells of *Chlorella vulgaris* 211/11c had not recovered to 100% of their previous oxygen evolution rates determined at 20 $\mu\text{mol s}^{-1}\text{m}^{-2}$ which suggested that the cytochrome oxidase had to some degree (60%) become

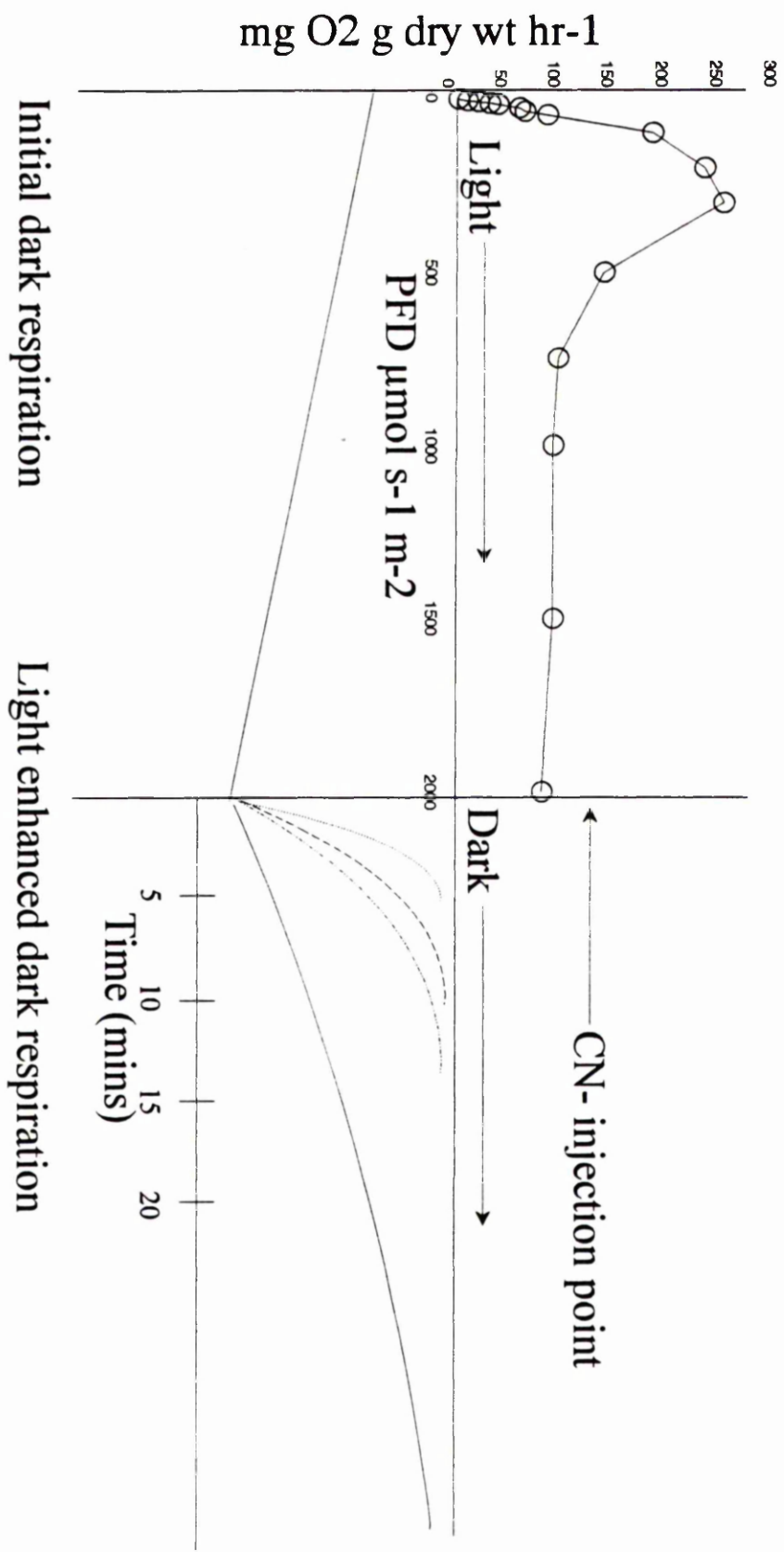


Figure 268. The effect of CN⁻ on the light enhanced dark respiration rates of *Scenedesmus*
sp., — control, ···· 100 μmol CN⁻, ---- 50 μmol CN⁻, -·-·- 10 μmol CN⁻.

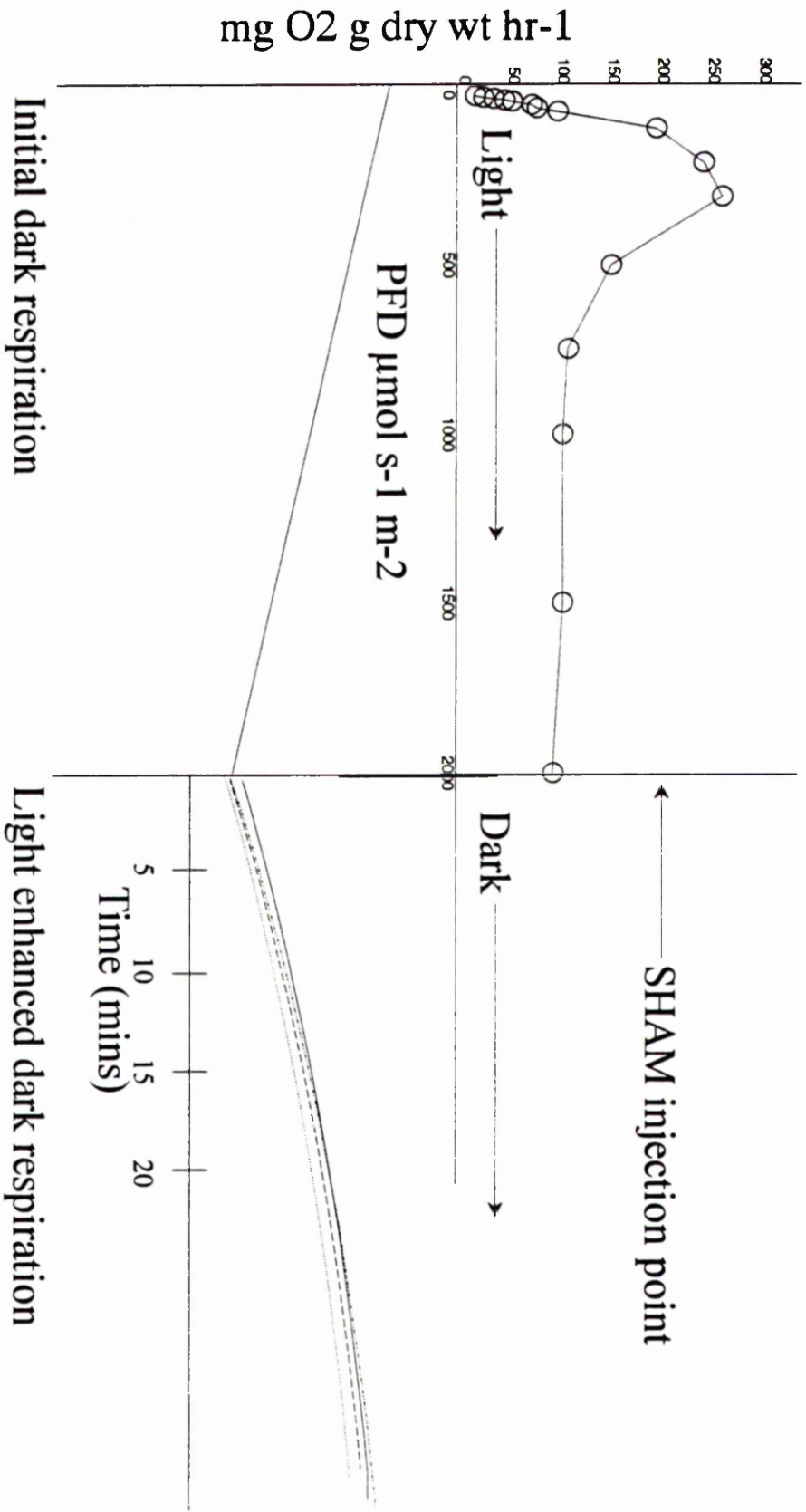


Figure 269. The effect of SHAM on the light enhanced dark respiration of *Scenedesmus* sp.,
 — control, ···· 10 μmol SHAM, ···· 50 μmol SHAM, ···· 100 μmol SHAM.

mg oxygen g dry wt-1 hr-1

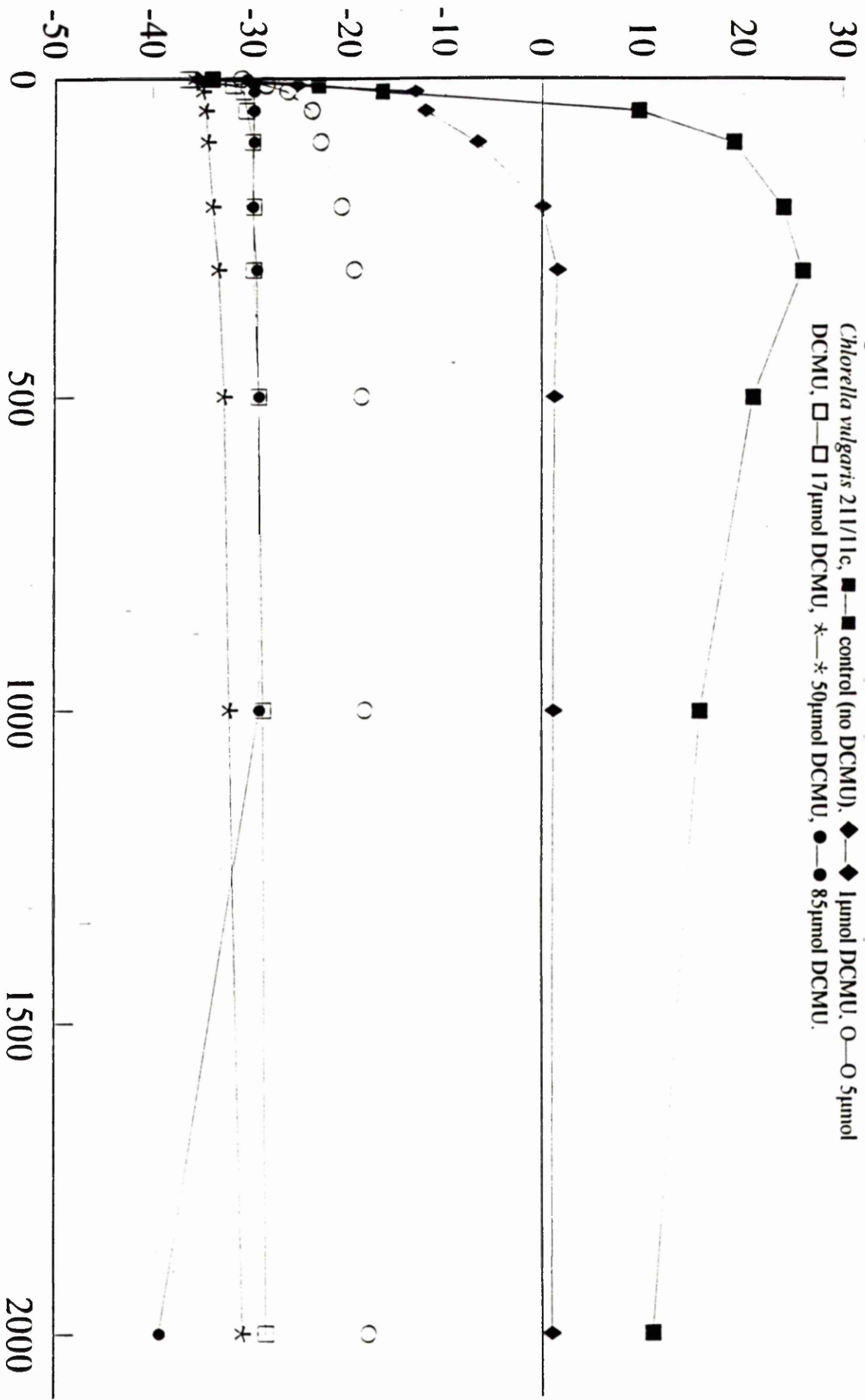


Figure 270. The effect of DCMU on the photosynthesis / irradiance response curves of *Chlorella vulgaris* 211/1c. ■—■ control (no DCMU), ◆—◆ 1μmol DCMU, ○—○ 5μmol DCMU, □—□ 17μmol DCMU, *—* 50μmol DCMU, ●—● 85μmol DCMU.

PFD μmol s-1 m-2

Table 113. The effect of SHAM concentration on the respiration of *Scenedesmus* sp.

SHAM	Control	10 μ mol	50 μ mol	100 μ mol
Initial dark respiration (DR) (mg oxygen g dry wt ⁻¹ hr ⁻¹).	10.14	9.88	11.21	8.82
Light enhanced dark respiration (mg oxygen g dry wt ⁻¹ hr ⁻¹) t=0	22.14	22.25	21.28	20.57
Light enhanced dark respiration (mg oxygen g dry wt ⁻¹ hr ⁻¹) t=10 min	20.13	19.16	20.12	18.91

Table 114. The effect of DCMU concentration on the respiration of *Chlorella vulgaris* 211/11c.

	DCMU concentration (μ mol)						
	Control	1	5	17	50	85	100
Initial dark respiration (DR) (mg oxygen g dry wt ⁻¹ hr ⁻¹)	28.75	29.93	26.31	30.86	30.19	25.88	26.73
Light enhanced dark respiration (mg oxygen g dry wt ⁻¹ hr ⁻¹) t=0	47.30	44.77	49.50	46.04	47.81	49.92	44.52
LEDR after DCMU injection(mg oxygen g dry wt ⁻¹ hr ⁻¹) t=10 mins	45.12	41.96	46.17	42.91	45.12	44.16	39.71
LEDR after DCMU injection(mg oxygen g dry wt ⁻¹ hr ⁻¹) t=30 mins	39.25	35.67	41.09	38.62	40.06	37.53	35.74

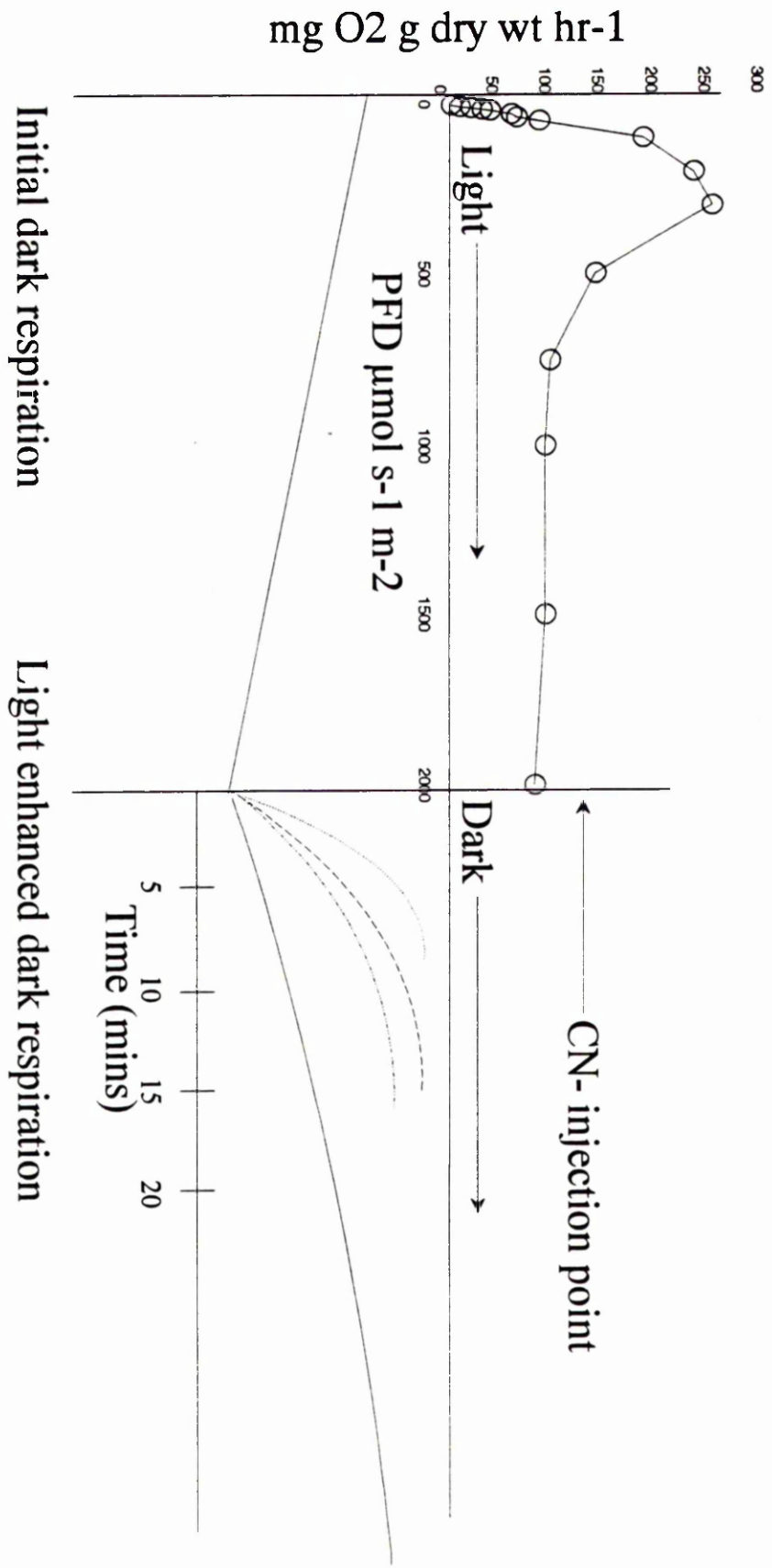


Figure 271. The effect of CN⁻ on the light enhanced dark respiration rates of *Chlorella vulgaris* 211/11c, — control, 100 μmol CN⁻, ---- 50 μmol CN⁻, -.-.- 10 μmol CN⁻.

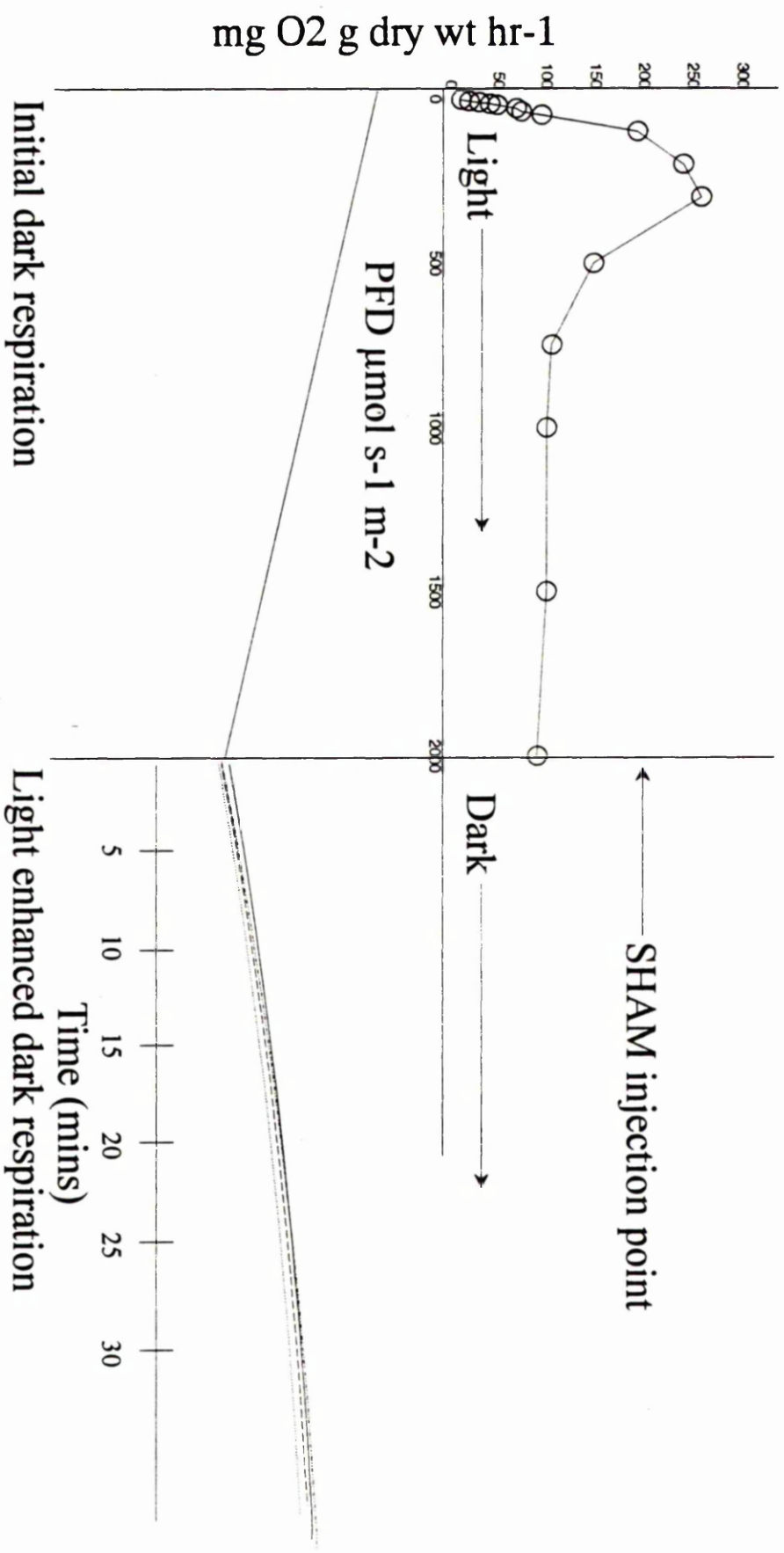


Figure 272. The effect of SHAM on the light enhanced dark respiration of *Chlorella vulgaris* 211/11c, — control, ····· 100 μmol SHAM, ····· 50 μmol SHAM, ····· 10 μmol SHAM.

irreversibly bound by the cyanide. Further attempts at revival including increasing the number of washes in 100mM sodium nitrate + 100% ASM had no effect on reversibility. *Scenedesmus sp.*, however, showed a higher recovery from the affects of cyanide with an 87% return to the control measurements prior to the addition of the cyanide. The non recoverability of the enzyme system of *Chlorella vulgaris* 211/11c and *Scenedesmus sp.* suggest that the oxidase systems of light enhanced dark respiration in micro-algae and cyanobacteria are very different

The observations made during incubation experiments of *Chlorella vulgaris* 211/11c and *Scenedesmus sp.* with SHAM and CN⁻ (Tables 112, 113, 115 and 116) are in agreement with Falkowski *et al.*, (1985) who found a 92% inhibition of enhanced post illumination respiration (EPIR) in the marine algae *Isochrysis galbana* when incubated in the presence of 100µmol CN⁻. They also reported that SHAM had no effect on EPIR but he could not account for the other 8% of EPIR. Experiments carried out by Sargent and Taylor, (1972), however, indicated the possibility of two oxidase enzymes in *Chlorella pyrenoidosa*. Their results suggested that the normal respiratory oxygen uptake is carried out mainly by cytochrome oxidase (65%) and that a second enzyme (possibly a cyanide resistant oxidase) accounted for the other 45% of respiration. The results in table 115 suggest that cells of *Chlorella vulgaris* 211/11c may be showing some elements of a double or multiple enzyme system as the cells are not 100% inhibited by 100µm cyanide. This is also supported by the observation that the reaction involving cells of *Chlorella vulgaris* 211/11c and cyanide was not 100% reversible. Since the cells did display some degree of reversibility, it is suggested that two or more enzymes are involved in the process of LEDR in *Chlorella vulgaris* 211/11c, one of which is reversibly bound by cyanide and the other that is irreversibly bound. With both *Scenedesmus sp.* and *Chlorella vulgaris* 211/11c it was found that low concentrations of DCMU <10µmol resulted in a decrease in the LEDR rate. Inhibition of oxygen uptake in the dark has also been reported by Glidewell and Raven, (1975) who found a 100% inhibition in oxygen uptake while incubating *Hydrodictyon africanum* in the presence of DCMU.

Inhibition of LEDR by DCMU has also been observed in mesophyl protoplasts from leaves of pea (Reddy *et al.*, 1991), however, Peltier and Thibault, (1985) reported that DCMU had no effect on the LEDR rate of *Chlamydomonas*.

Table 115. The effect of KCN on the respiration of *Chlorella vulgaris* 211/11c.

KCN	Control	10 μ mol	50 μ mol	100 μ mol
Initial dark respiration (DR) (mg oxygen g dry wt ⁻¹ hr ⁻¹).	28.75	29.00	25.21	26.73
Light enhanced dark respiration (mg oxygen g dry wt ⁻¹ hr ⁻¹) t=0	47.30	29.41	47.73	44.02
Light enhanced dark respiration (mg oxygen g dry wt ⁻¹ hr ⁻¹) t=10	43.77	15.81	7.63	4.84
% inhibition	0.0	68	84	89

Table 116. The effect of SHAM concentration on the respiration of *Chlorella vulgaris* 211/11c.

SHAM	Control	10 μ mol	50 μ mol	100 μ mol
Initial dark respiration (DR) (mg oxygen g dry wt ⁻¹ hr ⁻¹)	28.71	28.76	27.49	28.08
Light enhanced dark respiration (mg oxygen g dry wt ⁻¹ hr ⁻¹)	46.92	47.46	49.58	49.41
Light enhanced dark respiration (mg oxygen g dry wt ⁻¹ hr ⁻¹)	44.62	43.18	44.69	43.90
Recovery time LEDR=DR (mins)	60	54	65	60

Table 117. Reversibility of cyanide oxidase enzyme complex in *Scenedesmus sp.* and *Chlorella vulgaris* 211/11c.

Time (hours)	<i>Scenedesmus sp.</i> % recovery *		<i>Chlorella vulgaris</i> 211/11c % recovery *	
	Unwashed	Washed 3 times (ASM)	Unwashed	Washed (ASM)
0	4	14	3	11
1	6	21	7	16
3	13	44	10	29
5	17	81	13	35
6	24	87	18	40

Recovery assayed on oxygen evolution ($\text{mg oxygen g dry wt}^{-1} \text{ hr}^{-1}$) placed in a light field of $20 \mu\text{mol s}^{-1} \text{ m}^{-2}$ compared to control sample irradiated at same PFD.

There is still a great deal of uncertainty as to the exact number of oxidase systems involved in photosynthetic organisms and to the nature of binding the cyanide molecule. The results in Table 115 show some agreement with Syrett, (1951), in that the oxidase insensitive cells of *Chlorella vulgaris* 211/11c make up 40-50% of the total respiratory oxygen uptake. Glidewell and Raven, (1975) found that although oxygen uptake in the dark was inhibited by the action of 1mol KCN, light dependant oxygen consumption remained unaffected in *Hydrodictyon africanum*. It is possible that the process of LEDR is species dependent and may involve different configuration of enzymes linked to the mitochondria

When cells are irradiated with light of high PFD (greater than P_{max} or original growth irradiance) the rates of photosynthesis are increased and metabolites and respiratory substrates begin to build up in the cell. These compounds are subsequently removed via the TCA cycle resulting in an increased flux of electrons through the mitochondria (Beardall and Raven, 1989). Eukaryotic respiration in micro-algae is generally a combination of glycolysis, TCA cycle (Beardall and Raven, 1989; Weger and Turpin, 1989) and the oxidative pentose phosphate pathway (OPP). Other oxygen requiring processes include the oxidative phosphorylation (linked to the TCA cycle), the Mehler reaction and the newly termed 'chlororespiration' (Beardall and Raven, 1989). The basic outline to respiration is summed up in Figure 12. Most of these electron transport reactions are associated with the thylakoid membrane of the chloroplast (Sargent and Taylor, 1972). For most photosynthesis / irradiance measurements the dark respiration rate determined at the start of an experiment has always been assumed to be a constant. However this may not be the case and there is still great controversy over whether or not dark respiration does change while the cell is being irradiated with light. The data presented in this thesis concerned with the measurement of photosynthesis / irradiance curves has already shown that for several unicellular green eukaryotic micro-algae and unicellular cyanobacteria (although prokaryotic cells do not contain mitochondria), that increases in respiration do occur. The evidence that there are two or more oxidase systems in *Chlorella vulgaris* first proposed by Emerson, (1926) and more recently by Sargent and Taylor, (1972) is increased from the results presented here. *Chlorella vulgaris* 211/11c exhibited some cyanide

resistance and also demonstrated some reversibility of the enzyme system(s). Since only 40% of the *Chlorella vulgaris* 211/11c activity was restored after repeated washing, these findings would support the work Sargent and Taylor, (1972), that there were 2 oxidase systems, one of which accounts for between 35 and 65% of the total cytochrome oxidase activity.

It has also been found that certain key cycles may not proceed in the light due to the light inhibition of two important enzymes (Buchanan, 1980). The two enzymes, phospho-fructo-kinase (catalyses key sequence in glycolysis) and glucose-6-phosphate dehydrogenase (catalyses part of oxidative pentose phosphate pathway) are inhibited by light and thus prevent precursors from reaching the TCA cycle. Measurements made by Kanazawa *et al.*, (1970); and Raven, (1972) have shown that the carbon flux through the TCA cycle is the same in the light as it is in the dark thus contradicting the theory of Falkowski, *et al.*, (1985). If cells were to shut down the TCA cycle in the light, it would suggest that they would be unable to grow in continuous light. This is clearly not the case and if the above two enzymes are indeed non functional in the light there must be an alternative mechanism to supply the TCA cycle with triose carbon. The proposed route for the carbon is from the C₃-Calvin recycle cycle in which triose can enter the lower part of the glycolytic sequence by-passing the phospho-fructo-kinase enzyme system and thus enter the TCA cycle to drive the process (Beardall and Raven, 1990).

Carbon (HCO₃⁻) in the form of sodium hydrogen carbonate was added to the incubating medium of cells to saturate the system with carbon to ensure that the oxygenase activity of the Rubisco enzyme was completely inhibited due to carbon concentrating mechanisms. HCO₃⁻ was preferred over direct use of carbon dioxide since evidence suggests that this is the primary form of inorganic carbon found in cells of a marine cyanobacterium *Synechococcus sp.* (Badger and Andrews, 1982). With this inactivity of the Rubisco enzyme, the glycolytic pathway would be non functional and photo respiration could not occur. It has been suggested that the observation of light enhanced dark respiration or enhanced post illumination respiration has been due to the process of photorespiration (Burriss, 1980; Glover and Morris, 1981). However if photorespiration was to occur, it could not account for the length of time that LEDR continues (Beardall and Raven, 1989). Research presented here and elsewhere has demonstrated that in most cases, algal / cyanobacterial cells require several hours

to fully return their dark respiration rates to normal after being exposed to light of high PFDs (Brown and Van Norman, 1952; Heichel, 1970; Falkowski *et al.*, 1985). Contrary to the review of Graham (1980), cells of both *Chlorella vulgaris* 211/11c and *Scenedesmus sp.* did not display reduced dark respiration at low light intensities but in agreement with the review, the cells displayed high oxygen consumption at high light intensities. It is difficult to determine whether an increased oxygen uptake in the light occurs by the same mechanism as the increased oxygen uptake that occurs in cells displaying LEDR. By using ^{18}O isotope it has been demonstrated that light does stimulate an increase in oxygen uptake in *Hydrodictyon africanum* (Glidewell and Raven, 1975). Since the oxygen produced during photosynthesis is split from water the oxygen is mainly (99.76%) in the form of ^{16}O , and the oxygen uptake during respiration was in the form of molecular oxygen ^{18}O their experiments confirmed the uptake of ^{18}O at enhanced rates in the light. Although LEDR has been observed in many species of algae and higher plants, it is still not accepted as a factor worth considering when photosynthesis response curves are determined. .

3.11 Overall Discussion

The problem of poor light penetration and mixing in photobioreactors based on circular geometry resulting was resolved in the novel design of the flat plate air lift photobioreactor. Due to the nature of the flat plate design, the light field across the reactor surface was easily quantifiable and found to be extremely accurate in terms of photon flux density and spectral radiant flux. The cultures of *C. vulgaris* 211/11c, *Scenedesmus sp.* and *Synechococcus* 1479/5 had higher growth rates and maximum stationary phase biomass levels when cultured in the FPALR compared to the CSTR. Higher chlorophyll a and b levels and a lower growth rate and maximum stationary phase biomass were recorded from *C. vulgaris* 211/11c during illumination with quartz-halogen lights compared to the high pressure sodium lamp when grown in the FPALR (Ratchford and Fallowfield, 1991). This was primarily thought to be due to the weak spectral energy output of the 400W high pressure sodium lamp or possibly the age of the lamp itself. When replaced with a new 600W lamp the growth curves of *C. vulgaris* 211/11c and *Scenedesmus sp.* were similar with either the HPSL and QHL. The differences obtained in growth rates when using a 400W, 600W HPSLs and the quartz halogen lamps clearly indicates that light source is an important point to consider when selecting an appropriate lighting system for a photobioreactor since the spectral energy changes between source.

Although the FPALR was designed to provide a very accurately controlled light regime for photosynthetic studies, the air lift drive mechanism proved to be extremely valuable in ensuring that the culture was fully turbulent with Reynolds numbers as high as 6500. The requirement for high turbulence was evident from the experiments carried out on the effect of carbon dioxide concentration on the growth kinetics of micro-algae and cyanobacteria. Cells of *Scenedesmus sp.* and *Synechococcus* 1479/5 had much higher growth rates at the higher carbon dioxide concentrations of 8% v/v when cultured in the FPALR compared to the CSTR. This was probably due to the superior gas handling and mixing ability of the FPALR compared to the CSTR in ensuring that the carbon dioxide was fully mixed in the air stream prior to contact with the cells.

One unexpected effect of turbulence was the smaller diameter cells of *C. vulgaris* 211/11c when cultured in the FPALR operating at increasingly high Reynolds

numbers. This altered state in cellular dynamics demonstrated the extremely high shear forces that were known to exist in the FPALR when operated at high Reynolds numbers and how the cells responded to these high flow regimes. It also showed that there was a clear optimum flow rate at which increasing turbulence gave maximum cell diameter. No data was obtained on the changes in growth rate with respect to changes in Reynolds number.

Experiments were performed in the FPALR in an attempt to determine the effects of external parameters such as light source, PFD, nutrient availability and temperature on growth and photosynthesis of cells and apply this data to the future mathematical modelling of waste treatment systems. Mathematical modelling of the growth and productivity of micro-algae and cyanobacteria is seen as the only process by which the inorganic removal of nutrients can be economically achieved (Talbot *et al.*, 1991). For any given reactor system there is a given number of parameters that can be changed to achieve maximum efficiency. In HRAPs the most notable external parameters which are primarily examined are the availability of nutrients and the mixing ability of the system (Fallowfield and Martin, 1989; Talbot *et al.*, 1991). When these parameters, however, are not considered to be limiting, researchers examine light limitation and culture temperature as a means of improving removal / uptake rates and system efficiency.

The FPALR design allowed fully turbulent mixing within a sealed vessel in which light was the only limiting factor. Increases in temperature (up to a maximum of 35°C), light (up to a maximum PFD of 200 $\mu\text{mol s}^{-1} \text{m}^{-2}$) and carbon dioxide (up to a maximum concentration of 6% v/v in air) were all found to increase the growth rate of *C. vulgaris* 211/11c, *Scenedesmus sp.* and *Synechococcus* 1479/5 when cultured in the FPALR and CSTR. When cultured to a stationary phase in the FPALR, further additions of phosphate and nitrate were not found to affect the growth rate of *C. vulgaris* 211/11c. This indicated that the growth rate of a cell was only limited by light. Subsequent increasing of the PFD from 100 to 200 $\mu\text{mol s}^{-1} \text{m}^{-2}$ resulted in higher growth rates and an increase in the nutrient uptake rates. This increase in PFD was also accompanied by an increase in the protein levels when grown at a PFD of 200 $\mu\text{mol s}^{-1} \text{m}^{-2}$. It was observed that cells cultured at a PFD of 200 $\mu\text{mol s}^{-1} \text{m}^{-2}$ had higher resistance to the onset of photoinhibition than similar cells cultured at a PFD of 100 $\mu\text{mol s}^{-1} \text{m}^{-2}$. This suggested that although the cells cultured at the higher

PFD had higher growth rates, the increase in nutrient uptake levels (in particular the nitrate level), light enhanced dark respiration and protein synthesis was an indication of an increase in cellular maintenance whilst an increase in cellular division was occurring.

Much attention has been paid to the determination of photosynthesis / irradiance response curves and the subsequent interpretation of the resulting data throughout this presentation. Emphasis has been placed on the resulting photosynthesis / irradiance curves being directly related to the environment from which the cell had existed or was being cultured in. Generally carbon in the form of HCO_3^- was not found to significantly affect photosynthetic kinetics of micro-algae during P / I measurement, although *Scenedesmus sp.* had a significantly higher LEDR rate when incubated in the presence of 2mM HCO_3^- . The cyanobacterium *Synechococcus* 1479/5 did, however, produce different photosynthetic kinetics when in the presence of 2mM HCO_3^- . Similar findings have been reported by Sultemeyer *et al.*, (1989) for both green micro-algae and cyanobacteria. The study presented here, however, did not examine the effect of carbon dioxide directly on the cells.

Incubating cells of micro-algae and cyanobacteria in phosphate buffer resulted in significant differences in the photosynthetic response when compared to the same cells incubated in ASM. The main photosynthetic parameter that was altered when in the presence of phosphate buffer was the value of P_{max} for *C. vulgaris* 211/11c, *Scenedesmus sp.* and *Synechococcus* 1479/5. As cells were unable to grow entirely on phosphate it questions the use of phosphate buffer in determining the photosynthetic response curve from cells which have previously been growing on ASM or some other synthetic media. Further analysis of the ASM components revealed that nitrate was the important component of the media to cells during photosynthesis and appeared to have a function in preventing the onset of photoinhibition and aid recovery from the effects of photoinhibition when placed in the dark. It is still not clear whether the presence of nitrate resulted in greater availability of nitrogen for protein synthesis during photoinhibitive damage. Trace elements were not found to significantly affect the photosynthetic kinetics of micro-algae or cyanobacteria.

Investigation of the effect of centrifugation yielded some unexpected results. In all species of micro-algae and cyanobacteria, cells that had been centrifuged prior to

oxygen measurements had a higher initial dark respiration rate than uncentrifuged cells. In the case of *Scenedesmus sp.* the dark respiration rate was 3 times higher than normal after centrifugation. The time required for the respiration rate to return to normal after centrifugation was of the order of several hours (data not shown). Due to these increases in dark respiration all other photosynthetic kinetics were significantly affected, although this was species specific. As well as dark respiration, light enhanced dark respiration was also affected by the process of centrifugation. LEDR rates were higher in centrifuged cells indicating that although the cells from treated and untreated cells had received the same dosage of light, the cell stress caused by the high G forces was still evident and was responsible for the changes in photosynthesis / irradiance response curve determinations between centrifuged and uncentrifuged cells.

Generally, for comparison purposes cells should be measured in P / I incubation conditions which most accurately simulate those found in the environment from which they were removed; thus the only variable which is being examined is that of changes in PFD.

The process of LEDR was found to significantly increase in the light when the PFD exceeded $\frac{1}{2}P_{\max}$ (data not shown). LEDR is very rarely considered in net photosynthesis calculations since standard calculations assume dark respiration to be a constant (Hettler *et al.*, 1991). Figures 87, 88 and 89 show the changes in photosynthesis / irradiance response curve that are obtained when LEDR is considered in the calculation of oxygen production. The process of LEDR was found to alter the overall photosynthetic kinetics compared to those calculated with the initial constant dark respiration rate. Due to problems of measuring LEDR directly and the time required to generate P / I curves (Figs 87 to 89), an alternative would be to measure photosynthesis / irradiance responses and include the initial dark respiration and final LEDR rates, in order that a researcher may predict the changes in oxygen consumption with changes in light.

No problems of oxygen inhibition of photosynthesis were recorded in all the experiments carried out involving photosynthesis / irradiance response curve measurements. Separate experiments involving saturating ASM to 80-90% saturation were not found to result in an inhibition of photosynthesis (data not shown).

Section 3.4.1 examined the affect of light / temperature on the photosynthetic kinetics of micro-algae and cyanobacteria. It was generally found that increases in temperature increased the susceptibility of cell to photoinhibition. This has been recorded by several other workers (Harris and Piccinin, 1977; Belay and Fogg, 1978. Jensen and Knutsen (1993), however, reported that increasing the temperature of *Spirulina platensis* from 20°C to 30°C resulted in a reduction in the degree of photoinhibition. The conclusion was that the observation and measurement of photoinhibition was a reduction in oxygen evolution. No analysis of the changes in dark respiration accompanying the high irradiances were, however, reported. It is accepted that the mechanism associated with photoinhibition does cause a reduction in oxygen evolution but if LEDR is occurring at a high rate then a reduction in cellular oxygen levels could also indicate an increase in oxygen uptake. The reduction in oxygen evolution was considered to be a balance between the damage caused by high light and maintenance. It was suggested that a combination of light, temperature and dissolved oxygen concentration in high rate algal ponds would need to be continuously monitored in order to prevent problems associated with photoinhibition and photooxidation. Furthermore, increases in temperature were not observed to cause a reduction in photoinhibition as observed by Jensen and Knutsen (1993). From Figures 90 to 93, it can be seen that *C. vulgaris* 211/11c cells had higher rates of photoinhibition when the temperature was increased from 15°C to 35°C. Similar results were recorded with *Nannochloris atomus* (Figs 102 to 105), *Scenedesmus sp.* (Figs 114 to 117), *A. antarcticus* (Figs 126 to 129), *Synechococcus* 1479/5 (Figs 138-141) and *Synechococcus sp.* (Figs 150 to 153). The results are in agreement with those of Talbot *et al* (1991) who recorded lower growth rates and photosynthetic rates from *Oscillatoria agardhii* and *Ankistrodesmsu falcatius* when irradiated at high light intensities at high temperatures. All these observations may, however, be species specific.

As the culture growth temperature was increased to 35°C cells of *C. vulgaris* 211/11c (Fig 97), *Nannochloris atomus* (Fig 109), *Scenedesmus sp.* (Fig 121), *A. antarcticus* (Fig 133), *Synechococcus* 1479/5 (Fig145) and *Synechococcus sp.* (Fig157) all showed little change in respiration rates when the photosynthesis / irradiance incubation temperature was varied between 15°C and 35°C. This may have been expected since the respiration rate would be dictated by the enzymatic rate at a given temperature which should have been maximum at 35°C assuming optimum enzymatic

temperature of 35°C. It did, however, show that although respiration was assumed to be a constant in the computer modelling of waste water treatment using HRAPs (Martin personal communication), the temperature dependence of respiration was primarily determined by the previous culture temperature and light history. The rate of light enhanced dark respiration, however increased with increasing temperature for all cultures suggesting that although temperature does play a role (LEDR increases with increasing temperature), light intensity was the overall factor that significantly affected the rate of LEDR since they were higher at the initial culture PFD of $200\mu\text{mol s}^{-1} \text{m}^{-2}$ compared to $100\mu\text{mol s}^{-1} \text{m}^{-2}$.

The maintenance and repair rates of phytoplankton cells after exposure to photoinhibiting light intensities has been shown to have a major affect on overall photosynthetic recovery (Raven and Samuelsson, 1986; Raven, 1989). The process of respiration, however, has received little attention and should equally be considered as serious since increases in respiration during photosynthesis resulting in the phenomenon of light enhanced dark respiration are considered to be a process by which the polysaccharide synthesis is reversed (Beardall and Raven, 1990). As photosynthetic substrate is reduced the level of LEDR was also seen to fall (Ratchford unpublished data).

New factors, however, which include light / dark cycling have had a major impact on the modelling of micro-algal kinetics (Martin personal communication). Although considered separately on the basis of time cycles, light / dark cycles of medium frequency (seconds to minutes) are generally regarded as those which simulate cycles normally found in the photic zone of a water body (Denman and Gargett, 1983; Kirk, 1983; Walsh and Legendre, 1983; Grobbelaar, 1989; Kroon *et al.*, 1992). It was determined in the research carried out in this thesis that light / dark cycles of medium frequency do affect both the growth, physiology and photosynthetic kinetics of micro-algae and cyanobacteria which contradicts the findings of Grobbelaar, (1989), but supports results recorded by Richmond and Vonshak, (1978) and the later findings of Grobbelaar *et al.*, (1992) and Kroon *et al.*, (1992). The research carried out with short term incubations in the oxygen electrode supported the data obtained from the FPALR whilst operating under continuous kinetics which showed that similar responses to changes in the ratio of light to dark were extremely important in preventing photoinhibition. In order to maintain photosynthetic stability i.e. a constant

light saturated rate of photosynthesis when irradiated at light intensities above P_{\max}^{PFD} cells of *C. vulgaris* 211/11c and *Synechococcus* 1479/5 has to be cycled through a dark respiration period (or low enough PFD) long enough to prevent the onset of photoinhibition and photooxidation. Although not examined in this research the effect on the photosynthesis of micro-algae and cyanobacteria exposed to light at different wavelengths in a light / dark cycle would probably have a great influence on growth and photosynthesis. This would more accurately simulate both the changes in spectral composition and light attenuation that occur in lakes and HRAPs with increasing depth and is an area requiring further research.

C. vulgaris 211/11c and *Synechococcus* 1479/5 required a longer time period in the dark to recover from light of a photoinhibitive PFD. Dosage was not found (Figure 217) to be as important as the initial light intensity and duration of the exposure. As the exposure period to photoinhibiting light and the PFD of the photoinhibiting light was increased, the time required by cells of *C. vulgaris* 211/11c and *Synechococcus* 1479/5 in the dark to recover was increased.

From the experiments involving light / dark cycles of medium frequency measured over a period of 24 hours in the oxygen electrode (Section 3.5.1), it was apparent that recovery ratios (L / D cycle at a photoinhibiting PFD which did not result in photoinhibition) were dependent on the time exposure to the photoinhibiting PFD and in particular the intensity. A light / dark ratio of 2 : 1 measured at PFD of $300\mu\text{mol s}^{-1} \text{m}^{-2}$ for a light exposure of 1 minute would not necessarily mean that a 2 : 1 ratio would be sufficient at preventing the onset of photoinhibition at a PFD of $300\mu\text{mol s}^{-1} \text{m}^{-2}$ for a light exposure of 2 minutes. Hence Figure 218 only refers to recovery ratios of time exposure to the light of less than 280 seconds. For systems where the light / dark cycles are expected to exceed this time period in the light, further experiments would be required.

Overall phytoplankton productivity affects many of the biochemical processes and cycling of matter that occurs in the natural environment (Kirk, 1983). Small changes in productivity can effect important changes in this complex chain of events which leads to problems in long term predictions and modelling (Soeder *et al.*, 1985; Sager and Richman, 1991; Talbot *et al.*, 1991). The pathway through which cells of micro-algae, cyanobacteria, and particles of matter has largely been determined through the

use of mathematical equations and simulation vessels. These motions which cover both the vertical and horizontal movements, are only applied to short and medium time scales (months or even seasons) (Prezelin *et al.*, 1991). In high rate algal ponds, the photosynthetic organisms are circulated by a paddle wheel and it is considered that the vertical motion within the fluid layer is circular and that it passes through several complete cycles covering both the surface and the bottom of the fluid (Martin and Fallowfield unpublished data).

It has been previously shown that the change in depth profile has a major effect on the availability and usefulness of light in terms of photon flux density (Section 3.8) and spectral radiant flux. Cells of *C. vulgaris* 211/11c, had a higher growth rate when cultured in the FPALR in a light gradient of $800\mu\text{mol s}^{-1} \text{m}^{-2}$ (Table 90) compared to light gradients of lower initial PFD and this growth rate increased when the frequency of light / dark cycles was increased. This demonstrated that although the cells were exposed to light of photoinhibitive intensity, the length of time spent in the photoinhibition channel was not long enough to damage the cells. Subsequent movement through channels at lower PFDs (below those known to be photoinhibitory) allowed the cells time to recover. The results of the light / dark cycles in light gradients can be applied to high rate algal ponds and similar systems, although the light gradient in these systems is never fixed due to the changes in weather patterns which change both the temperature of the water body, the light / dark cycle ratios and the overall changes in the optical properties of the water. The data can, however, be used to predict the likely changes that occur during photosynthesis in a HRAP. The data may also be used to determine productivity in lake systems where forced turbulence is not a factor, since the light /dark cycles and fluctuations can vary from seconds to hours and are affected similarly by changing weather patterns and even by vertical migration by motile algal populations (Prezelin *et al.*, 1991).

The reduction in light with increasing depth was not the only major factor affecting photosynthesis. From Section (3.9.2) it was shown that cells of *C. vulgaris* 211/11c, *Scenedesmus sp.* and *Synechococcus* 1479/5 photosynthesise with higher oxygen evolution rates in full spectrum (300-800nm) > blue (350-475nm) light > red (600-800nm) light. As the depth of a water body increases the main areas of wavelength absorption increases corresponding to the maximum chlorophyll a and b absorption peaks of the cells (Kirk, 1983). Thus at a relatively shallow depth the photon flux

density may still be above $\frac{1}{2}P_{\max}$ (Kroon *et al.*, 1992), whereas the wavelength will not be available for photosynthesis. Light of different spectral radiant flux was also shown to affect the growth rates of *C. vulgaris* 211/11c, *Scenedesmus sp.* and *Synechococcus* 1479/5 when irradiated at identical PFDs (Section 3.9.1). Cells of the green micro-algae showed slightly higher growth rates when cultured in red light than in blue light, whereas, cells of *Synechococcus* 1479/5 had a very much higher growth rate when cultured in red light compared to blue light.

The discrepancy between growth and photosynthesis in red and blue light may be due to a number of factors. Firstly the products of photosynthesis, when cultured in red and blue light are notably different. Red light irradiated cells of *Chlorella* shunt carbon into the production of P-esters, free sugars and insoluble material (Ogasawara and Miyachi, 1970). Blue light irradiated cells of *Chlorella* have been reported to incorporate carbon into aspartic acid, glutamic acid, and malic acid; other effects of blue light include an increase in the activity of the enzyme PEP carboxylase and an increase in cellular respiration (Sargent and Taylor, 1975) thought to be due to an increase in chloroplast RNA and protein synthesis. This may explain why cells of *C. vulgaris* 211/11c, produced low growth rates when irradiated with red (600-800nm) light but had higher maximum rates of photosynthesis compared to blue light. *Synechococcus* 1479/5 and *Synechococcus sp.* are typical cyanobacteria and should be unable to grow in full blue light (375-500nm) (Dring personal communication). Although *Synechococcus* 1479/5 achieved a stationary phase biomass of 0.12 g l^{-1} whilst being irradiated with blue light, it suggests that other wavelengths of light were being transmitted through at the far red (>700nm) region of the spectrum (Dring personal communication). Although the chlorophyll a component of cyanobacteria is the principle absorption pigment and the major contributor to the light reactions of photosynthesis, it can receive energy from other light harvesting complexes (LHCs) present within the system. The LHCs from these cells thus expands the range of available wavelengths that the organism can derive energy from. Analysis on a scanning spectrophotometer showed that the blue filter was not filtering out the far red wavelengths of light (> 700nm). Since cyanobacteria contain phycocyanins which are able to intercept and utilise far red wavelengths, this may have been the determining factor behind why cyanobacteria grew in blue light. *Spirulina* produces large concentrations of carotenoids (the lipid soluble photopigments). These pigments principally absorb light in the wavelength region 300-500nm range. Changes in the

spectral quality of light has been shown to affect enzyme activity of *P.tricornutum* (Wynne and Rhee, 1988). Light intensity at saturating intensity and spectral quality (red light greater than blue light) was found to increase the activity of the enzyme alkaline phosphatase. It was found that the changes in rates of activity were not consistent with different species as red light increased the enzyme activity in *D.tertiolecta* compared to either blue or full spectrum light. Changes at the molecular level with respect to a cell's metabolic rate induced by changes in light quality has major implications on productivity as wavelengths of light are selectively filtered out as it penetrates the water column.

It is now commonly recognised by researchers that micro-algal and cyanobacterial cells respond to changes in the environment on a time scale of several hours (Prezelin *et al.*, 1991; Kroon *et al.*, 1992). This being the case, changes in both the water content and the mass of the supporting body will drastically effect the photosynthesis and overall productivity of a micro-algal / cyanobacterial cell (Prezelin, 1992). It was observed that daily variations in the productivity of phytoplankton are caused by diel periodicity's in the physiology of cells (Prezelin, 1992). This rhythmic response to the environment was also found to be related to photosystem II which has been noted to play a key role in both photoinhibition (Raven, 1989; Herbert, 1990) and light enhanced dark respiration (Ratchford and Fallowfield, 1992). These changes in the photosynthetic response to light based on a function of time may help explain why some HRAPs operated under batch kinetics appear to show no correlation between productivity and irradiance (Martin and Fallowfield, unpublished data). Although this data may be applicable to natural mixed cultures in terms of species, the observation of diel periodicity was not observed in the FPALR using axenic cultures of *C. vulgaris* 211/11c, *Synechococcus* 1479/5 or *Scenedesmus* sp.

The major drawbacks to batch kinetic work using chemostats is that these systems are usually based on circular geometry. Further problems include the accurate definition and measurement of the incident light field both in terms of photon flux density and spectral radiant flux. Finally the cells are usually mixed in light / dark cycles that do not correspond to those found in nature. It is quite common to see light / dark cycle ratios of 12:12 hours (Lee, 1987), 14:10 hours (Prezelin *et al.*, 1987); 16:8 hours (Kroon *et al.*, 1992). Although in terms of day and night length they agree, the changes associated with cycles in lake and HRAP systems are based on light / dark

cycles of a more complicated nature. Micro-algal cells and indeed any particle of matter in a lake system is circulated by both the external and internal forces of the environment and the water, cycles of varying medium frequency i.e. seconds to minutes (in varying PFD). The effect of medium light / dark cycles on the photosynthesis and respiration of micro-algae has been recently examined by Grobbelaar *et al.*, (1992). Using *C. pyrenoidosa* as the test organism, the effects of different light regimes on the light period of a diurnal cycle were examined. It was found that cells irradiated with light with an hourly oscillation were exposed to light of a more natural content compared to cells irradiated with sinusoidal or block light. The data also showed that the rates of photosynthesis either decreased or increased with decreasing frequency of light / dark cycling showing no consistent relationship between photosynthesis and light / dark cycle. This in part supports the measurements recorded in Section 3.8.1 which found that the overall productivity in terms of final stationary phase biomass and growth rates of *C. vulgaris* 211/11c decreased with increasing light / dark cycle frequency at the higher photoinhibitive light gradient intensities.

Although it is now generally accepted that light / dark cycles of medium frequency can affect the productivity and photosynthesis of micro-algal cells (Grobbelaar *et al.*, 1992; Kroon *et al.*, 1992), evidence is growing to suggest that the light harvesting complexes and photoreaction centres are to a greater degree affected by the light regime within the light / dark cycle. Kroon *et al.*, 1992 observed that cells of *C. pyrenoidosa* showed a decrease in the chlorophyll a to b ratio although the total chlorophyll content remained the same when irradiated with sinusoidal light on a 8 hour frequency compared to a 1 hour sinusoidal light curve with an 8 hour oscillation. This difference in the cellular oxygen evolution due to changes in the ratios of pigments has been attributed to changes in both the number and size of photosynthetic units. It is clearly evident from the results obtained in Section 3.6.1 that although chlorophyll a concentration decreased when the light intensity was doubled, the maximum rate of photosynthesis was found to increase. This discrepancy between chlorophyll a concentration and oxygen evolution may be explained by changes in the efficiency of the light harvesting pigments and / or the size and distribution of the photosynthetic units. Kirk, (1983) acknowledged that an increase in chlorophyll content resulting from growth at lower light intensities was probably due to an increase in both the number and size of photosynthetic units present within the cell.

This theory has been supported by a number of researchers who have found that the number of chlorophyll molecules does not actually change with changes in light intensity (Kirk, 1983) and that chlorophyll efficiency may be changing. Myers and Graham, (1971), however, recorded very large changes in the chlorophyll molecule content of *C. pyrenoidosa* when irradiated at different irradiances. The reduction in chlorophyll a content observed in *C. vulgaris* 211/11c (Section 3.6.1) was a direct result of increasing the light intensity, however, it remains unclear, however, if the number of photoreaction centres is directly affected by changes in light intensity. The latter point is particularly important since changes in photoreaction centre number has been observed by Falkowski and Owens 1980, in diatoms. A 26% reduction in the number of photosystem I reaction centres was measured in cells of *Skeletonema costatum* when the cells were cultured at $130\mu\text{mol s}^{-1} \text{m}^{-2}$ after being grown at $20\mu\text{mol s}^{-1} \text{m}^{-2}$. This change in photoreaction centre number, however, is not consistent in all micro-algae and cyanobacteria. Some researchers (Falkowski and Dubinsky, 1981) found no such difference in the number of photosystem I in exposed or shaded populations of the dinoflagellate *Stylophora pistillata* although the number of chlorophyll molecules was found to be 4-5 times higher in the shaded cells.

C. vulgaris 211/11c was cultured in the FPALR under different light regimes. It was found that an increased in dry matter production was observed when the light incident on the photostage was increase accordingly. Although the chlorophyll content of the cells decreased with an increase in light intensity, the maximum rate of photosynthesis increased. *C. vulgaris* 211/11c may be adapting itself to a new light regime and changing it's photosynthetic kinetics accordingly. The success at attempting to prevent photoadaptation by reducing the number of cell generations to 5 (Brand *et al.*, 1981) was not known but it is thought that some photoadaptation may have occurred in cells irradiated at a PFD of $400\mu\text{mol s}^{-1} \text{m}^{-2}$. Grobbelaar *et al.*, (1992) recorded a variation in the maximum chlorophyll specific productivity and respiration rates in *C. pyrenoidosa* measured at hourly intervals during the light period of a sinusoidal light exposure pattern. This variation in the $P_{\text{max}}^{\text{B}}$ rates was similar to the changes in the P_{max} rates observed in the FPALR when culturing *C. vulgaris* 211/11c in varying light intensity (stepped increases and decreases). These changes in photosynthetic kinetics have been reported by Harris (1978) and Fallowfield (unpublished data). One factor that remains unresolved is the process and time scale required for photoadaptation of cells to a new light environment. Cullen and Lewis, (1988) suggested that the time

scale of photoadaptation will be determined by the rate of change of mixing. Further analysis on the mechanisms of this process is required to understand the effects of changing PFD on cells cultured under continuous kinetics in varying light / dark cycles.

Changes in spectral radiant flux have a major influence on both the growth and photosynthetic kinetics of micro-algae and cyanobacteria. Spectral radiant flux in particular plays a major role in ocean productivity studies (Lewis *et al.*, 1985), since light attenuation decreases in both PFD and spectral radiant flux with increasing depth. The effect of wavelength of light on the respiration rates of micro-algae and cyanobacteria was found to be greatest in the red region of light (600-800nm). The LEDR rates of *C. vulgaris* 211/11c, *Scenedesmus* sp. and *Synechococcus* 1479/5 were all higher than similar cells irradiated with blue (375-500nm) or full spectrum (300-800nm) light.

Examination of the effect of LEDR presented in 3.10 found that there was no conclusive evidence that DCMU inhibited LEDR rates. The experiments involving potassium-cyanide, however, clearly indicated that cytochrome oxidase of the mitochondria was involved in the process as LEDR rates were partially or totally inhibited. The partial inhibition was due to the *C. vulgaris* 211/11c having possibly 2 or more oxidase systems which supports the observations made by Sargent and Taylor, (1972). In conclusion LEDR is an important process which can drastically alter the interpretation of photosynthetic kinetics and suggests that there is still much research to be carried out on its mode of action and mechanism.

-New experiments examining changes in light gradients and light / dark cycling of medium frequency simulating those induced by natural wave and wind action are providing new information on how cells respond to varying PFDs (Grobbelaar *et al.*, 1992). This data will enable the formulation of equations which can be used to refine computer models to more accurately predict productivity and understand the mechanisms of photosynthesis that occur at the various depths of water systems (Fallowfield and Martin, 1989). The research presented here has shown that respiration and light enhanced dark respiration play a much more important role than previously thought, in photosynthesis and that the initial rate of oxygen consumption although assumed to be constant throughout oxygen evolution, is in fact changing. As

photosynthesis / irradiance response curves measurement and interpretation have relied solely on a constant dark respiration rate it is essential that changes in LEDR are recorded and made available in the literature.

References

- Agusti, S. (1991a). Allometric scaling of light absorption and scattering by phytoplankton cells. *Can. J. Fish. Aquat. Sci.* **48**: 763-767.
- Agusti, S. and Philips, E.J. (1992). Light absorption by cyanobacteria: Implications of the colony growth form. *Limnol. Oceanogr.*, **37** (2): 434-441.
- Aparicio, P.J. and Quinones, M.A. (1991). Blue light, a positive switch signal for nitrate and nitrite uptake by the green alga *Monoraphidium braunii*. *Plant. Physiol.* **95**: 374-378.
- Arnold, K.E. and Murray, S.N. (1980). Relationships between irradiance and photosynthesis for marine benthic green algae (Chlorophyta) of differing morphologies. *J. Exp. Mar. Biol. Ecol.* **43**: 183-192.
- Babu, T.S., Kumar, A. and Varma, A.K. (1991). Effect of light quality on phycobilisoma components of the cyanobacterium *Spirulina platensis*. *Plant. Physiol.* **95**: 492-497.
- Badger, M.R. and Andrews, T.J. (1974). Effects of CO₂, O₂ and temperature on a high affinity form of ribulose diphosphate carboxylase-oxygenase from spinach. *Biochem. Biophys. Res. Commun.* **60**: 204-210.
- Badger, M.R., Kāplan, A. and Berry, J.A. (1980). Internal inorganic carbon pool of *Chlamydomonas reinhardtii*. Evidence for a carbon dioxide concentrating mechanism. *Plant. Physiol.* **66**: 407-413.
- Badger, M.R. and Andrews, T.J. (1982). Photosynthesis and inorganic carbon usage by the marine cyanobacterium *Synechococcus sp.* *Plant. Physiol.* **70**: 517-523.
- Badger, M.R., Bassett, M. and Comins, H.N. (1985). A model for HCO₃⁻ accumulation and photosynthesis in the cyanobacterium *Synechococcus sp.* *Plant. Physiol.* **77**: 465-471.
- Balfört, H.W., Bergman, T., Maestrini, S.Y., Wenzel, A. and Zohary, T. (1992). Flow cytometry: instrumentation and application in phytoplankton research. *Hydrobiologia.* **238**: 89-97.
- Baly, E.C.C. (1935). The kinetics of photosynthesis. *Proc. R. Soc. Lond. Ser B.* **117**: 218-239.
- Beardall, J. and Morris, I. (1976). The concept of light intensity adaptation in marine phytoplankton: some experiments with *Phaeodactylum tricorutum*. *Mar. Biol.* **37**: 3777-3787.

Beardall, J. (1989). Photosynthesis and photorespiration in marine phytoplankton. *Aquatic Botany*. **34**:105-130.

Beardall, J. and Raven, J.A. (1990). Pathways and mechanisms of respiration in microalgae. *Marine. Microbial. Food. Webs*. S.Y. Maestrini and F. Rassoulzadegan (eds.). "Microalgal growth : inputs and losses practical approaches." **4**: (1). 7-30.

Behrens, P.W., Scott, E.B., Scot, D.H., Cohoon, D.L. and Cox, J.C. (1989). Studies on the incorporation of CO₂ into starch by *Chlorella vulgaris*. *J. Appl. Phycol.* **1**: 123-130.

Belay, A. and Fogg, G.E. (1978). Photoinhibition of photosynthesis in *Asterionella formosa* (Bacillariophyceae). *J. Phycol.* **14**: 341-347.

Berry, J.A., Boynton, J., Kaplan, A. and Badger, M.R. (1976). Growth and photosynthesis of *Chlamydomonas reinhardtii* as a function of CO₂ concentration. Carnegie Institution of Washington Yearbook. **75**: 423-432.

Bidwell, R.G.S. (1976). Photosynthesis and light and dark respiration in freshwater algae. *Can. J. Bot.* **55**: 809-817.

Birmingham, B.C. and Colman, B. (1979). Measurement of carbon dioxide compensation points of freshwater algae. *Plant. Physiol.* **64**: 892-895.

Bishop, N.I. (1958). The influence of the herbicide DCMU on the oxygen evolving system of photosynthesis. *Biochim. Biophys. Acta.* **27**: 205-206.

Blackman, F.F. (1905). Optimas and limiting factors. *Ann. Bot.* **91**: 281-295.

Boing, J.T.P. (1982). Enzyme production. In Prescott and Dunne's Industrial Microbiology. 4th edition, pp 634-708. (ed. G. Reed). MacMillan, New York.

Borowitzka, M.A. & Borowitzka, L.J. (1988b). Micro-algal Biotechnology. Cambridge University Press, Cambridge.

Botton, R., Cosserat, D. and Charpentier, J.C. (1980). Mass transfer in bubble columns operating at high gas throughputs. *The Chemical Engineering Journal.* **20**: 87-94.

Bradford, M.M. (1976). A rapid and sensitive method for the quantitation of microgram quantities of protein utilising the principle of protein dye binding. *Anal. Biochem.* **72**: 248-254.

Brand, L.E., Guillard, R.R.L. and Murphy, L.S. (1981). A method for the rapid and precise determination of acclimated phytoplankton reproduction rates. *J. Plankton. Res.* **3**: 193-201.

- Brendan, C., Birmingham, J., Coleman, R. and Colman, B. (1982). Measurement of photorespiration in algae. *Plant. Physiol.* **69**: 259-262.
- Brown, A.H. and Van Norman, R.W. (1952). The relative rates of photosynthetic assimilation of isotopic forms of carbon dioxide. *Plant. Physiol.* **27**: 691-709.
- Brown, A.H. (1953). The effects of light on respiration using isotopically enriched oxygen. *Am. J. Bot.* **40**: 719-729.
- Brown, D.L. and Tregunna, E.B. (1966). Inhibition of respiration during photosynthesis by some algae. *Can. J. Bot.* **45**: 1135-1143.
- Buchanan, B.B. (1980). Role of light in the regulation of chloroplast enzymes. *Ann. Rev. Plant. Physiol.* **31**: 341-374.
- Burris, J.E. (1980). Respiration and photorespiration in marine algae. *In Primary Productivity in the Sea*. Falkowski, P.G. (ed). New York Plenum Press. 411-431.
- Cabecadas, G. and Brogueira, M.J. (1987). Primary production and pigments in 3 low alkalinity connected reservoirs receiving mine wastes. *Hydrobiologia.* **144**: 173-182.
- Cayle, T. and Emerson, R. (1957). Effect of wavelength on the distribution of carbon-14 in the early products of photosynthesis. *Nature.* **179**: 89-90.
- Cholet, R. and Ogren, W.L. (1975). Regulation of photorespiration in C3 and C4 species. *Bot. Rev.* **41**: 137-179.
- Clement-Metral, J.D., Gantt, E. and Redlinger, T. (1985). A photosystem II-phycobilisome preparation from the red alga *Porphyridium cruentum*: oxygen evolution, ultrastructure, and polypeptide resolution. *Arch. Biochem. Biophys.* **238**: 10-17.
- Clendenning, K.A. and Ehrmantraut, H.C. (1950). Photosynthesis and Hill reactions by whole *Chlorella* cells in continuous and flashing light. *Arch. Biochem.* **29**: 387-403.
- Coleman, J.R. and Colman, B. (1980). Effect of oxygen and temperature on the efficiency of photosynthetic carbon assimilation in two microscopic algae. *Plant. Physiol.* **65**: 980-983.
- Coleman, J.R. and Colman, B. (1981). Inorganic carbon accumulation and photosynthesis in a blue green algae as a function of external pH. *Plant. Physiol.* **67**: 917-921.
- Corman, H.S. (1975). A history of brewing. David and Charles Newton Abott.

- Cullen, J.J. and Lewis, M.R. (1988). The kinetics of algal photoadaptation in the context of vertical mixing. *J. Plankton. Res.* **10**:1039-1063.
- Cunningham, F.X., Dennenberg, R.J., Jursinic, P.A. and Gantt E. (1990). Growth under red light enhances photosystem II relative to photosystem I and phycobilisomes in the red alga *Porphyridium cruentum*. *Plant. Physiol.* **93**: 888-895.
- Danforth, W.F. (1967). Respiratory metabolism. In *Research in Protozoology*, Vol.1. Ed. T.T. Chen. Pergamon Press, Oxford, London, 205-306.
- Davis, E.A., Dedrick, J., French, C.S., Milner, H.W., Myers, J., Smith, J.H.C. & Spoehr, H.A. (1953). Laboratory experiments on *Chlorella* at the Carnegie Institution of Washington Department of Plant Biology. In: *Algal culture from Laboratory to Pilot Plant* (Ed. J.S. Burlew), pp. 105-153. Carnegie Institution, Washington.
- Decker, J.P. (1955). A rapid post illumination deceleration of respiration in green leaves. *Plant Physiol.* **30**: 82-84.
- Denman, K.L. and Gargett, A.E. (1983). Time and space scales of vertical mixing in the upper ocean. *Limnol. Oceanogr.* **28**: 801-815.
- Dera, J. (1970). On two layers of different light conditions in the euphotic zone of the sea. *Acta. Geophys.* **18**: 287-294.
- Dubinsky, Z., Falkowski, P.G., Post, A.F. & Hes, U.M. (1987). A system for measuring phytoplankton photosynthesis in a defined light field with an oxygen electrode. *J. Plankton Res.*, **9**: 607 - 612.
- Edwards, G. and Walker, D.A., 1983. *C₃, C₄: Mechanisms and cellular and environmental regulation of photosynthesis*. Oxford Blackwell Scientific 542p
- Emerson, R. (1926). The effect of certain respiratory inhibitors on the respiration of *Chlorella*. *J. Gen. Physiol.* **24**: 255-264.
- Espie, G.S. and Canvin, D.T. (1987). Evidence for Na⁺ independent HCO₃⁻ uptake by the cyanobacterium *Synechococcus leopoliensis*. *Plant. Physiol.* **84**: 125-130.
- Espie, G.S., Miller, A.G. and Canvin, D.T. (1991). High affinity transport of carbon dioxide in the cyanobacterium *Synechococcus* UTEX 625. *Plant. Physiol.* **97**: 943-953.
- Espie, G.S. and Kandasamy, R.A. (1992). Na⁺ independent HCO₃⁻ transport and accumulation in the cyanobacterium *Synechococcus* UTEX 625. *Plant. Physiol.* **98**: 560-568.

- Falkowski, P.G. and Owens, T.G. (1978). Effect of light intensity on photosynthesis and dark respiration in six species of marine phytoplankton. *Marine. Biology.* **45**: 289-295.
- Falkowski, P.G. and Owens, T.G. (1980). Light shade adaptation: two strategies in marine phytoplankton. *Plant. Physiol.* **66**: 592-595.
- Falkowski, P.G. and Dubinsky, Z. (1981). Light shade adaptation of *Stylophora pistillata*, a hermatypic coral from the Gulf of Eilat. *Nature.* **289**: 172-174.
- Falkowski, P.G., Dubinsky, Z. and Santostefano, G. (1985). Light enhanced dark respiration in phytoplankton. *Verh. Internat. Verein. Limnol.* **22**: 2830-2833.
- Falkowski, P.G., Sukenik, A., and Herzig, R. (1989). Nitrogen limitation in *Isochrysis galbana* (Haptophyceae). II. Relative abundance of chloroplast proteins. *J. Phycology* **23**: 471-478.
- Fallowfield, H.J. and Garret, M.K. (1985). The photosynthetic treatment of pig slurry in temperate climatic conditions: a pilot plant study. *Agric. Wastes.* **12**: 111-136.
- Fallowfield, H.J. and Martin, N.J. (1988). The operation performance and computer design of high rate algal ponds. In *Aquacultural Engineering: Technologies for the future.* Institute of Chemical Engineers Symposium series No. 111. EFCE Publication series No. 66. pp 389-403.
- Fallowfield, H.J., Martin, N.J., Foot, I.M. and Ratchford, I.A.J. (1990). A novel algal photobioreactor. *British. Phycol. Journal.* **25**: 87.
- Ferris, J.M. and Christian, R. (1991). Aquatic primary production in relation to microalgal responses to changing light: a review. *Aquatic. Sciences.* **53**: 187-217.
- Fork, D.C. and Satoh, K. (1986). The control of state transitions of the distribution of excitation energy in photosynthesis. *Annu. Rev. Plant. Physiol.* **37**: 335-361.
- Foy, R.H. and Gibson, C.E. (1982a). Photosynthetic characteristics of planktonic blue green algae: the response of twenty strains grown under high and low light. *Brit. Phycol. J.* **17**: 169-182.
- Gallegos, C.L., Church, M.R., Kelly, M.G. and Hornberger, G.M. (1983). Asynchrony between rates of oxygen production and inorganic carbon uptake in a mixed culture of phytoplankton. *Arch. Hydrobiol.* **96**: 164-175.
- Gallegos, C.L. and Platt, T. (1981). Photosynthesis measurements on natural populations of phytoplankton: Numerical analysis. *Can. Bull. Fish. Aquat. Sci.* **210**: 103-112.

- Gallon, J.R., Pederson, D.M. and Smith, G.D. (1993). The effect of temperature on the sensitivity of nitrogenase to oxygen in the cyanobacterium *Anabaena cylindrica* (Lemmermann) and *Gloeothoece* (Nägeli). *New Phytol.* **124**: 251-257.
- Geider, R.J. (1987). Light and Temperature dependence of the carbon to chlorophyll *a* ratio in micro-algae and cyanobacteria: Implications for physiology and growth of phytoplankton. *New Phytol.* **106**: 1-34.
- Geider, R.J. and Osborne, B.A. (1989). Respiration and micro-algal growth: a review of the quantitative relationship between dark respiration and growth. *New Phytol.* **112**: 327-341.
- Geider, R.J. and Osborne, B.A. (1992). *In*. Photosynthesis: the measurement of algal gas exchange. Current Phycology 2. Chapman and Hall. London.
- Geider, R.J., Osborne, B.A. and Raven, J.A. (1992). Light dependence of growth and photosynthesis in *Paedactylum tricornutum* (Bacillariophyceae). *Journal Applied Phycology*.
- Gibbs, M. (1962). Respiration. *In* : Physiology and Biochemistry of Algae, Ed. R.A. Lewin. Academic Press, London, New York, 61-90.
- Gibson, C.E. (1984). A comparison of captured and circulated phytoplankton by means of carbohydrate content and its relation to oxygen evolution. *Verh. Internat. Verein. Limnol.* **22**: 627-631.
- Glidewell, S.M. and Raven, J.A. (1975). Measurement of simultaneous oxygen evolution and uptake in *Hydrodictyon africanum*. *J. Exp. Botany.* **26**: 479-488.
- Glover, H.E. and Morris, I. (1981). Photosynthetic characteristic of coccoid marine cyanobacteria. *Arch. Microbiol.* **129**: 42-46.
- Graham, D. (1980). Effects of light on dark respiration. *In*. The biochemistry of plants. (Davies, D.D. ed). Academic Press, Inc., New York **2**: 525-579.
- Grande, K.D., Marra, J., Langdon, C., Heinemann, K. and Bender, M.L. (1989). Rates of respiration in the light measured in marine phytoplankton using an ¹⁸O isotope labelling technique. *J. Exp. Mar. Biol. Ecol.* **129**: 95-120.
- Grobbelaar, J.U. (1989). Do light / dark cycles of medium frequency enhance phytoplankton productivity. *Journal of Applied Phycology.* **1**: 333-340.
- Grobbelaar, J.U., Kroon, B.M.A., Burger-Wiersma, T. and Mur, L.R. (1992). Influence of medium frequency light / dark cycles of equal duration on the photosynthesis and respiration of *Chlorella pyrenoidosa*. *Hydrobiologia.* **238**: 53-62.

- Grumbach, K.H., Lichenthaler, H.K. and Erismann, K.H. (1978). Incorporation of carbon-14 labelled carbon dioxide in the photosynthetic pigments of *Chlorella pyrenoidosa*. *Planta*. **140**: 37-43.
- Harris, G.P. and Piccinin, B.B. (1977). Photosynthesis by natural phytoplankton populations. *Arch. Hydrobiol.* **80**: 405-457.
- Harris, G.P. (1978). Photosynthesis, productivity and growth: The physiological ecology of phytoplankton. *Arch. Hydrobiol. Beih. Ergebn. Limnol.* **10**: 1-128
- Hauschild, A.H.W., Nelson, C.D. and Krotkov, G. (1962). The effect of light quality on the products of photosynthesis in *Chlorella vulgaris*. *Can. J. Bot.* **40**: 179-184.
- Heichel, G.H. (1970). Prior illumination and the respiration of maize leaves in the dark. *Plant. Physiol.* **46**: 359-362.
- Heichel, G.H. (1972). Postillumination respiration of maize in relation to oxygen concentration and glycolic acid metabolism. *Plant. Physiol.* **49**: 490-496.
- Herbert (1971). *Methods in Microbiology*. **5B**, 265-278.
- Herbert, S.K. (1990). Photoinhibition resistance in the red alga *Porphyra perforata*. *Plant Physiol.* **92**: 514-519.
- Herzig, R. and Falkowski, P.G. (1989). Nitrogen limitation in *Isochrysis galbana* (Haptophyceae). Photosynthetic energy conversion and growth efficiencies. *J. Phycol.* **25**: 462-471.
- Hettler, H., Fallowfield, H.J., Martin, N.J. and Chrsitofi, N. (1991). The use of a novel oxygen probe to examine the affect of biocides on the photosynthesis and dark respiration of algae. *British. Phycol. J.* **26**: 199.
- Jassby, A.D. and Platt, T. (1976). Mathematical formulation of the relationship between photosynthesis and light for phytoplankton. *Limnol. Oceanogr.* **21**: 540-547.
- Jeffrey, S.W. and Humphrey, G.F. (1975). New spectrophotometric equations for determining chlorophylls a, b, c1 and c2 in higher plants, algae and natural phytoplankton. *Biochem. Physiol. Pflanz.* **167**: 191-194.
- Jensen, S. and Knutsen, G. (1993). Influence of light and temperature on photoinhibition of photosynthesis in *Spirulina platensis*. *J. Applied. Phycology.* **5**: 495-504.
- Jones, L.W. and Kok, B. (1966). Photoinhibition of chloroplast reactions. *Plant. Physiol.* **41**: 1037-1043

- Joshi, J.B. and Sharma, M.M. (1979). A circulation cell model for bubble columns. *Trans. Inst. Chem. Engrs.* **57**: 244-251.
- Kanazawa, T., Kanazawa, K., Kirk, M.R. and Bassham, J.A. (1970). Difference in nitrate reduction in light and dark stages of synchronously grown *Chlorella pyrenoidosa* and resultant metabolic changes. *Plant. Cell. Physiol.* **11**: 445-452.
- Kanazawa, T., Kanazawa, K., Kirk, M.R. and Bassham, J.A. (1972). Regulatory effects of ammonia on carbon metabolism in photosynthesizing *Chlorella pyrenoidosa*. during photosynthesis and respiration. *Biochim. Biophys. Acta.* **256**: 656-669.
- Kaplan, A., Badger, M.R. and Berry, J.A. (1980). Photosynthesis and the intracellular inorganic carbon pool in the blue green alga *Anabaena variabilis*. *Planta.* **149**: 219-226.
- Kirk, J.T.O. (1983), *In Light and photosynthesis in aquatic ecosystems*. Cambridge University Press, Cambridge, 1-401.
- Kirk, J.T.O. (1989). The upwelling light stream in natural waters. *Limnol. Oceanogr.* **34**: 1410-1425.
- Kok, B. (1948). A critical consideration of the quantum yield of *Chlorella* photosynthesis. *Enzymologia.* **13**: 1-56.
- Kowallik, W. and Schätzle, S. (1980). Enhancement of carbohydrate degradation by blue light. *In*. The blue light syndrome. (H. Jenger. ed). Springer, Berlin Heidelberg, New York.
- Kroon, M.B.A., Ketelaars, H.A.M., Fallowfield, H.J. and Mur, L.R. (1989). Modelling microalgal productivity in a high rate algal pond based on wavelength dependent optical properties. *J. Appl. Phycol.* **1**: 247-256.
- Kroon, B.M.A, van Hes, U.M. and Mur, L.R. (1992a). An algal cyclostat with computer controlled dynamic light regime. *Hydrobiologia.* **238**: 63-72.
- Kroon, B.M.A., Latassa, M., Ibelings, B.W. and Mur, L.R. (1992b). The effect of dynamic light regimes on *Chlorella*. I pigments and cross sections. *Hydrobiologia.* **238**: 71-78.
- Kroon, B.M.A., Burger-Wiersma, T., Viisser, P.M. and Mur, L.R. (1992c). The effect of dynamic light regimes on *Chlorella*. II minimum quantum requirement and photosynthetic-irradiance parameters. *Hydrobiologia.* **238**: 79-88.
- Kruger, G.H.J. & Eloff, J.N. (1981). Defined algal production systems for the culture of microalgae. University of Orange Free State Publication Series C, **3**: 16 - 24.

- Ku, S.B. and Edwards, G.E. (1977). Oxygen inhibition of photosynthesis. *Plant. Physiol.* **59**: 986-990.
- Kyle, D.J. (1987). The biochemical basis for photoinhibition of photosystem II. *In Topics in photosynthesis* (Kyle, D.J., Osmond, C.B. and Arntzen, C.J. eds). Elsevier Science Publishers. Amsterdam. **9**: 197-226.
- Laing, W.A., Ogren, W.L. and Hageman, R.H. (1974). Regulation of soybean net photosynthesis and carbon dioxide fixation by the interaction of CO₂, O₂ and ribulose-1, 5-diphosphate carboxylase. *Plant. Physiol.* **54**: 678-685.
- Latassa, M., Berdalet, E. and Estrada, M. (1992). Variations in biochemical parameters of *Heterocapsa sp.* and *Olisthodiscus luteus* grown in 12:12 light:dark cycles. *Hydrobiologia.* **238**: 149-157.
- Laws, E.A., Terry, K.L., Wickman, J. and Chalup, M.S. (1983). A simple algal production system designed to utilise the flashing light effect. *Biotechnol. Bioeng.* **25**: 2319-2335.
- Lee, Y.K. and Pirt, S.J. (1981). Energetics of photosynthetic algal growth: Influence of intermittent illumination in short (40s) cycles. *J. Gen. Microbiol.* **124**: 43-52.
- Lee, Y.K. (1987). Population growth kinetics of photosynthetic micro-organisms. *In Physiological models in microbiology* (Bazin, M.J. and Prosser, J.I. eds). CRC Press Florida. **1**: 91-111.
- Lee, E.T.Y. and Bazin, M.J., (1990). A laboratory scale air-lift helical photobioreactor to increase biomass output rate of photosynthetic algal cultures. *New Phycol.*, **116**: 331-335. Lembi and Waaland, 1988
- Lewis, M.R., Warnock, R.E. and Platt, T. (1985). Absorption and photosynthetic action spectra for natural phytoplankton populations: Implications for production in the open ocean. *Limnol. Oceanogr.* **30**: 794-806.
- Ley, A.C. and Butler, W.L. (1980). Effects of chromatic adaptation on the photochemical apparatus of photosynthesis in *Porphyridium cruentum*. *Plant. Physiol.* **65**: 714-722.
- Lin, T.Y. and Markhart, A.H. (1990). Temperature effects on mitochondrial respiration in *Phaseolus acutifolius* A. gray and *Phaseolus vulgaris* L. **94**: 54-58.
- Lloyd, D. (1974). Dark Respiration. *In Algal Physiology and Biochemistry*. Ed W.D.P. Stewart. Blackwell, Oxford. 505-529.
- Lloyd, N.D.H., Canvin, D.T. and Culver, D.A. (1977). Photosynthesis and photorespiration in Algae. *Plant. Physiol.* **59**: 936-940.

- Mangat, B.S., Levin, W.B. and Bidwell, R.G.S. (1974). The extent of dark respiration in illuminated leaves and its control by ATP levels. *Can. J. Bot.* **52**: 673-682.
- Mann, K.H., Britton, R.H. Kowalczewski, A., Lack, T.J., Mathews, C.P. and McDonald, I. (1972). Productivity and energy flow at all trophic levels in the River Thames, England. *In*. Productivity problems of freshwaters. (Kajak, Z. and Hillbricht-Ilkowska, A eds.). Polish Scientific Publ. 579-599.
- Marra, J. (1978). Phytoplankton photosynthetic response to vertical movement in a mixed layer. *Mar. Biol.* **46**: 203-208.
- Martin, N.J. and Fallowfield, H.J. (1989). Computer modelling of algal waste treatment systems. *Water. Science. Technology.* **22**: 277-287.
- Mavuti, K.M. (1992). Diel vertical distribution of zooplankton in Lake Naivasha, Kenya. *Hydrobiologia.* **232**: 31-41.
- Megard, R.O., Tonkyn, D.W. and Senft, W.H. (1984). Kinetics of oxygenic photosynthesis in planktonic algae. *J. Plankton. Res.* **6**: 325-337.
- Mehler, A.H. (1951). Studies on reactions of illuminated chloroplasts. I. Mechanism of the reduction of oxygen and other Hill reagents. *Arch. Biochem. Biophys.* **33**: 65-77.
- Miller, A.G., Cheng, K.H. and Colman, B. (1971). The uptake and oxidation of gluconic acid by blue green algae. *J. Phycol.* **7**: 97-100.
- Miller, A.G. and Colman, B. (1980). Evidence for HCO₃⁻ transport by the blue-green alga (Cyanobacterium) *Coccochloris peniocyctis*. *Plant. Physiol.* **65**: 397-402.
- Moo-Young, M. and Blanch, H.W., (1981). Design of bioreactors: Mass transfer criteria for simple and complex systems. *Adv. Biochem. Eng.*, **19**,1-69
- Mori, K., Ohya, H., Matsumoto, K., Furuune, H., Isozaki, K., and Siekmeier, P., (1989). Design for a Bioreactor with sunlight supply and operations systems for use in space environment, *Adv. Space. Res.*, **8**: 161-168.
- Myers, J. (1970). Genetic and adaptive physiological characteristics observed in the *Chlorellas*. *In* Prediction and measurement of photosynthetic production. Technical meeting, Trebon 1969. Wageningen, Pudoc. 447-454.
- Myers, J., Graham, J.R. (1971). The photosynthetic unit in *Chlorella* measured by repetitive short flashes. *Plant. Physiol.* **48**: 282-286.
- Myers, J., Graham, J.R. and Wang, R.T. (1980). Light harvesting in *Anacystis nidulans*. *Plant. Physiol.* **66**: 1144-1149.

Nielsen, E.S., Hansen, V.K. and Jorgensen, E.G. (1962). The adaptation to different light intensities in *Chlorella vulgaris* and the time dependence on transfer to a new light intensity. *Physiol. Planta*. **15**: 505-517.

Ogasawara, N. and Miyachi, S. (1970). Regulation of CO₂ fixation by *Chlorella* by light of varied wavelengths and intensities. *Plant & Cell Physiol*. Tokyo. **11**: 1-14.

Olaizola, M. and Duerr, E.O. (1990). Effects of light intensity and quality on the growth rate and photosynthetic pigment content of *Spirulina platensis*. *J. Appl. Phycol*. **2**: 97-104.

Oswald, W.J. (1986). *In Ponds as a wastewater treatment alternative*. (eds, Gloyna, E.F., Molina, J.F. and Davis, E.M.) pp 252-272. Austin: University of Texas centre for research water engineering, College of engineering.

Oswald, W.J. (1988). Micro-algae and waste water treatment. In *Micro-algal Biotechnology*. (Eds Borowitzka and Borowitzka) Cambridge Press pp 305-328

Owens, T.G., Riper, D.M. and Falkowski, P.G. (1978). Studies of delta-aminoievulinic acid dehydrase from *Skeletonema costatum* a marine plankton diatom. *Plant. Physiol*. **62**: 516-521.

Paasche, E. (1968). Marine plankton algae grown with light dark cycles. II *Ditylum brightwelli* and *Nitzschia turgidula*. *Physiol. Planta*. **21**: 66-77.

Palmqvist, K., Sundblad, L.G., Wingsle, G. and Samuelsson, G. (1990). Acclimation of photosynthetic light reactions during induction of inorganic carbon accumulation in the green alga *Chlamydomonas reinhardtii*. *Plant. Physiol*. **94**: 357-366.

Peltier, G. and Thibault, P. (1985). O₂ uptake in the light in *Chlamydomonas*. *Plant. Physiol*. **79**: 225-230.

Philippis, R.D., Margheri, M.C., Pelosi, E. and Ventura, S. (1993). Exopolysaccharide production by a unicellular cyanobacterium isolated from a hypersaline habitat. *J. Appl. Phycol*. **5**: 387-394.

Pirt, S.J. (1975). Principles of microbe and cell cultivation. Blackwell Scientific Publications. Oxford. 1-274.

Pirt, S.J., Lee, Y.K., Walach, M.R., Watts Pirt, M., Hushbang, H., Baluyuzi, M. and Bazin, M.J. (1983). A tubular bioreactor for photosynthetic production of biomass from carbon dioxide: design and performance. *Journal of Chemical Technology and Biotechnology*. **33B**: 35-58.

Platt, T., Denman, K.L and Jassby, A.D. (1975). The mathematical representation and prediction of phytoplankton productivity. *Fish. Mar. Serv. Tech. Rep*. **523**: 110

- Platt, T. and Jassby, A.D. (1976). The relationship between photosynthesis and light for natural assemblages of coastal marine phytoplankton. *J. Phycol.* **12**: 421-430.
- Platt, T and Gallegos, C.L. (1981). Modelling primary production. Brookhaven Symposia in Biology. **31**: 339-362.
- Platt, T., Gallegos, C.L. and Harrison, W.G. (1980). Photoinhibition of photosynthesis in natural assemblages of marine phytoplankton. *J. Mar. Res.* **38**: 687-701.
- Pollio, A., Pinto, G., Ligrone, R. and Aliotta, G. (1993). Effects of the potential alleochemical α -asaone on growth, physiology and ultrastructure of two unicellular green algae.
- Powles, S.B. (1984). Photoinhibition of photosynthesis induced by visible light. *Ann. Rev. Plant. Physiol.* **35**: 15-34.
- Prezelin, B.B. (1976). The role of peridinin-chlorophyll a proteins in the photosynthetic light adaptation of the marine dinoflagellate *Glenodinium sp.* *Planta (Berl.)*. **130**: 225-233.
- Prezelin, B.B., and Matlick, H.A. (1983). Nutrient dependent low light adaptation in the dinoflagellate, *Gonyaulax polyedra*. *Mar. Biol.* **74**: 141-150.
- Prezelin, B.B., Samuelsson, G. and Matlick, H.A. (1986). Nutrient dependent kinetics of photosynthesis parameters and photoinhibition of photosystem II during high light photoadaptation in *Gonyaulax polyedra*. *Mar. Biol.* **93**: 1-12.
- Prezelin, B.B., Glover, H.E. and Campbell, L. (1987). Effects of light intensity and nutrient availability on diel patterns of cell metabolism and growth in populations of *Synechococcus spp.* *Mar. Biol.* **95**: 469-480.
- Prezelin, B.B., Tilzer, M.M., Schofield, O. and Haese, C. (1991). The control of the production process of phytoplankton by the physical structure of the aquatic environment with special reference to its optical properties. *Aquatic. Sciences.* **53**: 137-184.
- Prezelin, B.B. (1992). Diel periodicity in phytoplankton productivity. *Hydrobiologia.* **238**: 1-35.
- Pronina, N.A., Avramova, S., Georiev, S. and Semenenko, V.E. (1981). Dynamics of carbonic anhydrase activity in *Chlorella* and *Scenedesmus* during adaptation of cells to light of high intensity and low CO₂ concentration. *Fiziol. Rast.* **28**: 43-52.
- Putt, M. and Prezelin, B.B. (1988). Diel periodicity of photosynthesis and cell division compared in *Thalassiosira weissflogii* (Bacillariophyceae). *J. Phycol.* **24**: 315-325.

- Radmer, R.J. and Kok, B. (1976). Photoreduction of O₂ primes and replaces CO₂ assimilation. *Plant. Physiol.* **58**: 336-340.
- Radmer, R.J. and Ollinger, O. (1980). Light driven uptake of oxygen, carbon dioxide and bicarbonate in the green alga *Scenedesmus*. *Plant. Physiol.* **65**: 723-729.
- Ramus, J. (1981). The capture and transduction of light energy. In: *The Biology of Seaweeds Botanical Monographs*. vol 17 (Ed. C.S.Lobban & M.J.Wynne), pp 458-492. Blackwell Scientific Publications, Oxford, England.
- Ratchford, I.A.J. and Fallowfield, H.J. (1991). A comparison of the growth kinetics of *Chlorella vulgaris* 211/11c grown in a flat plate multi-pass air lift reactor irradiated by quartz halogen or high pressure sodium lamps. *British. Phycological. Journal.* **26**: (2), 199.
- Ratchford, I.A.J. and Fallowfield, H.J. (1992a) Performance of a flat plate, air-lift reactor for the growth of high biomass algal cultures. *Journal of Applied Phycology* **4**: 1-9
- Ratchford, I.A.J. and Fallowfield, H.J. (1992b). The effect of culture wavelength on light enhanced dark respiration. *British. Phycological. Journal.* **27**: (1), 98.
- Raven, J.A. (1969). Effects of inhibitors on photosynthesis and the active influxes of K and CL in *Hydrodictyon africanum*. *New. Phytol.* **68**: 1089-1113.
- Raven, J.A. (1970). Endogenous in carbon sources in plant photosynthesis. *Biol. Rev.* **45**: 167-221.
- Raven, J.A. (1971). Cyclic and non-cyclic photophosphorylation as energy sources for active K influx in *Hydrodictyon africanum*. *J. Exp. Bot.* **22**: 420-433.
- Raven, J.A (1972a). Endogenous inorganic carbon sources in plant photosynthesis. Occurrence of dark respiratory pathways in illuminated green cells.
- Raven, J. A. (1984). *Energetics and Transport in Aquatic Plants*. New York, A.R. Liss, 596.
- Raven, J.A. and Samuelsson, G. (1986). Repair of photoinhibitory damage in *Anacystis nidulans* 625 (*Synechococcus* 6301): relation to catalytic capacity for and energy to, protein synthesis, and implications for μ_{max} and the efficiency of light limited growth. *New Phytol.* **103**: 625-643.
- Raven, J.A. (1989). Fight or flight: the economics of repair and avoidance of photoinhibition of photosynthesis. Essay Review. *Functional Ecology.* **3**: 5-19.

- Reddy, M.M., Vani, T. and Raghavendra, A.S. (1991). Light enhanced dark respiration in Mesophyl protoplasts from leaves of pea. *Plant. Physiol.* **96**: 1368-1371.
- Richardson, K., Beardall, J. and Raven, J.A. (1983). Adaptation of unicellular algae to irradiance: an analysis of strategies. *New. Phytol.* **93**: 157-191.
- Richmond, A. and Vonshak, A. (1978). *Spirulina* culture in Israel. *Arch. Hydrobiol. Beih., Ergebn. Limnol.* **11**: 274-280.
- Richmond, A., Vonshak, A. and Arad, S. (1980). Environmental limitations in outdoor production of algal biomass. *In. Algae Biomass.* (Shelef, G and Soeder, C.J., Eds). Elsevier North-Holland Biomedical Press, Amsterdam. 65-72.
- Richmond, A., Boussiba, S., Vonshak, A. and Kopel, R. (1992). A new tubular reactor for mass production of microalgae outdoors. *J. Applied. Phycol.* **5**: 327-332.
- Riper, D.M., Owens, T.G. and Falkowski, P.G. (1979). Chlorophyll turnover in *Skeletonema costatum*, a marine planktonic diatom. *Plant. Physiol.* **64**: 49-54.
- Rivkin, R.B., Voytek, M.A. and Seliger, H.H. (1982). Strategies of phytoplankton division rates in light limited environments. *Science.* **215** 1123-1125.
- Rodgers, P.W. and DePinto, J.V. (1981). Algae bacteria interaction in a light dark cycle. *J. Freshwater. Ecology.* **1**: 71-80.
- Sager, P.E. and Richman, S. (1991). Functional interaction of phytoplankton and zooplankton along the trophic gradient in Green Bay, Lake Michigan. *Can. J. Fish. Aquat. Sci.* **48**: 116-122.
- Samuelsson, G., Lonneborg, A., Rosenqvist, E., Gustafsson, P. and Oquist, G. (1985). Photoinhibition and reactivation of photosynthesis in the cyanobacterium *Anacystis nidulans*. *Plant. Physiol.* **79**: 992-995.
- Santillan, C. (1982). Mass production of *Spirulina*. *Experimentia.* **38**: 40-43.
- Sargent, D.F. and Taylor, P.S. (1972). Terminal oxidases of *Chlorella pyrenoidosa*. *Plant. Physiol.* **49**: 775-778.
- Sargent, D.F. and Taylor, C.P.S. (1975). On the respiratory enhancement in *Chlorella pyrenoidosa* by blue light. *Planta. (Berl.)* **127**: 171-175.
- Sathyendranath, S., Lazzara, L. and Prieur, L. (1987). Variations in the spectral values of specific absorption of phytoplankton. *Limnol. Oceanogr.* **32**: 403-415.

- Sato, K. (1970). Mechanism of photoinactivation in photosynthetic systems I. The dark reaction in photoinactivation. *Plant Cell Physiol.* **11**: 15-27.
- Sharkey, T.D. (1989). Evaluating the role of Rubisco regulation in photosynthesis of C3 plants. *Phil. Trans. R. Soc. Lond.* **B323**: 435-448.
- Sharpless, T.K. and Burrow, R.A. (1970). Phosphorylation sites, cytochrome complement and alternate pathways of coupled electron transport in *Euglena gracilis* mitochondria. *J. Biol. Chem.* **245**: 50-57.
- Shelp, J.B. and Canvin, D.T. (1980). Photorespiration and oxygen inhibition of photosynthesis in *Chlorella pyrenoidosa*. *Plant. Physiol.* **65**: 780-784.
- Shelp, J.B. and Canvin, D.T. (1985). Inorganic carbon accumulation and photosynthesis by *Chlorella pyrenoidosa*. *Can. J. Bot.* **63**: 1249-1254.
- Sheridan, R.P. (1972b). Adaptation to quantum flux by the Emerson photosynthetic unit. *Plant. Physiol.* **50**: 355-359.
- Shifrin, N.S. and Chisolm, S.W. (1981). Phytoplankton lipids: Interspecific differences and effects of nitrate, silicate and light dark cycles. *J. Phycol.* **17**: 374-384.
- Siefermann-Harms, D. (1980). The role of carotenoids in chloroplasts of higher plants. (Mazliak, P., Beneviste, P., Costes, C. and Douce, D. (editors)), *In Biogenesis and function of plant lipids*. Elsevier, North Holland Biochemical Press, Amsterdam, 331-340.
- Sironval, C. and Kandler, O. (1958). Photooxidation processes in normal green *Chlorella* cells. *Biochimica Et Biophysica Acta* **29**: 359-368.
- Smith, S.R.L. (1981). Some aspects of ICI's single cell protein process. *In Microbial growth on C₁ compounds*. (Eds, Dalton, H.) pp 342-348. Heyden, London.
- Soeder, C.J., Hegewald, E., Fiolitakis, E. and Grobbelaar, J.U. (1985). Temperature dependence of population growth in a green microalga: Thermodynamic characteristics of growth intensity and the influence of cell concentration. *Z. Naturforsch.* **40**: 227-233.
- Sorokin, C. (1957). Changes in photosynthetic activity in the course of cell development in *Chlorella*. *Physiol. Plant.* **10**: 659-666.
- Spalding, M.H., Spreitzer, R.J. and Owen, W.L. (1983a). Carbonic anhydrase deficient mutant of *Chlamydomonas reinhardtii* requires elevated carbon dioxide concentration for photoautotrophic growth. *Plant. Physiol.* **73**: 268-272.
- Stanbury, P.F. and Whitaker, A. (1984). *In Principles of fermentation technology*. Pergamon Press, Oxford.

- Stemann Nielsen, E., Hansen, V.K. and Jorgensen, E.G. (1962). The adaptation to different light intensities in *Chlorella vulgaris* and the time dependence to transfer to a new light intensity. *Physiol. Plant.* **15**: 505-517.
- Stemann Nielsen, E. and Jorgensen, E.G. (1968). The adaptation of plankton algae. *Plant. Physiol.* **21**: 401-413.
- Stemann Nielsen, E. (1975). *Marine Photosynthesis*. Amsterdam. Elsevier. 265-273.
- Steele, J.H. (1962). Environmental control of photosynthesis in the sea. *Limnol. Oceanogr.* **7**: 137-150.
- Stewart, D.E. and Farmer, F.H. (1984). Extraction, identification and quantification of phycobiliprotein pigments from phototrophic phytoplankton. *Limnol. Oceanogr.* **29**: 392-397.
- Stone, S.J.L. and Ganf, G.G. (1981). The influence of previous light history on the respiration of four species of freshwater phytoplankton. *Arch. Hydrobiol.* **91**: 435-462.
- Stuart, T.S. (1970). Hydrogen production by photosystem I of *Scenedesmus*: Effect of heat and Salicylaldehyde on electron transport and photophosphorylation. *Planta*. (Berl.). **96**: 81-92.
- Sültemeyer, D.F., Klug, K. and Fock, H.P. (1986). Effect of photon fluence rate on oxygen evolution and uptake in *Chlamydomonas reinhardtii* suspensions grown in ambient and CO₂ enriched air. *Plant. Physiol.* **81**: 372-375.
- Sültemeyer, D.F., Miller, A.G., Espie, G.S., Fock, H.P. and Canvin, D.T. (1989). Active CO₂ transport by the green alga *Chlamydomonas reinhardtii*. *Plant. Physiol.* **89**: 1213-1219.
- Sukenik, A., Bennett, J., Bertrand, A.M. and Falkowski, P.G. (1990). Adaptation of the photosynthetic apparatus to irradiance in *Dunaliella tertiolecta*. **92**: 891-898.
- Syrett, P.J. (1951). The effect of cyanide on the respiration and the oxidation assimilation of glucose by *C. vulgaris*. *Ann. Bot.* **15**: 473-492.
- Takahashi, M., Shimura, S., Yamaguchi, Y. and Fujita, Y. (1971). Photoinhibition of phytoplankton photosynthesis as a function of exposure time. *J. Ocean. Soc. Jap.* **27**: 43-50.
- Talbot, P., Thiebault, J.M., Dauta, A. and De La Noue, J. (1991). A comparative study and mathematical modelling of temperature, light and growth of three microalgae potentially useful for wastewater treatment. *Wat. Res.* **25**: 465-472.

- Tandeau de Marsac, N. (1977). Occurrence and nature of chromatic adaptation in cyanobacteria. *J. Bact.* **130**: 82-91.
- Terry, K.L. (1986). Photosynthesis in modulated light: Quantitative dependence of photosynthetic enhancement on flashing rate. *Biotech. Bioeng.* **28**: 988-995.
- Vincent, W.F. (1992). The daily pattern of nitrogen uptake by phytoplankton in dynamic mixed layer environments. *Hydrobiologia.* **238**: 37-52.
- Voskresenskaya, N.P. (1952). Influence of the spectral distribution of light on the products of photosynthesis. *Dokl. Akad. Nauk. SSSR.* **86**: 429.
- Walsh, P. and Legendre, L. (1983). Photosynthesis of natural phytoplankton under high frequency light fluctuations simulating those induced by sea surface waves *Limnol Oceanogr.* **28**: 688-697.
- Wang, W.Q., Chapman, D.J. and Barber, J. (1992). Inhibition of water splitting increases the susceptibility of photosystem II to photoinhibition. *Plant. Physiol.* **99**: 16-20
- Wang, R.T, Stevens, C.L.R. and Myers, J. (1977). Action spectra for photoreactions I and II of photosynthesis in the blue-green alga *Anacystis nidulans*. *Photochem. Photobiol.* **25**: 103-108.
- Warr, S.R.C., Reed, R.H. and Stewart, W.D.P. (1985). Blue green algae : interactions of temperature and salinity. *British. Phycol. Soc.* **100** : 285-292.
- Watts-Pirt, M. and Pirt, S.J. (1977). Photosynthetic production of biomass and starch by *Chlorella* in a chemostat culture. *J. Appl. Chem. Biotechnol.* **27**: 643-650.
- Webb, W.L., Newton, M. and Starr, D. (1974). Carbon dioxide exchange of *Alnus rubra*: a mathematical model. *Oecologia. (Berl).* **17**: 281-291.
- Wynne, D. and Rhee, G.Y. (1988). Changes in alkaline phosphatase activity and phosphate uptake in phosphorus limited phytoplankton induced by light intensity and spectral quality. *Hydrobiologia.* **160**: 173-178.
- Yentsch, C.S. and Lee, P.W. (1966). A study of the photosynthetic light reactions and a new interpretation of sun and shade phytoplankton. *J. Marine. Research.* **24**: 319-337.
- Zelitch, I. (1971). Photosynthesis, photorespiration and plant productivity. Academic Press. New York. 173-214.